ISSN 1948-5204 (online)

World Journal of *Gastrointestinal Oncology*

World J Gastrointest Oncol 2022 October 15; 14(10): 1892-2087

Published by Baishideng Publishing Group Inc

World Journal of Gastrointestinal Oncology

Contents

Monthly Volume 14 Number 10 October 15, 2022

MINIREVIEWS

ORIGINAL ARTICLE

Basic Study

Retrospective Study

Observational Study

World Journal of Gastrointestinal Oncology

Monthly Volume 14 Number 10 October 15, 2022

Contents

World Journal of Gastrointestinal Oncology

Monthly Volume 14 Number 10 October 15, 2022

Contents

ABOUT COVER

Editorial Board of *World Journal of Gastrointestinal Oncology*, Sezer Saglam, MD, Full Professor, Medical Oncology, Demiroglu Bilim University, Istanbul 34349, Turkey. saglam@istanbul.edu.tr

AIMS AND SCOPE

The primary aim of *World Journal of Gastrointestinal Oncology* (*WJGO*, *World J Gastrointest Oncol*) is to provide scholars and readers from various fields of gastrointestinal oncology with a platform to publish high-quality basic and clinical research articles and communicate their research findings online.

WJGO mainly publishes articles reporting research results and findings obtained in the field of gastrointestinal oncology and covering a wide range of topics including liver cell adenoma, gastric neoplasms, appendiceal neoplasms, biliary tract neoplasms, hepatocellular carcinoma, pancreatic carcinoma, cecal neoplasms, colonic neoplasms, colorectal neoplasms, duodenal neoplasms, esophageal neoplasms, gallbladder neoplasms, *etc*.

INDEXING/ABSTRACTING

The *WJGO* is now abstracted and indexed in PubMed, PubMed Central, Science Citation Index Expanded (SCIE, also known as SciSearch®), Journal Citation Reports/Science Edition, Scopus, Reference Citation Analysis, China National Knowledge Infrastructure, China Science and Technology Journal Database, and Superstar Journals Database. The 2022 edition of Journal Citation Reports® cites the 2021 impact factor (IF) for *WJGO* as 3.404; IF without journal self cites: 3.357; 5-year IF: 3.250; Journal Citation Indicator: 0.53; Ranking: 162 among 245 journals in oncology; Quartile category: Q3; Ranking: 59 among 93 journals in gastroenterology and hepatology; and Quartile category: Q3. The *WJGO*'s CiteScore for 2021 is 3.6 and Scopus CiteScore rank 2021: Gastroenterology is 72/149; Oncology is 203/360.

RESPONSIBLE EDITORS FOR THIS ISSUE

Production Editor: *Ying-Yi Yuan*; **Production Department Director:** *Xiang Li*; **Editorial Office Director:** *Jia-Ru Fan*.

NAME OF JOURNAL
World Journal of Gastrointestinal Oncology

ISSN
ISSN 1948-5204 (online)

LAUNCH DATE
February 15, 2009

FREQUENCY
Monthly

EDITORS-IN-CHIEF
Monjur Ahmed, Florin Burada

EDITORIAL BOARD MEMBERS
https://www.wjgnet.com/1948-5204/editorialboard.htm

PUBLICATION DATE
October 15, 2022

INSTRUCTIONS TO AUTHORS
https://www.wjgnet.com/bpg/gerinfo/204

GUIDELINES FOR ETHICS DOCUMENTS
https://www.wjgnet.com/bpg/GerInfo/287

GUIDELINES FOR NON-NATIVE SPEAKERS OF ENGLISH
https://www.wjgnet.com/bpg/gerinfo/240

PUBLICATION ETHICS
https://www.wjgnet.com/bpg/GerInfo/288

PUBLICATION MISCONDUCT
https://www.wjgnet.com/bpg/gerinfo/208

ARTICLE PROCESSING CHARGE
https://www.wjgnet.com/bpg/gerinfo/242

STEPS FOR SUBMITTING MANUSCRIPTS
https://www.wjgnet.com/bpg/GerInfo/239

ONLINE SUBMISSION
https://www.f6publishing.com

World Journal of Gastrointestinal Oncology

Submit a Manuscript: https://www.f6publishing.com

World J Gastrointest Oncol 2022 October 15; 14(10): 1892-1902

DOI: 10.4251/wjgo.v14.i10.1892

ISSN 1948-5204 (online)

MINIREVIEWS

Go-Ichi-Ni-San 2: A potential biomarker and therapeutic target in human cancers

Dan-Dan Shan, Qiu-Xian Zheng, Zhi Chen

Specialty type: Oncology

Provenance and peer review: Unsolicited article; Externally peer reviewed.

Peer-review model: Single blind

Peer-review report's scientific quality classification

Grade A (Excellent): 0
Grade B (Very good): B
Grade C (Good): C, C
Grade D (Fair): 0
Grade E (Poor): 0

P-Reviewer: Fazilat-Panah D, Iran; Luo Y, China; Tousidonis M, Spain

Received: May 19, 2022
Peer-review started: May 19, 2022
First decision: July 13, 2022
Revised: July 15, 2022
Accepted: September 6, 2022
Article in press: September 6, 2022
Published online: October 15, 2022

Dan-Dan Shan, Qiu-Xian Zheng, Zhi Chen, State Key Laboratory for Diagnosis and Treatment of Infectious Diseases, National Clinical Research Center for Infectious Diseases, National Medical Center for Infectious Diseases, Collaborative Innovation Center for Diagnosis and Treatment of Infectious Diseases, The First Affiliated Hospital, Zhejiang University School of Medicine, Hangzhou 310003, Zhejiang Province, China

Corresponding author: Zhi Chen, MD, PhD, Professor, State Key Laboratory for Diagnosis and Treatment of Infectious Diseases, National Clinical Research Center for Infectious Diseases, National Medical Center for Infectious Diseases, Collaborative Innovation Center for Diagnosis and Treatment of Infectious Diseases, The First Affiliated Hospital, Zhejiang University School of Medicine, No. 79 Qingchun Road, Shangcheng District, Hangzhou 310003, Zhejiang Province, China. zjuchenzhi@zju.edu.cn

Abstract

Cancer incidence and mortality are increasing globally, leading to its rising status as a leading cause of death. The Go-Ichi-Ni-San (GINS) complex plays a crucial role in DNA replication and the cell cycle. The GINS complex consists of four subunits encoded by the GINS1, GINS2, GINS3, and GINS4 genes. Recent findings have shown that GINS2 expression is upregulated in many diseases, particularly tumors. For example, increased GINS2 expression has been found in cervical cancer, gastric adenocarcinoma, glioma, non-small cell lung cancer, and pancreatic cancer. It correlates with the clinicopathological characteristics of the tumors. In addition, high GINS2 expression plays a pro-carcinogenic role in tumor development by promoting tumor cell proliferation and migration, inhibiting tumor cell apoptosis, and blocking the cell cycle. This review describes the upregulation of GINS2 expression in most human tumors and the pathway of GINS2 in tumor development. GINS2 may serve as a new marker for tumor diagnosis and a new biological target for therapy.

Key Words: Go-Ichi-Ni-San; Go-Ichi-Ni-San 2; Cancer; Biomarker; Clinicopathological characteristics; Molecular mechanism

Core Tip: The Go-Ichi-Ni-San (GINS) complex plays a crucial role in DNA replication and the cell cycle. The GINS complex consists of four subunits encoded by the GINS1, GINS2, GINS3, and GINS4 genes. This review explores the differential expression of GINS2 as a novel target in human cancers. GINS2 is upregulated in most tumors and can influence tumorigenesis and progression through competing endogenous RNA effects and signaling pathways. Therefore, GINS2 may become a new target for the diagnosis and treatment of many cancers.

Citation: Shan DD, Zheng QX, Chen Z. Go-Ichi-Ni-San 2: A potential biomarker and therapeutic target in human cancers. *World J Gastrointest Oncol* 2022; 14(10): 1892-1902
URL: https://www.wjgnet.com/1948-5204/full/v14/i10/1892.htm
DOI: https://dx.doi.org/10.4251/wjgo.v14.i10.1892

INTRODUCTION

Cancer ranks as the second leading cause of death worldwide, and the burden of cancer is growing, with approximately 9.6 million deaths due to cancer in 2018. Unfortunately, many cancer patients worldwide do not have access to timely, high-quality diagnosis and treatment (World Health Organization, https://www.who.int/cancer/en/). It is therefore crucial to more fully understand how cancer develops and to identify new markers for its diagnosis and new targets for its treatment.

In 2003, Takayama *et al*[1] described Go-Ichi-Ni-San (GINS) for the first time. The GINS complex is conserved in eukaryotic cells and is essential for DNA replication. When the DNA replication fork is opened, GINS is required to maintain the association between the microchromosome maintenance protein (MCM) and Cdc45 in the large replicator complex[1]. The GINS complex acts as a replicative helicase that unlocks the double-stranded DNA prior to the moving replication fork[2]. The GINS complex consists of four subunits encoded by the GINS1, GINS2, GINS3, and GINS4 genes. GINS2, also known as Psf2, is located in regions 2 and 4 of the long arm of chromosome 16 with a length of 1196 bp [2], as shown in Figure 1. Recent results suggest that GINS2 expression is upregulated in many diseases, especially tumors, and adversely affects prognosis, such as in patients with cervical cancer (CC)[3], breast cancer (BC)[4,5], gastric adenocarcinoma[6], glioma[7], non-small cell lung cancer (NSCLC)[8,9], and pancreatic cancer[10,11].

In this review, we reviewed associated reports and searched the PubMed database from February 2008 to April 2022 using the keywords "GINS2" and "cancer". After excluding articles from letters, case reports, reviews, meta-analyses, or conference reports, 55 articles describing the expression of GINS2 in human cancers and its relevance to clinical features, as well as the pathways of GINS2 in tumors, were included for further analysis. We also cited high-quality articles in *Reference Citation Analysis* (https://www.referencecitationanalysis.com). It is reasonable to assume that GINS2 may become a marker in cancer diagnosis and a biological target for prognosis.

EXPRESSION PROFILES OF GINS2 IN CANCERS

Numerous studies have investigated the expression levels of GINS2 in human tissues. The results show that GINS2 expression is increased in most tumors compared to normal tissues and correlates with various clinicopathological features. It has been demonstrated that GINS2 is expressed at higher levels in tumor tissue than in adjacent normal tissue, such as in CC[3], gastric adenocarcinoma[6], glioma[7], NSCLC[8,9], pancreatic cancer[10,11], and thyroid cancer (TC)[12,13]. Specifically, analysis of potential correlations between GINS2 expression levels and clinicopathological features has indicated that high GINS2 expression levels are closely associated with tumor size[6,10], tumor nodal metastasis (TNM) stage[6,8], pathological grade[7] and vascular permeation[10]. These conclusions imply that GINS2 may act as a tumor promoter. A summary of data obtained from published studies is provided in Table 1.

MOLECULAR PATHWAYS INVOLVED IN GINS2

In most tumors, elevated levels of GINS2 expression can increase malignant features such as tumor cell proliferation[3-7], migration[8,13,14], invasion[8,13], epithelial-mesenchymal transition (EMT)[8,10], anti-apoptosis effects[12-16] and cell cycle arrest[7,9,11,12], as shown in Figure 2, which are related to the many mechanisms GINS2 is involved in, as shown in Figure 3 and Table 2.

Table 1 The expression and clinical significance of Go-Ichi-Ni-San 2 in cancer

Cancer types	Cases	Expression	Clinicopathologic parameters	Ref.
Cervical cancer	155 pairs	Upregulated	Pelvic lymph node metastasis, SCC-Ag, deep stromal invasion, vital status, recurrence	Ouyang *et al* [3]
Gastric adenocarcinoma	123 pairs	Upregulated	Tumor size, T stage, LN metastasis	Feng *et al*[6]
Glioma	120 pairs	Upregulated	Uathological grade	Shen *et al*[7]
Glioma	37 pairs	Upregulated	/	Chi *et al*[9]
Glioma	63 pairs	Upregulated	TNM stage, clinical stage	Liu *et al*[8]
Pancreatic cancer	74 pairs	Upregulated	Tumor size, T stage, vascular permeation	Huang *et al*[10]
Pancreatic cancer	46 pairs	Upregulated	/	Bu *et al*[11]
Ovarian cancer	30 pairs	Upregulated	/	Zhan *et al*[14]

TNM: Tumor nodal metastasis; LN: Lymph node; SCC-Ag: Squamous cell carcinoma antigen.

BC

BC has high morbidity and mortality rates. However, there is still no cure, and patients diagnosed at a late stage often have a poor survival rate, and therefore it is crucial to better understand the mechanisms of breast cancer development[20]. Matrix metalloproteinases (MMPs) are zinc (Zn^{2+})-dependent endopeptidases involved in the remodeling of the extracellular matrix during physiopathological processes[21]. MMPs play an important role in development, wound healing, tissue remodeling and angiogenesis, with angiogenesis playing a key role in the growth and development of tumors[22]. MMP9 is one of these MMPs and belongs to the gelatinase family[23]. It degrades gelatine and collagen types IV, V, XI and XVI in tissue remodeling and has a significant impact on tumor invasion and metastasis[24]. Peng *et al*[4] found that knockdown of GINS2 in breast cancer resulted in a significant reduction in MMP9, and GINS2 may regulate the invasive and stem cell-like properties of breast cancer cells through MMP9. The above findings suggest that the expression of GINS2 may be closely related to the prognosis and survival of BC patients.

Bladder cancer

Bladder cancer has a high incidence of cancer of the urinary system, and 150000 people die of bladder cancer each year[25]. Targets for the effective diagnosis and treatment of bladder cancer are vital. Tian *et al*[26] found that GINS2 mRNA was a downstream target of miR-22-3p in bladder cancer cells and that knockdown of GINS2 suppressed the phenotype of tumor cells. Similar results were found in bladder cancer cells by Dai *et al*[27].

Colon cancer

The incidence and mortality rate of colon cancer remain high and pose a substantial global burden[28]. Exploring new targets for colon cancer is particularly critical. In cells, protein tyrosine phosphatases (PTPs) have a vital role in regulating tyrosine phosphorylation levels and numerous physiological processes[29]. PTP4A1 belongs to the tripentenyl PTP subclass (PTP4A1/2/3)[30]. Hu *et al*[31] found that GINS2 interacted with PTP4A1 to regulate the proliferation and apoptosis of colon cancer cells. This finding indicates that GINS2 may be a potential new molecular target for colon cancer.

Ovarian cancer

In 2018, the worldwide incidence of ovarian cancer (OC) was 6.6 per 100000[32]. Zhan *et al*[14] found that miR-502-5p can inhibit GINS2 expression through the activity of a competing endogenous RNA, which inhibits OC progression by suppressing OC cell growth and promoting apoptosis. In summary, GINS2 can be used as a downstream molecule to influence OC development, and GINS2 may be a new OC target.

Glioma

Gliomas are the most commonly occurring primary malignancies in the brain, with significantly higher recurrence and mortality rates[33]. In addition, the prognosis of patients is poor, methods to significantly improve patient survival are lacking, and research into the mechanisms of glioma is urgently needed. Minichromosome maintenance complex component 2 (MCM2) belongs to the minichromosome maintenance protein complex and consists of 6 highly conserved proteins (MCM2-7)[34]. Ataxia telangiectasia mutated (ATM) is an important upstream signaling molecule that controls the

Table 2 The mechanism of action of Go-Ichi-Ni-San 2 in various cancers

Cancer types	Assessed cancer cell lines	Expression	Related genes and pathways	Biological significance	Ref.
Bladder cancer	5637, T24	Up	miR-515-5p	Proliferation, migration, invasion, EMT	Dai *et al*[27]
Bladder cancer	RT4, T24, J82, 5637	Up	miR-22-3p	Proliferation, colony formation, anti-apoptosis	Tian *et al*[26]
Breast cancer	MCF10A, T47D, MCF-7, SUM149, SUM159, MDA-MB-231, MDA-MB-468, HS578	Up	MMP9	Proliferation, cell cycle, migration, invasion, stem-like feature	Peng *et al*[4]
Breast cancer	HCC-1937, MCF-10A, MDA-MB-231, T-47D, JIMT-1	Up	/	Proliferation, cell cycle	Rantala *et al*[5]
Cervical cancer	SiHa, HeLa, C33A, Caski, MS751, ME180	Up	/	Proliferation, migration, invasion	Ouyang *et al*[3]
Colon cancer	HCT116, LS174T, HCT8, SW620	Up	PTP4A1	Proliferation, cell cycle, anti-apoptosis	Hu *et al*[31]
Ovarian cancer	SKOV3, CaOV3, OVCAR3	Up	miR-502-5p	Proliferation, migration, anti-apoptosis	Zhan *et al*[14]
Ovarian cancer	SKOV-3, OVCAR3	Up	/	Proliferation, anti-apoptosis, cell cycle	Yan *et al*[15]
Gastric adenocarcinoma	KATO-III, MKN45	Up	/	Proliferation	Feng *et al*[6]
Gliomas	U87, U251	Up	MCM2, ATM, CHEK2	Proliferation, cell cycle, anti-apoptosis	Shen *et al*[7]
Leukemia	HL60	Up	Bax, Bcl2, ATM, CHK2, P53	Proliferation, cell cycle, anti-apoptosis	Zhang *et al*[16]
Leukemia	K562, NB4	Up	p38/MAPK	Anti-apoptosis, cell cycle	Gao *et al*[19]
Lung cancer	95D, A549, NCI-H1299, NCI-H1975	Up	STAT	Proliferation, growth, colony formation, cell cycle	Sun *et al*[17]
Lung cancer	A549, H460	Up	p53/GADD45A	Proliferation, anti-apoptosis, cell cycle	Chi *et al*[9]
Lung cancer	H1975, H1299, A549, SPC-A1, H460	Up	PI3K/Akt, MAPK/ERK	Proliferation, migration, invasion, EMT	Liu *et al*[8]
Pancreatic cancer	PANC-1, BxPC-3	Up	MAPK/ERK	Proliferation, anti-apoptosis, cell cycle	Zhang *et al*[18]
Pancreatic cancer	Aspc-1, Bxpc-3, PANC-1, Miapaca-2	Up	MAPK/ERK	EMT	Huang *et al*[10]
Pancreatic cancer	PANC-1, AsPC-1	Up	/	Proliferation, cell cycle	Bu *et al*[11]
Thyroid cancer	K1, SW579	Up	CITED2, LOXL2	Proliferation, anti-apoptosis, cell cycle	Ye *et al*[12]
Thyroid cancer	K1, SW579	Up	MAPK	Proliferation, migration, invasion, anti-apoptosis	He *et al*[13]

EMT: Epithelial-mesenchymal transition; MMP9: Matrix metalloproteinase-9; PTP4A1: Protein tyrosine phosphatase 4A1; MCM2: Microchromosome maintenance protein 2; ATM: Ataxia telangiectasia mutated; CHEK2: Checkpoint kinase 2; Bax: BCL2-associated x; Bcl2: B-cell lymphoma 2; CHK2: Cell kinase cyclecheckpoint 2; MAPK: Mitogen-activated protein kinase; STAT: Signal transducer and activator of transcription; GADD45A: Growth arrest and DNA damage inducible alpha; ERK: Extracellular signal-regulated kinase; CITED2: Cbp/P300-interacting transcription factor 2; LOXL2: Lysine oxidase-like 2.

cell cycle and phosphorylates and activates CHEK2 during DNA replication or upon stimulation by other substances, halting the cell cycle[35-37]. Shen *et al*[7] used laser confocal microscopy to reveal the relationship between MCM2 and ATM in glioma cells. Additionally, it was reported that inhibition of GINS2 expression reduced cell proliferation and tumorigenicity and that GINS2 could block the cell cycle by regulating MCM2, ATM, CHEK2 and other downstream molecules[7]. GINS2 could be a prognostic indicator and potential therapeutic target for glioma.

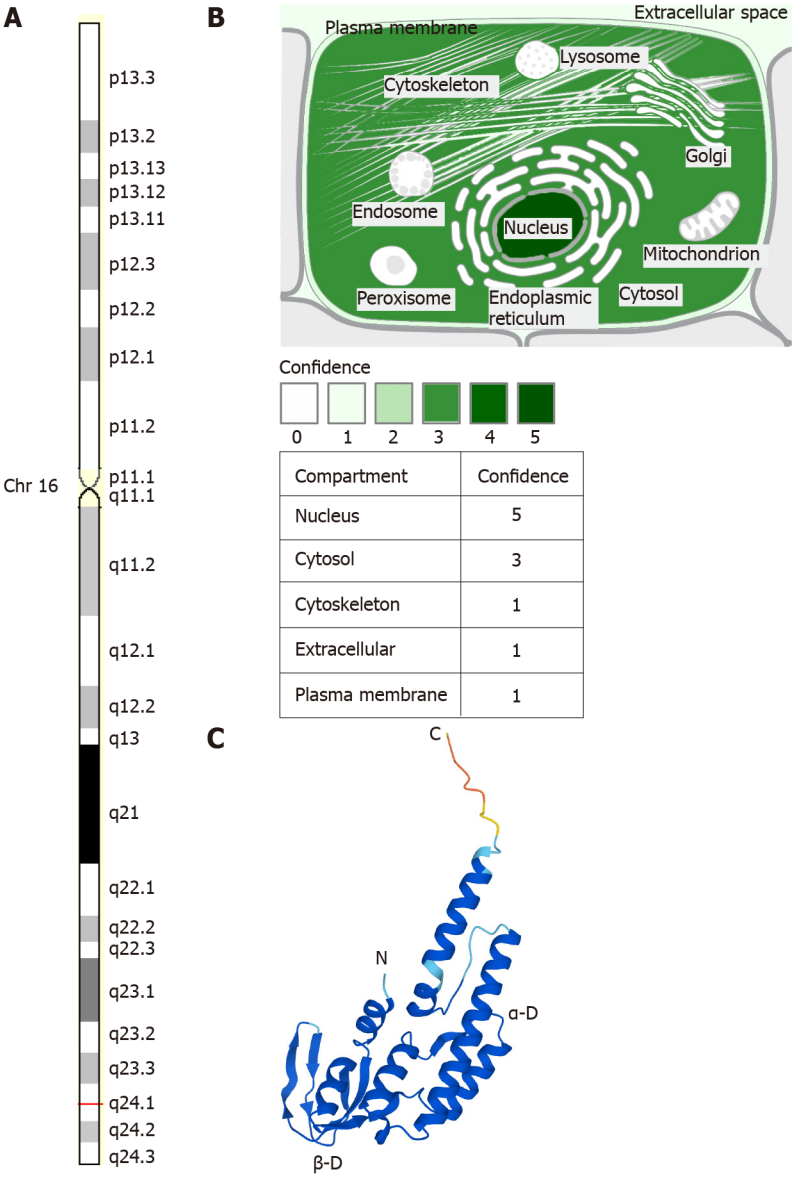

DOI: 10.4251/wjgo.v14.i10.1892

Figure 1 The position and structure of Go-Ichi-Ni-San 2. A: The chromosomal localization of Go-Ichi-Ni-San 2 (GINS2) (GeneCards, http://www.genecards.org); B: GINS2 expression is usually concentrated in the nucleus and cytosol (GeneCards, http://www.genecards.org); C: The structure of the GINS2 protein (AlphaFold Protein Structure Database, http://www.alphafold.ebi.ac.uk). The positions of the C- and N-termini and α-domains and β-domains in each subunit are indicated.

Leukaemia

Leukaemia is a blood cancer that originates in the bone marrow and is one of the leading causes of death from tumors in humans. In 2016, there were 467000 new cases of leukaemia and 310000 deaths from leukaemia worldwide. Early detection of effective treatment options for leukaemia can help reduce mortality[38]. Mitogen-activated protein kinase (MAPK) is a serine/threonine-protein kinase found in eukaryotic cells that can be activated by various internal and external stimuli. Upon activation, MAPK transmits extracellular signals to the nucleus and affects cellular functions by modulating the activity of transcription factors to alter the expression of related genes[39]. The p38/MAPK signaling pathway is a member of the MAPK superfamily. Gao *et al*[19] reported that GINS2 knockdown caused cell cycle arrest in chronic granulocytic leukaemia cells and acute promyelocytic leukaemia cells at the G2 phase through activation of p38/MAPK.

ATM-Chk2 and ATM-Chk1 are key signaling pathways that mediate the DNA damage response, and activation of these pathways is critical for the coordination of checkpoint and DNA repair processes. The DNA damage response is crucial to both cancer progression and treatment. p53 oncogene mutations are a way to evade the oncogenic barrier during tumor progression[40]. The findings of Zhang *et al*[16] suggest that the ATM, Chk2 and p53 genes may play a role in the pathogenic signaling pathway of human acute promyelocytic leukaemia when the GINS2 gene is downregulated. The above studies suggest that GINS2 contributes to the diagnosis and treatment of leukaemia.

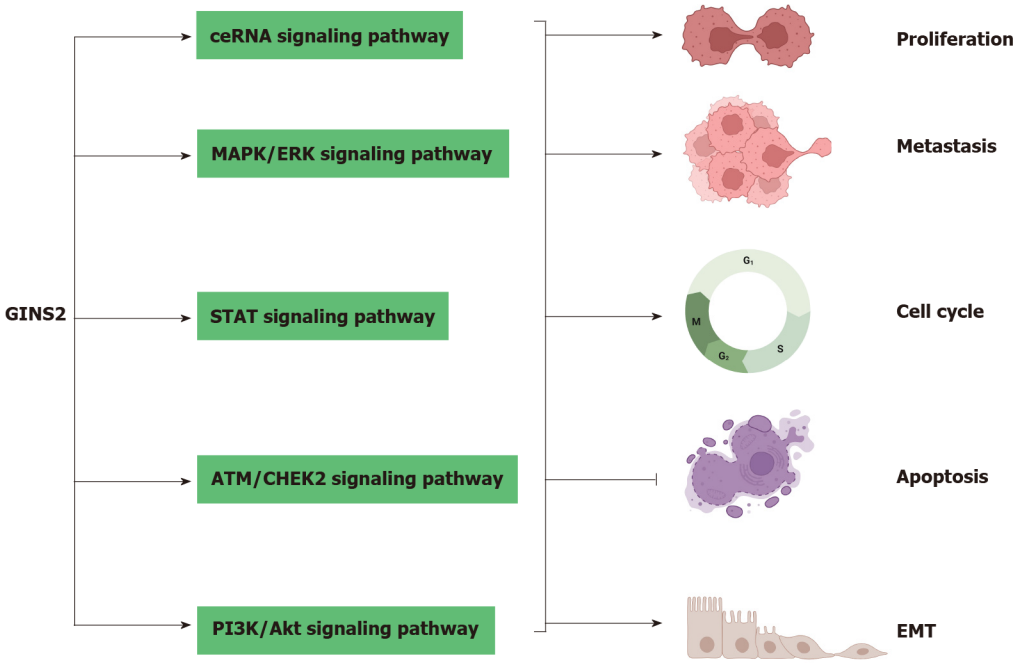

DOI: 10.4251/wjgo.v14.i10.1892

Figure 2 The effect of Go-Ichi-Ni-San 2 on the malignant characteristics of tumour cells. GINS2: Go-Ichi-Ni-San 2; MAPK: Mitogen-activated protein kinase; ERK: Extracellular signal-regulated kinase; STAT: Signal transducers and activator; EMT: Epithelial-mesenchymal transition; ATM: Ataxia telangiectasia mutated.

NSCLC

Lung cancer is the leading cause of cancer deaths, with NSCLC accounting for approximately 85% of all lung cancers[41]. Patients with NSCLC are often at an advanced stage at the time of detection. A better understanding of the development and evolution of NSCLC is needed to improve this situation. GADD45A is a protein whose expression is regulated over the entire cell cycle, with levels of this protein at their highest in the G1 phase and significantly reduced in the S phase. p53 is a member of the GADD45 (growth arrest and DNA damage induction) family and is responsible for maintaining genomic stability. Wild-type p53 protein arrests cell proliferation, inhibits cell division at the G1 checkpoint and contributes to the repair of damaged DNA. p53 mutations predispose cells to cellular malignancy and tumor formation during the S-phase of damaged DNA. GADD45A-mediated G2-M arrest was found to be dependent on wild-type p53, which controls cell proliferation/apoptosis by regulating cell cycle phases[42]. The results of Chi *et al*[9] showed that GINS2 expression was increased in NSCLC tissues and cell lines and could promote cell proliferation and inhibit apoptosis *via* the p53/GADD45A pathway.

Studies have shown that noncanonical nuclear factor-kappaB (NF-κB) transcription factors regulate several normal cellular and tissue processes, such as inflammatory responses, immunity, cell growth, and apoptosis[43,44]. NF-κB is an important "transcription factor", and aberrant activation of NF-κB signaling has been implicated in the pathogenesis of many diseases, especially tumors[45-47]. Tumor necrosis factor-inducible protein 3 (TNFAIP3) encodes TNFAIP3 (also known as A20) and is a critical negative regulator of NF-κB signaling[48]. Family members of transcription signal transducers and activators (STATs) have been identified as key proteins involved in cytokine signaling and interferon-related antiviral activity[49-51]. Their signaling activities are involved in many normal physiological cellular processes, including proliferation, differentiation, apoptosis, and angiogenesis. However, aberrant STAT regulation can lead to various pathological events, such as malignant cell transformation and metastasis[52]. Sun *et al*[17] found that after GINS2 gene knockout, the expression of STAT1 and STAT2 proteins increased, which inhibited tumor migration and proliferation. The protein expression of TNFAIP3 increased, suggesting that TNFAIP3 participates in the activity of GINS2 and could be involved in the spread and migration of NSCLC.

Both the PI3K/Akt and MEK/extracellular signal-regulated kinase (ERK) pathways have been reported to be associated with EMT in tumors[53,54]. Liu *et al*[8] also found that GINS2 could enhance the proliferation, migration, invasion and EMT of NSCLC cells *in vivo* and *in vitro* and further demonstrated that GINS2 could regulate the PI3K/Akt and MEK/ERK signaling pathways. In conclusion, GINS2 may be a therapeutic target for NSCLC.

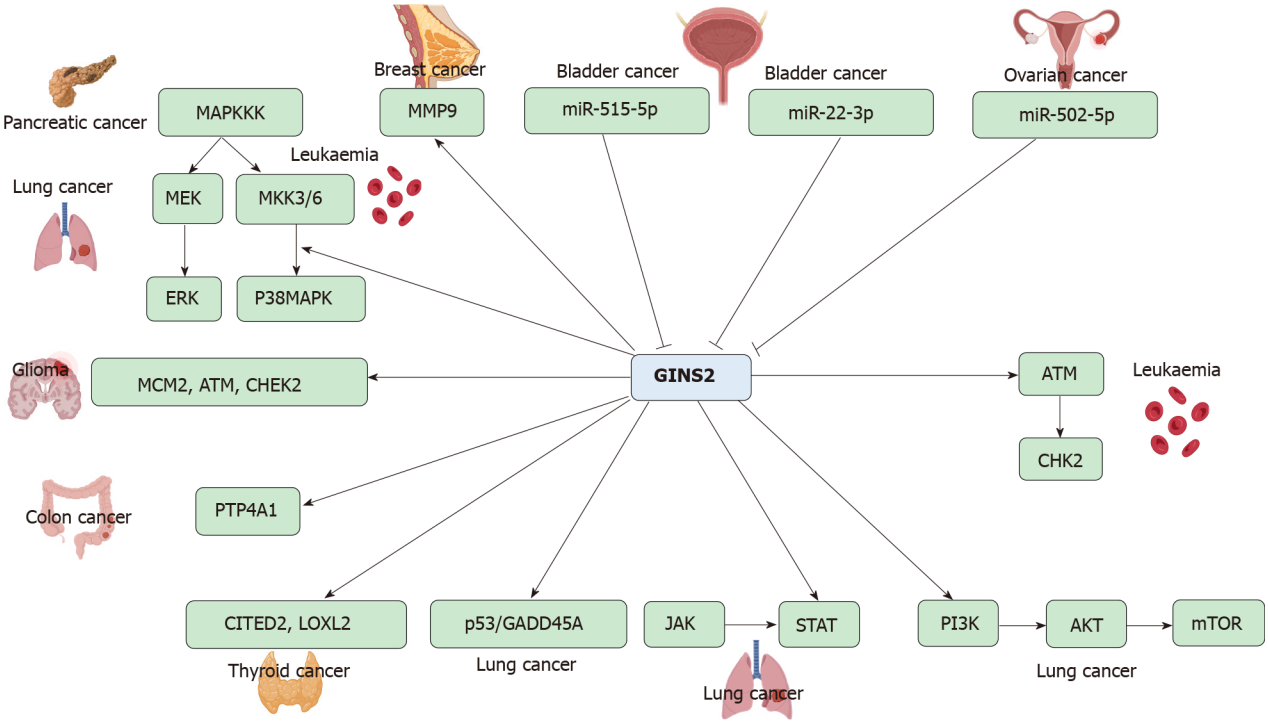

DOI: 10.4251/wjgo.v14.i10.1892

Figure 3 The participating pathways of Go-Ichi-Ni-San 2. GINS2: Go-Ichi-Ni-San 2; MAPK: Mitogen-activated protein kinase; ERK: Extracellular signal-regulated kinase; STAT: Signal transducers and activator; EMT: Epithelial-mesenchymal transition; MAPKKK: MAP kinase kinase kinase; MMPs: Matrix metalloproteinases; MEK: Mitogen-activated protein kinase; MKK3/6: MAP kinase kinase 3/6; MCM2: Minichromosome maintenance complex component 2; CHEK2: Checkpoint kinase 2; ATM: Ataxia telangiectasia mutated; CHK2: Cell kinase cyclecheckpoint2; PTP4A1: Protein tyrosine phosphatase 4A1; CITED2: Cbp/P300-interacting transcription factor 2; LOXL2: Lysyl oxidase like 2; GADD45A: Growth arrest and DNA damage inducible alpha; JAK: Janus kinase; mTOR: Mammalian target of rapamycin.

Pancreatic cancer

Due to the adverse survival prognosis of pancreatic cancer, the number of deaths is almost as high as the number of patients, and morbidity and mortality rates have remained stable or increased slightly in many countries[55]. It is therefore of interest to identify new targets for the diagnosis and treatment of pancreatic cancer. ERKs belong to the MAPK family and function in signaling cascades that transmit extracellular signals to cells. MAPK cascades are key signaling elements that regulate key processes such as cell proliferation, differentiation, and stress responses[56-58]. The ERK cascade is a tightly controlled cascade responsible for fundamental cellular processes. Excessive activation of proteins and kinases in the ERK pathway has been shown to contribute to a variety of diseases, including cancer, inflammation, developmental disorders, and neurological disorders[59,60]. Huang *et al*[10] found that overexpression of GINS2 in pancreatic cancer could stimulate EMT *in vitro*. In MiaPaCa-2 and PANC-1 cells with high GINS2 expression, GINS2 colocalized and coprecipitated with ERK, suggesting that GINS2 interacts closely with the MAPK/ERK pathway. Zhang *et al*[18] used small interfering RNA to reduce GINS2 expression and explored its mechanism of action in pancreatic cancer. Their results showed that GINS2 interference inhibited pancreatic cancer cell viability through the MAPK/ERK pathway, induced cell cycle arrest and promoted apoptosis in pancreatic cancer cell lines. The above findings suggest that GINS2 may play a negative role in pancreatic cancer and has a guiding role in treating pancreatic cancer.

TC

Since the 1980s, the incidence of TC has increased rapidly in most parts of the world. However, the aetiology of TC is not well understood, and the study of its development is particularly critical in its prevention and treatment[55]. Cbp/p300-interacting transcription factor 2 (CITED2) has a Glu/asp-rich carboxy-terminal domain and is a non-DNA-binding transcriptional coregulator. CITED2 can directly bind to host transcription factors and coactivators, interacting with them to activate gene transcription and affect their function[61]. Several studies have demonstrated that interference with CITED2 can induce apoptosis[62]. Lysine oxidase class 2 (LOXL2) is a member of the lysine oxidase (LOX) family, and some researchers have found that overexpression of LOXL2 activates cell growth in BC. In addition, LOXL2 can directly bind to substrate-like 1 of myristoylation alanine-rich kinase (MARCKSL1), activate the FAK/Akt/mTOR signaling pathway, and inhibit MARCKSL1-induced apoptosis[63]. Ye *et al*[12] found that GINS2 plays a role in TC cell proliferation and apoptosis by regulating the expression of

CITED2 and LOXL2 in TC cells. He *et al*[13] reported that GINS2 plays a vital role in the survival, migration and invasion of TC cells and regulates the MAPK signaling pathway. GINS2 may be a potential biomarker for TC diagnosis or prognosis and a drug target for treatment.

CONCLUSION

Most studies have shown that GINS2 expression is upregulated in tumor tissues such as CC, gastric adenocarcinoma, glioma, pancreatic cancer and OC compared to adjacent normal tissues, while GINS2 expression levels correlate with various clinicopathological parameters such as tumor size and TNM stage. These findings suggest that GINS2 can promote tumor progression by regulating tumor cell proliferation, apoptosis, migration, the cell cycle and EMT. In addition, at the cellular level, GINS2 affects the function of several pro- or oncogenic molecules through several signaling pathways, leading to poor patient prognosis. These results imply that GINS2 may be a new target in the diagnosis and treatment of certain tumors.

Currently, there are few publications on interfering with GINS2 in tumor therapy, and no corresponding inhibitors have been reported. In contrast, GINS2 expression is increased in the vast majority of tumors compared to normal tissues, which may make it possible to interfere with GINS2 expression and inhibit GINS2 protein function as an effective way to control tumor development. In future research, potent agents can be explored through molecular docking based on the GINS2 structure, for example.

In conclusion, a better understanding of the role of GINS2 in clinicopathological features and mechanisms of tumor development may help improve diagnostic and therapeutic outcomes. Further studies on GINS2 and its regulatory mechanisms may help improve prevention and treatment based on patient biological and pathological characteristics.

ACKNOWLEDGEMENTS

The authors gratefully acknowledge all the people that have made this study.

FOOTNOTES

Author contributions: Chen Z carried out the concepts and designed the definition of intellectual content; Shan DD carried out the literature search and manuscript editing; Zheng QX performed manuscript review; and all authors have read and approved the content of the manuscript.

Supported by the National Science and Technology Major Project of China, No. 2018ZX10302-206.

Conflict-of-interest statement: All the authors report no relevant conflicts of interest for this article.

Country/Territory of origin: China

ORCID number: Dan-Dan Shan 0000-0003-4761-7385; Qiu-Xian Zheng 0000-0001-5609-7380; Zhi Chen 0000-0002-0848-1502.

S-Editor: Wang JJ
L-Editor: A
P-Editor: Wang JJ

REFERENCES

1 **Takayama Y**, Kamimura Y, Okawa M, Muramatsu S, Sugino A, Araki H. GINS, a novel multiprotein complex required for chromosomal DNA replication in budding yeast. *Genes Dev* 2003; **17**: 1153-1165 [PMID: 12730134 DOI: 10.1101/gad.1065903]

2 **Gambus A**, Jones RC, Sanchez-Diaz A, Kanemaki M, van Deursen F, Edmondson RD, Labib K. GINS maintains association of Cdc45 with MCM in replisome progression complexes at eukaryotic DNA replication forks. *Nat Cell Biol* 2006; **8**: 358-366 [PMID: 16531994 DOI: 10.1038/ncb1382]

3 **Ouyang F**, Liu J, Xia M, Lin C, Wu X, Ye L, Song L, Li J, Wang J, Guo P, He M. GINS2 is a novel prognostic biomarker and promotes tumor progression in early-stage cervical cancer. *Oncol Rep* 2017; **37**: 2652-2662 [PMID: 28405687 DOI: 10.3892/or.2017.5573]
4 **Peng L**, Song Z, Chen D, Linghu R, Wang Y, Zhang X, Kou X, Yang J, Jiao S. GINS2 regulates matrix metallopeptidase 9 expression and cancer stem cell property in human triple negative Breast cancer. *Biomed Pharmacother* 2016; **84**: 1568-1574 [PMID: 27829549 DOI: 10.1016/j.biopha.2016.10.032]
5 **Rantala JK**, Edgren H, Lehtinen L, Wolf M, Kleivi K, Vollan HK, Aaltola AR, Laasola P, Kilpinen S, Saviranta P, Iljin K, Kallioniemi O. Integrative functional genomics analysis of sustained polyploidy phenotypes in breast cancer cells identifies an oncogenic profile for GINS2. *Neoplasia* 2010; **12**: 877-888 [PMID: 21082043 DOI: 10.1593/neo.10548]
6 **Feng H**, Zeng J, Gao L, Zhou Z, Wang L. GINS Complex Subunit 2 Facilitates Gastric Adenocarcinoma Proliferation and Indicates Poor Prognosis. *Tohoku J Exp Med* 2021; **255**: 111-121 [PMID: 34629365 DOI: 10.1620/tjem.255.111]
7 **Shen YL**, Li HZ, Hu YW, Zheng L, Wang Q. Loss of GINS2 inhibits cell proliferation and tumorigenesis in human gliomas. *CNS Neurosci Ther* 2019; **25**: 273-287 [PMID: 30338650 DOI: 10.1111/cns.13064]
8 **Liu X**, Sun L, Zhang S, Li W. GINS2 facilitates epithelial-to-mesenchymal transition in non-small-cell lung cancer through modulating PI3K/Akt and MEK/ERK signaling. *J Cell Physiol* 2020; **235**: 7747-7756 [PMID: 31681988 DOI: 10.1002/jcp.29381]
9 **Chi F**, Wang Z, Li Y, Chang N. Knockdown of GINS2 inhibits proliferation and promotes apoptosis through the p53/GADD45A pathway in non-small-cell lung cancer. *Biosci Rep* 2020; **40** [PMID: 32181475 DOI: 10.1042/BSR20193949]
10 **Huang L**, Chen S, Fan H, Ji D, Chen C, Sheng W. GINS2 promotes EMT in pancreatic cancer *via* specifically stimulating ERK/MAPK signaling. *Cancer Gene Ther* 2021; **28**: 839-849 [PMID: 32747685 DOI: 10.1038/s41417-020-0206-7]
11 **Bu F**, Zhu X, Yi X, Luo C, Lin K, Zhu J, Hu C, Liu Z, Zhao J, Huang C, Zhang W, Huang J. Expression Profile of GINS Complex Predicts the Prognosis of Pancreatic Cancer Patients. *Onco Targets Ther* 2020; **13**: 11433-11444 [PMID: 33192076 DOI: 10.2147/OTT.S275649]
12 **Ye Y**, Song YN, He SF, Zhuang JH, Wang GY, Xia W. GINS2 promotes cell proliferation and inhibits cell apoptosis in thyroid cancer by regulating CITED2 and LOXL2. *Cancer Gene Ther* 2019; **26**: 103-113 [PMID: 30177819 DOI: 10.1038/s41417-018-0045-y]
13 **He S**, Zhang M, Ye Y, Song Y, Ma X, Wang G, Zhuang J, Xia W, Zhao B. GINS2 affects cell proliferation, apoptosis, migration and invasion in thyroid cancer *via* regulating MAPK signaling pathway. *Mol Med Rep* 2021; **23** [PMID: 33537829 DOI: 10.3892/mmr.2021.11885]
14 **Zhan L**, Yang J, Liu Y, Cheng Y, Liu H. MicroRNA miR-502-5p inhibits ovarian cancer genesis by downregulation of GINS complex subunit 2. *Bioengineered* 2021; **12**: 3336-3347 [PMID: 34288816 DOI: 10.1080/21655979.2021.1946347]
15 **Yan T**, Liang W, Jiang E, Ye A, Wu Q, Xi M. GINS2 regulates cell proliferation and apoptosis in human epithelial ovarian cancer. *Oncol Lett* 2018; **16**: 2591-2598 [PMID: 30013653 DOI: 10.3892/ol.2018.8944]
16 **Zhang X**, Zhong L, Liu BZ, Gao YJ, Gao YM, Hu XX. Effect of GINS2 on proliferation and apoptosis in leukemic cell line. *Int J Med Sci* 2013; **10**: 1795-1804 [PMID: 24273454 DOI: 10.7150/ijms.7025]
17 **Sun D**, Zong Y, Cheng J, Li Z, Xing L, Yu J. GINS2 attenuates the development of lung cancer by inhibiting the STAT signaling pathway. *J Cancer* 2021; **12**: 99-110 [PMID: 33391406 DOI: 10.7150/jca.46744]
18 **Zhang M**, He S, Ma X, Ye Y, Wang G, Zhuang J, Song Y, Xia W. GINS2 affects cell viability, cell apoptosis, and cell cycle progression of pancreatic cancer cells *via* MAPK/ERK pathway. *J Cancer* 2020; **11**: 4662-4670 [PMID: 32626512 DOI: 10.7150/jca.38386]
19 **Gao Y**, Wang S, Liu B, Zhong L. Roles of GINS2 in K562 human chronic myelogenous leukemia and NB4 acute promyelocytic leukemia cells. *Int J Mol Med* 2013; **31**: 1402-1410 [PMID: 23589040 DOI: 10.3892/ijmm.2013.1339]
20 **Salod Z**, Singh Y. A five-year (2015 to 2019) analysis of studies focused on breast cancer prediction using machine learning: A systematic review and bibliometric analysis. *J Public Health Res* 2020; **9**: 1792 [PMID: 32642458 DOI: 10.4081/jphr.2020.1772]
21 **Vu HT**, Hoang TX, Kim JY. All-Trans Retinoic Acid Enhances Matrix Metalloproteinase 2 Expression and Secretion in Human Myeloid Leukemia THP-1 Cells. *Biomed Res Int* 2018; **2018**: 5971080 [PMID: 30225259 DOI: 10.1155/2018/5971080]
22 **Gialeli C**, Theocharis AD, Karamanos NK. Roles of matrix metalloproteinases in cancer progression and their pharmacological targeting. *FEBS J* 2011; **278**: 16-27 [PMID: 21087457 DOI: 10.1111/j.1742-4658.2010.07919.x]
23 **Bronisz E**, Kurkowska-Jastrzębska I. Matrix Metalloproteinase 9 in Epilepsy: The Role of Neuroinflammation in Seizure Development. *Mediators Inflamm* 2016; **2016**: 7369020 [PMID: 28104930 DOI: 10.1155/2016/7369020]
24 **Curran S**, Dundas SR, Buxton J, Leeman MF, Ramsay R, Murray GI. Matrix metalloproteinase/tissue inhibitors of matrix metalloproteinase phenotype identifies poor prognosis colorectal cancers. *Clin Cancer Res* 2004; **10**: 8229-8234 [PMID: 15623598 DOI: 10.1158/1078-0432.CCR-04-0424]
25 **Sanli O**, Dobruch J, Knowles MA, Burger M, Alemozaffar M, Nielsen ME, Lotan Y. Bladder cancer. *Nat Rev Dis Primers* 2017; **3**: 17022 [PMID: 28406148 DOI: 10.1038/nrdp.2017.22]
26 **Tian Y**, Guan Y, Su Y, Yang T, Yu H. TRPM2-AS Promotes Bladder Cancer by Targeting miR-22-3p and Regulating GINS2 mRNA Expression. *Onco Targets Ther* 2021; **14**: 1219-1237 [PMID: 33658791 DOI: 10.2147/OTT.S282151]
27 **Dai G**, Huang C, Yang J, Jin L, Fu K, Yuan F, Zhu J, Xue B. LncRNA SNHG3 promotes bladder cancer proliferation and metastasis through miR-515-5p/GINS2 axis. *J Cell Mol Med* 2020; **24**: 9231-9243 [PMID: 32596993 DOI: 10.1111/jcmm.15564]
28 **Siegel RL**, Miller KD, Jemal A. Cancer statistics, 2019. *CA Cancer J Clin* 2019; **69**: 7-34 [PMID: 30620402 DOI: 10.3322/caac.21551]
29 **Alonso A**, Sasin J, Bottini N, Friedberg I, Osterman A, Godzik A, Hunter T, Dixon J, Mustelin T. Protein tyrosine phosphatases in the human genome. *Cell* 2004; **117**: 699-711 [PMID: 15186772 DOI: 10.1016/j.cell.2004.05.018]
30 **Sacchetti C**, Bai Y, Stanford SM, Di Benedetto P, Cipriani P, Santelli E, Piera-Velazquez S, Chernitskiy V, Kiosses WB, Ceponis A, Kaestner KH, Boin F, Jimenez SA, Giacomelli R, Zhang ZY, Bottini N. PTP4A1 promotes TGFβ signaling and

fibrosis in systemic sclerosis. *Nat Commun* 2017; **8**: 1060 [PMID: 29057934 DOI: 10.1038/s41467-017-01168-1]

31 **Hu H**, Ye L, Liu Z. GINS2 regulates the proliferation and apoptosis of colon cancer cells through PTP4A1. *Mol Med Rep* 2022; **25** [PMID: 35137928 DOI: 10.3892/mmr.2022.12633]

32 **Ferlay J**, Colombet M, Soerjomataram I, Mathers C, Parkin DM, Piñeros M, Znaor A, Bray F. Estimating the global cancer incidence and mortality in 2018: GLOBOCAN sources and methods. *Int J Cancer* 2019; **144**: 1941-1953 [PMID: 30350310 DOI: 10.1002/ijc.31937]

33 **Wiedmann MKH**, Brunborg C, Di Ieva A, Lindemann K, Johannesen TB, Vatten L, Helseth E, Zwart JA. The impact of body mass index and height on the risk for glioblastoma and other glioma subgroups: a large prospective cohort study. *Neuro Oncol* 2017; **19**: 976-985 [PMID: 28040713 DOI: 10.1093/neuonc/now272]

34 **Zheng G**, Kanchwala M, Xing C, Yu H. MCM2-7-dependent cohesin loading during S phase promotes sister-chromatid cohesion. *Elife* 2018; **7** [PMID: 29611806 DOI: 10.7554/eLife.33920]

35 **Li Y**, Li L, Wu Z, Wang L, Wu Y, Li D, Ma U, Shao J, Yu H, Wang D. Silencing of ATM expression by siRNA technique contributes to glioma stem cell radiosensitivity in vitro and in vivo. *Oncol Rep* 2017; **38**: 325-335 [PMID: 28560406 DOI: 10.3892/or.2017.5665]

36 **Han B**, Cai J, Gao W, Meng X, Gao F, Wu P, Duan C, Wang R, Dinislam M, Lin L, Kang C, Jiang C. Loss of ATRX suppresses ATM dependent DNA damage repair by modulating H3K9me3 to enhance temozolomide sensitivity in glioma. *Cancer Lett* 2018; **419**: 280-290 [PMID: 29378238 DOI: 10.1016/j.canlet.2018.01.056]

37 **Blake SM**, Stricker SH, Halavach H, Poetsch AR, Cresswell G, Kelly G, Kanu N, Marino S, Luscombe NM, Pollard SM, Behrens A. Inactivation of the ATMIN/ATM pathway protects against glioblastoma formation. *Elife* 2016; **5** [PMID: 26984279 DOI: 10.7554/eLife.08711]

38 **Global Burden of Disease Cancer Collaboration**, Fitzmaurice C, Akinyemiju TF, Al Lami FH, Alam T, Alizadeh-Navaei R, Allen C, Alsharif U, Alvis-Guzman N, Amini E, Anderson BO, Aremu O, Artaman A, Asgedom SW, Assadi R, Atey TM, Avila-Burgos L, Awasthi A, Ba Saleem HO, Barac A, Bennett JR, Bensenor IM, Bhakta N, Brenner H, Cahuana-Hurtado L, Castañeda-Orjuela CA, Catalá-López F, Choi JJ, Christopher DJ, Chung SC, Curado MP, Dandona L, Dandona R, das Neves J, Dey S, Dharmaratne SD, Doku DT, Driscoll TR, Dubey M, Ebrahimi H, Edessa D, El-Khatib Z, Endries AY, Fischer F, Force LM, Foreman KJ, Gebrehiwot SW, Gopalani SV, Grosso G, Gupta R, Gyawali B, Hamadeh RR, Hamidi S, Harvey J, Hassen HY, Hay RJ, Hay SI, Heibati B, Hiluf MK, Horita N, Hosgood HD, Ilesanmi OS, Innos K, Islami F, Jakovljevic MB, Johnson SC, Jonas JB, Kasaeian A, Kassa TD, Khader YS, Khan EA, Khan G, Khang YH, Khosravi MH, Khubchandani J, Kopec JA, Kumar GA, Kutz M, Lad DP, Lafranconi A, Lan Q, Legesse Y, Leigh J, Linn S, Lunevicius R, Majeed A, Malekzadeh R, Malta DC, Mantovani LG, McMahon BJ, Meier T, Melaku YA, Melku M, Memiah P, Mendoza W, Meretoja TJ, Mezgebe HB, Miller TR, Mohammed S, Mokdad AH, Moosazadeh M, Moraga P, Mousavi SM, Nangia V, Nguyen CT, Nong VM, Ogbo FA, Olagunju AT, Pa M, Park EK, Patel T, Pereira DM, Pishgar F, Postma MJ, Pourmalek F, Qorbani M, Rafay A, Rawaf S, Rawaf DL, Roshandel G, Safiri S, Salimzadeh H, Sanabria JR, Santric Milicevic MM, Sartorius B, Satpathy M, Sepanlou SG, Shackelford KA, Shaikh MA, Sharif-Alhoseini M, She J, Shin MJ, Shiue I, Shrime MG, Sinke AH, Sisay M, Sligar A, Sufiyan MB, Sykes BL, Tabarés-Seisdedos R, Tessema GA, Topor-Madry R, Tran TT, Tran BX, Ukwaja KN, Vlassov VV, Vollset SE, Weiderpass E, Williams HC, Yimer NB, Yonemoto N, Younis MZ, Murray CJL, Naghavi M. Global, Regional, and National Cancer Incidence, Mortality, Years of Life Lost, Years Lived With Disability, and Disability-Adjusted Life-Years for 29 Cancer Groups, 1990 to 2016: A Systematic Analysis for the Global Burden of Disease Study. *JAMA Oncol* 2018; **4**: 1553-1568 [PMID: 29860482 DOI: 10.1001/jamaoncol.2018.2706]

39 **Mariani E**, Pulsatelli L, Facchini A. Signaling pathways in cartilage repair. *Int J Mol Sci* 2014; **15**: 8667-8698 [PMID: 24837833 DOI: 10.3390/ijms15058667]

40 **Smith J**, Tho LM, Xu N, Gillespie DA. The ATM-Chk2 and ATR-Chk1 pathways in DNA damage signaling and cancer. *Adv Cancer Res* 2010; **108**: 73-112 [PMID: 21034966 DOI: 10.1016/B978-0-12-380888-2.00003-0]

41 **Herbst RS**, Heymach JV, Lippman SM. Lung cancer. *N Engl J Med* 2008; **359**: 1367-1380 [PMID: 18815398 DOI: 10.1056/NEJMra0802714]

42 **Jin S**, Mazzacurati L, Zhu X, Tong T, Song Y, Shujuan S, Petrik KL, Rajasekaran B, Wu M, Zhan Q. Gadd45a contributes to p53 stabilization in response to DNA damage. *Oncogene* 2003; **22**: 8536-8540 [PMID: 14627995 DOI: 10.1038/sj.onc.1206907]

43 **Hoffmann A**, Baltimore D. Circuitry of nuclear factor kappaB signaling. *Immunol Rev* 2006; **210**: 171-186 [PMID: 16623771 DOI: 10.1111/j.0105-2896.2006.00375.x]

44 **Gilmore TD**, Kalaitzidis D, Liang MC, Starczynowski DT. The c-Rel transcription factor and B-cell proliferation: a deal with the devil. *Oncogene* 2004; **23**: 2275-2286 [PMID: 14755244 DOI: 10.1038/sj.onc.1207410]

45 **Qiao L**, Zhang H, Yu J, Francisco R, Dent P, Ebert MP, Röcken C, Farrell G. Constitutive activation of NF-kappaB in human hepatocellular carcinoma: evidence of a cytoprotective role. *Hum Gene Ther* 2006; **17**: 280-290 [PMID: 16544977 DOI: 10.1089/hum.2006.17.280]

46 **Mann AP**, Verma A, Sethi G, Manavathi B, Wang H, Fok JY, Kunnumakkara AB, Kumar R, Aggarwal BB, Mehta K. Overexpression of tissue transglutaminase leads to constitutive activation of nuclear factor-kappaB in cancer cells: delineation of a novel pathway. *Cancer Res* 2006; **66**: 8788-8795 [PMID: 16951195 DOI: 10.1158/0008-5472.CAN-06-1457]

47 **Prasad S**, Ravindran J, Aggarwal BB. NF-kappaB and cancer: how intimate is this relationship. *Mol Cell Biochem* 2010; **336**: 25-37 [PMID: 19823771 DOI: 10.1007/s11010-009-0267-2]

48 **Yu MP**, Xu XS, Zhou Q, Deuitch N, Lu MP. Haploinsufficiency of A20 (HA20): updates on the genetics, phenotype, pathogenesis and treatment. *World J Pediatr* 2020; **16**: 575-584 [PMID: 31587140 DOI: 10.1007/s12519-019-00288-6]

49 **Wegenka UM**, Lütticken C, Buschmann J, Yuan J, Lottspeich F, Müller-Esterl W, Schindler C, Roeb E, Heinrich PC, Horn F. The interleukin-6-activated acute-phase response factor is antigenically and functionally related to members of the signal transducer and activator of transcription (STAT) family. *Mol Cell Biol* 1994; **14**: 3186-3196 [PMID: 8164674 DOI: 10.1128/mcb.14.5.3186-3196.1994]

50 **Sadowski HB**, Shuai K, Darnell JE Jr, Gilman MZ. A common nuclear signal transduction pathway activated by growth

factor and cytokine receptors. *Science* 1993; **261**: 1739-1744 [PMID: 8397445 DOI: 10.1126/science.8397445]

51 **Darnell JE Jr**, Kerr IM, Stark GR. Jak-STAT pathways and transcriptional activation in response to IFNs and other extracellular signaling proteins. *Science* 1994; **264**: 1415-1421 [PMID: 8197455 DOI: 10.1126/science.8197455]

52 **Bowman T**, Garcia R, Turkson J, Jove R. STATs in oncogenesis. *Oncogene* 2000; **19**: 2474-2488 [PMID: 10851046 DOI: 10.1038/sj.onc.1203527]

53 **Pan H**, Jiang T, Cheng N, Wang Q, Ren S, Li X, Zhao C, Zhang L, Cai W, Zhou C. Long non-coding RNA BC087858 induces non-T790M mutation acquired resistance to EGFR-TKIs by activating PI3K/AKT and MEK/ERK pathways and EMT in non-small-cell lung cancer. *Oncotarget* 2016; **7**: 49948-49960 [PMID: 27409677 DOI: 10.18632/oncotarget.10521]

54 **Ha GH**, Park JS, Breuer EK. TACC3 promotes epithelial-mesenchymal transition (EMT) through the activation of PI3K/Akt and ERK signaling pathways. *Cancer Lett* 2013; **332**: 63-73 [PMID: 23348690 DOI: 10.1016/j.canlet.2013.01.013]

55 **Sung H**, Ferlay J, Siegel RL, Laversanne M, Soerjomataram I, Jemal A, Bray F. Global Cancer Statistics 2020: GLOBOCAN Estimates of Incidence and Mortality Worldwide for 36 Cancers in 185 Countries. *CA Cancer J Clin* 2021; **71**: 209-249 [PMID: 33538338 DOI: 10.3322/caac.21660]

56 **Sabio G**, Davis RJ. TNF and MAP kinase signalling pathways. *Semin Immunol* 2014; **26**: 237-245 [PMID: 24647229 DOI: 10.1016/j.smim.2014.02.009]

57 **Plotnikov A**, Zehorai E, Procaccia S, Seger R. The MAPK cascades: signaling components, nuclear roles and mechanisms of nuclear translocation. *Biochim Biophys Acta* 2011; **1813**: 1619-1633 [PMID: 21167873 DOI: 10.1016/j.bbamcr.2010.12.012]

58 **Keshet Y**, Seger R. The MAP kinase signaling cascades: a system of hundreds of components regulates a diverse array of physiological functions. *Methods Mol Biol* 2010; **661**: 3-38 [PMID: 20811974 DOI: 10.1007/978-1-60761-795-2_1]

59 **Kim JY**, Lee SG, Chung JY, Kim YJ, Park JE, Koh H, Han MS, Park YC, Yoo YH, Kim JM. Ellipticine induces apoptosis in human endometrial cancer cells: the potential involvement of reactive oxygen species and mitogen-activated protein kinases. *Toxicology* 2011; **289**: 91-102 [PMID: 21843585 DOI: 10.1016/j.tox.2011.07.014]

60 **Gupta J**, Nebreda AR. Roles of p38α mitogen-activated protein kinase in mouse models of inflammatory diseases and cancer. *FEBS J* 2015; **282**: 1841-1857 [PMID: 25728574 DOI: 10.1111/febs.13250]

61 **Chou YT**, Yang YC. Post-transcriptional control of Cited2 by transforming growth factor beta. Regulation *via* Smads and Cited2 coding region. *J Biol Chem* 2006; **281**: 18451-18462 [PMID: 16675452 DOI: 10.1074/jbc.m601720200]

62 **Minemura H**, Takagi K, Sato A, Takahashi H, Miki Y, Shibahara Y, Watanabe M, Ishida T, Sasano H, Suzuki T. CITED2 in breast carcinoma as a potent prognostic predictor associated with proliferation, migration and chemoresistance. *Cancer Sci* 2016; **107**: 1898-1908 [PMID: 27627783 DOI: 10.1111/cas.13081]

63 **Kim BR**, Dong SM, Seo SH, Lee JH, Lee JM, Lee SH, Rho SB. Lysyl oxidase-like 2 (LOXL2) controls tumor-associated cell proliferation through the interaction with MARCKSL1. *Cell Signal* 2014; **26**: 1765-1773 [PMID: 24863880 DOI: 10.1016/j.cellsig.2014.05.010]

World Journal of Gastrointestinal Oncology

Submit a Manuscript: https://www.f6publishing.com

World J Gastrointest Oncol 2022 October 15; 14(10): 1903-1917

DOI: 10.4251/wjgo.v14.i10.1903

ISSN 1948-5204 (online)

MINIREVIEWS

Neoadjuvant therapy in resectable pancreatic cancer: A promising curative method to improve prognosis

Hao-Qi Zhang, Jing Li, Chun-Lu Tan, Yong-Hua Chen, Zhen-Jiang Zheng, Xu-Bao Liu

Specialty type: Oncology

Provenance and peer review: Unsolicited article; Externally peer reviewed.

Peer-review model: Single blind

Peer-review report's scientific quality classification

Grade A (Excellent): 0
Grade B (Very good): 0
Grade C (Good): C, C
Grade D (Fair): 0
Grade E (Poor): 0

P-Reviewer: Merz V, Italy; Ryckman JM, Unite States

Received: June 26, 2022
Peer-review started: June 26, 2022
First decision: July 25, 2022
Revised: August 5, 2022
Accepted: September 8, 2022
Article in press: September 8, 2022
Published online: October 15, 2022

Hao-Qi Zhang, Chun-Lu Tan, Yong-Hua Chen, Zhen-Jiang Zheng, Xu-Bao Liu, Department of Pancreatic Surgery, West China Hospital, Sichuan University, Chengdu 610041, Sichuan Province, China

Jing Li, Department of Operating Room/West China School of Nursing, West China Hospital, Sichuan University, Chengdu 610041, Sichuan Province, China

Corresponding author: Chun-Lu Tan, MD, PhD, Associate Professor, Surgeon, Department of Pancreatic Surgery, West China Hospital, Sichuan University, No. 37 Guoxue Lane, Wuhou District, Chengdu 610041, Sichuan Province, China. chunlutan@163.com

Abstract

Currently, 15 randomized controlled trials (RCTs) have been designed to investigate whether neoadjuvant therapy (NAT) benefits patients with resectable pancreatic adenocarcinoma (R-PA) compared to surgery alone. Five of them have acquired results so far; however, corresponding conclusions have not been obtained. We speculated that the reason for this phenomenon could be that some prognostic factors had proven to be adverse through upfront surgery curative patterns, but some of them were not regarded as independent baseline characteristics, which is important to obtaining comparability between the NAT and upfront surgery groups. This fact could cause bias and lead to the difference in the outcomes of RCTs. In this review, we collate data about risk factors (such as tumor size, resection margin, and lymph node status) influencing the prognoses of patients with R-PA from five RCTs and discuss the possible reasons for the varying outcomes.

Key Words: Neoadjuvant therapy; Resectable; Pancreatic cancer; Prognosis

Core Tip: In this review, we collate data about risk factors influencing the prognoses of patients with resectable pancreatic cancer from five randomized controlled trials (RCTs) and discuss the possible reasons for the varying outcomes. By comparing the overall survival of two RCTs, we speculated that neoadjuvant therapy might actually benefit patients with low-risk factors for long-term survival. Moreover, we address some suggestions for the RCTs in the future.

Citation: Zhang HQ, Li J, Tan CL, Chen YH, Zheng ZJ, Liu XB. Neoadjuvant therapy in resectable pancreatic cancer: A promising curative method to improve prognosis. *World J Gastrointest Oncol* 2022; 14(10): 1903-1917
URL: https://www.wjgnet.com/1948-5204/full/v14/i10/1903.htm
DOI: https://dx.doi.org/10.4251/wjgo.v14.i10.1903

INTRODUCTION

Pancreatic cancer (PC) is a malignancy with a very high mortality and poor prognosis. Patients usually die in a short time due to the progression of the tumor. To moderate progression, curative-intent surgery is necessary. Unfortunately, not all PC patients are eligible for resection, and only approximately 15% to 20% of patients have resectable PC[1]. To improve survival outcomes, adjuvant chemotherapy and neoadjuvant therapy (NAT) have been used in selected patients with pancreatic ductal adenocarcinoma (PDAC). NAT includes neoadjuvant chemotherapy (NACT), neoadjuvant radiotherapy, and neoadjuvant chemoradiotherapy (NACRT). According to the National Comprehensive Cancer Network (NCCN) guidelines, pancreatic tumors are classified as resectable when there is no arterial contact [celiac axis, superior mesenteric artery (SMA), or common hepatic artery (CHA)] and no venous tumor contact with the superior mesenteric vein (SMV) or portal vein (PV). If there is venous contact, there must be less than 180° of contact without any vein contour irregularities to classify the case as resectable pancreatic adenocarcinoma (R-PA). Borderline resectable pancreatic adenocarcinoma (BR-PA) is defined as tumors that have tumor contact with the PV or SMV or with the peripancreatic major arteries, including the celiac artery (CA), the CHA, and the SMA. Tumors with contact with the SMA or CA > 180° or an unreconstructable SMV or PV due to tumor involvement or occlusion are classified as locally advanced. Although NAT has been proved to be beneficial in patients with either BR-PA or locally advanced tumors[2-4], there is no specific standard for NAT for R-PA. The main controversy is that the progression of PC might occur during NAT, which would preclude surgical resection. In addition, it remains questionable whether NAT actually benefits R-PA. According to the NCCN guidelines, R-PA patients should receive surgery first, and only those R-PA with some risk factors, such as a high carbohydrate antigen 19-9 (CA19-9) level, large tumor size, and positive lymph nodes, are recommended to undergo NAT. The regimens of NAT for PDAC patients are based on regimens that were proved to significantly improve disease-free survival (DFS) and overall survival (OS), such as gemcitabine plus albumin-bound nab-paclitaxel, oxaliplatin, gemcitabine plus cisplatin, and 5 fluorouracil, but there have not yet been studies of which is better. The NCCN guidelines recommend FOLFIRINOX or modified FOLFIRINOX ± subsequent chemoradiation or gemcitabine + albumin-bound paclitaxel ± subsequent chemoradiation for R-PA. In R-PA patients with known BRCA1/2 or PALB2 mutations, FOLFIRINOX or modified FOLFIRINOX ± subsequent chemoradiation or gemcitabine + cisplatin (≥ 2–6 cycles) ± subsequent chemoradiation is preferred.

The conclusions have been inconsistent after analyzing the outcomes of all of the current randomized controlled trials (RCTs); for example, the results from the phase II FRENCH SFRO-FFCD 97-04 trial showed that NACRT is feasible for patients with R-PA[5], but in another previous meta-analysis, NACRT could not be recommended for patients with R-PA[6]. Some prognostic factors have been proved to be adverse through upfront surgery curative patterns, but some of them have not been regarded as independent baseline characteristics, which is important for obtaining comparability between the NAT and upfront surgery groups. This fact could cause bias and lead to the differences in the outcomes of RCTs. Moreover, the NAT regimens are out of date in some research, which could also lead to negative outcomes.

This review focuses on the deficiencies of and data from current high-quality RCTs and provides suggestions for future RCTs.

STUDIES OF NAT IN RESECTABLE PANCREATIC CARCINOMA

The RCTs on NAT in resectable PC included in this review are listed in Table 1. There are ten other registered RCTs comparing NAT and upfront surgery for R-PA patients: One is not yet recruiting, three are recruiting, two are active but not recruiting, two are terminated, and two are completed. Information about these RCTs is listed in Table 2.

Five RCTs are introduced in detail as follows. The first is a German trial (NCT00335543), which was completed in 2013[7]. This study was the first prospective, randomized, phase II trial. A total of 254 patients were initially enrolled, but only 66 were actually enrolled until the trial was completed. Thirty-three patients were allocated to the NAT group, and another 33 were allocated to the upfront surgery group. The NAT regimen was gemcitabine and cisplatin plus radiotherapy. However, resectability was defined as no organ infiltration except the duodenum and maximal involvement of the peripancreatic vessels ≤ 180° confirmed by high-resolution CT. Thus, some patients who should have been regarded as

Table 1 Outcomes of randomized controlled trials included in the review

Ref.	Country	NCT number/Name	Treatment arm	N	mOS (mo)	pN0 rate	Resection rate	R0 rate	ITT R0 rate
Golcher *et al*[7]	Germany	NCT00335543	Upfront surgery	33	14.4	10/33 (30%)	23/33 (70%)	16/23 (70%)	16/33 (48%)
			GEM/CIS + RT	33	17.4	13/33 (39%)	19/33 (58%)	17/19 (89%)	17/33 (52%)
Versteijne *et al* [8]	Netherlands	PREOPANC	Upfront surgery	68	14.6	NM	54/68 (79%)	32/54 (59%)	32/68 (47%)
			GEM + RT	65	15.6	NM	44/65 (68%)	29/44 (66%)	29/65 (45%)
Casadei *et al*[9]	Italy	-	Upfront surgery	20	19.5	2/20 (10%)	15/20 (75%)	5/15 (33%)	5/20 (25%)
			GEM + RT	18	22.4	5/18 (28%)	11/18(61%)	7/11 (64%)	7/18 (39%)
Reni *et al*[10]	Italy	PACT-15	Upfront surgery (GEM)	26	20.4	6/22 (27%)	22/26 (84%)	6/22 (27%)	6/26 (23%)
			Upfront surgery (PEXG)	30	26.4	7/27 (26%)	27/30 (90%)	10/27 (37%)	10/30 (33%)
			PEXG	32	38.2	13/27 (48%)	27/32 (84%)	17/27 (63%)	17/32 (53%)
Satoi *et al*[11]	Japan	Prep-02/JSAP-05	Upfront surgery	180	26.3	NM	72%	NM	NM
			GEM + S-1	182	36.7	NM	77%	NM	NM

CIS: Cisplatin; GEM: Gemcitabine; RT: Radiotherapy; PEXG: Cisplatin, epirubicin, capecitabine, and gemcitabine; mOS: Median overall survival; pN0: Pathological N0; NM: Not mentioned; ITT: Intention to treat.

BR-PA cases according to the latest NCCN guidelines were deemed to be R-PA cases.

The second is a Dutch randomized, phase III PREOPANC trial[8]. Notably, this trial included both R-PA and BR-PA patients, and only data about R-PA are discussed in this review. The largest difference in this study compared to three other trials was that it excluded T1 resectable tumors (< 2 cm, without vascular involvement). The planned number of subjects to be included was 244, but 246 eligible patients were ultimately enrolled, and 133 were eligible for resection. After random assignment, 68 R-PA patients were allocated to the upfront surgery group and another 65 to the NAT group. The NAT regimen was gemcitabine plus radiotherapy. Nevertheless, the resectability was also different from the latest NCCN guidelines. In this research, a tumor without arterial involvement and with venous involvement < 90° was considered resectable, and a tumor with arterial involvement < 90° and/or venous involvement between 90° and 270° without occlusion was considered borderline resectable. This categorization meant that some patients who should have been regarded as R-PA cases (venous involvement between 90° and 180°) were classified as BR-PA cases.

The third is an Italian trial that required 32 patients *per* group, but only 38 were eventually enrolled overall[9]. The protocol or the registration number of this trial was not found. Twenty patients were assigned to the upfront surgery group, and 18 were assigned to the NAT group. The regimen was gemcitabine plus radiotherapy. Resectability corresponded to the latest NCCN guidelines.

The fourth is a phase II Italian trial (PACT-15)[10]. The enrollment was also less than expected; only 98 eligible patients were included, while it was estimated that 1040 patients would be enrolled. Finally, only 88 patients were randomly assigned to three groups: 26 in Group A received postoperative adjuvant intravenous gemcitabine, 30 in Group B received postoperative adjuvant PEXG (intravenous cisplatin, epirubicin, gemcitabine, and oral capecitabine), and 32 in Group C received preoperative and postoperative PEXG. The resectability criteria were stricter than the latest NCCN guidelines; only tumors without contact with arteries or veins were regarded as resectable, so some R-PA cases (with venous invasion < 180° without vein contour irregularities) was deemed BR-PA.

The last is a Japanese phase III trial that has not been published but was reported at the 2019 ASCO annual meeting[11]. A total of 360 patients were needed, and a total of 362 eligible patients were randomly allocated to the NAT group (n = 182) or the upfront surgery group (n = 180). The NAT regimen was gemcitabine plus S-1. Patients with PV involvement and without arterial involvement were deemed resectable in this research; furthermore, those with PV involvement > 180° were regarded as BR-PA cases according to the latest NCCN guidelines. However, details such as baseline characteristics or the proportion of patients with BR-PA were not posted. Thus, the outcomes might not be authoritative.

Table 2 Ongoing randomized controlled trials comparing surgery alone with neoadjuvant therapy followed by surgery for resectable pancreatic cancer

Trial name	NCT number	Phase	Status	Estimated enrollment	Treatment arm	Primary endpoint	Study start date	Estimated primary completion date	Estimated study completion date
ICI20-00047	NCT05181605	II/III	Not yet recruiting	116	FOLFIRINOX and SBRT with surgery Upfront surgery	OS	January 2022	January 2023	December 2024
CISPD-1	NCT03750669	II	Recruiting	416	nPt/GEM and mFOLFIRINOX with surgery Upfront surgery	DFS	October 2018	October 2023	October 2024
A021806	NCT04340141	III	Recruiting	352	mFOLFIRINOX with surgery Upfront surgery	OS	July 2020	January 2026	November 2030
PREOPANC	NCT04927780	III	Recruiting	378	mFOLFIRINOX with surgery Upfront surgery	OS	September 2021	February 2026	July 2029
AIO-PAK-0313	NCT02047513	II	Active, not recruiting	127[1]	nPt/GEM with surgery Upfront surgery	DFS	July 2015	April 2021[2]	October 2022[3]
NorPACT-1	NCT02919787	II/III	Active, not recruiting	140	FOLFIRINOX with surgery Upfront surgery	1-yr OS	September 2016	October 2022	April 2026
NEOPAC	NCT01314027	III	Terminated	38[1]	GEM/oxaliplatin with surgery Upfront surgery	PFS	September 2009	December 2018[2]	May 2019[3]
NEOPA	NCT01900327	III	Terminated	32[1]	GEM and EBRT with surgery Upfront surgery	3-yr survival rate	February 2014	November 2016[2]	July 2017[3]
NEOPAC/IPC 2011-002	NCT01521702	III	Completed	2[1]	GEM/Oxaliplatin with surgery Upfront surgery	PFS	December 2011	February 2015[2]	February 2015[3]
NEPAFOX	NCT02172976	II/III	Completed	40[1]	FOLFIRINOX with surgery Upfront surgery	mOS	November 2014	January 2020[2]	May 2020[3]

[1]Actual enrollment.
[2]Actual primary completion date.
[3]Actual study completion date.
SBRT: Stereotactic body radiotherapy; OS: Overall survival; nPt: Nab-paclitaxel; GEM: Gemcitabine; DFS: Disease-free survival; PFS: Progression-free survival; EBRT: External beam radiation.

Data about the median OS (mOS) of these RCTs are listed in Table 3. In the NCT00335543 trial[7], the mOS was 14.4 mo in the surgery group compared to 17.4 mo in the NAT group. In the Dutch trial[8], the mOS was comparable between the NAT group (15.6 mo) and the surgery group (14.6 mo). The outcome was similar in another RCT, in which the mOS was 19.5 and 22.4 mo in the upfront surgery group and the NAT group, respectively[9]. In the PACT-15 trial[10], the mOS in the NAT group (38.2 mo) was better than that in the upfront surgery groups (20.4 and 26.4 mo, respectively). However, data from the Prep-02/JSAP-05 study were inspiring; the mOS was 36.7 mo in the NAT group compared to 26.6 mo in the upfront surgery group (P = 0.015)[11].

The reasons for the different outcomes of these RCTs could include the following. First, three RCTs (the NCT00335543 trial, the Italian single-center trial, and the PACT-15 trial) obtained smaller enrollment than initially expected, and they terminated early due to the poor recruitment rates. The

Table 3 Comparison of median overall survival between the upfront surgery group and the neoadjuvant therapy plus surgery group

Ref.	Country	NCT number/Name	Variable	Upfront surgery	NAT plus surgery	*P* value
Golcher *et al*[7]	Germany	NCT00335543	mOS; mo	14.4	17.4	0.96
Versteijne *et al*[8]	Netherlands	PREOPANC	mOS; mo	14.6	15.6	0.83
Casadei *et al*[9]	Italy	-	mOS; mo	19.5	22.4	0.97
Reni *et al*[10]	Italy	PACT-15	mOS; mo	20.4,26.4	38.2	NM
Satoi *et al*[11]	Japan	Prep-02/JSAP-05	mOS; mo	26.6	36.7	0.015

NAT: Neoadjuvant therapy; mOS: Median overall survival; NM: Not mentioned.

poor sample sizes could have caused bias and led to inaccurate outcomes.

Second, the five RCTs adopted different resectability criteria. Referring to the latest NCCN guidelines, some patients actually with BR-PA cases (tumor contact with peripancreatic artery of ≤ 180°) were regarded as R-PA cases in the NCT00335543 trial and the Prep-02/JSAP-05 study, and some patients actually with R-PA cases (no arterial involvement and venous involvement ≤ 180°) were deemed to be BR-PA cases in the Dutch trial and the PACT-15 trial. This difference might have influenced the outcomes and caused the differences in the results of these RCTs.

Third, the regimens for NAT were also different. Although the regimens of these five RCTs were based on gemcitabine, two adopted gemcitabine alone, while the other three used gemcitabine combined with cisplatin or other agents. In addition, all of these RCTs combined preoperative radiotherapy with chemotherapy except the PACT-15 trial and the Prep-02/JSAP-05 study. However, the regimens (based on FOLFIRINOX or modified FOLFIRINOX or gemcitabine plus albumin-bound paclitaxel) that were recommended by the NCCN guidelines were not adopted in these RCTs. The German trial and the PACT-15 trial adopted regimens of gemcitabine and cisplatin, which are recommended for patients with known BRCA1/2 or PALB2 mutations, but these mutations were not mentioned in these two trials. The different efficiencies of these regimens could be another factor leading to various outcomes.

NAT might actually benefit patients with low-risk factors for long-term survival. According to the OS of the Dutch trial (Figure 1A), the 1-, 2-, 3-, and 4-year OS rates were comparable between the NAT group and the upfront surgery group[8]. The latest results of the PREOPANC trial showed that the hazard ratio (HR) of OS was 0.79 for patients with R-PA (P = 0.23)[12]. The reason for this outcome might be that this trial excluded T1 tumors (2 cm, without vascular involvement). Because patients with high-risk factors always die due to recurrence within 2 years, almost the only patients who were in the long-term follow-up were those with low-risk factors. Thus, when patients with low-risk factors were excluded, the benefit of NAT on long-term OS disappeared.

In the PACT-15 trial[10], the 1- and 2-year OS rates were similar between the NAT group and the upfront surgery group (Figure 1B). However, the NAT group showed better 3-year OS (55%) and 5-year OS (49%) than the surgery alone group (3-year OS: 35% and 43%; 5-year OS: 13% and 24%). The reason for this difference could be that T1 tumors were included. Tumors with low-risk factors could benefit from NAT and obtain better 3- and 5-year OS.

According to a recent meta-analysis, the NAT groups showed superior 1-, 2-, 3-, 4-, and 5-year survival rates compared to the upfront surgery group[13].

SAFETY AND FEASIBILITY

Postoperative complications

The lack of postoperative complications was an important prognostic factor of survival[14-16]. Lubrano *et al*[17] analyzed 942 patients with PDAC and found that the mOS and DFS decreased statistically when severe postoperative complications occurred[17]; the reason for this result could be that postoperative complications lead to failure of adjuvant therapy.

Data about postoperative complications are shown in Table 4.

In the German trial (NCT00335543)[7], postoperative complications were graded according to the Clavien-Dindo classification. In arm A (surgery alone), 17 patients suffered from grade I-II postoperative complications, and 15 patients suffered from grade III-V postoperative complications; in arm B (NACRT), 16 patients suffered from grade I-II postoperative complications, and 6 suffered from grade III-V postoperative complications.

Casadei *et al*[9] found that life-threatening complications were less frequent in the NAT group than in the surgery alone group. This could be attributed to pancreatic fibrosis as a result of NAT, which decreased the risk of pancreatic anastomotic leakage.

Table 4 Comparison of postoperative complications between the upfront surgery group and the neoadjuvant therapy plus surgery group

Ref.	Country	NCT number/Name	Variable	Upfront surgery	NAT plus surgery	*P* value
Golcher *et al*[7]	Germany	NCT00335543	Clavien-Dindo I-II complications	17/33 (52%)	16/33 (48%)	NM
			Clavien-Dindo III-V complications	15/33 (45%)	6/33 (18%)	NM
Versteijne *et al*[8]	Netherlands	PREOPANC	Postoperative complications	NM	NM	NM
Casadei *et al*[9]	Italy	-	Post-treatment morbidity	9/20 (45%)	10/18 (56%)	0.746
Reni *et al*[10]	Italy	PACT-15	Minor complications (Clavien-Dindo I–II)	21/49 (43%)	13/27 (48%)	NM
			Major complications (Clavien-Dindo III–IV)	10/49 (20%)	3/27 (11%)	NM

NAT: Neoadjuvant therapy; NM: Not mentioned.

In the PACT-15 trial[10], minor complications (Clavien-Dindo I-II) in Group C (NACT) were observed in 13 of 27 (48%) patients, compared to 9 of 22 (41%) and 12 of 27 (44%) in Groups A and B, respectively. Major complications (Clavien-Dindo III-IV) in Group C were observed in 3 of 27 (11%) patients, compared to 5 of 22 (23%) and 5 of 27 (19%) in Groups A and B, respectively[10].

No significant difference in postoperative morbidity was found between the two groups in the Prep-02/JSAP-05 study[11].

Postoperative complications occurred in 31 of 63 (49%) patients in the Japanese trial[18], which seemed comparable to those in the RCTs.

No significant difference was observed in the comparison of postoperative complications, indicating that NAT did not increase the risk of postoperative complications. Moreover, Golcher *et al*[7] and Casadei *et al*[9] agreed that NAT could decrease severe complications by inducing fibrosis[7,9].

Another three studies supported that the probability of postoperative complications occurring in patients who received NAT was not different from that in patients who underwent upfront surgery[19-21]. One study found that patients with R-PA who underwent NAT obtained a lower rate of postoperative complications than those who did not (30% *vs* 63%, $P = 0.001$)[4].

Postoperative adjuvant therapy

In a recent retrospective study, Nipp *et al*[22] found that the absence of adjuvant therapy was correlated with a high risk of early mortality[22]. Additional adjuvant therapy was linked to a reduction in mortality[23]. The results from a randomized, phase III trial attributed prolonged DFS to adjuvant therapy[24].

In the NCT00335543 trial[7], 10 of 23 (43%) patients in the surgery alone group underwent adjuvant chemotherapy, which was comparable to 7 of 19 (37%) patients in the NAT group.

Although there are no data for the R-PA subgroup regarding the difference in this factor between the two groups in the Dutch trial, data based on R-PA plus BR-PA patients showed no significant difference [8].

According to the PACT-15 trial[10], one patient among 18 in Group A (postoperative gemcitabine) was unable to receive adjuvant gemcitabine because his clinical condition did not completely recover after surgery. Moreover, ten patients did not complete the whole adjuvant gemcitabine treatment. Factors were similar in Groups B (postoperative adjuvant PEXG) and C (preoperative and postoperative adjuvant PEXG), and some patients did not complete the adjuvant therapy. Thus, preoperative chemoradiotherapy appears to be particularly essential.

Regardless of whether we consider the surgery alone group or the NAT group, some patients lost the opportunity for adjuvant therapy, which is essential for controlling recurrence. Considering this point, NAT is necessary to guarantee that more patients receive perioperative adjuvant therapy.

One study indicated that patients with R-PA who received NACRT had fewer chances of undergoing postoperative adjuvant therapy than those who merely underwent surgery[25]. Compared to NACRT patients, NACT patients were more likely to receive adjuvant chemotherapy after resection (41.3% *vs* 24.7%, $P < 0.001$)[26].

Duration of intervention

Some studies have explored whether operative duration correlates with the OS of patients with R-PA. Garcea *et al*[27] found that operative duration is not associated with survival[27]. In contrast, the results from another study showed that a short operative duration improved long-term survival by reducing the presence of hypoalbuminemia at 1 mo postoperatively[28]. However, overall, it was believed that the increased operative time was associated with a poorer long-term survival[29].

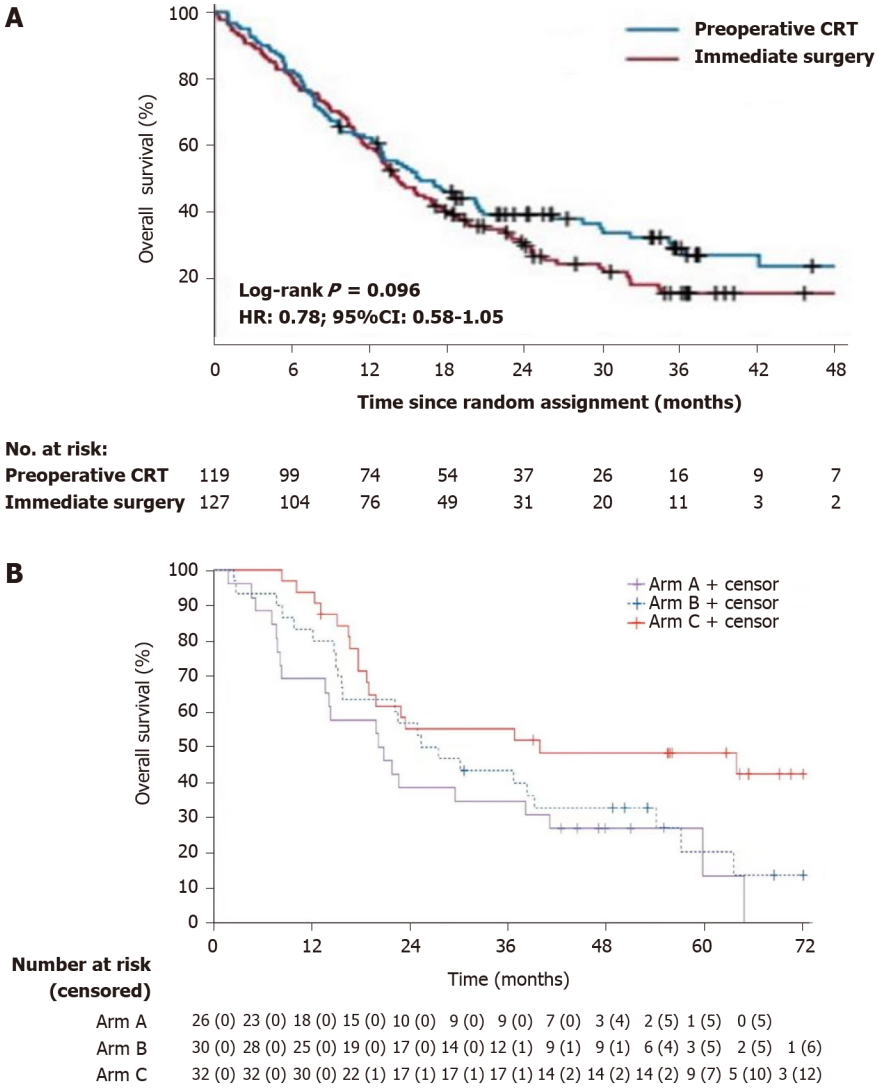

Figure 1 Overall survival. A: Comparison between NAT group and upfront surgery group; B: Comparison among different arms. Arm A: Upfront surgery (GEM); Arm B: Upfront surgery (PEXG); Arm C: PEXG. GEM: Gemcitabine; PEXG: Cisplatin, epirubicin, capecitabine, and gemcitabine. A: Citation: Versteijne E, Suker M, Groothuis K, Akkermans-Vogelaar JM, Besselink MG, Bonsing BA, Buijsen J, Busch OR, Creemers GM, van Dam RM, Eskens FALM, Festen S, de Groot JWB, Groot Koerkamp B, de Hingh IH, Homs MYV, van Hooft JE, Kerver ED, Luelmo SAC, Neelis KJ, Nuyttens J, Paardekooper GMRM, Patijn GA, van der Sangen MJC, de Vos-Geelen J, Wilmink JW, Zwinderman AH, Punt CJ, van Eijck CH, van Tienhoven G; Dutch Pancreatic Cancer Group. Preoperative Chemoradiotherapy Versus Immediate Surgery for Resectable and Borderline Resectable Pancreatic Cancer: Results of the Dutch Randomized Phase III PREOPANC Trial. *J Clin Oncol* 2020; 38: 1763-1773. Copyright ©The Author(s) 2020. Published by Wolters Kluwer Health Inc. B: Reni M, Balzano G, Zanon S, Zerbi A, Rimassa L, Castoldi R, Pinelli D, Mosconi S, Doglioni C, Chiaravalli M, Pircher C, Arcidiacono PG, Torri V, Maggiora P, Ceraulo D, Falconi M, Gianni L. Safety and efficacy of preoperative or postoperative chemotherapy for resectable pancreatic adenocarcinoma (PACT-15): a randomised, open-label, phase 2–3 trial. *Lancet Gastroenterol Hepatol* 2018; 3: 413-423. Copyright ©The Author(s) 2018. Published by Elsevier.

Only the Prep-02/JSAP-05 study showed no significant difference in operation time between the two groups, while no other RCTs focused on this factor.

Two retrospective studies indicated that there was a significant difference between NAT and upfront surgery in patients deemed to have resectable PDAC[19,20]. Patients who received NAT had a longer operative time than those who underwent upfront surgery.

Nutritional status

There have been limited studies of the relationship between nutritional status and survival of R-PA patients. A recent retrospective study indicated that the controlling nutritional status score, which is used to evaluate immune-nutritional status, had an independent correlation with survival in resected patients with PDAC[30]. No significant difference was shown between weight loss from the time of diagnosis and survival after resection[31]. Ueda *et al*[28] regarded hypoalbuminemia occurring within 1 mo after surgery as a predictor of survival in PDAC patients[28].

RCTs are needed to explore the correlation between nutritional status and NAT.

According to a retrospective study[21], the prognostic nutritional index (PNI), which was used to assess nutritional status, decreased in patients with R-PA from 48.2 ± 7.1 to 42.7 ± 6.0 ($P < 0.0001$) after

NACRT. Poor preoperative PNI is a predictor of poor survival in PDAC patients.

In summary, NAT is safe and feasible for patients with R-PA. First, NAT did not increase postoperative complications, and it might even decrease severe complications by inducing pancreatic fibrosis. Furthermore, comparable postoperative morbidity indicates that NAT does not limit adjuvant therapy; in contrast, it provides systemic therapy for those who are ineligible for adjuvant therapy, mostly due to postoperative complications. Moreover, NAT did not prolong the operation time.

FACTORS RELATED TO LOCAL RECURRENCE

Tumor diameter

Tumor size is important for the assessment of prognosis. According to the 8th AJCC TNM staging of PC, tumors ≤ 2 cm in diameter are defined as T1, tumors > 2 cm and ≤ 4 cm are defined as T2, and tumors > 4 cm are classified as T3 when there is no arterial invasion. Phoa *et al*[32] found an HR of 1.375 [95% confidence interval (CI): 1.267-1.492] for the T1 stage compared with the T2 stage and 1.796 (95%CI: 1.629-1.982) with the T3 stage, indicating a significant prognostic advantage for smaller tumor sizes (P < 0.001). Survival was longest for patients with a tumor diameter < 2 cm, and poor survival was observed in patients with resected tumors > 3 cm in diameter[32]. In addition, tumor size was associated with an increased risk of lymph node metastases and influenced the rate of margin positivity following resection [33]. NAT can reduce tumor size[25,34].

Tumor size was decreased in patients who underwent NAT according to the data from three RCTs, and there was a statistically significant advantage for NAT in one study (Table 5).

The results of the NCT00335543 trial showed that pT1-2 was more frequently observed in arm B (NACRT + surgery) than in those who underwent surgery only (arm A)[7]. Four of 19 (21%) patients in arm B were pT1-2 cases, while only 2 of 23 (9%) patients in arm A were at this stage.

The same conclusion was obtained in another RCT[9]. Pathologic T staging was significantly different between arm A (surgery alone) and arm B (NACRT plus surgery) (P = 0.016). Nine patients had pT1-2 stage disease in arm B, while none belonged to this stage in arm A.

In the PACT-15 trial, the tumor size in Group C (NACT) after resection was 2.0 cm, compared to 2.1 cm and 2.5 cm in Groups B and A, respectively[10].

In the Japanese phase II trial[18], the median tumor size before treatment was 24 mm, compared to 19 mm after receiving GSRT (gemcitabine and S-1 concurrently with radiation therapy).

A retrospective review showed that patients who underwent NACRT obtained smaller tumors in resection specimens (mean 2.5 cm) than those who underwent surgical exploration first (mean 3.1 cm, P = 0.04), although they had larger tumors prior to treatment (mean 2.5 cm *vs* 2.1 cm)[25].

NAT can reduce the tumor size and thus make it easier to obtain R0 resection. The anterior and posterior surfaces render it difficult to obtain R0 resection in large tumors.

Resection margins

According to the NCCN guidelines, resection margins are classified as R0 when the tumor is completely and microscopically removed within 1 mm. R1 denotes microscopic residual tumor, and R2 indicates macroscopic residual tumor. Most studies have supported that R1 resection leads to a worse outcome than R0 resection[29,34-36]. Positive margins can lead to local recurrence. The margins of the Whipple specimen include the SMA, portal vein, pancreatic neck, bile duct, and proximal (gastric or enteric) and distal enteric margins. The most important margin is the SMA margin, which consists of the soft tissue that connects the uncinate process to the right lateral border of the proximal 3–4 cm of the SMA.

The data about resection margins status are listed in Table 6.

In the NCT00335543 trial, 23 of 33 (70%) patients in arm A (upfront surgery group) underwent resection *vs* 19 of 33 (58%) in arm B (NAT group). R0 resection was obtained in 16 of 23 (70%) patients in arm A *vs* 17 of 19 (89%) in arm B. The intention-to-treat (ITT) R0 rate was 48% (16/33) in arm A compared to 52% (17/33) in arm B[7]. The time to progression was comparable between the two groups.

In the Dutch trial, 44 patients in the NACRT group (44/65, 68%) had successful resection, and 54 in the immediate surgery group (54/68, 79%) achieved resection[8]. The R0 resection rate was 66% (29 of 44) in patients who received NACRT *vs* 59% (32 of 54) in patients assigned to immediate surgery. The ITT R0 rate was 45% (29/65) in the NACRT group compared to 47% (32/68) in the immediate surgery group. The R0 rate increased in the NACRT group, while the resection rate decreased compared to the immediate surgery group. The locoregional failure-free interval (LFFI) was similar in the two groups.

In the Italian trial[9], R0 resection was defined as all PDAC with a clearance > 1 mm from each margin. R0 resection criteria were not mentioned in the other RCTs. Fifteen of 20 (75%) patients in arm A (upfront surgery group) underwent resection compared to 11 of 18 (61%) in arm B (NAT group). The R0 rate was 33% (5/15) in arm A *vs* 64% (7/11) in arm B. The ITT R0 resection rate was higher in arm B (7/18, 39%) than in arm A (5/20, 25%). No data about local recurrence were mentioned.

In the PACT-15 trial[10], the resection rates were 84% (22/26), 90% (27/30), and 84% (27/32) in Groups A (adjuvant gemcitabine), B (adjuvant PEXG), and C (neoadjuvant PEXG), respectively. The R0 resection rates were 27% (6/22), 37% (10/27), and 63% (17/27) in Groups A, B, and C, respectively. The

Table 5 Comparison of tumor size between the upfront surgery group and the neoadjuvant therapy plus surgery group

Ref.	Country	NCT number/Name	Variable	Upfront surgery	NAT plus surgery	*P* value
Golcher *et al*[7]	Germany	NCT00335543	Tumoral diameter (cm)	NM	NM	NM
			T1-2 stage	2	4	NM
			T3-4 stage	21	15	NM
Versteijne *et al*[8]	Netherlands	PREOPANC	Tumoral diameter (cm)	NM	NM	NM
			T1-2 stage	NM	NM	NM
			T3-4 stage	NM	NM	NM
Casadei *et al*[9]	Italy	-	Tumoral diameter (cm)	NM	NM	NM
			T1-2 stage	0	9	0.016
			T3-4 stage	20	8	
Reni *et al*[10]	Italy	PACT-15	Tumoral diameter (cm)	2.1-2.5	2	NM
			T1-2 stage	3	5	NM
			T3-4 stage	46	22	NM

NAT: Neoadjuvant therapy; NM: Not mentioned.

Table 6 Comparison of resection margin status between the upfront surgery group and the neoadjuvant therapy plus surgery group

Ref.	Country	NCT number/Name	Variable	Upfront surgery	NAT plus surgery	*P* value
Golcher *et al*[7]	Germany	NCT00335543	Resection rate	23/33 (70%)	19/33 (58%)	0.31
			R0 rate	16/23 (70%)	17/19 (89%)	NM
			ITT R0 rate	16/33 (48%)	17/33 (52%)	0.81
Versteijne *et al*[8]	Netherlands	PREOPANC	Resection rate	54/68 (79%)	44/65 (68%)	0.17
			R0 rate	32/54 (59%)	29/44 (66%)	0.54
			ITT R0 rate	32/68 (47%)	29/65 (45%)	NM
Casadei *et al*[9]	Italy	-	Resection rate	15/20 (75%)	11/18 (61%)	0.489
			R0 rate	5/15 (33%)	7/11 (64%)	NM
			ITT R0 rate	5/20 (25%)	7/18 (39%)	0.489
Reni *et al*[10]	Italy	PACT-15	Resection rate	49/56 (88%)	27/32 (84%)	NM
			R0 rate	16/49 (33%)	17/27 (63%)	NM
			ITT R0 rate	16/56 (29%)	17/32 (53%)	NM

NAT: Neoadjuvant therapy; NM: Not mentioned; ITT: Intention to treat.

ITT R0 resection rates were 23% (6/26), 33% (10/30), and 53% (17/32) in Groups A, B, and C, respectively. The rates of local failure were comparable between the NAT group and the two upfront surgery groups.

In the Prep-02/JSAP-05 study, no significant difference was observed in the R0 resection rate between the two groups[11].

In the Japanese trial[18], R0 resection was defined as the absence of cancer cells at the cut end of any specimen slice. Fifty-four of 63 patients underwent surgery, and all 54 patients who underwent resection achieved R0 resection.

An observational study showed that patients with R-PA who underwent NACRT obtained fewer positive microscopic resection margins than those who underwent upfront surgery (14% *vs* 30%; P = 0.042)[19].

Although the data from these five RCTs seem to indicate that the resection rates were lower in the NAT groups, and R0 resection rates were higher compared to the upfront surgery groups, there was no significant difference.

In the Prep-02/JSAP-05 study[11], a significant decrease in viable tumor cells was observed in primary tumors after NAT compared to upfront surgery ($P < 0.01$). Fewer viable tumor cells might be helpful in promoting response and limiting progression.

Although smaller tumors made it easier to obtain R0 resections, the margin status was also influenced by other factors. The SMA margin made it difficult to obtain R0 resection in tumors with vascular invasion, although they were small in size. NAT could reduce the tumor size and thus benefit the margin status, but it might be meaningless for improving the biological behavior of tumors (invasion of vessels, high differentiation grade, and so on); thus, R0 resection was not approved in some trials. Moreover, patients with BR-PA were deemed R-PA cases in the German trial, and the Prep-02/JSAP-05 study also influenced the rate of R0 resection. In addition, assessments of R0 were performed after surgery rather than after completing the whole treatment, and the benefit of systemic treatment could only be detected after all treatments were completed.

FACTORS RELATED TO METASTASIS

Lymph node status

Lymph node metastasis is regarded as a factor for poor prognosis congruously, and lymph node status has been proved to be one of the most effective prognostic factors in some recent studies. Furthermore, the ratio of positive nodes to total examined nodes is more valuable for prognosis than merely evaluating the number of positive lymph nodes[29,35]. Elshaer *et al*[37] found that most studies indicated that lymph node ratio and number of positive nodes, but not total nodes examined, correlated with OS in PDAC[37]. Recently, Shi *et al*[38] proposed a modification of the 8th AJCC staging system for PDAC[38]. Compared to the 8th AJCC staging system, it weakens the influences of positive lymph nodes, and small tumors with positive nodes are divided into earlier stages.

Most studies have shown that lymph node positivity is less frequently observed in patients with R-PA who received NAT than in those who underwent surgery only[19-23,25,34,39]. Data about lymph node status are listed in Table 7. In the German trial, there were 22 of 33 (67%) patients with clinical N0 in the NAT group compared to 30 of 33 (91%) in the primary surgery group before treatment ($P = 0.03$), but a higher (y)pN0 rate was observed in the NAT group (39%, 13/33) than in the primary surgery group (30%, 10/33) after treatment[7]. The preoperative clinical N0 rate was not comparable, which might have caused the negativity of the difference in pN0. The rate of (y)pM0 was comparable. The Italian single-center RCT also indicated that the NAT group obtained a higher pN0 rate (28%, 5/18) than the surgery group (10%, 2/20)[9]. The rate of pM0 was also comparable in this research. In addition, in the PACT-15 trial, the pN0 rates were 27% (6/22), 26% (7/27), and 48% (13/27) in patients who underwent resection in Groups A (adjuvant intravenous gemcitabine), B (adjuvant PEXG), and C (preoperative and postoperative PEXG), respectively[10]. However, the number of patients with liver metastasis in the NAT group decreased by half compared to that in the upfront surgery groups (64%, 42%, and 33% in Groups A, B, and C, respectively). No data about this factor in the NACRT subgroup were mentioned in the Dutch trial[8]. However, the median distant metastasis-free intervals were similar between the two groups.

No significant difference was found in the data from the above four RCTs, indicating that NAT did not improve the lymph node status. However, in the Prep-02/JSAP-05 study, resected patients in the NAT group obtained a significantly decreased nodal positive rate compared with the upfront surgery group ($P < 0.01$)[11]. This finding could indicate that patients who completed NAT and resection obtained better nodal status. The reason for this phenomenon could be that some patients were ineligible for surgery due to progression during NAT, and node positivity was observed more frequently in these patients, leading to a nonsignificant difference in ITT analysis between the two groups. Regarding the subgroup analysis of resected patients, a significant decrease was observed in the NAT group. Moreover, hepatic recurrence after surgery was significantly decreased in the NAT group (30.0%) compared to the upfront surgery group (47.5%).

In the Japanese trial[18], 37 of 63 (59%) patients were in the N0 stage.

A randomized, phase II trial indicated that R-PA patients who received NACT with gemcitabine plus cisplatin exhibited less node positivity than those who received NACT with gemcitabine[40]. In another study[26], postoperative pathology showed that R-PA patients who received NACRT prior to surgery had a higher rate of node-negative pathology than those who received NACT (68.0% *vs* 42.7%, $P < 0.001$), indicating that neoadjuvant external beam radiation is beneficial for reducing the rates of node-positive pathology.

Invasion of vessels and perineural spread

Tumors with poor biological behavior often invade vessels or nerves.

Direct invasion of the venous vasculature indicates distant spread and nodal or hematogenous metastasis, while perineural spread is associated with local recurrence[41]. At the same time, severe venous invasion leads to a poor prognosis[29].

Table 7 Comparison of lymph node status between the upfront surgery group and the neoadjuvant therapy plus surgery group

Ref.	Country	NCT number/Name	Variable	Upfront surgery	NAT plus surgery	*P* value
Golcher *et al*[7]	Germany	NCT00335543	pN0	10/33 (30%)	13/33 (39%)	0.44
Versteijne *et al*[8]	Netherlands	PREOPANC	pN0	NM	NM	NM
Casadei *et al*[9]	Italy	-	pN0	2/20 (10%)	5/18 (28%)	0.095
Reni *et al*[10]	Italy	PACT-15	pN0	13/49 (27%)	13/27 (48%)	NM

NAT: Neoadjuvant therapy; pN0: Pathological N0; NM: Not mentioned.

The Dutch trial and the PACT-15 trial considered this factor, and they enrolled patients with less venous invasion (< 90° and no venous contact, respectively). The Italian trial specifically regarded the grade of superior mesenteric and portal vein involvement as independent baseline characteristics. However, most RCTs did not research this factor, and only the Dutch trial focused on it[8]. Perineural invasion was less frequent in patients treated with NACRT (39% *vs* 73%; $P < 0.001$), as was venous invasion (19% *vs* 36%; $P = 0.024$). Based on the latest results from the Dutch trial, vascular invasion was less frequently observed in the NAT group (36% *vs* 65%; $P < 0.001$)[12]. Nevertheless, the results were based on patients with R-PA and BR-PA, and there were no specific data about the venous or perineural invasion in the R-PA subgroup.

Barbier *et al*[34] found that there were fewer vascular and perineural invasions in PDAC patients who underwent NACRT than in those who underwent surgery first ($P < 0.001$)[34]. The same conclusion was shown in two other studies[19,22].

CA19-9 levels

Tumors with elevated CA19-9 levels could indicate poor biological behavior and subclinical metastasis.

A national cancer database study enrolled 28074 PDAC patients with reported CA19-9[42]. Among early-stage (I/II) patients ($n = 10806$), there were 957 (8.8%) nonsecretors, 2708 (25.1%) with normal levels, and 7141 (66.1%) with elevated levels (CA19-9 > 37 U/mL). Survival was disappointing in patients with elevated CA-19-9, regardless of stage. Early-stage patients with elevated CA19-9 had worse survival at 1, 2, and 3 years than patients with normal levels. Nonsecretors and patients with normal levels had similar survival. High preoperative CA19-9 levels are regarded as a predictor of local and early (defined as relapse < 6 mo after resection) recurrence[25,43]. However, compared to preoperative CA19-9 levels, postoperative CA19-9 levels have more prognostic value because they can reflect the quality of tumor resection[44].

In the PACT-15 trial[10], the CA19-9 response was evaluated in 22 of 23 (96%) patients in the NACRT group. One patient obtained a decrease of more than 89%, 12 had decreases of 50% to 89%, and 9 had decreases less than 50%. In several previous studies, the median decrease in CA19-9 was 26%. The results indicated that NAT could decrease CA19-9 levels, but more authoritative evidence is needed to prove this deduction.

In the Japanese trial, median CA19-9 level decreased from 261 to 61 U/mL after patients received GSRT[18].

PDAC patients with CA19-9 levels that decreased during NAT had a better OS[45]. A phase I trial and a phase II trial demonstrated that PDAC patients had decreased median CA19-9 levels after achieving NAT[46,47].

Tumor differentiation grade

The majority of studies have supported that there is a statistically significant correlation between well-differentiated tumors and improved prognosis. The degree of differentiation is inversely associated with tumor aggressiveness[29]. High-grade tumors usually demonstrate poor biological behavior.

The latest results of the PREOPANC trial showed that tumor differentiation was similar between the NAT group and the upfront surgery group ($P = 0.91$). The data were based on patients with R-PA and BR-PA, and there were no data about the R-PA subgroup.

Improved nodal status accompanied by less hepatic metastasis was shown in the PACT-15 trial and Prep-02/JSAP-05 study, but the other RCTs did not obtain significant differences. The probable reason for this finding is that, although NAT can improve nodal status, it does not influence the biological behavior of tumors. In fact, NAT could benefit patients by controlling micrometastasis and allowing for systemic therapy.

CONCLUSION

The primary factors influencing the outcomes were as follows. First, the actual sample sizes were less than expected in some trials. In addition, the criteria for resectability were different in the studies. Moreover, the regimens varied in the different RCTs. Finally, how NAT influences the biological behavior of PC is still unknown, and no research has regarded it as an independent baseline characteristic to assign. NAT might not be useful for improving it, and poor biological behavior would offset the benefits from NAT (such as improving R0 resection and nodal status), leading to negative outcomes.

NAT is feasible and safe because it does not increase postoperative complications or prolong the operation time, and some experts have supported that it decreases the occurrence of severe postoperative complications by inducing fibrosis of pancreatic and peripancreatic tissue. Moreover, NAT reduces tumor diameter and provides an opportunity for perioperative adjuvant therapy for patients who cannot undergo postoperative adjuvant therapy. More evidence is needed to verify whether NAT actually decreases CA19-9 concentrations. More RCTs are needed to determine whether NAT worsens nutritional status. How NAT influences tumor differentiation remains unknown.

Some other advantages of NAT are as follows: (1) NAT might treat micrometastases and prevent local recurrence. However, in the Dutch trial, although the median LFFI was higher in the NAT group (17 mo) than in the immediate surgery group (13.5 mo), there was no significant difference (P = 0.067)[8]. In the PACT-15 trial[10], the local and distant recurrence rates were comparable between the NAT group and the surgery group. However, liver metastases were found less frequently in the NAT group (33%) than in the two adjuvant groups (64% and 42%, respectively); and (2) NAT provides sufficient time to expose metastases related to the progression of micrometastases that could not be detected previously and screens for patients who cannot benefit from surgery. Casadei *et al*[9] found that distant micrometastases had already occurred in some patients but were not detected. With the development of the diseases, they were found during NAT and avoided surgery, which was meaningless. Nevertheless, progression would occur if the NAT regimens were not effective. Currently, there is no RCT design for exploring these deductions, and more RCTs are needed to verify them in the future.

In general, the benefit of NAT outweighs the disadvantages. However, the majority of studies about NAT for R-PA patients have been retrospective; although there have been several prospective studies, their sample sizes have been too limited to obtain a conclusive outcome. In addition, more phase III trials and RCTs are needed to verify the conclusions.

It is essential to select patients who could mostly benefit from NAT. Some novel predictive factors in R-PA were addressed recently, such as molecular profiles, tumor microenvironments, immune cell infiltration, microRNAs, circulating tumor DNA, organoids, and the gut microbiome[48]. In the future, the RCT study design should likely be refined in patients with three types of resectable PC. The first group should include patients without risk factors for poor prognosis. The second category should include patients with a small tumor diameter who are prone to distant metastasis, as suggested by imaging or tumor biology-related examinations. The third group should include patients who could not easily obtain radical treatment of R0 disease by imaging evaluation.

FOOTNOTES

Author contributions: Tan CL and Liu XB designed the study; Zheng ZJ and Chen YH acquired the data; Zhang HQ and Li J analyzed and interpreted the data; Zhang HQ wrote the paper; Tan CL and Liu XB critically revised the manuscript for important intellectual content.

Supported by 1.3.5 Project for Disciplines of Excellence, West China Hospital, Sichuan University, No. ZY2017302 1-3-5; Key Research and Development Projects of Sichuan Province, No. 2019YFS0042; Post-Doctor Research Project, West China Hospital, Sichuan University, No. 2020HXBH168; and Key R&D Project of Science and Technology Department of Sichuan Province, No. 2021YFS0107.

Conflict-of-interest statement: All the authors report no relevant conflicts of interest for this article.

Country/Territory of origin: China

ORCID number: Chun-Lu Tan 0000-0002-7315-1964; Yong-Hua Chen 0000-0001-8485-0755.

S-Editor: Fan JR
L-Editor: Wang TQ

P-Editor: Fan JR

REFERENCES

1 **Li D**, Xie K, Wolff R, Abbruzzese JL. Pancreatic cancer. *Lancet* 2004; **363**: 1049-1057 [PMID: 15051286 DOI: 10.1016/S0140-6736(04)15841-8]

2 **Golcher H**, Brunner T, Grabenbauer G, Merkel S, Papadopoulos T, Hohenberger W, Meyer T. Preoperative chemoradiation in adenocarcinoma of the pancreas. A single centre experience advocating a new treatment strategy. *Eur J Surg Oncol* 2008; **34**: 756-764 [PMID: 18191528 DOI: 10.1016/j.ejso.2007.11.012]

3 **Murakami Y**, Uemura K, Sudo T, Hashimoto Y, Kondo N, Nakagawa N, Takahashi S, Sueda T. Survival impact of neoadjuvant gemcitabine plus S-1 chemotherapy for patients with borderline resectable pancreatic carcinoma with arterial contact. *Cancer Chemother Pharmacol* 2017; **79**: 37-47 [PMID: 27878355 DOI: 10.1007/s00280-016-3199-z]

4 **Sho M**, Akahori T, Tanaka T, Kinoshita S, Nagai M, Tamamoto T, Ohbayashi C, Hasegawa M, Kichikawa K, Nakajima Y. Importance of resectability status in neoadjuvant treatment for pancreatic cancer. *J Hepatobiliary Pancreat Sci* 2015; **22**: 563-570 [PMID: 25921623 DOI: 10.1002/jhbp.258]

5 **Mornex F**, Girard N, Scoazec JY, Bossard N, Ychou M, Smith D, Seitz JF, Valette PJ, Roy P, Rouanet P, Ducreux M, Partensky C. Feasibility of preoperative combined radiation therapy and chemotherapy with 5-fluorouracil and cisplatin in potentially resectable pancreatic adenocarcinoma: The French SFRO-FFCD 97-04 Phase II trial. *Int J Radiat Oncol Biol Phys* 2006; **65**: 1471-1478 [PMID: 16793214 DOI: 10.1016/j.ijrobp.2006.02.054]

6 **Gillen S**, Schuster T, Meyer Zum Büschenfelde C, Friess H, Kleeff J. Preoperative/neoadjuvant therapy in pancreatic cancer: a systematic review and meta-analysis of response and resection percentages. *PLoS Med* 2010; **7**: e1000267 [PMID: 20422030 DOI: 10.1371/journal.pmed.1000267]

7 **Golcher H**, Brunner TB, Witzigmann H, Marti L, Bechstein WO, Bruns C, Jungnickel H, Schreiber S, Grabenbauer GG, Meyer T, Merkel S, Fietkau R, Hohenberger W. Neoadjuvant chemoradiation therapy with gemcitabine/cisplatin and surgery versus immediate surgery in resectable pancreatic cancer: results of the first prospective randomized phase II trial. *Strahlenther Onkol* 2015; **191**: 7-16 [PMID: 25252602 DOI: 10.1007/s00066-014-0737-7]

8 **Versteijne E**, Suker M, Groothuis K, Akkermans-Vogelaar JM, Besselink MG, Bonsing BA, Buijsen J, Busch OR, Creemers GM, van Dam RM, Eskens FALM, Festen S, de Groot JWB, Groot Koerkamp B, de Hingh IH, Homs MYV, van Hooft JE, Kerver ED, Luelmo SAC, Neelis KJ, Nuyttens J, Paardekooper GMRM, Patijn GA, van der Sangen MJC, de Vos-Geelen J, Wilmink JW, Zwinderman AH, Punt CJ, van Eijck CH, van Tienhoven G; Dutch Pancreatic Cancer Group. Preoperative Chemoradiotherapy Versus Immediate Surgery for Resectable and Borderline Resectable Pancreatic Cancer: Results of the Dutch Randomized Phase III PREOPANC Trial. *J Clin Oncol* 2020; **38**: 1763-1773 [PMID: 32105518 DOI: 10.1200/JCO.19.02274]

9 **Casadei R**, Di Marco M, Ricci C, Santini D, Serra C, Calculli L, D'Ambra M, Guido A, Morselli-Labate AM, Minni F. Neoadjuvant Chemoradiotherapy and Surgery Versus Surgery Alone in Resectable Pancreatic Cancer: A Single-Center Prospective, Randomized, Controlled Trial Which Failed to Achieve Accrual Targets. *J Gastrointest Surg* 2015; **19**: 1802-1812 [PMID: 26224039 DOI: 10.1007/s11605-015-2890-4]

10 **Reni M**, Balzano G, Zanon S, Zerbi A, Rimassa L, Castoldi R, Pinelli D, Mosconi S, Doglioni C, Chiaravalli M, Pircher C, Arcidiacono PG, Torri V, Maggiora P, Ceraulo D, Falconi M, Gianni L. Safety and efficacy of preoperative or postoperative chemotherapy for resectable pancreatic adenocarcinoma (PACT-15): a randomised, open-label, phase 2-3 trial. *Lancet Gastroenterol Hepatol* 2018; **3**: 413-423 [PMID: 29625841 DOI: 10.1016/S2468-1253(18)30081-5]

11 **Satoi S**, Unno M, Motoi F, Matsuyama Y, Matsumoto I, Aosasa S, Shirakawa H, Wada K, Fujii T, Yoshitomi H, Takahashi S, Sho M, Ueno H, Yamamoto T, Kosuge T. The effect of neoadjuvant chemotherapy with gemcitabine and S-1 for resectable pancreatic cancer (randomized phase II/III trial; Prep-02/JSAP-05). *J Clin Oncol* 2019; **37**: 2 [DOI: 10.1200/jco.2019.37.15_suppl.4126]

12 **Versteijne E**, van Dam JL, Suker M, Janssen QP, Groothuis K, Akkermans-Vogelaar JM, Besselink MG, Bonsing BA, Buijsen J, Busch OR, Creemers GM, van Dam RM, Eskens FALM, Festen S, de Groot JWB, Groot Koerkamp B, de Hingh IH, Homs MYV, van Hooft JE, Kerver ED, Luelmo SAC, Neelis KJ, Nuyttens J, Paardekooper GMRM, Patijn GA, van der Sangen MJC, de Vos-Geelen J, Wilmink JW, Zwinderman AH, Punt CJ, van Tienhoven G, van Eijck CHJ; Dutch Pancreatic Cancer Group. Neoadjuvant Chemoradiotherapy Versus Upfront Surgery for Resectable and Borderline Resectable Pancreatic Cancer: Long-Term Results of the Dutch Randomized PREOPANC Trial. *J Clin Oncol* 2022; **40**: 1220-1230 [PMID: 35084987 DOI: 10.1200/JCO.21.02233]

13 **Bradley A**, Van Der Meer R. Upfront Surgery versus Neoadjuvant Therapy for Resectable Pancreatic Cancer: Systematic Review and Bayesian Network Meta-analysis. *Sci Rep* 2019; **9**: 4354 [PMID: 30867522 DOI: 10.1038/s41598-019-40951-6]

14 **Evans DB**, Varadhachary GR, Crane CH, Sun CC, Lee JE, Pisters PW, Vauthey JN, Wang H, Cleary KR, Staerkel GA, Charnsangavej C, Lano EA, Ho L, Lenzi R, Abbruzzese JL, Wolff RA. Preoperative gemcitabine-based chemoradiation for patients with resectable adenocarcinoma of the pancreatic head. *J Clin Oncol* 2008; **26**: 3496-3502 [PMID: 18640930 DOI: 10.1200/JCO.2007.15.8634]

15 **Howard TJ**, Krug JE, Yu J, Zyromski NJ, Schmidt CM, Jacobson LE, Madura JA, Wiebke EA, Lillemoe KD. A margin-negative R0 resection accomplished with minimal postoperative complications is the surgeon's contribution to long-term survival in pancreatic cancer. *J Gastrointest Surg* 2006; **10**: 1338-45; discussion 1345 [PMID: 17175452 DOI: 10.1016/j.gassur.2006.09.008]

16 **Tzeng CW**, Tran Cao HS, Lee JE, Pisters PW, Varadhachary GR, Wolff RA, Abbruzzese JL, Crane CH, Evans DB, Wang H, Abbott DE, Vauthey JN, Aloia TA, Fleming JB, Katz MH. Treatment sequencing for resectable pancreatic cancer: influence of early metastases and surgical complications on multimodality therapy completion and survival. *J Gastrointest*

Surg 2014; **18**: 16-24; discussion 24 [PMID: 24241967 DOI: 10.1007/s11605-013-2412-1]
17 **Lubrano J**, Bachelier P, Paye F, Le Treut YP, Chiche L, Sa-Cunha A, Turrini O, Menahem B, Launoy G, Delpero JR. Severe postoperative complications decrease overall and disease free survival in pancreatic ductal adenocarcinoma after pancreaticoduodenectomy. *Eur J Surg Oncol* 2018; **44**: 1078-1082 [PMID: 29685757 DOI: 10.1016/j.ejso.2018.03.024]
18 **Eguchi H**, Takeda Y, Takahashi H, Nakahira S, Kashiwazaki M, Shimizu J, Sakai D, Isohashi F, Nagano H, Mori M, Doki Y. A Prospective, Open-Label, Multicenter Phase 2 Trial of Neoadjuvant Therapy Using Full-Dose Gemcitabine and S-1 Concurrent with Radiation for Resectable Pancreatic Ductal Adenocarcinoma. *Ann Surg Oncol* 2019; **26**: 4498-4505 [PMID: 31440928 DOI: 10.1245/s10434-019-07735-8]
19 **Fujii T**, Satoi S, Yamada S, Murotani K, Yanagimoto H, Takami H, Yamamoto T, Kanda M, Yamaki S, Hirooka S, Kon M, Kodera Y. Clinical benefits of neoadjuvant chemoradiotherapy for adenocarcinoma of the pancreatic head: an observational study using inverse probability of treatment weighting. *J Gastroenterol* 2017; **52**: 81-93 [PMID: 27169844 DOI: 10.1007/s00535-016-1217-x]
20 **Motoi F**, Unno M, Takahashi H, Okada T, Wada K, Sho M, Nagano H, Matsumoto I, Satoi S, Murakami Y, Kishiwada M, Honda G, Kinoshita H, Baba H, Hishinuma S, Kitago M, Tajima H, Shinchi H, Takamori H, Kosuge T, Yamaue H, Takada T. Influence of preoperative anti-cancer therapy on resectability and perioperative outcomes in patients with pancreatic cancer: project study by the Japanese Society of Hepato-Biliary-Pancreatic Surgery. *J Hepatobiliary Pancreat Sci* 2014; **21**: 148-158 [PMID: 23913634 DOI: 10.1002/jhbp.15]
21 **Sho M**, Akahori T, Tanaka T, Kinoshita S, Tamamoto T, Nomi T, Yamato I, Hokuto D, Yasuda S, Kawaguchi C, Nishiofuku H, Marugami N, Enomonoto Y, Kasai T, Hasegawa M, Kichikawa K, Nakajima Y. Pathological and clinical impact of neoadjuvant chemoradiotherapy using full-dose gemcitabine and concurrent radiation for resectable pancreatic cancer. *J Hepatobiliary Pancreat Sci* 2013; **20**: 197-205 [PMID: 22766692 DOI: 10.1007/s00534-012-0532-8]
22 **Nipp RD**, Zanconato A, Zheng H, Ferrone CR, Lillemoe KD, Wo JY, Hong TS, Clark JW, Ryan DP, Fernández-Del Castillo C. Predictors of Early Mortality After Surgical Resection of Pancreatic Adenocarcinoma in the Era of Neoadjuvant Treatment. *Pancreas* 2017; **46**: 183-189 [PMID: 27846142 DOI: 10.1097/MPA.0000000000000731]
23 **Mokdad AA**, Minter RM, Zhu H, Augustine MM, Porembka MR, Wang SC, Yopp AC, Mansour JC, Choti MA, Polanco PM. Neoadjuvant Therapy Followed by Resection Versus Upfront Resection for Resectable Pancreatic Cancer: A Propensity Score Matched Analysis. *J Clin Oncol* 2017; **35**: 515-522 [PMID: 27621388 DOI: 10.1200/JCO.2016.68.5081]
24 **Ueno H**, Kosuge T, Matsuyama Y, Yamamoto J, Nakao A, Egawa S, Doi R, Monden M, Hatori T, Tanaka M, Shimada M, Kanemitsu K. A randomised phase III trial comparing gemcitabine with surgery-only in patients with resected pancreatic cancer: Japanese Study Group of Adjuvant Therapy for Pancreatic Cancer. *Br J Cancer* 2009; **101**: 908-915 [PMID: 19690548 DOI: 10.1038/sj.bjc.6605256]
25 **Papalezova KT**, Tyler DS, Blazer DG 3rd, Clary BM, Czito BG, Hurwitz HI, Uronis HE, Pappas TN, Willett CG, White RR. Does preoperative therapy optimize outcomes in patients with resectable pancreatic cancer? *J Surg Oncol* 2012; **106**: 111-118 [PMID: 22311829 DOI: 10.1002/jso.23044]
26 **Lutfi W**, Talamonti MS, Kantor O, Wang CH, Stocker SJ, Bentrem DJ, Roggin KK, Winchester DJ, Marsh R, Prinz RA, Baker MS. Neoadjuvant external beam radiation is associated with No benefit in overall survival for early stage pancreatic cancer. *Am J Surg* 2017; **213**: 521-525 [PMID: 28089341 DOI: 10.1016/j.amjsurg.2016.11.039]
27 **Garcea G**, Dennison AR, Ong SL, Pattenden CJ, Neal CP, Sutton CD, Mann CD, Berry DP. Tumour characteristics predictive of survival following resection for ductal adenocarcinoma of the head of pancreas. *Eur J Surg Oncol* 2007; **33**: 892-897 [PMID: 17398060 DOI: 10.1016/j.ejso.2007.02.024]
28 **Ueda M**, Endo I, Nakashima M, Minami Y, Takeda K, Matsuo K, Nagano Y, Tanaka K, Ichikawa Y, Togo S, Kunisaki C, Shimada H. Prognostic factors after resection of pancreatic cancer. *World J Surg* 2009; **33**: 104-110 [PMID: 19011933 DOI: 10.1007/s00268-008-9807-2]
29 **Neuzillet C**, Sauvanet A, Hammel P. Prognostic factors for resectable pancreatic adenocarcinoma. *J Visc Surg* 2011; **148**: e232-e243 [PMID: 21924695 DOI: 10.1016/j.jviscsurg.2011.07.007]
30 **Kato Y**, Yamada S, Suenaga M, Takami H, Niwa Y, Hayashi M, Iwata N, Kanda M, Tanaka C, Nakayama G, Koike M, Fujiwara M, Kodera Y. Impact of the Controlling Nutritional Status Score on the Prognosis After Curative Resection of Pancreatic Ductal Adenocarcinoma. *Pancreas* 2018; **47**: 823-829 [PMID: 29975352 DOI: 10.1097/MPA.0000000000001105]
31 **Perini MV**, Montagnini AL, Jukemura J, Penteado S, Abdo EE, Patzina R, Cecconello I, Cunha JE. Clinical and pathologic prognostic factors for curative resection for pancreatic cancer. *HPB (Oxford)* 2008; **10**: 356-362 [PMID: 18982152 DOI: 10.1080/13651820802140752]
32 **Phoa SS**, Tilleman EH, van Delden OM, Bossuyt PM, Gouma DJ, Laméris JS. Value of CT criteria in predicting survival in patients with potentially resectable pancreatic head carcinoma. *J Surg Oncol* 2005; **91**: 33-40 [PMID: 15999356 DOI: 10.1002/jso.20270]
33 **Midha S**, Chawla S, Garg PK. Modifiable and non-modifiable risk factors for pancreatic cancer: A review. *Cancer Lett* 2016; **381**: 269-277 [PMID: 27461582 DOI: 10.1016/j.canlet.2016.07.022]
34 **Barbier L**, Turrini O, Grégoire E, Viret F, Le Treut YP, Delpero JR. Pancreatic head resectable adenocarcinoma: preoperative chemoradiation improves local control but does not affect survival. *HPB (Oxford)* 2011; **13**: 64-69 [PMID: 21159106 DOI: 10.1111/j.1477-2574.2010.00245.x]
35 **Åkerberg D**, Ansari D, Andersson R. Re-evaluation of classical prognostic factors in resectable ductal adenocarcinoma of the pancreas. *World J Gastroenterol* 2016; **22**: 6424-6433 [PMID: 27605878 DOI: 10.3748/wjg.v22.i28.6424]
36 **Butler JR**, Ahmad SA, Katz MH, Cioffi JL, Zyromski NJ. A systematic review of the role of periadventitial dissection of the superior mesenteric artery in affecting margin status after pancreatoduodenectomy for pancreatic adenocarcinoma. *HPB (Oxford)* 2016; **18**: 305-311 [PMID: 27037198 DOI: 10.1016/j.hpb.2015.11.009]
37 **Elshaer M**, Gravante G, Kosmin M, Riaz A, Al-Bahrani A. A systematic review of the prognostic value of lymph node ratio, number of positive nodes and total nodes examined in pancreatic ductal adenocarcinoma. *Ann R Coll Surg Engl* 2017; **99**: 101-106 [PMID: 27869496 DOI: 10.1308/rcsann.2016.0340]
38 **Shi S**, Hua J, Liang C, Meng Q, Liang D, Xu J, Ni Q, Yu X. Proposed Modification of the 8th Edition of the AJCC Staging

System for Pancreatic Ductal Adenocarcinoma. *Ann Surg* 2019; **269**: 944-950 [PMID: 29334560 DOI: 10.1097/SLA.0000000000002668]

39 **Moutardier V**, Turrini O, Huiart L, Viret F, Giovannini MH, Magnin V, Lelong B, Bories E, Guiramand J, Sannini A, Giovannini M, Houvenaeghel G, Blache JL, Moutardier JC, Delpero JR. A reappraisal of preoperative chemoradiation for localized pancreatic head ductal adenocarcinoma in a 5-year single-institution experience. *J Gastrointest Surg* 2004; **8**: 502-510 [PMID: 15120377 DOI: 10.1016/j.gassur.2003.11.013]

40 **Palmer DH**, Stocken DD, Hewitt H, Markham CE, Hassan AB, Johnson PJ, Buckels JA, Bramhall SR. A randomized phase 2 trial of neoadjuvant chemotherapy in resectable pancreatic cancer: gemcitabine alone versus gemcitabine combined with cisplatin. *Ann Surg Oncol* 2007; **14**: 2088-2096 [PMID: 17453298 DOI: 10.1245/s10434-007-9384-x]

41 **Garcea G**, Dennison AR, Pattenden CJ, Neal CP, Sutton CD, Berry DP. Survival following curative resection for pancreatic ductal adenocarcinoma. A systematic review of the literature. *JOP* 2008; **9**: 99-132 [PMID: 18326920]

42 **Bichoo RA**, Jha CK, Mishra A. Letter to editor in response to the article entitled "Successful Completion of the Pilot Phase of a Randomized Controlled Trial Comparing Sentinel Lymph Node Biopsy to No Further Axillary Staging in Patients with Clinical T1-T2 N0 Breast Cancer and Normal Axillary Ultrasound" by Cyr AE et al. in J Am Coll Surg 2016; 223 (2): 399-407. *Am J Surg* 2017; **214**: 979-980 [PMID: 28132719 DOI: 10.1016/j.amjsurg.2016.10.039]

43 **Osayi SN**, Bloomston M, Schmidt CM, Ellison EC, Muscarella P. Biomarkers as predictors of recurrence following curative resection for pancreatic ductal adenocarcinoma: a review. *Biomed Res Int* 2014; **2014**: 468959 [PMID: 25050350 DOI: 10.1155/2014/468959]

44 **Ferrone CR**, Finkelstein DM, Thayer SP, Muzikansky A, Fernandez-delCastillo C, Warshaw AL. Perioperative CA19-9 levels can predict stage and survival in patients with resectable pancreatic adenocarcinoma. *J Clin Oncol* 2006; **24**: 2897-2902 [PMID: 16782929 DOI: 10.1200/JCO.2005.05.3934]

45 **Lim KH**, Chung E, Khan A, Cao D, Linehan D, Ben-Josef E, Wang-Gillam A. Neoadjuvant therapy of pancreatic cancer: the emerging paradigm? *Oncologist* 2012; **17**: 192-200 [PMID: 22250057 DOI: 10.1634/theoncologist.2011-0268]

46 **Tajima H**, Kitagawa H, Tsukada T, Nakanuma S, Okamoto K, Sakai S, Makino I, Furukawa H, Nakamura K, Hayashi H, Oyama K, Inokuchi M, Nakagawara H, Miyashita T, Fujita H, Itoh H, Takamura H, Ninomiya I, Fushida S, Fujimura T, Ohta T. A phase I study of neoadjuvant chemotherapy with gemcitabine plus oral S-1 for resectable pancreatic cancer. *Mol Clin Oncol* 2013; **1**: 768-772 [PMID: 24649244 DOI: 10.3892/mco.2013.133]

47 **Talamonti MS**, Small W Jr, Mulcahy MF, Wayne JD, Attaluri V, Colletti LM, Zalupski MM, Hoffman JP, Freedman GM, Kinsella TJ, Philip PA, McGinn CJ. A multi-institutional phase II trial of preoperative full-dose gemcitabine and concurrent radiation for patients with potentially resectable pancreatic carcinoma. *Ann Surg Oncol* 2006; **13**: 150-158 [PMID: 16418882 DOI: 10.1245/ASO.2006.03.039]

48 **Merz V**, Mangiameli D, Zecchetto C, Quinzii A, Pietrobono S, Messina C, Casalino S, Gaule M, Pesoni C, Vitale P, Trentin C, Frisinghelli M, Caffo O, Melisi D. Predictive Biomarkers for a Personalized Approach in Resectable Pancreatic Cancer. *Front Surg* 2022; **9**: 866173 [PMID: 35599791 DOI: 10.3389/fsurg.2022.866173]

World Journal of Gastrointestinal Oncology

Submit a Manuscript: https://www.f6publishing.com

World J Gastrointest Oncol 2022 October 15; 14(10): 1918-1932

DOI: 10.4251/wjgo.v14.i10.1918

ISSN 1948-5204 (online)

ORIGINAL ARTICLE

Basic Study

Transcriptional factor III A promotes colorectal cancer progression by upregulating cystatin A

Jing Wang, Yuan Tan, Qun-Ying Jia, Fa-Qin Tang

Specialty type: Oncology

Provenance and peer review: Unsolicited article; Externally peer reviewed.

Peer-review model: Single blind

Peer-review report's scientific quality classification

Grade A (Excellent): A
Grade B (Very good): B
Grade C (Good): C
Grade D (Fair): 0
Grade E (Poor): 0

P-Reviewer: Sahin TT, Turkey; Thummer RP, India

Received: May 7, 2022
Peer-review started: May 7, 2022
First decision: July 13, 2022
Revised: July 23, 2022
Accepted: September 8, 2022
Article in press: September 8, 2022
Published online: October 15, 2022

Jing Wang, Yuan Tan, Qun-Ying Jia, Fa-Qin Tang, Hunan Key Laboratory of Oncotarget Gene, Hunan Cancer Hospital & The Affiliated Cancer Hospital of Xiangya School of Medicine, Central South University, Changsha 410013, Hunan Province, China

Corresponding author: Fa-Qin Tang, MD, PhD, Doctor, Professor, Hunan Key Laboratory of Oncotarget Gene, Hunan Cancer Hospital & The Affiliated Cancer Hospital of Xiangya School of Medicine, Central South University, No. 283 Tongzipo Road, Changsha 410013, Hunan Province, China. tangfq@hnca.org.cn

Abstract

BACKGROUND

Advanced colorectal cancer (CRC) generally has poor outcomes and high mortality rates. Clarifying the molecular mechanisms underlying CRC progression is necessary to develop new diagnostic and therapeutic strategies to improve CRC outcome and decrease mortality. Transcriptional factor III A (GTF3A), an RNA polymerase III transcriptional factor, is a critical driver of tumorgenesis and aggravates CRC cell growth.

AIM

To confirm whether GTF3A promotes CRC progression by regulating the expression of cystatin A (*Csta*) gene and investigate whether GTF3A can serve as a prognostic biomarker and therapeutic target for patients with CRC.

METHODS

Human tissue microarrays containing 90 pairs of CRC tissues and adjacent non-tumor tissues, and human tissue microarrays containing 20 pairs of CRC tissues, adjacent non-tumor tissues, and metastatic tissues were examined for GTF3A expression using immunohistochemistry. The survival rates of patients were analyzed. Short hairpin GTF3As and CSTAs were designed and packaged into the virus to block the expression of *Gtf3a* and *Csta* genes, respectively. *In vivo* tumor growth assays were performed to confirm whether GTF3A promotes CRC cell proliferation *in vivo*. Electrophoretic mobility shift assay and fluorescence *in situ* hybridization assay were used to detect the interaction of GTF3A with *Csta*, whereas luciferase activity assay was used to evaluate the expression of the *Gtf3a* and *Csta* genes. RNA-Sequencing (RNA-Seq) and data analyses were used to screen for target genes of GTF3A.

RESULTS

The expression of GTF3A was higher in CRC tissues and lymph node metastatic tissues than in the adjacent normal tissues. GTF3A was associated with CRC prognosis, and knockdown of the *Gtf3a* gene impaired CRC cell proliferation, invasion, and motility *in vitro* and *in vivo*. Moreover, RNA-Seq analysis revealed that GTF3A might upregulate the expression of *Csta*, whereas the luciferase activity assay showed that GTF3A bound to the promoter of *Csta* gene and increased *Csta* transcription. Furthermore, CSTA regulated the expression of epithelial-mesenchymal transition (EMT) markers.

CONCLUSION

GTF3A increases CSTA expression by binding to the *Csta* promoter, and increased CSTA level promotes CRC progression by regulating the EMT. Inhibition of GTF3A prevents CRC progression. Therefore, GTF3A is a potential novel therapeutic target and biomarker for CRC.

Key Words: Transcription factor IIIA; Cystatin A; Colorectal cancer; Epithelial-mesenchymal transition

Core Tip: Transcriptional factor III A (GTF3A) is highly expressed in colorectal cancer (CRC) tissues, and GTF3A expression is associated with CRC prognosis. GTF3A binds to the promoter of cystatin (*Csta*) gene to facilitate *Csta* transcription, which regulates the expression of epithelial-mesenchymal transition markers and promotes CRC progression. Blocking GTF3A significantly inhibits CRC cell growth. Therefore, GTF3A is a potential novel therapeutic target and prognostic biomarker for CRC.

Citation: Wang J, Tan Y, Jia QY, Tang FQ. Transcriptional factor III A promotes colorectal cancer progression by upregulating cystatin A. *World J Gastrointest Oncol* 2022; 14(10): 1918-1932
URL: https://www.wjgnet.com/1948-5204/full/v14/i10/1918.htm
DOI: https://dx.doi.org/10.4251/wjgo.v14.i10.1918

INTRODUCTION

Colorectal cancer (CRC) is the third most commonly diagnosed cancer and the leading cause of cancer-related death worldwide[1]. CRC has distant invasive and metastatic abilities, such as liver and lung metastases, resulting in a poor survival[2]. Clarifying the molecular mechanisms underlying CRC progression is necessary for the development of new therapeutic strategies. Transcriptional factor III A (GTF3A), an RNA polymerase III transcriptional factor, specifically binds to the internal control region of the 5S rRNA gene from nucleotides +43 to +96[3], initiating the assembly of the transcription initiation complex (5S rDNA-TFIIIA-TFIIIC2-TFIIIBbeta complex). Complex formation is not proportional to the amount of TFIIIA[4]. GTF3A is present in all human organs. GTF3A shares a common conserved transcription activating signal, nuclear localization signal, and nuclear export signal, but lacks initiated Met and accompanying conserved residues in the N-terminal regions[5]. GTF3A regulates the 5S rRNA synthesis network by binding to 5S rDNA and 5S rRNA[6]. GTF3A binds to 5S rRNA to form the 7S ribonucleoprotein particle (RNP) complex, and the complex functions as a nuclear export signal (NES) to transfer 5S rRNA to the cytoplasm depending on the NES sequence, which protects the 5S rRNA from degradation[7,8]. Several studies have suggested that 5S rRNA binds to L5 and L11 to form the 5S RNP complex, regulating the MDM2-p53 checkpoint[9-12]. Alterations in ribosome biogenesis are critical drivers of tumorgenesis, and are closely associated with increased CRC cell growth[13]. These findings suggest that GTF3A regulates CRC progression.

Cystatin A (CSTA), a cysteine proteinase inhibitor, is a type 1 cystain (stefin). CSTA is a cornified cell envelope constituent of keratinocytes that plays a critical role in epidermal development and maintenance. The high expression of CSTA is associated with the invasion and metastasis of various malignant tumors, such as pancreatic ductal adenocarcinoma[14], esophageal squamous cell carcinoma [15], lung cancer[16], hepatocellular carcinoma (HCC)[17], and nasopharyngeal carcinoma (NPC)[18]. An increasing number of studies have shown that CSTA is a potential prognostic and diagnostic biomarker for cancer progression. The activity of the *Csta* promoter is positively regulated by the active Ras/MEKK1/MKK7/JNK signal transduction pathway, but negatively regulated by the negative Ras/Raf-1/MEK1/ERK pathway in human keratinocytes[19]. Other cysteine protease inhibitors, cystatin SN (CST1) and cystatin S (CST4), are type 2 cystatin proteins, which enhance the metastasis of various malignant tumors and contribute to a poor patient survival[20,21]. CST1 overexpression increases cell migration and invasion by mediating the epithelial-mesenchymal transition (EMT) in breast cancer and HCC[22,23] and contributes to CRC cell proliferation[24]. CST1 is also considered an

early diagnostic biomarker and potential therapeutic target in breast cancer, CRC, and gastric cancer[25, 26]. In the present study, we showed that GTF3A was highly expressed in CRC, and it bound to the promoter of *Csta* to facilitate *Csta* transcription, which then regulated EMT marker expression and promoted CRC progression. Therefore, GTF3A is a potential novel therapeutic target and a prognostic biomarker for CRC.

MATERIALS AND METHODS

Reagents and antibodies

Dulbecco's modified Eagle's medium (DMEM), Cell Counting Kit (CCK8), and other supplements were obtained from Life Technologies (Rockville, MD, United States). GTF3A antibody for Western blot analysis was purchased from Bethyl Laboratories, Inc (Suzhou, China). CSTA antibody was purchased from Novus (CO, United States). CST1 antibody was purchased from Invitrogen (Shanghai, China). CST4 antibody was purchased from R&D Systems (Minneapolis, MN, United States). GTF3A antibody used for the immunofluorescence assay was purchased from Bioss Antibodies (Beijing, China). The dual-luciferase reporter assay system was purchased from Promega (Madison, WI, United States). Antibodies against Snail, E-cadherin, and beta-catenin were purchased from Abcam (Cambridge, United Kingdom). Glyceraldehydes-3-phosphate dehydrogenase (GAPDH) and secondary antibodies were purchased from Proteintech Company (Wuhan, Hubei, China).

Tissue microarray and immunohistochemical staining

Human tissue microarrays (HCol-Ade180Sur-08) containing 90 pairs of CRC tissues and adjacent non-tumor tissues, and human tissue microarrays (HCol-Ade060Lym-01) containing 20 pairs of CRC tissues, adjacent non-tumor tissues, and lymph node metastatic tissues, were purchased from Outdo Biotech Company (Shanghai, China). Immunohistochemical (IHC) staining was performed to detect the expression of GTF3A as described previously[27]. These tissue microarrays were stained with GTF3A antibody (1:300 dilution). The use of patient materials was approved by the ethics committee of Hunan Cancer Hospital (No. KYJJ-2020-004). All IHC results were evaluated based on the semi-quantitative histological scoring (HSCORE) system using the following formula: H-SCORE = $\sum$ (pi × i) ["pi" represents the percentage of stained cells in an intensity area, whereas "I" represents the staining intensity (0, no labeling; 1, weak; 2, moderate; and 3, strong)].

Cell lines

Human CRC cell lines (HCT116, SW480, DLD1, SW620, and HT29) were obtained from the American Type Culture Collection (Manassas, VA, United States) and were purchased from the Shanghai Cell Center (Shanghai, China). All cell lines were cultured in high-glucose DMEM supplemented with 10% fetal bovine serum (FBS) at 37 °C with 5% CO_2.

Real-time quantitative polymerase chain reaction

Real-time quantitative polymerase chain reaction (RT-qPCR) was performed as described previously [28]. Briefly, the total RNA of cultured cells was extracted using a total RNA kit (R6834, OMEGA), and 1 μg of DNase-treated RNA was reverse transcribed using the Revert Aid First Strand cDNA Synthesis Kit (Thermo Fisher Scientific, Shanghai, China) according to the manufacturer's instructions. The threshold cycle (Ct) values were measured using Hieff quantitative PCR SYBR Green Mix (Yeasen, Shanghai, China) in A LightCycler 96 qPCR System (Roche). Primer sequences used are listed in Supplementary Table 1. The relative mRNA levels of each gene were normalized to those of the housekeeping gene GAPDH. Relative transcript levels were calculated as two power values of ΔCt (the differential value of Ct between GAPDH and the target cDNA).

Plasmid transfection

The designed short hairpin RNAs (shRNAs) shGTF3A#1, shGTF3A#2, shGTF3A#3, shGTF3A#4, and shscramble were cloned into the lentivirus vector GV112 by Shanghai GeneKai Company (Shanghai, China). The shRNA sequences for *Gtf3a* are listed in Supplementary Table 2. The shRNAs for the *Csta* gene were designed to knock down the expression of CSTA. The shRNA sequences for *Csta* are shown in Supplementary Table 3. Synthetic plasmids were verified by sequence analysis and PCR and then cloned into GV493. Lipofectamine 3000 (Thermo Fisher Scientific, Carlsbad, CA, United States) was used to transfect the plasmids into HEK293T cells; 1×10^5 cells were transfected with shscramble, shGTF3A#1, shGTF3A#2, shGTF3A#3, shGTF3A#4, shCSTA#1, and shCSTA#2. The knockdown efficiency was filtered using RT-qPCR.

Stable cell lines

shGTF3As, shCSTAs, and negative control lentiviruses were packaged by the Shanghai GeneKai Company (Shanghai, China). The lentivirus titers were quantified (≥ 10^8 TU/mL). Following the

manufacturer's protocol, 2 × 10^5 of SW480 and HCT116 cells were seeded in six-well culture plates, and cultivated at 37 °C and 5% CO_2. After 24 h, the cells were transfected with the appropriate amount of lentivirus at a multiplicity of infection of 20 TU/mL. After being incubated for 10 h, the culture medium was removed, and fresh DMEM containing 10% FBS was added. Next, antibiotic-free medium containing 3 μg/mL puromycin was used to screen the stable cells for 3-4 wk. Ultimately, the knockdown and negative control stable cell lines shscramble-SW480, shGTF3A#1-SW480, shGTF3A#4-SW480, shGTF3A#1-HCT116, and shGTF3A#4-HCT116 were obtained.

Western blot analysis

Western blotting was performed as previously described[29]. Briefly, 1 × 10^6 cells were lysed with a radioimmunoprecipitation assay lysis buffer [50 mmol/L Tris pH 7.4, 150 mmol/L NaCl, 1% Triton X-100, 1% sodium deoxycholate, and 0.1% sodium dodecyl sulfate (SDS)] containing 100 × protease inhibitor cocktail and 100 × phosphatase inhibitor cocktail (CWBIO, Beijing, China). Following the manufacturer's instructions, the crude lysate was centrifuged and the supernatant was collected to measure the protein concentration using the BCA Protein Assay Kit (CWBIO, Beijing, China). After being boiled at 100 °C for 5 min, 20-60 μg of protein was separated by 10% SDS- polyacrylamide gel electrophoresis and transferred to a 0.2 μm PVDF membrane (Millipore). The protein membrane was blocked with 5% non-fat milk, incubated with the primary antibody, and incubated with an appropriate peroxidase conjugated secondary antibody. The signal was detected on a gel imager using an enhanced chemiluminescence (ECL) Western blotting kit (CWBIO, Beijing, China). GAPDH was used as an internal control to verify basal expression. The ratio of specific proteins to GAPDH was calculated.

Cell proliferation and colony formation assays

shGTF3A#1-HCT116, shGTF3A#4-HCT116, shscramble-HCT116, shGTF3A#1-SW480, shGTF3A#4-SW480, and shscramble-SW480 cells were seeded in 96-well plates, and CCK8 (ApexBio) was used to examine cell viability following the manufacturer's protocol. Briefly, CCK8 was added to the cell plates, and incubated for 4 h. Then, the optical density at 450 nm was measured using a microplate reader. Cell viability was calculated daily for 5 d. For the colony formation assay, shGTF3A#1-HCT116, shGTF3A#4-HCT116, shscramble-HCT116, shGTF3A#1-SW480, shGTF3A#4-SW480, and shscramble-SW480 cells were seeded in 6-well plates with each well containing 1000 cells, and cultured for 16 d. The cell colonies were fixed in methanol, stained with 0.5% gentian violet, and counted automatically using a computerized microscope system.

Cell invasion and motility assays

Cell invasion and motility assays *in vitro* were performed using previously described methods[29]. Briefly, for the invasion assay, Matrigel (25 mg/50mL, Collaborative Biomedical Products, Bedford, MA, United States) was added to the upper chamber with 8 mm pore polycarbonate membrane filters. shGTF3A#1-HCT116, shGTF3A#4-HCT116, shscramble-HCT116, shGTF3A#1-SW480, shGTF3A#4-SW480, and shscramble-SW480 cells were seeded in the upper chamber (Neuro Probe, cabin John, MD) at a density of 1.5 × 10^4 cells/well in 100 μL of serum-free medium, and then incubated at 37 °C for 48 h. The bottom chamber contained standard medium with 20% FBS. Cells that invaded the lower surface of the membrane were fixed with 37% paraformaldehyde, and stained with crystal violet. Invading cells were counted under a light microscope. The motility assay was performed in a similar manner to the invasion assay without Matrigel coating.

Wound healing assay

A wound healing assay was used to measure the cell migration potential. Briefly, 2 × 10^5 of shGTF3A#1-HCT116, shGTF3A#4-HCT116, shscramble-HCT116, shGTF3A#1-SW480, shGTF3A#4-SW480, and shscramble-SW480 cells were seeded in 6-well plates. After the cells reached 95% confluence, the surface of the cell layer was wounded using a sterile 10 μL pipette tip. The cells were then rinsed three times with phosphate buffered saline (PBS) to move detached cells and incubated in DMEM containing 1% FBS for 48 h. Wound closure was observed under a microscope at 0, 24, and 48 h.

Tumor growth assay in vivo

In vivo tumor growth assays were performed as previously described[30]. Briefly, female nude mice (aged 4-5 wk) were obtained from Hunan SJA Laboratory Animal Co. Ltd. (Changsha, China). Experiments involving animal subjects and protocols for animal studies were approved by the Laboratory Animal Research Center of Hunan Cancer Hospital (No. 2020-118). Nude mice were subcutaneously injected with 3 × 10^6 shGTF3A#1-SW480, shGTF3A#4-SW480, or shscramble-SW480 cells (5 mice per group). The size of the tumor that developed in the mice was measured every 3 d, and a tumor growth curve was drawn. After 4 wk, the mice were euthanized with pentobarbital sodium at 20 mg/mL, and the tumor weights were measured.

RNA sequencing and data analysis

After harvesting shGTF3A#1-SW480, shGTF3A#4-SW480, and shscramble-SW480 cells, total RNA was extracted using TRIzol reagent (Invitrogen). After the rRNA was removed, the enriched longRNA (> 200 nt) was interrupted, reversely transcribed into cDNA, and repaired, and RNA sequencing (RNA-Seq) was performed to build a chain-specific database. The clean data were obtained by quality testing of Bioptic Qsep100, and then comparative mapping of genomes was acquired between clean data and the hg38 Ensemble transcriptome using HISAT2 software. The differentially expressed genes between groups were analyzed using the DESeq2 R package, and the default screening criteria were: (1) Log2 (fold change) >1; and (2) False discovery rate < 0.05.

Fluorescence in situ hybridization assay

Fluorescence *in situ* hybridization (FISH) assays were performed as previously described[31]. FISH probes for *Csta* promoter sequence were designed and synthesized by Well Bio (Guangzhou, China). The IncRNA FISH kit (C10910) was purchased from Wellbio (Guangzhou, China). The cell slides were fixed with 4% paraformaldehyde for 30 min at 25 °C, permeabilized with proteinase K for 30 min at 37 °C, and blocked for 30 min at 37 °C with 200 μL of pre-hybridization solution. After removing the pre-hybridization solution, 100 μL of the probe hybridization solution was added to the cell slides overnight at 37 °C in the dark. After being washed three times for 5 min each with 4 × SSC, 2 × SSC, 1 × SSC, and PBS, the cell slides were incubated with the appropriately diluted primary antibody (anti-GTF3A) overnight at 4 °C. After washing three times with PBS, the slides were incubated with the secondary antibody (fluorescence labelled anti-rabbit immunoglobulin G) for 90 min at 37 °C. Finally, the slides were stained with 4′,6-diamidino-2-phenylidole for 10 min at 37 °C and sealed with 90% glycerin. All images were acquired using a fluorescence microscope.

Electrophoretic mobility shift assay

A biotin labeled *Csta* promoter DNA probe (5′-biotin-agctagtgacgccttttaaaacacgt ccaccattccttcctttttttc-3′) was synthesized by Sangon (Shanghai, China). Both sense and antisense strands were diluted to a concentration of 0.2 μM, mixed at 1:1, denatured at 95 °C for 5 min, maintained at 70 °C for 20 min, and formed into a double-stranded probe (diluted 10 times when used) after being cooled to room temperature. Following the instructions of the electrophoretic mobility shift assay (EMSA) kit (CWBIO, Beijing, China), the protein supernatant for each sample was separated on a 4% polyacrylamide gel, and transferred to a nylon membrane (CWBIO). The protein membrane was cross-linked using UV radiation, blocked with a confining liquid, and incubated with the indicated streptavidin-horseradish peroxidase conjugate. The signal was detected on a gel imager using the ECL Western blotting kit (CWBIO, Beijing, China).

Luciferase activity assay

A dual-luciferase reporter assay system (Promega) was used to detect the expression of *Csta* following the manufacturer's instructions. Briefly, the *Csta* promoter was cloned into the firefly luciferase plasmid, and *Csta* promoter-luc was obtained. Then, 1×10^5 of HCT116 cells were cultured in 48-well plates. *Csta* promoter-luc, plasmid-Renilla, and plasmid-GTF3A were co-transfected into HCT116 cells with X-tremeGene HP. After 48 h of culture, the cells were harvested, lysed with Passive Lysis Buffer, and treated with Luciferase Assay Reagent. Firefly luciferase and renilla luciferase were measured. The ratio of firefly luciferase to renilla luciferase represents the expression of *Csta*.

Statistical analysis

All experiments were performed at least three times. The results are presented as the mean ± SD of three independent experiments and were analyzed using Student's *t*-test. The differences between groups are reported as follows: $^aP < 0.05$, $^bP < 0.01$, $^cP < 0.001$, and $P > 0.05$. All statistical data were calculated using GraphPad Prism software (version7.0).

RESULTS

High expression of GTF3A in CRC and metastatic tissues

To determine the expression of GTF3A in CRC tissues, two sets of CRC tissue microarray were used to detect GTF3A expression by IHC. GTF3A was found to have higher expression in the cancer tissues than in the adjacent tissues of HCol-Ade180Sur-08 microarray. To further probe whether metastatic cancers had higher expression and analyze the association of GTF3A expression with metastasis, HCol-Ade060Lym-01 microarray containing CRC cancer, metastatic tissues, and adjacent tissues was also used to detect GTF3A, and observe GTF3A expression in metastatic tissues. These two microarrays had a total of 110 cancer tissues, 110 adjacent tissues, and 20 metastatic tissues, some of which were chipped off and could not be used; 102 cases in the cancer group, 106 in the adjacent group, and 20 in the metastatic group were calculated by gray scanning and scored, and survival time and survival curve

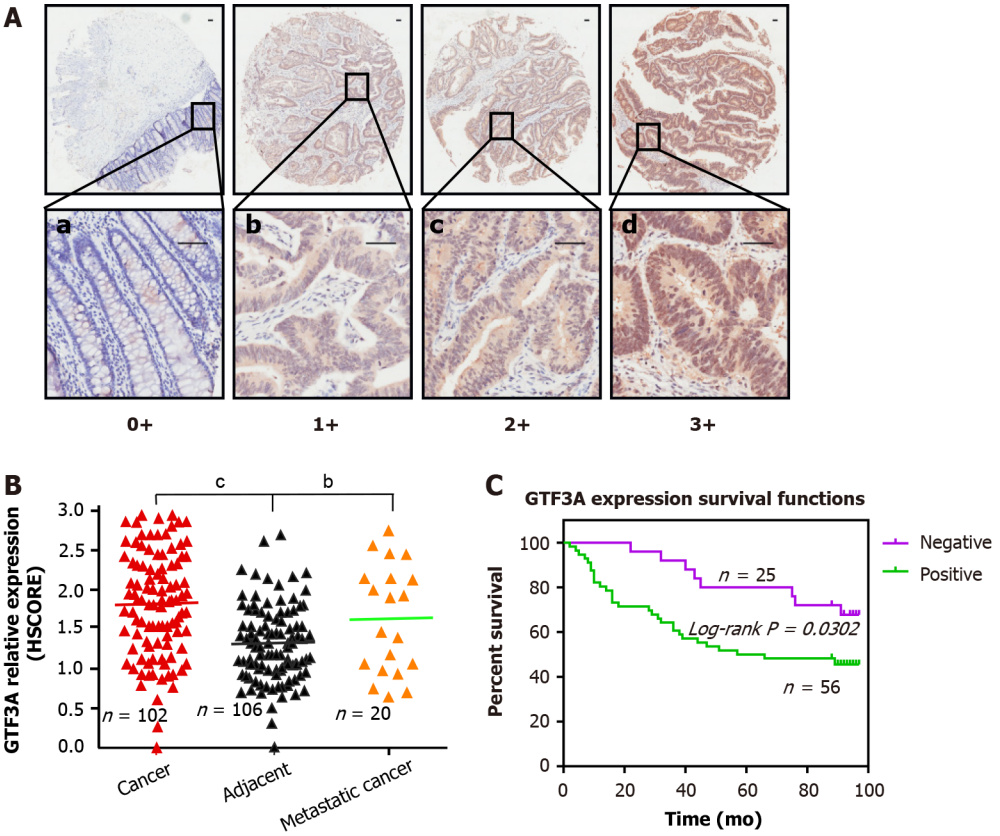

Figure 1 Transcriptional factor III A expression in colorectal cancer and survival analysis of patients with colorectal cancer. A: Transcriptional factor III A (GTF3A) expression in adjacent normal, colorectal cancer (CRC), and metastatic tissues were detected using immunohistochemical staining. The grading standards were: (1) Negative, a, scored as 0; (2) Weakly positive, b, scored as 1; (3) Moderately positive, c, scored as 2; and (4) Strongly positive, d, scored as 3. Scale bar, 50 μm; B: GTF3A expression in adjacent normal, CRC, and metastatic tissues was quantified using semi-quantitative histological score. Scored dots expression groups were statistically analyzed using unpaired *t* test; C: Overall survival of patients with GTF3A negative ($n = 25$) or GTF3A positive ($n = 56$) expression was analyzed by log-rank (Mantel-Cox) test. $^{b}P < 0.01$; $^{c}P < 0.001$. GTF3A: Transcriptional factor III A; HSCORE: Semi-quantitative histological score.

were analyzed. The expression of GTF3A in CRC and metastatic tissues was higher than that in adjacent normal tissues (Figures 1A and B, $P < 0.01$). To analyze whether GTF3A expression was relevant to survival time, patients with CRC were divided into GTF3A negative and positive groups, and the survival curve of CRC patients showed that the negative group had a longer overall survival than the positive group (Figure 1C, $P < 0.05$). These clinical data suggested that GTF3A expression is associated with CRC progression.

Knockdown of the Gtf3a gene inhibits CRC cell proliferation

Five CRC cell lines, HCT116, SW480, DLD1, SW620, and HT-29, were used to detect the expression of GTF3A using Western blot. The results showed that SW480 cells had high expression of GTF3A, whereas HCT116, DLD1, SW620, and HT-29 cells had low expression of GTF3A (Figure 2A). To clarify the role of *Gtf3a* in CRC, shGTF3A#1, #2, #3, and #4 were designed and packaged into the virus. Their inhibitory effects on *Gtf3a* were screened, and the results showed that shGTF3A#1 and shGTF3A#4 had high knockdown efficiencies. HCT116 and SW480 cells were stably transfected with shscramble, shGTF3A#1, or shGTF3A#4. RT-qPCR was performed to evaluate knockdown efficiency, and the results showed that shGTF3A#1 and shGTF3A#4 induced effective knockdown of *Gtf3a* in HCT116 and SW480 cells (Figure 2B). Consistently, Western blot results showed that GTF3A protein expression was effectively decreased in shGTF3A#1 and #4-HCT116 and shGTF3A#1 and #4-SW480 cells (Figure 2B). The cell viability of HCT116 and SW480 cells was detected using the CCK8 assay after knockdown of the *Gtf3a* gene, and the cell proliferation of HCT116 and SW480 cells was significantly decreased in the knockdown group (Figure 2B). Furthermore, the cell colony formation assay showed that colony size and number were dramatically diminished in *Gtf3a*-knockdown cells (Figure 2C, $P < 0.01$). These data indicated that knockdown of *Gtf3a* inhibits the growth of CRC cells.

Knockdown of Gtf3a inhibits CRC cell motility and invasion

Gtf3a-knockdown SW480 and HCT116 cells were used to determine whether *Gtf3a* is involved in CRC cell motility and invasion. Results of the wound healing assay showed that shGTF3A#1 and #4-HCT116

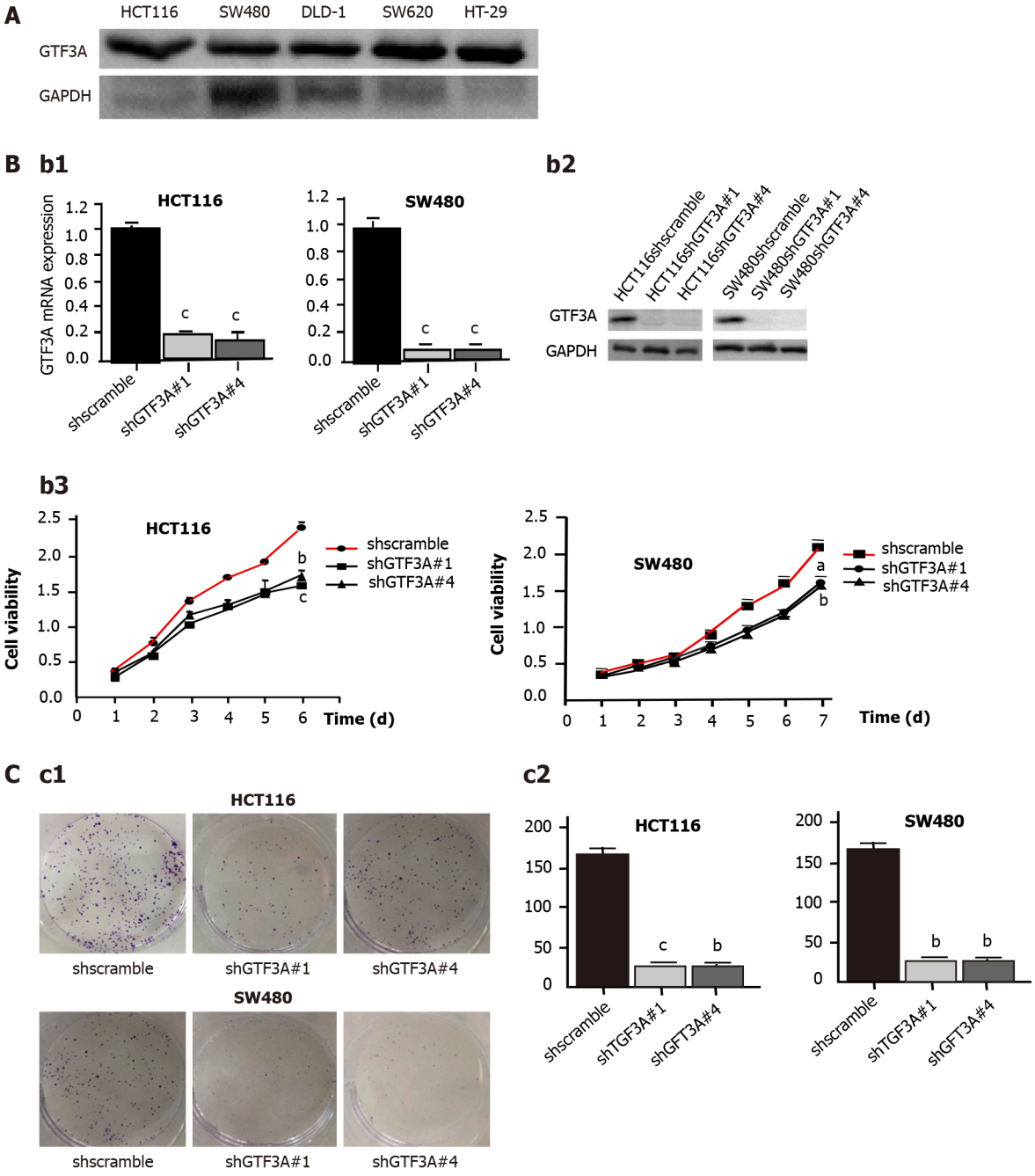

Figure 2 Knockdown of transcriptional factor III A gene inhibits colorectal cancer cell proliferation. A: The expression of transcriptional factor III A (GTF3A) in HCT116, SW480, DLD-1, SW620, and HT-29 cells was detected by Western blot; B: HCT116 and SW480 cells were stably transfected with short hairpin (sh) shscramble and shGTF3A#1 and #4-GV112 virus, respectively. *Gtf3a* mRNA (b1) and GTF3A protein (b2) expression were detected using real-time quantitative polymerase chain reaction and Western blot, respectively. The cell viability of HCT116 and SW480-shscramble as well as shGTF3A#1 and #4 cells was detected using Cell Counting Kit assay (b3); C: Colony formation of the transfected HCT116 and SW480 cells was detected using colony formation assay (c1), and the colony number was counted (c2). *Gtf3a* mRNA expression, cell colony number, and cell viability are expressed as the mean ± SEM of three independent experiments. $^{a}P < 0.05$; $^{b}P < 0.01$; $^{c}P < 0.001$. GTF3A: Transcriptional factor III A; GAPDH: Glyceraldehydes-3-phosphate dehydrogenase.

and shGTF3A#1 and #4-SW480 cells had impaired migratory capability compared with shscramble cells (Figure 3A). In addition, the transwell assay showed that invasion and metastasis in the *Gtf3a*-knockdown groups were significantly repressed compared with those in the controls (Figure 3B), and the number of invaded or migrated cells in the knockdown groups dramatically decreased (Figure 3B). Collectively, these results highlighted that knockdown of *Gtf3a* suppressed CRC cell invasion and metastasis in *vitro*, whereas the *Gtf3a* gene promoted the progression of CRC.

GTF3A protein regulates CSTA by binding to the CSTA promoter

To explore the molecular mechanisms of GTF3A in CRC progression, RNA-Seq was used to screen the target genes of GTF3A, and the differential genes between SW480 *Gtf3a*-knockdown and scramble control cells were analyzed. The RNA-Seq results are shown in Figures 4A and 4B; several differentially

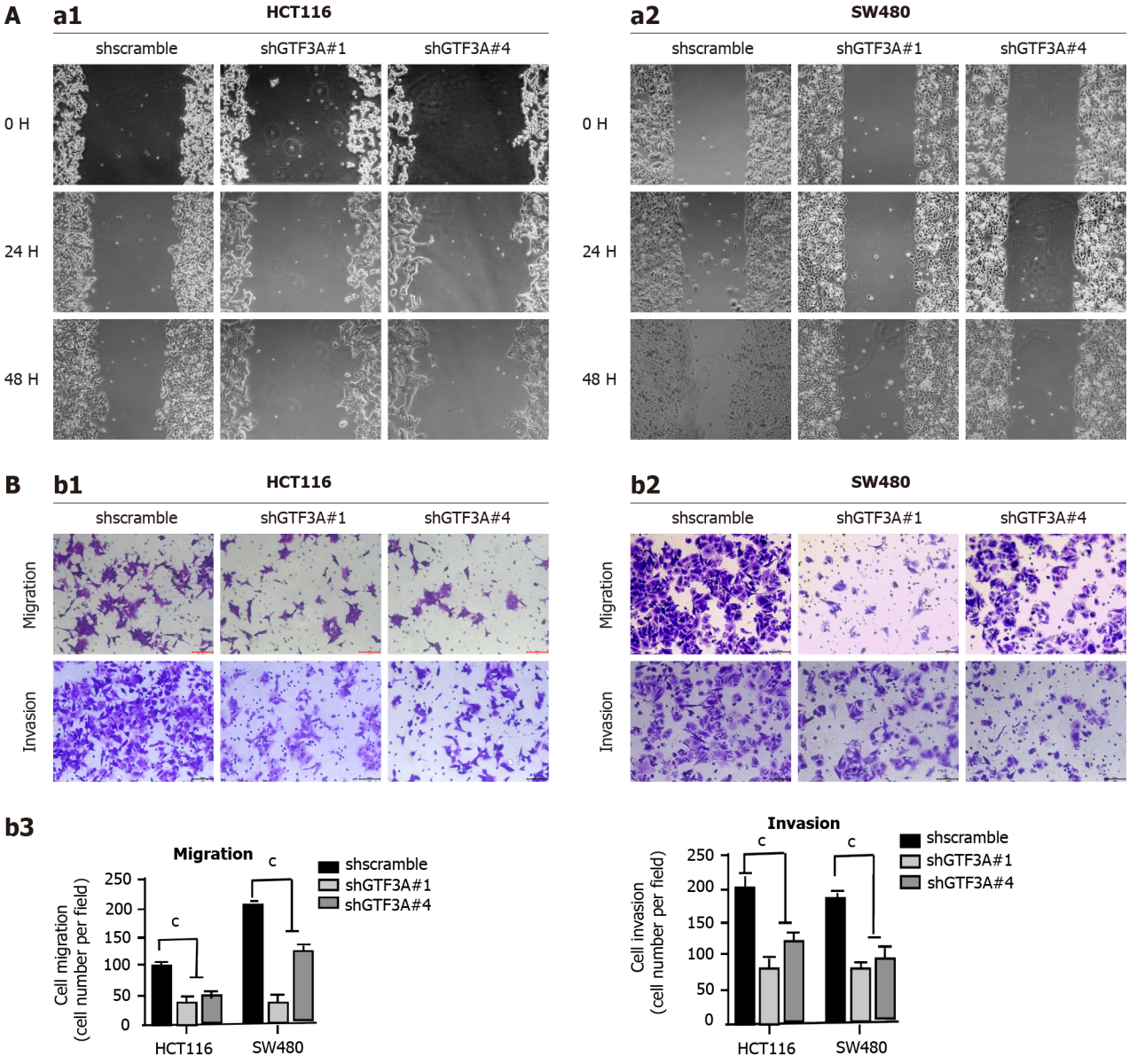

Figure 3 Knockdown of transcriptional factor III A gene inhibits the invasion and migration of colorectal cancer cell *in vitro*. A: The migratory abilities of short hairpin (sh) GTF3A#1 and #4-HCT116 cells were detected using wound-healing assay (a1). The migratory abilities of shGTF3A#1 and #4-SW480 cells were detected as above (a2); B: The migratory and invasive capabilities of shGTF3A#1 and #4-HCT116 (b1) and shGTF3A#1 and #4-SW480 cells (b2) were detected using transwell assay. The migrated and invaded cells were counted (b3). Migratory and invasive capabilities are expressed as the mean ± SEM of three independent experiments. $^{c}P < 0.001$.

expressed genes were found between the groups (Figures 4A and 4B, Supplementary Table 4). In particular, the expression of *Csta/Cst1/Cst4* genes in *Gtf3a*-knockdown cells was dramatically lower than that in the control group (Supplementary Table 4). *Csta/Cst1/Cst4* genes, members of the cystatin superfamily that encode cysteine protease inhibitors, are overexpressed in various types of cancers, subsequently promoting cancer cell metastasis and resulting in a poor prognosis[14-16]. RT-qPCR and Western blot results showed that the expression of *Csta/Cst1/Cst4* genes was significantly decreased in *Gtf3a*-knockdown cells (Figures 4C and 4D).

The results of the RNA-Seq showed that CSTA had the largest difference after knockdown of *Gtf3a* in FISH experiments; the sequence probe of the *Csta* promoter was labeled with red fluorescence, whereas GTF3A was labeled with green fluorescence. The fluorescence staining of the GTF3A and *Csta* promoters was colocalized to a large extent as indicated by an orange-yellow fused fluorescence (Figure 4E), suggesting that GTF3A binds with the *Csta* promoter. To confirm the interaction between GTF3A and the *Csta* promoter, EMSA was performed to directly observe the interaction of GTF3A and the *Csta* promoter. The results showed that GTF3A interacted with the *Csta* promoter (Figure 4F). Next, a dual-luciferase assay was carried out to determine whether the interaction of GTF3A with *Csta* promoter increased *Csta* expression, and the results showed that the transcript activity of the *Csta* gene was significantly increased after transfection with CSTA (Figure 4G, $P < 0.05$). These data suggested that GTF3A binds to the *Csta* promoter to regulate its transcription and translation.

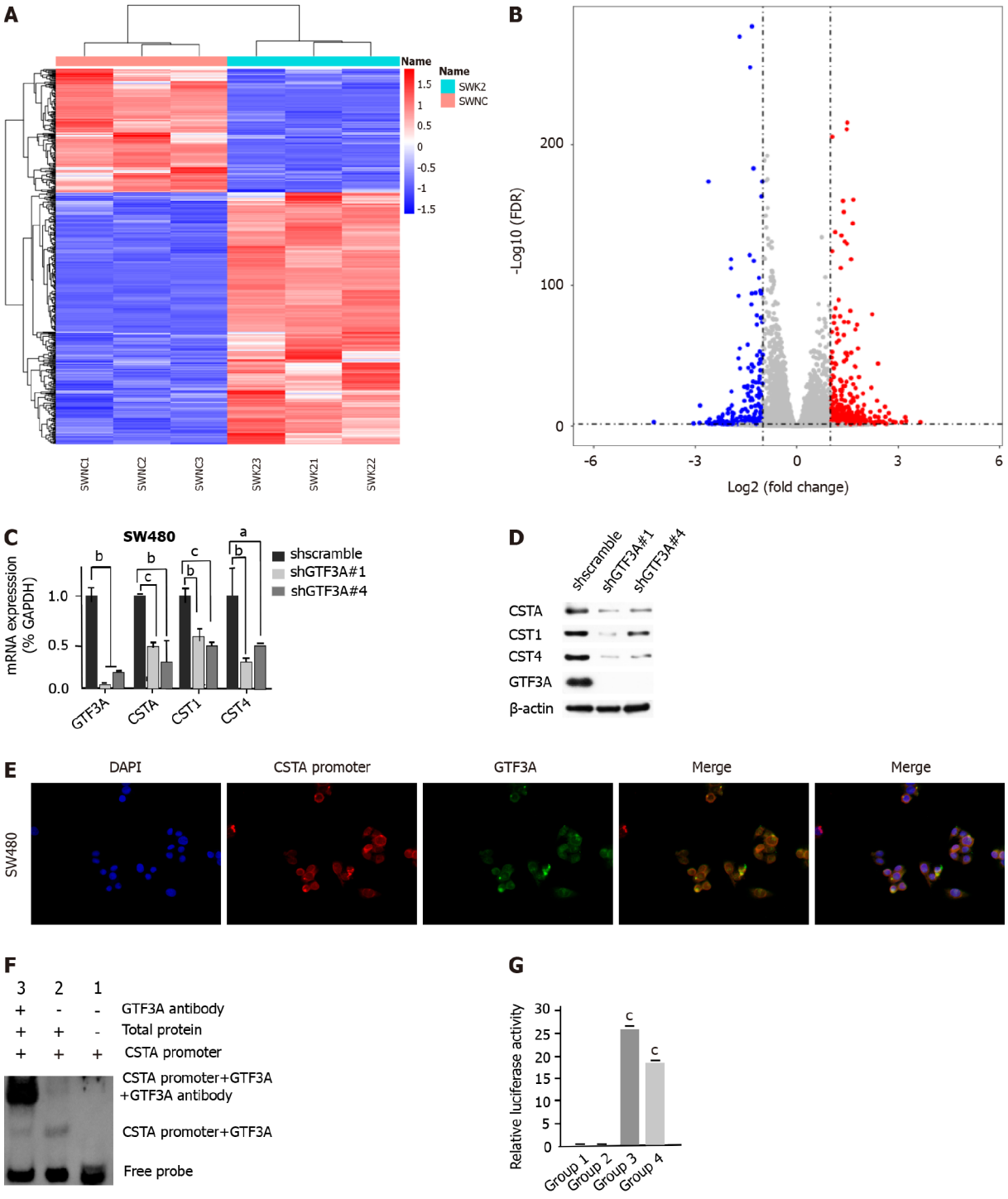

Figure 4 Transcriptional factor III A regulates cystatin A by binding to the promoter of cystatin A gene. A: Heat map of RNA-sequencing (RNA-Seq) for transcriptional factor III A *gene (Gtf3a)*-knockdown and scramble control cells; B: Volcano plot of RNA-Seq for *Gtf3a*-knockdown and scramble control cells; C: mRNA expression of *Gtf3a*, cystatin A (*Csta*), cystatin SN gene (*Cst1*), and cystatin S genes (*Cst4*) in short hairpin (sh)scramble-SW480 and shGTF3A#1 and #4-SW480 cells were detected using real-time quantitative polymerase chain reaction; D: GTF3A, CSTA, CST1, and CST4 in shscramble-SW480 and shGTF3A#1 and #4-SW480 cells were detected using Western blot; E: RNA fluorescence *in situ* hybridization was performed to verify the locations of the *Csta* promoter probe (lncRNA) and GTF3A in SW480 cells; F: Electrophoretic mobility shift assay (EMSA) was used to test the interaction of the *Csta* promoter and GTF3A. The *Csta* promoter plus GTF3A antibody as the super shift in EMSA; G: Luciferase activity assay was used to detect the interaction of GTF3A with the *Csta* promoter and the transcription of *Csta*. Group 1 (*Csta* promoter-luc blank vector plus GTF3A blank plasmid) and group 2 (*Csta* promoter-luc blank vector plus GTF3A-plasmid) served as the control groups, and group 3 (*Csta* promoter-luc plus GTF3A) and group 4 (*Csta* promoter-luc plus GTF3A blank vector) as experimental groups. *Csta* expression is expressed as the mean ± SEM of three independent experiments. $^{c}P < 0.001$. GTF3A: Transcriptional factor III A; GAPDH: Glyceraldehydes-3-phosphate dehydrogenase; CSTA: Cystatin A; CST1: Cystatin SN; CST4: Cystatin S.

GTF3A mediates CRC cell EMT by regulating the expression of CSTA

The above results indicated that GTF3A promoted CRC cell invasion and metastasis. To investigate the underlying mechanisms, EMT markers, such as Snail, E-cadherin, and beta-catenin, were detected in

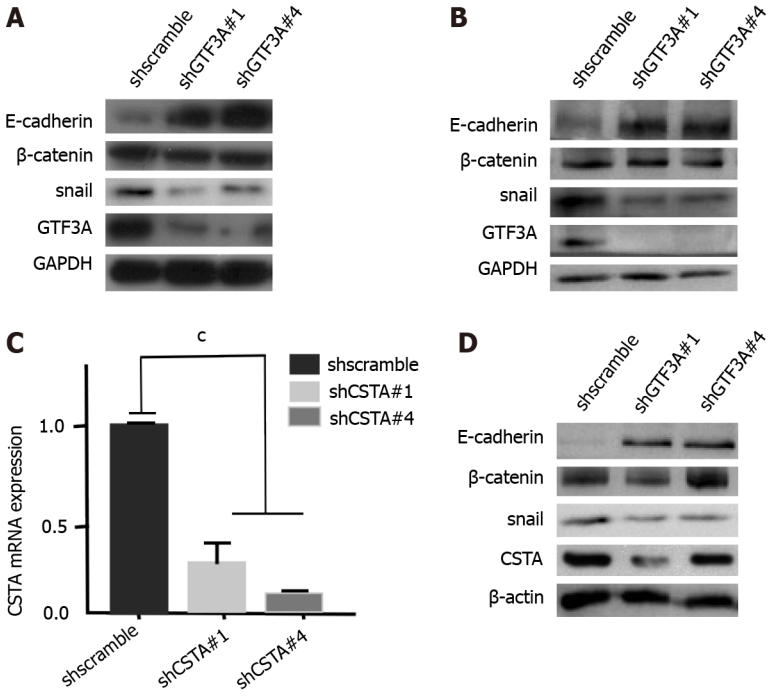

Figure 5 Transcriptional factor III A mediates epithelial-mesenchymal transition of colorectal cancer cells by regulating cystatin A. A: Epithelial-mesenchymal transition (EMT) biomarkers E-cadherin, beta-catenin, and snail in short hairpin of transcriptional factor III A (shGTF3A) #1 and #4-HCT116 cells and the control group were detected by Western blot; B: EMT biomarkers were tested in shGTF3A#1 and #4-SW480 cells and the control group; C: mRNA expression of cystatin A (*Csta*) gene in shCSTA#1,2-SW480 and the control group was detected using real-time quantitative polymerase chain reaction; D: EMT biomarkers were analyzed in *Csta*-knockdown SW480 and the control cells. Cystatin A mRNA expression is expressed as the mean ± SEM of three independent experiments. There were statistically significant differences between shCSTA#1,2-SW480 and the control group. °$P < 0.001$. GTF3A: Transcriptional factor III A; GAPDH: Glyceraldehydes-3-phosphate dehydrogenase; CSTA: Cystatin A; shscramble: Short hairpin scramble; shCSTA: Short hairpin of transcriptional factor III A.

scrambled control and *Gtf3a*-knockdown cells. Western blot results showed that *Gtf3a*-knockdown HCT116 and SW480 cells had decreased Snail expression and increased E-cadherin expression compared with the scrambled control (Figures 5A and 5B). Moreover, GTF3A regulates the expression of CSTA/CST1/CST4, and CST1 promotes the migration and invasion of breast cancer cells by up-regulating E-cadherin[23]. Consistent with these results, *Csta*-knockdown cells were constructed (Figure 5C), and Snail, E-cadherin, and beta-catenin were detected in these cells. The cells showed down-regulated Snail expression and upregulated E-cadherin expression (Figure 5D). Collectively, GTF3A may mediate the EMT to promote CRC cell metastasis by regulating CSTA and CST1 expression.

GTF3A promotes CRC cell growth in vivo

The above results showed that GTF3A promoted the proliferation, invasion, and metastasis of CRC cells *in vitro*. To verify whether GTF3A promotes CRC progression *in vivo*, nude mice were subcutaneously injected with the *Gtf3a*-knockdown and control cells to examine the function of *Gtf3a*. After 28 d, the *Gtf3a*-knockdown group had a significantly smaller tumor size (Figures 6A and 6B) and slower tumor growth (Figure 6C, $P < 0.05$) than the control group. In addition, the *Gtf3a*-knockdown group showed a reduction in tumor weights (Figure 6D, $P < 0.05$). *In vivo* experiments demonstrated that GTF3A promoted the growth of CRC cells.

DISCUSSION

As a transcription factor of RNA polymerase III, GTF3A is homologous to TFIIIB and TFIIIC, which guides the accurate transcription of 5S RNA genes[32]. RNA polymerase III is responsible for the transcription of non-coding genes including U6 snRNA, tRNA, and 5S RNA[33]. Deregulation of RNA polymerase III leads to the development of a large variety of human disorders[34], and upregulation of RNA polymerase III transcription has been observed in various types of cancer[35,36]. TFIIIB and TFIIIC can enhance the transcriptional activity of RNA polymerase III and mediate cellular transformation and tumor formation[37-40]. In addition, TFIIIA-mediated 5S rRNA is an essential component of 5S RNP that regulates the Hdm^2-p53 checkpoint to affect ribosome biosynthesis and cancer progression[9-13], indicating that GTF3A participates in the occurrence and development of various cancer types. Overexpression of GTF3A has been observed in CRC tumors and metastatic tissues using CRC tissue arrays, and clinical data analysis suggests that GTF3A is associated with CRC progression and metastasis.

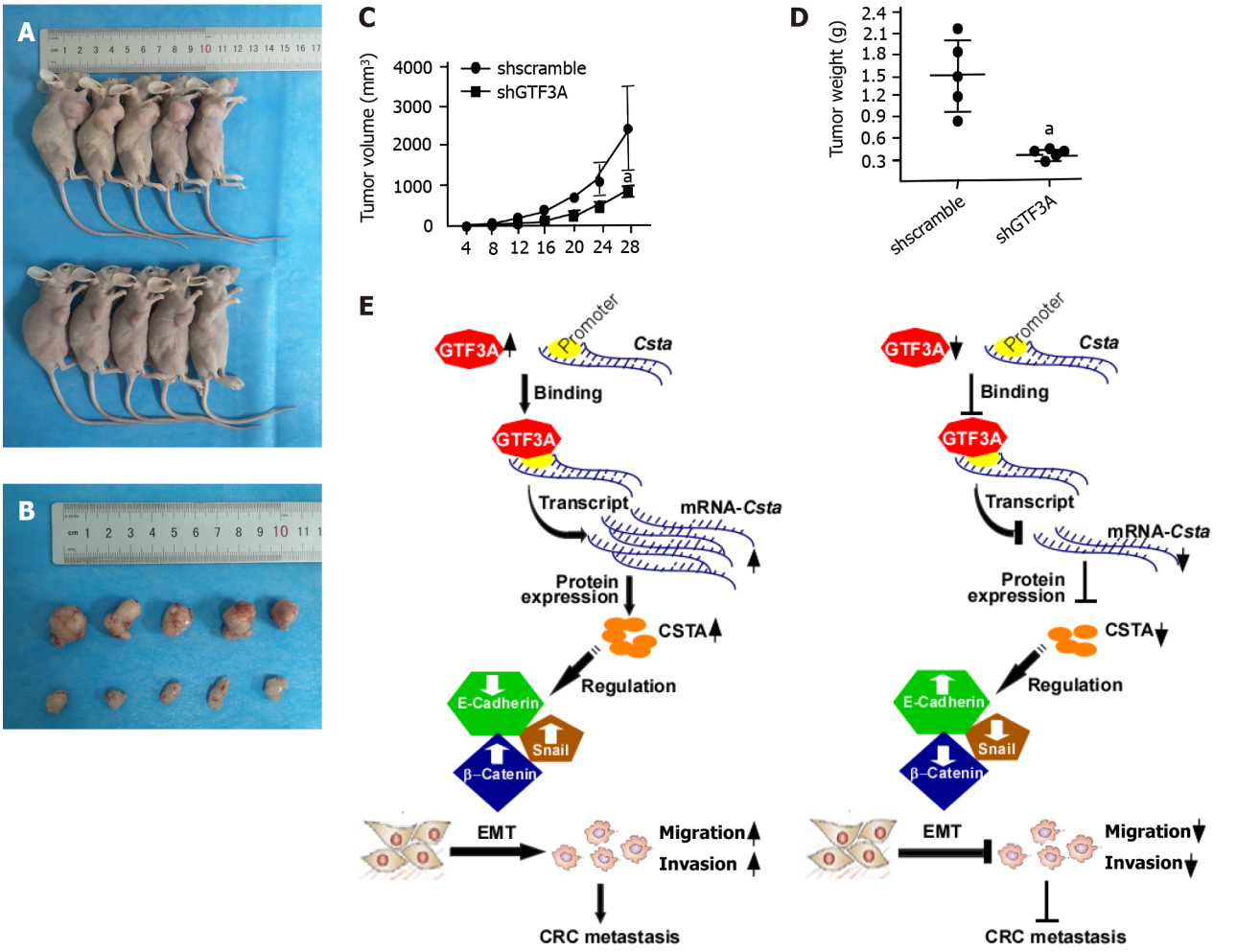

Figure 6 Transcriptional factor III A promotes colorectal cancer growth *in vivo*. A: Short hairpin of transcriptional factor III A (shGTF3A)-HCT116 and short hairpin of scramble (shscramble)-HCT116 cells were subcutaneously injected into the right armpit of nude mice. After 28 d, the mice were euthanized, and the images of the representative nude mice are shown; B: Tumors were stripped from the nude mouse; C: The tumor growth curve of shGTF3A-HCT116 and shscramble-HCT116 cells was calculated by tumor volume; D: The removed tumors of shGTF3A-HCT116 and shscramble-HCT116 cells were weighed; E: Schematic diagram of GTF3A-promoting CRC metastasis. GTF3A bound to the promoter of cystatin A (*Csta*) gene to increase *Csta* gene transcription and protein expression, increased CSTA regulated the epithelial-mesenchymal transition (EMT) to promote invasion and metastasis of colorectal cancer (CRC) cells, while knockdown of *Gtf3a* decreased CSTA expression, inhibited the EMT, and reduced CRC cell invasion and metastasis. $^{a}P < 0.05$. shscramble: Short hairpin scramble; shCSTA: Short hairpin of transcriptional factor III A; EMT: Epithelial-mesenchymal transition; CRC: Colorectal cancer; CSTA: Cystatin A.

A series of *in vitro* and *in vivo* experiments was performed to examine the role of GTF3A in CRC development. The results showed that the knockdown of *Gtf3a* inhibited the proliferation, invasion, and metastasis of CRC cells. Generally, cancer metastasis is mostly related to the EMT[41]. We hypothesized that GTF3A promotes CRC cell metastasis by mediating the EMT. Thus, the EMT biomarkers Snail, vimentin, beta-catenin, and E-cadherin were detected. These changes in Snail and E-cadherin levels were in accordance with our hypothesis. The vimentin had no changed after knockdown of GTF3A (not shown). Both RNA-Seq and RT-qPCR showed that *Csta* expression was dramatically decreased in *Gtf3a*-knockdown cells. Furthermore, the luciferase activity assay suggested that GTF3A regulates the *Csta* transcription and translation by binding to the *Csta* promoter, therefore, *Csta* is a target gene of GTF3A.

CSTA is associated with invasion and metastasis in various cancer types[17,19,22], and *in vitro* experiments have shown that CSTA modulates the invasion and metastasis of NPC cells[18]. Based on our data, GTF3A may regulate *Csta* expression to mediate the EMT and promote CRC metastasis. FISH and EMSA results suggested that GTF3A binds with the promoter of the *Csta* gene, and the luciferase activity assay showed that GTF3A upregulated *Csta* transcription by binding to the *Csta* promoter. In addition, CSTA regulates E-cadherin and Snail expression, there mediating the EMT shift. Collectively, GTF3A upregulates CSTA expression to promote CRC metastasis by accelerating EMT shift. CST1 is associated with the progression and prognosis of various cancer types[20,25], and its overexpression modulates EMT progression by modulating the PI3K/AKT pathway *in vivo* and *in vitro*[22].

CONCLUSION

GTF3A increases *Csta* gene transcription and protein expression by binding to the *Csta* promoter, increases the expression of CSTA, enhances the EMT process, and facilitates CRC cell invasion and metastasis. However, knockdown of *Gtf3a* decreases CSTA expression, inhibits the EMT, and suppresses CRC cell invasion and metastasis (Figure 6E). Therefore, GTF3A is a potential novel therapeutic target and prognostic biomarker in human CRC.

ARTICLE HIGHLIGHTS

Research background

Advanced colorectal cancer (CRC) generally has poor outcomes and high mortality rates. Clarifying the molecular mechanisms underlying CRC progression is necessary to develop new diagnostic and therapeutic strategies to improve CRC outcome and decrease mortality.

Research motivation

Transcriptional factor III A (GTF3A), an RNA polymerase III transcriptional factor, is a critical driver of tumorgenesis and aggravates CRC cell growth. The mechanism of GTF3A participating in CRC is not clear.

Research objectives

To confirm whether GTF3A aggravates CRC progression and investigate molecular mechanisms underlying CRC progression.

Research methods

Immunohistochemistry was used to detect GTF3A expression in CRC tissues. Short hairpin GTF3As and CSTAs were designed and packaged into the virus to block the expression of *Gtf3a* and *Csta* genes. RNA sequencing and data analysis was used to screen the target genes of GTF3A. Fluorescence *in situ* hybridization assay was used to detect the interaction of GTF3A with *Csta,* and luciferase activity assay was used to evaluate the expression of *Gtf3a* and *Csta* genes.

Research results

GTF3A was highly expressed in CRC tissues and metastatic tissues, and its expression was associated with CRC prognosis. Knockdown of the *Gtf3a* gene impaired CRC cell proliferation, invasion, and motility *in vitro* and *in vivo*. GTF3A increased *Csta* transcription, and increased CSTA upregulated epithelial-mesenchymal transition (EMT) markers.

Research conclusions

GTF3A increases CSTA expression by binding to the *Csta* promoter, and increased CSTA levels promote CRC progression by regulating EMT. Inhibition of GTF3A prevents CRC progression.

Research perspectives

GTF3A may be a potential novel therapeutic target and biomarker for CRC.

ACKNOWLEDGEMENTS

The authors would like to acknowledge the members in Clinical Laboratory Center of Hunan Cancer Hospital and Xiangya Medical School of Central South University for contributions.

FOOTNOTES

Author contributions: Tang FQ designed and coordinated the study; Wang J, Tan Y, and Jia QY performed the experiments, and acquired and analyzed data; Wang J and Tang FQ wrote the manuscript; and all authors approved the final version of the article.

Supported by the National Natural Science Foundation of China, No. 81872226; Changsha Science and Technology Project, No. 2019TP1046; and the Research Projects of Hunan Health Commission, No. B2019084.

Institutional review board statement: The study was reviewed and approved by the Hunan Cancer Hospital Institutional Review Board (Approval No. KYJJ-2020-004).

Institutional animal care and use committee statement: All procedures involving animals were reviewed and approved by the Institutional Animal Care and Use Committee of the Hunan Cancer Hospital (No. 2020-118).

Conflict-of-interest statement: All the authors report no relevant conflicts of interest for this article.

Data sharing statement: No additional data are available.

ARRIVE guidelines statement: The authors have read the ARRIVE Guidelines, and the manuscript was prepared and revised according to the ARRIVE Guidelines.

Country/Territory of origin: China

ORCID number: Jing Wang 0000-0002-6594-3494; Yuan Tan 0000-0003-0362-4073; Qun-Ying Jia 0000-0003-4660-3790; Fa-Qin Tang 0000-0001-5794-4975.

S-Editor: Wang JJ
L-Editor: Wang TQ
P-Editor: Yuan YY

REFERENCES

1 **Jemal A**, Bray F, Center MM, Ferlay J, Ward E, Forman D. Global cancer statistics. *CA Cancer J Clin* 2011; **61**: 69-90 [PMID: 21296855 DOI: 10.3322/caac.20107]
2 **Riihimäki M**, Hemminki A, Sundquist J, Hemminki K. Patterns of metastasis in colon and rectal cancer. *Sci Rep* 2016; **6**: 29765 [PMID: 27416752 DOI: 10.1038/srep29765]
3 **Seifart KH**, Wang L, Waldschmidt R, Jahn D, Wingender E. Purification of human transcription factor IIIA and its interaction with a chemically synthesized gene encoding human 5 S rRNA. *J Biol Chem* 1989; **264**: 1702-1709 [PMID: 2912980]
4 **Weser S**, Riemann J, Seifart KH, Meissner W. Assembly and isolation of intermediate steps of transcription complexes formed on the human 5S rRNA gene. *Nucleic Acids Res* 2003; **31**: 2408-2416 [PMID: 12711686 DOI: 10.1093/nar/gkg345]
5 **Hanas JS**, Hocker JR, Cheng YG, Lerner MR, Brackett DJ, Lightfoot SA, Hanas RJ, Madhusudhan KT, Moreland RJ. cDNA cloning, DNA binding, and evolution of mammalian transcription factor IIIA. *Gene* 2002; **282**: 43-52 [PMID: 11814676 DOI: 10.1016/s0378-1119(01)00796-x]
6 **Schulman DB**, Setzer DR. Identification and characterization of transcription factor IIIA from Schizosaccharomyces pombe. *Nucleic Acids Res* 2002; **30**: 2772-2781 [PMID: 12087160 DOI: 10.1093/nar/gkf385]
7 **Fridell RA**, Fischer U, Lührmann R, Meyer BE, Meinkoth JL, Malim MH, Cullen BR. Amphibian transcription factor IIIA proteins contain a sequence element functionally equivalent to the nuclear export signal of human immunodeficiency virus type 1 Rev. *Proc Natl Acad Sci U S A* 1996; **93**: 2936-2940 [PMID: 8610146 DOI: 10.1073/pnas.93.7.2936]
8 **Layat E**, Probst AV, Tourmente S. Structure, function and regulation of Transcription Factor IIIA: From Xenopus to Arabidopsis. *Biochim Biophys Acta* 2013; **1829**: 274-282 [PMID: 23142779 DOI: 10.1016/j.bbagrm.2012.10.013]
9 **Sloan KE**, Bohnsack MT, Watkins NJ. The 5S RNP couples p53 homeostasis to ribosome biogenesis and nucleolar stress. *Cell Rep* 2013; **5**: 237-247 [PMID: 24120868 DOI: 10.1016/j.celrep.2013.08.049]
10 **Donati G**, Peddigari S, Mercer CA, Thomas G. 5S ribosomal RNA is an essential component of a nascent ribosomal precursor complex that regulates the Hdm2-p53 checkpoint. *Cell Rep* 2013; **4**: 87-98 [PMID: 23831031 DOI: 10.1016/j.celrep.2013.05.045]
11 **Onofrillo C**, Galbiati A, Montanaro L, Derenzini M. The pre-existing population of 5S rRNA effects p53 stabilization during ribosome biogenesis inhibition. *Oncotarget* 2017; **8**: 4257-4267 [PMID: 28032591 DOI: 10.18632/oncotarget.13833]
12 **Nishimura K**, Kumazawa T, Kuroda T, Katagiri N, Tsuchiya M, Goto N, Furumai R, Murayama A, Yanagisawa J, Kimura K. Perturbation of ribosome biogenesis drives cells into senescence through 5S RNP-mediated p53 activation. *Cell Rep* 2015; **10**: 1310-1323 [PMID: 25732822 DOI: 10.1016/j.celrep.2015.01.055]
13 **Nait Slimane S**, Marcel V, Fenouil T, Catez F, Saurin JC, Bouvet P, Diaz JJ, Mertani HC. Ribosome Biogenesis Alterations in Colorectal Cancer. *Cells* 2020; **9** [PMID: 33120992 DOI: 10.3390/cells9112361]
14 **Komura T**, Takabatake H, Harada K, Yamato M, Miyazawa M, Yoshida K, Honda M, Wada T, Kitagawa H, Ohta T, Kaneko S, Sakai Y. Clinical features of cystatin A expression in patients with pancreatic ductal adenocarcinoma. *Cancer Sci* 2017; **108**: 2122-2129 [PMID: 28898495 DOI: 10.1111/cas.13396]
15 **Shiba D**, Terayama M, Yamada K, Hagiwara T, Oyama C, Tamura-Nakano M, Igari T, Yokoi C, Soma D, Nohara K, Yamashita S, Dohi T, Kawamura YI. Clinicopathological significance of cystatin A expression in progression of esophageal squamous cell carcinoma. *Medicine (Baltimore)* 2018; **97**: e0357 [PMID: 29642180 DOI: 10.1097/MD.0000000000010357]

16 **Butler MW**, Fukui T, Salit J, Shaykhiev R, Mezey JG, Hackett NR, Crystal RG. Modulation of cystatin A expression in human airway epithelium related to genotype, smoking, COPD, and lung cancer. *Cancer Res* 2011; **71**: 2572-2581 [PMID: 21325429 DOI: 10.1158/0008-5472.CAN-10-2046]

17 **Lin YY**, Chen ZW, Lin ZP, Lin LB, Yang XM, Xu LY, Xie Q. Tissue Levels of Stefin A and Stefin B in Hepatocellular Carcinoma. *Anat Rec (Hoboken)* 2016; **299**: 428-438 [PMID: 26753874 DOI: 10.1002/ar.23311]

18 **Chang KP**, Wu CC, Chen HC, Chen SJ, Peng PH, Tsang NM, Lee LY, Liu SC, Liang Y, Lee YS, Hao SP, Chang YS, Yu JS. Identification of candidate nasopharyngeal carcinoma serum biomarkers by cancer cell secretome and tissue transcriptome analysis: potential usage of cystatin A for predicting nodal stage and poor prognosis. *Proteomics* 2010; **10**: 2644-2660 [PMID: 20461718 DOI: 10.1002/pmic.200900620]

19 **Takahashi H**, Honma M, Ishida-Yamamoto A, Namikawa K, Kiyama H, Iizuka H. Expression of human cystatin A by keratinocytes is positively regulated *via* the Ras/MEKK1/MKK7/JNK signal transduction pathway but negatively regulated *via* the Ras/Raf-1/MEK1/ERK pathway. *J Biol Chem* 2001; **276**: 36632-36638 [PMID: 11451947 DOI: 10.1074/jbc.m102021200]

20 **Cao X**, Li Y, Luo RZ, Zhang L, Zhang SL, Zeng J, Han YJ, Wen ZS. Expression of Cystatin SN significantly correlates with recurrence, metastasis, and survival duration in surgically resected non-small cell lung cancer patients. *Sci Rep* 2015; **5**: 8230 [PMID: 25648368 DOI: 10.1038/srep08230]

21 **Jiang J**, Liu HL, Liu ZH, Tan SW, Wu B. Identification of cystatin SN as a novel biomarker for pancreatic cancer. *Tumour Biol* 2015; **36**: 3903-3910 [PMID: 25577248 DOI: 10.1007/s13277-014-3033-3]

22 **Cui Y**, Sun D, Song R, Zhang S, Liu X, Wang Y, Meng F, Lan Y, Han J, Pan S, Liang S, Zhang B, Guo H, Liu Y, Lu Z, Liu L. Upregulation of cystatin SN promotes hepatocellular carcinoma progression and predicts a poor prognosis. *J Cell Physiol* 2019; **234**: 22623-22634 [PMID: 31106426 DOI: 10.1002/jcp.28828]

23 **Dai DN**, Li Y, Chen B, Du Y, Li SB, Lu SX, Zhao ZP, Zhou AJ, Xue N, Xia TL, Zeng MS, Zhong Q, Wei WD. Elevated expression of CST1 promotes breast cancer progression and predicts a poor prognosis. *J Mol Med (Berl)* 2017; **95**: 873-886 [PMID: 28523467 DOI: 10.1007/s00109-017-1537-1]

24 **Jiang J**, Liu HL, Tao L, Lin XY, Yang YD, Tan SW, Wu B. Let7d inhibits colorectal cancer cell proliferation through the CST1/p65 pathway. *Int J Oncol* 2018; **53**: 781-790 [PMID: 29845224 DOI: 10.3892/ijo.2018.4419]

25 **Yoneda K**, Iida H, Endo H, Hosono K, Akiyama T, Takahashi H, Inamori M, Abe Y, Yoneda M, Fujita K, Kato S, Nozaki Y, Ichikawa Y, Uozaki H, Fukayama M, Shimamura T, Kodama T, Aburatani H, Miyazawa C, Ishii K, Hosomi N, Sagara M, Takahashi M, Ike H, Saito H, Kusakabe A, Nakajima A. Identification of Cystatin SN as a novel tumor marker for colorectal cancer. *Int J Oncol* 2009; **35**: 33-40 [PMID: 19513549 DOI: 10.3892/ijo_00000310]

26 **Choi EH**, Kim JT, Kim JH, Kim SY, Song EY, Kim JW, Yeom YI, Kim IH, Lee HG. Upregulation of the cysteine protease inhibitor, cystatin SN, contributes to cell proliferation and cathepsin inhibition in gastric cancer. *Clin Chim Acta* 2009; **406**: 45-51 [PMID: 19463800 DOI: 10.1016/j.cca.2009.05.008]

27 **Hong J**, Hu K, Yuan Y, Sang Y, Bu Q, Chen G, Yang L, Li B, Huang P, Chen D, Liang Y, Zhang R, Pan J, Zeng YX, Kang T. CHK1 targets spleen tyrosine kinase (L) for proteolysis in hepatocellular carcinoma. *J Clin Invest* 2012; **122**: 2165-2175 [PMID: 22585575 DOI: 10.1172/JCI61380]

28 **Xu S**, Wu Y, Chen Q, Cao J, Hu K, Tang J, Sang Y, Lai F, Wang L, Zhang R, Li SP, Zeng YX, Yin Y, Kang T. hSSB1 regulates both the stability and the transcriptional activity of p53. *Cell Res* 2013; **23**: 423-435 [PMID: 23184057 DOI: 10.1038/cr.2012.162]

29 **Lu J**, Li Y, Wu Y, Zhou S, Duan C, Dong Z, Kang T, Tang F. MICAL2 Mediates p53 Ubiquitin Degradation through Oxidating p53 Methionine 40 and 160 and Promotes Colorectal Cancer Malignance. *Theranostics* 2018; **8**: 5289-5306 [PMID: 30555547 DOI: 10.7150/thno.28228]

30 **Tang FQ**, Duan CJ, Huang DM, Wang WW, Xie CL, Meng JJ, Wang L, Jiang HY, Feng DY, Wu SH, Gu HH, Li MY, Deng FL, Gong ZJ, Zhou H, Xu YH, Tan C, Zhang X, Cao Y. HSP70 and mucin 5B: novel protein targets of N,N'-dinitrosopiperazine-induced nasopharyngeal tumorigenesis. *Cancer Sci* 2009; **100**: 216-224 [PMID: 19068094 DOI: 10.1111/j.1349-7006.2008.01028.x]

31 **Tang F**, Zou F, Peng Z, Huang D, Wu Y, Chen Y, Duan C, Cao Y, Mei W, Tang X, Dong Z. N,N'-dinitrosopiperazine-mediated ezrin protein phosphorylation *via* activation of Rho kinase and protein kinase C is involved in metastasis of nasopharyngeal carcinoma 6-10B cells. *J Biol Chem* 2011; **286**: 36956-36967 [PMID: 21878630 DOI: 10.1074/jbc.M111.259234]

32 **Birkenmeier EH**, Brown DD, Jordan E. A nuclear extract of Xenopus laevis oocytes that accurately transcribes 5S RNA genes. *Cell* 1978; **15**: 1077-1086 [PMID: 569551 DOI: 10.1016/0092-8674(78)90291-x]

33 **Abascal-Palacios G**, Ramsay EP, Beuron F, Morris E, Vannini A. Structural basis of RNA polymerase III transcription initiation. *Nature* 2018; **553**: 301-306 [PMID: 29345637 DOI: 10.1038/nature25441]

34 **Yeganeh M**, Hernandez N. RNA polymerase III transcription as a disease factor. *Genes Dev* 2020; **34**: 865-882 [PMID: 32611613 DOI: 10.1101/gad.333989.119]

35 **Ramsay EP**, Abascal-Palacios G, Daiß JL, King H, Gouge J, Pilsl M, Beuron F, Morris E, Gunkel P, Engel C, Vannini A. Structure of human RNA polymerase III. *Nat Commun* 2020; **11**: 6409 [PMID: 33335104 DOI: 10.1038/s41467-020-20262-5]

36 **Cabarcas S**, Schramm L. RNA polymerase III transcription in cancer: the BRF2 connection. *Mol Cancer* 2011; **10**: 47 [PMID: 21518452 DOI: 10.1186/1476-4598-10-47]

37 **Lei J**, Chen S, Zhong S. Abnormal expression of TFIIIB subunits and RNA Pol III genes is associated with hepatocellular carcinoma. *Liver Res* 2017; **1**: 112-120 [PMID: 29276645 DOI: 10.1016/j.livres.2017.08.005]

38 **Zhong Q**, Xi S, Liang J, Shi G, Huang Y, Zhang Y, Levy D, Zhong S. The significance of Brf1 overexpression in human hepatocellular carcinoma. *Oncotarget* 2016; **7**: 6243-6254 [PMID: 26701855 DOI: 10.18632/oncotarget.6668]

39 **Bellido F**, Sowada N, Mur P, Lázaro C, Pons T, Valdés-Mas R, Pineda M, Aiza G, Iglesias S, Soto JL, Urioste M, Caldés T, Balbín M, Blay P, Rueda D, Durán M, Valencia A, Moreno V, Brunet J, Blanco I, Navarro M, Calin GA, Borck G, Puente XS, Capellá G, Valle L. Association Between Germline Mutations in BRF1, a Subunit of the RNA Polymerase III Transcription Complex, and Hereditary Colorectal Cancer. *Gastroenterology* 2018; **154**: 181-194.e20 [PMID: 28912018

DOI: 10.1053/j.gastro.2017.09.005]

40 **Gouge J**, Guthertz N, Kramm K, Dergai O, Abascal-Palacios G, Satia K, Cousin P, Hernandez N, Grohmann D, Vannini A. Molecular mechanisms of Bdp1 in TFIIIB assembly and RNA polymerase III transcription initiation. *Nat Commun* 2017; **8**: 130 [PMID: 28743884 DOI: 10.1038/s41467-017-00126-1]

41 **Georgakopoulos-Soares I**, Chartoumpekis DV, Kyriazopoulou V, Zaravinos A. EMT Factors and Metabolic Pathways in Cancer. *Front Oncol* 2020; **10**: 499 [PMID: 32318352 DOI: 10.3389/fonc.2020.00499]

World Journal of Gastrointestinal Oncology

Submit a Manuscript: https://www.f6publishing.com

World J Gastrointest Oncol 2022 October 15; 14(10): 1933-1948

DOI: 10.4251/wjgo.v14.i10.1933

ISSN 1948-5204 (online)

ORIGINAL ARTICLE

Basic Study

VCAN, expressed highly in hepatitis B virus-induced hepatocellular carcinoma, is a potential biomarker for immune checkpoint inhibitors

Mu-Qi Wang, Ya-Ping Li, Meng Xu, Yan Tian, Yuan Wu, Xin Zhang, Juan-Juan Shi, Shuang-Suo Dang, Xiao-Li Jia

Specialty type: Oncology

Provenance and peer review: Unsolicited article; Externally peer reviewed.

Peer-review model: Single blind

Peer-review report's scientific quality classification

Grade A (Excellent): 0
Grade B (Very good): B
Grade C (Good): C
Grade D (Fair): 0
Grade E (Poor): 0

P-Reviewer: Gupta T, India; Yao YQ, China

Received: May 21, 2022
Peer-review started: May 21, 2022
First decision: July 13, 2022
Revised: July 23, 2022
Accepted: September 12, 2022
Article in press: September 12, 2022
Published online: October 15, 2022

Mu-Qi Wang, Ya-Ping Li, Yan Tian, Xin Zhang, Juan-Juan Shi, Shuang-Suo Dang, Xiao-Li Jia, Department of Infectious Diseases, The Second Affiliated Hospital of Xi'an Jiaotong University, Xi'an 710004, Shaanxi Province, China

Meng Xu, Department of General Surgery, The Second Affiliated Hospital of Xi'an Jiaotong University, Xi'an 710004, Shaanxi Province, China

Yuan Wu, Department of Critical Care Medicine, The Second Affiliated Hospital of Xi'an Jiaotong University, Xi'an 710004, Shaanxi Province, China

Corresponding author: Xiao-Li Jia, Doctor, Chief Doctor, Department of Infectious Diseases, The Second Affiliated Hospital of Xi'an Jiaotong University, No. 157 Xiwu Road, Xincheng District, Xi'an 710004, Shaanxi Province, China. drjxl.123@xjtu.edu.cn

Abstract

BACKGROUND

As a proteoglycan, VCAN exists in the tumor microenvironment and regulates tumor proliferation, invasion, and metastasis, but its role in hepatocellular carcinoma (HCC) has not yet been elucidated.

AIM

To investigate the expression and potential mechanism of action of VCAN in HCC.

METHODS

Based on The Cancer Genome Atlas Liver Hepatocellular Carcinoma dataset, we explored the correlation between VCAN expression and clinical features, and analyzed the prognosis of patients with high and low VCAN expression. The potential mechanism of action of VCAN was explored by Gene Ontology analysis, Kyoto Encyclopedia of Genes and Genomes analysis, and gene set enrichment analysis. We also explored immune cell infiltration, immune checkpoint gene expression, and sensitivity of immune checkpoint [programmed cell death protein 1 (PD-1)/cytotoxic T lymphocyte antigen 4 (CTLA4)] inhibitor therapy in patients with different VCAN expression. VCAN mRNA expression and VCAN methylation in peripheral blood were tested in 100 hepatitis B virus (HBV)-related

patients (50 HCC and 50 liver cirrhosis).

RESULTS

VCAN was highly expressed in HCC tissues, which was associated with a poor prognosis in HCC patients. No significant difference was found in VCAN mRNA expression in blood between patients with HBV-related cirrhosis and those with HCC, but there was a significant difference in VCAN methylation between the two groups. The correlation between VCAN and infiltrations of several different tumor immune cell types (including B cells, $CD8^+$ T cells, and eosinophils) was significantly different. VCAN was strongly related to immune checkpoint gene expression and tumor mutation burden, and could be a biomarker of sensitivity to immune checkpoint (PD1/CTLA4) inhibitors. In addition, VCAN mRNA expression was associated with hepatitis B e antigen, HBV DNA, white blood cells, platelets, cholesterol, and coagulation function.

CONCLUSION

High VCAN level could be a possible biomarker for poor prognosis of HCC, and its immunomodulatory mechanism in HCC warrants investigation.

Key Words: VCAN; Hepatocellular carcinoma; Hepatitis B virus; Immune checkpoints; Tumor microenvironment

Core Tip: VCAN expression is significantly higher in hepatocellular carcinoma (HCC) tumor tissue than in adjacent tissue, and high VCAN level may be a possible biomarker for the diagnosis and prognosis of HCC. VCAN is associated with hepatitis B e antigen in hepatitis B virus infected patients. VCAN may play a role in HCC through the extracellular matrix signaling pathway and inflammatory immune response, and is a potential biomarker for immune checkpoint (programmed cell death protein 1/cytotoxic T lymphocyte antigen 4) inhibitors.

Citation: Wang MQ, Li YP, Xu M, Tian Y, Wu Y, Zhang X, Shi JJ, Dang SS, Jia XL. VCAN, expressed highly in hepatitis B virus-induced hepatocellular carcinoma, is a potential biomarker for immune checkpoint inhibitors. *World J Gastrointest Oncol* 2022; 14(10): 1933-1948
URL: https://www.wjgnet.com/1948-5204/full/v14/i10/1933.htm
DOI: https://dx.doi.org/10.4251/wjgo.v14.i10.1933

INTRODUCTION

According to the GLOBOCAN 2020 estimates, the number of new liver cancer cases in China (410038) accounted for 45.7% of the global total (905077), and the fatality rate ranks second among malignant tumors in China[1,2]. In contrast to Western countries, 92.6% of liver cancer in China is caused by chronic hepatitis B virus (HBV) infection [86% pure HBV infection and 6.7% coinfection of HBV and hepatitis C virus (HCV)], which often occurs with cirrhosis and has a worse prognosis[3].

Due to a strong correlation between the occurrence of hepatocellular carcinoma (HCC) and the continuous immune inflammatory response, it is necessary to explore whether and how the tumor microenvironment (TME) acts on the progression of HCC[4]. The TME is where tumor cells exist and includes the extracellular matrix (ECM), fibroblasts, blood vessels, and various immune cells[5]. The ECM supports the structure of connective tissues and regulates cell functions, which consists of fibers, proteoglycans, hyaluronic acid, and glycoproteins[6]. In the TME, nonmalignant cells can help tumor cells proliferate, invade, and metastasize[7]. The TME in HCC plays an important role in promoting tumor progression and inhibiting antitumor immunity. For example, tumor-associated macrophages (TAMs) are important immune cells involved in the microenvironment of HCC, and the low presence of CD86+ TAMs and high presence of CD206+ TAMs are significantly associated with aggressive tumor phenotypes, poor overall survival (OS), and shortened recurrence time[8]. The use of various targeted TME drugs for advanced unresectable HCC has been written into the guidelines[9-11]. VCAN is a proteoglycan that exists in the ECM of the TME, binds to integrins and integrin receptors or other ECM components on the cell surface, interacts with various cells in the TME, and participates in the adhesion, proliferation, migration, and angiogenesis of tumor cells[12]. VCAN promotes the invasion and metastasis of HCC in cell experiments[13,14], but the mechanism is still unclear. In addition, VCAN mRNA expression in human liver cancer tissues is higher than that in adjacent tissues[15], but whether VCAN could be a marker for the early diagnosis of HCC needs confirmation.

This study enrolled 100 patients with HBV-related liver diseases, including 50 with HCC and 50 with liver cirrhosis. VCAN mRNA expression and DNA methylation in serum were detected to analyze their correlation with clinical features. By using public datasets, we explored VCAN mRNA expression in HCC patients, the impact of VCAN on the clinical characteristics of patients, and the possible immune mechanism of VCAN in HBV-related HCC. Figure 1 more clearly describes the content of our study. We hope that this research will help to clarify the role of VCAN in HCC.

MATERIALS AND METHODS

Dataset download

The RNA expression profiles and corresponding clinicopathological information of The Cancer Genome Atlas Liver Hepatocellular Carcinoma (TCGA-LIHC) were downloaded from TCGA database (https://portal.gdc.cancer.gov/repository?facetTab=cases) on May 30, 2021. The transcriptome data of 374 cancer tissues and 50 paracancer tissues were annotated to extract the expression of VCAN.

Correlation between VCAN expression and clinical characteristics

VCAN mRNA expression in different cancer types was analyzed online with TIMER[16] (https://cistrome.shinyapps.io/timer/). R3.6.1 was used to perform differential analysis of VCAN mRNA in tumor tissues and adjacent tissues of patients from TCGA-LIHC. The Kruskal-Wallis test was performed to evaluate the correlation between VCAN expression and the clinical characteristics of TCGA-LIHC patients. The OS of HCC patients with high and low expression of VCAN was compared by Kaplan-Meier analysis and the log-rank test with the survival package in R3.6.1.

Clinical validation of VCAN expression in HBV related cirrhosis and HCC patients

During September 2021 to April 2022, 100 hospitalized HBV-related patients (50 with HCC and 50 with liver cirrhosis) were enrolled in the Second Affiliated Hospital of Xi'an Jiaotong University. Patients with HCC and liver cirrhosis had to meet the diagnostic criteria of Guidelines for Diagnosis and Treatment of Primary Liver Cancer in China (2019 edition)[17] and The Guidelines of Prevention and Treatment for Chronic Hepatitis B (2019 version)[18]. Among 50 HBV-related HCC patients, we collected ten pairs of tumor tissues and adjacent tissues of patients who underwent surgical therapy, and tumor-adjacent tissues were used as a control group to perform immunohistochemistry. The study was reviewed and approved by the Medical Ethics Committees of the Second Affiliated Hospital of Xi'an Jiaotong University (Approval No. 2019-1093). Informed consent was required from all participants.

Quantitative real-time polymerase chain reaction

Total RNA was extracted from the mononuclear cells of collected peripheral blood with TRIzol reagent (Invitrogen, United States). Using total RNA as a template, cDNA was synthesized by reverse transcription, and then real-time fluorescent quantitative polymerase chain reaction (PCR) was performed using the SYBR® Premix Ex Taq™ II kit (Takara, Japan). The primer sequences of VCAN (primers synthesized by the Shanghai Shenggong Biological Engineering Co. Ltd.) are: Forward, 5'-TGGCATGAGAATGGCCAGTGGA-3' and reverse, 5'- AAGCCAGAGACCCTCCCCCA-3'. OAZ1 was used as the internal reference. The primer sequences of OAZ1 (primers synthesized by the Shanghai Shenggong Biological Engineering) are: Forward, 5'-AGCAAGGACAGCTTTGCAGTTCTC-3' and reverse, 5'- GATGCCCCGGTCTCACAATC-3'. The final Ct value of the target gene was the average of the Ct values of three replicate wells. The relative expression of VCAN mRNA was calculated according to the following formula: Relative expression of the target gene = $2^{-\Delta Ct}$, Δ Ct = Ct(VCAN) - Ct(OAZ1).

DNA extraction and methylation detection

The peripheral venous blood of the participants was collected, and genomic DNA was extracted with a blood DNA extraction kit (Tiangen, Beijing, China). The extracted genomic DNA was treated with bisulfite using an EZ DNA Methylation-Gold Kit (Zymo, Irvine, CA, United States) and then subjected to high-throughput sequencing after PCR amplification to obtain DNA methylation results.

Immunohistochemistry

Tissue samples were boiled in Tris/EDTA buffer (pH 9.0) for antigen retrieval, and immunohistochemistry was performed with primary antibody (EPR12277; Abcam, The United Kingdom), according to the SP Rabbit HRP Kit instructions (CE2035S, CWBIO, China).

VCAN function prediction

VENNY 2.1.0 (https://bioinfogp.cnb.csic.es/tools/venny/index.html) was used to draw a Venn diagram containing coexpressed genes of VCAN ($P < 0.05$, $r > 0.6$), and differentially expressed genes between the high VCAN group and low VCAN group (median cut off, $|\log_2$Fold change$| > 2$, $P < 0.05$).

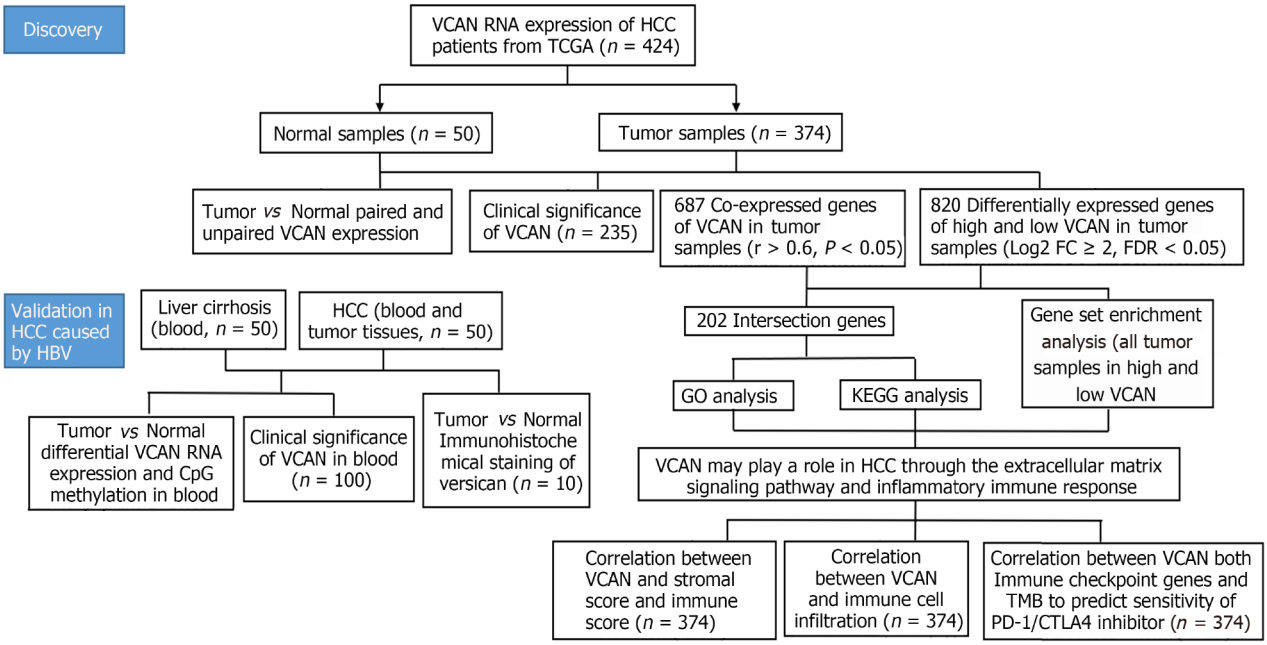

DOI: 10.4251/wjgo.v14.i10.1933

Figure 1 Experimental design of the study. HCC: Hepatocellular carcinoma; TCGA: The Cancer Genome Atlas; FC: Fold change; FDR: False discovery rate; GO: Gene Ontology; KEEG: Kyoto Encyclopedia of Genes and Genomes; TMB: Tumor mutation burden; PD-1: Programmed cell death protein 1; CTLA4: Cytotoxic T lymphocyte-associated antigen-4.

These intersection genes were strongly related to the potential immune mechanism of VCAN in HCC, which were considered as VCAN-related genes. VCAN-related genes were annotated by Gene Ontology (GO) analysis and Kyoto Encyclopedia of Genes and Genomes (KEEG) gene set function using the clusterProfiler package of R3.6.1.

Gene set enrichment analysis (GSEA) was performed on the group with high and low expression (median as the cutoff) of VCAN in TCGA-LIHC using GSEA 4.0.3. KEGG gene set (c2.cp.kegg.v7.4.symbols.gmt) was applied to explore the potential signaling pathway of VCAN in HCC (false discovery rate < 0.05)[19]. The proteins that may interact with VCAN were obtained with STRING (https://www.string-db.org/), and a corresponding protein-protein interaction (PPI) network diagram was drawn.

TME immune score and stroma score of TCGA-LIHC liver cancer tissues were calculated based on estimated algorithm using the R3.6.1 package estimate. Different algorithms (ssGSEA, CIBERSORTx, and TIMER) were used to evaluate intratumoral immune cell composition in patients with high and low expression of VCAN in TCGA-LIHC[16,20,21]. Tumor mutation burden (TMB) was calculated using the TCGA mutations package of R3.6.1. An immune checkpoint genes list was obtained from the published literature[22]. These gene expression data were extracted from transcripts of TCGA-LIHC to perform correlation analysis with VCAN expression.

Statistical analysis

All analyses and image preparation were performed using SPSS 22.0 (SPSS Inc., Chicago, IL), GraphPad Prism 5.0 (GraphPad, United States), Origin 2021b (OriginLab, United States), and R3.6.1. Normally distributed measurement data are represented by the mean ± SD, and those with a skewed distribution by the median (25%, 75%). Numerical data are represented by the number of cases. The means of two groups were compared by the *t*-test or Wilcoxon rank-sum test, and those of multiple groups were compared by analysis of variance or Kruskal-Wallis nonparametric test. The rates of multiple groups were compared by the χ^2 test. $P < 0.05$ indicated that the difference was statistically significant.

RESULTS

Clinical characteristics and VCAN expression in HCC patients in public databases

VCAN was highly expressed in a variety of tumor tissues, including breast cancer, cholangiocarcinoma, colon cancer, esophageal cancer, glioma, head and neck squamous cell carcinoma, renal chromophore cell carcinoma, renal papillary cell carcinoma, HCC, lung adenocarcinoma, lung squamous cell carcinoma, gastric cancer, and thyroid cancer (Figure 2A). VCAN was significantly overexpressed in tumors in both paired and independent samples for patients from TCGA-LIHC (Figures 2B and C).

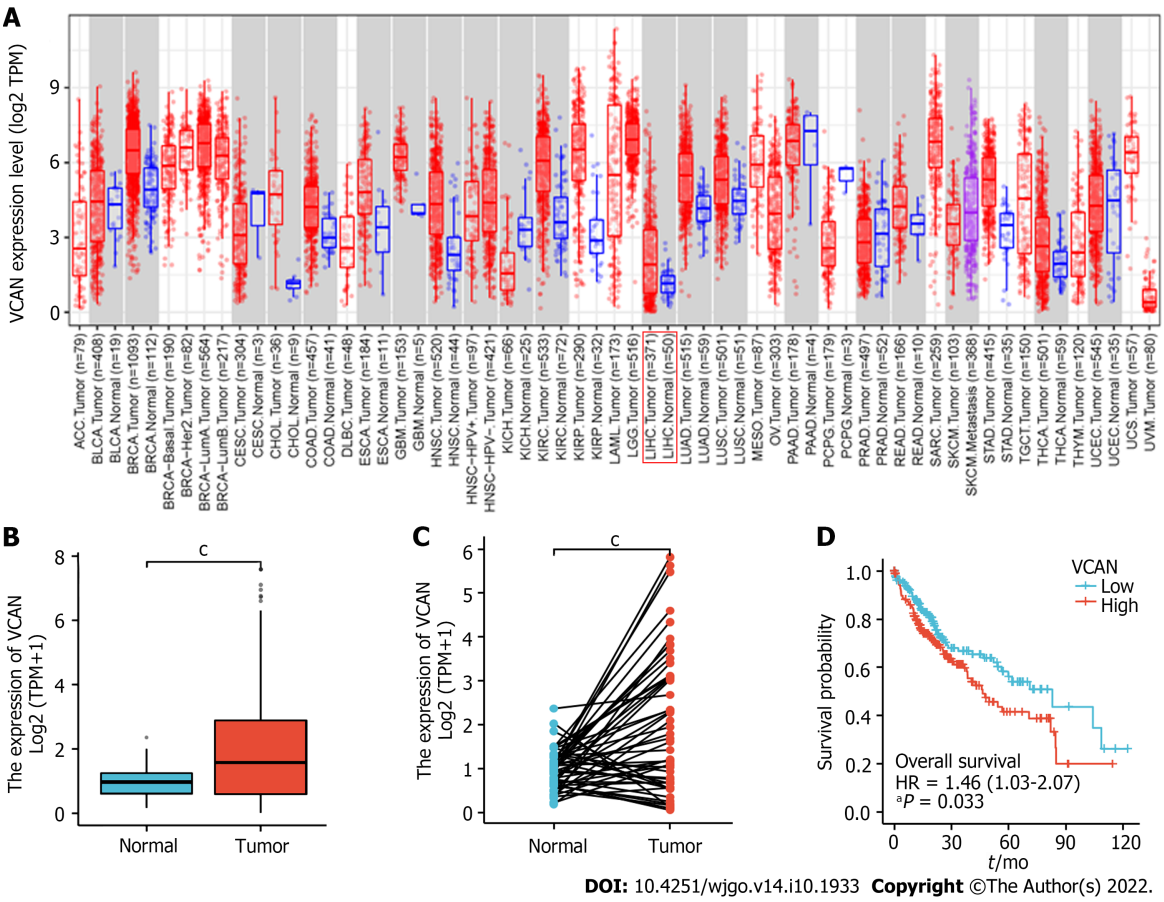

DOI: 10.4251/wjgo.v14.i10.1933

Figure 2 VCAN mRNA expression in tumor tissue and adjacent tissue in The Cancer Genome Atlas Liver Hepatocellular Carcinoma. A: VCAN mRNA expression in different types of tumors; B: VCAN mRNA expression in 374 tumor tissues and 50 normal tissues from The Cancer Genome Atlas Liver Hepatocellular Carcinoma (TCGA-LIHC); C: VCAN mRNA expression in 50 paired tumor tissues and normal tissues from TCGA-LIHC; D: Kaplan-Meier analysis for low VCAN and high VCAN expression (median as cutoff) in TCGA-LIHC. $^{a}P < 0.05$, $^{b}P < 0.01$, $^{c}P < 0.001$. TPM: Transcripts per kilobase of exon model per million mapped reads; HR: Hazard ratio.

Relationship between VCAN mRNA and clinical features in HCC patients in public databases

The patients were divided into two groups by the median of VCAN mRNA expression, and Kaplan-Meier analysis indicated that the survival rate of the low VCAN expression group was significantly higher than that of the high-VCAN expression group in patients from TCGA-LIHC (Figure 2D). Univariate regression analysis showed that high level of VCAN was a marker of poor prognosis in HCC patients (Figure 3). There were significant differences in VCAN mRNA according to age, gender, pathological stage, and a-fetoprotein level of patients from TCGA-LIHC (Table 1).

Clinical characteristics of HBV-related HCC and cirrhosis, and VCAN mRNA and methylation levels

The clinical characteristics and relevant VCAN mRNA levels in the HBV-related HCC and cirrhosis patients are shown in Table 2. The baseline data including age, sex, antiviral therapy within 6 mo, hepatitis B e antigen (HBeAg), and Child-Pugh class were not significantly different between the two groups. There was no significant difference in VCAN mRNA between the two groups (Figure 4A), but there was a significant difference in VCAN methylation (Figure 4B). The methylation levels of each CpG site in the two groups of patients are shown in Figure 4C, which indicates that cg82767790, cg82767780, and cg82768850 differed significantly ($P < 0.05$). The correlation analysis between VCAN mRNA expression and the methylation levels of each site is shown in Figure 4D, which indicates that VCAN mRNA expression was not significantly related to any CpG sites of VCAN.

According to the immunohistochemical results in the Human Protein Atlas (HPA)[23], VCAN is mainly expressed in the ECM in liver tumor tissues (Figure 5A). Immunohistochemical results of hepatocellular and adjacent tumor tissue showed that VCAN was expressed more in tumor tissue than in adjacent tissue, and VCAN was mainly distributed in the ECM (Figure 5B), which was similar to the result in the HPA (Figure 5A).

Correlation between VCAN expression and clinical features in HBV-related HCC and cirrhosis

The participants were divided into either a group of patients with high VCAN mRNA expression or a group of patients with low VCAN mRNA expression in blood using the median as the cutoff.

Table 1 Correlation between VCAN expression and clinical characteristics in The Cancer Genome Atlas Liver Hepatocellular Carcinoma

Characteristic	Low VCAN	High VCAN	*P* value
n	187	187	
Age, *n* (%)			0.020
60	77 (20.6)	100 (26.8)	
> 60	110 (29.5)	86 (23.1)	
Gender, *n* (%)			0.015
Female	49 (13.1)	72 (19.3)	
Male	138 (36.9)	115 (30.7)	
Pathologic stage, *n* (%)			0.042
I & II	138 (39.4)	122 (34.8)	
III & IV	41 (11.7)	45 (14.0)	
Histologic grade, *n* (%)			0.090
G1	34 (9.2)	21 (5.7)	
G2	88 (23.8)	90 (24.4)	
G3	54 (14.6)	70 (19)	
G4	8 (2.2)	4 (1.1)	
AFP (ng/mL), median (IQR)	9 (3.5, 140)	23 (5, 419)	0.039

AFP: Alpha-fetoprotein; IQR: Interquartile range.

Table 2 Clinical features and VCAN expression in patients with hepatocellular carcinoma and liver cirrhosis caused by hepatitis B virus

Clinical feature	HCC (*n* = 50)	Liver cirrhosis (*n* = 50)	*P* value
Age	57.55 ± 1.80	54.05 ± 2.22	0.227
Sex (male/female)	8/32	30/10	0.705
Anti-virus treatment (yes/no)	26/14	20/20	0.337
HBeAg (+/-)	7/33	6/34	0.144
HBV-DNA (IU/mL): ≤ 10^2/> 10^2	22/18	11/29	0.100
Child-Pugh: A/B&C	28/17	8/32	0.168
VCAN mRNA (%)	4.45 ± 0.56	3.83 ± 0.61	0.147
VCAN methylation	0.056 ± 0.009	0.047 ± 0.005	0.022

HCC: Hepatocellular carcinoma; HBV: Hepatitis B virus; HBeAg: Hepatitis B e antigen.

Table 3 Correlation between VCAN mRNA expression and clinical features

Variable	VCAN RNA expression (median as cutoff)		*P* value
	Low	High	
Age	56.60 ± 8.45	55.00 ± 9.82	0.552
Male/female	39/11	38/12	0.705
Anti-viral treatment/no treatment	23/27	35/15	0.110
HBeAg (+)/(-)	21/29	5/45	0.028
HBV-DNA (IU/mL): ≤ 10^2/> 10^2	13/37	34/16	0.025

Child-Pugh: A/B&C	35/15	31/19	0.490
AFP (ng/mL)	11.59 (3.47, 135.68)	21.43 (1.84, 210.88)	0.698
Total bilirubin (μmol/L)	26.37 (18.70, 50.25)	16.26 (11.47, 29.14)	0.035
Direct bilirubin (μmol/L)	8.44 (6.64, 27.92)	5.28 (3.51, 13.96)	0.043
Indirect bilirubin (μmol/L)	17.21 (12.23, 22.83)	10.51 (6.78, 13.39)	0.007
Total cholesterol (mmol/L)	2.90 ± 0.82	3.56 ± 0.81	0.015
LDL-C (mmol/L)	1.74 ± 0.59	2.25 ± 0.59	0.009
WBC (× 10^9/L)	3.54 ± 1.40	6.12 ± 2.40	< 0.001
Neutrophil (%)	58.69 ± 13.24	57.31 ± 14.48	0.302
Platelet (× 10^9/L)	76.60 ± 49.14	172.6 ± 87.01	< 0.001
Prothrombin time (s)	11.85 (10.85, 15.55)	11.15 (10.43, 11.83)	0.030
Prothrombin activity (%)	75.64 ± 21.15	89.37 ± 12.74	0.018
Fibrinogen (mg/dL)	186.00 ± 49.53	267.55 ± 111.17	0.006

LDL-C: Low density lipoprotein cholesterol; WBC: White blood cells; HBV: Hepatitis B virus; HBeAg: Hepatitis B e antigen; AFP: Alpha-fetoprotein.

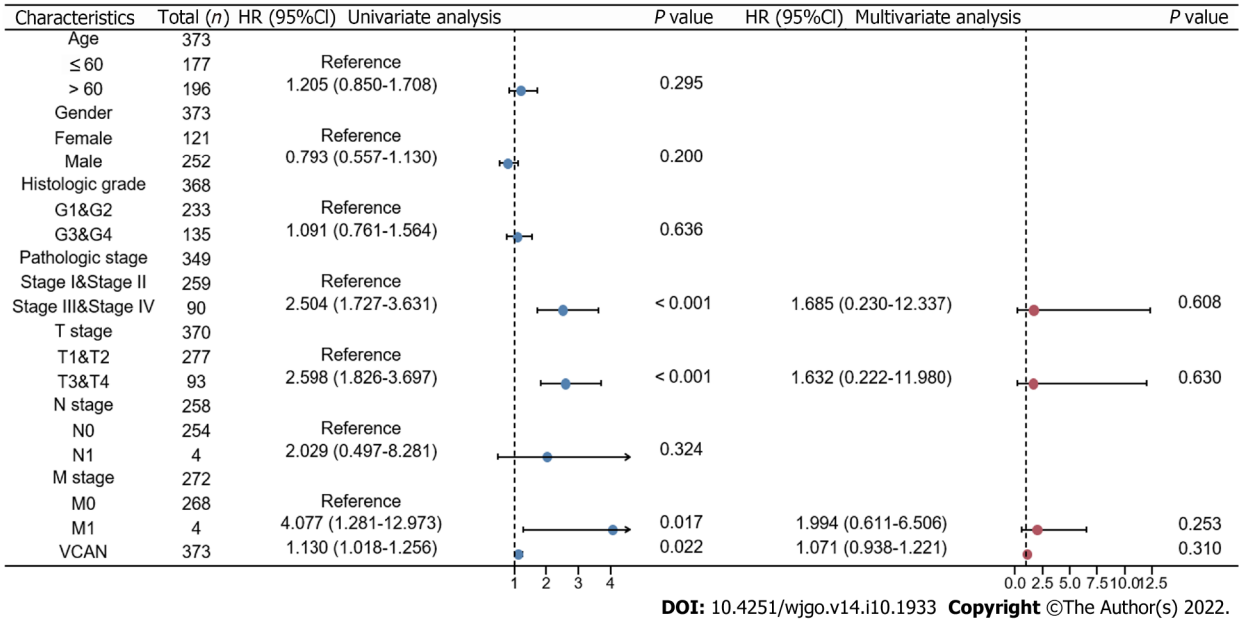

Figure 3 Univariate and multivariate Cox regression forest plots of The Cancer Genome Atlas Liver Hepatocellular Carcinoma. HR: Hazard ratio; CI: Confidence interval.

Comparison of clinical characteristics between the two groups showed that the expression of VCAN was associated with HBeAg, HBV DNA, total cholesterol, low density lipoprotein-cholesterol, white blood cells, platelets, and prothrombin activity (Table 3).

Prediction of mechanism of action of VCAN

The PPI network diagram (Figure 6A) consists of proteins potentially interacting with VCAN, which are mainly proteoglycan molecules, ECM molecules, and inflammatory factors. After co-expression analysis and differential expression analysis of high and low expression of VCAN, we obtained 687 VCAN co-expressed genes and 820 differentially expressed genes; 202 intersection genes (VCAN-related genes) are listed in Figure 6B.

GO analysis, KEGG analysis, and GSEA

The 202 intersection genes were subjected to functional annotation (Figure 6C). These genes mainly participate in biological processes involved in ECM organization, extracellular structure organization, and connective tissue development. VCAN-related genes participate in the formation of cellular

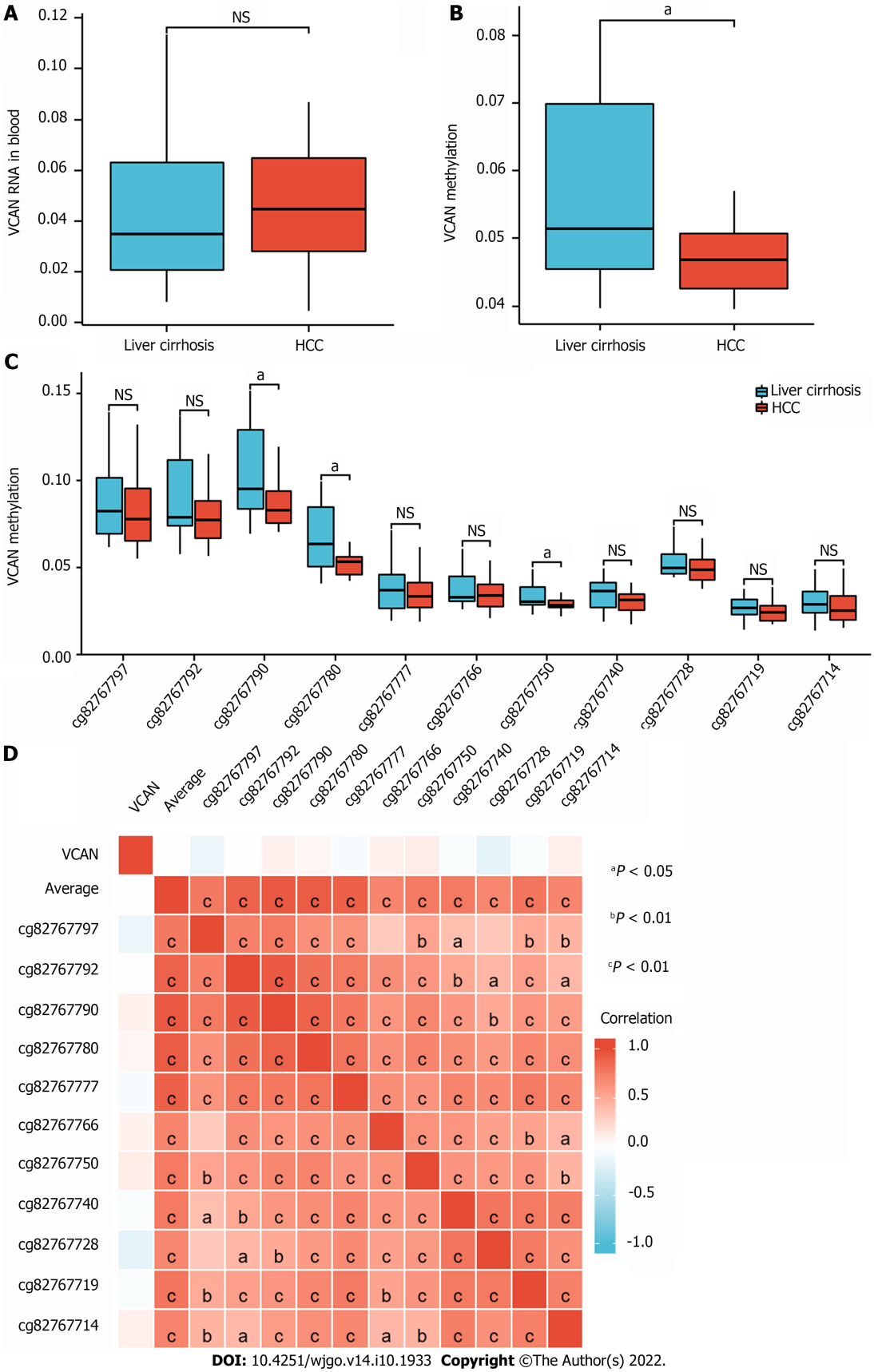

DOI: 10.4251/wjgo.v14.i10.1933

Figure 4 Expression of VCAN mRNA and DNA methylation in patients with hepatitis B virus-related hepatocellular carcinoma and cirrhosis. A: VCAN mRNA expression in the serum of hepatitis B virus (HBV)-related patients and controls; B: VCAN DNA methylation in the blood of HBV-related patients; C: Box diagram of VCAN CpG methylation in HBV-related patients; D: Correlation heatmap between VCAN mRNA and the methylation of each CpG site in blood. ns: $P > 0.05$, $^{a}P < 0.05$. HCC: Hepatocellular carcinoma.

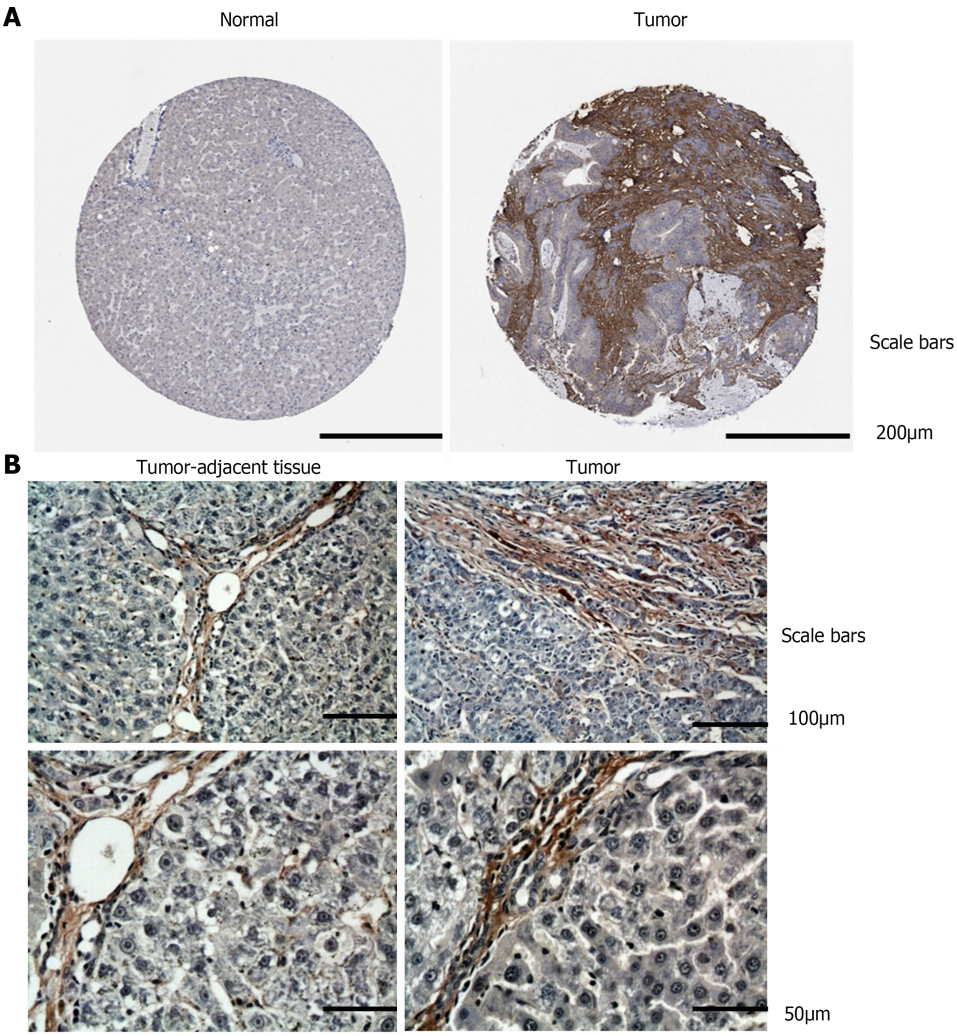

DOI: 10.4251/wjgo.v14.i10.1933

Figure 5 Immunohistochemical staining for VCAN in tumor tissue and adjacent tissue. A: Immunohistochemical results of VCAN in normal liver tissue and liver tumor tissue in the Human Protein Atlas; B: Immunohistochemical results of VCAN in liver tumor tissue and tumor-adjacent tissue from patients.

components including collagen-containing ECM, endoplasmic reticulum lumen, collagen trimer, and basement membrane, and they performed molecular functions such as ECM structural constituents, glycosaminoglycan binding, and sulfur compound binding. KEGG analysis and GSEA showed that VCAN-related genes were mainly enriched in the PI3K-AKT signaling pathway, focal adhesion, protein digestion and absorption, ECM-receptor interaction, and proteoglycans in cancer (Table 4, Figure 6D).

VCAN participates in immunomodulatory function in HCC

The results of three different algorithms showed that immune cell infiltration was significantly different between the high and low VCAN expression groups (Figures 7A-C). The stromal score, immune score, and tumor purity of TCGA-LIHC tumor tissues were significantly different between the two groups (Figures 8A and B). VCAN was significantly correlated to all 47 immune checkpoint genes (Figure 8C). In addition, TMB in the low VCAN group was significantly higher than that in the high VCAN group (Figure 8D). Programmed cell death protein 1 (PD-1) and cytotoxic T lymphocyte antigen 4 (CTLA4) were significantly related to VCAN mRNA expression (Figure 8E). Based on the significant correlation between VCAN and immune checkpoint genes and TMB[24], VCAN is possible to predict sensitivity to immune checkpoint inhibitor (ICI) therapy in HCC.

DISCUSSION

Our study found no significant difference in VCAN mRNA in serum mononuclear cells between HBV-related patients and controls, but the analysis based on BBCancer database showed that VCAN in HCC patients was significantly higher than that in normal controls (Supplementary Figure 1A). The possible reasons were as follows: The public database detected VCAN expression levels in extracellular vesicles

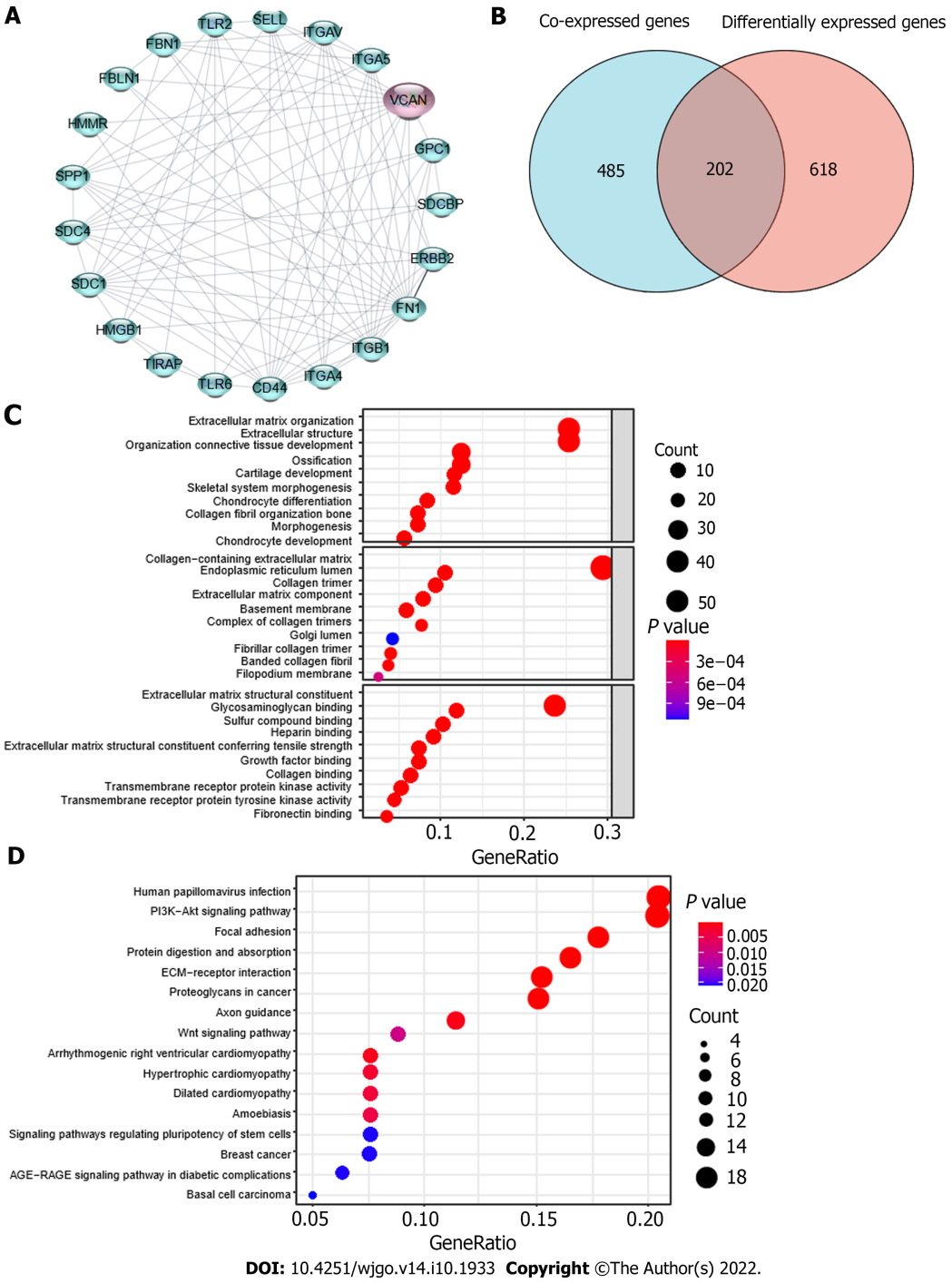

DOI: 10.4251/wjgo.v14.i10.1933

Figure 6 Possible mechanism of action of VCAN in hepatocellular carcinoma. A: Protein-protein interaction analysis of VCAN on STRING; B: Venn diagram for VCAN co-expressed genes and differentially expressed genes in high VCAN group and low VCAN group; C: Gene Ontology analysis of the 202 intersection genes; D: Kyoto Encyclopedia of Genes and Genomes analysis of the 202 intersection genes. HMMR: Hyaluronan mediated motility receptor; FBLN1: Fibulin-1; FBN1: Fibrillin-1; TLR2: Toll-like receptor 2; SELL: L-selectin; ITGAV: Integrin alpha-V; ITGA5: Integrin alpha-5; GPC1: Glypican-1; SDCBP: Syntenin-1; ERBB2: Receptor tyrosine-protein kinase erbB-2; FN1: Fibronectin 1; ITGB1: Integrin beta-1; ITGA4: Integrin alpha-4; CD44: CD44 antigen; TIRAP: Toll/interleukin-1 receptor domain-containing adapter protein; HMGB1: High mobility group protein B1; SDC: Syndecan; SPP1: Secreted phosphoprotein 1.

in serum, while we detected VCAN expression levels in peripheral blood mononuclear cells, considering that VCAN is mainly expressed on the cell surface. Exosomes are vesicles secreted by a variety of living cells, which contain a variety of components such as protein and RNA. Tumor-derived or tumor-related exosomes play an important role in the regulation of tumor development, especially through the TME, so the result would have been different if we had collected plasma exosomes from patients to measure VCAN RNA levels[25]. The reason why we made the assumption that VCAN methylation was significantly lower in HCC patients' blood, which is consistent with the result from TCGA-LIHC, was that VCAN is highly expressed in tumor tissue.

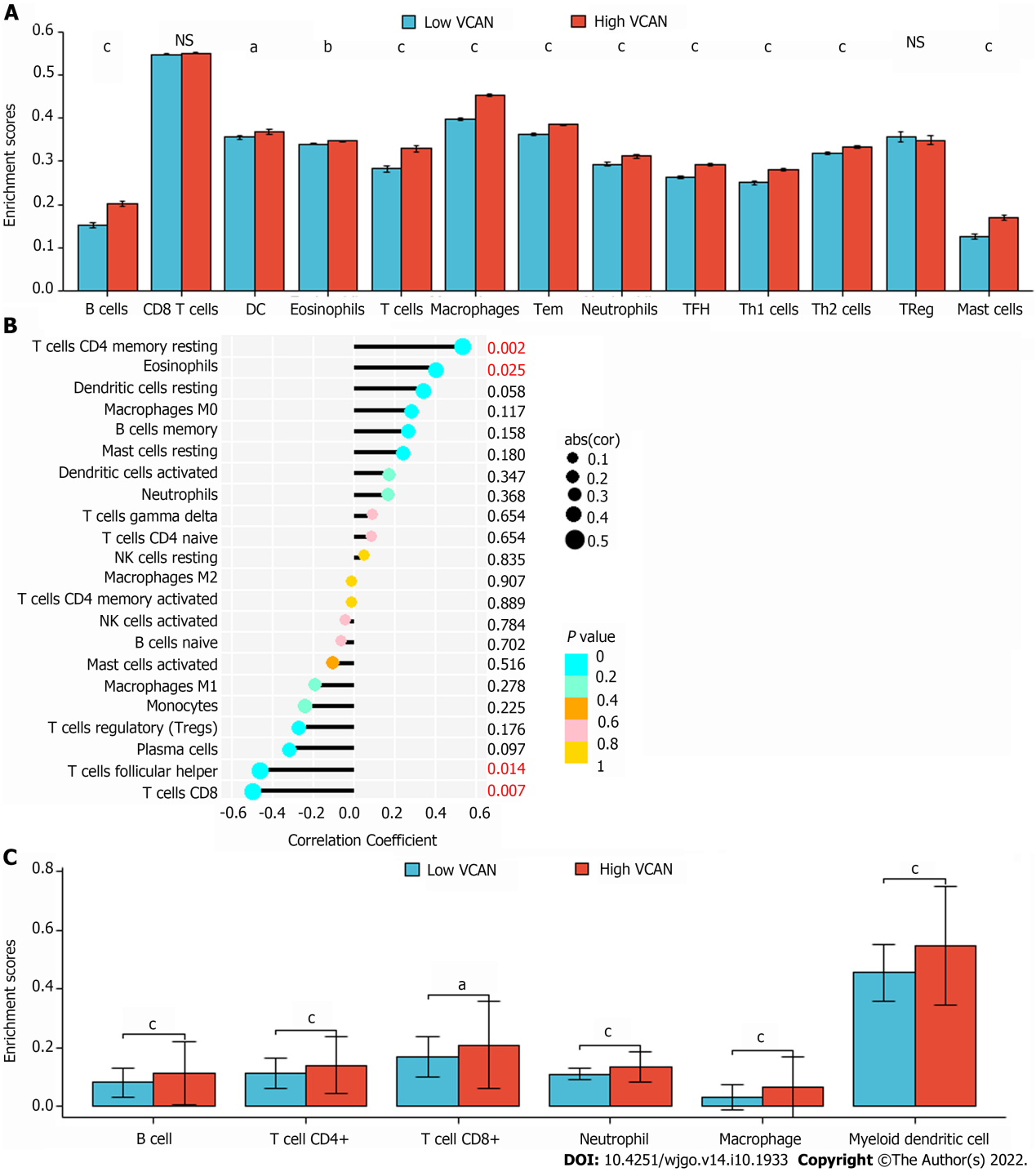

DOI: 10.4251/wjgo.v14.i10.1933

Figure 7 Immune cell infiltration in low VCAN group and high VCAN group. A: Immune cell infiltration calculated by ssGSEA algorithm; B: Immune cell infiltration calculated by CIBERSORTx algorithm; C: Immune cell infiltration calculated by TIMER algorithm. ns: $P > 0.05$; $^{a}P < 0.05$, $^{b}P < 0.01$, $^{c}P < 0.001$.

VCAN is highly expressed in tumor tissues, but especially higher in tumor tissues of HCC associated with viruses (Liver Cancer-RIKEN, Japan Project from International Cancer Genome Consortium) compared with HCC secondary to alcohol consumption and adiposity (ICGA-LICA-FR, Supplementary Figures 1B-D). In addition, when there is cirrhosis of the liver, viral hepatitis (including HBV and HCV) is more likely to progress to liver cancer than fatty hepatitis (including alcoholic and nonalcoholic), but when there is no cirrhosis of the liver, the opposite is true[26], which suggests that different causes have different mechanisms of progression from liver cirrhosis to cancer. VCAN expression in serum mononuclear cells is related to the characterization of HBeAg, which has been confirmed to promote the progression of HCC. This also proves that VCAN may promote the occurrence of liver cancer through interaction with HBeAg.

To investigate why VCAN is highly expressed in HCC tumor tissue or how it works, we also predicted VCAN-interacting proteins. The proteins that may interact with VCAN obtained by STRING

Table 4 Top 20 gene enrichment sets of highly expressed VCAN

Name	Size	ES	NES	NOM *P* value	FDR *Q* value
KEGG_FC_GAMMA_R_MEDIATED_PHAGOCYTOSIS	96	-0.739	-2.154	< 0.001	5.13E-04
KEGG_PATHOGENIC_ESCHERICHIA_COLI_INFECTION	56	-0.720	-2.046	< 0.001	5.91E-04
KEGG_ECM_RECEPTOR_INTERACTION	84	-0.716	-2.162	< 0.001	8.55E-04
KEGG_AXON_GUIDANCE	129	-0.695	-2.191	< 0.001	0.0015376
KEGG_DILATED_CARDIOMYOPATHY	90	-0.680	-2.112	< 0.001	4.91E-04
KEGG_APOPTOSIS	87	-0.678	-2.042	< 0.001	6.26E-04
KEGG_CHEMOKINE_SIGNALING_PATHWAY	188	-0.678	-2.127	< 0.001	3.83E-04
KEGG_LEUKOCYTE_TRANSENDOTHELIAL_MIGRATION	116	-0.677	-2.187	< 0.001	7.69E-04
KEGG_FOCAL_ADHESION	199	-0.675	-2.148	< 0.001	4.28E-04
KEGG_HYPERTROPHIC_CARDIOMYOPATHY_HCM	83	-0.673	-2.128	< 0.001	4.30E-04
KEGG_CELL_ADHESION_MOLECULES_CAMS	131	-0.663	-2.076	< 0.001	7.01E-04
KEGG_REGULATION_OF_ACTIN_CYTOSKELETON	213	-0.659	-2.158	< 0.001	6.42E-04
KEGG_GAP_JUNCTION	90	-0.656	-2.052	< 0.001	6.23E-04
KEGG_ENDOCYTOSIS	181	-0.656	-2.084	< 0.001	8.02E-04
KEGG_MELANOGENESIS	101	-0.630	-2.129	< 0.001	4.92E-04
KEGG_VASCULAR_SMOOTH_MUSCLE_CONTRACTION	114	-0.629	-2.097	< 0.001	7.21E-04
KEGG_CYTOKINE_CYTOKINE_RECEPTOR_INTERACTION	264	-0.625	-2.119	< 0.001	3.44E-04
KEGG_PATHWAYS_IN_CANCER	325	-0.621	-2.111	< 0.001	4.50E-04
KEGG_MAPK_SIGNALING_PATHWAY	267	-0.602	-2.080	< 0.001	7.48E-04
KEGG_CALCIUM_SIGNALING_PATHWAY	177	-0.582	-2.057	< 0.001	6.60E-04

ES: Enrichment score; NES: Normalized enrichment score; NOM: Nominal; FDR: False discovery rate; KEEG: Kyoto Encyclopedia of Genes and Genomes.

online (Figure 5A) include three main types: Decorin, biglycan, and other ECM components mainly involved in collagen production, physiological activities such as cell adhesion, apoptosis, and cellular immunity; Toll-like receptor (TLR)1 and TLR2, factors involved in immune response and inflammatory response; and integrin/integrin receptors and various protein kinases, which participate in angiogenesis and cell adhesion. A similar conclusion was drawn by the GO analysis, KEGG analysis, and the GSEA of patients with high VCAN expression (Figures 5C and D, Table 4), which showed that VCAN affects the occurrence of HCC mainly through ECM-related signaling pathways and the immune inflammatory response.

To explore the role of VCAN in immunoregulation of liver cancer, we analyzed the correlation between VCAN expression and tumor immune cell infiltration of TCGA-LIHC (Figures 6A-C), which indicated that VCAN plays a role in T-cell regulation in HCC. PD-1 regulates the immune system and promotes tolerance by inhibiting T-cell inflammatory activity. Clinical trials of nivolumab, pembrolizumab, and atezolizumab (PD-1 inhibitors) have shown they prolong OS of HCC patients and delay tumor progression[27-29], and tremelimumab (CTLA-4 inhibitor) has shown similar results[30]. Several guidelines recommend ICIs in combination with antiangiogenic agents as first-line therapy for advanced HCC[9-11]. The efficacy of ICIs can be predicted by TMB and immune checkpoint gene expression levels[31,32]. In our study, differential expression of PD-1 and CTLA-4 in the high and low VCAN groups, as well as significantly different TMB, showed that VCAN could be a potential biomarker of sensitivity to ICIs in HCC. However, only transcription data of a cohort of HCC patients treated with ICIs could directly explain whether VCAN could be a biomarker for the efficacy of such immunotherapy.

In addition, CD44 deserves attention when studying the role of VCAN in immunoregulation of liver cancer. PPI shows that CD44 is the most likely immune-related protein to interact with VCAN. Both VCAN and CD44 are involved in the adhesion and migration of T cells through the ECM, and both of their intermediate molecules are hyaluronic acid[33]. The immune cells in the TME of HCC interact with effector molecules to alter the immune system and promote or inhibit the growth of HCC[34]. Immunotherapy has been listed as a fourth-line treatment after surgery, radiotherapy, and chemotherapy, and has been promoted as a first-line treatment for advanced unresectable liver cancer. Immune checkpoints

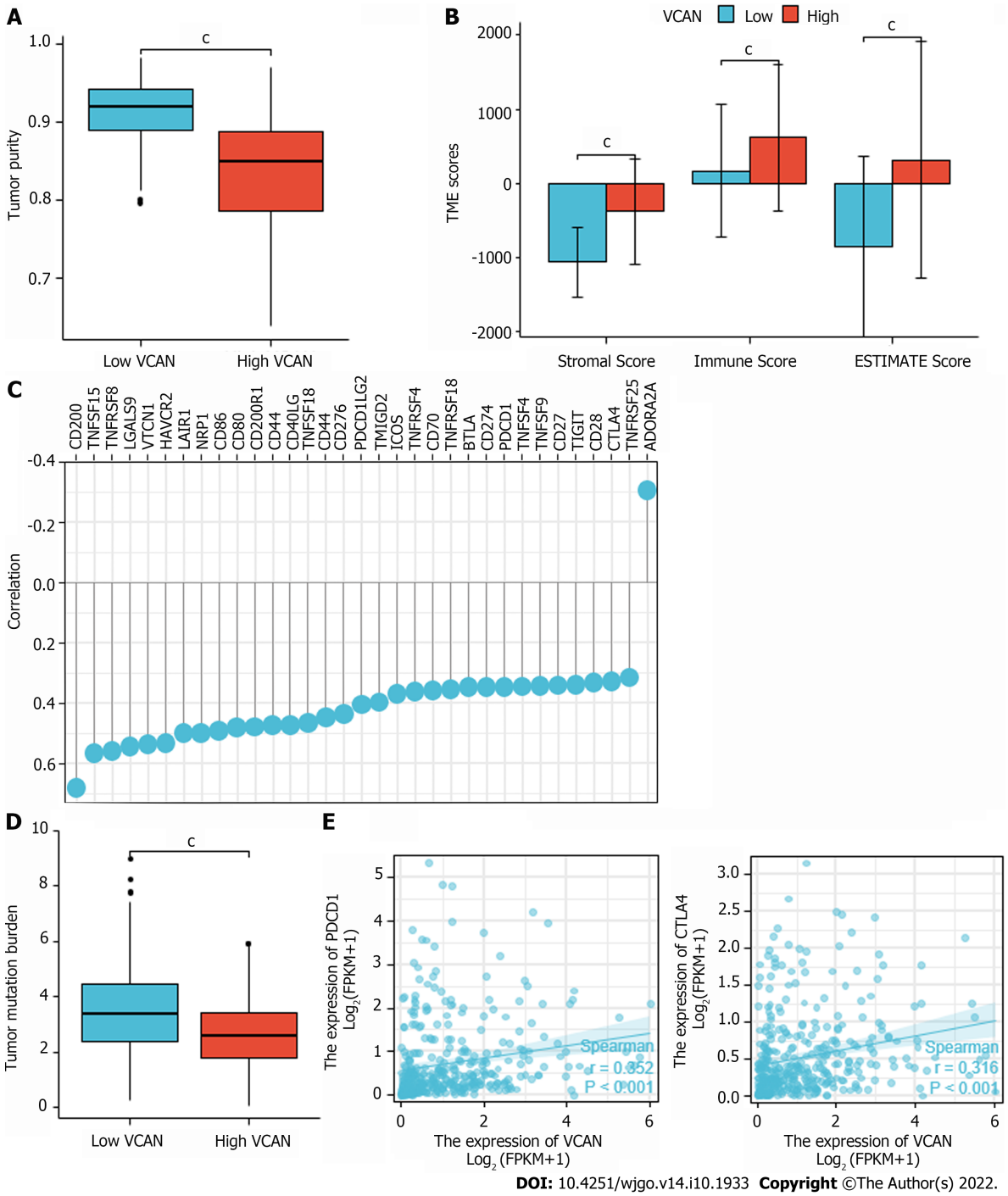

DOI: 10.4251/wjgo.v14.i10.1933

Figure 8 Correlation between VCAN and tumor microenvironment score, tumor mutation burden, or immune checkpoint genes. A: Tumor purity of low VCAN group and high VCAN group; B: Stromal score, immune score, and ESTIMATE score of low VCAN group and high VCAN group; C: Significant VCAN-related immune checkpoint genes ($r > 0.3$, $P < 0.05$); D: Tumor mutation burden of low VCAN group and high VCAN group; E: Correlation between VCAN and programmed cell death protein 1/cytotoxic T lymphocyte antigen 4. °$P < 0.001$. TME: Tumor microenvironment.

block T-cell activation and promote T-cell failure to regulate immune escape in cancer[35]. ICIs have been widely used in melanoma, nonsmall cell lung cancer, *etc.* Immune and inflammatory responses play a key role in the development and progression of HCC, so ICIs are supposed to be effective in HCC. Several clinical trials of PD-1/CTLA4 inhibitors in HCC are under way, and have proved their efficacy[27-29]. VCAN deserves attention due to its potential prediction of sensitivity to PD-1/CTLA4 inhibitors.

In this study, we found that VCAN was highly expressed in HCC tumor tissues and could possibly be a biomarker of prognosis and sensitivity to ICIs in HCC patients. Our study had the following limitations: Due to the lack of follow-up for HCC patients, survival data were not available for analysis. In addition, we did not extract exosomes from patients' serum for detection. We will further study the effects of the above defects on VCAN and its related genes in HBV-related liver diseases.

CONCLUSION

We analyzed VCAN expression and corresponding clinical features of patients from the public database and our HBV-related patients, and concluded that VCAN may affect the occurrence of liver cancer and the prognosis of HCC patients through ECM signaling pathways and inflammatory immune response signaling pathways. In addition, VCAN may be a biomarker for sensitivity to ICIs, which needs to be verified.

ARTICLE HIGHLIGHTS

Research background

Existing studies have shown that chondroitin sulfate proteoglycan, including VCAN, is a key component in the tumor microenvironment and may play an important role in hepatocellular carcinoma (HCC).

Research motivation

The role of VCAN in HCC has not yet been elucidated, especially in hepatitis B virus (HBV)-related HCC.

Research objectives

This study aimed to investigate the expression and potential mechanism of action of VCAN in HCC.

Research methods

We tested VCAN expression in serum of patients with HBV-associated HCC and cirrhosis, and explore the underlying mechanism of VCAN in HCC by bioinformatics methods.

Research results

VCAN may be a possible biomarker for the prognosis of HCC. VCAN was associated with HBV e antigen in HBV infected patients. VCAN may play a role in HCC through the extracellular matrix signaling pathway and inflammatory immune response.

Research conclusions

High VCAN level could be a possible biomarker for the poor prognosis of HCC, and its immunomodulatory mechanism in HCC deserves attention.

Research perspectives

Future studies will be conducted to explore the immune mechanism of VCAN in HBV-associated HCC.

FOOTNOTES

Author contributions: Jia XL and Dang SS designed the study; Zhang X, Wu Y, Li YP, and Jia XL collected all samples in the study; Wang MQ, Wu Y, and Tian Y collected the data; Wang MQ and Xu M performed the statistical analysis; Wang MQ, Li YP, and Jia XL drafted the manuscript; Xu M, Jia XL, and Li YP made critical revisions to the manuscript; Jia XL, Xu M and Shi JJ provided financial support; and all authors read and approved the manuscript.

Supported by the National Natural Science Foundation of China, No. 31500650 and 81902449; the Key Research & Development Program-Social Development of Shaanxi Province, No. 2020SF-063; and Shaanxi Key Research and Development Plans, No. 2021SF-227.

Institutional review board statement: The study was reviewed and approved by the Medical Ethics Committees of the Second Affiliated Hospital of Xi'an Jiaotong University (Approval No. 2019-1093).

Conflict-of-interest statement: All the authors report no relevant conflicts of interest for this article.

Data sharing statement: No additional data are available.

Country/Territory of origin: China

ORCID number: Mu-Qi Wang 0000-0003-2314-8983; Ya-Ping Li 0000-0002-0900-5559; Meng Xu 0000-0002-6118-9965; Yan Tian 0000-0002-5967-6887; Yuan Wu 0000-0002-0413-4204; Xin Zhang 0000-0002-5966-0471; Juan-Juan Shi 0000-0002-5626-9821; Shuang-Suo Dang 0000-0003-0918-9535; Xiao-Li Jia 0000-0001-8865-9771.

S-Editor: Wang JJ
L-Editor: Wang TQ
P-Editor: Cai YX

REFERENCES

1 **Sung H**, Ferlay J, Siegel RL, Laversanne M, Soerjomataram I, Jemal A, Bray F. Global Cancer Statistics 2020: GLOBOCAN Estimates of Incidence and Mortality Worldwide for 36 Cancers in 185 Countries. *CA Cancer J Clin* 2021; **71**: 209-249 [PMID: 33538338 DOI: 10.3322/caac.21660]
2 **Zheng RS**, Sun KX, Zhang SW, Zeng HM, Zou XN, Chen R, Gu XY, Wei WW, He J. [Report of cancer epidemiology in China, 2015]. *Zhonghua Zhong Liu Za Zhi* 2019; **41**: 19-28 [PMID: 30678413 DOI: 10.3760/cma.j.issn.0253-3766.2019.01.005]
3 **Wang M**, Wang Y, Feng X, Wang R, Zeng H, Qi J, Zhao H, Li N, Cai J, Qu C. Contribution of hepatitis B virus and hepatitis C virus to liver cancer in China north areas: Experience of the Chinese National Cancer Center. *Int J Infect Dis* 2017; **65**: 15-21 [PMID: 28935244 DOI: 10.1016/j.ijid.2017.09.003]
4 **Affo S**, Yu LX, Schwabe RF. The Role of Cancer-Associated Fibroblasts and Fibrosis in Liver Cancer. *Annu Rev Pathol* 2017; **12**: 153-186 [PMID: 27959632 DOI: 10.1146/annurev-pathol-052016-100322]
5 **Zeltz C**, Primac I, Erusappan P, Alam J, Noel A, Gullberg D. Cancer-associated fibroblasts in desmoplastic tumors: emerging role of integrins. *Semin Cancer Biol* 2020; **62**: 166-181 [PMID: 31415910 DOI: 10.1016/j.semcancer.2019.08.004]
6 **Paolillo M**, Schinelli S. Extracellular Matrix Alterations in Metastatic Processes. *Int J Mol Sci* 2019; **20** [PMID: 31591367 DOI: 10.3390/ijms20194947]
7 **Lu C**, Rong D, Zhang B, Zheng W, Wang X, Chen Z, Tang W. Current perspectives on the immunosuppressive tumor microenvironment in hepatocellular carcinoma: challenges and opportunities. *Mol Cancer* 2019; **18**: 130 [PMID: 31464625 DOI: 10.1186/s12943-019-1047-6]
8 **Dong P**, Ma L, Liu L, Zhao G, Zhang S, Dong L, Xue R, Chen S. $CD86^+/CD206^+$, Diametrically Polarized Tumor-Associated Macrophages, Predict Hepatocellular Carcinoma Patient Prognosis. *Int J Mol Sci* 2016; **17**: 320 [PMID: 26938527 DOI: 10.3390/ijms17030320]
9 **Gordan JD**, Kennedy EB, Abou-Alfa GK, Beg MS, Brower ST, Gade TP, Goff L, Gupta S, Guy J, Harris WP, Iyer R, Jaiyesimi I, Jhawer M, Karippot A, Kaseb AO, Kelley RK, Knox JJ, Kortmansky J, Leaf A, Remak WM, Shroff RT, Sohal DPS, Taddei TH, Venepalli NK, Wilson A, Zhu AX, Rose MG. Systemic Therapy for Advanced Hepatocellular Carcinoma: ASCO Guideline. *J Clin Oncol* 2020; **38**: 4317-4345 [PMID: 33197225 DOI: 10.1200/JCO.20.02672]
10 **Greten TF**, Abou-Alfa GK, Cheng AL, Duffy AG, El-Khoueiry AB, Finn RS, Galle PR, Goyal L, He AR, Kaseb AO, Kelley RK, Lencioni R, Lujambio A, Mabry Hrones D, Pinato DJ, Sangro B, Troisi RI, Wilson Woods A, Yau T, Zhu AX, Melero I. Society for Immunotherapy of Cancer (SITC) clinical practice guideline on immunotherapy for the treatment of hepatocellular carcinoma. *J Immunother Cancer* 2021; **9** [PMID: 34518290 DOI: 10.1136/jitc-2021-002794]
11 **Sun HC**, Zhou J, Wang Z, Liu X, Xie Q, Jia W, Zhao M, Bi X, Li G, Bai X, Ji Y, Xu L, Zhu XD, Bai D, Chen Y, Dai C, Guo R, Guo W, Hao C, Huang T, Huang Z, Li D, Li T, Li X, Liang X, Liu J, Liu F, Lu S, Lu Z, Lv W, Mao Y, Shao G, Shi Y, Song T, Tan G, Tang Y, Tao K, Wan C, Wang G, Wang L, Wang S, Wen T, Xing B, Xiang B, Yan S, Yang D, Yin G, Yin T, Yin Z, Yu Z, Zhang B, Zhang J, Zhang S, Zhang T, Zhang Y, Zhang A, Zhao H, Zhou L, Zhang W, Zhu Z, Qin S, Shen F, Cai X, Teng G, Cai J, Chen M, Li Q, Liu L, Wang W, Liang T, Dong J, Chen X, Wang X, Zheng S, Fan J; Alliance of Liver Cancer Conversion Therapy, Committee of Liver Cancer of the Chinese Anti-Cancer Association. Chinese expert consensus on conversion therapy for hepatocellular carcinoma (2021 edition). *Hepatobiliary Surg Nutr* 2022; **11**: 227-252 [PMID: 35464283 DOI: 10.21037/hbsn-21-328]
12 **Wu YJ**, La Pierre DP, Wu J, Yee AJ, Yang BB. The interaction of versican with its binding partners. *Cell Res* 2005; **15**: 483-494 [PMID: 16045811 DOI: 10.1038/sj.cr.7290318]
13 **Zhangyuan G**, Wang F, Zhang H, Jiang R, Tao X, Yu D, Jin K, Yu W, Liu Y, Yin Y, Shen J, Xu Q, Zhang W, Sun B. VersicanV1 promotes proliferation and metastasis of hepatocellular carcinoma through the activation of EGFR-PI3K-AKT pathway. *Oncogene* 2020; **39**: 1213-1230 [PMID: 31605014 DOI: 10.1038/s41388-019-1052-7]
14 **Xia L**, Huang W, Tian D, Zhang L, Qi X, Chen Z, Shang X, Nie Y, Wu K. Forkhead box Q1 promotes hepatocellular carcinoma metastasis by transactivating ZEB2 and VersicanV1 expression. *Hepatology* 2014; **59**: 958-973 [PMID: 24005989 DOI: 10.1002/hep.26735]
15 **Naboulsi W**, Megger DA, Bracht T, Kohl M, Turewicz M, Eisenacher M, Voss DM, Schlaak JF, Hoffmann AC, Weber F, Baba HA, Meyer HE, Sitek B. Quantitative Tissue Proteomics Analysis Reveals Versican as Potential Biomarker for Early-Stage Hepatocellular Carcinoma. *J Proteome Res* 2016; **15**: 38-47 [PMID: 26626371 DOI: 10.1021/acs.jproteome.5b00420]
16 **Li T**, Fan J, Wang B, Traugh N, Chen Q, Liu JS, Li B, Liu XS. TIMER: A Web Server for Comprehensive Analysis of Tumor-Infiltrating Immune Cells. *Cancer Res* 2017; **77**: e108-e110 [PMID: 29092952 DOI: 10.1158/0008-5472.CAN-17-0307]
17 **Department of Medical Administration**, National Health and Health Commission of the People's Republic of China.

[Guidelines for diagnosis and treatment of primary liver cancer in China (2019 edition)]. *Zhonghua Gan Zang Bing Za Zhi* 2020; **28**: 112-128 [PMID: 32164061 DOI: 10.3760/cma.j.issn.1007-3418.2020.02.004]

18 **Chinese Society of Infectious Diseases**; Chinese Medical Association; Chinese Society of Hepatology, Chinese Medical Association. [The guidelines of prevention and treatment for chronic hepatitis B (2019 version)]. *Zhonghua Gan Zang Bing Za Zhi* 2019; **27**: 938-961 [PMID: 31941257 DOI: 10.3760/cma.j.issn.1007-3418.2019.12.007]

19 **Subramanian A**, Tamayo P, Mootha VK, Mukherjee S, Ebert BL, Gillette MA, Paulovich A, Pomeroy SL, Golub TR, Lander ES, Mesirov JP. Gene set enrichment analysis: a knowledge-based approach for interpreting genome-wide expression profiles. *Proc Natl Acad Sci U S A* 2005; **102**: 15545-15550 [PMID: 16199517 DOI: 10.1073/pnas.0506580102]

20 **Newman AM**, Steen CB, Liu CL, Gentles AJ, Chaudhuri AA, Scherer F, Khodadoust MS, Esfahani MS, Luca BA, Steiner D, Diehn M, Alizadeh AA. Determining cell type abundance and expression from bulk tissues with digital cytometry. *Nat Biotechnol* 2019; **37**: 773-782 [PMID: 31061481 DOI: 10.1038/s41587-019-0114-2]

21 **Barbie DA**, Tamayo P, Boehm JS, Kim SY, Moody SE, Dunn IF, Schinzel AC, Sandy P, Meylan E, Scholl C, Fröhling S, Chan EM, Sos ML, Michel K, Mermel C, Silver SJ, Weir BA, Reiling JH, Sheng Q, Gupta PB, Wadlow RC, Le H, Hoersch S, Wittner BS, Ramaswamy S, Livingston DM, Sabatini DM, Meyerson M, Thomas RK, Lander ES, Mesirov JP, Root DE, Gilliland DG, Jacks T, Hahn WC. Systematic RNA interference reveals that oncogenic KRAS-driven cancers require TBK1. *Nature* 2009; **462**: 108-112 [PMID: 19847166 DOI: 10.1038/nature08460]

22 **Xu D**, Liu X, Wang Y, Zhou K, Wu J, Chen JC, Chen C, Chen L, Zheng J. Identification of immune subtypes and prognosis of hepatocellular carcinoma based on immune checkpoint gene expression profile. *Biomed Pharmacother* 2020; **126**: 109903 [PMID: 32113055 DOI: 10.1016/j.biopha.2020.109903]

23 **Uhlén M**, Fagerberg L, Hallström BM, Lindskog C, Oksvold P, Mardinoglu A, Sivertsson Å, Kampf C, Sjöstedt E, Asplund A, Olsson I, Edlund K, Lundberg E, Navani S, Szigyarto CA, Odeberg J, Djureinovic D, Takanen JO, Hober S, Alm T, Edqvist PH, Berling H, Tegel H, Mulder J, Rockberg J, Nilsson P, Schwenk JM, Hamsten M, von Feilitzen K, Forsberg M, Persson L, Johansson F, Zwahlen M, von Heijne G, Nielsen J, Pontén F. Proteomics. Tissue-based map of the human proteome. *Science* 2015; **347**: 1260419 [PMID: 25613900 DOI: 10.1126/science.1260419]

24 **Chan TA**, Yarchoan M, Jaffee E, Swanton C, Quezada SA, Stenzinger A, Peters S. Development of tumor mutation burden as an immunotherapy biomarker: utility for the oncology clinic. *Ann Oncol* 2019; **30**: 44-56 [PMID: 30395155 DOI: 10.1093/annonc/mdy495]

25 **Seo N**, Akiyoshi K, Shiku H. Exosome-mediated regulation of tumor immunology. *Cancer Sci* 2018; **109**: 2998-3004 [PMID: 29999574 DOI: 10.1111/cas.13735]

26 **Mittal S**, El-Serag HB, Sada YH, Kanwal F, Duan Z, Temple S, May SB, Kramer JR, Richardson PA, Davila JA. Hepatocellular Carcinoma in the Absence of Cirrhosis in United States Veterans is Associated With Nonalcoholic Fatty Liver Disease. *Clin Gastroenterol Hepatol* 2016; **14**: 124-31.e1 [PMID: 26196445 DOI: 10.1016/j.cgh.2015.07.019]

27 **Yau T**, Kang YK, Kim TY, El-Khoueiry AB, Santoro A, Sangro B, Melero I, Kudo M, Hou MM, Matilla A, Tovoli F, Knox JJ, Ruth He A, El-Rayes BF, Acosta-Rivera M, Lim HY, Neely J, Shen Y, Wisniewski T, Anderson J, Hsu C. Efficacy and Safety of Nivolumab Plus Ipilimumab in Patients With Advanced Hepatocellular Carcinoma Previously Treated With Sorafenib: The CheckMate 040 Randomized Clinical Trial. *JAMA Oncol* 2020; **6**: e204564 [PMID: 33001135 DOI: 10.1001/jamaoncol.2020.4564]

28 **Finn RS**, Ryoo BY, Merle P, Kudo M, Bouattour M, Lim HY, Breder V, Edeline J, Chao Y, Ogasawara S, Yau T, Garrido M, Chan SL, Knox J, Daniele B, Ebbinghaus SW, Chen E, Siegel AB, Zhu AX, Cheng AL; KEYNOTE-240 investigators. Pembrolizumab As Second-Line Therapy in Patients With Advanced Hepatocellular Carcinoma in KEYNOTE-240: A Randomized, Double-Blind, Phase III Trial. *J Clin Oncol* 2020; **38**: 193-202 [PMID: 31790344 DOI: 10.1200/JCO.19.01307]

29 **Sonbol MB**, Riaz IB, Naqvi SAA, Almquist DR, Mina S, Almasri J, Shah S, Almader-Douglas D, Uson Junior PLS, Mahipal A, Ma WW, Jin Z, Mody K, Starr J, Borad MJ, Ahn DH, Murad MH, Bekaii-Saab T. Systemic Therapy and Sequencing Options in Advanced Hepatocellular Carcinoma: A Systematic Review and Network Meta-analysis. *JAMA Oncol* 2020; **6**: e204930 [PMID: 33090186 DOI: 10.1001/jamaoncol.2020.4930]

30 **Duffy AG**, Ulahannan SV, Makorova-Rusher O, Rahma O, Wedemeyer H, Pratt D, Davis JL, Hughes MS, Heller T, ElGindi M, Uppala A, Korangy F, Kleiner DE, Figg WD, Venzon D, Steinberg SM, Venkatesan AM, Krishnasamy V, Abi-Jaoudeh N, Levy E, Wood BJ, Greten TF. Tremelimumab in combination with ablation in patients with advanced hepatocellular carcinoma. *J Hepatol* 2017; **66**: 545-551 [PMID: 27816492 DOI: 10.1016/j.jhep.2016.10.029]

31 **Ott PA**, Bang YJ, Piha-Paul SA, Razak ARA, Bennouna J, Soria JC, Rugo HS, Cohen RB, O'Neil BH, Mehnert JM, Lopez J, Doi T, van Brummelen EMJ, Cristescu R, Yang P, Emancipator K, Stein K, Ayers M, Joe AK, Lunceford JK. T-Cell-Inflamed Gene-Expression Profile, Programmed Death Ligand 1 Expression, and Tumor Mutational Burden Predict Efficacy in Patients Treated With Pembrolizumab Across 20 Cancers: KEYNOTE-028. *J Clin Oncol* 2019; **37**: 318-327 [PMID: 30557521 DOI: 10.1200/JCO.2018.78.2276]

32 **Marabelle A**, Fakih M, Lopez J, Shah M, Shapira-Frommer R, Nakagawa K, Chung HC, Kindler HL, Lopez-Martin JA, Miller WH Jr, Italiano A, Kao S, Piha-Paul SA, Delord JP, McWilliams RR, Fabrizio DA, Aurora-Garg D, Xu L, Jin F, Norwood K, Bang YJ. Association of tumour mutational burden with outcomes in patients with advanced solid tumours treated with pembrolizumab: prospective biomarker analysis of the multicohort, open-label, phase 2 KEYNOTE-158 study. *Lancet Oncol* 2020; **21**: 1353-1365 [PMID: 32919526 DOI: 10.1016/S1470-2045(20)30445-9]

33 **Evanko SP**, Potter-Perigo S, Bollyky PL, Nepom GT, Wight TN. Hyaluronan and versican in the control of human T-lymphocyte adhesion and migration. *Matrix Biol* 2012; **31**: 90-100 [PMID: 22155153 DOI: 10.1016/j.matbio.2011.10.004]

34 **Oura K**, Morishita A, Tani J, Masaki T. Tumor Immune Microenvironment and Immunosuppressive Therapy in Hepatocellular Carcinoma: A Review. *Int J Mol Sci* 2021; **22** [PMID: 34071550 DOI: 10.3390/ijms22115801]

35 **Abril-Rodriguez G**, Ribas A. SnapShot: Immune Checkpoint Inhibitors. *Cancer Cell* 2017; **31**: 848-848.e1 [PMID: 28609660 DOI: 10.1016/j.ccell.2017.05.010]

World Journal of Gastrointestinal Oncology

Submit a Manuscript: https://www.f6publishing.com

World J Gastrointest Oncol 2022 October 15; 14(10): 1949-1967

DOI: 10.4251/wjgo.v14.i10.1949

ISSN 1948-5204 (online)

ORIGINAL ARTICLE

Basic Study

Overexpression of ELL-associated factor 2 suppresses invasion, migration, and angiogenesis in colorectal cancer

Ming-Liang Feng, Can Wu, Hui-Jing Zhang, Huan Zhou, Tai-Wei Jiao, Meng-Yuan Liu, Ming-Jun Sun

Specialty type: Oncology

Provenance and peer review: Unsolicited article; Externally peer reviewed.

Peer-review model: Single blind

Peer-review report's scientific quality classification

Grade A (Excellent): 0
Grade B (Very good): B
Grade C (Good): C, C, C, C
Grade D (Fair): D
Grade E (Poor): E

P-Reviewer: Imai Y, Japan; Jeong KY, South Korea; Linnebacher M, Germany; Naserian S, France

Received: May 19, 2022
Peer-review started: May 19, 2022
First decision: June 6, 2022
Revised: June 20, 2022
Accepted: September 21, 2022
Article in press: September 21, 2022
Published online: October 15, 2022

Ming-Liang Feng, Can Wu, Hui-Jing Zhang, Huan Zhou, Tai-Wei Jiao, Meng-Yuan Liu, Ming-Jun Sun, Department of Endoscopy, The First Hospital Affiliated to China Medical University, Shenyang 110001, Liaoning Province, China

Corresponding author: Ming-Jun Sun, Doctor, PhD, Chief Physician, Professor, Department of Endoscopy, The First Hospital Affiliated to China Medical University, No. 155 Nanjing North Street, Shenyang 110001, Liaoning Province, China. sunydyy@163.com

Abstract

BACKGROUND

The androgen responsive gene, ELL-associated factor 2 (EAF2), expressed in benign prostate tissues, has been shown to play an important role in tumor suppression in a variety of malignant tumors. In addition, some scholars found that EAF2 frameshift mutations are associated with intratumor heterogeneity in colorectal cancer (CRC) and inactivation of EAF2 in microsatellite instability-high CRC. However, the molecular mechanism by which EAF2 is involved in CRC invasion and metastasis remains unclear.

AIM

To determine the clinical value of expression of EAF2 protein in CRC, and to study the effects of EAF2 on the invasion, migration, and angiogenesis of CRC cells *in vitro*.

METHODS

In this study, we collected colorectal adenocarcinoma and corresponding adjacent tissues to investigate the clinical expression of EAF2 protein in patients with advanced CRC. Subsequently, we investigated the effect of EAF2 on the invasion, migration, and angiogenesis of CRC cells *in vitro* using plasmid transfection.

RESULTS

EAF2 protein was lowly expressed in cancer tissues of patients with advanced CRC. Kaplan-Meier survival analysis showed that the survival rate of the high EAF2 level group was higher than that of the low EAF2 level group.

CONCLUSION

Our results demonstrated that EAF2, as a tumor suppressor, may inhibit the invasion, metastasis, and angiogenesis of CRC cells by regulating the signal transducer and activator of transcription 3/transforming growth factor-β1

crosstalk pathway, and play a cancer suppressive and protective role in the occurrence and development of CRC. Our findings are of great significance to provide a new idea and theoretical basis for the targeted diagnosis and treatment of CRC.

Key Words: ELL-associated factor 2; Transforming growth factor-β1; Signal transducer and activator of transcription 3; Colorectal cancer; Invasion; Migration; Angiogenesis

Core Tip: Androgen-responsive gene ELL-associated factor 2 (EAF2) plays an important role in tumor suppression in a variety of malignant tumors. We found that EAF2 protein was lowly expressed in colorectal cancer (CRC) tissues. Kaplan-Meier survival analysis showed that the survival rate of the group with high EAF2 level was higher than that of the group with low EAF2 level. Moreover, EAF2 may play a tumor suppressive and protective role in CRC by inhibiting the invasion, metastasis, and angiogenesis *via* regulating the signal transducer and activator of transcription 3/transforming growth factor beta 1 crosstalk pathway. Our findings are of great significance to provide a new idea and theoretical basis for targeting diagnosis and therapy of CRC.

Citation: Feng ML, Wu C, Zhang HJ, Zhou H, Jiao TW, Liu MY, Sun MJ. Overexpression of ELL-associated factor 2 suppresses invasion, migration, and angiogenesis in colorectal cancer. *World J Gastrointest Oncol* 2022; 14(10): 1949-1967
URL: https://www.wjgnet.com/1948-5204/full/v14/i10/1949.htm
DOI: https://dx.doi.org/10.4251/wjgo.v14.i10.1949

INTRODUCTION

Colorectal cancer (CRC) is one of the tumors with high morbidity and mortality in the world. The Global Cancer Statistics 2020 revealed that CRC was estimated to be the third most diagnosed malignant tumor (10%) and the second leading cause of cancer death (9.4%) worldwide[1]. As an important process in the development of CRC, tumor metastasis is a key factor affecting the survival rate of CRC patients. Approximately 35% of newly diagnosed CRC patients present metastatic disease, and about 50% of patients with non-metastatic disease eventually develop metastatic disease[2]. Most regrettably, the 5-year survival rate of patients with metastatic CRC is less than 10%[3]. There is a great need to elucidate the molecular mechanism of CRC invasion and metastasis, which is beneficial to explore new potential molecular markers and the direction of targeted therapy of CRC.

ELL-associated factor 2 (EAF2) was first identified as an androgen-responsive gene expressed by luminal epithelial cells in benign prostatic tissue[4,5]. Interestingly, EAF2 has been found to inhibit cell proliferation and tumor size in prostate cancer *in vivo*[6], and corresponding to that, knockdown of EAF2 in prostate cancer cells resulted in increased proliferation and migration[7]. In recent years, more and more studies have shown that EAF2 plays an important role in tumor suppression in a variety of malignant tumors[8]. Furthermore, scholars have identified intratumor heterogeneity (ITH) of EAF2 frameshift mutations in CRC and the inactivation of EAF2 in microsatellite instability (MSI)-high CRC [9]. This finding suggests that EAF2 inactivation may occur during tumor progression rather than tumorigenesis. Besides, EAF2 gene silencing could modulate the cytotoxic response of colon cancer cell line HCT116 to statins[10]. However, studies on the expression and role of EAF2 protein in CRC are still lacking. The molecular mechanism of involvement of EAF2 in CRC invasion and metastasis remains unclear.

EAF2 has been shown to attenuate transforming growth factor beta 1 (TGF-β1)-induced G1 cell cycle arrest and cell migration in a variety of tumor cells, such as renal carcinoma cells, human hepatocellular carcinoma cells, and breast cancer cells[11]. It is worth noting that blocking the TGF-β1 signaling pathway may be a therapeutic strategy for attenuating tumor metastasis in CRC metastatic models[12]. In addition, the signal transducer and activator of transcription 3 (STAT3) pathway is involved in the process of TGF-β1-induced epithelial-mesenchymal transition (EMT), and cell migration and invasion in malignant tumor[13,14]. As well, EAF2 knockout induced STAT3 phosphorylation (Tyr705) in prostate cancer cells, which drove tumor progression in prostate cancer[15]. Therefore, in this study, we investigated the effect of EAF2 on the STAT3/TGF-β1 pathway in CRC cells to explore the possible mechanism of action of EAF2 in CRC.

All tissues in the body need blood vessels to provide nutrients and oxygen to maintain growth and function[16], so angiogenesis provides necessary functions in normal growth and biological development processes, such as embryonic development, bone formation, and the function of ovaries

and other endocrine glands[17]. Not only that, tumor growth and metastasis also require angiogenesis [18]. Abnormalities in vasculogenesis and spermatogenesis have been found in EAF2 knockout mice [19]. Besides, EAF2 negatively regulated the activity of angiogenic factor hypoxia inducible factor (HIF)-1α[20]. Therefore, exploring the regulatory role of EAF2 in CRC angiogenesis may provide a theoretical basis for anti-angiogenic treatment. Activation of the JAK2/STAT3 (Tyr705) signaling pathway in CRC cells promoted cell proliferation and angiogenesis by positively regulating HIF-1α/vascular endothelial growth factor A (VEGFA)[21,22]. Meanwhile, HIF-1α sumoylation may elevate the microvascular density and lumen size and promote tumor growth by amplifying TGF-β/Smad signaling in tumor cells [23,24]. Therefore, we further investigated the role of EAF2 in CRC angiogenesis *via* the STAT3/TGF-β1 pathway.

In this study, we aimed to determine the clinical value of expression of EAF2 protein in CRC. Furthermore, we studied the effects of EAF2 on the invasion, migration, and angiogenesis of CRC cells *in vitro*. In addition, we preliminarily explored the mechanism by which EAF2 affects the biological function and angiogenesis of CRC cells *via* regulating the STAT3/TGF-β1 pathway. Our findings are of great significance to provide a new idea and theoretical basis for the targeted diagnosis and therapy of CRC.

MATERIALS AND METHODS

CRC patients and tissue samples

We selected 70 cases of advanced CRC from the First Affiliated Hospital of China Medical University (Liaoning, China) between 2012 and 2015. This study was approved by the Institutional Review Board of the First Affiliated Hospital of China Medical University (Registration No. 2021-68-2; informed consent was waived). Seventy pairs of histological sections of colorectal adenocarcinomas and corresponding paracancerous tissue that had been surgically removed were studied. In addition, another eight pairs of fresh cancer and adjacent tissue were selected for western blot assay. None of patients received radiotherapy or chemotherapy prior to surgical resection. We defined tumor stages according to the American Joint Committee on Cancer/Union for International Cancer Control TNM staging system (8th Edition).

Reagents

Recombinant human TGF-β1 (mammalian derived) was bought from PeproTech (100-21) (United States). The antibodies used in this study include: Rabbit monoclonal anti-EAF2 (ab237753) (for IHC-P), rabbit monoclonal anti-EAF2 [EPR7117(2)] (ab151692) (for western blot) (Abcam, United Kingdom); rabbit monoclonal anti-TGF-β1 (56E4) (#3709), rabbit monoclonal anti-phospho-STAT3 (Tyr705) (#9145), rabbit monoclonal anti-STAT3 (#30835) (Cell Signaling, Danvers, MA, United States); rabbit polyclonal anti-glyceraldehyde-3-phosphate dehydrogenase (GAPDH) (FL-335) (Santa Cruz, CA, United States).

Cell culture

CRC cell lines (SW480, RKO, HCT116, HT29, and HIEC) and the human normal colon cell line NCM460 were purchased from the Cell Bank of the Chinese Academy of Science (Shanghai, China). And these cells were cultured in RPMI-1640 medium (Gibco, Grand Island, NY, United States) containing 10% fetal bovine serum (FBS) (Gibco) at 37 °C with 5% CO_2 in a humidified incubator. Human umbilical vein endothelial cells (HUVECs) were also purchased from the Cell Bank of the Chinese Academy of Science (Shanghai, China) and cultured in DMEM medium (Gibco) containing 10% FBS at 37 °C with 5% CO_2 in a humidified incubator.

Cell transfection

The plasmid for overexpressing human EAF2 (GenBank No. NM_018456) was designed and synthesized by GeneChem (Shanghai, China). And three plasmid targets for silencing human STAT3 (GenBank No. NM_139276) were also provided by GeneChem. The sequences are listed in Table 1. The cell transfection was performed using the Lipofectamine 2000 Kit (Invitrogen, Carlsbad, CA, United States). Cells were plated into six-well plates and transfected with 4.0 μg plasmid DNA. Six hours after transfection, cells were treated with medium containing 10% FBS.

Immunohistochemistry

Typical CRC tissues and corresponding paracancer tissues were selected. The sections were dewaxed, rehydrated, and heated using a pressure-cooker for antigen retrieval. And then antigenic repair was performed with citric acid. Subsequently, the sections were incubated overnight at 4 °C with rabbit monoclonal anti-EAF2 antibody (1:200 dilution, ab237753), followed by incubation with the secondary antibody for 40 min at 37 °C. Finally, the slides were stained with diaminobenzidine, counter-stained with hematoxylin, air-dried, dehydrated, and mounted.

Table 1 Gene sequences used for transfection

Gene	Sequences	
STAT3-siRNA	1-siRNA	5′-CCGGGCTGACCAACAATCCCAAGAACTCGAGTTCTTGGGATTGTTGGTCAGCTTTTT G-3′
	Anti-sense	5′-AATTCAAAAAGCTGACCAACAATCCCAAGAACTCGAGTTCTTGGGATTGTTGGTCAGC-3′
	2-siRNA	5′-CCGGGCACAATCTACGAAGAATCAACTCGAGTTGATTCTTCGTAGATTGTGCTTTTTG-3′
	Anti-sense	5′-AATTCAAAAAGCACAATCTACGAAGAATCAACTCGAGTTGATTCTTCGTAGATTGTGC-3′
	3-siRNA	5′-CCGGGCTGAAATCATCATGGGCTATCTCGAGATAGCCCATGATGATTTCAGCTTTTTG-3′
	Anti-sense	5′-AATTCAAAAAGCTGAAATCATCATGGGCTATCTCGAGATAGCCCATGATGATTTCAGC-3′

STAT3: Signal transducer and activator of transcription 3.

Double blind reading was performed by two experienced pathologists. We calculated the final staining score by multiplying the positive expression score by the intensity score. Five high-power fields (magnification at 200 ×) were observed on each section. We divided the immunostaining intensity into four categories: 0 (negative immunostaining), 1 (weak immunostaining), 2 (moderate immunostaining), and 3 (strong immunostaining). And the proportion of positive cells scored from 0 to 4 as follows: (1) 0 (positive cells < 5%); (2) 1 (positive cells 5% to 25%); (3) 2 (positive cells 26% to 50%); (4) 3 (positive cells 51% to 75%); and (5) 4 (positive cells > 75%).

Western blot assay

The tissues and cells were lysed in RIPA lysis buffer containing protease inhibitors such as phenylmethylsulfonyl fluoride. Protein concentrations were measured with a BCA kit (Beyotime Institute of Biotechnology, China). Equal amounts of protein (50 μg per sample) were separated by 10% sodium dodecyl sulfate/polyacrylamide gel electrophoresis and then transferred onto polyvinylidene difluoride membranes at a 200 mA constant current. Primary antibodies for EAF2 (ab151692), TGF-β1, phospho-STAT3 (Tyr705), STAT3, and GAPDH were used at a dilution ratio of 1:1000. Then, anti-rabbit immunoglobulin G secondary antibody (1:5000) was used to incubate the membranes at 37 °C for 2 h. The immunoreactive bands were detected with ECL-Plus chemiluminescent detection reagents (Beyotime Institute of Biotechnology) and using the Microchemi 4.2 Bio-imaging system. The expression of proteins of interest was normalized to that of GAPDH. Experiments were repeated at least three times under the same experimental conditions.

Transwell invasion and migration assays

Before invasion assay, Matrigel (BD Biosciences, San Diego, CA, United States) diluted at a ratio of 1:8 with serum-free medium was used to block the membranes at 37 °C for 6 h. A total of 4 × 10^4 cells/well in 200 μL serum-free medium were seeded in the upper chambers of 8-μM pore transwell plates (3422; Corning Incorporated, NY, United States), and 600 μL medium containing 20% FBS was added to the lower chambers. For migration assay, 2 × 10^5 cells/well were seeded into the upper chambers of 8-μM pore transwell plates (3422) in 200 μL serum-free medium. The lower chambers were filled with 600 μL medium with 10% FBS.

After incubation for 72h, the non-invaded or non-migrated cells on the inner surface of the filter membrane were removed by scrubbing with a cotton swab, and the invaded or migrated cells were fixed by methanol. Next, the cells were stained with 0.1% crystal violet. The membranes were moved from the chambers and fixed on cover slides. Invading or metastasizing cells were counted from five random fields under a light microscope (magnification at 200 ×). The experiments were repeated at least three times under the same experimental conditions.

Wound healing assay

A total of 2 × 10^5 cells/well were seeded into 6-well plates. Scratch wounds were generated using a 200 μL pipette tip when the cells reached 90% confluence. Afterwards, the cells were washed with phosphate buffered saline (PBS) three times, and then incubated in medium containing 2% serum. The scratch wounds were photographed at 0 h, 6 h, 12 h, 24 h, 48 h, and 72 h in five selected regions. ImageJ software (Version 1.46r) was used to measure the wound area (magnification at 40 ×). The experiments were repeated at least three times under the same experimental conditions.

Tube formation assay

Before tube formation assay, Matrigel was placed in a 96-well plate at 37 °C for 1 h. And the conditioned medium from treated RKO cells was collected and centrifuged at 2000 rpm for 10 min to remove debris. HUVECs at 1.0 × 10^4 cells/well were seeded in a Matrigel coated 96-well plate and cultured in

conditioned medium. After 6 h, capillary morphogenesis was evaluated by inverted microscopy (magnification at 100 ×). Then, we analyzed the images for evaluating the branch points by means of the angiogenesis analyzer that was developed for the Image J software (Version 1.46r).

HUVEC transwell migration assay

For HUVEC migration assay, 1 × 10^5 HUVECs were plated in the upper chambers of 8-μM pore transwell plates (3422) with 200 μL serum-free medium; 600 μL conditioned medium was placed in the lower chambers. After 6 h, the cells were fixed with methanol and non-migrated cells were removed from the inner surface of the filter membrane. The cells on the lower surface of the membrane were stained with 0.1% crystal violet, and the number of migrated cells was counted from five fields (magnification at 200 ×) under an optical microscope. The experiments were repeated at least three times under the same experimental conditions.

HUVEC scratch assay

For scratch assay, 2 × 10^5 HUVECs/well were seeded in 6-well plate. When cells reached about 90% confluence, a 200 μL tip was used to scratch the cells. The cells were then washed with PBS three times and incubated with 2 mL conditioned medium per well. The scratch was photographed at 0 h, 12 h, and 24 h time points under a microscope in five selected regions (magnification at 40 ×). ImageJ software (Version 1.46r) was used to measure the wound area. Experiments were repeated at least three times under the same experimental conditions.

Statistical analysis

The results in this study were analyzed with SPSS software (Version 26). Pearson's chi-squared test was adopted to evaluate the correlation between EAF2 protein and clinicopathological parameters. The expression differences of EAF2 between paired adenocarcinoma and paracancerous tissues were analyzed by Wilcoxon sign rank test. Receiver operating characteristic (ROC) curve was used to determine the Youden index to delimit the high and low expression of EAF2 in tissues. The data are shown as the mean ± SD. Student's *t* test was used for analyzing the differences between two groups, while for differences among three or more groups, one-way ANOVA was performed. The Kaplan-Meier method was used to estimate the cumulative survival of patients, and the Log-rank test was used to test the significance of the differences in survival. Cox proportional hazards regression model was used for multivariate analysis to evaluate the independent prognostic effect of EAF2 protein on survival. All the statistics were subjected to ANOVA followed by Bonferroni test. Two-sided *P* values < 0.05 were considered statistically significant.

RESULTS

EAF2 protein expression is decreased in advanced CRC tissue

To assess the expression and localization of EAF2 protein in CRC specimens, we examined the expression of EAF2 at the protein level in paired adenocarcinoma and paracancerous tissues by immunohistochemical analysis and western blot assay. Immunohistochemical analysis showed that EAF2 protein was mainly localized in the cytoplasm of colorectal epithelial cells (Figure 1A). The median EAF2 score was 6.0 in tumor tissue and 6.8 in adjacent non-tumor tissue, with a median difference of -2.0. Moreover, Wilcoxon signed-rank test of paired samples showed that EAF2 expression was lower in tumor tissue than in non-tumor tissue ($Z = -3.727$, $P < 0.001$). Additionally, we used western blot assay to measure the level of EAF2 protein expression in eight matched pairs of fresh colorectal adenocarcinoma and corresponding paracancerous tissue. The results also revealed a lower level of EAF2 protein expression ($P = 0.012$) in tumor tissue compared with adjacent non-tumor tissue (Figure 1B). According to the Youden index determined by ROC curve, the cut-off value delimiting high and low expression of EAF2 (dependent variable is non-cancer) was determined to be 6.2 ($P < 0.001$). In this study, we found low EAF2 expression in 58 of 70 CRC tissues.

We then assessed the relationship between EAF2 protein expression and major clinicopathological characteristics. Statistical results showed that the expression of EAF2 protein in CRC tissue was negatively correlated with distant metastasis ($r = -0.268$, $P = 0.025$) and carcinoembryonic antigen (CEA) ($r = -0.249$, $P = 0.038$), but not with other clinical characteristics, such as age, sex, primary tumor site, tumor size, tumor histological differentiation, degree of differentiation, vasculolymphatic and/or perineural invasion, tumor stage, tumor invasion depth, lymph node status, carbohydrate antigen 19-9 (CA19-9), P53, or CDX2 (Table 2). High expression of CEA, CA19-9, P53, and CDX2 was defined as a score of ≥ 3, and their low expression was defined as a score of < 3.

Survival analysis of EAF2 expression in patients with advanced CRC

Kaplan-Meier survival analysis and Log-rank testing for overall survival (OS) showed that the survival rate of the group with high EAF2 level was higher than that of the group with low EAF2 level (*P* =

Table 2 Baseline characteristics of patients with advanced colorectal cancer and their correlation with immunohistochemical expression of ELL-associated factor 2

Clinicopathologic characteristic	Cases, *n* (%)	EAF2		*P* value
		Low (*n* = 58)	High (*n* = 12)	
Age (yr)				0.831
< 61 (median)	47.14	27	6	
≥ 61	52.86	31	6	
Gender				0.589
Male	57.14	34	6	
Female	42.86	24	6	
Tumor site				0.162
Colon	34.29	22	2	
Rectum	65.71	36	10	
Size of the tumor (cm)				0.726
≤ 4	37.14	21	5	
> 4	62.86	37	7	
Histological type				0.210
Mucinous	20.00	10	4	
Non-mucinous	80.00	48	8	
Degree of differentiation				0.318
Well/moderate	62.86	38	6	
Poor/mucinous	37.14	20	6	
Angiolymphatic and/or perineural invasion				0.113
Absent	45.71	24	8	
Present	54.29	34	4	
Tumor stage (TNM)				0.240
I-II	42.86	23	7	
III-IV	57.14	35	5	
Tumor invasion depth				0.682
T2-T3	52.86	30	7	
T4	47.14	28	5	
Lymph node status				0.210
N0	50.00	27	8	
N1-N2	50.00	31	4	
Distant metastasis				0.025
Absent	74.29	40	12	
Present	25.71	18	0	
CEA				0.038
Normal	65.71	35	11	
High	34.29	23	1	
CA19-9				0.445
Normal	40.00	22	6	
High	60.00	36	6	

P53				0.589
Normal	42.86	24	6	
High	57.14	34	6	
CDX2				0.350
Normal	22.86	12	4	
High	77.14	46	8	

EAF2: ELL-associated factor 2; TNM: Tumor-node-metastasis; CEA: Carcinoembryonic antigen; CA19-9: Carbohydrate antigen 19-9.

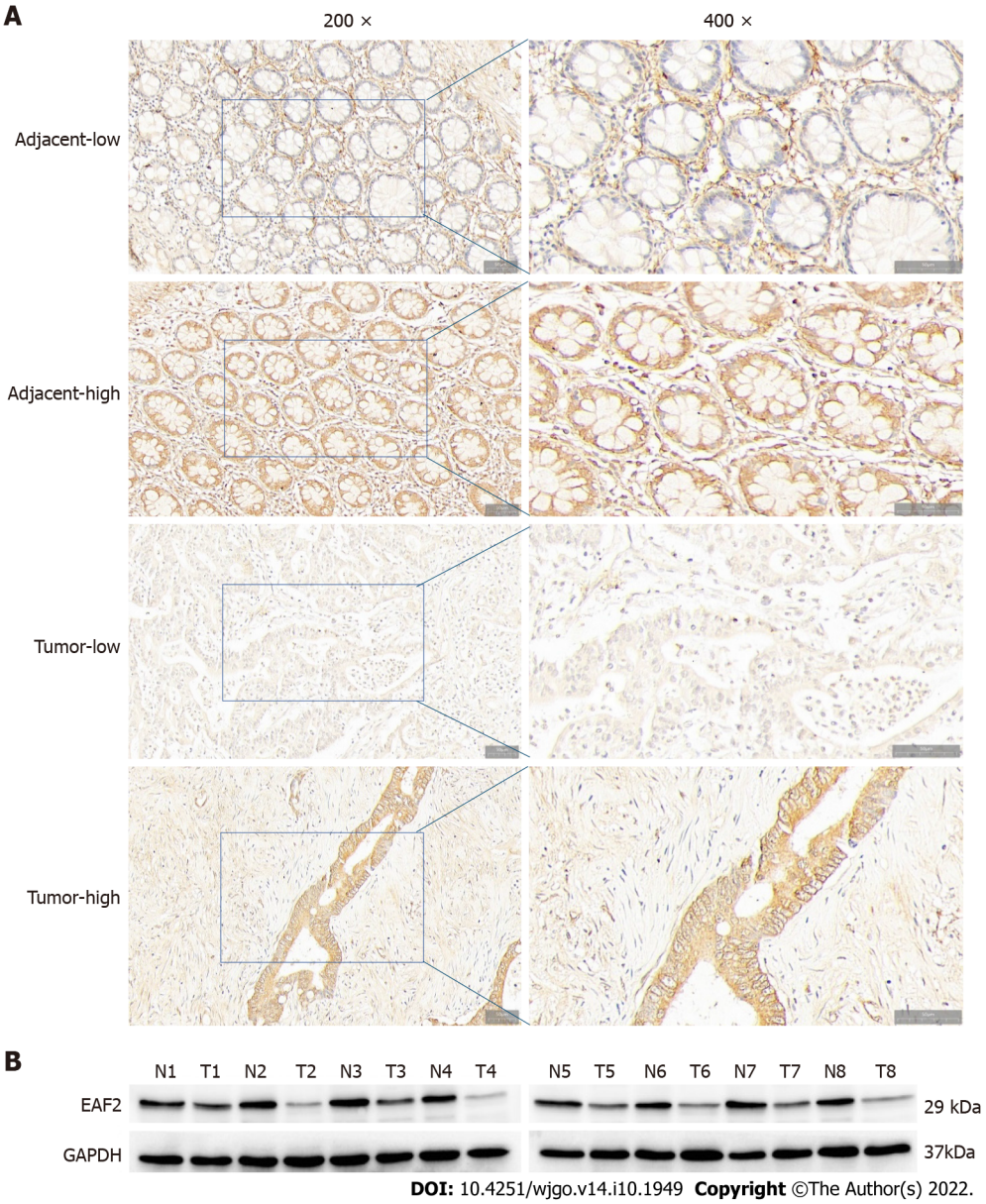

DOI: 10.4251/wjgo.v14.i10.1949

Figure 1 ELL-associated factor 2 protein is decreased in colorectal cancer tissue. A: Representative immunohistochemical staining for ELL-associated factor 2 (EAF2) in colorectal adenocarcinoma tissue and adjacent tissue (magnification, 200 × and 400 ×); B: western blot showing lower EAF2 level in colorectal adenocarcinoma fresh tissue than in corresponding para-cancerous tissue (T, colorectal adenocarcinoma tissue; N, adjacent non-tumor tissue). EAF2: ELL-associated factor 2; GAPDH: Glyceraldehyde-3-phosphate dehydrogenase.

0.026). Figure 2 shows the Kaplan-Meier survival curves of advanced CRC patients with high and low EAF2 expression. We used Cox proportional-hazards model to evaluate the effect of EAF2 protein on OS in patients with advanced CRC. From univariate analysis, we found that angiolymphatic and/or perineural invasion (P = 0.003), tumor stage (P = 0.012), tumor invasion depth (P = 0.011), lymph node

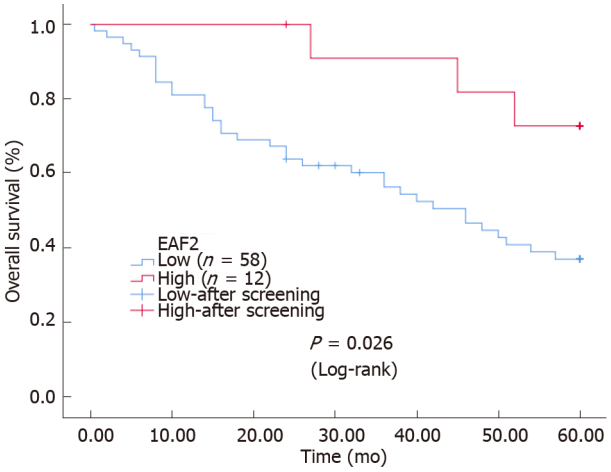

DOI: 10.4251/wjgo.v14.i10.1949

Figure 2 Kaplan-Meier survival curves for ELL-associated factor 2 expression in colorectal cancer tissue. The survival rate of the group with high ELL-associated factor 2 (EAF2) levels was higher than that of the group with low EAF2 levels. EAF2: ELL-associated factor 2.

status (P = 0.017), distant metastasis (P < 0.001), and EAF2 protein expression level (P = 0.038) were significantly correlated with OS (Table 3). The clinicopathological characteristics with P < 0.3 in univariate analysis were included in multivariate analysis, and the independent prognostic effect of EAF2 protein on OS was assessed by adjusting for confounding factors. However, multivariate analysis proved that tumor invasion depth (P = 0.035) and distal metastasis (P < 0.001) were independent prognostic factors for OS (Table 3).

Overexpression of EAF2 inhibits invasion and migration of CRC cells

We cultured CRC cells *in vitro* to determine the expression of EAF2 protein and further investigate its effects on the biological function of CRC cells. The expression level of EAF2 protein in human CRC cell lines (SW480, RKO, HCT116, HT29, and HIEC) were observably lower than that in normal colorectal epithelial cells (NCM460) (Figure 3). There was a considerable decrease (64.11%) in EAF2 protein expression in colon cancer RKO cells (P < 0.001) (Figure 3). Thus, we used RKO cells in subsequent experiments.

Subsequently, we overexpressed EAF2 protein by plasmid transfection technique to investigate the effects of EAF2 overexpression on the invasion and migration of RKO cells. EAF2 overexpression significantly increased the protein expression level in RKO cells, which was 2.25-fold higher than that of the control group (Figure 4A, P < 0.001). Results of transwell invasion assay showed that EAF2 overexpression significantly weakened the invasion ability of RKO cells (Figure 4B, P < 0.001). Analogously, cells transfected with EAF2-overexpressing plasmid also showed a poorer migration capacity than the control group in the transwell migration assay (Figure 4B, P < 0.001). In addition, as shown in Figure 4C, EAF2 overexpression reduced the wound healing ability of RKO cells (P < 0.001).

Overexpression of EAF2 suppresses the activity of STAT3/TGF-β1 crosstalk pathway

In this study, we set out to investigate the molecular mechanism of EAF2 on RKO cells *in vitro*. Phosphorylated STAT3 (Tyr705) and TGF-β1 protein expression levels were significantly increased in human CRC cell lines (SW480, RKO, HCT116, HT29, and HIEC) compared with normal colorectal epithelial cells (NCM460) (Figure 3). The upregulation of phosphorylated STAT3 protein (Tyr705) (with a 1.585-fold increase, P < 0.001) and TGF-β1 protein (with a 2.485-fold increase, P < 0.001) in RKO cells was statistically significant.

Compared with control cells, TGF-β1 protein expression level was significantly decreased in RKO cells transfected with EAF2-overexpressing plasmid (Figure 5A). Meanwhile, we also found that overexpression of EAF2 remarkably decreased phosphorylated STAT3 (Tyr705) levels in RKO cells, but not total STAT3 levels (Figure 5A).

And then we knocked down STAT3 gene by transfecting with STAT3 siRNA (Figure 6A). We found that inhibition of STAT3 phosphorylation (with a reduction of 60.25%, P < 0.001) resulted in a significant decrease in TGF-β1 protein expression (P < 0.001) in RKO cells but not in EAF2 (P = 0.228) (Figure 6B). Furthermore, we treated RKO cells with TGF-β1 recombinant protein to clarify the regulatory effect of TGF-β1 on EAF2 protein expression and STAT3 phosphorylation. The results revealed that TGF-β1 recombinant protein reversed the decrease of phosphorylated STAT3 (Tyr705) induced by EAF2 overexpression (P < 0.001) (Figure 5A). However, our results showed that TGF-β1 recombinant protein did not affect the expression of EAF2 protein (P = 0.099) in RKO cells (Figure 5A).

Table 3 Univariate and multivariate survival analyses of overall survival for colorectal cancer by Cox regression

Variable	Univariate analysis			Multivariate analysis		
	HR	95%CI	*P* value	HR	95%CI	*P* value
Age (yr) (≥ 61/< 61)	1.203	0.633-2.284	0.573			
Gender (female/male)	0.894	0.472-1.695	0.732			
Tumor site (colon/rectum)	1.524	0.791-2.935	0.208	0.682	0.288-1.618	0.386
Size of the tumor, cm (> 4/≤ 4)	0.929	0.479-1.799	0.827			
Histological type (mucinous/non-mucinous)	1.481	0.619-3.544	0.378			
Degree of differentiation (poor/mucinous, well/moderate)	0.863	0.446-1.670	0.661			
Angiolymphatic and/or perineural invasion (present/absent)	0.342	0.169-0.693	0.003	0.194	0.036-1.042	0.056
Tumor stage (III-IV/I-II)	0.404	0.200-0.816	0.012	4.199	0.603-29.234	0.147
Tumor invasion depth (T4/T2-T3)	0.426	0.221-0.822	0.011	0.253	0.071-0.908	0.035
Lymph node status (N1-N2/N0)	0.447	0.231-0.867	0.017	3.138	0.766-12.863	0.112
Distant metastasis (present/absent)	0.203	0.105-0.393	< 0.001	0.149	0.056-0.397	< 0.001
EAF2 (low/high)	3.481	1.069-11.341	0.038	2.261	0.653-7.829	0.198
CEA (high/low)	1.092	0.559-2.136	0.796			
CA19-9 (high/low)	0.740	0.378-1.446	0.378			
P53 (high/low)	0.579	0.295-1.134	0.111	0.697	0.336-1.448	0.333
CDX2 (high/low)	0.694	0.305-1.576	0.383			

HR: Hazard ratio; CI: Confidence interval; EAF2: ELL-associated factor 2; CEA: Carcinoembryonic antigen; CA19-9: Carbohydrate antigen 19-9.

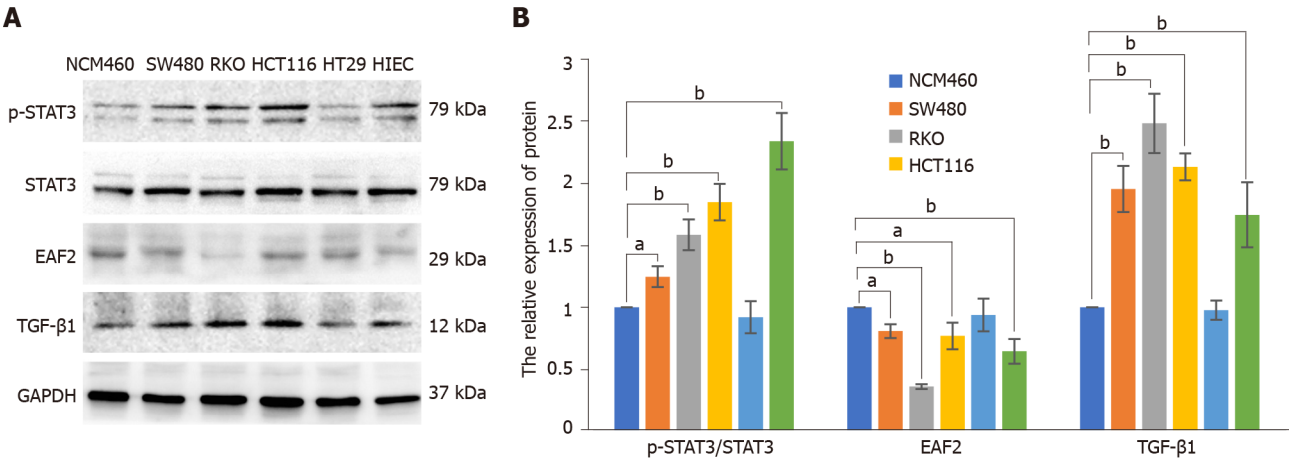

DOI: 10.4251/wjgo.v14.i10.1949

Figure 3 Protein levels of ELL-associated factor 2, phosphorylated-signal transducer and activator of transcription 3, and transforming growth factor-β1 in colorectal cancer cell lines (SW480, RKO, HCT116, HT29, and HIEC) and normal colorectal epithelial cells (NCM460) by western blot assay. A: Western blot results of proteins in in colorectal cancer cell lines (SW480, RKO, HCT116, HT29, and HIEC) and normal colorectal epithelial cells (NCM460); B: Relative expression of the proteins. The data are shown as the mean ± SD. $^{a}P < 0.05$, $^{b}P < 0.001$. p-STAT3: Phosphorylated-signal transducer and activator of transcription 3; TGF-β1: Transforming growth factor-β1; EAF2: ELL-associated factor 2; GAPDH: Glyceraldehyde-3-phosphate dehydrogenase.

Overexpression of EAF2 inhibits invasion and migration of CRC cells by down-regulating the activity of STAT3/TGF-β1 crosstalk pathway

We attempted to further determine whether EAF2 regulates the biological function of CRC cells by regulating the activity of STAT3/TGF-β1 crosstalk pathway. We used TGF-β1 recombinant protein to treat the RKO cells transfected with EAF2-overexpressing plasmid for 24 h. As a result, the invasiveness and metastasis capability of RKO cells weakened by EAF2 overexpression was partially reversed by

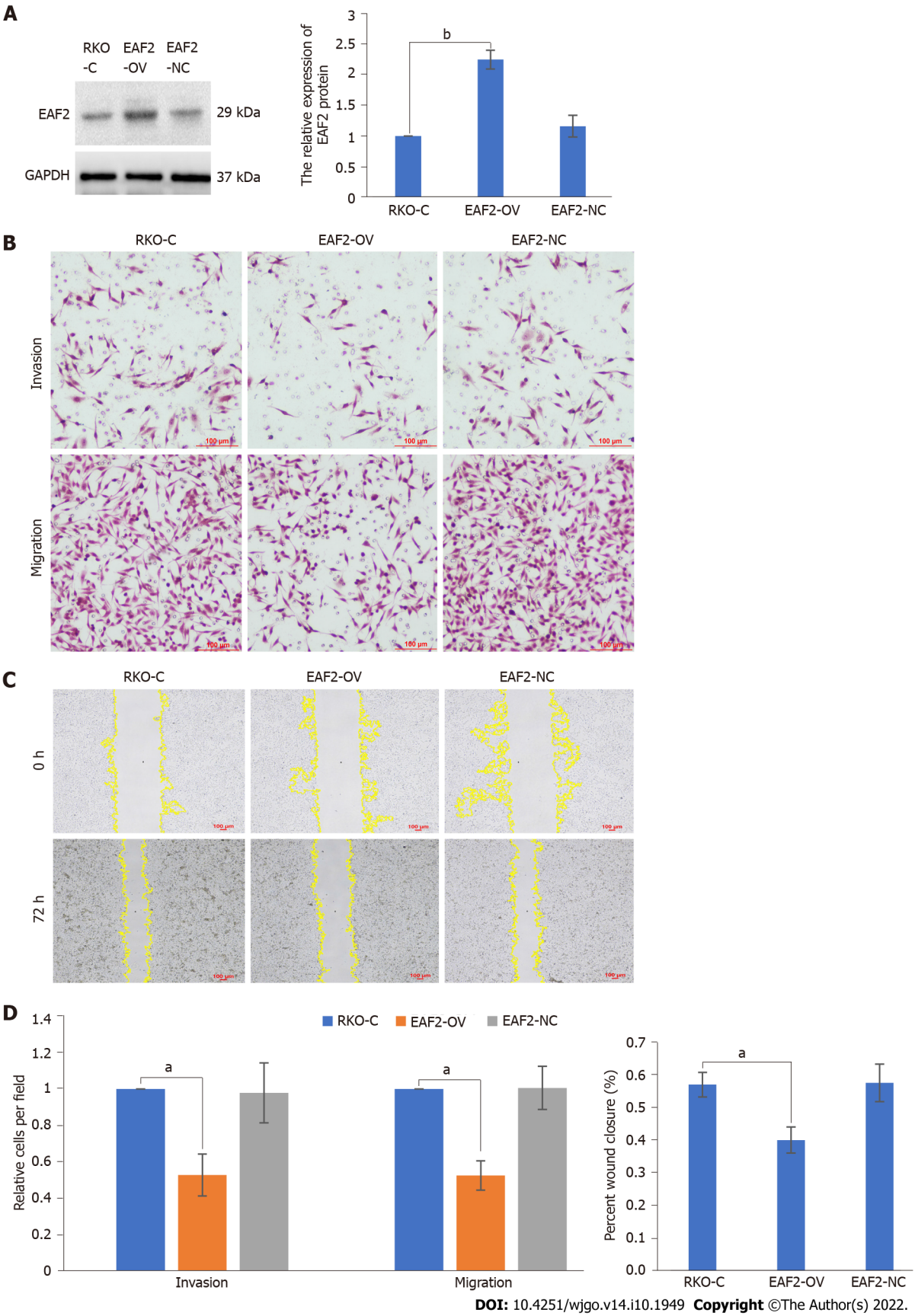

DOI: 10.4251/wjgo.v14.i10.1949

Figure 4 Overexpression of ELL-associated factor 2 inhibits the invasion and migration of RKO cells. A: Protein levels of ELL-associated factor 2 (EAF2) in RKO cells transfected with EAF2 overexpression vector by western blot assay; B: Invasion and migration abilities evaluated by transwell assay; C: Migration ability analyzed by wound healing assay after 72 h; D: Migration and invasion abilities of RKO cells measured using ImageJ software. The data are shown as the mean ± SD. $^{a}P < 0.001$; $^{b}P < 0.05$. RKO-C: The group of RKO control cells; EAF2-OV: The group of RKO cells transfected with ELL-associated factor 2 overexpression vector; EAF2-NC: The group of RKO cells transfected empty vector; EAF2: ELL-associated factor 2; GAPDH: Glyceraldehyde-3-phosphate

dehydrogenase.

TGF-β1 recombinant protein (Figures 5B and 5C).

Overexpression of EAF2 inhibits CRC angiogenesis

In this study, we preliminarily investigated the effects of RKO cells overexpressing EAF2 on the migration and tube formation abilities of HUVECs. First, HUVECs were cultured with DMEM medium containing 10% serum[25]. After 2-6 passages of cells, HUVECs were subcultured into corresponding petri dishes. We then treated HUVECs with conditioned medium from RKO cells transfected with EAF2-overexpressed plasmid (EAF2-OV group) or empty control plasmid (EAF2-NC group) for 24 h. Compared with the control group (RKO-C group), whose conditioned medium was collected from RKO cells cultured with 10% serum for 24 h, the tube formation (Figure 7A) and migration (Figures 7B and 7C) of HUVECs in the EAF2-OV group were significantly reduced, while the differences in the EAF2-NC group were not statistically significant. Our results indicated that overexpression of EAF2 protein may inhibit angiogenesis induced by CRC cells *in vitro*.

Overexpression of EAF2 regulates CRC angiogenesis via STAT3/TGF-β1 signaling pathway

STAT3-related pathway and non-specific angiogenic factor TGF-β1 play a proangiogenic role in tumor angiogenesis. Our study showed that overexpression of EAF2 inhibits the activity of the STAT3/TGF-β1 crosstalk pathway in RKO cells. Hence, we next investigated whether EAF2 inhibits CRC angiogenesis through the STAT3/TGF-β1 signaling pathway. We used TGF-β1 recombinant protein to treat RKO cells transfected with or without EAF2-overexpressing plasmid for 24 h, and collected conditioned medium to culture HUVECs. We aimed to investigate whether TGF-β1-related pathways are involved in the molecular mechanism of EAF2 overexpression regulating angiogenesis in RKO cells *in vitro*. Compared with the RKO-C group, the tube formation (Figure 8A) and migration (Figures 8B and 8C) of HUVECs in the EAF2-OV group were significantly decreased. Interestingly, when HUVECs were cultured with conditioned medium from EAF2-overexpressing RKO cells treated with TGF-β1 recombinant protein, the inhibition of EAF2 overexpression on tube formation (Figure 8A) and migration (Figures 8B and 8C) of HUVECs was reversed. Together, these data confirmed our hypothesis that EAF2 overexpression inhibits CRC angiogenesis by suppressing the activity of the STAT3/TGF-β1 crosstalk pathway *in vitro*.

DISCUSSION

Previous studies have supported the role of EAF2 as a tumor suppressor in multiple human tissues[6]. EAF2 knockout mice developed a higher frequency of B-cell lymphoma, lung adenocarcinoma, hepatocellular carcinoma, and prostatic intraepithelial neoplasia[6]. EAF2 and its homologue EAF1 were originally identified as binding partners of the fusion protein ELL (11-19 lysine-rich leukemia) associated with myeloid leukemia[26,27], stimulating the extension activity of ELL. However, EAF2 mutations produce truncated EAF2 mutants, which may be associated with the pathogenesis of MSI-high cancers[9]. Recently, further studies have found ITH in EAF2 frameshift mutations in CRC and the inactivation of EAF2 in MSI-high CRC[9], suggesting that EAF2 mutations may occur during tumor progression rather than during tumorigenesis. However, the expression, role, and molecular mechanism of EAF2 protein in CRC remain unclear.

This study collected colorectal adenocarcinoma and paired adjacent tissues to investigate the clinical expression of EAF2 protein in patients with advanced CRC. Compared with non-tumor tissue, the results of immunohistochemistry and western blot assay showed that the level of EAF2 protein in CRC tissue was significantly lower. And immunohistochemical results indicated that EAF2 protein was mainly expressed in the cytoplasm. Meanwhile, *in vitro* experiments also confirmed that EAF2 expression level in CRC cells was lower than that in normal colorectal epithelial cells. Further analysis of the correlation between EAF2 expression level and clinicopathological characteristics revealed that EAF2 protein level was negatively correlated with distant metastasis and CEA expression level in CRC tissues. These results suggest that EAF2 protein may be related to the invasion and metastasis of CRC. However, further studies are needed to determine the mechanism of decreased EAF2 protein expression in CRC.

Besides, Kaplan-Meier survival analysis showed that the survival rate of the group with high EAF2 levels was higher than that of the group with low EAF2 levels. Although multivariate analysis did not suggest that EAF2 expression level was an independent survival prognostic marker in patients with advanced CRC, univariate analysis suggested that it was an influential factor of survival and prognosis in patients with advanced CRC. However, more cases and more comprehensive clinical studies are needed to further explore this question.

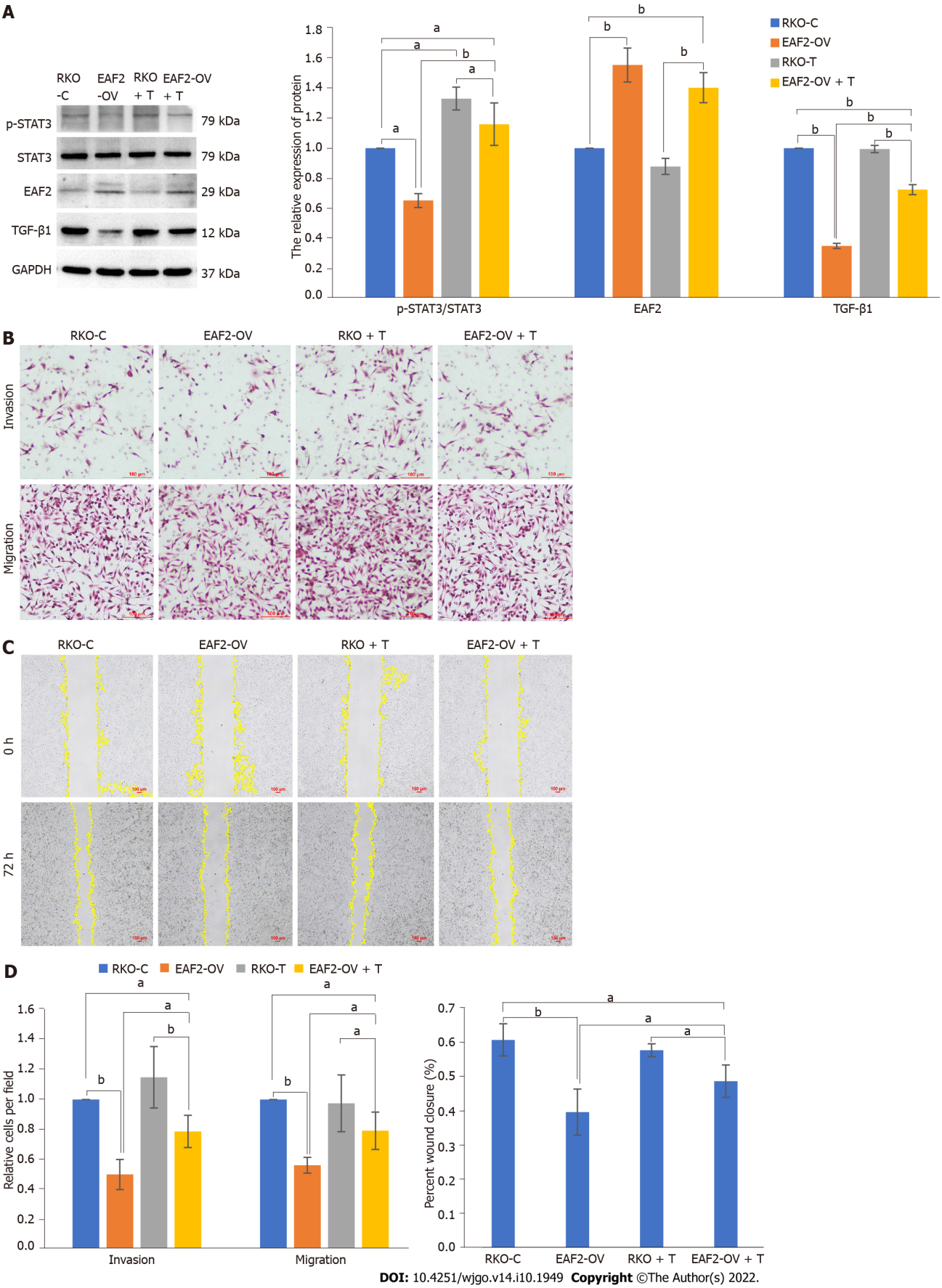

DOI: 10.4251/wjgo.v14.i10.1949

Figure 5 Overexpression of ELL-associated factor 2 suppresses the activity of the signal transducer and activator of transcription 3/transforming growth factor-β1 pathway to inhibit the invasion and migration of RKO cells. A: Overexpression of ELL-associated factor 2 (EAF2) inhibited the signal transducer and activator of transcription 3/transforming growth factor-β1 (STAT3/TGF-β1) pathway measured by western blot assay. And TGF-β1

recombinant protein abolished EAF2 overexpression-reduced the phosphorylation (Tyr705) of STAT3 protein; B: Invasion and migration abilities evaluated by transwelll assay; C: Migration ability analyzed by wound healing assay after 72 h; D: Migration and invasion abilities of RKO cells measured using ImageJ software. The data are shown as the mean ± SD. $^{a}P < 0.05$, $^{b}P < 0.001$. RKO-C: The group of RKO control cells; EAF2-OV: The group of RKO cells transfected with ELL-associated factor 2 overexpression vector; RKO + T: The group of RKO cells treated with 5 ng/mL transforming growth factor-β1 recombinant protein for 24 h; EAF2-OV + T: The group of RKO cells were transfected with EAF2-OV plasmid for 24 h and then cultured with 5 ng/mL transforming growth factor-β1 recombinant protein for 24 h; p-STAT3: Phosphorylated-signal transducer and activator of transcription 3; TGF-β1: Transforming growth factor-β1; EAF2: ELL-associated factor 2; GAPDH: Glyceraldehyde-3-phosphate dehydrogenase.

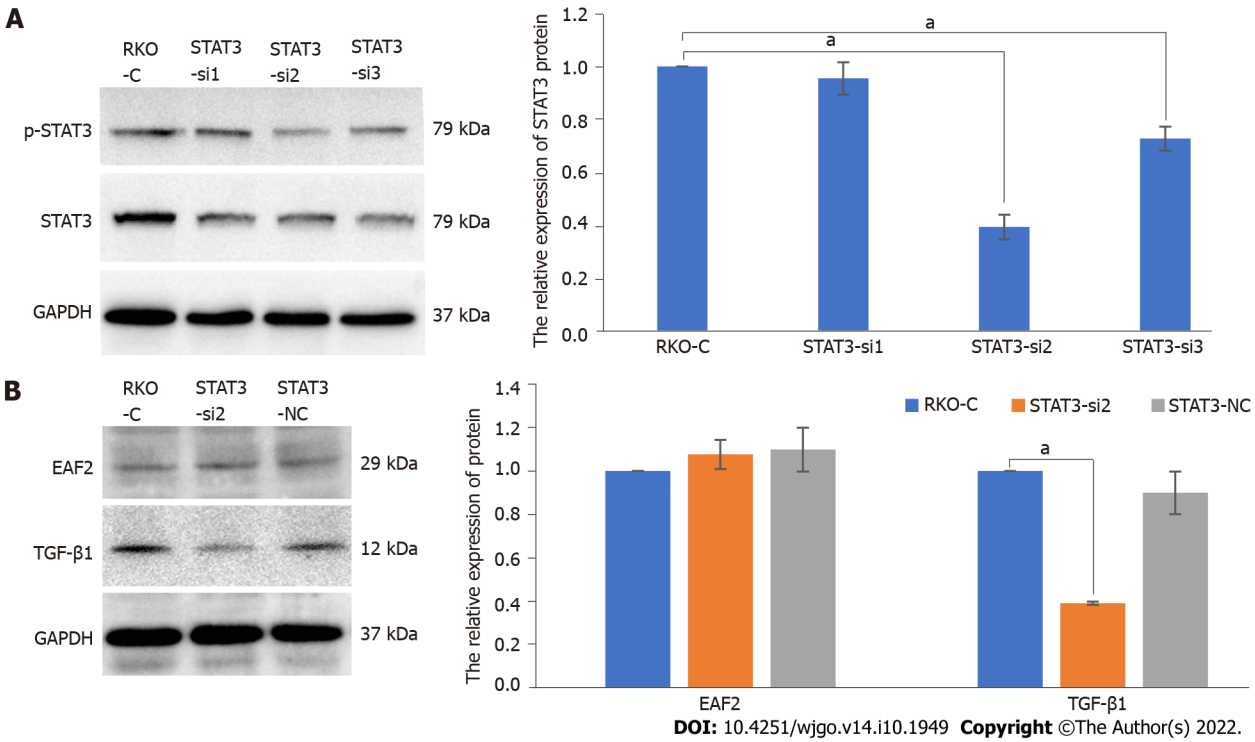

DOI: 10.4251/wjgo.v14.i10.1949

Figure 6 Silencing signal transducer and activator of transcription 3 decreases transforming growth factor-β1 protein expression in RKO cells. A: Protein levels of phosphorylated-signal transducer and activator of transcription 3 (p-STAT3) in RKO cells transfected with STAT3 siRNA plasmid by western blot assay; B: Knockdown of STAT3 decreased the levels of transforming growth factor-β1 protein but not ELL-associated factor 2 protein in RKO cells. The data are shown as the mean ± SD. $^{a}P < 0.01$. RKO-C: The group of RKO control cells; STAT3-si: The group of RKO cells transfected with signal transducer and activator of transcription 3 siRNA plasmid. STAT3-NC: The group of RKO cells transfected empty vector; p-STAT3: Phosphorylated-signal transducer and activator of transcription 3; TGF-β1: Transforming growth factor-β1; EAF2: ELL-associated factor 2; GAPDH: Glyceraldehyde-3-phosphate dehydrogenase.

In addition, phospho-STAT3 (Tyr705) and TGF-β1 protein were highly expressed in CRC cells in this study. Studies have shown that TGF-β1 is highly expressed in CRC tissue, and overexpression of TGF-β1 facilitates the invasion and migration of CRC cells *in vitro*[28]. Furthermore, blocking the TGF-β1 signaling pathway in CRC metastatic models may serve as a therapeutic strategy to weaken tumor metastasis *in vivo*[20]. Importantly, STAT3 acts as a positive regulator to activate TGF-β1 to induce tumor EMT and metastasis[14]. Meanwhile, STAT3 is one of the major oncogenic pathways activated in CRC, and its activation can be detected in CRC tissue, primary CRC cells, or CRC cell lines[29-31].

Further studies have revealed that EAF2 attenuates TGF-β1-induced G1 cell cycle arrest and cell migration, which has been demonstrated in renal carcinoma cells, human hepatocellular carcinoma cells, and breast cancer cells[11]. Besides, phospho-STAT3 (Tyr705) immunostaining is correlated with down-regulation of EAF2 in human prostate cancer specimens[15]. EAF2 knockout induces STAT3 phosphorylation (Tyr705) *in vivo* and *in vitro*, suggesting that EAF2 is a repressor of the STAT3 signaling pathway[15]. In our study, we found that overexpression of EAF2 decreased the levels of phosphorylated STAT3 (Tyr705) and TGF-β1 protein in CRC cells. In addition to this, we also found that silencing STAT3 reduced TGF-β1 protein expression. More than that, TGF-β1 recombinant protein eliminated the reduction of phosphorylated STAT3 (Tyr705) induced by EAF2 overexpression. Together, these results indicate that EAF2 overexpression may inhibit the activity of STAT3/TGF-β1 crosstalk pathway in CRC cells.

We found that EAF2 overexpression restrains the invasion and metastasis of CRC cells. It makes sense to further explore the role of EAF2 in regulating the activity of the STAT3/TGF-β1 crosstalk pathway in CRC cell invasion and metastasis. The results revealed that the invasiveness and metastasis capability of CRC cells weakened by EAF2 overexpression could be partially reversed by TGF-β1

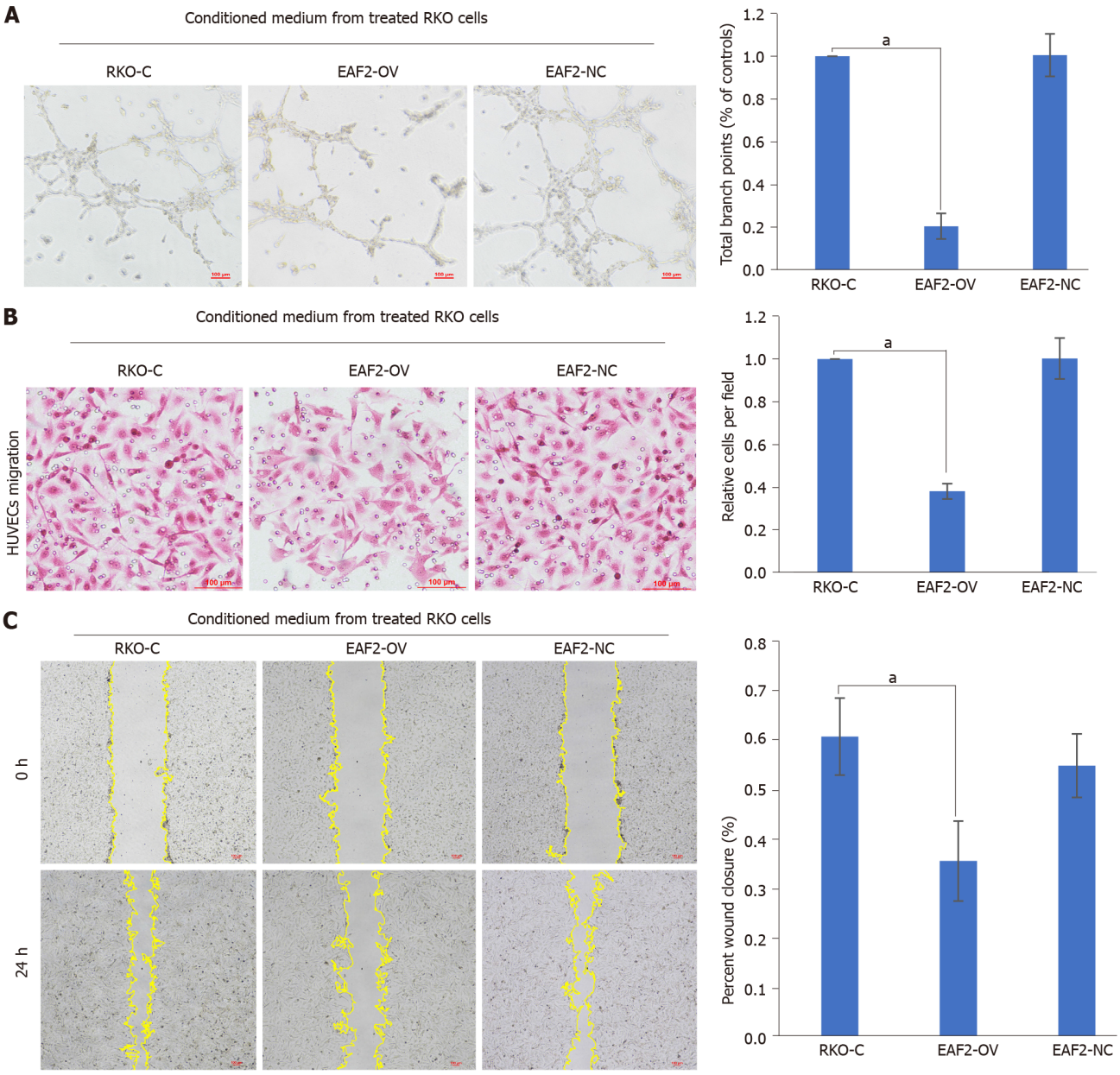

DOI: 10.4251/wjgo.v14.i10.1949

Figure 7 Overexpression of ELL-associated factor 2 in RKO cells inhibits tumor-induced angiogenesis. A: Conditioned medium from RKO cells transfected with ELL-associated factor 2-overexpressed plasmids or empty control plasmids was collected to perform tube formation assay; B: Migration ability of human umbilical vein endothelial cells (HUVECs) analyzed by transwell migration assay; C: Migration ability of HUVECs analyzed by wound healing assay. And the results were measured with ImageJ software. The data are shown as the mean ± SD. $^{a}P < 0.001$. HUVECs: Human Umbilical Vein Endothelial Cells; RKO-C: The group of Human Umbilical Vein Endothelial Cells cultured with conditioned medium from RKO cells cultured with 10% serum for 24 h; EAF2-OV: The group of human umbilical vein endothelial cells cultured with conditioned medium from RKO cells transfected with ELL-associated factor 2-overexpressed plasmids for 24 h; EAF2-NC: The group of human umbilical vein endothelial cells cultured with conditioned medium from RKO cells transfected with empty control plasmids for 24 h.

protein. Therefore, it was concluded that EAF2 overexpression inhibited the invasion and migration of CRC cells by down-regulating the activity of the STAT3/TGF-β1 crosstalk pathway. It is possible that therapeutic drugs targeting the STAT3/TGF-β1 signaling pathway may be effective for CRC subsets with down-regulated EAF2, elevated STAT3 phosphorylation, and up-regulated TGF-β1.

Tumor angiogenesis is critical not only for tumor growth, but also for tumor progression and metastasis[32]. Tumor angiogenesis is regulated by multiple angiogenic factors and angiogenic inhibitors[21]. The activation of the STAT3 pathway contributes to angiogenesis by increasing the expression of angiogenic factors, such as VEGFA, interleukin (IL)-8, HIF-1α, or IL-6[33]. The non-specific angiogenic factor TGF-β1 plays a proangiogenic role in CRC angiogenesis[34]. TGF-β1 signaling inactivation caused by dnTGFBR1 in tumor cells can reduce microvessel density and lumen sizes, and decrease tumor growth[35]. In keloid tissues, sumoylation of HIF-1α may increase the stability and an amplified effect on TGF-β/SMAD signaling[23]. Matrigel plug angiogenesis assay showed that EAF2 knockout mice responded to VEGF with significantly enhanced neovascularization[19]. And EAF2 is a

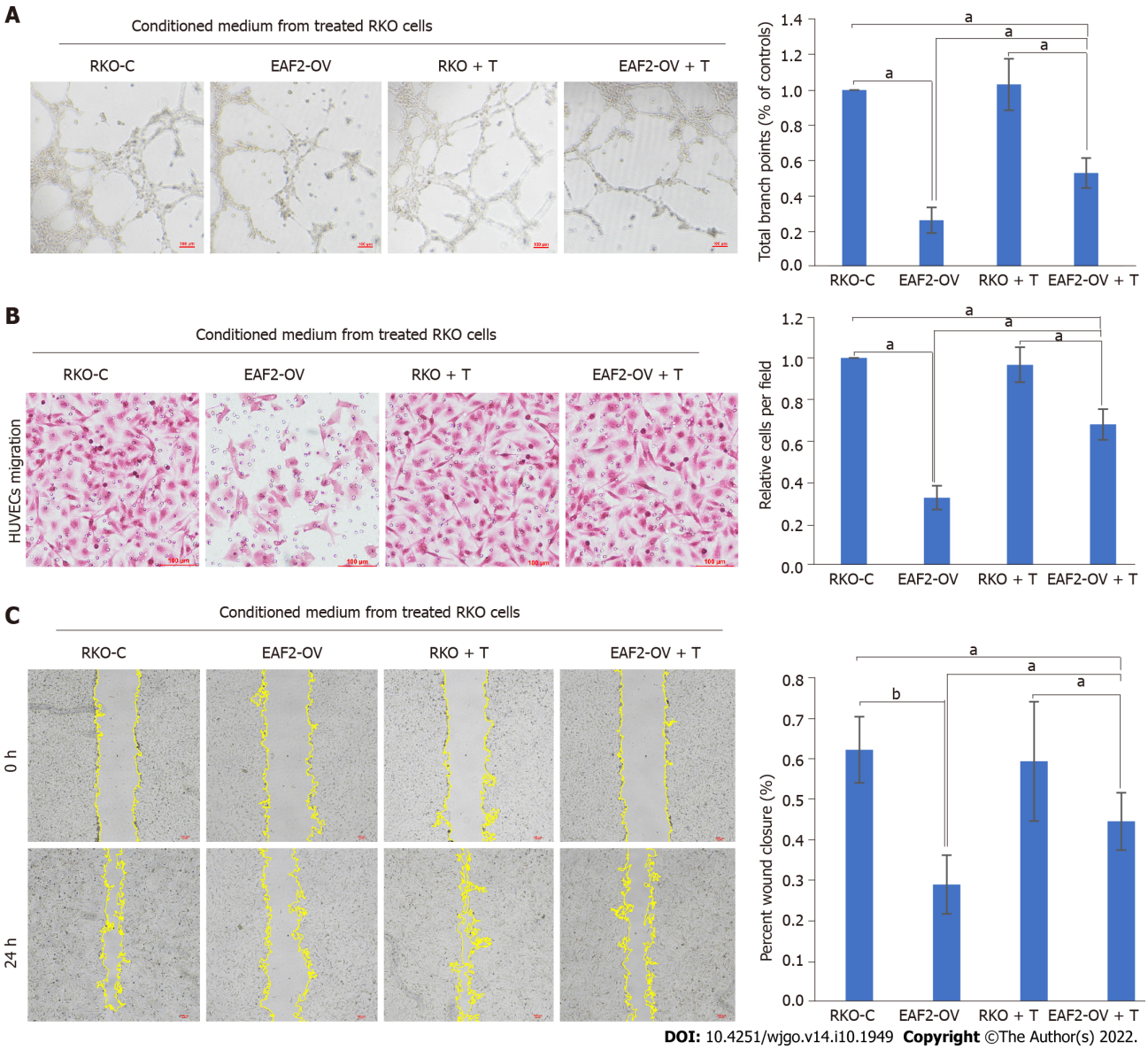

DOI: 10.4251/wjgo.v14.i10.1949

Figure 8 Overexpression of ELL-associated factor 2 inhibited tumor-induced angiogenesis in RKO cells *via* the signal transducer and activator of transcription 3/transforming growth factor beta 1 pathway. A: Conditioned medium from RKO cells transfected with ELL-associated factor 2-overexpressed plasmids or treated with transforming growth factor beta 1 recombinant protein was collected to perform tube formation assay; B: Migration ability of human umbilical vein endothelial cells (HUVECs) analyzed by transwell migration assay; C: Migration ability of HUVECs analyzed by wound healing assay. And the results were measured with ImageJ software. The data are shown as the mean ± SD. $^{a}P < 0.05$, $^{b}P < 0.001$. RKO-C: The group of human umbilical vein endothelial cells cultured with conditioned medium from RKO cells cultured with 10% serum for 24 h; EAF2-OV: The group of human umbilical vein endothelial cells cultured with conditioned medium from RKO cells transfected with ELL-associated factor 2-overexpressed plasmids for 24 h; RKO + T: The group of human umbilical vein endothelial cells cultured with conditioned medium from RKO cells treated with 5 ng/mL transforming growth factor-β1 pathway recombinant protein for 24 h; EAF2-OV + T: The group of human umbilical vein endothelial cells cultured with conditioned medium from RKO cells which were transfected with EAF-OV plasmid for 24 h and then cultured with 5 ng/mL transforming growth factor beta 1 pathway recombinant protein for 24 h.

negative regulator of HIF-1α activity[20]. EAF2 binds to and stabilizes von Hippel-Lindau protein and then disrupts the HIF-1α-mediated hypoxia signaling pathway[19,36]. Abnormal vasculogenesis occurred in EAF2 knockout mice[19]. We hypothesized that EAF2 may regulate CRC angiogenesis through the STAT3/TGF-β1 pathway. HUVECs were used in this study for evaluating the impact of RKO cells on angiogenesis. Besides, endothelial progenitor cells are also a good endothelial model for studying tumor-induced angiogenesis[37].

In this study, our results show that EAF2-overexpressing CRC cells can inhibit tube formation and migration of HUVECs. Besides, the inhibition of EAF2 overexpression on tube formation and migration of HUVECs may be reversed by TGF-β1 recombinant protein. This suggests that EAF2 overexpression inhibited CRC angiogenesis by suppressing the activity of the STAT3/TGF-β1 crosstalk pathway. However, this study still has some limitations, and lacks further studies on vascular regulatory factors released by vascular endothelial cells and changes in tumor microenvironment mediated by EAF2 and its downstream STAT3/TGF-β1 crosstalk pathway.

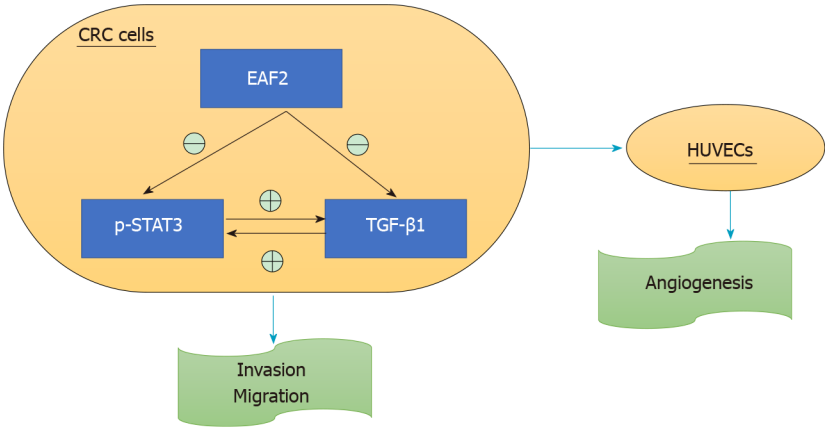

DOI: 10.4251/wjgo.v14.i10.1949

Figure 9 Schematic depiction of ELL-associated factor 2 regulating the signal transducer and activator of transcription 3/transforming growth factor beta 1 crosstalk pathway in this study. EAF2: ELL-associated factor 2; p-STAT3: Phosphorylated-signal transducer and activator of transcription 3; TGF-β1: Transforming growth factor beta 1; CRC: Colorectal cancer; HUVECs: Human umbilical vein endothelial cells.

CONCLUSION

In conclusion, our findings suggest that EAF2 protein is under-expressed in cancer tissue of patients with advanced CRC. And Kaplan-Meier survival analysis showed that the survival rate of the group with high EAF2 levels was higher than that of the group with low EAF2 levels. Moreover, as a tumor suppressor, EAF2 may play a tumor suppressive and protective role in the development of CRC by inhibiting the invasion, metastasis, and angiogenesis of CRC cells. The regulatory effect of EAF2 on the biological functions of CRC cells may be realized by regulating the STAT3/TGF-β1 crosstalk pathway (Figure 9). Further research on methods and technologies to increase EAF2 in CRC will be one of the future research directions, and exploration of upstream factors such as related non-coding RNAs may provide new diagnostic markers and novel therapeutic targets for CRC.

ARTICLE HIGHLIGHTS

Research background

There are few studies on the expression and role of ELL-associated factor 2 (EAF2) protein in colorectal cancer (CRC). The molecular mechanism of involvement of EAF2 in CRC invasion and metastasis remains unclear.

Research motivation

EAF2 may play a tumor suppressive and protective role in the development of CRC by inhibiting the invasion, metastasis, and angiogenesis of CRC cells.

Research objectives

We assessed the expression and localization of EAF2 protein in CRC specimens. Meanwhile, we cultured CRC cells *in vitro* to determine the expression of EAF2 protein and further investigate its effects on the biological function of CRC cells.

Research methods

We used immunohistochemistry and western blot assay to detect the expression of EAF2 protein in CRC tissues from 70 patients. In addition, we applied plasmid transfection technology to study the effects of EAF2 on the invasion, migration, and angiogenesis of CRC cells *in vitro*.

Research results

EAF2 protein was lowly expressed in cancer tissues of patients with advanced CRC. Kaplan-Meier survival analysis showed that the survival rate of the group with high EAF2 level was higher than that of the group with low EAF2 level. In addition, EAF2 affected the biological functions of CRC cells by regulating the STAT3/TGF-β1 crosstalk pathway.

Research conclusions

As a tumor suppressor, EAF2 may play a tumor suppressive and protective role in the development of CRC by inhibiting the invasion, metastasis, and angiogenesis of CRC cells *via* regulating the signal transducer and activator of transcription 3/transforming growth factor beta 1 crosstalk pathway. These findings may provide new diagnostic markers and novel therapeutic targets for CRC.

Research perspectives

Our data is beneficial to elucidate the molecular mechanism of CRC invasion and metastasis as well as explore new potential molecular markers and the direction of targeted therapy.

FOOTNOTES

Author contributions: Feng ML and Wu C designed the research study; Zhang HJ and Jiao TW performed the research; Zhou H and Liu MY contributed new reagents and analytic tools; Feng ML and Sun MJ analyzed the data and wrote the manuscript; and all authors have read and approved the final manuscript.

Supported by the Natural Science Foundation of Liaoning Province, No. 2019-BS-279.

Institutional review board statement: This study was approved by the Institutional Review Board of The First Affiliated Hospital of China Medical University (Registration No. 2021-68-2).

Informed consent statement: Patients were not required to give informed consent to the study because the analysis used anonymous data that were obtained after each patient agreed to treatment by written consent.

Conflict-of-interest statement: All the authors report no relevant conflicts of interest for this article.

Data sharing statement: No additional data are available.

Country/Territory of origin: China

ORCID number: Ming-Liang Feng 0000-0001-6624-9624; Can Wu 0000-0002-9532-8767; Hui-Jing Zhang 0000-0002-6322-2335; Huan Zhou 0000-0002-6299-2514; Tai-Wei Jiao 0000-0002-7679-6354; Meng-Yuan Liu 0000-0002-5058-1558; Ming-Jun Sun 0000-0003-0072-2575.

S-Editor: Wang JJ
L-Editor: Wang TQ
P-Editor: Wang JJ

REFERENCES

1 **Sung H**, Ferlay J, Siegel RL, Laversanne M, Soerjomataram I, Jemal A, Bray F. Global Cancer Statistics 2020: GLOBOCAN Estimates of Incidence and Mortality Worldwide for 36 Cancers in 185 Countries. *CA Cancer J Clin* 2021; **71**: 209-249 [PMID: 33538338 DOI: 10.3322/caac.21660]

2 **Zacharakis M**, Xynos ID, Lazaris A, Smaro T, Kosmas C, Dokou A, Felekouras E, Antoniou E, Polyzos A, Sarantonis J, Syrios J, Zografos G, Papalambros A, Tsavaris N. Predictors of survival in stage IV metastatic colorectal cancer. *Anticancer Res* 2010; **30**: 653-660 [PMID: 20332485]

3 **McQuade RM**, Stojanovska V, Bornstein JC, Nurgali K. Colorectal Cancer Chemotherapy: The Evolution of Treatment and New Approaches. *Curr Med Chem* 2017; **24**: 1537-1557 [PMID: 28079003 DOI: 10.2174/0929867324666170111152436]

4 **Xiao W**, Zhang Q, Jiang F, Pins M, Kozlowski JM, Wang Z. Suppression of prostate tumor growth by U19, a novel testosterone-regulated apoptosis inducer. *Cancer Res* 2003; **63**: 4698-4704 [PMID: 12907652]

5 **Ai J**, Pascal LE, O'Malley KJ, Dar JA, Isharwal S, Qiao Z, Ren B, Rigatti LH, Dhir R, Xiao W, Nelson JB, Wang Z. Concomitant loss of EAF2/U19 and Pten synergistically promotes prostate carcinogenesis in the mouse model. *Oncogene* 2014; **33**: 2286-2294 [PMID: 23708662 DOI: 10.1038/onc.2013.190]

6 **Xiao W**, Zhang Q, Habermacher G, Yang X, Zhang AY, Cai X, Hahn J, Liu J, Pins M, Doglio L, Dhir R, Gingrich J, Wang Z. U19/Eaf2 knockout causes lung adenocarcinoma, B-cell lymphoma, hepatocellular carcinoma and prostatic intraepithelial neoplasia. *Oncogene* 2008; **27**: 1536-1544 [PMID: 17873910 DOI: 10.1038/sj.onc.1210786]

7 **Guo W**, Keener AL, Jing Y, Cai L, Ai J, Zhang J, Fisher AL, Fu G, Wang Z. FOXA1 modulates EAF2 regulation of AR

transcriptional activity, cell proliferation, and migration in prostate cancer cells. *Prostate* 2015; **75**: 976-987 [PMID: 25808853 DOI: 10.1002/pros.22982]

8 **Zang Y**, Dong Y, Yang D, Xue B, Li F, Gu P, Zhao H, Wang S, Zhou S, Ying R, Wang Z, Shan Y. Expression and prognostic significance of ELL-associated factor 2 in human prostate cancer. *Int Urol Nephrol* 2016; **48**: 695-700 [PMID: 26895851 DOI: 10.1007/s11255-015-1210-y]

9 **Jo YS**, Kim SS, Kim MS, Yoo NJ, Lee SH. Candidate Tumor Suppressor Gene EAF2 is Mutated in Colorectal and Gastric Cancers. *Pathol Oncol Res* 2019; **25**: 823-824 [PMID: 30088132 DOI: 10.1007/s12253-018-0461-1]

10 **Savas S**, Azorsa DO, Jarjanazi H, Ibrahim-Zada I, Gonzales IM, Arora S, Henderson MC, Choi YH, Briollais L, Ozcelik H, Tuzmen S. NCI60 cancer cell line panel data and RNAi analysis help identify EAF2 as a modulator of simvastatin and lovastatin response in HCT-116 cells. *PLoS One* 2011; **6**: e18306 [PMID: 21483694 DOI: 10.1371/journal.pone.0018306]

11 **Liu X**, Chen Z, Ouyang G, Song T, Liang H, Liu W, Xiao W. ELL Protein-associated Factor 2 (EAF2) Inhibits Transforming Growth Factor β Signaling through a Direct Interaction with Smad3. *J Biol Chem* 2015; **290**: 25933-25945 [PMID: 26370086 DOI: 10.1074/jbc.M115.663542]

12 **Villalba M**, Evans SR, Vidal-Vanaclocha F, Calvo A. Role of TGF-β in metastatic colon cancer: it is finally time for targeted therapy. *Cell Tissue Res* 2017; **370**: 29-39 [PMID: 28560691 DOI: 10.1007/s00441-017-2633-9]

13 **Liu RY**, Zeng Y, Lei Z, Wang L, Yang H, Liu Z, Zhao J, Zhang HT. JAK/STAT3 signaling is required for TGF-β-induced epithelial-mesenchymal transition in lung cancer cells. *Int J Oncol* 2014; **44**: 1643-1651 [PMID: 24573038 DOI: 10.3892/ijo.2014.2310]

14 **Wang B**, Liu T, Wu JC, Luo SZ, Chen R, Lu LG, Xu MY. STAT3 aggravates TGF-β1-induced hepatic epithelial-to-mesenchymal transition and migration. *Biomed Pharmacother* 2018; **98**: 214-221 [PMID: 29268242 DOI: 10.1016/j.biopha.2017.12.035]

15 **Pascal LE**, Wang Y, Zhong M, Wang D, Chakka AB, Yang Z, Li F, Song Q, Rigatti LH, Chaparala S, Chandran U, Parwani AV, Wang Z. EAF2 and p53 Co-Regulate STAT3 Activation in Prostate Cancer. *Neoplasia* 2018; **20**: 351-363 [PMID: 29518696 DOI: 10.1016/j.neo.2018.01.011]

16 **Jain RK**. Normalization of tumor vasculature: an emerging concept in antiangiogenic therapy. *Science* 2005; **307**: 58-62 [PMID: 15637262 DOI: 10.1126/science.1104819]

17 **Ferrara N**. Vascular endothelial growth factor: basic science and clinical progress. *Endocr Rev* 2004; **25**: 581-611 [PMID: 15294883 DOI: 10.1210/er.2003-0027]

18 **Folkman J**. Role of angiogenesis in tumor growth and metastasis. *Semin Oncol* 2002; **29**: 15-18 [PMID: 12516034 DOI: 10.1053/sonc.2002.37263]

19 **Xiao W**, Ai J, Habermacher G, Volpert O, Yang X, Zhang AY, Hahn J, Cai X, Wang Z. U19/Eaf2 binds to and stabilizes von hippel-lindau protein. *Cancer Res* 2009; **69**: 2599-2606 [PMID: 19258512 DOI: 10.1158/0008-5472.CAN-08-2595]

20 **Pang B**, Zheng XR, Tian JX, Gao TH, Gu GY, Zhang R, Fu YB, Pang Q, Li XG, Liu Q. EZH2 promotes metabolic reprogramming in glioblastomas through epigenetic repression of EAF2-HIF1α signaling. *Oncotarget* 2016; **7**: 45134-45143 [PMID: 27259264 DOI: 10.18632/oncotarget.9761]

21 **Liu JF**, Deng WW, Chen L, Li YC, Wu L, Ma SR, Zhang WF, Bu LL, Sun ZJ. Inhibition of JAK2/STAT3 reduces tumor-induced angiogenesis and myeloid-derived suppressor cells in head and neck cancer. *Mol Carcinog* 2018; **57**: 429-439 [PMID: 29215754 DOI: 10.1002/mc.22767]

22 **Zhang ZH**, Li MY, Wang Z, Zuo HX, Wang JY, Xing Y, Jin C, Xu G, Piao L, Piao H, Ma J, Jin X. Convallatoxin promotes apoptosis and inhibits proliferation and angiogenesis through crosstalk between JAK2/STAT3 (T705) and mTOR/STAT3 (S727) signaling pathways in colorectal cancer. *Phytomedicine* 2020; **68**: 153172 [PMID: 32004989 DOI: 10.1016/j.phymed.2020.153172]

23 **Lin X**, Wang Y, Jiang Y, Xu M, Pang Q, Sun J, Yu Y, Shen Z, Lei R, Xu J. Sumoylation enhances the activity of the TGF-β/SMAD and HIF-1 signaling pathways in keloids. *Life Sci* 2020; **255**: 117859 [PMID: 32474020 DOI: 10.1016/j.lfs.2020.117859]

24 **Zonneville J**, Safina A, Truskinovsky AM, Arteaga CL, Bakin AV. TGF-β signaling promotes tumor vasculature by enhancing the pericyte-endothelium association. *BMC Cancer* 2018; **18**: 670 [PMID: 29921235 DOI: 10.1186/s12885-018-4587-z]

25 **Beldi G**, Bahiraii S, Lezin C, Nouri Barkestani M, Abdelgawad ME, Uzan G, Naserian S. TNFR2 Is a Crucial Hub Controlling Mesenchymal Stem Cell Biological and Functional Properties. *Front Cell Dev Biol* 2020; **8**: 596831 [PMID: 33344453 DOI: 10.3389/fcell.2020.596831]

26 **Liu JX**, Zhang D, Xie X, Ouyang G, Liu X, Sun Y, Xiao W. Eaf1 and Eaf2 negatively regulate canonical Wnt/β-catenin signaling. *Development* 2013; **140**: 1067-1078 [PMID: 23364330 DOI: 10.1242/dev.086157]

27 **Simone F**, Luo RT, Polak PE, Kaberlein JJ, Thirman MJ. ELL-associated factor 2 (EAF2), a functional homolog of EAF1 with alternative ELL binding properties. *Blood* 2003; **101**: 2355-2362 [PMID: 12446457 DOI: 10.1182/blood-2002-06-1664]

28 **An Y**, Zhang S, Zhang J, Yin Q, Han H, Wu F, Zhang X. Overexpression of lncRNA NLIPMT Inhibits Colorectal Cancer Cell Migration and Invasion by Downregulating TGF-β1. *Cancer Manag Res* 2020; **12**: 6045-6052 [PMID: 32765103 DOI: 10.2147/CMAR.S247764]

29 **Morikawa T**, Baba Y, Yamauchi M, Kuchiba A, Nosho K, Shima K, Tanaka N, Huttenhower C, Frank DA, Fuchs CS, Ogino S. STAT3 expression, molecular features, inflammation patterns, and prognosis in a database of 724 colorectal cancers. *Clin Cancer Res* 2011; **17**: 1452-1462 [PMID: 21310826 DOI: 10.1158/1078-0432.CCR-10-2694]

30 **Rokavec M**, Öner MG, Li H, Jackstadt R, Jiang L, Lodygin D, Kaller M, Horst D, Ziegler PK, Schwitalla S, Slotta-Huspenina J, Bader FG, Greten FR, Hermeking H. IL-6R/STAT3/miR-34a feedback loop promotes EMT-mediated colorectal cancer invasion and metastasis. *J Clin Invest* 2014; **124**: 1853-1867 [PMID: 24642471 DOI: 10.1172/JCI73531]

31 **Zhang X**, Yue P, Page BD, Li T, Zhao W, Namanja AT, Paladino D, Zhao J, Chen Y, Gunning PT, Turkson J. Orally bioavailable small-molecule inhibitor of transcription factor Stat3 regresses human breast and lung cancer xenografts. *Proc Natl Acad Sci U S A* 2012; **109**: 9623-9628 [PMID: 22623533 DOI: 10.1073/pnas.1121606109]

32 **Naumov GN**, Akslen LA, Folkman J. Role of angiogenesis in human tumor dormancy: animal models of the angiogenic

switch. *Cell Cycle* 2006; **5**: 1779-1787 [PMID: 16931911 DOI: 10.4161/cc.5.16.3018]

33 **Sun W**. Angiogenesis in metastatic colorectal cancer and the benefits of targeted therapy. *J Hematol Oncol* 2012; **5**: 63 [PMID: 23057939 DOI: 10.1186/1756-8722-5-63]

34 **Yang L**, Liu Z, Wen T. Multiplex fluorescent immunohistochemistry quantitatively analyses microvascular density (MVD) and the roles of TGF-β signalling in orchestrating angiogenesis in colorectal cancer. *Transl Cancer Res* 2019; **8**: 429-438 [PMID: 35116775 DOI: 10.21037/tcr.2019.02.09]

35 **Du YE**, Tu G, Yang G, Li G, Yang D, Lang L, Xi L, Sun K, Chen Y, Shu K, Liao H, Liu M, Hou Y. MiR-205/YAP1 in Activated Fibroblasts of Breast Tumor Promotes VEGF-independent Angiogenesis through STAT3 Signaling. *Theranostics* 2017; **7**: 3972-3988 [PMID: 29109792 DOI: 10.7150/thno.18990]

36 **Pascal LE**, Ai J, Rigatti LH, Lipton AK, Xiao W, Gnarra JR, Wang Z. EAF2 loss enhances angiogenic effects of Von Hippel-Lindau heterozygosity on the murine liver and prostate. *Angiogenesis* 2011; **14**: 331-343 [PMID: 21638067 DOI: 10.1007/s10456-011-9217-1]

37 **Abdelgawad ME**, Desterke C, Uzan G, Naserian S. Single-cell transcriptomic profiling and characterization of endothelial progenitor cells: new approach for finding novel markers. *Stem Cell Res Ther* 2021; **12**: 145 [PMID: 33627177 DOI: 10.1186/s13287-021-02185-0]

World Journal of Gastrointestinal Oncology

Submit a Manuscript: https://www.f6publishing.com

World J Gastrointest Oncol 2022 October 15; 14(10): 1968-1980

DOI: 10.4251/wjgo.v14.i10.1968

ISSN 1948-5204 (online)

ORIGINAL ARTICLE

Basic Study

Interleukin-34 promotes the proliferation and epithelial-mesenchymal transition of gastric cancer cells

Chuan-Hong Li, Zhang-Ming Chen, Pei-Feng Chen, Lei Meng, Wan-Nian Sui, Song-Cheng Ying, A-Man Xu, Wen-Xiu Han

Specialty type: Oncology

Provenance and peer review: Unsolicited article; Externally peer reviewed.

Peer-review model: Single blind

Peer-review report's scientific quality classification

Grade A (Excellent): A
Grade B (Very good): B, B, B
Grade C (Good): C, C
Grade D (Fair): 0
Grade E (Poor): 0

P-Reviewer: Imai Y, Japan; Nath L, India; Qin Y; Tanabe S, Japan; Zhang Z, China

Received: May 30, 2022
Peer-review started: May 30, 2022
First decision: June 21, 2022
Revised: July 4, 2022
Accepted: August 21, 2022
Article in press: August 21, 2022
Published online: October 15, 2022

Chuan-Hong Li, Zhang-Ming Chen, Pei-Feng Chen, Lei Meng, Wan-Nian Sui, A-Man Xu, Wen-Xiu Han, Department of General Surgery, The First Affiliated Hospital of Anhui Medical University, Hefei 230022, Anhui Province, China

Song-Cheng Ying, Department of Immunology, College of Basic Medicine, Anhui Medical University, Hefei 230022, Anhui Province, China

Corresponding author: Wen-Xiu Han, MD, PhD, Professor, Department of General Surgery, The First Affiliated Hospital of Anhui Medical University, No. 218 Jixi Avenue, Shushan District, Hefei 230022, Anhui Province, China. hwxhbh@126.com

Abstract

BACKGROUND

Interleukin (IL)-34 is a pro-inflammatory cytokine involved in tumor development. The role of IL-34 in the proliferation and epithelial-mesenchymal transition (EMT) of gastric cancer (GC) remains to be investigated.

AIM

To investigate whether and how IL-34 affects the proliferation of GC cells and EMT.

METHODS

Using immunohistochemical staining, the expression of IL-34 protein was detected in 60 paired GC and normal paracancerous tissues and the relationship between IL-34 and clinicopathological factors was analyzed. The expression of IL-34 mRNA and protein in normal gastric epithelial cell lines and GC was detected using quantitative real-time polymerase chain reaction (qRT-PCR) and western blotting, respectively. Stable IL-34 knockdown and overexpression in AGS cell lines were established by lentiviral infection and validated by qRT-PCR and western blotting. The cholecystokinin-8 assay, clone formation assay, cell scratch assay, and transwell system were used to detect GC cell proliferation, clone formation, migration, and invasion capacity, respectively. The effects of IL-34 on the growth of GC transplant tumors were assessed using a subcutaneous transplant tumor assay in nude mice. The effects of IL-34 on the expression level of EMT-associated proteins in AGS cells were examined by western blotting.

RESULTS

Expression of IL-34 protein and mRNA was higher in GC cell lines than in GES-1 cells. Compared to matched normal paraneoplastic tissues, the expression of IL-34 protein was higher in 60 GC tissues, which was correlated with tumor size, T-stage, N-stage, tumor, node and metastasis stage, and degree of differentiation. Knockdown of IL-34 expression inhibited the proliferation, clone formation, migration, and invasion of AGS cells, while overexpression of IL-34 promoted cell proliferation, clone formation, migration, and invasion. Furthermore, the reduction of IL-34 promoted the expression of E-cadherin in AGS cells but inhibited the expression of vimentin and N-cadherin. Overexpression of IL-34 inhibited E-cadherin expression but promoted expression of vimentin and N-cadherin in AGS cells. Overexpression of IL-34 promoted the growth of subcutaneous transplanted tumors in nude mice.

CONCLUSION

IL-34 expression is increased in GC tissues and cell lines compared to normal gastric tissues or cell lines. In GC cells, IL-34 promoted proliferation, clone formation, migration, and invasion by regulating EMT-related protein expression cells. Interference with IL-34 may represent a novel strategy for diagnosis and targeted therapy of GC.

Key Words: Gastric cancer; Interleukin-34; Proliferation; Epithelial-mesenchymal transition; Metastasis

Core Tip: Our study provides novel evidence that interleukin (IL)-34 contribute the growth and metastasis of gastric cancer (GC). IL-34 is up-regulated in GC cell lines and tissues, which is correlated with tumor size, grade of differentiation and tumor, node and metastasis stage. IL-34 enhances the ability of proliferation, clone formation, migration and invasion of GC cells and regulates the expression levels of epithelial-mesenchymal transition-associated proteins, suggesting that IL-34 may be an effective target for the therapy of GC.

Citation: Li CH, Chen ZM, Chen PF, Meng L, Sui WN, Ying SC, Xu AM, Han WX. Interleukin-34 promotes the proliferation and epithelial-mesenchymal transition of gastric cancer cells. *World J Gastrointest Oncol* 2022; 14(10): 1968-1980

URL: https://www.wjgnet.com/1948-5204/full/v14/i10/1968.htm

DOI: https://dx.doi.org/10.4251/wjgo.v14.i10.1968

INTRODUCTION

Gastric cancer (GC) is one of the most aggressive cancers, with approximately 1 million new cases diagnosed worldwide in 2020 and an estimated 769000 deaths, ranking fifth in incidence and fourth in mortality globally[1]. Rates are two-fold higher in men than in women[1]. East Asia, including China, Japan, and Korea, is the hotspot of incidence and mortality of GC[2]. In Japan and Korea, screening programs have led to substantial reductions in GC-associated mortality[2]. However, in China, due to the lack of extensive initial screening for early GC, most patients present with advanced GC[3]. Radial surgery is the main modality for the treatment of locally progressive GC, and the combination of chemotherapy and targeted therapy can improve the prognosis. During 2007-2021, the 5-year relative survival rate of patients with GC continued to increase[4]. The overall 5-year age-standardized relative survival rates in 2007-2011, 2012-2016, and 2017-2021 were 38.3%, 40.6%, and 42.9%, respectively[4]. However, the overall relative survival of patients with GC remains low[4]. In particular, the survival rate of patients with distant-stage GC remains very low (10%)[4]. Targeted therapy alone or in combination with chemotherapy has shown potential advantages in the treatment of advanced GC[5]. Trastuzumab is a targeted therapy that effectively improves the prognosis of HER2-positive patients with GC; however, less than 20% of patients with GC are HER2-positive, which means that the remaining 80% of patients with GC do not benefit from the drug[1]. Therefore, identifying more effective targets will provide new ideas for targeted therapy for GC.

Epithelial-mesenchymal transition (EMT) refers to the biological process in which epithelial cells are transformed into cells with mesenchymal properties through a complex series of mechanisms in response to relevant factors[6-8]. In cancer, EMT is associated with tumorigenesis, invasion, metastasis, and resistance to therapy. Different states of EMT exhibit different functional characteristics in cancer and are associated with tumor proliferation, propagation, plasticity, invasion, and metastasis[9]. Exosomes have been proposed as a therapeutic tool to control the development of EMT and influence

the progression of cancer[10]. In addition, Pinin induces EMT and malignant progression in hepatocellular carcinoma[11]. Furthermore, Wu *et al*[12] found that interleukin (IL)-6 secreted by cancer-associated fibroblasts promotes EMT and GC metastasis through the JAK2/STAT3 signaling pathway, Li *et al*[13] reported that tumor-associated neutrophils induce EMT by IL-17a to promote migration and invasion in GC cells, and Tian *et al*[14] reported that SERPINH1 regulates EMT and GC metastasis through the Wnt/β-catenin signaling pathway. Clarifying the regulatory mechanism of EMT in the development of GC is of great practical importance in attempting to understand the occurrence and metastasis of GC.

IL-34 is a new cytokine discovered in 2008 that binds to its functional receptor and plays a role in the regulation of cell differentiation, proliferation, angiogenesis, inflammation, and the immune response [15-17]. IL-34 has been found to play a pro-cancer role in a variety of tumors, including thyroid, colorectal, and liver cancers[18-20]. In particular, Zhang *et al*[18] found that IL-34 promotes tumor proliferation and activates the ERK signaling pathway in papillary thyroid cancer cells. However, it remains unclear whether IL-34 regulates GC cell migration and invasion. Furthermore, it is also unknown whether IL-34 can regulate GC proliferation *in vitro* and *in vivo*. This study aimed to elucidate the relationship between IL-34 and the clinicopathological characteristics of patients with GC and the role of IL-34 in the proliferation and the EMT of GC cells.

MATERIALS AND METHODS

Patients and samples

A total of 60 patients diagnosed with GC (age >18 years) were collected from patients who underwent surgical resection at The First Affiliated Hospital of Anhui Medical University from November 2019 to June 2020. Patients with a history of preoperative radiotherapy, long-term drug treatment, inflammatory diseases, rheumatic immune diseases, and genetic-related diseases were excluded. Information collected included sex, age, tumor diameter, T-stage, N-stage, M-stage, tumor, node and metastasis (TNM) stage, and grade (well, moderate, and poor). All tumors were staged according to the Eighth Edition of American Joint Committee on Cancer TNM classification. All procedures performed in studies with human participants were reviewed and approved by the Ethics Committee of The First Affiliated Hospital of Anhui Medical University and were carried out in accordance with the Declaration of Helsinki of 1964 and its subsequent amendments or comparable ethical standards. Written informed consent was obtained from all individual participants included in the study. Approval for the ethical use of clinical samples was obtained from the Institutional Review Board (No: Quick-PJ2019-09-11).

Immunohistochemical staining

Tumor tissues collected from patients with GC were fixed in 4.0% paraformaldehyde, embedded in paraffin, and sliced into 4-μm sections. The sections were incubated with 3.0% hydrogen peroxide to inactivate endogenous peroxidase and then blocked in 5.0% bovine serum albumin after antigen retrieval. After blocking, sections were incubated with anti-IL-34 monoclonal antibody (863800; ZEN-BIOSCIENCE; 1:150) overnight at 4°C, followed by secondary antibody (ab150077; Abcam; 1:500). Sections were visualized with a diaminobenzidine solution and hematoxylin counterstain. Images were acquired with a microscope (Nikon Eclipse E200). Two pathologists blinded to clinical data independently scored tissue staining. The percentage of staining was evaluated and scored as follows: 0, < 1% staining; 1, 1%-25% staining; 2, 26%-50% staining; 3, 51%-75% staining; and 4, > 75% staining. The intensity of staining was defined as follows: 0, no signal; 1, weak; 2, moderate; and 3, strong. Scoring formula = percentage of positive tumor cell score × positive cell staining score. A total score of < 5 was considered negative and > 6 was considered positive.

RNA isolation and quantitative real-time polymerase chain reaction

Total RNA was isolated from tissues and cells with the TRIzol reagent (Thermo Fisher). Reverse transcription was achieved using Vazyme Biotech kits. The cDNA amplification was then performed using SYBR Premix Ex Taq (Vazyme Biotech) using a Roche 480 light cycler. PCR was carried out for 40 cycles according to the following procedure: 95°C for 60 s, and 60°C for 30 s. Relative mRNA expression of target genes were calculated using the $2^{-\Delta\Delta Ct}$ method after normalization with GAPDH expression. Primer sequences were as follows: IL-34, 5′-TTGACGCAGAATGAGGAGTG-3′(forward); 5′-CCCTCGTAAGGCACACTG AT-3′(reverse); GAPDH,5′-CAGGAGGCATTGCTGATGAT-3′(forward); 5′-GAAGG CTGGGGCTCATTT-3′(reverse).

Western blotting

Protein was obtained by lysis of tissues or cells using RIPA buffer containing protease inhibitors (Thermo Fisher), and protein concentration was quantified using the BCA Protein Assay kit (Beyotime Biotechnology). Protein was separated by SDS-PAGE and transferred to a polyvinylidene fluoride

membrane according to standard protocols and then blocked with 5% skim milk in TBST for 1 h. The membranes were incubated overnight at 4°C with the following antibodies: anti-E-cadherin (1:5000, Abcam), anti-N-cadherin (1:5000, Abcam), anti-Vimentin (1:5000, Abcam), anti-GAPDH (1:5000, Abcam), anti-Vimentin (1:5000, Abcam), anti-GAPDH (1:5000, Abcam), anti-IL-34 (1:1000, ZEN-BIOSCIENCE) and then incubated with horseradish peroxidase conjugated secondary antibodies (1:2000, Proteintech Group) at room temperature for 1 h after washing 3 times using TBST. The relative band density was determined with the ECL Western Blotting Substrate Kit (EMD Millipore) using Tanon 5200 Multifunctional Imaging System (Shanghai, China). GAPDH was used as an internal control.

Cell culture and transfection

The human normal gastric mucosal epithelial cell line (GES-1) and human GC cell lines (AGS, MKN-45 and HGC-27) were provided by Prof. Aman Xu (The First Affiliated Hospital of Anhui Medical University). Cells were grown in RPMI 1640 medium supplemented with 10% FBS (BI), 100 U/mL penicillin (Gibco). The cells were kept in a humidified incubator at 37°C with a mixture of 95% air and 5% CO_2.

The short hairpin RNA (shRNA) and IL-34 overexpression plasmid sequences were synthesized by the Public Protein/Plasmid Library. The shRNA sequences were as follows: shRNA-IL-34, 5′-CAGAGC-CCTCATTGCAGTATG-3′ and Negative control, 5′-GTTCTCCGAACGTGTCACGTT-3′. The IL-34 overexpression plasmid is a lentiviral expression vector for human IL-34 with an inserted sequence size of 729 bp and no fused CopGFP protein at its C-terminus. Target plasmids with IL-34, shRNA-IL-34, or shRNA control were transfected into AGS cells using lentivirus and selected by adding puromycin after 48 h, then viable cells were diluted to 50 cells/mL and inoculated into 96-well plates, respectively, and continued to be screened with drugs until satisfactory monoclonal cell lines were selected.

Cell proliferation and clone formation assay

For the cholecystokinin (CCK) assay, cells were seeded in 96-well culture plates at about 3000 cells per well. At 0, 24, 48, 72, and 96 h, CCK-8 agent was added to each well and cells were treated for 2 h. Absorbance values at 450 nm were measured using an enzyme labeler (USCN KIT INC, China). For the clone formation assay, cells were seeded in six-well plates at 400 cells per well and then cultured for 2 wk. Cells were fixed and stained for 30 min in a 35% methanol solution with 1% crystal violet, and then the number of stained cells was counted.

Cell migration and invasion assays

The cells were seeded in six-well plates (2×10^4/well). A scratch was made through the cell layer along the central axis using a sterile plastic tip after complete cell attachment. After scratching, the cells were washed 3 times with PBS to remove floating cells and to make the scratch visible, and then the medium was replaced with fresh medium to continue the culture. The scratch was photographed at 0 h and 24 h. The photos were imported into Image J software and the cell closure was calculated according to the software instructions.

The cell invasion assay was performed using Transwell chambers with a pore size of 8 μm. A 200 μL cell suspension (2×10^3/L) was added to the upper chamber with Matrigel and placed in a 24-well plate containing 700 μL medium with 10% FBS. After 24 h of incubation at 37°C and 5% CO_2, cells that invaded toward the lower surface of the membrane were fixed with 4% paraformaldehyde, stained with 0.1% crystal violet, and counted.

Animal experiments

All applicable national and institutional guidelines for the care and use of animals were followed. The ethics approval for the animal protocols for this study was obtained by the Animal Research Committee of Anhui Medical University (No. SC20200513). Ten 4-wk-old female nude mice purchased from Shanghai SLAC Laboratory Animal Co., Ltd were randomly divided into two groups (experimental and control groups), five in each group. Pre-cultured AGS cells (overexpression group and control group) in good growth condition were digested separately using trypsin, centrifuged, and a cell suspension (1×10^6 cells) was injected into the inguinal region of mice. The mice in both groups were maintained in the same feeding environment and nutritional conditions. The animals were sacrificed at the end of the experiments for an observation period of 28 d. Tumor weights were recorded per mouse and tumor volumes were calculated using the modified formula of (length × width^2)/2.

Statistical analyses

SPSS statistical software (version 22.0) statistical software was used for statistical analysis and GraphPad Prism (version 8.0.2) was used for graphing. Measurement data were first examined using the Kolmogorov-Smirnov test to check whether the measurement data of each group had a normal distribution. Results are expressed as the mean ± SE for measurement data with a normal distribution. Comparisons between two groups were performed using the two-tailed Student's *t* test. One-way analysis of variance was used for multiple group comparisons, and the LSD-*t* test was used for pairwise

comparisons. All results are from three independent replicate experiments. *P* values < 0.05 were used to indicate statistically significant differences.

RESULTS

IL-34 expression increased in GC tissues and cell lines

The results of immunohistochemical staining showed that IL-34 expression increased in GC tissues compared to paired normal gastric tissues (Figure 1A and B, $P < 0.01$). Meanwhile, as shown in Figure 1C-E, the expression of IL-34 mRNA and protein in GC cell lines (AGS, HGC-27, and MKN-45) were higher than in normal gastric mucosal cells GES-1 ($P < 0.01$). Furthermore, the relationship between IL-34 and clinicopathological characteristics was also analyzed, and the results showed that tumor size in GC patients with higher expression of IL-34 was greater than with lower expression of IL-34 ($P < 0.05$, Table 1). Furthermore, IL-34 expression correlated with the depth of invasion, the degree of differentiation, lymph node metastasis, and the TNM stage of GC patients, but not with age, sex, or distant metastasis ($P > 0.05$, Table 1). Altogether, these findings suggested that IL-34 might function as an oncogene in the development of GC.

IL-34 accelerated the formation and proliferation of clones of GC cells

AGS cell lines with stable knockdown or overexpression of IL-34 were successfully obtained by introducing plasmids containing shRNA-IL-34 or the cds fragment (coding sequence) of the IL-34 gene into AGS cells by lentiviral infection, followed by puromycin pressurization screening. As shown in Figure 1F-J. To identify the effects of IL-34 on GC cell proliferation, we evaluated the formation of CCK-8 and plate clones in AGS cells with different expression of IL-34. The results showed that the number of AGS cell clones in the stable knockdown group (shRNA-1) was less than in the control group (shNC) (Figure 2A and B, $P < 0.01$). Meanwhile, the proliferation rate of AGS cells in the shRNA-1 group was also slowed compared to the shNC group (Figure 2C, $P < 0.05$). Furthermore, as shown in Figure 2C and D, the clone formation was significantly increased following the stable overexpression of the IL-34 compared to cells transfected with Vector alone (Figure 2E, $P < 0.05$). In addition, the CCK-8 assay also showed that the proliferation ability of AGS cells in the stable IL-34 overexpression group was significantly enhanced compared to the Vector-transfected cells, and the difference was statistically significant (Figure 2F, $P < 0.05$). Therefore, IL-34 accelerated the proliferation and clone formation of AGS cells.

IL-34 improved the migration and invasion of AGS cells

To verify the effect of IL-34 on GC migration and invasion ability, we examined the migration and invasion capacity of AGS cell lines in the shNC group and in the shRNA-1 group. As shown in Figure 3A and B, the migration capacity of AGS cells in the shRNA-1 group was reduced compared to the shNC group ($P < 0.05$). Meanwhile, the transwell assay showed that the invasion of AGS cells in the shRNA-1 group was weaker than that of the shNC group (Figure 3C and D, $P < 0.05$). As shown in Figure 3E-H, the migration and invasion of AGS cell lines was enhanced following the stable overexpression of IL-34 compared to cells transfected with Vector alone ($P < 0.05$). Taken together, IL-34 overexpression promoted migration and invasiveness of AGS cells.

Overexpression of IL-34 accelerated the growth of subcutaneous transplantation tumors in nude mice

To further verify the effects of IL-34 on GC transplant tumors *in vivo*, we constructed a subcutaneous transplant tumor model in nude mice. As shown in Figure 4A and B, the tumors of the nude mice in the IL-34 group grew faster compared to the Vector implanted group ($P < 0.05$). Furthermore, tumor weight in the IL-34 group was higher than in the Vector group (Figure 4C, $P < 0.05$). Therefore, IL-34 overexpression promoted the growth of subcutaneous transplantation tumors in nude mice.

IL-34 regulated the expression of EMT-associated proteins

The EMT process is characterized by a decreased expression of the epithelial cell marker (E-cadherin) and an elevated expression of the mesenchymal cell marker (vimentin) and the tumor invasion promoter marker (N-cadherin)[24]. As shown in Figure 5A-D, knockdown increased the expression of the E-cadherin protein expression but decreased the expression of vimentin and N-cadherin in AGS cells ($P < 0.01$). In contrast, overexpression of IL-34 suppressed E-cadherin expression and increased vimentin and N-cadherin protein expression in AGS cells (Figure 5E-H, $P < 0.01$). Overall, IL-34 promoted the migration and invasion of AGS cells by regulating the expression of EMT-associated proteins.

Table 1 Correlations between expression of interleukin-34 proteins and clinicopathologic features in 60 patients with gastric cancer

Characteristics	Expression of IL-34		χ^2/t	*P* value
	Lower (*n* = 29)	Higher (*n* = 31)		
Age (yr)	62.14 ± 11.23	63.87 ± 10.642	0.976	0.945
Tumor size (cm)	4.69 ± 1.74	6.52 ± 3.06	0.003	0.006
Sex				
Male	16	21	1.001	0.317
Female	13	10		
T-stage				
T1 + T2	13	4	7.520	0.006
T3 + T4	16	27		
N-stage				
N0	17	8	6.638	0.010
N1 + N2 + N3	12	23		
M0 stage				
Yes	1	2	0.000	1.000
No	28	29		
TNM stages				
I + II	17	10	4.207	0.040
III + IV	12	21		
Grade				
Well + moderate	11	4	5.006	0.025
Poor	18	27		

IL: Interleukin; TNM: Tumor, node and metastasis.

DISCUSSION

In recent years, IL-34, a newly discovered cytokine, has been reported to influence tumorigenesis and progression by binding to receptors triggering multiple intracellular pathways, which mediate cellular processes such as cell proliferation, the cell cycle, and protein phosphorylation[16]. Zhou *et al*[17] found that IL-34 binds to the colony stimulating factor 1 receptor (CSF-1R) to control the survival, proliferation, and differentiation of tumor-associated macrophages, and patients with higher expression of IL-34 and higher density of tumor-associated macrophages had a poorer prognosis and shorter overall survival and recurrence-free period. Additionally, Zhang *et al*[18] found that IL-34 Levels were significantly up-regulated in serum and tissue samples from patients with thyroid cancer, which were strongly correlated with tumor size, TNM stage, and lymph node metastasis. Kobayashi *et al*[19] found that IL-34 is a prognostic factor in colorectal cancer. Irie *et al*[20] found that IL-34 promotes hepatoblastoma cells progression *via* autocrine and paracrine mechanisms. Kajihara *et al*[21] found that IL-34 expression was upregulated in triple-negative breast cancer and that overall survival was worse in patients with triple-negative breast cancer with high expression of IL-34. Consistent with the above findings, we found that IL-34 expression levels were correlated with the clinicopathological characteristics of the patients, including tumor size, T-stage, N-stage, stage TNM, and tumor grade of differentiation. More specifically, patients with GC with lower expression of IL-34 had smaller tumors, earlier tumor stages (T-stage and N-stage, and TNM stage) and well-differentiated tumors. Additionally, CCK-8 assays and plate clone formation assays showed that the capacity for proliferation and clone formation of GC cells was enhanced after IL-34 overexpression, while the knockdown of IL-34 suppressed the proliferation and clone formation of GC cells. Similarly, Franzè *et al*[22] also found that IL-34 promoted colorectal cancer cell proliferation by regulating the growth of tumor-associated macrophages. In this study, we also attempted to further validate the effects of IL-34 on GC growth *in vivo* by constructing subcutaneous tumor nude mice models. The results showed that the overexpression of IL-34 accelerated the growth rate of GC tumors compared to cell xenograft containing only Vector. Regrettably, due to the limitations of nude mouse subcutaneous tumor models, no supporting evidence was observed with

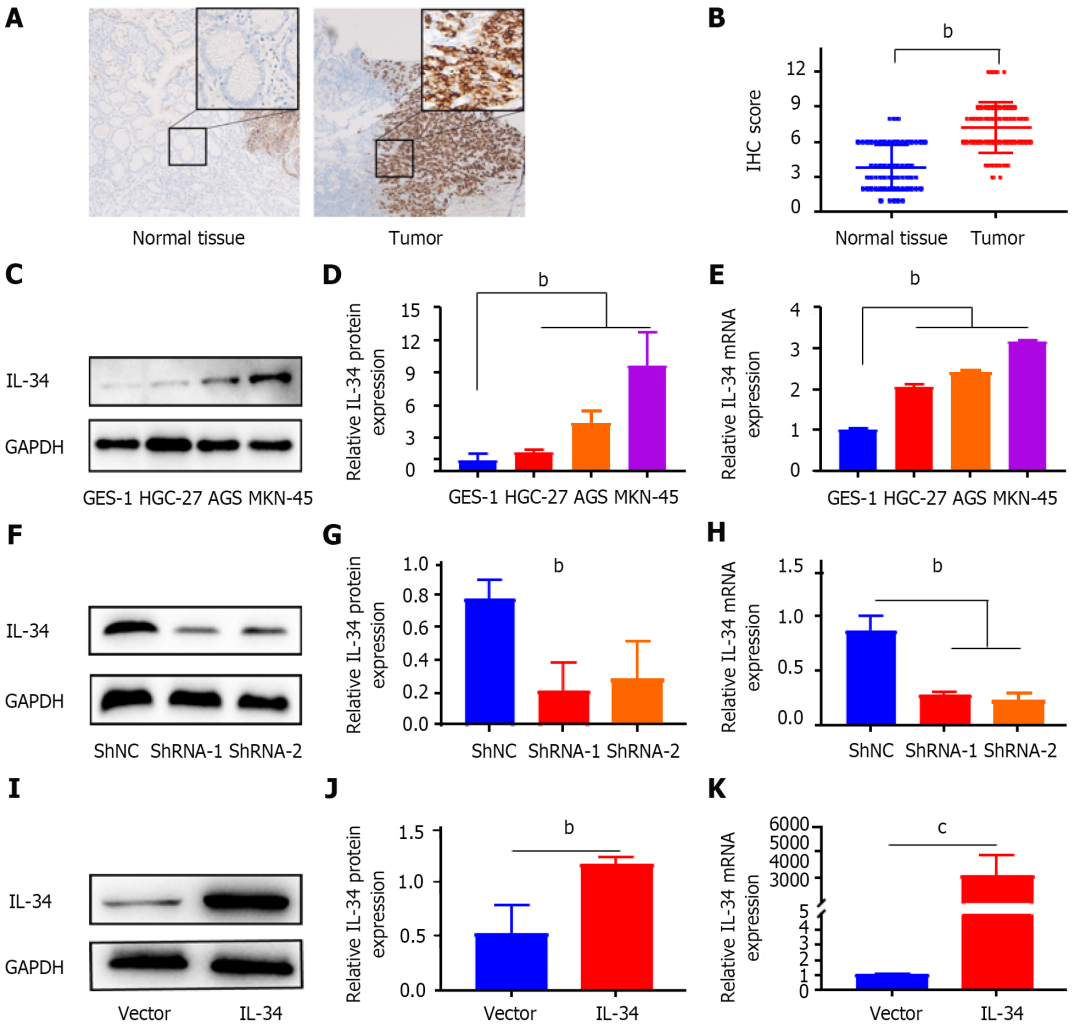

DOI: 10.4251/wjgo.v14.i10.1968

Figure 1 Expression of interleukin-34 in gastric cancer tissues and cell lines, and construction of AGS cell lines with stable knockdown or overexpression of interleukin-34. A: Representative immunohistochemistry (IHC) staining of interleukin (IL)-34 in adjacent normal tissue, gastric cancer (GC) tissues, (scale bar = 25 μm); B: IHC staining scores were used to evaluate IL-34 expression in GC tissues and adjacent normal tissue; C: Western blotting was used to detect IL-34 protein expression in gastric normal epithelial cells (GES-1) and GC cell lines (AGS, HGC-27, and MKN-45); D: The relative densitometric analysis of protein bands was calculated; E: IL-34 mRNA expression was detected by quantitative real-time polymerase chain reaction (qRT-PCR); F and G: Western blotting was used to verify the downregulation of IL-34 in AGS cell lines; H: qRT-PCR was used to verify the downregulation of IL-34 in AGS cell lines; I and J: Western blotting was used to verify the overexpression of IL-34 in AGS cell lines; K: qRT-PCR was used to verify the overexpression of IL-34 in AGS cell lines. $^{b}P < 0.01$, $^{c}P < 0.001$.

regard to macrophage and lymphocyte infiltration into tumors (data was not shown), making it difficult to investigate the role of tumor-associated macrophages in IL-34 mediating GC progression.

It is well known that EMT is involved in GC metastasis, which is characterized by changes in migration, invasion, and expression of proteins associated with EMT, including E-cadherin, vimentin, and N-cadherin[6,23-25]. Previous studies have found that EMT is strongly associated with the proliferation and metastasis of GC[12-14]. For example, cancer-associated fibroblasts promote EMT and GC metastasis *via* the JAK2/STAT3 signaling pathway[12], while tumor neutrophils induce EMT to promote migration and invasion in GC cells[13]. SERPINH1 regulates the progression of EMT and GC through the Wnt/β-catenin pathway[14]. Furthermore, ZMYM1 promotes EMT and metastasis of GC cells by recruiting the CtBP/LSD1/CoREST complex to bind to the E-cadherin promoter and mediating its repression[26]. IL-34 has been reported to promote EMT and activate the ERK signaling pathway in papillary thyroid cancer cells[15]. However, it remains unclear whether IL-34 regulates the EMT process of GC. In the present study, overexpression of IL-34 enhanced migration and invasion ability, while knockdown of IL-34 impaired metastasis in GC cells. Furthermore, we also found that the N-cadherin and vimentin proteins were up-regulated in GC cells after overexpression of IL-34, while the knockdown of IL-34 decreased the expression of N-cadherin and vimentin. In human papillary thyroid cancer, it has also been reported that IL-34 regulates the expression of E-cadherin, vimentin, and N-cadherin, which is consistent with our results.

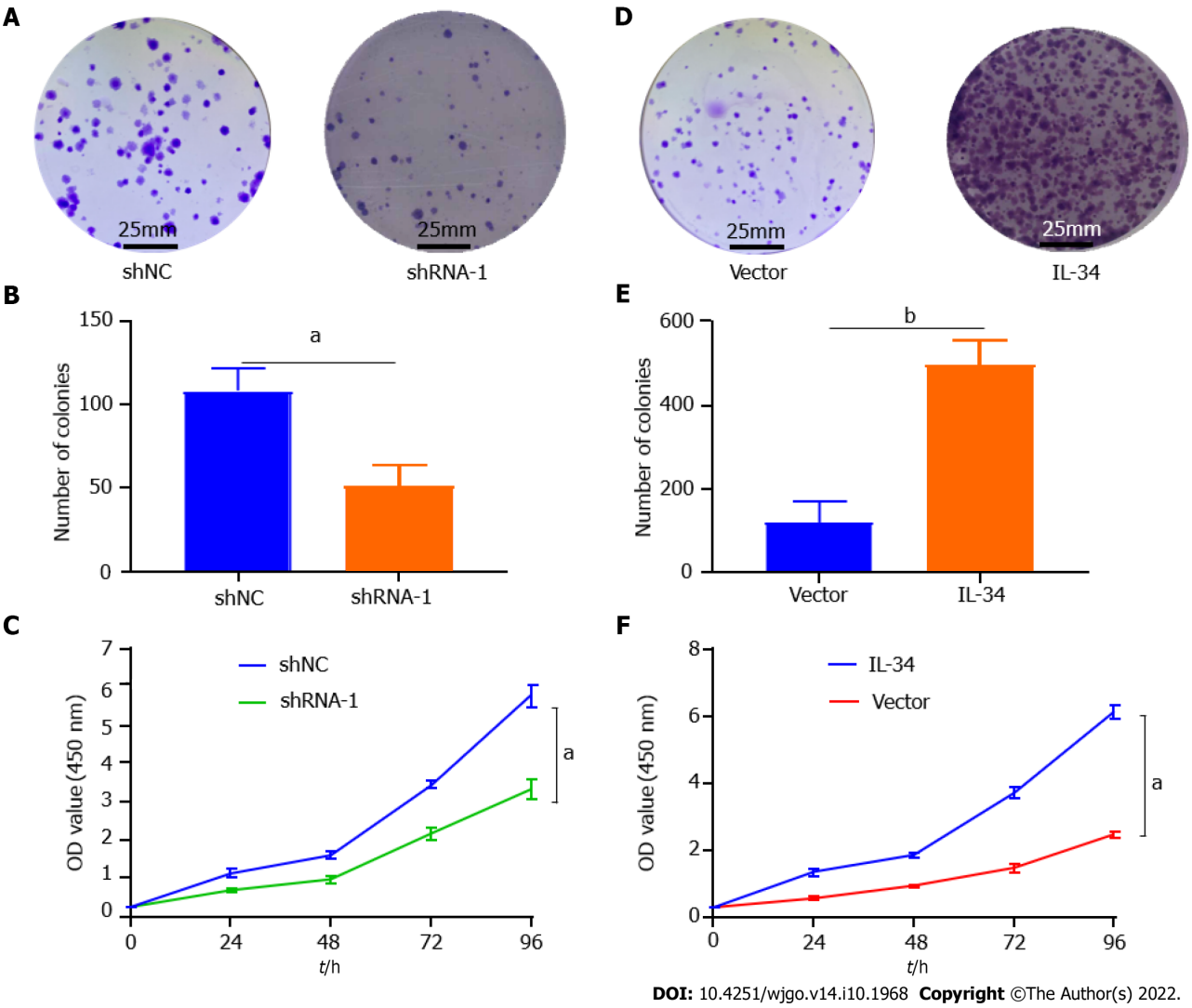

DOI: 10.4251/wjgo.v14.i10.1968

Figure 2 Interleukin-34 modulates clone formation and proliferation in AGS cells. A and B: Downregulation of endogenous interleukin (IL)-34 reduced the mean colony number in the colony formation assay; C: Downregulation of endogenous IL-34 reduced the mean number of AGS cells in the proliferation assay; D and E: Upregulation of endogenous COL5A2 increased the number of invasion cells in the colony formation assay; F: Upregulation of endogenous IL-34 increased the mean number of AGS cells in the proliferation assay. Data shown on graphs were obtained from three independent replicates of the experiments and expressed as mean ± SD, $^{a}P < 0.05$, $^{b}P < 0.01$.

Previous studies have shown that interactions between IL-34 and its functional receptors trigger several intracellular pathways that ultimately control the growth and progression of many types of cancers. For example, multiple studies have found that IL-34 promotes tumor cell growth and invasion through the activation of the ERK signaling pathway[27-29], while inhibition of the ERK signaling pathway inhibits the tumor-promoting effects of IL-34[30]. Currently, the factors and molecular mechanisms that regulate IL-34 in cancer cells are still unknown. We speculate that IL-34 induction is associated with oncogenic mutations that trigger signal that sustain carcinogenesis, and that production of cytokines and chemokines sustains carcinogenesis[31]. Furthermore, it is possible that the altered synthesis of IL-34 depends on changes in miRNA expression, a class of small noncoding RNAs that regulate a wide range of biological processes by altering the expression and translation of their target messenger RNA genes[32]. Finally, immune and stromal cells present in the tumor microenvironment secrete many inflammatory mediators, growth factors such as TNF- a, IL-1b, and IL-6, and these small molecules stimulate tumor cells to secrete IL-34[33,34].

A limitation of the present study is that we did not further investigate the mechanism of action of IL-34 in GC. During the novel coronavirus epidemic, we were temporarily unable to conduct further mechanistic studies due to lack of time and funding constraints. However, we have identified nuclear factor-kappa B as a potential mechanism that may regulate IL-34 expression in GC by single cell sequencing. In the next step, we will continue to validate the mechanism of IL-34 regulation of proliferation, migration and EMT expression in GC.

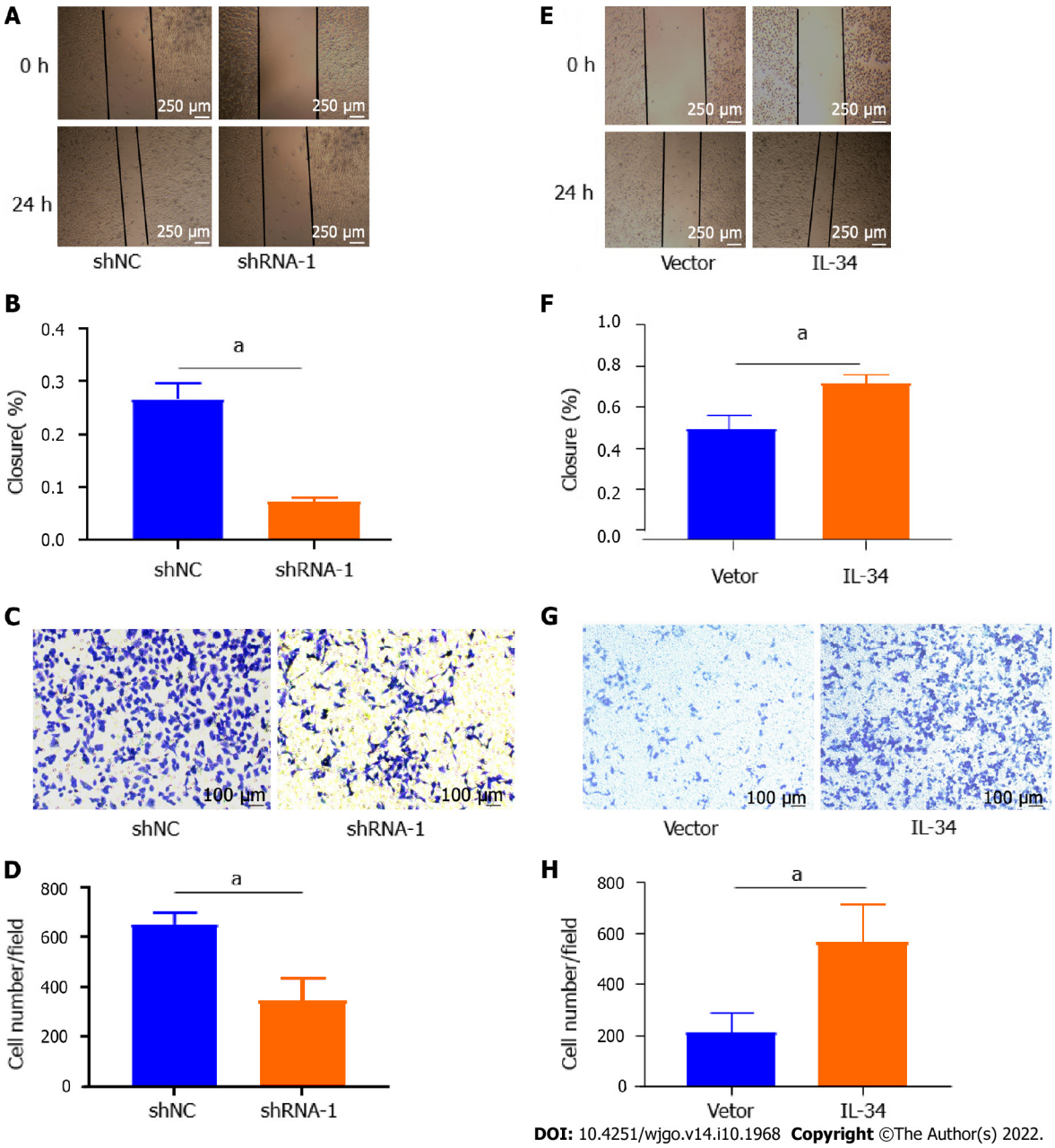

Figure 3 Interleukin-34 regulates the migration and invasiveness of AGS cells. A and B: Wound-healing assay revealed that downregulation of endogenous interleukin (IL)-34 significantly reduced the migration rate; C and D: Downregulation of endogenous IL-34 reduced the number of invaded cells in the transwell assay; E and F: Wound-healing assay revealed that upregulation of endogenous IL-34 significantly increased the migration rate; G and H: Upregulation of endogenous IL-34 increased the number of invaded cells in the transwell assay. Data derived from three independent experiments performed in triplicate and expressed as mean ± SD, and $^{a}P < 0.05$.

CONCLUSION

Our study provides novel evidence that IL-34 contributes to GC growth and metastasis. IL-34 is up-regulated in GC cell lines and tissues, and is correlated with tumor size, grade of differentiation, and TNM stage. IL-34 enhances the capacity for cancer cell proliferation, clone formation, migration, and invasion, and regulates the expression of EMT-associated proteins, suggesting that IL-34 may be an effective target for the therapy of GC.

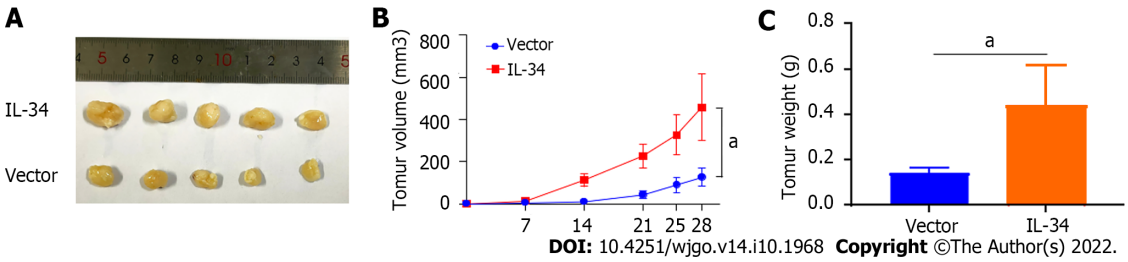

DOI: 10.4251/wjgo.v14.i10.1968

Figure 4 Interleukin-34 regulates the growth of subcutaneous transplantation tumors in nude mice. A-C: Upregulation of endogenous interleukin-34 promotes the growth of transplanted tumors in nude mice. [a]*P* < 0.05.

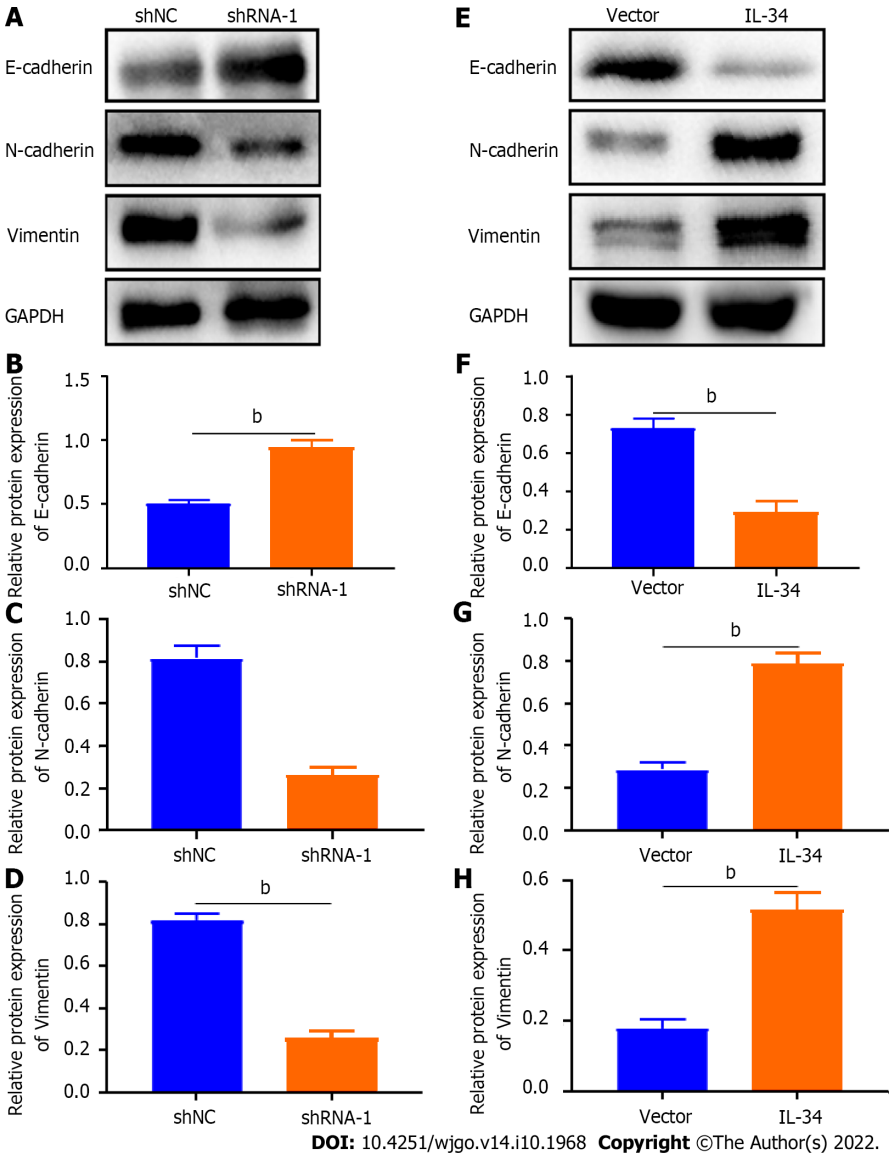

DOI: 10.4251/wjgo.v14.i10.1968

Figure 5 Interleukin-34 regulates the expression of epithelial-mesenchymal transition-related proteins in AGS cells. A-D: Downregulation of endogenous interleukin (IL)-34 increases E-cadherin expression, and reduces the expression of N-cadherin and vimentin in AGS cells; E-H: Upregulation of endogenous IL-34 reduces the E-cadherin expression, but increases the expression of N-cadherin and vimentin in AGS cells. Data was experiments performed in triplicate and expressed as mean ± standard deviation. [b]*P* < 0.01.

ARTICLE HIGHLIGHTS

Research background

Interleukin (IL)-34 is an inflammatory cytokine that is also involved in the development of several tumors. However, the role of IL-34 in the proliferation and epithelial-mesenchymal transition (EMT) of gastric cancer (GC) remains to be investigated.

Research motivation

To investigate the effect of IL-34 on the proliferation of GC cells and to find new therapeutic targets for the treatment of GC.

Research objectives

To clarify the effect of IL-34 on the prognosis of GC patients and the effect of IL-34 on the proliferation and EMT of GC cells.

Research methods

The expression of IL-34 protein in GC tissues and cells was detected using immunohistochemical staining and Western blotting. *In vitro*, stable IL-34 knockdown and overexpressed GC cell lines were cultured, and the proliferation, clone formation, migration and invasion ability of GC cells were examined using cholecystokinin-8 assay, clone formation assay, cell scratch assay and transwell assay, respectively. *In vivo*, the effect of IL-34 on GC transplantation tumor growth was assessed using a subcutaneous tumor transplantation assay in nude mice. Western blotting was used to detect the association of IL-34 protein with EMT-related protein expression levels.

Research results

IL-34 expression is elevated in GC cells and tissues, and IL-34 expression levels correlated with tumor size, T stage, N stage, tumor, node and metastasis stage, and degree of differentiation. *In vitro*, endogenous upregulation of IL-34 promoted GC cell proliferation and EMT. *In vivo*, IL-34 overexpression promoted subcutaneous graft tumor growth in nude mice.

Research conclusions

IL-34 expression is increased in GC tissues and cell lines. IL-34 promotes the proliferation and epithelial-mesenchymal transition of GC cells.

Research perspectives

IL-34 may represent a new strategy for the diagnosis and targeted treatment of GC. Further search for potential cancer-promoting mechanisms of IL-34 is needed in the future.

FOOTNOTES

Author contributions: Li CH, Chen ZM, and Chen PF collected the data and wrote the manuscript; Sui WN participated in data analysis; Ying SC participated in discussion and language editing; Xu AM provided funding support; Han WX reviewed the manuscript and provided funding support; All authors contributed to the article and approved the submitted version.

Supported by the Natural Science Project of Anhui Province, No. KJ2021ZD0022; and the Key Research and Development Program of Anhui Province, No. 202104J07020029.

Institutional review board statement: The study was reviewed and approved by the Institutional Review Board of The First Affiliated Hospital of Anhui Medical University (Quick PJ 2019-09-01).

Institutional animal care and use committee statement: All procedures involving animals were reviewed and approved by the Institutional Animal Care and Use Committee of the Anhui Medical University (SC20200513).

Informed consent statement: All study participants, or their legal guardian, provided informed written consent prior to study enrollment.

Conflict-of-interest statement: There is no conflict of interest in this study.

Data sharing statement: Technical appendix, statistical code, and dataset available from the corresponding author at email address hwxhbh@126.com. Participants gave informed consent for data sharing.

ARRIVE guidelines statement: The authors have read the ARRIVE Guidelines, and the manuscript was prepared and revised according to the ARRIVE Guidelines.

Country/Territory of origin: China

ORCID number: Chuan-Hong Li 0000-0002-3945-972X; Zhang-Ming Chen 0000-0002-4830-0745; Pei-Feng Chen 0000-0003-2843-425X; Lei Meng 0000-0002-1089-1228; Wan-Nian Sui 0000-0002-4337-5238; Song-Cheng Ying 0000-0002-3446-4482; A-Man Xu 0000-0002-7171-5295; Wen-Xiu Han 0000-0002-5335-9645.

S-Editor: Zhang H
L-Editor: A
P-Editor: Zhang XD

REFERENCES

1 **Sung H**, Ferlay J, Siegel RL, Laversanne M, Soerjomataram I, Jemal A, Bray F. Global Cancer Statistics 2020: GLOBOCAN Estimates of Incidence and Mortality Worldwide for 36 Cancers in 185 Countries. *CA Cancer J Clin* 2021; **71**: 209-249 [PMID: 33538338 DOI: 10.3322/caac.21660]
2 **Smyth EC**, Nilsson M, Grabsch HI, van Grieken NC, Lordick F. Gastric cancer. *Lancet* 2020; **396**: 635-648 [PMID: 32861308 DOI: 10.1016/S0140-6736(20)31288-5]
3 **Feng RM**, Zong YN, Cao SM, Xu RH. Current cancer situation in China: good or bad news from the 2018 Global Cancer Statistics? *Cancer Commun (Lond)* 2019; **39**: 22 [PMID: 31030667 DOI: 10.1186/s40880-019-0368-6]
4 **Li Y**, Feng A, Zheng S, Chen C, Lyu J. Recent Estimates and Predictions of 5-Year Survival in Patients with Gastric Cancer: A Model-Based Period Analysis. *Cancer Control* 2022; **29**: 10732748221099227 [PMID: 35499497 DOI: 10.1177/10732748221099227]
5 **Zhang X**, Liang H, Li Z, Xue Y, Wang Y, Zhou Z, Yu J, Bu Z, Chen L, Du Y, Wang X, Wu A, Li G, Su X, Xiao G, Cui M, Wu D, Wu X, Zhou Y, Zhang L, Dang C, He Y, Zhang Z, Sun Y, Li Y, Chen H, Bai Y, Qi C, Yu P, Zhu G, Suo J, Jia B, Li L, Huang C, Li F, Ye Y, Xu H, Yuan Y, E JY, Ying X, Yao C, Shen L, Ji J; RESOLVE study group. Perioperative or postoperative adjuvant oxaliplatin with S-1 *vs* adjuvant oxaliplatin with capecitabine in patients with locally advanced gastric or gastro-oesophageal junction adenocarcinoma undergoing D2 gastrectomy (RESOLVE): an open-label, superiority and non-inferiority, phase 3 randomised controlled trial. *Lancet Oncol* 2021; **22**: 1081-1092 [PMID: 34252374 DOI: 10.1016/S1470-2045(21)00297-7]
6 **Babaei G**, Aziz SG, Jaghi NZZ. EMT, cancer stem cells and autophagy; The three main axes of metastasis. *Biomed Pharmacother* 2021; **133**: 110909 [PMID: 33227701 DOI: 10.1016/j.biopha.2020.110909]
7 **Puisieux A**, Brabletz T, Caramel J. Oncogenic roles of EMT-inducing transcription factors. *Nat Cell Biol* 2014; **16**: 488-494 [PMID: 24875735 DOI: 10.1038/ncb2976]
8 **Zhang J**, Tian XJ, Zhang H, Teng Y, Li R, Bai F, Elankumaran S, Xing J. TGF-β-induced epithelial-to-mesenchymal transition proceeds through stepwise activation of multiple feedback loops. *Sci Signal* 2014; **7**: ra91 [PMID: 25270257 DOI: 10.1126/scisignal.2005304]
9 **Pastushenko I**, Blanpain C. EMT Transition States during Tumor Progression and Metastasis. *Trends Cell Biol* 2019; **29**: 212-226 [PMID: 30594349 DOI: 10.1016/j.tcb.2018.12.001]
10 **Jiang J**, Li J, Zhou X, Zhao X, Huang B, Qin Y. Exosomes Regulate the Epithelial-Mesenchymal Transition in Cancer. *Front Oncol* 2022; **12**: 864980 [PMID: 35359397 DOI: 10.3389/fonc.2022.864980]
11 **Qiao K**, Chen C, Liu H, Qin Y. Pinin Induces Epithelial-to-Mesenchymal Transition in Hepatocellular Carcinoma by Regulating m6A Modification. *J Oncol* 2021; **2021**: 7529164 [PMID: 34917148 DOI: 10.1155/2021/7529164]
12 **Wu X**, Tao P, Zhou Q, Li J, Yu Z, Wang X, Li C, Yan M, Zhu Z, Liu B, Su L. IL-6 secreted by cancer-associated fibroblasts promotes epithelial-mesenchymal transition and metastasis of gastric cancer *via* JAK2/STAT3 signaling pathway. *Oncotarget* 2017; **8**: 20741-20750 [PMID: 28186964 DOI: 10.18632/oncotarget.15119]
13 **Li S**, Cong X, Gao H, Lan X, Li Z, Wang W, Song S, Wang Y, Li C, Zhang H, Zhao Y, Xue Y. Tumor-associated neutrophils induce EMT by IL-17a to promote migration and invasion in gastric cancer cells. *J Exp Clin Cancer Res* 2019; **38**: 6 [PMID: 30616627 DOI: 10.1186/s13046-018-1003-0]
14 **Tian S**, Peng P, Li J, Deng H, Zhan N, Zeng Z, Dong W. SERPINH1 regulates EMT and gastric cancer metastasis *via* the Wnt/β-catenin signaling pathway. *Aging (Albany NY)* 2020; **12**: 3574-3593 [PMID: 32091407 DOI: 10.18632/aging.102831]
15 **Garceau V**, Smith J, Paton IR, Davey M, Fares MA, Sester DP, Burt DW, Hume DA. Pivotal Advance: Avian colony-stimulating factor 1 (CSF-1), interleukin-34 (IL-34), and CSF-1 receptor genes and gene products. *J Leukoc Biol* 2010; **87**: 753-764 [PMID: 20051473 DOI: 10.1189/jlb.0909624]
16 **Ségaliny AI**, Brion R, Brulin B, Maillasson M, Charrier C, Téletchéa S, Heymann D. IL-34 and M-CSF form a novel heteromeric cytokine and regulate the M-CSF receptor activation and localization. *Cytokine* 2015; **76**: 170-181 [PMID: 26095744 DOI: 10.1016/j.cyto.2015.05.029]
17 **Zhou SL**, Hu ZQ, Zhou ZJ, Dai Z, Wang Z, Cao Y, Fan J, Huang XW, Zhou J. miR-28-5p-IL-34-macrophage feedback loop modulates hepatocellular carcinoma metastasis. *Hepatology* 2016; **63**: 1560-1575 [PMID: 26754294 DOI: 10.1002/hep.28445]

18 **Zhang P**, Zhang H, Dong W, Wang Z, Qin Y, Wu C, Dong Q. IL-34 is a potential biomarker for the treatment of papillary thyroid cancer. *J Clin Lab Anal* 2020; **34**: e23335 [PMID: 32573824 DOI: 10.1002/jcla.23335]

19 **Kobayashi T**, Baghdadi M, Han N, Murata T, Hama N, Otsuka R, Wada H, Shiozawa M, Yokose T, Miyagi Y, Takano A, Daigo Y, Seino KI. Prognostic value of IL-34 in colorectal cancer patients. *Immunol Med* 2019; **42**: 169-175 [PMID: 31762401 DOI: 10.1080/25785826.2019.1691429]

20 **Irie T**, Yoshii D, Komohara Y, Fujiwara Y, Kadohisa M, Honda M, Suzu S, Matsuura T, Kohashi K, Oda Y, Hibi T. IL-34 in hepatoblastoma cells potentially promote tumor progression *via* autocrine and paracrine mechanisms. *Cancer Med* 2022; **11**: 1441-1453 [PMID: 35132816 DOI: 10.1002/cam4.4537]

21 **Kajihara N**, Kitagawa F, Kobayashi T, Wada H, Otsuka R, Seino KI. Interleukin-34 contributes to poor prognosis in triple-negative breast cancer. *Breast Cancer* 2020; **27**: 1198-1204 [PMID: 32578004 DOI: 10.1007/s12282-020-01123-x]

22 **Franzè E**, Di Grazia A, Sica GS, Biancone L, Laudisi F, Monteleone G. Interleukin-34 Enhances the Tumor Promoting Function of Colorectal Cancer-Associated Fibroblasts. *Cancers (Basel)* 2020; **12**: 3537 [PMID: 33260828 DOI: 10.3390/cancers12123537]

23 **Mittal V**. Epithelial Mesenchymal Transition in Tumor Metastasis. *Annu Rev Pathol* 2018; **13**: 395-412 [PMID: 29414248 DOI: 10.1146/annurev-pathol-020117-043854]

24 **Sun L**, Fang J. Epigenetic regulation of epithelial-mesenchymal transition. *Cell Mol Life Sci* 2016; **73**: 4493-4515 [PMID: 27392607 DOI: 10.1007/s00018-016-2303-1]

25 **Xu J**, Liu D, Niu H, Zhu G, Xu Y, Ye D, Li J, Zhang Q. Resveratrol reverses Doxorubicin resistance by inhibiting epithelial-mesenchymal transition (EMT) through modulating PTEN/Akt signaling pathway in gastric cancer. *J Exp Clin Cancer Res* 2017; **36**: 19 [PMID: 28126034 DOI: 10.1186/s13046-016-0487-8]

26 **Yue B**, Song C, Yang L, Cui R, Cheng X, Zhang Z, Zhao G. METTL3-mediated N6-methyladenosine modification is critical for epithelial-mesenchymal transition and metastasis of gastric cancer. *Mol Cancer* 2019; **18**: 142 [PMID: 31607270 DOI: 10.1186/s12943-019-1065-4]

27 **Xia H**, Chen J, Shi M, Gao H, Sekar K, Seshachalam VP, Ooi LL, Hui KM. EDIL3 is a novel regulator of epithelial-mesenchymal transition controlling early recurrence of hepatocellular carcinoma. *J Hepatol* 2015; **63**: 863-873 [PMID: 25980764 DOI: 10.1016/j.jhep.2015.05.005]

28 **Hu J**, Li L, Chen H, Zhang G, Liu H, Kong R, Wang Y, Li Y, Tian F, Lv X, Li G, Sun B. MiR-361-3p regulates ERK1/2-induced EMT *via* DUSP2 mRNA degradation in pancreatic ductal adenocarcinoma. *Cell Death Dis* 2018; **9**: 807 [PMID: 30042387 DOI: 10.1038/s41419-018-0839-8]

29 **Wang K**, Ji W, Yu Y, Li Z, Niu X, Xia W, Lu S. FGFR1-ERK1/2-SOX2 axis promotes cell proliferation, epithelial-mesenchymal transition, and metastasis in FGFR1-amplified lung cancer. *Oncogene* 2018; **37**: 5340-5354 [PMID: 29858603 DOI: 10.1038/s41388-018-0311-3]

30 **Franzè E**, Dinallo V, Rizzo A, Di Giovangiulio M, Bevivino G, Stolfi C, Caprioli F, Colantoni A, Ortenzi A, Grazia AD, Sica G, Sileri PP, Rossi P, Monteleone G. Interleukin-34 sustains pro-tumorigenic signals in colon cancer tissue. *Oncotarget* 2018; **9**: 3432-3445 [PMID: 29423057 DOI: 10.18632/oncotarget.23289]

31 **Wellenstein MD**, de Visser KE. Cancer-Cell-Intrinsic Mechanisms Shaping the Tumor Immune Landscape. *Immunity* 2018; **48**: 399-416 [PMID: 29562192 DOI: 10.1016/j.immuni.2018.03.004]

32 **Treiber T**, Treiber N, Meister G. Regulation of microRNA biogenesis and its crosstalk with other cellular pathways. *Nat Rev Mol Cell Biol* 2019; **20**: 5-20 [PMID: 30228348 DOI: 10.1038/s41580-018-0059-1]

33 **Franzè E**, Monteleone I, Cupi ML, Mancia P, Caprioli F, Marafini I, Colantoni A, Ortenzi A, Laudisi F, Sica G, Sileri P, Pallone F, Monteleone G. Interleukin-34 sustains inflammatory pathways in the gut. *Clin Sci (Lond)* 2015; **129**: 271-280 [PMID: 25800277 DOI: 10.1042/CS20150132]

34 **Baghdadi M**, Ishikawa K, Nakanishi S, Murata T, Umeyama Y, Kobayashi T, Kameda Y, Endo H, Wada H, Bogen B, Yamamoto S, Yamaguchi K, Kasahara I, Iwasaki H, Takahata M, Ibata M, Takahashi S, Goto H, Teshima T, Seino KI. A role for IL-34 in osteolytic disease of multiple myeloma. *Blood Adv* 2019; **3**: 541-551 [PMID: 30782613 DOI: 10.1182/bloodadvances.2018020008]

World Journal of Gastrointestinal Oncology

Submit a Manuscript: https://www.f6publishing.com

World J Gastrointest Oncol 2022 October 15; 14(10): 1981-2003

DOI: 10.4251/wjgo.v14.i10.1981

ISSN 1948-5204 (online)

ORIGINAL ARTICLE

Basic Study

Cuproptosis-related long non-coding RNAs model that effectively predicts prognosis in hepatocellular carcinoma

En-Min Huang, Ning Ma, Tao Ma, Jun-Yi Zhou, Wei-Sheng Yang, Chuang-Xiong Liu, Ze-Hui Hou, Shuang Chen, Zhen Zong, Bing Zeng, Ying-Ru Li, Tai-Cheng Zhou

Specialty type: Mathematical and computational biology

Provenance and peer review: Unsolicited article; Externally peer reviewed.

Peer-review model: Single blind

Peer-review report's scientific quality classification

Grade A (Excellent): 0
Grade B (Very good): 0
Grade C (Good): C, C, C
Grade D (Fair): 0
Grade E (Poor): 0

P-Reviewer: Li ZZ, China; Nath L, India

Received: June 24, 2022
Peer-review started: June 24, 2022
First decision: July 18, 2022
Revised: July 29, 2022
Accepted: August 17, 2022
Article in press: August 17, 2022
Published online: October 15, 2022

En-Min Huang, Ning Ma, Tao Ma, Wei-Sheng Yang, Chuang-Xiong Liu, Ze-Hui Hou, Shuang Chen, Bing Zeng, Ying-Ru Li, Tai-Cheng Zhou, Department of Gastroenterological Surgery and Hernia Center, The Sixth Affiliated Hospital, Sun Yat-sen University, Guangzhou 510655, Guangdong Province, China

En-Min Huang, Ning Ma, Tao Ma, Jun-Yi Zhou, Wei-Sheng Yang, Chuang-Xiong Liu, Ze-Hui Hou, Shuang Chen, Bing Zeng, Ying-Ru Li, Tai-Cheng Zhou, Guangdong Provincial Key Laboratory of Colorectal and Pelvic Floor Diseases, The Sixth Affiliated Hospital, Sun Yat-sen University, Guangzhou 510655, Guangdong Province, China

Jun-Yi Zhou, Department of Gastrointestinal Surgery, The Sixth Affiliated Hospital, Sun Yat-sen University, Guangzhou 510655, Guangdong Province, China

Zhen Zong, Department of Gastroenterological Surgery, The Second Affiliated Hospital, Nanchang University, Nanchang 330006, Jiangxi Province, China

Corresponding author: Tai-Cheng Zhou, MD, PhD, Associate Professor, Doctor, Surgeon, Surgical Oncologist, Department of Gastroenterological Surgery and Hernia Center, The Sixth Affiliated Hospital, Sun Yat-sen University, No. 26 Erheng Road, Yuancun, Guangzhou 510655, Guangdong Province, China. zhoutch3@mail.sysu.edu.cn

Abstract

BACKGROUND

Cuproptosis has recently been considered a novel form of programmed cell death. To date, long-chain non-coding RNAs (lncRNAs) crucial to the regulation of this process remain unelucidated.

AIM

To identify lncRNAs linked to cuproptosis in order to estimate patients' prognoses for hepatocellular carcinoma (HCC).

METHODS

Using RNA sequence data from The Cancer Genome Atlas Live Hepatocellular Carcinoma (TCGA-LIHC), a co-expression network of cuproptosis-related genes and lncRNAs was constructed. For HCC prognosis, we developed a cuproptosis-related lncRNA signature (CupRLSig) using univariate Cox, lasso, and multivariate Cox regression analyses. Kaplan-Meier analysis was used to compare

overall survival among high- and low-risk groups stratified by median CupRLSig risk score. Furthermore, comparisons of functional annotation, immune infiltration, somatic mutation, tumor mutation burden (TMB), and pharmacologic options were made between high- and low-risk groups.

RESULTS

Three hundred and forty-three patients with complete follow-up data were recruited in the analysis. Pearson correlation analysis identified 157 cuproptosis-related lncRNAs related to 14 cuproptosis genes. Next, we divided the TCGA-LIHC sample into a training set and a validation set. In univariate Cox regression analysis, 27 LncRNAs with prognostic value were identified in the training set. After lasso regression, the multivariate Cox regression model determined the identified risk equation as follows: Risk score = (0.2659 × PICSAR expression) + (0.4374 × FOXD2-AS1 expression) + (-0.3467 × AP001065.1 expression). The CupRLSig high-risk group was associated with poor overall survival (hazard ratio = 1.162, 95%CI = 1.063-1.270; $P < 0.001$) after the patients were divided into two groups depending upon their median risk score. Model accuracy was further supported by receiver operating characteristic and principal component analysis as well as the validation set. The area under the curve of 0.741 was found to be a better predictor of HCC prognosis as compared to other clinicopathological variables. Mutation analysis revealed that high-risk combinations with high TMB carried worse prognoses (median survival of 30 mo *vs* 102 mo of low-risk combinations with low TMB group). The low-risk group had more activated natural killer cells (NK cells, $P = 0.032$ by Wilcoxon rank sum test) and fewer regulatory T cells (Tregs, $P = 0.021$) infiltration than the high-risk group. This finding could explain why the low-risk group has a better prognosis. Interestingly, when checkpoint gene expression (CD276, CTLA-4, and PDCD-1) and tumor immune dysfunction and rejection (TIDE) scores are considered, high-risk patients may respond better to immunotherapy. Finally, most drugs commonly used in preclinical and clinical systemic therapy for HCC, such as 5-fluorouracil, gemcitabine, paclitaxel, imatinib, sunitinib, rapamycin, and XL-184 (cabozantinib), were found to be more efficacious in the low-risk group; erlotinib, an exception, was more efficacious in the high-risk group.

CONCLUSION

The lncRNA signature, CupRLSig, constructed in this study is valuable in prognostic estimation of HCC. Importantly, CupRLSig also predicts the level of immune infiltration and potential efficacy of tumor immunotherapy.

Key Words: Hepatocellular carcinoma; Cuproptosis; Long-chain non-coding RNAs; Prognosis; Tumor microenvironment; Immunotherapy

Core Tip: Factors crucial to the regulation of cuproptosis remain unelucidated. Using transcriptome data from The Cancer Genome Atlas (TCGA-LIHC), we developed a cuproptosis- and prognosis-related long-chain non-coding RNAs signature (CupRLSig) for hepatocellular carcinoma. The high-risk group identified by CupRLSig was associated with poorer overall survival and progression-free survival. Less activation of natural killer cells and more infiltration of regulatory T cells in the high-risk group may explain the worse outcomes. Interestingly, based on checkpoint gene expression (CD276, CTLA-4, and PDCD-1) and tumor immune dysfunction and rejection, high-risk patients may respond better to immunotherapy.

Citation: Huang EM, Ma N, Ma T, Zhou JY, Yang WS, Liu CX, Hou ZH, Chen S, Zong Z, Zeng B, Li YR, Zhou TC. Cuproptosis-related long non-coding RNAs model that effectively predicts prognosis in hepatocellular carcinoma. *World J Gastrointest Oncol* 2022; 14(10): 1981-2003
URL: https://www.wjgnet.com/1948-5204/full/v14/i10/1981.htm
DOI: https://dx.doi.org/10.4251/wjgo.v14.i10.1981

INTRODUCTION

The second most deadly tumor type after pancreatic cancer, liver cancer has a 5-year survival rate of only 18% and a median survival time of just one year[1]. Around 80% of those primary liver tumors are hepatocellular carcinomas (HCC)[2]. Surgery, ablation, and orthotopic liver transplantation remain the

most popular locoregional treatment options for HCC[3]. However, as most HCC patients are diagnosed at a late stage in the illness and often have metastases on diagnosis, surgical resection is rarely a viable treatment option. Such patients can only be treated with systemic therapies such as targeted therapies[4]. Despite the availability of several tyrosine kinase inhibitors for first- and second-line treatment, the overall survival (OS) of patients with advanced HCC remains poor owing to drug resistance and has not improved over the past decade[5]. Although the recent approval by the Food and Drug Administration of immune checkpoint inhibitors has transformed the clinical management of HCC, only a small proportion of patients are sensitive to this therapy owing to a lack of relevant selective biomarkers[6]. As a result, there is a pressing necessity to investigate novel treatment modalities and biomarkers in order to improve patient outcomes.

Levels of copper, including the complex form of ceruloplasmin, are significantly elevated in serum and tumors of cancer patients[7]. Excess copper acts as a powerful oxidant, promoting the intracellular production of reactive oxygen species (ROS) and apoptosis[8]. Malignant cells naturally possess higher basal ROS levels compared with normal cells[8] as they use mechanisms such as compensatory upregulation of the NRF2 gene to counter increases in ROS resulting from copper accumulation[2]. Thus, utilization of the altered copper distribution to generate an intolerable increase in ROS stress in malignant cells warrants consideration as a potential anticancer strategy[7]. Prior to the clinical utilization of spatial copper distribution for cancer treatment, however, the genes involved in copper metabolism and their regulatory networks must be elucidated. For example, alterations in copper bioavailability in KRAS-mutant tumors have been investigated in preclinical studies[9]. Copper has a dual function, being an essential enzyme cofactor but also producing toxicity that causes cell death. Thus, copper has been proposed as a new therapeutic target for use in strategies to specifically kill cancer cells by increasing intracellular copper accumulation[10,11]. Recently, researchers found that some cancer cells die when carrier molecules such as FDX1 import substantial levels of copper into the cytoplasm[12]. By blocking alternative cell death pathways, this was proved to be a specific type of cell death; further research revealed that cells more reliant on mitochondria for energy production were more sensitive to this copper-induced death, which was named cuproptosis[12]. Lipid acylation, a major target of cuproptosis for cytotoxicity, is widespread and conserved in nature[11]. This metabolic profile indicates the promise of copper-ion-targeted therapies for tumors. There is thus an urgent need for methods for reliable and accurate detection of biomarkers of cuproptosis in human tumor tissues.

Long non-coding RNAs (lncRNAs) are involved in a variety of biological processes. Several HCC-related lncRNAs have been discovered to be deregulated in tumor tissues and to play critical roles in shaping the tumor microenvironment *via* epigenetic regulation[13]. Similarly, lncRNAs have been reported to have crucial roles in the regulation of metabolism of metal ion homeostasis. Some 2564 LncRNAs were found to be significantly upregulated, whereas 1052 were downregulated, in a recently constructed toxic milk mouse model of Wilson's disease (WD), which is characterized by a mutation of the ATP7B gene that affects copper transport[14]. The cytosolic lncRNA P53RRA was found to displace p53 from the G3BP1-p53 complex, resulting in increased intranuclear p53 retention and manifestation of ferroptosis, another ion-induced form of programmed cell death[15]. Although the mechanism characterizing the lncRNA-mediated epigenetic regulation of ferroptosis has been widely investigated[16], the lncRNA regulatory network associated with cuproptosis remains almost completely unknown. Given that lncRNAs play a role in a variety of biological processes, such as ferroptosis, they are highly likely to be involved in the regulation of cuproptosis. Thus, identification of transcriptional changes in lncRNAs will be critical for the characterization of cuproptosis and for determining its relevance in malignancy.

Here, we developed a cuproptosis-related lncRNA signature (CupRLSig) and demonstrated its ability to predict prognosis of HCC patients. Furthermore, we constructed a nomogram based on CupRLSig as well as a number of clinical features and compared gene enrichment, mutations, immune cell infiltration, and potential responses to targeted therapy and immunotherapy between CupRLSig-defined high- and low-risk groups. This study provides insight into the cuproptosis regulatory network, the understanding of which is critical for improving the efficacy of individualized HCC treatment.

MATERIALS AND METHODS

Dataset and sample extraction

RNA-sequencing data (RNA-seq), clinical characteristics, and mutation data of HCC patients were obtained from The Cancer Genome Atlas-Live Hepatocellular Carcinoma Database (TCGA-LIHC, https://portal.gdc.cancer.gov/). Initially, data from 424 HCC patients were collected. Patients with incomplete follow-up data or survival < 30 d and those lacking complete clinicopathological data were excluded from follow-up analysis; 343 patients were ultimately included. The 19 cuproptosis-related genes, listed in Supplementary Table 1, were obtained from the available literature[2,9,12,17-19] reporting findings of gene manipulation studies, and are genes that were found to either induce or inhibit cuproptosis. The present study was conducted in accordance with the Declaration of Helsinki as revised in 2013.

Identification of CupRLSig for prediction of HCC patient prognosis

Based on gene names, transcriptional expression profile data were classified as lncRNA or mRNA, and lncRNAs associated with 19 cuproptosis-related genes (mRNAs) were identified using the "limma" R package and the Pearson correlation test. The absolute value of the Pearson correlation coefficient (> 0.4) and $P < 0.05$ were used as thresholds for the establishment of a cuproptosis-related mRNA-lncRNA co-expression network to identify lncRNAs relevant in cuproptosis. The network was visualized using a Sankey diagram generated by the R software package "ggalluvial." The entire TCGA-LIHC sample was subsequently randomly divided into a training group and a validation group (Table 1); univariate Cox regression analysis was used to determine whether these lncRNAs were associated with patient prognosis in the training group. Lasso regression analysis was also performed to avoid over-fitting and eliminate tightly correlated genes. The minimal penalty term (lambda) was chosen using ten-fold cross-validation. The aforementioned lncRNAs were subsequently used to construct a multivariate Cox regression model and determine correlation coefficients. The following formula was used to calculate risk scores based on the model: risk score = explncRNA1 × coef lncRNA1 + explncRNA2 × coef lncRNA2 + ... + explncRNAi × coef lncRNAi. We termed this predictive lncRNA signature CupRLSig. Risk scores were calculated for all patients in the training set, test set, and entire TCGA-LIHC set, and According to the median risk score in the training group, HCC samples from all three datasets were split into high- and low-risk groups. The CupRLSig model was tested using Kaplan-Meier curves, risk curves, survival status analyses, and heatmap analyses to see if it could effectively identify patients with different risk levels. The accuracy of the model was quantified using progression-free survival (PFS) analysis, the concordance index (C-index), independent prognostic analysis, and receiver operating characteristic (ROC) curves. The R software package "pheatmap" was used to visualize clinicopathological variables in the high- and low-risk groups from the entire TCGA-LIHC sample set; the distribution of patients with varying risk scores was evaluated using principal component analysis (PCA) and visualized using the R software package "scatterplot3d." Finally, stratified analyses were performed using various pathological parameters to determine whether the model's distinction between high- and low-risk groups significantly correlated with other clinical parameters.

Construction of the nomogram

A nomogram was constructed using the R software packages "rms" and "regplot" for the prediction of HCC patient survival at 1, 3, and 5 years based on a combination of the risk score with other clinicopathological data. Calibration curves were used to evaluate whether the predicted survival rates were consistent with actual survival rates. A patient was randomly selected to confirm the predictive utility of the nomogram.

Analysis of functional enrichment of genes and lncRNAs with differential expression in different-risk CupRLSig groups

Differentially expressed genes and lncRNAs between the high- and low-risk CupRLSig groups were identified using the R software package "limma" with the criteria of $\log_2$ fold change absolute value greater than 1 and false discovery rate less than 0.05. Functional enrichment analysis of the differentially expressed genes and lncRNAs was then performed using the Gene Ontology (GO) and the Kyoto Encyclopedia of Genes and Genomes (KEGG) databases.

Analysis of somatic mutation data and TMB

The number of somatic non-synonymous point mutations in each sample was counted and visualized using the R software package "maftools"[20]. The TMB was calculated as the number of somatic, coding, base replacement, and insert-deletion mutations discovered per megabase of genome using non-synonymous and code-shifting indels with a 5% detection limit. In addition, TMB was compared between the high- and low-risk groups, and survival curves for TMB and risk score integration were plotted.

Estimation of immune infiltration

The CIBERSORT algorithm[21] was used to estimate the infiltration proportions of 22 immune cell types in HCC samples. The proportions of immune cells in different groups were compared using the Wilcoxon rank-sum test. Single-sample gene set enrichment analysis was performed using the R software package "GSVA"[22] to assess the activity of 13 immune-related functions and compare differences between the two groups.

Potential relationships of CupRLSig with immunotherapy, chemotherapy, and target therapy

First, differential expression of 47 immune checkpoint genes in the CupRLSig high- and low-risk groups was compared. The tumor immune dysfunction and exclusion (TIDE, http://tide.dfci.harvard.edu/) module was used to distinguish potential immunotherapy responses between groups. This module predicts anti-PD1 and anti-CTLA4 treatment response based on patients' pre-treatment genome transcriptional expression profiles. The role of CupRLSig in predicting the therapeutic response of HCC

Table 1 Clinical characteristics of The Cancer Genome Atlas Live Hepatocellular Carcinoma sample training and test groups (*n* = 343)

Covariates	Sub type	Entire TCGA-LIHC, *n* (%)	Test group, *n* (%)	Training group, *n* (%)	*P* value
Age (yr)	≤ 65	216 (62.97)	103 (60.23)	113 (65.70)	0.3493
	> 65	127 (37.03)	68 (39.77)	59 (34.30)	
Gender	Female	110 (32.07)	59 (34.50)	51 (29.65)	0.3971
	Male	233 (67.93)	112 (65.50)	121 (70.35)	
Grade	G1	53 (15.45)	27 (15.79)	26 (15.12)	0.3
	G2	161 (46.94)	85 (49.71)	76 (44.19)	
	G3	112 (32.65)	54 (31.58)	58 (33.72)	
	G4	12 (3.50)	3 (1.75)	9 (5.23)	
	Unknown	5 (1.46)	2 (1.17)	3 (1.74)	
Stage	Stage I	161 (46.94)	81 (47.37)	80 (46.51)	0.9079
	Stage II	77 (22.45)	39 (22.81)	38 (22.09)	
	Stage III	80 (23.32)	38 (22.22)	42 (24.42)	
	Stage IV	3 (0.87)	2 (1.17)	1 (0.58)	
	Unknown	22 (6.41)	11 (6.43)	11 (6.40)	
T	T1	168 (48.98)	86 (50.29)	82 (47.67)	0.5683
	T2	84 (24.49)	42 (24.56)	42 (24.42)	
	T3	75 (21.87)	37 (21.64)	38 (22.09)	
	T4	13 (3.79)	4 (2.34)	9 (5.23)	
	Unknown	3 (0.87)	2 (1.17)	1 (0.58)	
M	M0	245 (71.43)	118 (69.01)	127 (73.84)	0.9551
	M1	3 (0.87)	2 (1.17)	1 (0.58)	
	Unknown	95 (27.70)	51 (29.82)	44 (25.58)	
N	N0	239 (69.68)	111 (64.91)	128 (74.42)	0.9081
	N1	3 (0.87)	2 (1.17)	1 (0.58)	
	Unknown	101 (29.45)	58 (33.92)	43 (25.00)	

T: Tumor; N: Lymph node; M: Metastasis. The *P* value is indicated for the chi-square test and Kruskal-Wallis test among the three groups.

was further evaluated by calculation of the half-maximal inhibitory concentration (IC_{50}) values of drugs commonly used for chemotherapy and targeted therapy. The Wilcoxon signed-rank test and R software package "pRRophetic" were used to compare and visualize IC_{50} values in the high- and low-risk groups.

Statistical analysis

The Kaplan-Meier method were used to compare OS and PFS of different groups of patients. The R "survivalROC" package was used to construct ROC curves and calculate the area under the curve (AUC). The Kruskal-Wallis test was used to compare differences between groups, and clinical data were analyzed using either chi-squared or Fisher's exact tests. Relationships between lncRNA expression, immune infiltration, and immune checkpoint gene expression were assessed using Spearman or Pearson correlation coefficients. All statistical analyses were performed using R software (version 4.1.2); a *P* value < 0.05 was considered to indicate statistical significance. The statistical methods used in this study were reviewed by Dr. GanFeng Luo from the Department of Epidemiology and Health Statistics, School of Public Health, Sun Yat-sen University.

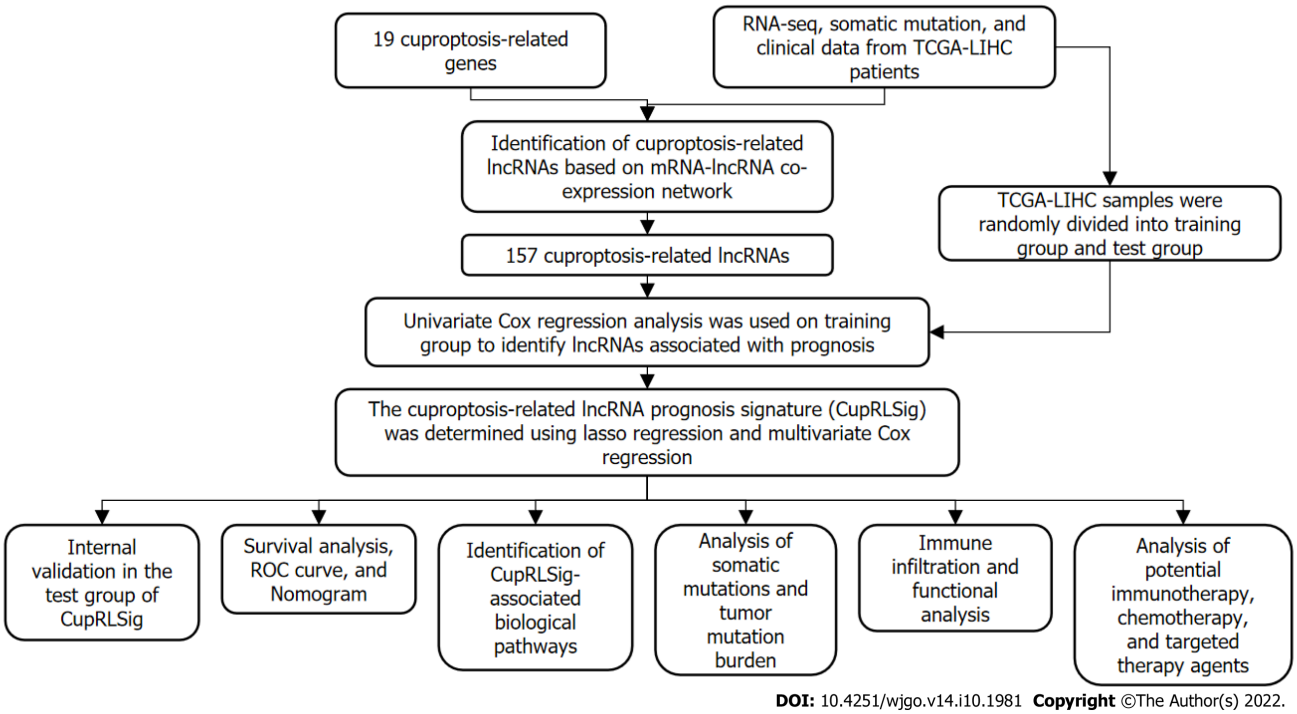

DOI: 10.4251/wjgo.v14.i10.1981

Figure 1 Study flowchart. RNA-seq: RNA sequencing; TCGA-LIHC: The Cancer Genome Atlas-Live Hepatocellular Carcinoma; lncRNAs: Long non-coding RNAs; ROC: Receiver operating characteristic.

RESULTS

Characteristics of the datasets and construction of the CupRLSig model

Figure 1 presents a flow chart of the present study. First, Pearson correlation analysis identified 157 cuproptosis-related lncRNAs related to 14 cuproptosis genes, with correlation coefficient > 0.4 and P < 0.05 (Figure 2A and Supplementary Table 2). We collected 343 samples with complete clinicopathological data from the TCGA-LIHC database. The samples and data were from 233 males and 110 females, 224 of whom were still alive. The age of HCC patients ranged from 16 to 90 years, and their survival after diagnosis ranged from 30 to 3675 d. More detailed characteristics are shown in Table 1.

The entire TCGA-LIHC sample was subsequently randomly divided into a training group and a validation group (Table 1). Univariate Cox regression analysis revealed a total of 27 LncRNAs that had prognostic significance in the training group (Figure 2B). Following Lasso regression analysis (Figure 2C and D), three lncRNAs in the training group were retained and used to construct a multivariate Cox regression model. The correlations between these three lncRNAs (collectively termed CupRLSig) and the 19 cuproptosis-related genes are shown in Figure 2E. A formula for the CupRLSig risk score was established as follows: risk score = (0.2659 × PICSAR expression) + (0.4374 × FOXD2-AS1 expression) + (-0.3467 × AP001065.1 expression). Based on the median risk score in the training group, patients were divided into two risk groups using this formula. Finally, 86, 80, and 166 patients from the training, test, and entire set, respectively, were assigned to the high-risk group; and 86, 91, and 177 patients were assigned to the low-risk group (Figure 3A-C). Kaplan-Meier analysis revealed a significantly shorter OS in the high-risk group compared with the low-risk group for both datasets (Figure 3A-C). Individual patient risk scores and survival statistics are detailed in Figure 3D-I; notably, the risk score rose along with the number of deaths. The expression status of the three lncRNAs in each group is detailed in Figure 3J-L.

Evaluation of the accuracy of the CupRLSig model

We further evaluated the PFS of 343 HCC patients using data downloaded from http://xena.ucsc.edu/ to assess the prediction accuracy of our CupRLSig prognostic model among HCC patients. High-risk patients were noted to have significantly shorter PFS (P = 0.001; Figure 4A). According to the C-index values, the model's prognostic prediction performance was comparable with that of disease stage (Figure 4B). Univariate and multivariate Cox regression analyses revealed CupRLSig risk score to be an independent prognostic factor (Figure 4C and D); its AUC of 0.741 indicated that it was a better predictor of HCC prognosis than other clinicopathological variables (Figure 4E). The 1-, 3-, and 5-year ROC AUCs were 0.741, 0.636, and 0.649, respectively, indicating that CupRLSig exhibited good prognostic performance (Figure 4F).

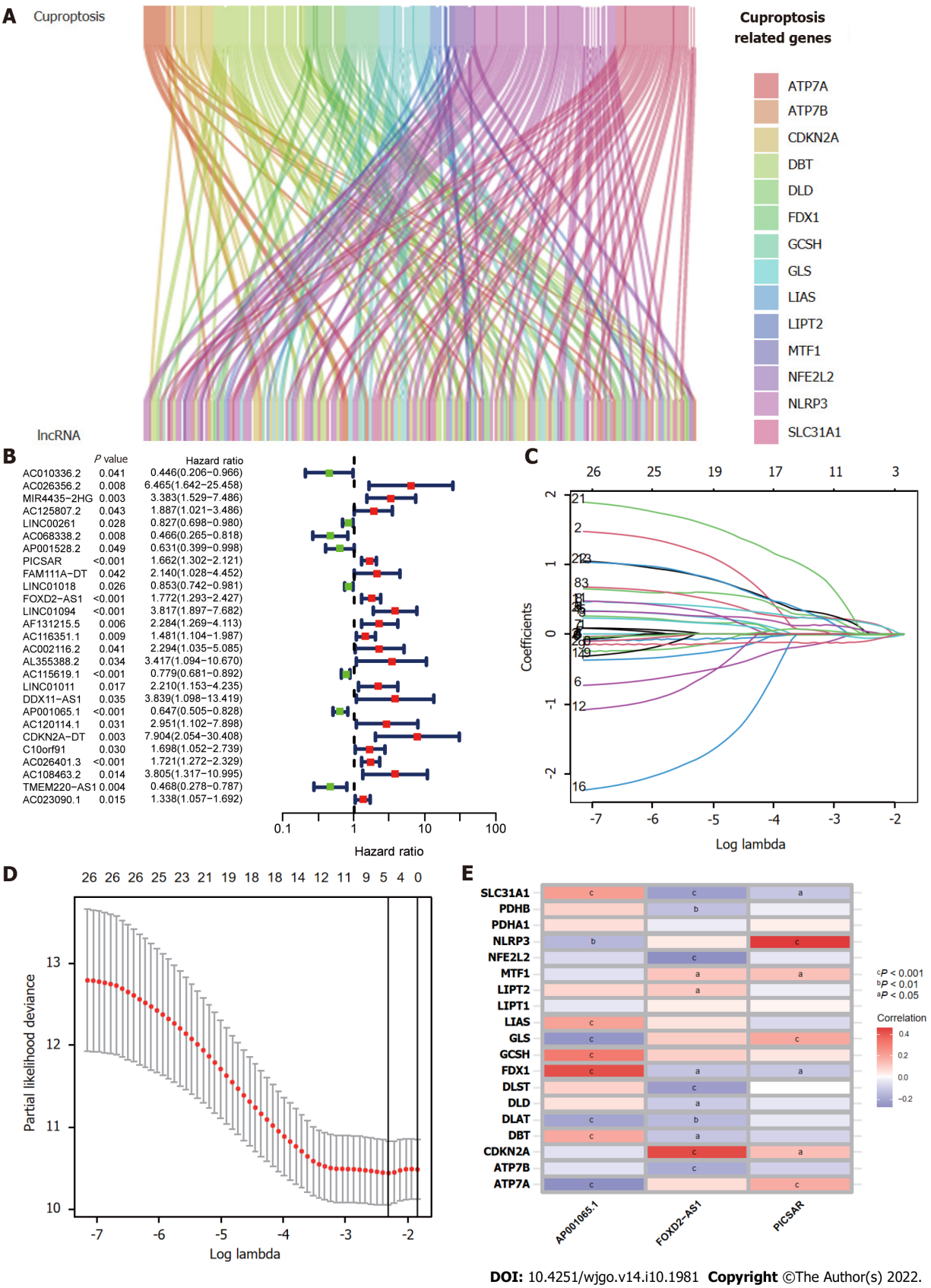

DOI: 10.4251/wjgo.v14.i10.1981

Figure 2 Construction of the cuproptosis-related long-chain non-coding RNA signature (CupRLSig) model. A: Sankey diagram showing the associations between cuproptosis-related long-chain non-coding RNAs (lncRNAs) and mRNAs; B: Forest plot showing 27 LncRNAs with hazard ratios (95% confidence intervals) and *P* values for association with HCC prognosis based on univariate Cox proportional-hazards analysis; C: Lasso coefficient profiles; D: Selection of the tuning parameter (lambda) in the Lasso model by ten-fold cross-validation based on minimum criteria for overall survival; E: Heatmap showing the correlations of the three lncRNAs incorporated into the cuproptosis-related long-chain non-coding RNA signature model (CupRLSig) model and 19 cuproptosis-related genes. $^{a}P < 0.05$; $^{b}P < 0.01$; $^{c}P < 0.001$.

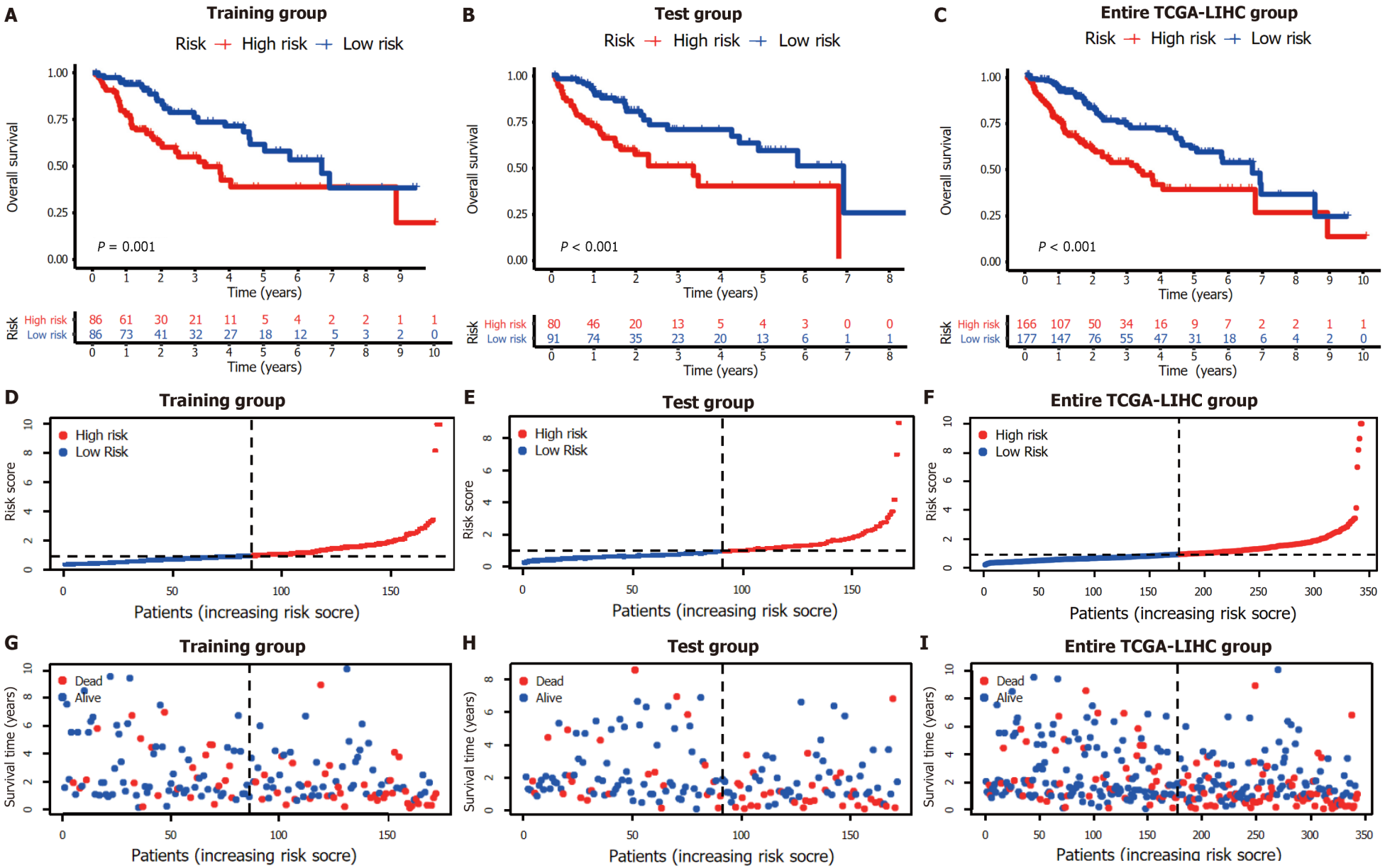
A
Training group
Risk High risk Low risk
Overall survival
P = 0.001
Time (years)
Risk High risk 86 61 30 21 11 5 4 2 2 1 1
Low risk 86 73 41 32 27 18 12 5 3 2 0
B
Test group
Risk High risk Low risk
Overall survival
P < 0.001
Time (years)
Risk High risk 80 46 20 13 5 4 3 0 0
Low risk 91 74 35 23 20 13 6 1 1
C
Entire TCGA-LIHC group
Risk High risk Low risk
Overall survival
P < 0.001
Time (years)
Risk High risk 166 107 50 34 16 9 7 2 2 1 1
Low risk 177 147 76 55 47 31 18 6 4 2 0
D
Training group
High risk
Low Risk
Risk score
Patients (increasing risk socre)
E
Test group
High risk
Low Risk
Risk score
Patients (increasing risk socre)
F
Entire TCGA-LIHC group
High risk
Low Risk
Risk score
Patients (increasing risk socre)
G
Training group
Dead
Alive
Survival time (years)
Patients (increasing risk socre)
H
Test group
Dead
Alive
Survival time (years)
Patients (increasing risk socre)
I
Entire TCGA-LIHC group
Dead
Alive
Survival time (years)
Patients (increasing risk socre)

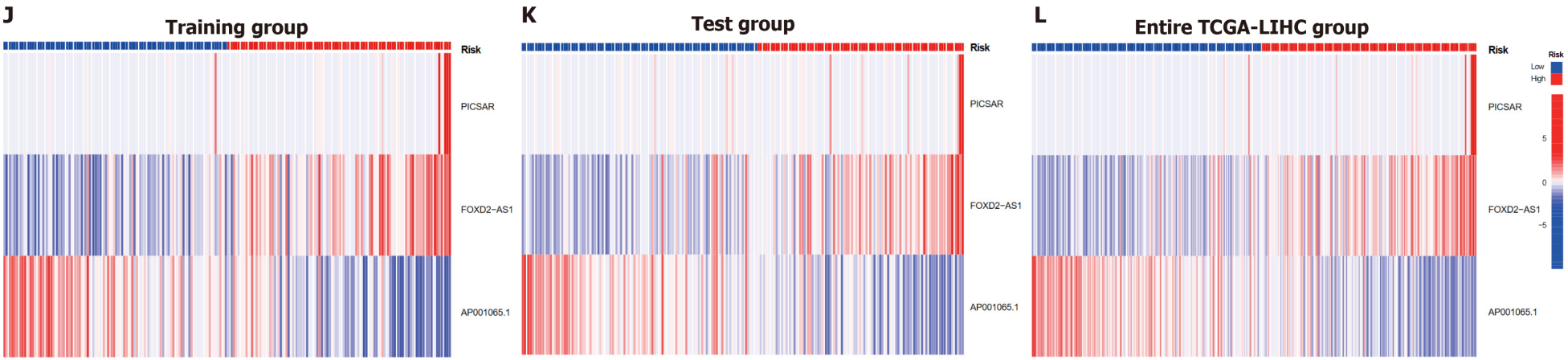

DOI: 10.4251/wjgo.v14.i10.1981

Figure 3 Internal validation of cuproptosis-related long-chain non-coding RNA signature (CupRLSig) model for determination of overall survival in training, test, and entire The Cancer Genome Atlas-Live Hepatocellular Carcinoma groups. A-C: Kaplan-Meier survival curves in the high- and low-risk groups stratified by median CupRLSig risk scores for overall survival in the training set (A), test set (B), and entire The Cancer Genome Atlas-Live Hepatocellular Carcinoma (TCGA-LIHC) dataset (C); *P* values were determined using the log-rank test; D-F: Risk curves were based on the risk score for each sample in the training (D), test (E), and entire TCGA-LIHC (F) sets, where red and blue dots indicate high- and low-risk samples, respectively; G-I: The scatter plot was based on the survival status of each sample from the training (G), test (H), and entire TCGA-LIHC (I) sets, where red and blue dots indicate death and survival, respectively; J-L: Heatmaps detailing the expression levels of the three cuproptosis-related long-chain non-coding RNA (lncRNA) signature (CupRLSig) lncRNAs in each group. TCGA-LIHC: The Cancer Genome Atlas-Live Hepatocellular Carcinoma.

Expression levels of the three lncRNAs from the CupRLSig model, as well as clinicopathological factors, are detailed in Figure 5A. PCA was performed for whole genes, cuproptosis-related genes, cuproptosis-related lncRNAs, and risk-related lncRNAs from the CupRLSig model to determine their ability to distinguish between high- and low-risk patients (Figure 5B-E). The CupRLSig (Figure 5E) model was found to effectively distinguish between patients in the low- and high-risk groups, underscoring the accuracy of the model.

Subgroup analysis was also performed to determine whether CupRLSig had prognostic value in subgroups with different clinicopathological parameters (Figure 6). Risk score showed significant correlations with age (Figure 6A and B), sex (Figure 6C and D), tumor grade (Figure 6E and F), tumor stage (Figure 6G and H), and T stage (Figure 6I and J) in the assessment of correlations among risk score and clinicopathological factors. The numbers of cases in the M and N stage subgroups were too small for evaluation. Overall, the CupRLSig risk score was found to be an independent prognostic risk factor in HCC patients.

Construction of a predictive nomogram

The CupRLSig risk score, in combination with other clinicopathological factors, was used to develop a nomogram to guide clinical assessment of prognosis and estimate 1-, 3-, and 5-year survival probability of HCC patients (Figure 7A). Patient 53 was randomly chosen for evaluation of the predictive utility of the nomogram. As shown in Figure 7A, the risk score of this patient was 175 points; the 5-year survival

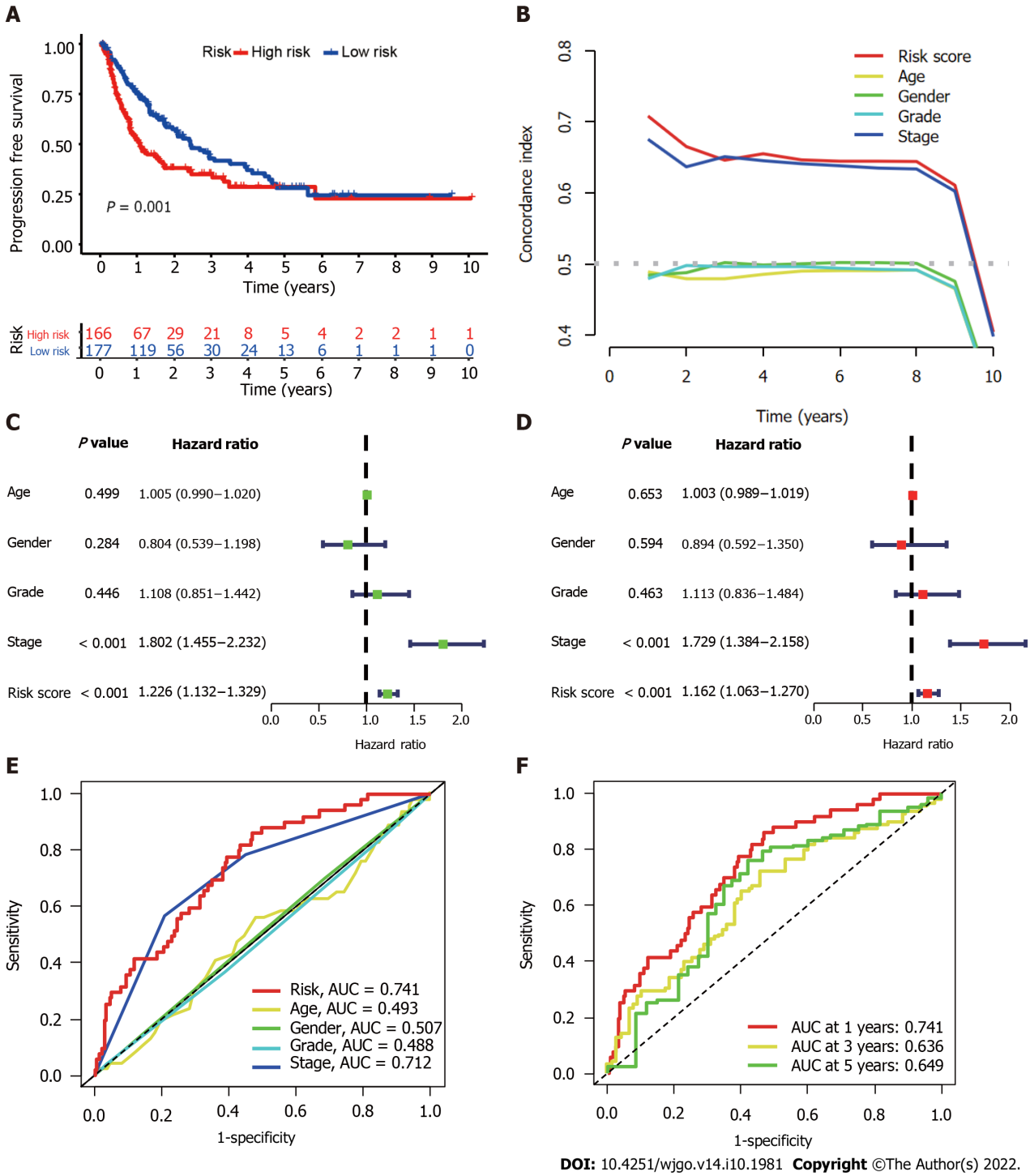

DOI: 10.4251/wjgo.v14.i10.1981

Figure 4 Evaluation of predictive accuracy of the cuproptosis-related long-chain non-coding RNAs signature (CupRLSig) model using the entire The Cancer Genome Atlas-Live Hepatocellular Carcinoma dataset. A: Kaplan-Meier curves for progression-free survival in high- and low-risk groups stratified by median value of cuproptosis-related long-chain non-coding RNAs signature (CupRLSig) risk score; B: Concordance index curves depicting CupRLSig risk scores and other clinical parameters relevant to predicting hepatocellular carcinoma patient prognosis; C and D: Forest plots for univariate (C) and multivariate (D) Cox proportional-hazards analysis for determination of the independent prognostic value of the CupRLSig risk score; E: Area under the curve (ROC) curves for the CupRLSig risk score and other clinicopathological variables; F: Time-dependent ROC curves for 1-, 3-, and 5-year survival for the CupRLSig signature. ROC: Receiver operating characteristic; AUC: Area under the curve.

rate was 0.642, the 3-year survival rate was 0.738, and the 1-year survival rate was 0.875. The nomogram was found to accurately estimate mortality (Figure 7B).

Identification of biological pathways linked to CupRLSig

The R software "enrichplot" package was used for gene set functional annotation of differentially expressed genes and lncRNAs (n = 523, Supplementary Table 3) among the high- and low-risk HCC groups. The five biological processes with the highest enrichment according to GO analysis were mitotic

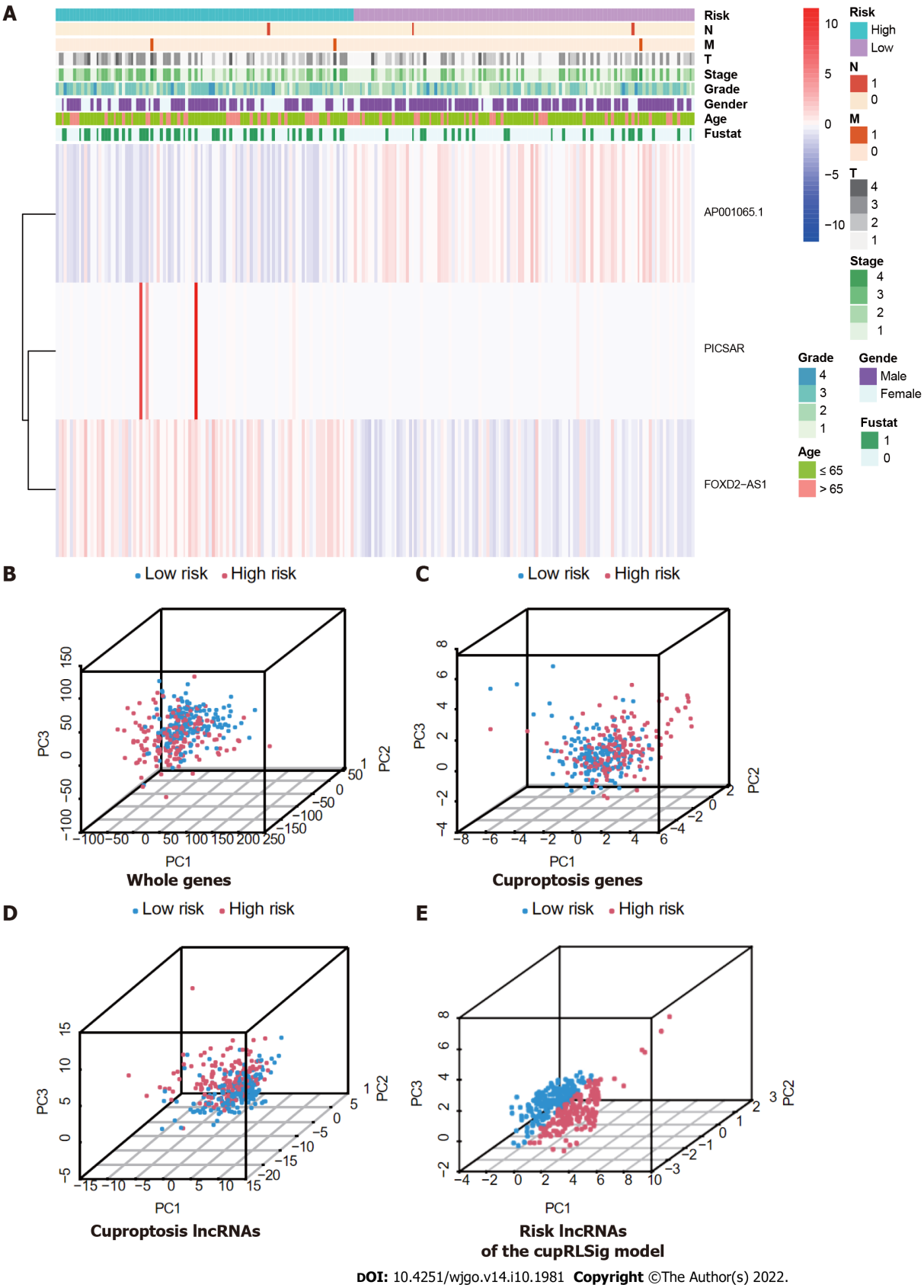

DOI: 10.4251/wjgo.v14.i10.1981

Figure 5 Visualization of expression levels of the three component long-chain non-coding RNAs of the cuproptosis-related long-chain non-coding RNA signature (CupRLSig) model based on clinicopathological variable stratification and principal component analysis of different gene sets performed for classification of patient risk. A: Heatmaps of expression of the three long-chain non-coding RNAs (lncRNAs) and clinical characteristics for different risk groups; B-E: PCA of low- and high-risk groups based on (B) whole-genome genes, (C) cuproptosis-related genes, (D) cuproptosis-related lncRNAs, and (E) cuproptosis-related lncRNA signature (CupRLSig) model risk lncRNAs. Patients with high risk scores are denoted by red, while those with low risk scores are denoted by blue. N: Lymph node metastasis; M: Mistant metastasis; T: Tumor.

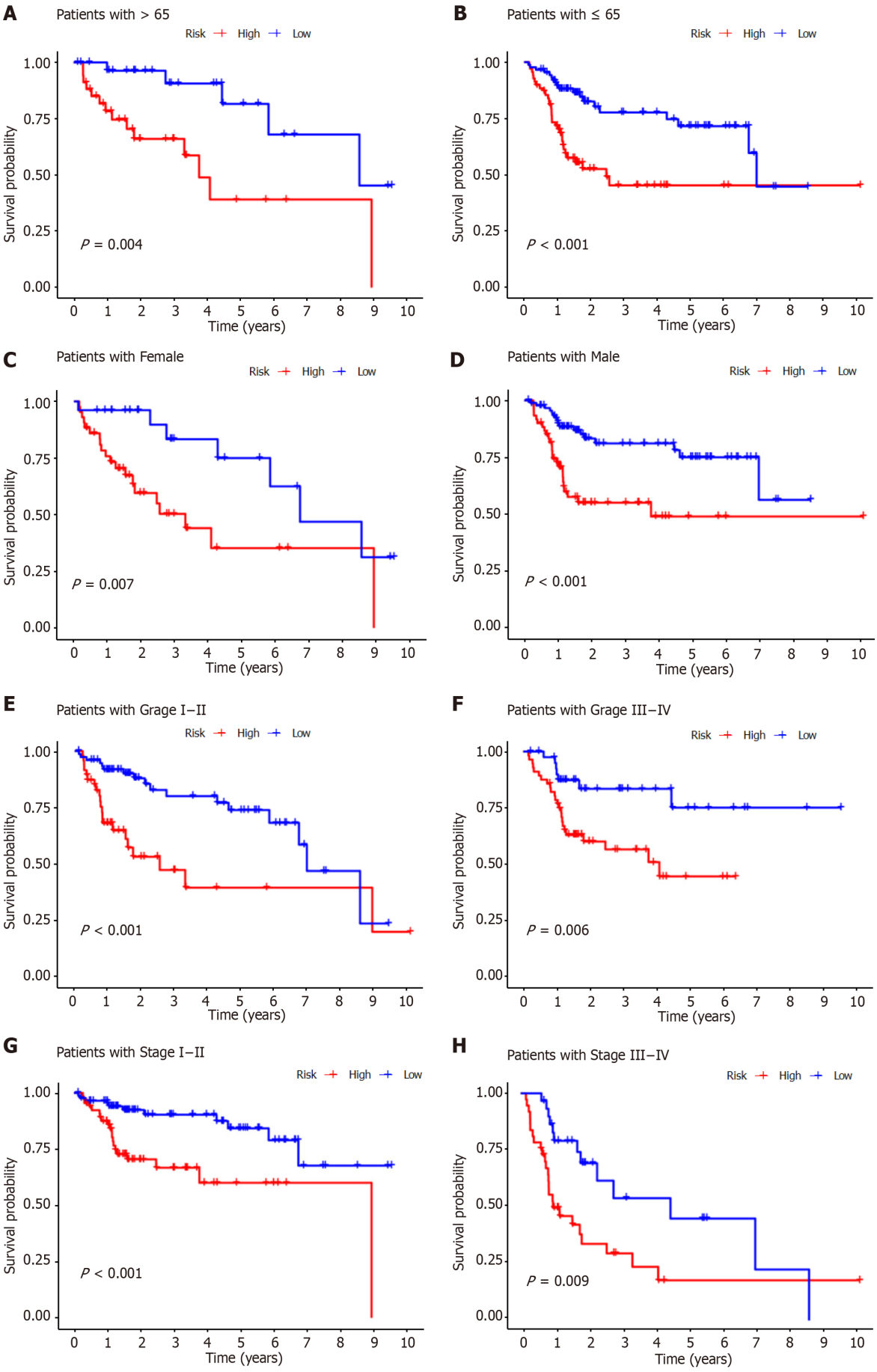
A
Patients with > 65
Risk High Low
Survival probability
P = 0.004
Time (years)
B
Patients with ≤ 65
Risk High Low
Survival probability
P < 0.001
Time (years)
C
Patients with Female
Risk High Low
Survival probability
P = 0.007
Time (years)
D
Patients with Male
Risk High Low
Survival probability
P < 0.001
Time (years)
E
Patients with Grage I–II
Risk High Low
Survival probability
P < 0.001
Time (years)
F
Patients with Grage III–IV
Risk High Low
Survival probability
P = 0.006
Time (years)
G
Patients with Stage I–II
Risk High Low
Survival probability
P < 0.001
Time (years)
H
Patients with Stage III–IV
Risk High Low
Survival probability
P = 0.009
Time (years)

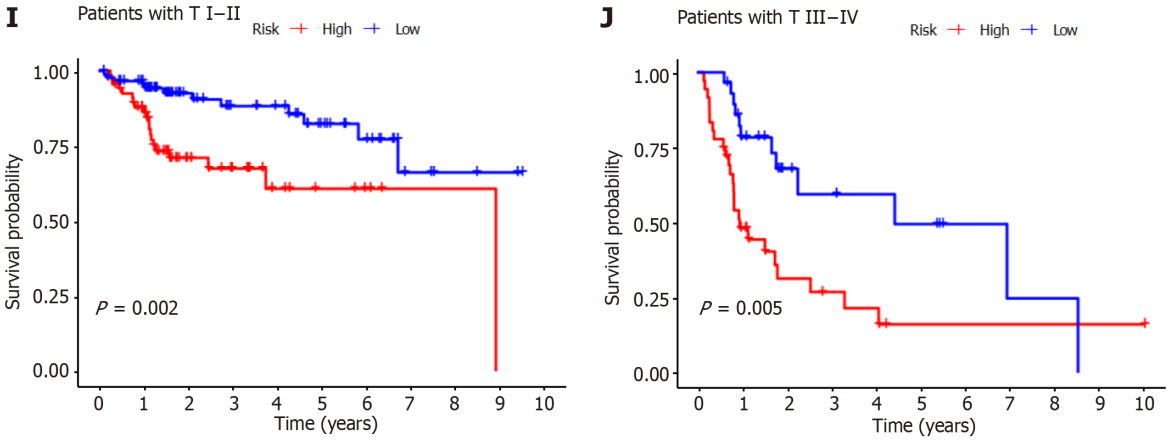

DOI: 10.4251/wjgo.v14.i10.1981

Figure 6 Kaplan-Meier survival curves for high- and low-risk patient groups sorted by clinicopathological variables. A and B: Age; C and D: Sex; E and F: Grade; G and H: Overall stage; I and J: T stage. T: Tumor.

nuclear division, mitotic sister chromatid segregation, nuclear division, chromosome segregation, and sister chromatid segregation (Figure 8A). The five cellular components with the highest enrichment were condensed chromosomes, kinetochores, spindle, chromosomes, and condensed chromosomes (Figure 8A). Finally, the most enriched molecular functions were steroid hydroxylase activity, oxidoreductase activity, microtubule binding, aromatase activity, and tubulin binding (Figure 8A). The five most enriched KEGG pathways were retinol metabolism, cytochrome P450 drug metabolism, cytochrome P450 xenobiotic metabolism, the cell cycle, and chemical carcinogenesis-DNA adducts (Figure 8B).

Relationships of CupRLSig risk score with somatic mutation and TMB

Somatic mutations in patients in the low- and high-risk subgroups were assessed separately (Figure 9A and B); TP53 (36% *vs* 17%) had a higher rate of somatic mutation in the high-risk group than the low-risk group, whereas CTNNB1 (30% *vs* 20%) and TTN (25% *vs* 20%) had higher rates of somatic mutation in the low-risk group. Furthermore, although no difference in TMB between the two groups (Figure 9C) was found, the survival time of patients with higher TMB was significantly reduced (Figure 9D). High TMB in high-risk group patients led to an even worse prognosis (Figure 9E), highlighting a significant synergistic effect between these two indicators.

Immune infiltration in different risk subgroups

According to analysis using the CIBERSORT algorithm, the infiltration ratios of M2 macrophages (P = 0.007), resting mast cells (P = 0.002), monocytes (P = 0.002), and activated NK cells (P = 0.032) in the low-risk group were significantly higher than those in the high-risk group (Figure 10A). Ratios of resting NK cells (P = 0.018), regulatory T cells (Tregs; P = 0.021), CD4 memory activated T cells (P = 0.025), and M0 macrophages (P = 0.007) exhibited the opposite pattern (Figure 10A). Scores for immune functions including C-C chemokine receptor, check points, and major histocompatibility complex class I were significantly higher in high-risk group patients than in those in the low-risk group, although response to interferon type II exhibited the opposite pattern (Figure 10B). These findings reveal differences in immune infiltration between the two groups. As immunotherapy is understood to depend on the existence of a "hot" immune microenvironment[23], such differences highlight the potential of immunotherapy.

Potential relationships of CupRLSig with immunotherapy, chemotherapy, and targeted therapy in HCC

Twenty-eight of a total of 47 immune checkpoint genes evaluated were found to differ in terms of expression levels between the high- and low-risk groups (Figure 11A). Immunotherapy markers including CD276, CTLA-4, and PDCD-1, which are currently in widespread clinical use, were found to have markedly elevated expression in the high-risk group (Figure 11A), implying potential immunotherapeutic responses in high-risk patients. Moreover, when the online software TIDE was used to predict the outcomes of cancer patients treated with anti-PD1 or anti-CTLA4 therapies, higher TIDE scores were found in the low-risk group compared with the high-risk group (Figure 11B). Importantly, a higher TIDE score suggests a greater likelihood of tumor immune escape and a poorer response to immunotherapy. Based on the results for immune infiltration, checkpoint gene expression, and TIDE score, HCC patients with high cuproptosis-related risk scores are likely to respond better to immunotherapy.

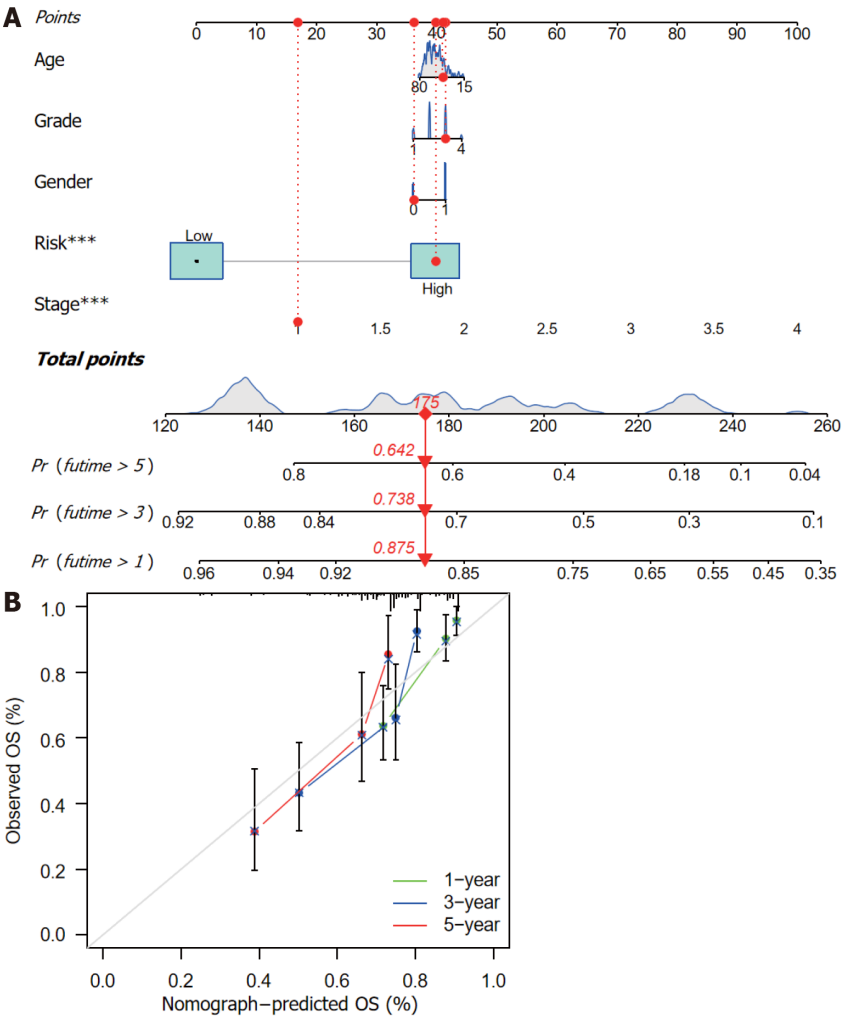

DOI: 10.4251/wjgo.v14.i10.1981

Figure 7 Nomogram construction and verification. A: Nomogram combining clinicopathological parameters and risk scores to predict 1-, 3-, and 5-year survival probabilities of hepatocellular carcinoma (HCC) patients. Multivariate Cox proportional-hazards analysis was used to determine each parameter's independent prognostic value. Red dots, diamonds, triangles, and dashed lines represent the 53rd patient, randomly selected for illustration of the nomogram; B: Calibration curves to assess the consistency between actual observed and nomogram-predicted overall survival (OS) at 1-, 3-, and 5-years.

Finally, the relationships between CupRLSig risk score and the efficacies of chemotherapy and targeted therapy for HCC were evaluated. Most drugs commonly used in preclinical and clinical systemic therapies for HCC, including 5-fluorouracil (Figure 11C), gemcitabine (Figure 11D), paclitaxel (Figure 11E), imatinib (Figure 11F), sunitinib (Figure 11G), rapamycin (Figure 11H), and XL-184 (cabozantinib, Figure 11I) were found to be more efficacious in the low-risk group; erlotinib (Figure 11J), an exception, was more efficacious in the high-risk group. Our findings highlight the potential of CupRLSig for future clinical development of personalized treatment strategies.

DISCUSSION

Widespread hepatitis B vaccination in China has led to a gradual decline in the incidence of HCC, from 29.2/100000 in 1998 to 21.9/100000 in 2012[24]. However, the prognosis of HCC patients remains poor, in large part owing to a lack of therapeutic and prognostic biomarkers. Markers currently considered in clinical practice, such as alpha fetoprotein (AFP), can be used as diagnostic markers or for monitoring recurrence, but they do not provide treatment or prognostic data[25]. The combination of several biomarkers into a single model improves both therapeutic and prognostic prediction accuracy compared with a single biomarker[26].

Serum and tissue copper levels are known to be elevated in various malignancies, with this elevation being directly related to cancer progression[7]. As such, we hypothesized that abnormal expression of genes relevant to the copper metabolism pathway could serve as prognostic and therapeutic markers in HCC. Cuproptosis, a form of programmed cell death recently shown to result from the binding of accumulated intracellular copper to aliphatic components of the tricarboxylic acid cycle, causes

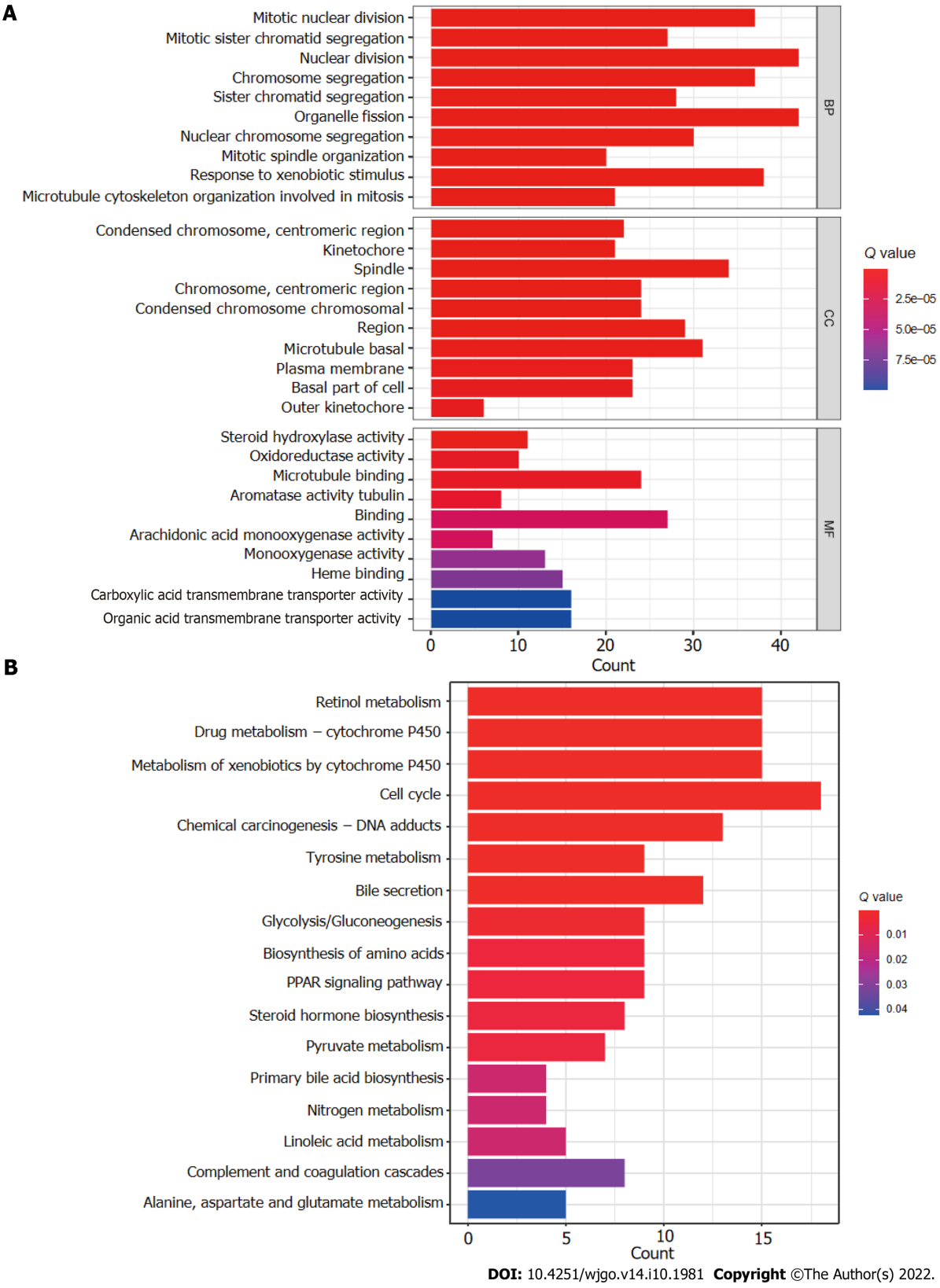

DOI: 10.4251/wjgo.v14.i10.1981

Figure 8 Gene set functional annotation of differentially expressed genes and long-chain non-coding RNAs in high- and low-risk hepatocellular carcinoma groups. A: In gene ontology analysis, differentially expressed genes and long-chain non-coding RNAs (lncRNAs) were found to be most enriched in biological process terms mitotic nuclear division, mitotic sister chromatid segregation, nuclear division, chromosome segregation, and sister chromatid segregation; in cellular component terms condensed chromosomes, kinetochores, spindles, chromosomes, and condensed chromosomes; and in molecular function terms steroid hydroxylase activity, oxidoreductase activity, microtubule binding, aromatase activity, and tubulin binding; B: Differentially expressed genes and lncRNAs were found to be most enriched in the following five Kyoto Encyclopedia of Genes and Genomes (KEGG) pathways: retinol metabolism, cytochrome P450 drug metabolism, cytochrome P450 xenobiotic metabolism, cell cycle, and chemical carcinogenesis-DNA adducts. BP: Biological process; CC: Cellular component; MF: Molecular function.

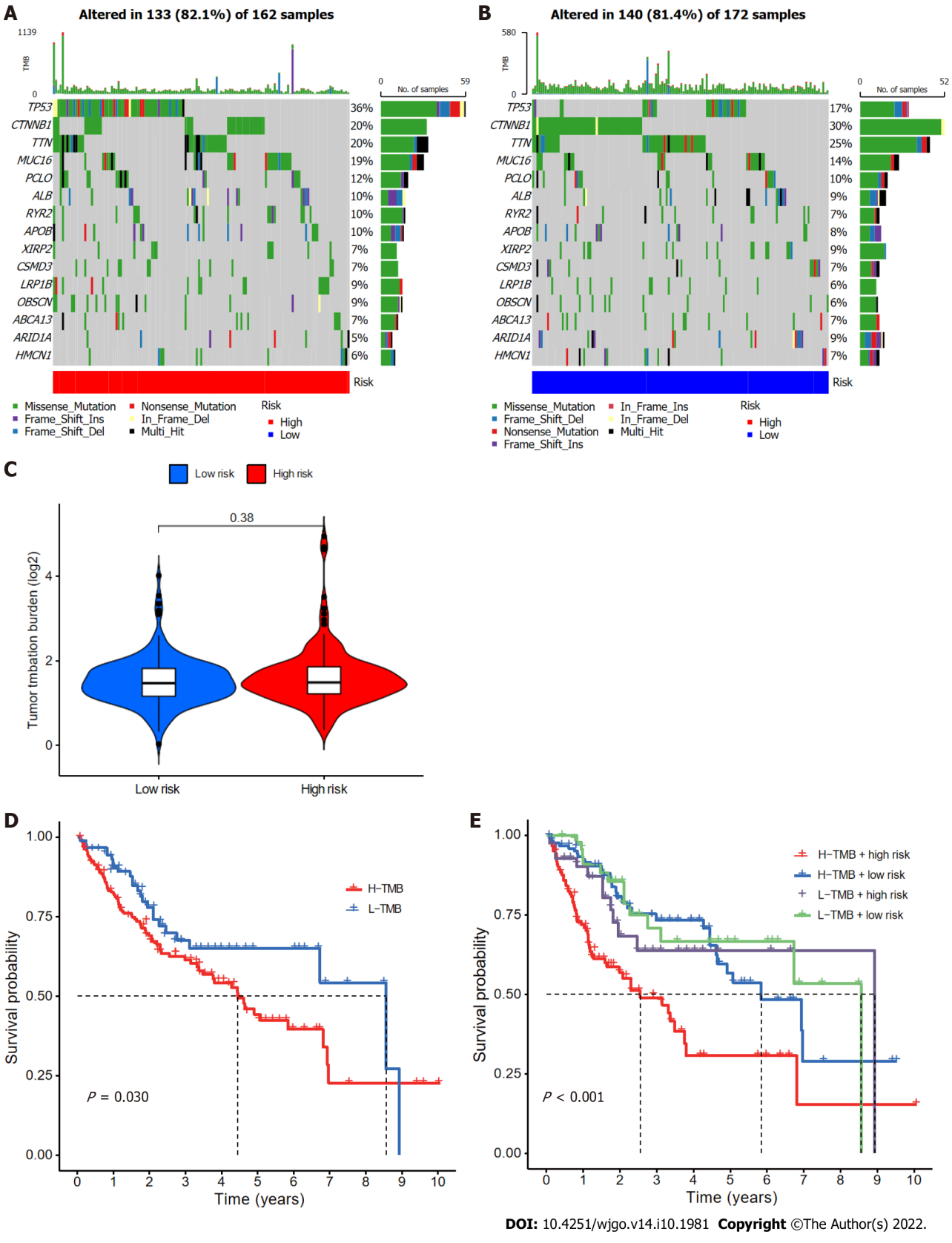

DOI: 10.4251/wjgo.v14.i10.1981

Figure 9 Relationships between cuproptosis-related long-chain non-coding RNA signature (CupRLSig) risk scores and somatic mutation and tumor mutation burden. A and B: Waterfall plots showing somatic mutations of the most significant 15 genes among high-risk (A) and low-risk (B) hepatocellular carcinoma (HCC) patients; C: Comparison of tumor mutation burden (TMB) between low- and high-risk subgroups; D: Kaplan-Meier curves for high- and low-TMB groups; E: Kaplan-Meier curves for subgroup analyses of patients stratified by TMB and risk score. The *P* value is representative of the results of the analysis of variance test among subgroups.

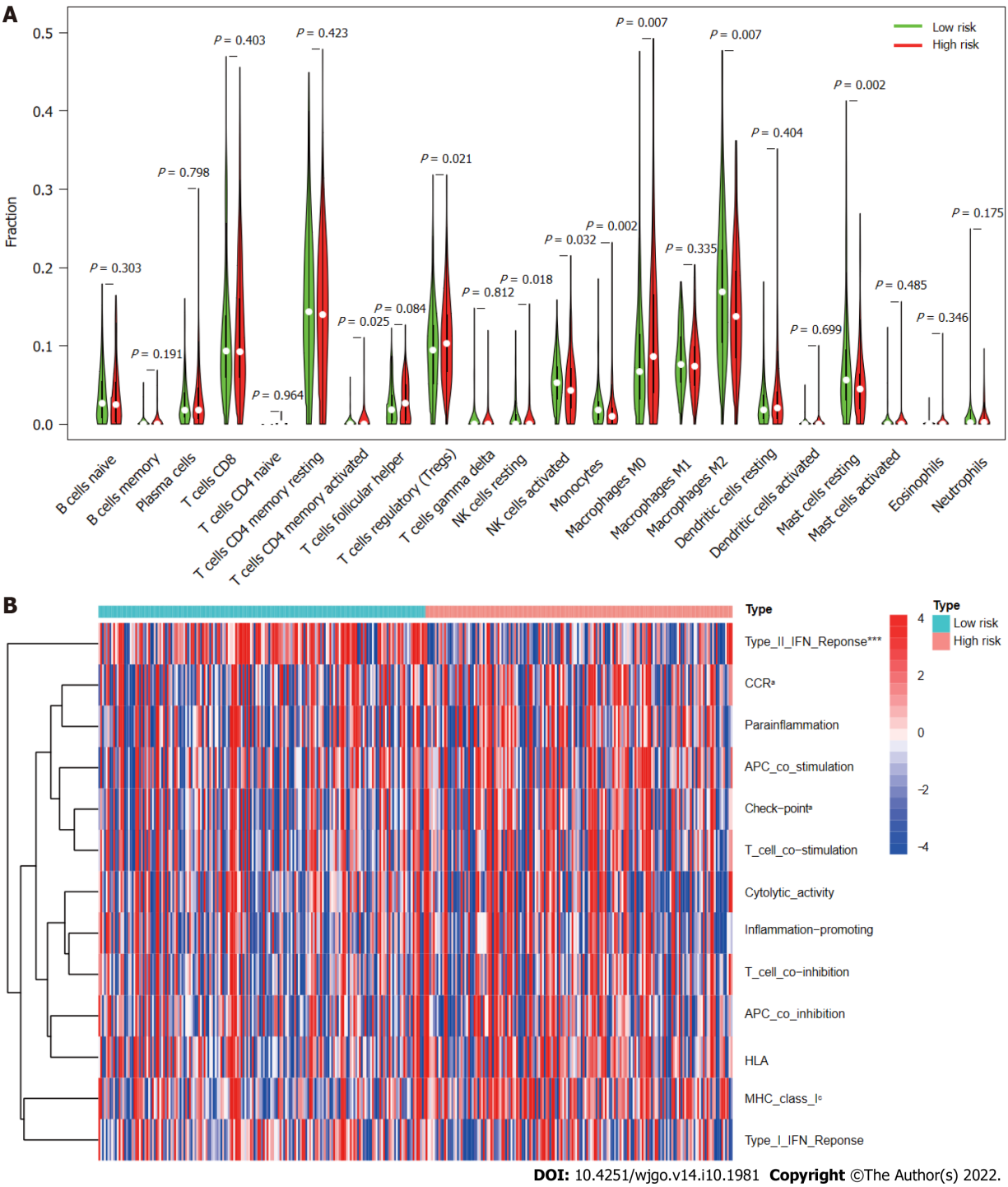

DOI: 10.4251/wjgo.v14.i10.1981

Figure 10 Immune cell infiltration and immune-related functions in different risk groups. A: Violin plot showing whether there were significant differences in immune infiltration among 22 types of cells between high- and low-risk subgroups; B: Heatmap showing whether there were significant differences in 13 immune-related functions between high- and low-risk subgroups. NK: Natural killer; CCR: C-C chemokine receptor; APC: Antigen-presenting cell; HLA: Human leukocyte antigen; MHC: Major histocompatibility complex; IFN: Interferon. $^{a}P < 0.05$; $^{c}P < 0.001$.

aggregation of lipoacylated proteins and loss of iron-sulfur cluster proteins[12]. Although many pivotal genes in cuproptosis have been identified, the overall regulatory landscape of this process in HCC remains unclear. Here, we incorporated three cuproptosis-related lncRNAs into a CupRLSig signature capable of addressing both cuproptosis and HCC prognosis.

The ROC curves indicated that CupRLSig showed adequate predictive utility for the evaluation of OS of HCC patients. Additionally, our novel nomogram has the potential to direct the formulation of therapeutic approaches and enhance clinical decision-making. Both FOXD2-AS1 and PICSAR (components of the CupRLSig model) have been previously identified as oncogenes in HCC; FOXD2-AS1 aggravates HCC tumorigenesis by regulating the miR-206/MAP3K1 axis[27], whereas PICSAR accelerates disease progression by regulating the miR-588/PI3K/AKT/mTOR axis[28]. However, there

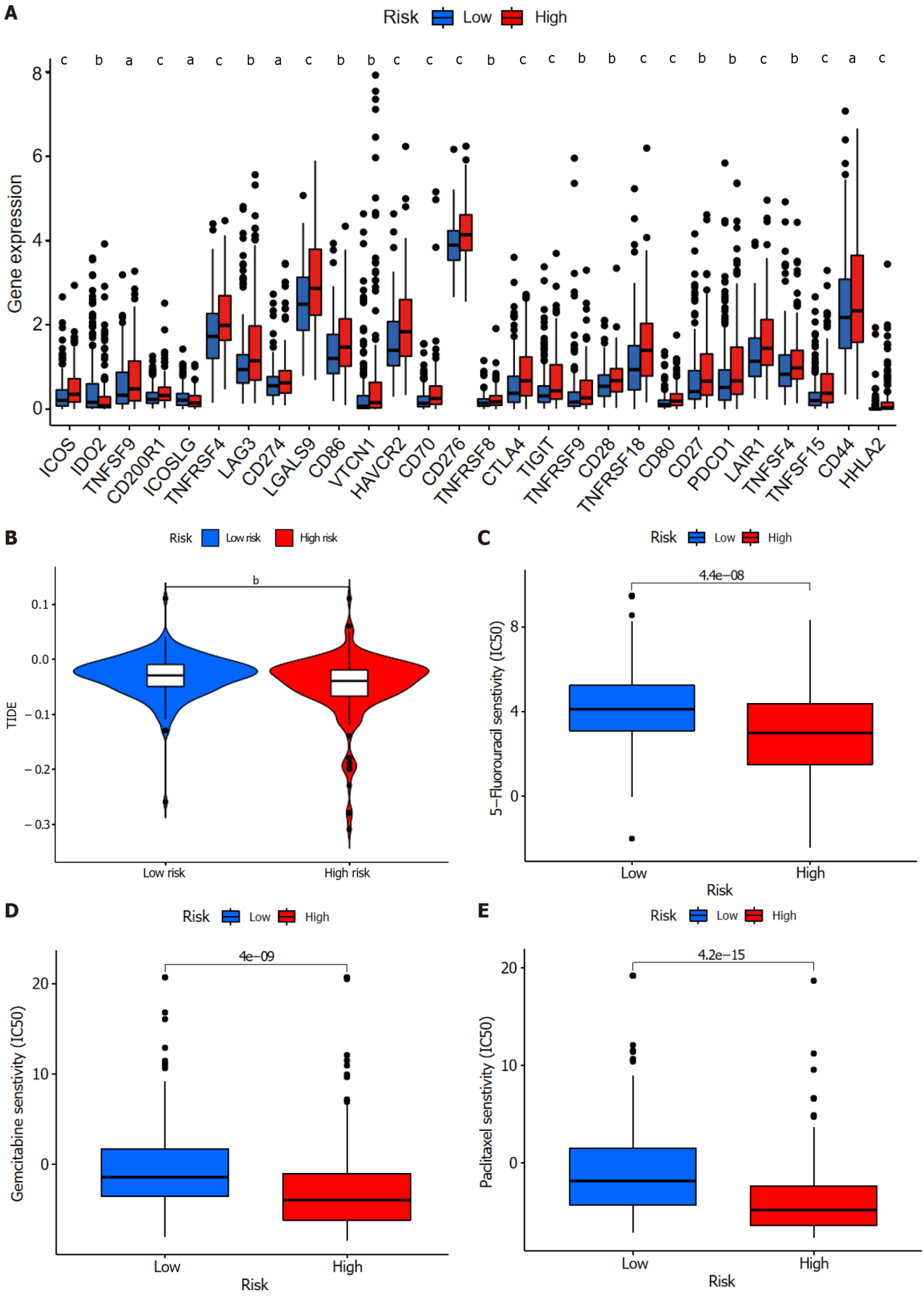
A
Risk Low High
Gene expression
ICOS IDO2 TNFSF9 CD200R1 ICOSLG TNFRSF4 LAG3 CD274 LGALS9 CD86 VTCN1 HAVCR2 CD70 CD276 TNFRSF8 CTLA4 TIGIT TNFRSF9 CD28 TNFRSF18 CD80 CD27 PDCD1 LAIR1 TNFSF4 TNFSF15 CD44 HHLA2
B
Risk Low risk High risk
TIDE
b
Low risk
High risk
C
Risk Low High
5−Fluorouracil senstivity (IC50)
4.4e−08
Low
High
Risk
D
Risk Low High
Gemcitabine senstivity (IC50)
4e−09
Low
High
Risk
E
Risk Low High
Paclitaxel senstivity (IC50)
4.2e−15
Low
High
Risk

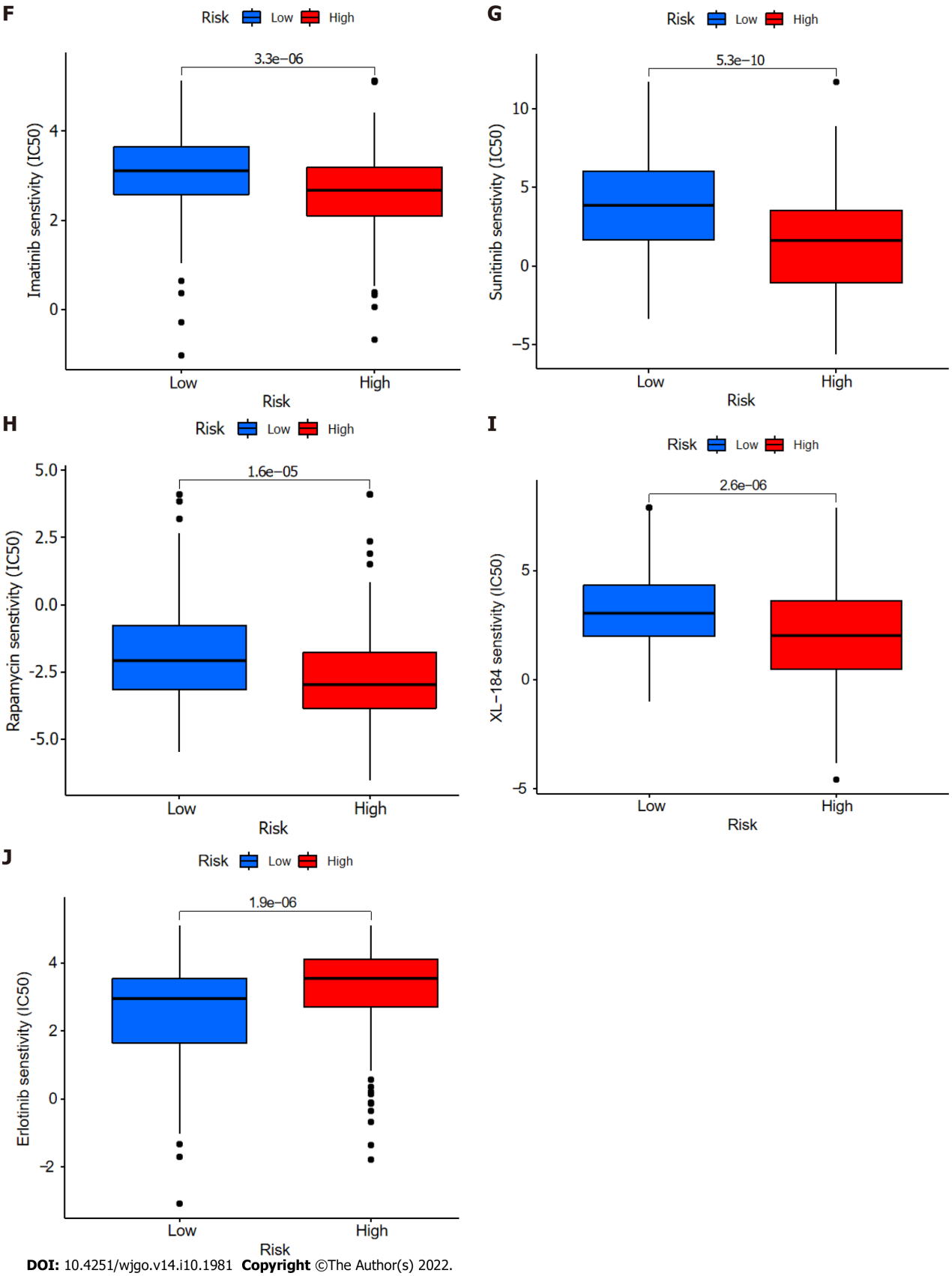

DOI: 10.4251/wjgo.v14.i10.1981

Figure 11 Comparison of immune checkpoints, tumor immune dysfunction, and exclusion module scores, and chemotherapy and targeted therapy drug efficacy in high- and low-risk groups. A: Expression of 28 immune checkpoint genes differed between the high- and low-risk groups. Red and blue boxes represent high- and low-risk patients, respectively; B: Online software tumor immune dysfunction (TIDE) predictions of outcomes in HCC subgroups treated with either anti-PD1 or anti-CTLA4 therapy. A higher TIDE score suggests a greater likelihood of tumor immune escape and a poorer response to immunotherapy; C-J: IC_{50} values for (C) 5-fluorouracil, (D) gemcitabine, (E) paclitaxel, (F) imatinib, (G) sunitinib, (H) rapamycin, (I) XL-184 (cabozantinib), and (J)

erlotinib in high- and low-risk groups. IC_{50}, half-maximal inhibitory concentration. $^{a}P < 0.05$; $^{b}P < 0.01$; $^{c}P < 0.001$. NS: Not significant.

has been a lack of research on the prognostic value of AP001065.1 and the extent of its involvement in cuproptosis; further study of this lncRNA is warranted.

This study also explored the important relationship between cuproptosis and treatment decisions in the management of HCC. Endogenous oxidative stress levels are known to be elevated in a variety of tumors, probably owing to a combination of active metabolism, mitochondrial mutations, cytokine activity, and inflammation[7]. Under constant oxidative stress, cancer cells tend to make extensive use of adaptive mechanisms and may deplete the intracellular ROS buffer capacity[7]. Thus, increased copper levels in cancer cells, as well as the resulting increase in oxidative stress, facilitate a novel cancer-specific therapeutic strategy. The liver is the most important organ for copper metabolism, with the biliary tract excreting 80% of copper ions[29]. The induction of cuproptosis in the setting of HCC thus offers a basis for effective management of this illness. The design of preclinical studies of this concept first requires a detailed understanding of the expression of regulatory genes of the cuproptosis pathway in HCC. A study using a WD mouse model revealed that ATP7B-deficient hepatocytes, such as those found in WD patients, activated autophagy in response to copper overload to prevent copper-induced apoptosis[17]. Inhibition of the autophagy pathway, and consequent further copper overload and elevated ROS, is thus likely to activate the cuproptosis pathway and lead to the death of copper-rich tumor cells. Notably, the efficacy of chemotherapeutic agents designed to induce ROS, such as paclitaxel, differed between patients in the high- and low-risk groups as defined by the CupRLSig model. The CupRLSig model was also shown to have a relationship with the HCC immune microenvironment. According to CupRLSig stratification, expression of most immune checkpoints, activation of immune pathways, and infiltration of immune cells were higher in the high-risk group compared with the low-risk group, while TIDE score showed the opposite pattern. These findings suggest that high-risk patients have more to benefit from immunotherapy. Taken together, these results confirm that CupRLSig has potential utility as an adjunctive selection tool for pharmacotherapy.

There were several limitations to this study. First, only TCGA datasets were used. Use of additional external data, such as data from the Gene Expression Omnibus, should be considered in future studies to further confirm the predictive utility of CupRLSig. Second, owing to a lack of complete data, prognostic factors such as surgical data were not considered in the construction of the nomogram. This may have affected the accuracy of the model. Third, functional studies are required to better understand the molecular mechanisms associated with the effects of cuproptosis-related lncRNAs.

CONCLUSION

This study proposes a novel CupRLSig lncRNA signature, as well as a nomogram based on that signature, which could be useful in predicting HCC patient prognosis. Importantly, CupRLSig also appears likely to predict levels of immune infiltration and indicate the potential efficacy of tumor immunotherapy, chemotherapy, and targeted therapy.

ARTICLE HIGHLIGHTS

Research background

Cuproptosis, a form of programmed cell death recently found to result from the binding of accumulated intracellular copper to aliphatic components of the tricarboxylic acid cycle, causes aggregation of lipoacylated proteins and loss of iron-sulfur cluster proteins. However, factors crucial to the regulation of cuproptosis remain unelucidated.

Research motivation

We hypothesized that abnormal expression of genes relevant to the copper metabolism pathway could serve as prognostic and therapeutic markers in hepatocellular carcinoma (HCC).

Research objectives

To identify long-chain non-coding RNAs (lncRNAs) associated with cuproptosis in order to predict the prognosis of patients with HCC.

Research methods

Using RNA sequencing data from The Cancer Genome Atlas Live Hepatocellular Carcinoma (TCGA-LIHC), a co-expression network of cuproptosis-related genes and lncRNAs was constructed. For HCC

prognosis, we developed a cuproptosis-related lncRNA signature (CupRLSig) using univariate Cox, Lasso, and multivariate Cox regression analyses. Kaplan-Meier analysis was used to compare overall survival among high- and low-risk groups stratified by median CupRLSig risk score. Furthermore, comparisons of functional annotation, immune infiltration, somatic mutation, tumor mutation burden (TMB), and pharmacologic options were made between high- and low-risk groups.

Research results

The high-risk group identified by CupRLSig was associated with poorer overall survival and progression-free survival. Less activation of natural killer cells and more infiltration of regulatory T cells in the high-risk group may explain the worse outcomes. Based on checkpoint gene expression (CD276, CTLA-4, and PDCD-1) and tumor immune dysfunction and rejection (TIDE) scores, high-risk patients may respond better to immunotherapy.

Research conclusions

The lncRNA signature, CupRLSig, constructed in this study is valuable in prognostic estimation in the setting of HCC. Importantly, CupRLSig probably also predicts levels of immune infiltration and the potential efficacy of tumor immunotherapy, chemotherapy, and targeted therapy.

Research perspectives

We believe that we can expand the bulk-sequencing-generated lncRNA model to the standard care of HCC patients if sufficient external data is available to validate the predictive efficacy of CupRLSig.

ACKNOWLEDGEMENTS

The authors would like to thank The Cancer Genome Atlas (TCGA) for providing useful RNA-seq data with detailed accompanying clinical information (https://tcga-data.nci.nih.gov/tcga/); and Dr. Luo Ganfeng for his biostatistical review.

FOOTNOTES

Author contributions: Zhou TC, Li YR, Zeng B, Zong Z, and Chen S conceived the study and its design, and provided administrative support; Huang EM, Ma N, and Ma T were involved in data analyses and wrote, reviewed, and edited the manuscript; Zhou JY, Yang WS, Liu CX, and Hou ZH contributed data analysis and reviewed the manuscript; all authors read and approved the final manuscript, and contributed to the article and approved the submitted version for publication.

Supported by the National Key Clinical Discipline, the Basic and Applied Basic Research Fund Project of Guangdong Province, No. 2021A1515410004 and No. 2019A1515011200; National Natural Science Foundation of China, No. 81973858 and No. 82172790; and Science and Technology Plan Project of Qingyuan City, No. 2019A028.

Institutional review board statement: The study was conducted in accordance with the Declaration of Helsinki (as revised in 2013). Since the present study is a bioinformatics work that did not involve animal or human specimens, there is no requirement for ethical permission from our institution or an ethics number.

Conflict-of-interest statement: There are no conflicts of interest to report.

Data sharing statement: Publicly available datasets were analyzed in this study. These data can be found here: https://portal.gdc.cancer.gov/repository. Technical appendix, statistical code, and dataset available from the corresponding author at zhoutch3@mail.sysu.edu.cn.

Country/Territory of origin: China

ORCID number: En-Min Huang 0000-0003-0570-3138; Ning Ma 0000-0002-6305-7915; Tao Ma 0000-0002-6890-0289; Jun-Yi Zhou 0000-0002-0024-9338; Wei-Sheng Yang 0000-0001-9314-8191; Chuang-Xiong Liu 0000-0002-4103-9062; Ze-Hui Hou 0000-0003-0298-0236; Shuang Chen 0000-0002-7013-5774; Zhen Zong 0000-0001-8953-7792; Bing Zeng 0000-0003-4167-5330; Ying-Ru Li 0000-0003-0583-703X; Tai-Cheng Zhou 0000-0003-0582-1150.

S-Editor: Chen YL
L-Editor: A
P-Editor: Guo X

REFERENCES

1 **Jemal A**, Ward EM, Johnson CJ, Cronin KA, Ma J, Ryerson B, Mariotto A, Lake AJ, Wilson R, Sherman RL, Anderson RN, Henley SJ, Kohler BA, Penberthy L, Feuer EJ, Weir HK. Annual Report to the Nation on the Status of Cancer, 1975-2014, Featuring Survival. *J Natl Cancer Inst* 2017; **109** [PMID: 28376154 DOI: 10.1093/jnci/djx030]
2 **Ren X**, Li Y, Zhou Y, Hu W, Yang C, Jing Q, Zhou C, Wang X, Hu J, Wang L, Yang J, Wang H, Xu H, Li H, Tong X, Wang Y, Du J. Overcoming the compensatory elevation of NRF2 renders hepatocellular carcinoma cells more vulnerable to disulfiram/copper-induced ferroptosis. *Redox Biol* 2021; **46**: 102122 [PMID: 34482117 DOI: 10.1016/j.redox.2021.102122]
3 **Zhang FJ**, Yang JT, Tang LH, Wang WN, Sun K, Ming Y, Muhammad KG, Zheng YF, Yan M. Effect of X-ray irradiation on hepatocarcinoma cells and erythrocytes in salvaged blood. *Sci Rep* 2017; **7**: 7995 [PMID: 28801583 DOI: 10.1038/s41598-017-08405-z]
4 **El-Serag HB**. Hepatocellular carcinoma. *N Engl J Med* 2011; **365**: 1118-1127 [PMID: 21992124 DOI: 10.1056/NEJMra1001683]
5 **Giraud J**, Chalopin D, Blanc JF, Saleh M. Hepatocellular Carcinoma Immune Landscape and the Potential of Immunotherapies. *Front Immunol* 2021; **12**: 655697 [PMID: 33815418 DOI: 10.3389/fimmu.2021.655697]
6 **Sangro B**, Gomez-Martin C, de la Mata M, Iñarrairaegui M, Garralda E, Barrera P, Riezu-Boj JI, Larrea E, Alfaro C, Sarobe P, Lasarte JJ, Pérez-Gracia JL, Melero I, Prieto J. A clinical trial of CTLA-4 blockade with tremelimumab in patients with hepatocellular carcinoma and chronic hepatitis C. *J Hepatol* 2013; **59**: 81-88 [PMID: 23466307 DOI: 10.1016/j.jhep.2013.02.022]
7 **Gupte A**, Mumper RJ. Elevated copper and oxidative stress in cancer cells as a target for cancer treatment. *Cancer Treat Rev* 2009; **35**: 32-46 [PMID: 18774652 DOI: 10.1016/j.ctrv.2008.07.004]
8 **Fruehauf JP**, Meyskens FL Jr. Reactive oxygen species: a breath of life or death? *Clin Cancer Res* 2007; **13**: 789-794 [PMID: 17289868 DOI: 10.1158/1078-0432.ccr-06-2082]
9 **Aubert L**, Nandagopal N, Steinhart Z, Lavoie G, Nourreddine S, Berman J, Saba-El-Leil MK, Papadopoli D, Lin S, Hart T, Macleod G, Topisirovic I, Gaboury L, Fahrni CJ, Schramek D, Meloche S, Angers S, Roux PP. Copper bioavailability is a KRAS-specific vulnerability in colorectal cancer. *Nat Commun* 2020; **11**: 3701 [PMID: 32709883 DOI: 10.1038/s41467-020-17549-y]
10 **Ge EJ**, Bush AI, Casini A, Cobine PA, Cross JR, DeNicola GM, Dou QP, Franz KJ, Gohil VM, Gupta S, Kaler SG, Lutsenko S, Mittal V, Petris MJ, Polishchuk R, Ralle M, Schilsky ML, Tonks NK, Vahdat LT, Van Aelst L, Xi D, Yuan P, Brady DC, Chang CJ. Connecting copper and cancer: from transition metal signalling to metalloplasia. *Nat Rev Cancer* 2022; **22**: 102-113 [PMID: 34764459 DOI: 10.1038/s41568-021-00417-2]
11 **Zhang G**, Sun J, Zhang X. A novel Cuproptosis-related LncRNA signature to predict prognosis in hepatocellular carcinoma. *Sci Rep* 2022; **12**: 11325 [PMID: 35790864 DOI: 10.1038/s41598-022-15251-1]
12 **Tsvetkov P**, Coy S, Petrova B, Dreishpoon M, Verma A, Abdusamad M, Rossen J, Joesch-Cohen L, Humeidi R, Spangler RD, Eaton JK, Frenkel E, Kocak M, Corsello SM, Lutsenko S, Kanarek N, Santagata S, Golub TR. Copper induces cell death by targeting lipoylated TCA cycle proteins. *Science* 2022; **375**: 1254-1261 [PMID: 35298263 DOI: 10.1126/science.abf0529]
13 **Huang Z**, Zhou JK, Peng Y, He W, Huang C. The role of long noncoding RNAs in hepatocellular carcinoma. *Mol Cancer* 2020; **19**: 77 [PMID: 32295598 DOI: 10.1186/s12943-020-01188-4]
14 **Zhang J**, Ma Y, Xie D, Bao Y, Yang W, Wang H, Jiang H, Han H, Dong T. Differentially expressed lncRNAs in liver tissues of TX mice with hepatolenticular degeneration. *Sci Rep* 2021; **11**: 1377 [PMID: 33446761 DOI: 10.1038/s41598-020-80635-0]
15 **Mao C**, Wang X, Liu Y, Wang M, Yan B, Jiang Y, Shi Y, Shen Y, Liu X, Lai W, Yang R, Xiao D, Cheng Y, Liu S, Zhou H, Cao Y, Yu W, Muegge K, Yu H, Tao Y. A G3BP1-Interacting lncRNA Promotes Ferroptosis and Apoptosis in Cancer *via* Nuclear Sequestration of p53. *Cancer Res* 2018; **78**: 3484-3496 [PMID: 29588351 DOI: 10.1158/0008-5472.CAN-17-3454]
16 **Wu Y**, Zhang S, Gong X, Tam S, Xiao D, Liu S, Tao Y. The epigenetic regulators and metabolic changes in ferroptosis-associated cancer progression. *Mol Cancer* 2020; **19**: 39 [PMID: 32103754 DOI: 10.1186/s12943-020-01157-x]
17 **Polishchuk EV**, Merolla A, Lichtmannegger J, Romano A, Indrieri A, Ilyechova EY, Concilli M, De Cegli R, Crispino R, Mariniello M, Petruzzelli R, Ranucci G, Iorio R, Pietrocola F, Einer C, Borchard S, Zibert A, Schmidt HH, Di Schiavi E, Puchkova LV, Franco B, Kroemer G, Zischka H, Polishchuk RS. Activation of Autophagy, Observed in Liver Tissues From Patients With Wilson Disease and From ATP7B-Deficient Animals, Protects Hepatocytes From Copper-Induced Apoptosis. *Gastroenterology* 2019; **156**: 1173-1189.e5 [PMID: 30452922 DOI: 10.1053/j.gastro.2018.11.032]
18 **Kahlson MA**, Dixon SJ. Copper-induced cell death. *Science* 2022; **375**: 1231-1232 [PMID: 35298241 DOI: 10.1126/science.abo3959]
19 **Dong J**, Wang X, Xu C, Gao M, Wang S, Zhang J, Tong H, Wang L, Han Y, Cheng N. Inhibiting NLRP3 inflammasome activation prevents copper-induced neuropathology in a murine model of Wilson's disease. *Cell Death Dis* 2021; **12**: 87 [PMID: 33462188 DOI: 10.1038/s41419-021-03397-1]
20 **Mayakonda A**, Lin DC, Assenov Y, Plass C, Koeffler HP. Maftools: efficient and comprehensive analysis of somatic variants in cancer. *Genome Res* 2018; **28**: 1747-1756 [PMID: 30341162 DOI: 10.1101/gr.239244.118]
21 **Newman AM**, Liu CL, Green MR, Gentles AJ, Feng W, Xu Y, Hoang CD, Diehn M, Alizadeh AA. Robust enumeration of cell subsets from tissue expression profiles. *Nat Methods* 2015; **12**: 453-457 [PMID: 25822800 DOI: 10.1038/nmeth.3337]

22 **Rooney MS**, Shukla SA, Wu CJ, Getz G, Hacohen N. Molecular and genetic properties of tumors associated with local immune cytolytic activity. *Cell* 2015; **160**: 48-61 [PMID: 25594174 DOI: 10.1016/j.cell.2014.12.033]

23 **Mlecnik B**, Bindea G, Angell HK, Maby P, Angelova M, Tougeron D, Church SE, Lafontaine L, Fischer M, Fredriksen T, Sasso M, Bilocq AM, Kirilovsky A, Obenauf AC, Hamieh M, Berger A, Bruneval P, Tuech JJ, Sabourin JC, Le Pessot F, Mauillon J, Rafii A, Laurent-Puig P, Speicher MR, Trajanoski Z, Michel P, Sesboüe R, Frebourg T, Pagès F, Valge-Archer V, Latouche JB, Galon J. Integrative Analyses of Colorectal Cancer Show Immunoscore Is a Stronger Predictor of Patient Survival Than Microsatellite Instability. *Immunity* 2016; **44**: 698-711 [PMID: 26982367 DOI: 10.1016/j.immuni.2016.02.025]

24 **Ferlay J**, Colombet M, Bray F. Cancer incidence in five continents, CI5plus: IARC CancerBase No. 9. Lyon. France: International Agency for Research on Cancer, 2018

25 **Zhang JS**, Wang ZH, Guo XG, Zhang J, Ni JS. A nomogram for predicting the risk of postoperative recurrence of hepatitis B virus-related hepatocellular carcinoma in patients with high preoperative serum glutamyl transpeptidase. *J Gastrointest Oncol* 2022; **13**: 298-310 [PMID: 35284131 DOI: 10.21037/jgo-21-450]

26 **Guo Y**, Qu Z, Li D, Bai F, Xing J, Ding Q, Zhou J, Yao L, Xu Q. Identification of a prognostic ferroptosis-related lncRNA signature in the tumor microenvironment of lung adenocarcinoma. *Cell Death Discov* 2021; **7**: 190 [PMID: 34312372 DOI: 10.1038/s41420-021-00576-z]

27 **Hu W**, Feng H, Xu X, Huang X, Chen W, Hao L, Xia W. Long noncoding RNA FOXD2-AS1 aggravates hepatocellular carcinoma tumorigenesis by regulating the miR-206/MAP3K1 axis. *Cancer Med* 2020; **9**: 5620-5631 [PMID: 32558350 DOI: 10.1002/cam4.3204]

28 **Liu Z**, Mo H, Sun L, Wang L, Chen T, Yao B, Liu R, Niu Y, Tu K, Xu Q, Yang N. Long noncoding RNA PICSAR/miR-588/EIF6 axis regulates tumorigenesis of hepatocellular carcinoma by activating PI3K/AKT/mTOR signaling pathway. *Cancer Sci* 2020; **111**: 4118-4128 [PMID: 32860321 DOI: 10.1111/cas.14631]

29 **Valko M**, Morris H, Cronin MT. Metals, toxicity and oxidative stress. *Curr Med Chem* 2005; **12**: 1161-1208 [PMID: 15892631 DOI: 10.2174/0929867053764635]

World Journal of Gastrointestinal Oncology

Submit a Manuscript: https://www.f6publishing.com

World J Gastrointest Oncol 2022 October 15; 14(10): 2004-2013

DOI: 10.4251/wjgo.v14.i10.2004

ISSN 1948-5204 (online)

ORIGINAL ARTICLE

Retrospective Study

Multi-slice spiral computed tomography in differential diagnosis of gastric stromal tumors and benign gastric polyps, and gastric stromal tumor risk stratification assessment

Xiao-Long Li, Peng-Fei Han, Wei Wang, Li-Wei Shao, Ying-Wei Wang

Specialty type: Radiology, nuclear medicine and medical imaging

Provenance and peer review: Unsolicited article; Externally peer reviewed.

Peer-review model: Single blind

Peer-review report's scientific quality classification

Grade A (Excellent): 0
Grade B (Very good): B, B
Grade C (Good): C
Grade D (Fair): 0
Grade E (Poor): 0

P-Reviewer: Jusakul A, Thailand; Krishnan U, Australia; Shroff RT, United States

Received: June 22, 2022
Peer-review started: June 22, 2022
First decision: July 12, 2022
Revised: July 18, 2022
Accepted: September 13, 2022
Article in press: September 13, 2022
Published online: October 15, 2022

Xiao-Long Li, Peng-Fei Han, Wei Wang, Ying-Wei Wang, Diagnostic Radiology Department, The First Medical Center of PLA General Hospital, Beijing 100853, China

Li-Wei Shao, Pathology Department, The Seventh Medical Center of PLA General Hospital, Beijing 100700, China

Corresponding author: Ying-Wei Wang, PhD, Attending Doctor, Diagnostic Radiology Department, The first medical center of PLA General Hospital, No. 28 Fuxing Road, Haidian District, Beijing 100853, China. wangyw301@163.com

Abstract

BACKGROUND

The biological characteristics of gastric stromal tumors are complex, and their incidence has increased in recent years. Gastric stromal tumors (GST) have potential malignant tendencies, and the probability of transformation into malignant tumors is as high as 20%-30%.

AIM

To investigate the value of multi-slice spiral computed tomography (MSCT) in the differential diagnosis of GST and benign gastric polyps, and GST risk stratification assessment.

METHODS

We included 64 patients with GST (GST group) and 60 with benign gastric polyps (control group), confirmed by pathological examination after surgery in PLA General Hospital, from January 2016 to June 2021. The differences in the MSCT imaging characteristic parameters and enhanced CT values between the two groups before surgery were compared. According to the National Institutes of Health's standard, GST is divided into low- and high-risk groups for MSCT imaging characteristic parameters and enhanced CT values.

RESULTS

The incidences of extraluminal growth, blurred boundaries, and ulceration in the GST group were significantly higher than those in the control group ($P < 0.05$). The CT values and enhanced peak CT values in the arterial phase in the CST group were higher than those in the control group ($P < 0.05$). The MSCT differ-

ential diagnosis of GST and gastric polyp sensitivity, specificity, misdiagnosis rate, missed diagnosis rate, and areas under the curve (AUCs) were 73.44 %, 83.33%, 26.56%, 16.67%, 0.784, respectively. The receiver operating characteristic curves were plotted with the arterial CT value and enhanced peak CT value, with a statistical difference. The results showed that the sensitivity, specificity, misdiagnosis rate, missed diagnosis rate, and AUC value of arterial CT in the differential diagnosis of GST and gastric polyps were 80.18%, 62.20%, 19.82%, 37.80%, and 0.710, respectively. The sensitivity, specificity, misdiagnosis rate, missed diagnosis rate, and AUC value of the enhanced peak CT value in the differential diagnosis of GST and gastric polyps were 67.63%, 60.40%, 32.37%, 39.60%, and 0.710, respectively. The incidence of blurred lesion boundaries and ulceration in the high-risk group was significantly higher than that in the low-risk group ($P < 0.05$). The arterial phase and enhanced peak CT values in the high-risk group were significantly higher than those in the low-risk group ($P < 0.05$).

CONCLUSION

Presurgical MSCT examination has important value in the differential diagnosis of GST and gastric benign polyps and can effectively evaluate the risk grade of GST patients.

Key Words: Multi-slice spiral computed tomography; Differential diagnosis; Gastric stromal tumor; Benign gastric polyps; Risk stratification

Core Tip: Gastric stromal tumors (GSTs) are common gastrointestinal tumors and have a certain possibility of malignant change. Therefore, surgical intervention is important. However, the signs of early patients are not obvious, and difficult to distinguish from benign gastric tumors. Imaging examinations have always been the main methods for diagnosing GSTs. The degree of risk to patients can be evaluated by performing a computed tomography (CT) examination. In this study, a CT examination was performed to analyze the difference in CT performance between GSTs and gastric polyps, to provide the corresponding basis for early diagnosis of GSTs and reasonable selection of treatment methods.

Citation: Li XL, Han PF, Wang W, Shao LW, Wang YW. Multi-slice spiral computed tomography in differential diagnosis of gastric stromal tumors and benign gastric polyps, and gastric stromal tumor risk stratification assessment. *World J Gastrointest Oncol* 2022; 14(10): 2004-2013
URL: https://www.wjgnet.com/1948-5204/full/v14/i10/2004.htm
DOI: https://dx.doi.org/10.4251/wjgo.v14.i10.2004

INTRODUCTION

Gastric stromal tumors (GSTs) are mesenchymal tumors originating from Cahar mesenchymal cells, with malignant potential. At present, the most effective treatment is surgical resection; however, there is a risk of postoperative recurrence and metastasis. Gastric polyps are benign tumors of gastric epithelium or gastric interstitial origin, and endoscopic resection can be performed. The two tumors have different treatment methods, but their clinical symptoms and signs are similar[1]. Imaging examination has always been a common means for clinically diagnosing GSTs, which can locate the lesion, clarify morphological characteristics, and evaluate local invasiveness. Computed tomography (CT) is a commonly used diagnostic method in clinical practice. In recent years, enhanced CT examination has been determined to evaluate the risk of GSTs. CT examination can effectively avoid the influence of gastrointestinal gas and the superposition of surrounding organs on the preliminary diagnosis of lesions and reduce the missed diagnosis rate of lesions[2]. In this study, the imaging characteristics of gastric stromal tumors and gastric polyps in this region were analyzed using multi-slice spiral CT (MSCT), and the GST risk stratification was also evaluated. The purpose of this study was to provide a basis for the early diagnosis of GST in the clinic.

MATERIALS AND METHODS

General information

Sixty-four patients (GST group), with GST confirmed by pathological examination after surgery in PLA

General Hospital, from January 2016 to June 2021 and 60 patients with benign gastric polyps (control group) were selected.

The inclusion criteria were: (1) Patients aged 19–79 years were included in the study; (2) The diagnostic criteria for GST and benign gastric polyps refer to the criteria in the eighth edition of the 'Surgery' of the People's Health Press[3]; (3) All patients underwent endoscopic or surgical resection in our hospital for gastrointestinal surgery, as confirmed by postoperative pathological examination; (4) All patients underwent MSCT examination before surgery, and their imaging data were preserved completely; and (5) The research program was reviewed and approved by the medical ethics committee of our hospital. Exclusion criteria: (1) A history of chemoradiotherapy; (2) Additional with malignant tumors in other parts of the gastrointestinal tract; and (3) Patients with missing imaging data that could not be included in the statistical analysis.

MSCT inspection method

Inspection instrument: Siemens 64-row dual-source CT was used to perform the whole abdominal CT plain scan + enhanced examination. The scanning parameters were set as follows: tube voltage 120 kV, tube current, using automatic mA technology; pitch, 1.0; collimation, 128 mm × 0.6 mm, scanning layer thickness 3 mm, recombination layer thickness 3 mm; and matrix, 512 × 512. In the supine position, 80–120 mL (iodine content 320 mg/mL, 1.5 mL/kg body weight) of high-pressure injector was injected intravenously, through the median elbow. The injection flow rate was 3–4 mL/s. The abdominal aorta was monitored using an injection contrast agent (trigger threshold, 100 HU) for arterial phase scanning, and portal venous phase and delayed phase scanning were delayed for 45 s and 90 s.

All images were entered into a medical imaging workstation, and image analysis was performed by two imaging physicians with more than five years of experience. The tumor location, size, growth mode, morphology, lesion necrosis, calcification, and lymph node hyperplasia were analyzed. The CT value was measured at the same level in all four stages. ROI mapping should try to avoid the surrounding blood vessels, fat spaces, calcification, and necrotic areas in the tumor, and the average value of each patient was measured three times.

GST pathological risk assessment criteria

The risk classification standard of gastrointestinal stromal tumors was based on the National Institutes of Health (NIH) standard, as shown in Table 1.

Statistical analysis

The age, body mass index, lesion diameter, and other measurement indices of the patients were tested by normal distribution, which were in accordance with the approximate normal distribution or normal distribution, and expressed as mean ± SD. The *t*-test was used for comparisons between two groups. The non-grade count data were expressed as a percentage, and the statistical analysis was performed using the χ^2 test; diagnostic analysis was performed using a 2 × 2 four-fold table, diagnostic indicators were calculated, and a receiver operating characteristic curve was drawn. The professional SPSS21.0 software was used for data processing, test level $\alpha = 0.05$.

RESULTS

Comparison of baseline data between GST group and control group

Age, BMI, lesion diameter, gender, smoking, drinking and comorbidity were compared between GST group and control group ($P > 0.05$, Table 2).

Comparison of CT signs and parameters between GST group and control group

The lesion location, tumor shape, calcification and enhancement pattern of GST group and control group were compared ($P > 0.05$). The incidence of extraluminal growth, blurred boundary and ulcer in CST group was significantly higher than that in control group ($P < 0.05$) (Table 3).

Comparison of CT values between GST group and control group

CT values of GST group and control group in venous phase and delayed phase were compared ($P > 0.05$); the CT values and enhanced peak CT values in the arterial phase in the CST group were higher than those in the control group ($P < 0.05$) (Table 4).

Value of MSCT in differential diagnosis of GST and gastric polyps

The pathological results and the diagnostic results of MSCT signs parameters were used to draw a 2 × 2 quadrangle, and the results showed that the sensitivity of MSCT in the differential diagnosis of GST and gastric polyps was 73.44%, the specificity was 83.33%, the misdiagnosis rate was 26.56%, the missed diagnosis rate was 16.67%, and the AUC value was 0.784 (Table 5, Figure 1A).

Table 1 National Institutes of Health evaluation criteria for gastric stromal tumor pathological risk

GST Hazard classification	Lesion diameter (cm)	Mitosis (/50HPF)	Primary tumor location
Very low risk	< 2.0	≤ 5.0	Any position
Low risk	2.1 - 5.0	≤ 5.0	Any position
Medium risk	2.1 - 5.0	> 5.0	Stomach
	< 5.0	6.0 - 1.0	Any position
	5.0 - 10.0	≤ 5.0	Stomach
High risk	Any case	Any case	Tumor rupture
	> 10.0	Any case	Any position
	Any case	> 10.0	Any position
	> 5.0	> 5.0	Any position
	2.1 - 5.0	> 5.0	Non-stomach
	5.0 - 10.0	≤ 5.0	Non-stomach

GST: Gastric stromal tumor.

Table 2 Comparison of baseline data between gastric stromal tumor group and control group, *n* (%)

Normal information	GST group (*n* = 64)	Control group (*n* = 60)	t/χ^2 value	*P* value
Age (yr)	56.9 ± 8.2	59.0 ± 7.5	-1.485	0.140
BMI (kg/m^2)	24.7 ± 2.4	24.4 ± 2.3	0.710	0.479
Lesion diameter (cm)	2.98 ± 0.77	3.05 ± 0.80	-0.496	0.620
Gender			1.542	0.214
Male	37 (57.81)	28 (46.67)		
Female	27 (42.19)	32 (53.33)		
Smoking			1.663	0.197
Yes	24 (37.5)	16 (26.67)		
No	40 (62.5)	44 (73.33)		
Drinking			1.592	0.207
Yes	25 (39.06)	17 (28.33)		
No	39 (60.94)	43 (71.67)		
Diabetes			0.776	0.378
Yes	9 (14.06)	12 (20.00)		
No	55 (85.94)	48 (80.00)		
Hypertension			2.940	0.086
Yes	15 (23.44)	7 (11.67)		
No	49 (76.56)	53 (88.33)		

GST: Gastric stromal tumor; BMI: Body mass index.

Receiver operating characteristic (ROC) curve was drawn by arterial phase CT value and enhanced peak CT value, respectively. The results showed that the sensitivity, specificity, misdiagnosis rate, missed diagnosis rate and AUC value of arterial phase CT value in the differential diagnosis of GST and gastric polyps were 80.18%, 62.20%, 19.82%, 37.80% and 0.710, respectively. The sensitivity, specificity, misdiagnosis rate, missed diagnosis rate and AUC value of enhanced peak CT value in the differential diagnosis of GST and gastric polyps were 67.63%, 60.40%, 32.37%, 39.60% and 0.710, respectively (Figure 1B).

Table 3 Comparison of computed tomography signs and parameters between gastric stromal tumor group and control group, *n* (%)

CT signs	GST group (*n* = 64)	Control group (*n* = 60)	χ^2 value	*P* value
Lesion location			4.174	0.383
Fundus of stomach	12 (18.75)	14 (23.33)		
Cardia	6 (9.38)	8 (13.33)		
Greater curvature of the stomach	26 (40.63)	17 (28.33)		
Lesser curvature of stomach	11 (17.19)	7 (11.67)		
Gastric antrum	9 (14.06)	14 (23.33)		
Tumor shape			3.228	0.072
Smooth	50 (78.13)	54 (90.00)		
Lobulated	14 (21.88)	6 (10.00)		
Growth pattern			41.177	0.000
Intraluminal	22 (34.38)	54 (90.00)		
Extraluminal	32 (50.00)	6 (10.00)		
Mixed way	10 (15.63)	0 (0.00)		
Calcification			1.166	0.280
Yes	5 (7.81)	2 (3.33)		
No	59 (92.19)	58 (96.67)		
Lesion border			31.312	0.000
Clear	11 (17.19)	40 (66.67)		
Blurry	53 (82.81)	20 (33.33)		
Reinforcement			3.725	0.054
Uniform	54 (84.38)	57 (95.00)		
Uneven	10 (15.63)	3 (5.00)		
Ulcer			9.771	0.002
Yes	18 (28.13)	4 (6.67)		
No	46 (71.88)	56 (93.33)		

GST: Gastric stromal tumor; CT: Computed tomography.

Table 4 Comparison of computed tomography values between gastric stromal tumor group and control group (mean ± SD, HU)

Groups	*n*	Arterial phase	Venous phase	Delay period	Reinforcement peak
GST group	64	63.98 ± 14.38	59.04 ± 12.74	66.58 ± 11.47	75.58 ± 12.88
Control group	60	47.61 ± 11.04	56.48 ± 14.20	64.72 ± 9.83	64.46 ± 10.94
t value		-7.137	-1.054	-0.971	-5.192
P value		0.000	0.294	0.333	0.000

GST: Gastric stromal tumor.

Comparison of CT sign parameters in GST groups with different risk classifications

According to NIH classification standard, there were 23 high-risk patients, 17 middle-risk patients and 24 Low-risk patients in GST group. The incidence of blurred lesion boundary and ulceration in the high-risk group was significantly higher than that in the low-risk group ($P < 0.05$) (Table 6).

Table 5 Multi-slice spiral computed tomography differential diagnosis of gastric stromal tumor and gastric polyps 2 × 2 four-table table

MSCT	Pathology		Total
	GST	Benign polyp	
GST	47	10	57
Benign polyp	17	50	67
Total	64	60	124

MDCT: Multi-slice spiral computed tomography; GST: Gastric stromal tumor.

Table 6 Comparison of computed tomography sign parameters in gastric stromal tumor groups with different risk classes, *n* (%)

CT signs	Low-intermediate-risk group (*n* = 41)	High-risk group (*n* = 23)	χ^2 value	*P* value
Lesion location			2.180	0.703
Fundus of stomach	7 (17.07)	5 (21.74)		
Cardia	4 (9.76)	2 (8.70)		
Greater curvature of the stomach	15 (36.59)	11 (47.83)		
Lesser curvature of stomach	9 (21.95)	2 (8.70)		
Gastric antrum	6 (14.63)	3 (13.04)		
Tumor shape			1.539	0.215
Smooth	34 (82.93)	16 (69.57)		
Lobulated	7 (17.07)	7 (30.43)		
Growth pattern			5.520	0.063
Intraluminal	17 (41.46)	5 (21.74)		
Extraluminal	16 (39.02)	16 (69.57)		
Mixed way	8 (19.51)	2 (8.70)		
Calcification			0.039	0.844
Yes	3 (7.32)	2 (8.70)		
No	38 (92.68)	21 (91.3)		
Lesion border			4.158	0.041
Clear	10 (24.39)	1 (4.35)		
Blurry	31 (75.61)	22 (95.65)		
Reinforcement			0.181	0.670
Uniform	34 (82.93)	20 (86.96)		
Uneven	7 (17.07)	3 (13.04)		
Ulcer			4.187	0.041
Yes	8 (19.51)	10 (43.48)		
No	33 (80.49)	13 (56.52)		

CT: Computed tomography.

Comparison of CT values of patients in GST groups with different risk classifications

The arterial phase CT value and enhanced peak CT value in the high-risk group were significantly higher than those in the low-risk group ($P < 0.05$) (Table 7).

Table 7 Comparison of computed tomography values of patients in gastric stromal tumor groups with different risk classes (mean ± SD)

Group	*n*	Arterial phase	Venous phase	Delay period	Reinforcement peak
Low-intermediate-risk group	41	55.71 ± 13.77	57.94 ± 12.51	64.83 ± 11.20	72.66 ± 12.46
High-risk group	23	78.72 ± 12.66	61.00 ± 11.96	69.70 ± 10.85	80.79 ± 12.37
t value		-6.598	-0.954	-1.688	-2.511
P value		0.000	0.344	0.097	0.015

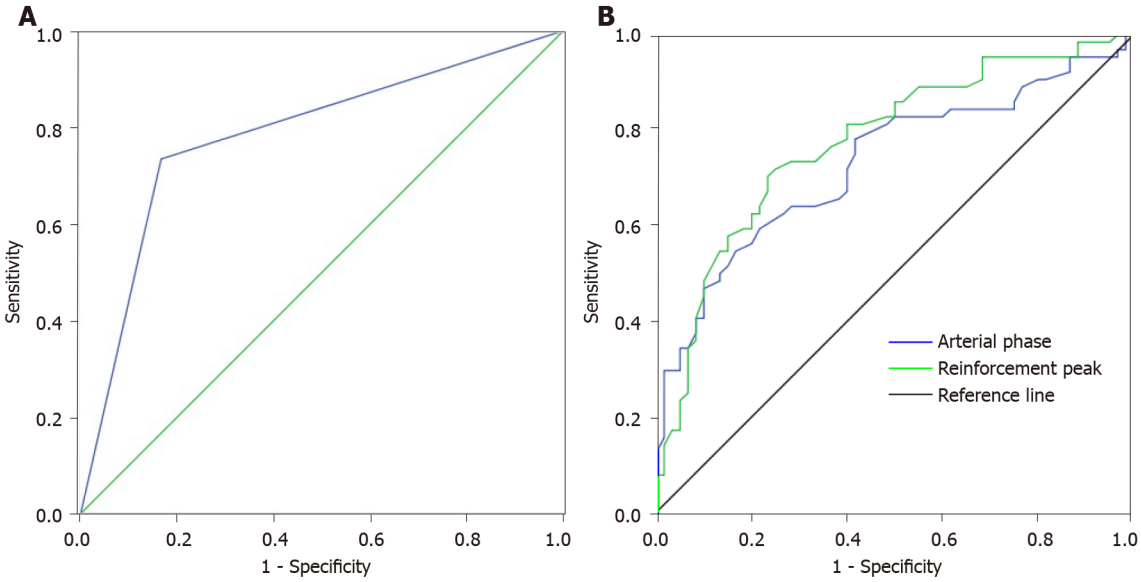

DOI: 10.4251/wjgo.v14.i10.2004

Figure 1 Receiver operating characteristic curve. A: Receiver operating characteristic (ROC) curve of multi-slice spiral computed tomography (MSCT) in differential diagnosis of gastric stromal tumor (GST) and gastric polyps; B: ROC curve of differential diagnosis of GST and gastric polyps by peak CT value of arterial phase enhancement.

DISCUSSION

GSTs are common mesenchymal tumors of the digestive system. Benign gastric polyps are common benign tumors of the stomach, but their clinical symptoms are not distinguished. Therefore, if an accurate diagnosis is not made prior to surgery, the treatment options will be affected[3]. CT has always been an important method for the clinical diagnosis of gastrointestinal tumors. It can distinguish the location, size, shape, and internal structure of the tumor and also distinguish the relationship between the tumor and the surrounding tissue structure. In particular, enhanced CT can be used to analyze the lesion details[4,5].

This study analyzed the differences between GSTs and benign tumors on CT scans. GSTs are rich in blood supply; therefore, they are prone to bleeding and cause cystic necrosis within the tumor, and calcification is relatively common with the progression of the disease. Benign tumors, owing to their slow growth, show homogeneous soft tissue masses with relatively clear boundaries and regular morphology. Cystic necrosis and calcification of tumors are rare[6,7]. In this study, the incidence of extraluminal growth, blurred boundaries, and ulcers in the CST group was significantly higher than that in the benign tumor group, indicating that GSTs show extraluminal growth, blurred boundaries, and ulcers, which is of great significance for the identification of GSTs and benign tumors. Some scholars have reported that malignant tumors grow rapidly and have different rates of extension in various directions, resulting in irregular shapes such as lobulation. Benign tumors are mostly round, oval, and other regular shapes, owing to the uniform expansion of the growth mode around them. The higher the risk, the more irregular the shape; the more uneven the internal density and the greater the probability of necrosis, liquefaction, and bleeding. These results are consistent with those of this study[8,9].

This study also analyzed the difference between contrast-enhanced CT in the differential diagnosis of gastric stromal and benign tumors. Previous studies have found that contrast-enhanced CT has little significance in the differential diagnosis of gastric stromal and benign tumors. The main reason is that both tumors originate from the gastric submucosa interstitial tissue, and there is little difference in

blood supply between tumors, which leads to obvious enhancement in contrast-enhanced CT[10]. In this study, there was no difference in CT values between the GST and control groups in the venous and delayed phases, but the CT values and enhanced peak CT values of the CST group were higher than those of the control group in the arterial phase. We believe that the enhancement examination can reveal a cluster-like small vascular shadow around the tumor. Previous studies have suggested that enhancement may be related to the malignant degree of the tumor, and a low malignant degree of the tumor may lead to uniform and moderate enhancement, or tumor necrosis and cystic degeneration[11-14]. ROC curve analysis showed that the arterial CT value and enhanced peak CT value had a certain sensitivity and specificity in the differential diagnosis of GST and gastric polyps.

The NIH grading standard has been commonly used for assessing the risk of GSTs in clinical practice. The degree of risk is mainly divided according to mitosis, tumor size, primary site, and rupture. In this study, the lesion boundary of the high-risk group was blurred, and the incidence of ulceration in the lesion was significantly higher than that in the low-risk group[15,16]. Further analysis of the enhanced CT results showed that the arterial phase CT value and enhanced peak CT value of the high-risk group were significantly higher than those of the low-risk group, indicating that the blood supply in GSTs was rich, mainly due to the rapid proliferation of malignant tumor blood vessels. Therefore, in addition to vascular penetration, blood vessels can also be observed on CT examination[17,18]. Some scholars have reported that GSTs show mild-to-moderate homogeneous enhancement on contrast-enhanced scanning. With different degrees of malignancy, homogeneous or inhomogeneous enhancement was observed. Especially, the enhancement degree less than 15.4 Hu in the arterial phase was an important indicator for distinguishing benign tumors from GSTs, which was primarily consistent with the results of this study[19,20].

This study analyzed the differences between GSTs and benign gastric polyps on contrast-enhanced CT examination and confirmed that CT examination has a certain reference value for the identification of the two diseases. Concurrently, it also confirmed the difference in the degree of disease risk in CT examinations, which could provide the corresponding diagnostic basis for clinical differential diagnosis and risk assessment of GSTs. However, the number of samples included in this study was relatively small, and this was a single-center study, which may have regional differences. Moreover, it is not possible to analyze the CT texture differences and whether there is a difference in the size of the GSTs on CT examination. Therefore, it is necessary to expand the sample size and conduct stratified research to further demonstrate and analyze our results.

CONCLUSION

In conclusion, preoperative MSCT examination has important value in the differential diagnosis of GST and benign gastric polyps and can effectively evaluate the risk classification of GST patients.

ARTICLE HIGHLIGHTS

Research background

The malignant tendency and complex features of gastric stromal tumors (GSTs) seriously threaten human health.

Research motivation

Multi-slice spiral computed tomography (MSCT) is widely used in clinical practice. We try to apply it in the differential diagnosis and risk stratification of GSTs and benign gastric polyps, hoping to obtain valuable clues that can guide the clinical practice.

Research objectives

This study aimed to clarify the manifestations of GSTs and benign gastric polyps in multi-slice computed tomography, including diagnostic value and risk stratification.

Research methods

The differences and risk stratification characteristics of MSCT imaging parameters and contrast-enhanced CT between patients with GST confirmed by pathological examination after surgery and patients with benign gastric polyps were retrospectively analyzed.

Research results

There are significant differences in MSCT characteristics and enhancement characteristics between GST and gastric polyps, and the MSCT characteristics and enhancement characteristics of GST in different risk stratifications are also different. MSCT has higher value in the identification and risk stratification

of GST and gastric polyps.

Research conclusions

Preoperative application of MSCT to distinguish GST from benign gastric polyps is of high value, and it is also feasible to classify the risk level of GST patients.

Research perspectives

We recommend preoperative MSCT to distinguish GST from benign gastric polyps and to classify GST patients at risk.

FOOTNOTES

Author contributions: Li XL and Han PF contributed equally to this article and should be considered as co-first authors; Li XL, Han PF and Wang YW wrote the paper; Li XL, Han PF and Shao LW were responsible for sorting the data.

Institutional review board statement: The study was reviewed and approved by the First Medical Center of PLA General Hospital.

Informed consent statement: All study participants, or their legal guardian, provided informed written consent prior to study enrollment.

Conflict-of-interest statement: The authors report no conflict of interest.

Data sharing statement: No additional data are available.

Country/Territory of origin: China

ORCID number: Xiao-Long Li 0000-0002-3911-0448; Peng-Fei Han 0000-0002-2287-6340; Wei Wang 0000-0002-3886-4723; Li-Wei Shao 0000-0001-7763-2506; Ying-Wei Wang 0000-0002-5611-0458.

S-Editor: Wang JL
L-Editor: A
P-Editor: Wang JL

REFERENCES

1 **Papke DJ Jr**, Hornick JL. Recent developments in gastroesophageal mesenchymal tumours. *Histopathology* 2021; **78**: 171-186 [PMID: 33382494 DOI: 10.1111/his.14164]
2 **Wang MX**, Devine C, Segaran N, Ganeshan D. Current update on molecular cytogenetics, diagnosis and management of gastrointestinal stromal tumors. *World J Gastroenterol* 2021; **27**: 7125-7133 [PMID: 34887632 DOI: 10.3748/wjg.v27.i41.7125]
3 **Zimmer V**, Bier B. Loop ligation-assisted endoscopic resection of a gastrointestinal stromal tumor in the gastric fundus. *Dig Liver Dis* 2021; **53**: 245-247 [PMID: 32616460 DOI: 10.1016/j.dld.2020.06.028]
4 **Kawabata K**, Takahashi T, Nakajima K, Tanaka K, Miyazaki Y, Makino T, Kurokawa Y, Yamasaki M, Mori M, Doki Y. [Laparoscopic Resection of a Huge Gastric Gastrointestinal Stromal Tumor after Neoadjuvant Chemotherapy-A Case Report]. *Gan To Kagaku Ryoho* 2020; **47**: 670-672 [PMID: 32389979]
5 **Inukai M**, Shibasaki S, Suzuki K, Tsuru Y, Matsuo K, Goto A, Nakamura K, Tanaka T, Kikuchi K, Suda K, Inaba K, Uyama I. [Preoperative Imatinib Therapy Followed by Laparoscopic Local Gastrectomy for a Giant Gastric Gastrointestinal Stromal Tumor-A Case Report]. *Gan To Kagaku Ryoho* 2020; **47**: 2062-2064 [PMID: 33468801]
6 **Gu JY**, Shi HT, Yang LX, Shen YQ, Wang ZX, Feng Q, Wang M, Cao H. [Clinical significance of the deep learning algorithm based on contrast-enhanced CT in the differential diagnosis of gastric gastrointestinal stromal tumors with a diameter ≤ 5 cm]. *Zhonghua Wei Chang Wai Ke Za Zhi* 2021; **24**: 796-803 [PMID: 34530561 DOI: 10.3760/cma.j.cn.441530-20210706-00267]
7 **Hamman SM**, Biyyam DR, Mandell GA. Gastric Gastrointestinal Stromal Tumor Incidentally Detected With Meckel Scintigraphy. *Clin Nucl Med* 2020; **45**: 372-373 [PMID: 32149788 DOI: 10.1097/RLU.0000000000002974]
8 **Namikawa T**, Maeda M, Yokota K, Tanioka N, Iwabu J, Munekage M, Uemura S, Maeda H, Kitagawa H, Nagata Y, Kobayashi M, Hanazaki K. Laparoscopic Distal Gastrectomy for Synchronous Gastric Cancer and Gastrointestinal Stromal

Tumor With Situs Inversus Totalis. *In Vivo* 2021; **35**: 913-918 [PMID: 33622883 DOI: 10.21873/invivo.12331]

9 **Li C**, Fu W, Huang L, Chen Y, Xiang P, Guan J, Sun C. A CT-based nomogram for predicting the malignant potential of primary gastric gastrointestinal stromal tumors preoperatively. *Abdom Radiol (NY)* 2021; **46**: 3075-3085 [PMID: 33713161 DOI: 10.1007/s00261-021-03026-7]

10 **Wu E**, Son SY, Gariwala V, O'Neill C. Gastric gastrointestinal stromal tumor (GIST) with co-occurrence of pancreatic neuroendocrine tumor. *Radiol Case Rep* 2021; **16**: 1391-1394 [PMID: 33912253 DOI: 10.1016/j.radcr.2021.03.014]

11 **Taguchi T**, Nagase H, Noguchi K, Hirota M, Oshima K, Tanida T, Noura S, Kawase T, Imamura H, Iwazawa T, Akagi K, Andou H, Tamura Y, Adachi S, Douno K. [Gastric Gastrointestinal Stromal Tumor Appearing Nine Years after Resection of a Duodenal Gastrointestinal Stromal Tumor-A Case Report]. *Gan To Kagaku Ryoho* 2020; **47**: 144-146 [PMID: 32381886]

12 **Zhao H**, Chen C, Yang C, Mo S, Zhao H, Tian Y. Prefoldin and prefoldin-like complex subunits as predictive biomarkers for hepatocellular carcinoma immunotherapy. *Pathol Res Pract* 2022; **232**: 153808 [PMID: 35217267 DOI: 10.1016/j.prp.2022.153808]

13 **Zhang Y**, Zhou F, Yang H, Gong X, Gao J. Current Status of Fear of Disease Progression in Patients with Advanced Cancer and Usefulness of Dignity Therapy Intervention. *J Healthc Eng* 2022; **2022**: 6069060 [PMID: 35356618 DOI: 10.1155/2022/6069060]

14 **Xu JX**, Ding QL, Lu YF, Fan SF, Rao QP, Yu RS. A scoring model for radiologic diagnosis of gastric leiomyomas (GLMs) with contrast-enhanced computed tomography (CE-CT): Differential diagnosis from gastrointestinal stromal tumors (GISTs). *Eur J Radiol* 2021; **134**: 109395 [PMID: 33310552 DOI: 10.1016/j.ejrad.2020.109395]

15 **Xiao F**, Zhang L, Yang S, Peng K, Hua T, Tang G. Quantitative analysis of the MRI features in the differentiation of benign, borderline, and malignant epithelial ovarian tumors. *J Ovarian Res* 2022; **15**: 13 [PMID: 35062992 DOI: 10.1186/s13048-021-00920-y]

16 **Mazzei MA**, Cioffi Squitieri N, Vindigni C, Guerrini S, Gentili F, Sadotti G, Mercuri P, Righi L, Lucii G, Mazzei FG, Marrelli D, Volterrani L. Gastrointestinal stromal tumors (GIST): a proposal of a "CT-based predictive model of Miettinen index" in predicting the risk of malignancy. *Abdom Radiol (NY)* 2020; **45**: 2989-2996 [PMID: 31506758 DOI: 10.1007/s00261-019-02209-7]

17 **Sugiyama Y**, Shimbara K, Sasaki M, Kouyama M, Tazaki T, Takahashi S, Nakamitsu A. Solitary peritoneal metastasis of gastrointestinal stromal tumor: A case report. *World J Gastroenterol* 2020; **26**: 5527-5533 [PMID: 33024403 DOI: 10.3748/wjg.v26.i36.5527]

18 **Li J**, Jiang Y, Chen C, Tan W, Li P, Chen G, Peng Q, Yin W. Integrin β4 Is an Effective and Efficient Marker in Synchronously Highlighting Lymphatic and Blood Vascular Invasion, and Perineural Aggression in Malignancy. *Am J Surg Pathol* 2020; **44**: 681-690 [PMID: 32044807 DOI: 10.1097/PAS.0000000000001451]

19 **Wang J**, Xie Z, Zhu X, Niu Z, Ji H, He L, Hu Q, Zhang C. Differentiation of gastric schwannomas from gastrointestinal stromal tumors by CT using machine learning. *Abdom Radiol (NY)* 2021; **46**: 1773-1782 [PMID: 33083871 DOI: 10.1007/s00261-020-02797-9]

20 **Dhali A**, Ray S, Khamrui S, Dhali GK. Mucinous cystadenocarcinoma of pancreas mimicking gastrointestinal stromal tumor of stomach: Case report. *Int J Surg Case Rep* 2021; **85**: 106240 [PMID: 34343789 DOI: 10.1016/j.ijscr.2021.106240]

World Journal of Gastrointestinal Oncology

Submit a Manuscript: https://www.f6publishing.com

World J Gastrointest Oncol 2022 October 15; 14(10): 2014-2024

DOI: 10.4251/wjgo.v14.i10.2014

ISSN 1948-5204 (online)

ORIGINAL ARTICLE

Retrospective Study

Predictive value of a serum tumor biomarkers scoring system for clinical stage II/III rectal cancer with neoadjuvant chemoradiotherapy

Jie-Yi Zhao, Qing-Qing Tang, Yu-Ting Luo, Shu-Min Wang, Xiao-Rui Zhu, Xiao-Yu Wang

Specialty type: Gastroenterology and hepatology

Provenance and peer review: Unsolicited article; Externally peer reviewed.

Peer-review model: Single blind

Peer-review report's scientific quality classification

Grade A (Excellent): 0
Grade B (Very good): 0
Grade C (Good): C, C
Grade D (Fair): 0
Grade E (Poor): 0

P-Reviewer: Dulskas A, Lithuania; Elkady N, Egypt

Received: June 8, 2022
Peer-review started: June 8, 2022
First decision: June 23, 2022
Revised: July 6, 2022
Accepted: August 22, 2022
Article in press: August 22, 2022
Published online: October 15, 2022

Jie-Yi Zhao, Xiao-Yu Wang, Department of Neurosurgery, West China Hospital, Sichuan University, Chengdu 610041, Sichuan Province, China

Qing-Qing Tang, Department of Ophthalmology, West China Hospital, Sichuan University, Chengdu 610041, Sichuan Province, China

Yu-Ting Luo, Shu-Min Wang, Xiao-Rui Zhu, West China Medical School, Sichuan University, Chengdu 610041, Sichuan Province, China

Corresponding author: Xiao-Yu Wang, MD, Doctor, Department of Neurosurgery, West China Hospital, Sichuan University, No. 37 Guo Xue Alley, Chengdu 610041, Sichuan Province, China. yuxixi1052006@126.com

Abstract

BACKGROUND

Multiple classes of molecular biomarkers have been studied as potential predictors for rectal cancer (RC) response. Carcinoembryonic antigen (CEA) is the most widely used blood-based marker of RC and has proven to be an effective predictive marker. Cancer antigen 19-9 (CA19-9) is another tumor biomarker used for RC diagnosis and postoperative monitoring, as well as monitoring of the therapeutic effect. Using a panel of tumor markers for RC outcome prediction is a practical approach.

AIM

To assess the predictive effect of pre-neoadjuvant chemoradiotherapy (NCRT) CEA and CA19-9 levels on the prognosis of stage II/III RC patients.

METHODS

CEA and CA19-9 levels were evaluated 1 wk before NCRT. According to the receiver operating characteristic curve analysis, the optimal cut-off point of CEA and CA19-9 levels for the prognosis were 3.55 and 19.01, respectively. The novel serum tumor biomarker (NSTB) scores were as follows: score 0: Pre-NCRT CEA < 3.55 and CA19-9 < 19.01; score 2: Pre-NCRT CEA > 3.55 and CA19-9 > 19.01; score 1: Other situations. Pathological information was recorded according to histopathological reports after the operation.

RESULTS

In the univariate analysis, pre-NCRT CEA < 3.55 [P = 0.025 for overall survival

(OS), P = 0.019 for disease-free survival (DFS)], pre-NCRT CA19-9 < 19.01 (P = 0.014 for OS, P = 0.009 for DFS), a lower NSTB score (0-1 *vs* 2, P = 0.009 for OS, P = 0.005 for DFS) could predict a better prognosis. However, in the multivariate analysis, only a lower NSTB score (0-1 *vs* 2; for OS, HR = 0.485, 95%CI: 0.251-0.940, P = 0.032; for DFS, HR = 0.453, 95%CI: 0.234-0.877, P = 0.019) and higher pathological grade, node and metastasis stage (0-I *vs* II-III; for OS, HR = 0.363, 95%CI: 0.158-0.837, P = 0.017; for DFS, HR = 0.342, 95%CI: 0.149-0.786, P = 0.012) were independent predictive factors.

CONCLUSION

The combination of post-NCRT CEA and CA19-9 was a predictive factor for clinical stage II/III RC patients receiving NCRT, and the combined index had a stronger predictive effect.

Key Words: Rectal cancer; Neoadjuvant chemoradiotherapy; Scoring system; Carcinoembryonic antigen; Carbohydrate antigen 19-9; Predictive

Core Tip: Tumor microenvironment (TME) combined with neoadjuvant chemotherapy (NCRT) is the standard treatment for resectable stage II/III rectal cancer (RC). Multiple classes of molecular biomarkers have been studied as potential predictors for RC response but there is no sufficient evidence for any of them to be introduced into clinical practice. By retrospectively evaluating clinical stage II/III RC patients undergoing NCRT followed by standard TME, we found that the combination of NCRT carcinoembryonic antigen and carbohydrate antigen 19-9 levels could be a prognostic predictor for clinical stage II/III RC patients receiving NCRT, and the combined indexes had a stronger predictive effect than the index alone.

Citation: Zhao JY, Tang QQ, Luo YT, Wang SM, Zhu XR, Wang XY. Predictive value of a serum tumor biomarkers scoring system for clinical stage II/III rectal cancer with neoadjuvant chemoradiotherapy. *World J Gastrointest Oncol* 2022; 14(10): 2014-2024

URL: https://www.wjgnet.com/1948-5204/full/v14/i10/2014.htm

DOI: https://dx.doi.org/10.4251/wjgo.v14.i10.2014

INTRODUCTION

In the United States, tumor microenvironment (TME) combined with neoadjuvant chemotherapy (NCRT) is the standard treatment for resectable stage II/III rectal cancer (RC)[1-3]. Although numerous studies have shown that NCRT can reduce the rate of local recurrence, it is difficult to improve overall survival (OS)[4-6]. Multiple classes of molecular biomarkers have been studied as potential predictors for RC response but there is no sufficient evidence for any of them to be introduced into clinical practice [7]. Moreover, additional systematic chemotherapy could increase the toxicity [8,9]. Therefore, it is critical to identify predictive factors for clinical stage II/III patients and give additional chemotherapy or more aggressive treatment strategies.

Pathological indicators are generally considered to be the most effective predictive factors[10,11]. Unfortunately, pathological characteristics are difficult to obtain and quantitate and are usually affected by the operation and specimen-processing quality[8,9]. Moreover, the pathological indicators, which can only be obtained after surgery, do not assist in judging whether patients need additional chemotherapy before undergoing NCRT or surgery.

A glycoprotein, carcinoembryonic antigen (CEA), is the most widely used blood-based marker of RC and has proven to be an effective predictive marker[12-14]. According to You *et al*[15], the increment in postoperative serum CEA levels (CEA < 5 *vs* > 5) was an independent predictor of a poor prognosis. However, the major problem with the use of CEA as a marker of RC is its association with other types of cancer and benign diseases (inflammatory bowel disease)[16-18]. Cancer antigen 19-9 (CA19-9) is another tumor biomarker used for RC diagnosis and postoperative monitoring, as well as monitoring of the therapeutic effect[19,20]. Due to the highly heterogeneous nature of RC, a single tumor marker is unlikely to become a stand-alone predictive factor. Using a panel of tumor markers for RC outcome prediction is a practical approach.

In this study, we analyzed the predictive value of the combination of pre-NCRT serum tumor markers (CEA and CA19-9) in clinical stage II/III RC patients.

MATERIALS AND METHODS

Patients screening

We retrospectively evaluated clinical stage II/III RC patients undergoing NCRT followed by standard TME in our hospital from February 2011 to August 2020. We included the following categories of patients: (1) Patients receiving preoperative NCRT; (2) patients with colorectal adenocarcinoma confirmed by pathological biopsy; (3) patients whose serum CEA and CA19-9 levels were measured within one week before NCRT; and (4) patients undergoing NCRT followed by standard TME. We excluded the following categories of patients: (1) Patients with distal metastasis; (2) patients with other concomitant tumors; (3) patients with insufficient blood, clinicopathological, or follow-up data; and (4) patients with unresectable RC. The patient-screening flowchart is shown in Figure 1.

This retrospective study was approved by the ethics committee of our hospital. The requirement for patients' informed consent was waived due to the retrospective nature of the study.

Treatment and follow-up of patients

All patients in this study received NCRT followed by standard TME. Their CEA and CA19-9 levels were evaluated within 1 wk pre-NCRT. Pathological, node and metastasis (TNM) stages and histological grades were noted according to histopathological reports. The receiver operating characteristic (ROC) curve was adopted to determine the best cut-off values of pre-NCRT CEA and CA19-9 levels for predicting OS. The novel serum tumor biomarker (NSTB) scores were as follows: score 0: Pre-NCRT CEA < 3.55 and CA19-9 < 19.01; score 2: Pre-NCRT CEA > 3.55 and CA19-9 > 19.01; score 1: Pre-NCRT CEA < 3.55 and CA19-9 > 19.01 or pre-NCRT CEA > 3.55 and CA19-9 < 19.01.

Postoperative follow-up was performed according to the National Comprehensive Cancer Network guidelines[13]. Generally, patients were followed up clinically and radiographically at three-month intervals in the first 2 years after surgery, then every 6 mo for 3 years, and annually thereafter[13]. Follow-up data were obtained from medical records, telephone follow-ups, out-patient clinics, or visits.

OS was defined as the survival time until death by any reason[21]. DFS was defined as the time-lapse between surgery and either RC recurrence or death[22]. Patients lost to follow-up or still alive at the final follow-up were included in the analysis as censored data[21].

Statistical analysis

Data were analyzed using SPSS for Windows (IBM Corp. Released 2013. IBM SPSS Statistics for Windows, Version 22.0. Armonk, NY: IBM Corp.). Continuous data were described in terms of the median and interquartile range (IQR) whereas categorical variables were described in terms of frequencies and percentages. Significant parameters identified in the univariate analysis ($P < 0.05$) were entered into the multivariate Cox regression analysis to determine independent predictive factors[23, 24]. All statistical tests were two-sided, and a P value of < 0.05 was considered statistically significant [25].

In general, pathological characteristics have the strongest predictive value for patient outcomes[21]. To compare the predictive effect of the NSTB score, several pathological indicators were included. To prevent the effects of pre-NCRT CEA and CA19-9 levels on the NSTB score, two models, one including and the other excluding the NSTB score in the multivariate analysis, were established.

RESULTS

Patient characteristics

Eighty-seven (36.7%) patients were female and 150 (63.3%) were male. The distribution of the patients according to pathological evaluation was as follows: vascular invasion was detected in 13 (5.5%) patients, lymphatic invasion in 13 (5.5%) patients, perineural invasion in 41 (17.3%) patients, and circumferential resection margin (CRM) positivity in 8 (3.8%) patients. Regarding the pathological TNM classification, 45 (19.0%) patients were in stage 0, 57 (24.1%) were in stage I, 72 (30.4%) were in stage II, and 63 (26.6%) were in stage III (Table 1). A total of 118 (49.8%) patients were in pT stage 0-2 while 119 (50.2%) were in pT stage 3-4. Sixty (25.3%) patients had pN metastases while 177 (74.7%) did not have pN metastases. The median (IQR) level of pre-NCRT CEA was 4.15 (2.18-10.07) and that of pre-NCRT CA19-9 was 13.56 (7.80-25.40).

During follow-up, 9 (3.8%) patients were lost to follow-up and 36 (15.2%) developed cancer recurrence and died.

Kaplan-Meier curves stratified by pre-NCRT CEA, CA19-9, and the NSTB score

ROC curves identified the optimal cut-off for survival prediction by pre-NCRT CEA and CA19-9 were 3.55 and 19.01, respectively. They divided patients into different groups. Figures 2-4A show the OS of included patients stratified by pre-NCRT CEA, CA19-9, and the NSTB score, respectively, and Figures 2-4B show their DFS stratified by the same parameters. According to the Kaplan–Meier curves, increased

Table 1 Clinicopathological characteristics

Features	Median (IQR)
Pre-NCRT CEA	4.15 (2.18-10.07)
Pre-NCRT CA19-9	13.56 (7.80-25.40)
Age in yr	57.0 (50.0-66.5)
Sex	
Male	150
Female	87
Pathological T stage	
T0-2	118
T3-4	119
Pathological N stage	
N0	177
N+	60
Pathological TNM stage	
0	45
I	57
II	72
III	63
Pathological vascular invasion	
Yes	13
No	224
Pathological lymphatic invasion	
Yes	13
No	224
Pathological perineural invasion	
Yes	41
No	196
Pathological CRM	
Positive	8
Negative	229

NCRT: Neoadjuvant chemoradiotherapy; CEA: Carcinoembryonic antigen; CA19-9: Cancer antigen 19-9; TNM: Tumor, node and metastasis; CRM: Circumferential resection margin; IQR: Interquartile range.

pre-NCRT CEA and CA19-9 levels and higher NSTB scores were all associated with decreased OS and DFS.

Cox regression analysis of factors affecting the prognosis

Possible clinicopathological parameters that may predict patient outcome were reviewed. In the univariate analysis, pre-NCRT CEA > 3.55, pre-CA19-9 > 19.01, a higher pathological TNM stage, and a higher NSTB score were significantly associated with decreased OS (Table 2) and DFS (Table 3).

In the multivariate analysis of OS (Table 4), only a lower pathological TNM stage (stage 0-I *vs* II-III, HR = 0.363, 95%CI: 0.158-0.837, P = 0.017) and the NSTB score (score 0-1 *vs* 2, HR = 0.485, 95%CI: 0.251-0.940, P = 0.032) were significant predictors of a better outcome while pre-NCRT CEA < 3.55 (HR = 0.529, 95%CI: 0.23-1.205, P = 0.130) and CA19-9 < 19.01 (HR = 0.604, 95%CI: 0.300-1.215, P = 0.158) were not. In the multivariate analysis of DFS (Table 5), a lower pathological TNM stage (stage 0-I *vs* II–III, HR = 0.342, 95%CI: 0.149-0.786, P = 0.012) and the NSTB score (score 0-1 *vs* 2, HR = 0.453, 95%CI: 0.234-0.877, P = 0.019) could also predict a better outcome while pre-NCRT CEA < 3.55 (HR = 0.521, 95%CI:

Table 2 Univariate analysis of factors affecting the overall survival

Characteristics	HR (95%CI)	*P* value
Pre-NCRT CEA (< 3.55/> 3.55)	0.407 (0.185-0.893)	0.025
Pre-NCRT CA19-9 (< 19.01/> 19.01)	0.437 (0.225-0.849)	0.014
Sex (male/female)	0.478 (0.218-1.049)	0.066
Pathological TNM stage (0-I/II-III)	0.321 (0.141-0.732)	0.007
Pathological vascular invasion (absent/present)	0.556 (0.170-1.821)	0.332
Pathological lymphatic invasion (absent/present)	0.400 (0.141-1.136)	0.085
Pathological perineural invasion (absent/present)	0.534 (0.250-1.141)	0.105
Pathological CRM (negative/positive)	0.826 (0.198-3.449)	0.793
NSTB score (0-1/2)	0.416 (0.217-0.800)	0.009

NCRT: Neoadjuvant chemoradiotherapy; CEA: Carcinoembryonic antigen; CA19-9: Cancer antigen 19-9; TNM: Tumor, node and metastasis; CRM: Circumferential resection margin; NSTB: Novel serum tumor biomarker score.

Table 3 Univariate analysis of factors affecting disease-free survival

Characteristic	HR (95%CI)	*P* value
Pre-NCRT CEA (< 3.55/> 3.55)	0.391 (0.178-0.859)	0.019
Pre-NCRT CA19-9 (< 19.01/> 19.01)	0.413 (0.213-0.802)	0.009
Sex (male/female)	0.466 (0.213-1.023)	0.057
Pathological TNM stage (0-I/II-III)	0.302 (0.132-0.690)	0.005
Pathological vascular invasion (absent/present)	0.571 (0.175-1.863)	0.353
Pathological lymphatic invasion (absent/present)	0.435 (0.154-1.231)	0.117
Pathological perineural invasion (absent/present)	0.595 (0.279-1.265)	0.177
Pathological CRM (negative/positive)	0.657 (0.158-2.738)	0.564
NSTB score (0-1/2)	0.391 (0.203-0.751)	0.005

NCRT: Neoadjuvant chemoradiotherapy; CEA: Carcinoembryonic antigen; CA19-9: Cancer antigen 19-9; TNM: Tumor, node and metastasis; CRM: Circumferential resection margin; NSTB: Novel serum tumor biomarker score.

0.226-1.162, P = 0.109) and CA19-9 < 19.01 (HR = 0.570, 95%CI: 0.284-1.141, P = 0.112) could not. The nomogram of OS (Figure 5) and DFS (Figure 6) shows the precise prognosis.

DISCUSSION

Our data showed that the combination of pre-NCRT tumor markers had better predictive value than a single marker. Although univariate analyses demonstrated that lower pre-NCRT CEA and CA19-9 levels were potential indicators of a better prognosis, the multivariate analysis proved that only the NSTB score and pathological TNM stage could independently determine the prognosis. In general, pathological indicators had a more robust predictive value than other indicators in determining the prognosis[8]; however, the multivariate analysis revealed that the NSTB score could predict outcomes better than pathological characteristics of lymphatic invasion, vascular invasion, nerve infiltration, and CRM invasion. Thus, we propose that the NSTB score should be used to guide the treatment and determine the prognosis of patients with RC of clinical stage II/III.

Pathological findings were generally recognized as the most effective indicators to predict the prognosis[8]. A previous study revealed that lymphatic invasion, perineural invasion, vascular invasion, CRM invasion, LN metastasis, and a higher tumor invasion stage can predict a worse outcome[4]. However, pathological characteristics were difficult to identify as they are usually affected by the quality of surgery and specimen-processing, and their analysis is significantly subjective and difficult to quantitate[15]. Moreover, pathological indicators could only be obtained after surgery, which means

Table 4 Multivariate analysis of factors affecting the overall survival

Characteristic	Multivariate analysis			
	Model 1		Model 2	
	HR (95%CI)	*P* value	HR (95%CI)	*P* value
Pre-NCRT CEA (< 3.55/> 3.55)	0.529 (0.232-1.205)	0.130		
Pre-NCRT CA19-9 (< 19.01/> 19.01)	0.604 (0.300-1.215)	0.158		
Pathological TNM stage (0-I/II-III)	0.373 (0.162-0.859)	0.020	0.363 (0.158-0.837)	0.017
NSTB score (0-1/2)			0.485 (0.251-0.940)	0.032

Model 1: Including pre-neoadjuvant chemoradiotherapy (NCRT) carcinoembryonic antigen (CEA) and cancer antigen 19-9 (CA19-9) into multivariate analysis, not including novel serum tumor biomarker (NSTB) score; Model 2: Including NSTB score into multivariate analysis, not including pre-NCRT CEA and CA19-9. NCRT: Neoadjuvant chemoradiotherapy; CEA: Carcinoembryonic antigen; CA19-9: Cancer antigen 19-9; NSTB: Novel serum tumor biomarker score; TNM: Tumor, node and metastasis.

Table 5 Multivariate analysis of factors affecting the disease-free survival

Characteristic	Multivariate analysis			
	Model 1		Model 2	
	HR (95%CI)	*P* value	HR (95%CI)	*P* value
Pre-NCRT CEA (< 3.55/> 3.55)	0.512 (0.226-1.162)	0.109		
Pre-NCRT CA19-9 (< 19.01/> 19.01)	0.570 (0.284-1.141)	0.112		
Pathological TNM stage (0-I/II-III)	0.350 (0.152-0.806)	0.014	0.342 (0.149-0.786)	0.012
NSTB score (0-1/2)			0.453 (0.234-0.877)	0.019

Model 1: Including pre-neoadjuvant chemoradiotherapy (NCRT) carcinoembryonic antigen (CEA) and cancer antigen 19-9 (CA19-9) into multivariate analysis, not including novel serum tumor biomarker (NSTB) score; Model 2: Including NSTB score into multivariate analysis, not including pre-NCRT CEA and CA19-9. NCRT: Neoadjuvant chemoradiotherapy; CEA: Carcinoembryonic antigen; CA19-9: Cancer antigen 19-9; NSTB: Novel serum tumor biomarker score; TNM: Tumor, node and metastasis.

that it was impossible to judge whether patients needed additional chemotherapy before undergoing NCRT or surgery. Moreover, the NSTB score could be obtained before NCRT and surgery.

Some molecules or proteins can determine a patient's prognosis. Lin *et al*[26] reported that the high expression of EphA4 served as an independent adverse predictor for DFS. Rödel *et al*[27] found that an increase in survivin levels was a significant risk factor for local recurrence and decreased DFS. Hiyoshi *et al*[28] demonstrated that serum miR-143 was a non-invasive and novel predictive marker for locally advanced rectal cancer (LARC) patients. Unfortunately, all of these molecular or protein markers had the following disadvantages: First, the detection cost of these markers was high, which increased the economic burden for patients; second, these novel markers could only be detected in large medical centers, which made them difficult to be used widely in clinical practice; finally, these new indicators lack uniform standards, and the test results may vary a lot in different medical centers. CEA and CA19-9 levels are widely used clinically because they are cheap, convenient to detect, and have uniform standards in different hospitals.

CEA is currently one of the primary markers for the diagnosis and follow-up of RC[2,18,19]. We found that lower CEA levels could predict a better prognosis in a univariate analysis. CA19-9 has shown great value for the differential diagnosis of malignant tumors and disease monitoring and evaluation [19]. Compared to either CA19-9 or CEA alone, an essential advantage of the combination was that it could reduce the interference of other factors and increase the predictive effectiveness. Although some studies also focused on the influence of CEA and CA19-9 levels on the prognosis, the two markers were studied separately[2,18-20,29]. Consequently, they failed to identify CEA and CA19-9 as predictive factors, which was similar to our findings. However, the predictive value increased significantly and was even stronger than that of several pathological factors when they were combined.

Our study had a few strengths: Firstly, to the best of our knowledge, this is the first study that combined CEA and CA19-9 to evaluate the prognosis of clinical stage II/III patients undergoing NCRT. Secondly, we adopted an ROC curve to determine the cut-off point of CEA and CA19-9 instead of just evaluating whether they were higher than the normal values, which optimized the efficiency of the OS prediction. Ultimately, the NSTB score was cheap and easily accessible before treatment.

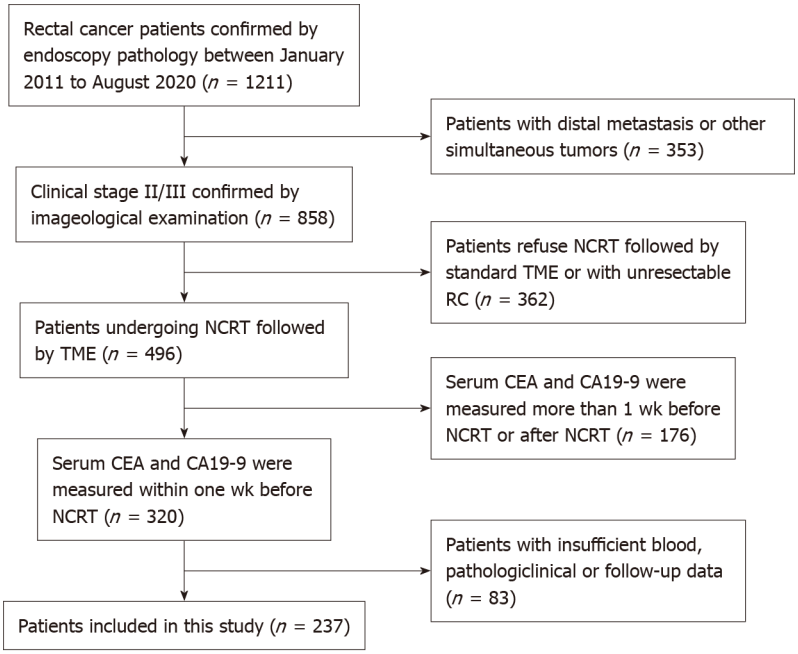

DOI: 10.4251/wjgo.v14.i10.2014

Figure 1 Patient-screening flowchart. NCRT: Neoadjuvant chemoradiotherapy; TME: Tumor microenvironment; RC: Rectal cancer; CEA: Carcinoembryonic antigen; CA19-9: Cancer antigen 19-9.

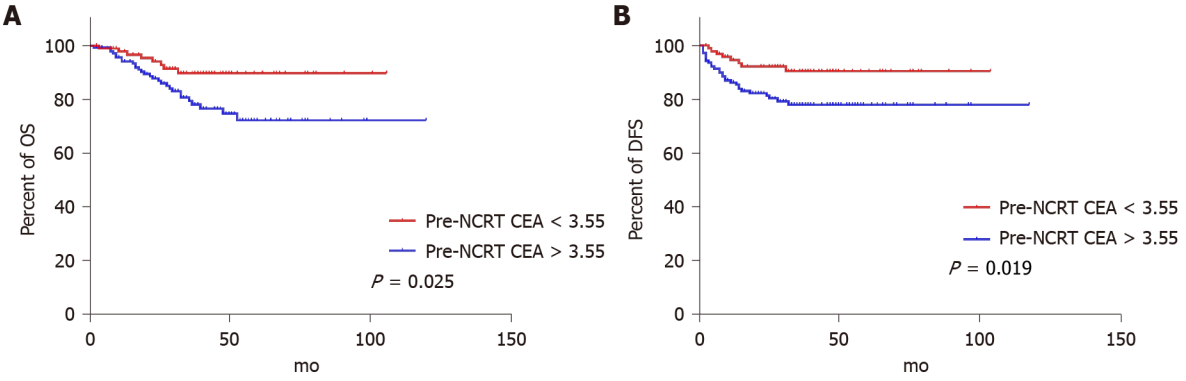

DOI: 10.4251/wjgo.v14.i10.2014

Figure 2 Overall survival curves and disease-free survival curves stratified by pre-neoadjuvant chemoradiotherapy carcinoembryonic antigen levels. A: Overall survival curves stratified by pre-neoadjuvant chemoradiotherapy carcinoembryonic antigen (CEA) levels; B: Disease-free survival curves stratified by pre-neoadjuvant chemoradiotherapy CEA levels. NCRT: Neoadjuvant chemoradiotherapy; CEA: Carcinoembryonic antigen; OS: Overall survival; DFS: Disease-free survival.

Our study also had some shortcomings. First, this was a retrospective study conducted in a single medical center. Second, the cut-off points of pre-NCRT CEA and CA19-9 levels in our center may not always be reproducible in other centers.

CONCLUSION

This study established a NSTB score by combining pre-NCRT CEA and CA19-9 levels. The NSTB score can independently predict the prognosis of patients with LARC of clinical stage II/III who underwent NCRT. Its predictive value was stronger than that of either marker alone, and even some pathologic characteristics.

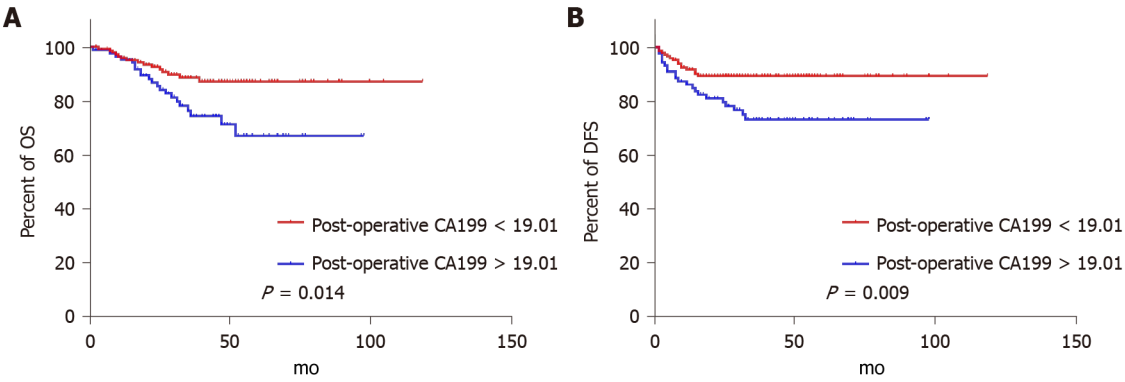

DOI: 10.4251/wjgo.v14.i10.2014 **Copyright** ©The Author(s) 2022.

Figure 3 Overall survival curves and disease-free survival curves stratified by pre-neoadjuvant chemoradiotherapy cancer antigen 19-9 levels. A: Overall survival curves stratified by pre-neoadjuvant chemoradiotherapy cancer antigen 19-9 (CA19-9) levels; B: Disease-free survival curves stratified by pre-neoadjuvant chemoradiotherapy CA19-9 levels. CA19-9: Cancer antigen 19-9; OS: Overall survival; DFS: Disease-free survival.

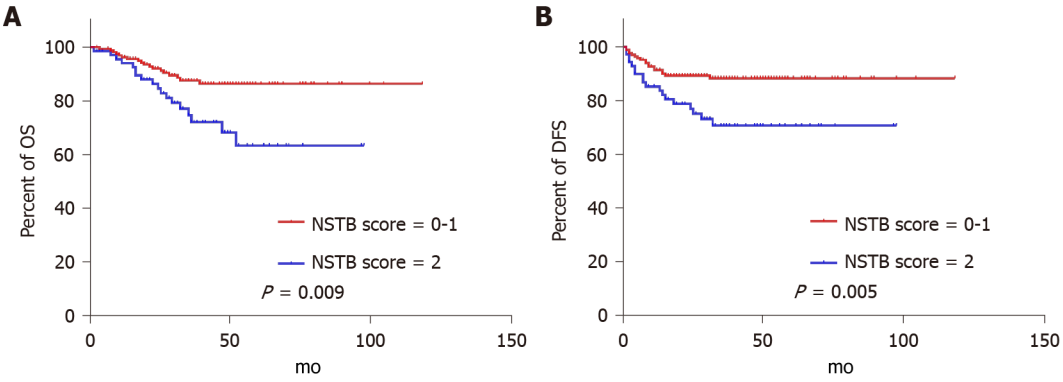

DOI: 10.4251/wjgo.v14.i10.2014 **Copyright** ©The Author(s) 2022.

Figure 4 Overall survival curves and disease-free survival curves stratified by novel serum tumor biomarker scores. A: Overall survival curves stratified by novel serum tumor biomarker scores; B: Disease-free survival curves stratified by novel serum tumor biomarker scores. NSTB: Novel serum tumor biomarker; OS: Overall survival; DFS: Disease-free survival.

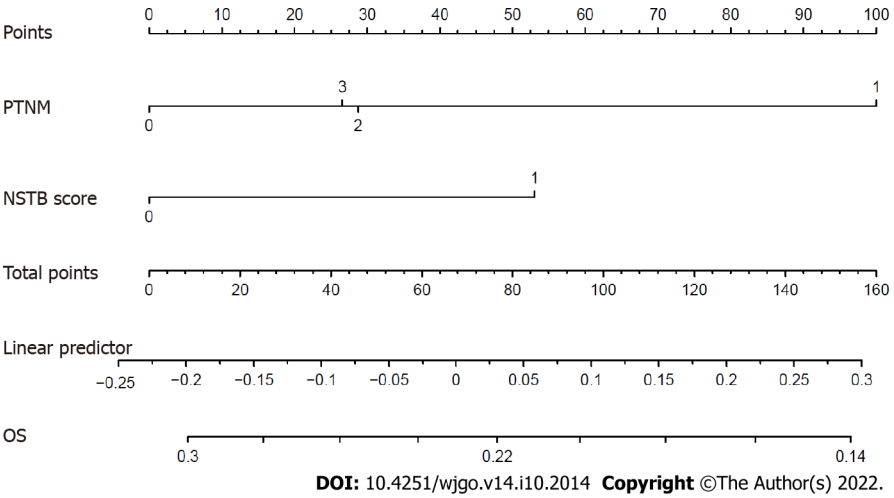

DOI: 10.4251/wjgo.v14.i10.2014 **Copyright** ©The Author(s) 2022.

Figure 5 Predictive nomogram predicting overall survival in clinical stage II/III RC patients undergoing NCRT. PTNM: Pathological tumor-node-metastasis; NSTB: Novel serum tumor biomarker; OS: Overall survival.

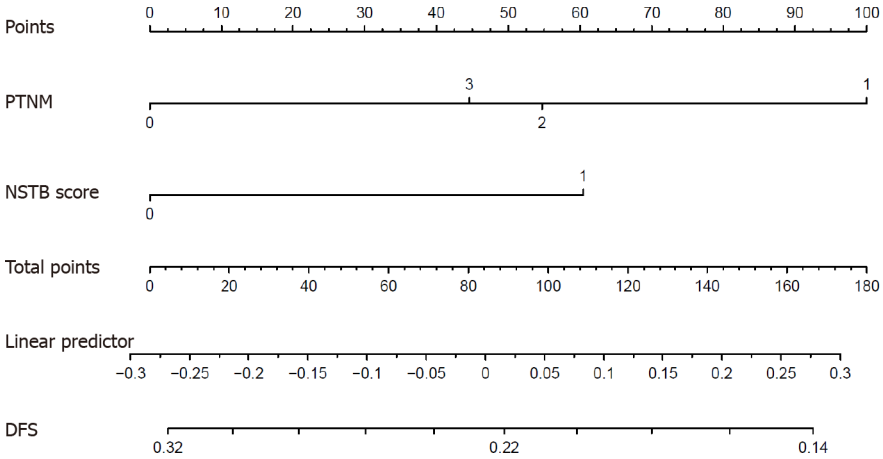

DOI: 10.4251/wjgo.v14.i10.2014

Figure 6 Predictive nomogram predicting disease-free survival in clinical stage II/III RC patients undergoing NCRT. PTNM: Pathological tumor-node-metastasis; NSTB: Novel serum tumor biomarker; DFS: Disease-free survival.

ARTICLE HIGHLIGHTS

Research background

Multiple classes of molecular biomarkers were studied as potential predictors for rectal cancer (RC) response but there was no sufficient evidence for any of them to be introduced into clinical practice.

Research motivation

To assess the predictive effect of pre-neoadjuvant chemoradiotherapy (NCRT) carcinoembryonic antigen (CEA) and cancer antigen 19-9 (CA19-9) levels on the prognosis of stage II/III RC patients.

Research objectives

The objective of this study is to establish a novel serum tumor biomarker score by combining pre-NCRT CEA and CA19-9 levels. The novel serum tumor biomarker (NSTB) score may predict the prognosis of patients with locally advanced rectal cancer (LARC) of clinical stage II/III who underwent NCRT independently.

Research methods

A total of 237 patients were included in this study. CEA and CA 19-9 levels were evaluated 1 wk before NCRT. The NSTB score was as follows: score 0: pre-NCRT CEA < 3.55 and CA19-9 < 19.01; score 2: pre-NCRT CEA > 3.55 and CA19-9 > 19.01; score 1: other situations. Pathological information was recorded according to histopathological reports after the operation.

Research results

In the univariate analysis, pre-NCRT CEA < 3.55, pre-NCRT CA19-9 < 19.01, and a lower NSTB score could predict a better prognosis. However, in the multivariate analysis, only a lower NSTB score and higher pathological tumor-node-metastasis (TNM) stage were independent predictive factors.

Research conclusions

We established a novel serum tumor biomarker score by combining pre-NCRT CEA and CA19-9 levels. The NSTB score can independently predict the prognosis of patients with LARC of clinical stage II/III who underwent NCRT.

Research perspectives

More accurate prediction models need to be established by studies with a larger number of patients.

FOOTNOTES

Author contributions: Zhao JY and Wang XY designed the research and wrote the manuscript; Tang QQ and Luo YT analyzed the data; Wang SM and Zhu XR performed data extraction; all authors have read and approved the final version.

Institutional review board statement: This study was reviewed and approved by the West China hospital, Sichuan University Institutional Review Board, Approval No. 2020.18.

Informed consent statement: The requirement for patients' informed consent was waived due to the retrospective nature of the study.

Conflict-of-interest statement: All author reports no conflict of interest.

Data sharing statement: Anyone who wants the data can connect to the corresponding author (yuxixi1052006@126.com).

Country/Territory of origin: China

ORCID number: Jie-Yi Zhao 0000-0001-8993-0121; Qing-Qing Tang 0000-0001-8993-0121; Yu-Ting Luo 0000-0002-2783-1643; Shu-Min Wang 0000-0001-8103-316X; Xiao-Rui Zhu 0000-0003-3611-0263; Xiao-Yu Wang 0000-0003-0936-2094.

S-Editor: Zhang H
L-Editor: Ma JY-MedE
P-Editor: Zhang H

REFERENCES

1 **Naffouje S**, Sabesan A, Powers BD, Dessureault S, Sanchez J, Schell M, Imanirad I, Sahin I, Xie H, Felder S. Patient Risk Subgroups Predict Benefit of Adjuvant Chemotherapy in Stage II Rectal Cancer Patients Following Neoadjuvant Chemoradiation and Total Mesorectal Excision. *Clin Colorectal Cancer* 2021; **20**: e155-e164 [PMID: 33775560 DOI: 10.1016/j.clcc.2021.02.006]

2 **Zhang S**, Zhang R, Li RZ, Wang QX, Chang H, Ding PR, Li LR, Wu XJ, Chen G, Zeng ZF, Xiao WW, Gao YH. Beneficiaries of radical surgery among clinical complete responders to neoadjuvant chemoradiotherapy in rectal cancer. *Cancer Sci* 2021; **112**: 3607-3615 [PMID: 34146368 DOI: 10.1111/cas.15039]

3 **Zhou S**, Jiang Y, Pei W, Zhou H, Liang J, Zhou Z. Neoadjuvant chemoradiotherapy followed by lateral pelvic lymph node dissection for rectal cancer patients: A retrospective study of its safety and indications. *J Surg Oncol* 2021; **124**: 354-360 [PMID: 33882149 DOI: 10.1002/jso.26509]

4 **Diefenhardt M**, Ludmir EB, Hofheinz RD, Ghadimi M, Minsky BD, Rödel C, Fokas E. Association of Treatment Adherence With Oncologic Outcomes for Patients With Rectal Cancer: A Post Hoc Analysis of the CAO/ARO/AIO-04 Phase 3 Randomized Clinical Trial. *JAMA Oncol* 2020; **6**: 1416-1421 [PMID: 32644104 DOI: 10.1001/jamaoncol.2020.2394]

5 **Kroon HM**, Malakorn S, Dudi-Venkata NN, Bedrikovetski S, Liu J, Kenyon-Smith T, Bednarski BK, Ogura A, van de Velde CJH, Rutten HJT, Beets GL, Thomas ML, Kusters M, Chang GJ, Sammour T. Local recurrences in western low rectal cancer patients treated with or without lateral lymph node dissection after neoadjuvant (chemo)radiotherapy: An international multi-centre comparative study. *Eur J Surg Oncol* 2021; **47**: 2441-2449 [PMID: 34120810 DOI: 10.1016/j.ejso.2021.06.004]

6 **Zhang YZ**, Song M, Geng JH, Zhu XG, Li S, Li YH, Cai Y, Wang WH. Patterns of failure and implications for clinical target volume definition of locally advanced T4b rectal cancer identified with magnetic resonance imaging and treated using neoadjuvant chemoradiotherapy and surgery. *Radiother Oncol* 2021; **161**: 132-139 [PMID: 34126137 DOI: 10.1016/j.radonc.2021.06.017]

7 **Smolskas E**, Mikulskytė G, Sileika E, Suziedelis K, Dulskas A. Tissue-Based Markers as a Tool to Assess Response to Neoadjuvant Radiotherapy in Rectal Cancer-Systematic Review. *Int J Mol Sci* 2022; **23** [PMID: 35682714 DOI: 10.3390/ijms23116040]

8 **Bauer PS**, Chapman WC Jr, Atallah C, Makhdoom BA, Damle A, Smith RK, Wise PE, Glasgow SC, Silviera ML, Hunt SR, Mutch MG. Perioperative Complications After Proctectomy for Rectal Cancer: Does Neoadjuvant Regimen Matter? *Ann Surg* 2022; **275**: e428-e432 [PMID: 32209914 DOI: 10.1097/SLA.0000000000003885]

9 **Petrelli F**, Trevisan F, Cabiddu M, Sgroi G, Bruschieri L, Rausa E, Ghidini M, Turati L. Total Neoadjuvant Therapy in Rectal Cancer: A Systematic Review and Meta-analysis of Treatment Outcomes. *Ann Surg* 2020; **271**: 440-448 [PMID: 31318794 DOI: 10.1097/SLA.0000000000003471]

10 **Xu T**, Zhang L, Yu L, Zhu Y, Fang H, Chen B, Zhang H. Log odds of positive lymph nodes is an excellent prognostic factor for patients with rectal cancer after neoadjuvant chemoradiotherapy. *Ann Transl Med* 2021; **9**: 637 [PMID: 33987335 DOI: 10.21037/atm-20-7590]

11 **Zhao Q**, Wan L, Zou S, Zhang C, E T, Yang Y, Ye F, Zhao X, Ouyang H, Zhang H. Prognostic risk factors and survival models for T3 locally advanced rectal cancer: what can we learn from the baseline MRI? *Eur Radiol* 2021; **31**: 4739-4750 [PMID: 34003351 DOI: 10.1007/s00330-021-08045-y]

12 **Cheong C**, Shin JS, Suh KW. Prognostic value of changes in serum carcinoembryonic antigen levels for preoperative chemoradiotherapy response in locally advanced rectal cancer. *World J Gastroenterol* 2020; **26**: 7022-7035 [PMID: 33311947 DOI: 10.3748/wjg.v26.i44.7022]

13 **You YN**, Hardiman KM, Bafford A, Poylin V, Francone TD, Davis K, Paquette IM, Steele SR, Feingold DL; On Behalf of the Clinical Practice Guidelines Committee of the American Society of Colon and Rectal Surgeons. The American Society of Colon and Rectal Surgeons Clinical Practice Guidelines for the Management of Rectal Cancer. *Dis Colon Rectum* 2020; **63**: 1191-1222 [PMID: 33216491 DOI: 10.1097/DCR.0000000000001762]

14 **Zheng Z**, Wang X, Huang Y, Lu X, Huang Z, Chi P. Defining and predicting early recurrence in patients with locally advanced rectal cancer treated with neoadjuvant chemoradiotherapy. *Eur J Surg Oncol* 2020; **46**: 2057-2063 [PMID: 32782202 DOI: 10.1016/j.ejso.2020.07.019]

15 **You W**, Yan L, Cai Z, Xie L, Sheng N, Wang G, Wu X, Wang Z. Clinical Significances of Positive Postoperative Serum CEA and Post-preoperative CEA Increment in Stage II and III Colorectal Cancer: A Multicenter Retrospective Study. *Front Oncol* 2020; **10**: 671 [PMID: 32509572 DOI: 10.3389/fonc.2020.00671]

16 **Doos WG**, Wolff WI, Shinya H, DeChabon A, Stenger RJ, Gottlieb LS, Zamcheck N. CEA levels in patients with colorectal polyps. *Cancer* 1975; **36**: 1996-2003 [PMID: 1203857 DOI: 10.1002/cncr.2820360911]

17 **Moore TL**, Kantrowitz PA, Zamcheck N. Carcinoembryonic antigen (CEA) in inflammatory bowel disease. *JAMA* 1972; **222**: 944-947 [PMID: 4678960 DOI: 10.1001/jama.1972.03210080028007]

18 **Rule AH**, Goleski-Reilly C, Sachar DB, Vandevoorde J, Janowitz HD. Circulating carcinoembryonic antigen (CEA): relationship to clinical status of patients with inflammatory bowel disease. *Gut* 1973; **14**: 880-884 [PMID: 4761608 DOI: 10.1136/gut.14.11.880]

19 **Huang D**, Lin Q, Song J, Xu B. Prognostic Value of Pretreatment Serum CA199 in Patients with Locally Advanced Rectal Cancer Treated with CRT Followed by TME with Normal Pretreatment Carcinoembryonic Antigen Levels. *Dig Surg* 2021; **38**: 24-29 [PMID: 33171467 DOI: 10.1159/000508442]

20 **Mizuno H**, Miyake H, Nagai H, Yoshioka Y, Shibata K, Asai S, Takamizawa J, Yuasa N. Optimal cutoff value of preoperative CEA and CA19-9 for prognostic significance in patients with stage II/III colon cancer. *Langenbecks Arch Surg* 2021; **406**: 1987-1997 [PMID: 34148158 DOI: 10.1007/s00423-021-02236-3]

21 **Dossa F**, Acuna SA, Rickles AS, Berho M, Wexner SD, Quereshy FA, Baxter NN, Chadi SA. Association Between Adjuvant Chemotherapy and Overall Survival in Patients With Rectal Cancer and Pathological Complete Response After Neoadjuvant Chemotherapy and Resection. *JAMA Oncol* 2018; **4**: 930-937 [PMID: 29710274 DOI: 10.1001/jamaoncol.2017.5597]

22 **Zhang XY**, Wang S, Li XT, Wang YP, Shi YJ, Wang L, Wu AW, Sun YS. MRI of Extramural Venous Invasion in Locally Advanced Rectal Cancer: Relationship to Tumor Recurrence and Overall Survival. *Radiology* 2018; **289**: 677-685 [PMID: 30152742 DOI: 10.1148/radiol.2018172889]

23 **Goh TS**, Lee JS, Il Kim J, Park YG, Pak K, Jeong DC, Oh SO, Kim YH. Prognostic scoring system for osteosarcoma using network-regularized high-dimensional Cox-regression analysis and potential therapeutic targets. *J Cell Physiol* 2019; **234**: 13851-13857 [PMID: 30604867 DOI: 10.1002/jcp.28065]

24 **Li Z**, Wang Q, Qiao Y, Wang X, Jin X, Wang A. Incidence and associated predictors of adverse pregnancy outcomes of maternal syphilis in China, 2016-19: a Cox regression analysis. *BJOG* 2021; **128**: 994-1002 [PMID: 33021043 DOI: 10.1111/1471-0528.16554]

25 **Hsu CH**, Yu M. Cox regression analysis with missing covariates *via* nonparametric multiple imputation. *Stat Methods Med Res* 2019; **28**: 1676-1688 [PMID: 29717943 DOI: 10.1177/0962280218772592]

26 **Lin CY**, Lee YE, Tian YF, Sun DP, Sheu MJ, Lin CY, Li CF, Lee SW, Lin LC, Chang IW, Wang CT, He HL. High Expression of EphA4 Predicted Lesser Degree of Tumor Regression after Neoadjuvant Chemoradiotherapy in Rectal Cancer. *J Cancer* 2017; **8**: 1089-1096 [PMID: 28529623 DOI: 10.7150/jca.17471]

27 **Rödel F**, Hoffmann J, Distel L, Herrmann M, Noisternig T, Papadopoulos T, Sauer R, Rödel C. Survivin as a radioresistance factor, and prognostic and therapeutic target for radiotherapy in rectal cancer. *Cancer Res* 2005; **65**: 4881-4887 [PMID: 15930309 DOI: 10.1158/0008-5472.CAN-04-3028]

28 **Hiyoshi Y**, Akiyoshi T, Inoue R, Murofushi K, Yamamoto N, Fukunaga Y, Ueno M, Baba H, Mori S, Yamaguchi T. Serum miR-143 levels predict the pathological response to neoadjuvant chemoradiotherapy in patients with locally advanced rectal cancer. *Oncotarget* 2017; **8**: 79201-79211 [PMID: 29108299 DOI: 10.18632/oncotarget.16760]

29 **Chen Y**, Gao SG, Chen JM, Wang GP, Wang ZF, Zhou B, Jin CH, Yang YT, Feng XS. Serum CA242, CA199, CA125, CEA, and TSGF are Biomarkers for the Efficacy and Prognosis of Cryoablation in Pancreatic Cancer Patients. *Cell Biochem Biophys* 2015; **71**: 1287-1291 [PMID: 25486903 DOI: 10.1007/s12013-014-0345-2]

World Journal of Gastrointestinal Oncology

Submit a Manuscript: https://www.f6publishing.com

World J Gastrointest Oncol 2022 October 15; 14(10): 2025-2037

DOI: 10.4251/wjgo.v14.i10.2025

ISSN 1948-5204 (online)

ORIGINAL ARTICLE

Observational Study

Role of sex on psychological distress, quality of life, and coping of patients with advanced colorectal and non-colorectal cancer

Vilma Pacheco-Barcia, David Gomez, Berta Obispo, Luka Mihic Gongora, Raquel Hernandez San Gil, Patricia Cruz-Castellanos, Mireia Gil-Raga, Vicente Villalba, Ismael Ghanem, Paula Jimenez-Fonseca, Caterina Calderon

Specialty type: Oncology

Provenance and peer review: Unsolicited article; Externally peer reviewed.

Peer-review model: Single blind

Peer-review report's scientific quality classification

Grade A (Excellent): A, A
Grade B (Very good): B
Grade C (Good): C
Grade D (Fair): 0
Grade E (Poor): 0

P-Reviewer: Gao W, China; Rwegerera GM, Botswana; Scurtu RR, Romania; Yu T, China

Received: April 25, 2022
Peer-review started: April 25, 2022
First decision: May 11, 2022
Revised: May 24, 2022
Accepted: August 25, 2022
Article in press: August 25, 2022
Published online: October 15, 2022

Vilma Pacheco-Barcia, Department of Medical Oncology, School of Medicine, Alcala University (UAH), Hospital Central de la Defensa Gómez Ulla, Madrid 28047, Spain

David Gomez, Department of Medical Oncology, Hospital Universitario de Navarra, Pamplona 31008, Spain

Berta Obispo, Department of Medical Oncology, Hospital Universitario Infanta Leonor, Madrid 28031, Spain

Luka Mihic Gongora, Department of Medical Oncology, Hospital Universitario Central de Asturias, Oviedo 33011, Spain

Raquel Hernandez San Gil, Department of Medical Oncology, Hospital Universitario de Canarias, Tenerife 38320, Spain

Patricia Cruz-Castellanos, Ismael Ghanem, Department of Medical Oncology, Hospital Universitario La Paz, Madrid 28046, Spain

Mireia Gil-Raga, Department of Medical Oncology, Hospital General Universitario de Valencia, CIBERONC, Valencia 46014, Spain

Vicente Villalba, Department of Clinical Psychology and Psychobiology, Faculty of Psychology, University of Barcelona, Barcelona 08007, Spain

Paula Jimenez-Fonseca, Department of Medical Oncology, Hospital Universitario Central de Asturias, ISPA, Oviedo 33007, Spain

Caterina Calderon, Department of Clinical Psychology and Psychobiology, University of Barcelona, Barcelona 08007, Spain

Corresponding author: Vilma Pacheco-Barcia, MD, MSc, PhD, Associate Professor, Doctor, Department of Medical Oncology, School of Medicine, Alcala University (UAH), Hospital Central de la Defensa Gómez Ulla, Glorieta del Ejercito 1, Madrid 28047, Spain.
vilmapbarcia@yahoo.es

Abstract

BACKGROUND

Patients with advanced gastrointestinal cancer must cope with the negative effects of cancer and complications.

AIM

To evaluate psychological distress, quality of life, and coping strategies in patients with advanced colorectal cancer compared to non-colorectal cancer based on sex.

METHODS

A prospective, transversal, multicenter study was conducted in 203 patients; 101 (50%) had a colorectal and 102 (50%) had digestive, non-colorectal advanced cancer. Participants completed questionnaires evaluating psychological distress (Brief Symptom Inventory-18), quality of life (EORTC QLQ-C30), and coping strategies (Mini-Mental Adjustment to Cancer) before starting systemic cancer treatment.

RESULTS

The study included 42.4% women. Women exhibited more depressive symptoms, anxiety, functional limitations, and anxious preoccupation than men. Patients with non-colorectal digestive cancer and women showed more somatization and physical symptoms than subjects with colorectal cancer and men. Men with colorectal cancer reported the best health status.

CONCLUSION

The degree of disease acceptance in gastrointestinal malignancies may depend on sex and location of the primary digestive neoplasm. Future interventions should specifically address sex and tumor site differences in individuals with advanced digestive cancer.

Key Words: Anxiety; Colorectal cancer; Depression; Gastrointestinal cancer; Sex

Core Tip: Patients with advanced gastrointestinal cancer must cope with the negative effects of cancer and complications. However, data on psychological distress, quality of life, and coping strategies in patients with advanced colorectal cancer compared to non-colorectal cancer based on sex is lacking. This was a multicenter study conducted in 203 patients that completed questionnaires evaluating psychological distress, quality of life, and coping strategies before starting systemic cancer treatment. Based on these data, the degree of disease acceptance in gastrointestinal malignancies may depend on sex and location of the primary digestive neoplasm.

Citation: Pacheco-Barcia V, Gomez D, Obispo B, Mihic Gongora L, Hernandez San Gil R, Cruz-Castellanos P, Gil-Raga M, Villalba V, Ghanem I, Jimenez-Fonseca P, Calderon C. Role of sex on psychological distress, quality of life, and coping of patients with advanced colorectal and non-colorectal cancer. *World J Gastrointest Oncol* 2022; 14(10): 2025-2037

URL: https://www.wjgnet.com/1948-5204/full/v14/i10/2025.htm

DOI: https://dx.doi.org/10.4251/wjgo.v14.i10.2025

INTRODUCTION

Background

Gastrointestinal cancers are among the most prevalent both worldwide and in Spain[1,2]. Colorectal cancer is the most frequent neoplasm in Spain in both sexes[2] with close to 65% survival at 5 years, although this rate declines in metastatic stages and in unresectable cancers[3]. The most common non-colorectal digestive cancers are pancreatic, gastric, and hepatocellular carcinoma, which are associated with a worse prognosis than colorectal cancer with a 5-year survival rate of < 5 years in the advanced scenery.

Individuals with advanced gastrointestinal cancer must face the negative effects (pain, malnutrition) and tumor-related complications (intestinal obstruction or hemorrhage). Advances made in recent years in anticancer treatment modalities to fight these cancers have managed to extend overall survival (OS) and control physical symptoms. Meanwhile, emotional distress in these cases has been correlated with diminished quality of life and with a negative impact on treatment compliance[4,5] and on oncological outcomes[6,7]. Furthermore, psychological suffering can aggravate vomiting and other side effects of systemic antineoplastic treatment and of the cancer itself[8-10]. For its part, the type of cancer and

surgery can affect the emotional distress and quality of life in individuals with a gastrointestinal neoplasm. In a Spanish prospective series, people with pancreatic-biliary cancer expressed more somatic complaints, depression, and anguish than those with colorectal cancer, whereas participants with gastroesophageal neoplasms suffered higher rates of depression, psychological distress, and hopelessness than those with colorectal cancer[11].

The relevance of contemplating sex and its influence on study outcomes is stated in the SAGER guidelines (Sex and Gender Equity in Research) designed to inform authors in preparing their manuscripts[12,13]. Sex, understood as going beyond its biological concept (chromosomal assignment) and founded on the basis of the roles and relationships established throughout the person's lifetime, is a sociodemographic variable that can give rise to differences in the evolution as well as the clinical and psychological aspects of cancer[14]. This is particularly relevant in cancers such as digestive neoplasms that have a higher incidence in men and in which there may be an underrepresentation of women who may experience a different evolution and coping style that call for specific approaches[15,16].

In the case of advanced gastroesophageal tumors, women have been seen to be less likely to receive systemic treatment with chemotherapy when the histology is adenocarcinoma with no difference among patients with squamous cell tumors. This impacts survival, in as much as men display increased OS in esophageal adenocarcinomas with no differences in survival rates by sex in cases of esophageal squamous cell carcinoma in some studies, while others attribute a higher incidence of cancers having an unfavorable and more aggressive histology among women[17-20]. As for pancreatic cancer, differences in the efficacy and toxicity of chemotherapy have been observed between men and women[21,22]. Women receiving FOLFIRINOX are older at the time of diagnosis and exhibit higher OS rates than men, despite requiring an earlier dose decrease due to early toxicity, which is possibly attributable to worse tolerance to systemic treatment. No study has investigated whether this poor tolerance is influenced by psychological factors[23].

Other clinical trials have revealed a trend toward higher progression-free survival and OS in women, although these findings were not statistically significant[23,24]. In individuals with localized colorectal cancer, a large-scale German study examined sex and found that the women were older than the men, had a more advanced stage at the time of diagnosis, and received a lower dose intensity of chemotherapy, despite having greater disease-free survival and OS[25]. The more advanced stage of disease among women might be due to the greater acceptance of endoscopic screening by men, among other reasons[26-28]. Therefore, women with digestive cancers are usually diagnosed at older ages than men and regardless of a lower rate of chemotherapy administration and greater toxicity in general, they display better survival rates without any study having been conducted to probe the cause behind such differences and whether psychological factors may play a role.

Three key psychological factors in cancer patients are psychological distress[6], quality of life[29-31], and coping[32,33]. Earlier studies have reported that up to 54% of people with colorectal cancer suffer anxiety and 27% suffer from depression[34-36] with higher incidences among women[37]. One study performed in subjects with gastrointestinal cancer in Spain reported that men with colorectal cancer have a worse quality of life, associated with physical performance and emotional and cognitive functioning[38]. Oppegaard *et al*[39] carried out a descriptive study focusing on sex differences in coping strategies and noted that women scored higher on positive reframing, religion, and instrumental support, while men scored higher for mood. Nevertheless, the question has never been studied as to whether these differences are due to the person's biological sex or if there are sex characteristics (acquired) or other biopsychosocial variables that modulate coping, emotional stress, and quality of life.

Objectives

The aim of our study was to analyze whether there were differences between colorectal and non-colorectal digestive cancer in sociodemographic and/or clinical conditions and compared mental health status, quality of life, and coping between colorectal and non-colorectal digestive cancer patients depending on sex. We believe that these results may be useful to design specific preventive programs for each group.

MATERIALS AND METHODS

Study design

NEOetic is a multi-institutional (22 Spanish hospitals), prospective, observational study and is part of a cancer patient research program funded by the Spanish Society of Medical Oncology. The study was approved by the Ethics Committee of each institution and by the Spanish Agency of Medicines and Medical Devices (identification code: ES14042015).

Participants

The study was a cohort study, and participants were 18 years of age or older with unresectable, locally advanced, or metastatic cancer and were candidates for systemic antineoplastic treatment. For the purposes of this analysis, subjects with digestive cancers were regarded and grouped as being colorectal

(colon and rectum) and non-colorectal digestive (esophagus, stomach, pancreas, biliary tract, liver, anal canal).

Setting

Patients were invited to participate in the study at the first visit with the oncologist where they were informed of the treatment alternatives for their cancer. Participation was voluntary, anonymous, and did not affect patient care. All patients included in the study signed an informed consent for their inclusion. The study was undertaken according to the Strengthening the Reporting of Observational studies in Epidemiology (STROBE) guidelines[40].

We screened 245 patients; 203 were eligible for this analysis and 42 were excluded (10 failed to meet the inclusion criteria, 13 met the exclusion criteria, and 19 had incomplete data at the time of analysis).

Variables and measures

Demographic and clinical data (age, sex, marital status, educational level, employment status, tumor location and stage, and treatment) were obtained and updated by the medical oncologist directly from the patients and from their records. The oncologist explained the questionnaires to the participant who completed them at home during the 1st month following diagnosis of advanced disease and prior to starting cancer treatment. The questionnaires used are validated and are described below.

Data sources/measurement

The Brief Symptom Inventory consists of 18 items divided into three dimensions (somatization, depression, and anxiety) as well as a total score, the Global Severity Index, which summarizes the respondent's overall emotional adjustment or psychological distress over the last 7 d[41]. Each item is rated on a 5-point Likert scale and Cronbach's alpha ranged between 0.81 and 0.90[42].

The European Organization for Research and Treatment of Cancer Quality of Life Questionnaire (EORTC QLQ-C30) contains 30 items comprising four subscales: functioning, symptoms, health status, and global quality of life[43]. The response choices range from 1 (not at all) to 4 (very much), except for the health status scale, where responses range from 1 (very poor) to 7 (excellent). All scale scores are linearly transformed into a 0-100 scale. Higher scores on the functioning scales and global quality of life scale represent a higher level of functioning or quality of life. For the symptom scales, the higher the score, the greater the symptom burden. In this sample $\alpha = 0.85$[44].

The Mini-Mental Adjustment to Cancer is a 29-item scale that assesses cancer-specific coping strategies as being adaptive (cognitive avoidance, fighting spirit, and fatalism) or maladaptive (helplessness and anxious preoccupation)[45]. When studying the psychometric properties of the Spanish translation of the scale, a 4-factor structure is found and used in this study; it includes helplessness, anxious preoccupation, and cognitive avoidance as well as a new subscale, positive attitude, that combines fighting spirit and fatalism[46]. Each item is rated on a 4-point Likert scale and Cronbach's alpha coefficients for each domain ranged from 0.62-0.88[46].

Statistical analysis

Descriptive statistics were used for demographic data and survey responses. Absolute frequencies were used for categorical data and mean and standard deviation for quantitative data. Additional descriptive analyses were performed, grouping patients by cancer type. We conducted bivariate χ^2 and *t* tests to examine differences between colorectal cancer and non-colorectal digestive cancer patients in terms of sociodemographic, clinical, and psychological characteristics.

A general linear model was created for each dependent variable (psychological distress, quality of life, and coping) with the different cancer type (colorectal and non-colorectal digestive); the effect of sex was probed, in addition to the interaction effect between sex and cancer type. All post-hoc tests were subjected to Bonferroni correction. All analyses were complemented with the corresponding effect size statistic. Reference values were established as 0.01, 0.06, and > 0.14 for small, medium, and large sizes, respectively, for the partial eta-square (η^2_p). Statistics were generated using a standard statistical software package IBM SPSS Statistics for Windows, version 23.0 (IBM Corp., Armonk, NY, United States).

RESULTS

Participants

The study admitted 203 patients recruited during 2021. There were 101 (50%) colorectal cancer sufferers, and 102 (50%) had a non-colorectal digestive malignance.

Descriptive data

The sociodemographic and clinical characteristics of both groups are displayed in Table 1. Of the total study population, 115 (56.7%) were men and 88 (43.3%) were women. The percentage of men *vs* women

Table 1 Patients' baseline characteristics, *n* = 203

Characteristic	Total		Colorectal, *n* = 101		Non-colorectal digestive cancer, *n* = 102		*P* value	λ
	n	%	*n*	%	*n*	%		
Sex							0.622	0.026
Men	115	56.7	60	59.4	55	53.9		
Women	88	43.3	41	40.6	47	46.1		
Age							0.028	0.081
≤ 65 yr	85	41.9	50	49.5	35	34.3		
> 65 yr	118	59.1	51	50.5	67	65.7		
Number of Elixhauser comorbidities (%)							0.344	0.033
≤ 4	81	39.9	37	36.6	44	43.1		
> 4	122	60.1	64	63.4	58	56.9		
ECOG							0.029	0.086
0	56	27.6	35	34.7	21	20.6		
1	138	68.0	62	61.4	76	74.5		
2	9	4.4	4	4.0	5	4.9		
Marital status							0.883	0.001
Married/partnered	167	86.6	87	86.2	92	87.0		
Not partnered	36	13.4	24	13.8	24	13.0		
Children							0.370	0.029
Do not have children	35	17.2	15	14.9	20	19.6		
Have children	168	82.8	86	85.1	82	81.4		
Educational level							0.521	0.010
Primary	112	55.2	58	57.4	54	52.9		
High school or higher	91	44.8	43	42.6	48	47.1		
Histology							0.001	0.129
Adenocarcinoma	180	88.7	98	97.0	82	80.4		
Others	23	11.3	3	3.0	20	19.6		
Metastasis							0.001	0.218
Locally advanced	32	15.8	1	1.0	31	30.4		
Metastatic disease	171	84.2	100	99.0	71	69.6		
Biomarker							0.001	0.196
No	161	79.3	66	65.3	95	93.1		
Yes	42	20.7	35	34.7	7	6.9		
Estimated survival							0.001	0.776
< 18 mo	108	53.2	14	13.9	94	92.2		
≥ 18 mo	95	4.8	87	86.1	8	7.8		
Treatment modality							0.001	0.339
Chemotherapy	139	68.5	45	44.6	94	92.2		
Combined	64	31.5	56	54.4	8	7.8		

ECOG: Eastern Cooperative Oncology Group.

in those with colorectal and non-colorectal digestive tract malignances was 60 (59.4%) to 41 (40.6%) and 55 (53.9%) to 47 (46.1%), respectively. The median age was 65.7 years (range: 34-88, standard deviation = 9.6).

Outcome data

Colorectal cancer patients tended to be younger than those with non-colorectal, gastrointestinal cancer ($P = 0.028$, $\lambda = 0.081$). Additionally, colorectal cancer patients had a better Eastern Cooperative Oncology Group performance status than non-colorectal digestive cancer patients, 34.7% *vs* 20.6%, respectively ($P = 0.029$, $\lambda = 0.086$). Most participants were married or partnered (86.6%) with children (82.2%) and had a primary level of education (55.2%). All subjects were either retired or unemployed.

Of the patients with non-colorectal digestive cancer, the most common primary tumor site was the pancreas (54.9%, $n = 56$), followed by the stomach (22.5%, $n = 23$), esophagus (8.8%, $n = 9$), biliary tract (6.9%, $n = 7$), liver (4.9%, $n = 5$), and anus (2%, $n = 2$). Individuals with colorectal cancer were diagnosed with metastatic disease more often than unresectable, locally advanced cancer ($P = 0.001$, $\lambda = 0.218$); biomarkers to guide treatment options were more often available in these subjects ($P = 0.001$, $\lambda = 0.196$), and most received combined, systemic treatment with chemotherapy and a targeted drug ($P = 0.001$, $\lambda = 0.339$). The estimated 18-mo survival rate was 86.1% in colorectal cancer patients compared to 7.8% in patients with non-colorectal digestive cancer ($P = 0.001$, $\lambda = 0.776$).

Psychological distress

The general linear model results indicated significant differences in the levels of somatization ($F_{(1,202)} = 5.0244$, $P = 0.026$, $\eta^2_p = 0.025$), depression ($F_{(1,202)} = 15.747$, $P = 0.001$, $\eta^2_p = 0.073$), and anxiety ($F_{(1,202)} = 19.697$, $P = 0.001$, $\eta^2_p = 0.090$). The post hoc test showed significant differences in mean scores by sex, *i.e.* women manifested more depressive symptoms ($\eta^2_p = 0.073$) and anxiety ($\eta^2_p = 0.061$) than men. Patients with non-colorectal digestive cancer ($\eta^2_p = 0.020$) and women ($\eta^2_p = 0.025$) displayed more somatization than subjects with colorectal cancer and men. The model parameters and significant categories of each predicted variable are presented in Table 2 and Figure 1.

Quality of life

Again, the general linear model results revealed significant differences on the functional ($F_{(1,202)} = 19.697$, $P = 0.001$, $\eta^2_p = 0.090$) and symptom ($F_{(1,202)} = 8.154$, $P = 0.005$, $\eta^2_p = 0.039$) scales. The post hoc test indicated that women presented more functional limitations than men ($\eta^2_p = 0.090$). Participants with non-colorectal, gastrointestinal cancer ($\eta^2_p = 0.030$) and women ($\eta^2_p = 0.039$) had more symptoms than those with colorectal cancer and who were men. The results revealed a significant effect of sex on symptom control. A statistically significant association between tumor type and sex in health status levels was observed, and men with colorectal cancer reported the best health status ($\eta^2_p = 0.025$) (Table 2 and Figure 1).

Coping strategies

In coping strategies, positive attitude and cognitive avoidance were the most widely used strategies by all patients included, and hopelessness was the least used (Table 2 and Figure 2). Differences were observed in the estimated mean scores for anxious preoccupation ($F_{(1,202)} = 6.722$, $P = 0.010$, $\eta^2_p = 0.033$) and positive attitude ($F_{(1,202)} = 4.389$, $P = 0.037$, $\eta^2_p = 0.022$). Post hoc tests showed that women presented more anxious preoccupation ($\eta^2_p = 0.033$) and less positive attitude ($\eta^2_p = 0.022$) than men.

DISCUSSION

Key results

In this study we analyzed the differences in emotional distress, quality of life, and coping by digestive tumor type and sex. Women displayed more depressive symptoms, anxiety, functional limitations, and anxious preoccupation than men. Individuals with non-colorectal digestive cancer and women exhibited more physical symptoms and somatization than patients with colorectal cancer and men, whereas men with colorectal cancer reported better health status. By type of cancer, participants with colorectal cancer are younger, treatment is more often adjusted by biomarkers, they receive more combined chemotherapy and a biological agent, their estimated survival is higher, and they have better general status at the time of diagnosis than subjects with non-colorectal digestive cancer.

Interpretation

As for coping strategy, women exhibited more anxious preoccupation and men exhibited positive attitude. These results might explain why women present more symptoms and worse functional status than men. Oppegaard *et al*[39] observed that women scored higher on denial, which has previously been associated with worse oncological outcomes, given the delay in seeking care, which in turn entails a diagnosis made at more advanced stages, with worse general status, and lower survival rates[47].

Table 2 Univariate general linear model for predicting psychological distress, quality of life, and coping strategies by tumor and sex

Scales	Colorectal cancer, *n* = 101		Non-colorectal digestive cancer, *n* = 102		ANOVA results, *F*		
	Men, mean (SD)	Women, mean (SD)	Men, mean (SD)	Women, mean (SD)	Tumor × sex	Tumor	Sex
Psych. distress (BSI)[1]							
Somatization	62.0 (6.3)	64.1 (8.0)	63.9 (6.7)	66.3 (8.1)	0.021	3.963	5.044
Depression	60.3 (6.6)	65.0 (6.6)	60.1 (5.5)	62.9 (7.5)	0.923	1.423	15.747
Anxiety	61.9 (7.8)	65.8 (8.3)	61.9 (6.8)	66.0 (8.3)	0.030	0.011	12.818
Quality of life (EORTC-QLQ-C30)[2]							
Functional scale	79.6 (17.4)	62.3 (23.0)	70.8 (22.6)	60.8 (24.0)	1.427	2.781	19.697
Symptom scale	24.4 (22.9)	29.8 (19.4)	28.6 (17.8)	40.0 (22.1)	1.044	6.067	8.154
Health status scale	67.6 (22.6)	53.7 (27.9)	51.9 (23.5)	55.1 (32.8)	5.185	3.547	2.059
Coping with cancer (M-MAC)[2]							
Helplessness	24.0 (22.9)	25.0 (21.9)	25.9 (22.8)	28.6 (25.6)	0.069	0.696	0.288
Anxious preoccupation	46.2 (24.4)	51.4 (18.8)	43.8 (19.0)	54.4 (23.6)	0.800	0.008	6.722
Positive attitude	83.4 (16.5)	76.8 (18.1)	79.2 (15.8)	74.9 (22.9)	0.186	1.364	4.389
Cognitive avoidance	66.6 (27.3)	60.6 (21.6)	64.3 (24.5)	60.2 (27.1)	0.036	0.192	1.758

[1]T score.

[2]Scale from 0 to 100.

ANOVA: Analysis of variance; BSI: Brief Symptom Inventory; EORTC-QLQ-C30: European Organization for Research and Treatment of Cancer Quality of Life Questionnaire; M-MAC: Mini-Mental Adjustment to Cancer; SD: Standard deviation.

Furthermore, Oppegaard *et al*[39] demonstrated that women scored higher on self-distraction as a detachment coping strategy, which had already been associated with a decreased sense of meaning of life in both women and men with cancer[48].

In our study, women suffered more psychological distress in the form of anxiety and depression compared to men, and women with non-colorectal digestive cancer displayed more somatization than men and than women with colorectal cancer. Most studies have encountered similar results. Aminisani *et al*[49] evaluated psychological distress in a cohort of 303 colorectal cancer survivors from Iran. One-third of the study population presented depression and more than half of them exhibited anxiety; both conditions were more common among women than men. Sex differences in psychological distress have been reported by Gonzalez-Saenz de Tejada *et al*[50], revealing that men had less depression and anxiety. In The Netherlands, Braamse *et al*[51] found that women had higher levels of depression but not anxiety. Mols *et al*[30] observed that men suffered less anxiety and depression over time. Linden *et al*[52] examined anxiety and depression in a large cohort of oncological patients (*n* = 10153), including breast and gynecological cancer, and detected that women had more anxiety and depression than men, similar to our findings. Women have already been reported to exhibit greater acceptance of cancer of the reproductive organs compared to patients with gastrointestinal neoplasms[53]. Shapiro *et al*[54] published similar levels of depressive symptoms in individuals of both sexes with advanced cancer, and Goldzweig *et al*[15], in a cohort of 339 subjects with stage I-III colorecta cancer, reported greater psychological distress and impotence in men than in women, without knowing the reason for this disparity with respect to other studies. One of the most relevant points of our work is that it focuses specifically on gastrointestinal neoplasms and reveals that not only women (in general) but specifically those with non-colorectal digestive cancer are the ones who exhibit greater psychological distress.

Trinquinato *et al*[55] appraised quality of life in Brazilian patients with colorectal cancer undergoing chemotherapy and reported that chemotherapy negatively impacted men and women differentially. In their study, they found that cognitive function led to worse quality of life in men compared to women and that symptoms varied according to sex. Men had worse quality of life, due to sexual impotence and fecal incontinence, while in women, poor quality of life was associated with body image, abdominal pain, and dry mouth. Similarly, the women in our study had more functional limitations and more symptoms compared to men, with the corresponding impact of sex on the type of symptoms.

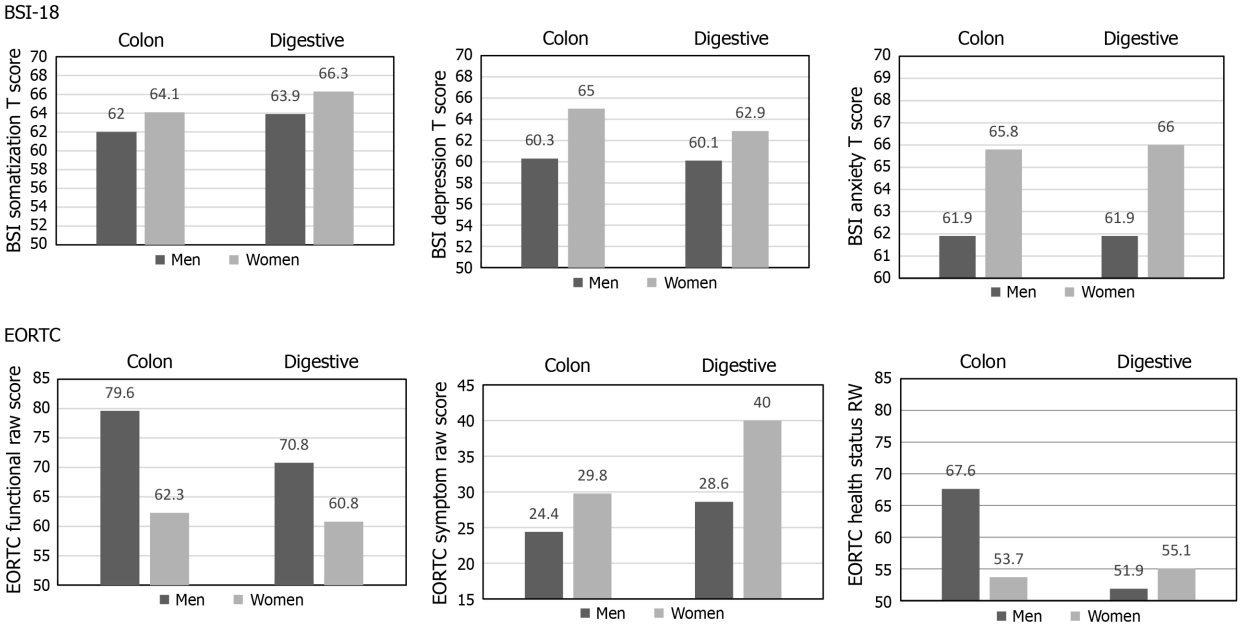

DOI: 10.4251/wjgo.v14.i10.2025

Figure 1 Scores obtained on the Brief Symptom Inventory-18, European Organization for Research and Treatment of Cancer Quality of Life Questionnaire for men *vs* women and for patients with colorectal *vs* digestive (non-colorectal) cancer. BSI: Brief Symptom Inventory; EORTC: European Organization for Research and Treatment of Cancer; RW: Raw.

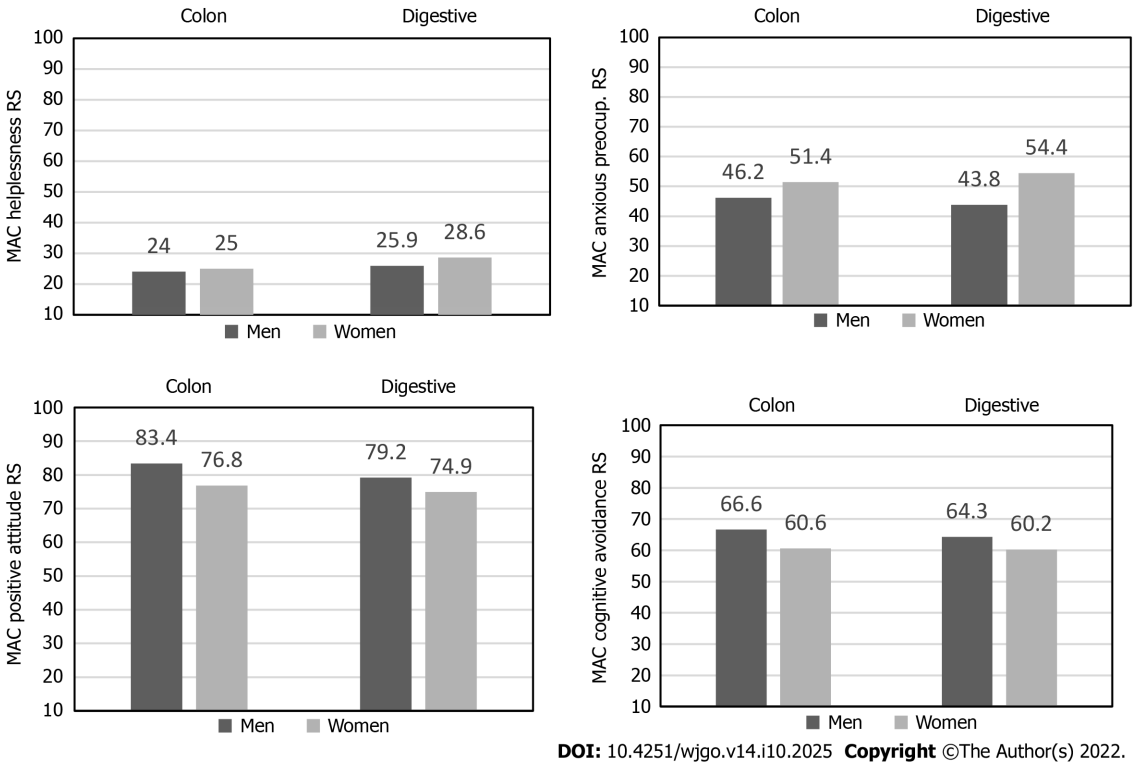

DOI: 10.4251/wjgo.v14.i10.2025

Figure 2 Scores obtained on the Mini-Mental Adjustment to Cancer scales for men *vs* women and for patients with colorectal *vs* digestive (non-colorectal) cancer. MAC: Mini-Mental Adjustment to Cancer; RS: Raw score.

Individuals with advanced colorectal cancer have a better prognosis than those with non-colorectal digestive cancer[2], and better patient-perceived quality of life might correlate with better acceptance of the disease, given the better prognosis and the presence of fewer symptoms. In our study, the participants with non-colorectal digestive cancers had more somatization symptoms than those with colorectal cancer, which may be attributable to the unfavorable prognosis. In a cohort of 378 individuals with colorectal, gastric, and pancreatic cancer, Czerw *et al*[56] reported that those with colorectal cancer

displayed an active behavior coping strategy compared to the subjects with non-colorectal cancer, who demonstrated a maladaptive coping behavior. In contrast, in our series, the strategies most widely used by the participants with advanced digestive tract cancers were positive attitude and cognitive avoidance, although the non-colorectal cancer group exhibited higher levels of helplessness, in line with outcomes observed by Czerw *et al*[56] in pancreatic cancer.

Colorectal cancer has the best prognosis among the main digestive tumors. However, neither the causes nor the prognostic differences in digestive cancers according to sex are well established. Colorectal cancer in women is located more often in the right colon than in men, which is a location associated with worse prognosis[57-59]. That being said, Schmuck *et al*[25] observed that the women included in a study of a cohort of people over 50 years of age had a better OS than men. The authors consider that these outcomes may have to do with the protective effect of women hormones against colorectal cancer, although there may be other causes for these prognostic disparities across sexes[60, 61]. In a sample of 13391 patients from a Norwegian cancer registry, men with gastroesophageal adenocarcinoma were more often assigned to potentially curative treatment compared to the women and had higher 5-year survival rates[16]. Kim *et al*[21] detected greater survival in women with advanced pancreatic cancer with worse tolerance of chemotherapy that has been linked to less clearance of cytotoxic drugs, such as 5-fluorouracil[62] and irinotecan[63-65], and with greater toxicity in women compared to men[66].

Generalisability

There are no data concerning sex differences in cancer perception among patients with advanced gastrointestinal malignancies, and previous studies that included patients with metastatic colorectal cancer and non-colorectal digestive cancer have not reported specific data in this regard[56,67]. Women have been underrepresented in gastrointestinal cancer research, and men have been underrepresented in cancer-associated psychosocial assessment[68]. The relevance of assessing sex differences stems from the fact that men and women have specific social, psychological, and physical characteristics that might compromise coping strategies and perceptions of quality of life.

Limitations

The present study has several limitations. First, the underrepresentation of some non-colorectal digestive cancer subtypes and the heterogeneity of the data could bias the overall estimates. Second, the questionnaires were completed during the appointment prior to beginning antineoplastic treatment, which does not capture the variation of parameters over time nor the causal relationship between variables. Third, the study only included patients from Spain and advanced stage cancers; thus, these results should be confirmed in patients from other countries and with cancers of other stages.

CONCLUSION

In conclusion, this study has detected differences in psychological distress, quality of life, and coping with cancer between women and men and between patients with colorectal and non-colorectal digestive cancers. Women and patients with non-colorectal gastrointestinal tract malignances have more physical symptoms and somatization, and women suffer more psychological distress. These findings, if confirmed, suggest that sex and location of the primary digestive neoplasm should be considered in individualized communication with the patient to achieve a suitable approach to their psychological situation. Future studies should factor in sex and primary tumor site differences in advanced gastrointestinal cancer patients.

ARTICLE HIGHLIGHTS

Research background

Patients with advanced gastrointestinal cancer must cope with the negative effects of cancer and complications. Sex is a sociodemographic variable that can give rise to differences in the evolution as well as the clinical and psychological aspects of cancer.

Research motivation

To analyze whether there are differences between colorectal and non-colorectal digestive cancer in sociodemographic and/or clinical conditions and coping depending on sex.

Research objectives

To evaluate psychological distress, quality of life, and coping strategies in patients with advanced colorectal cancer compared to non-colorectal cancer based on sex.

Research methods

This was a multi-institutional prospective, observational study that evaluated patients with advanced digestive cancers; 203 patients were eligible for this analysis. Demographic and clinical data were obtained and the association between psychological distress, quality of life, and coping strategies and the role of sex and primary tumor site were analyzed.

Research results

Women exhibited more depressive symptoms, anxiety, functional limitations, and anxious preoccupation than men. Non-colorectal digestive cancer patients and women showed more somatization and physical symptoms than colorectal cancer patients and men.

Research conclusions

Disease acceptance in patients with advanced cancer of the digestive tract may be sex dependent.

Research perspectives

Future interventions should evaluate primary tumor site and sex differences in patients with gastrointestinal malignancies.

ACKNOWLEDGEMENTS

The authors thank the Bioethics Section of the Spanish Society of Medical Oncology (SEOM) for their contribution to this study, Priscilla Chase Duran for editing the manuscript, and Natalia Cateriano, Miguel Vaquero, and IRICOM S.A. for supporting the registry website. The authors are indebted to all patients as well as to NEOetic-SEOM centers and investigators who participated in this research and made it possible.

FOOTNOTES

Author contributions: Pacheco-Barcia V, Calderon C, and Jimenez-Fonseca P developed the project, analyzed the data, and drafted the manuscript; The other authors recruited patients and provided clinical information, comments, and improvements to the manuscript; All authors participated in the interpretation and discussion of data and the critical review of the manuscript.

Supported by The FSEOM (Spanish Society of Medical Oncology Foundation) grant for Projects of the Collaborative Groups in 2018 and by an Astra Zeneca grant, No. ES2020-1939.

Institutional review board statement: The study was approved by the Research Ethics Committee of the Principality of Asturias (May 17, 2019) and by the Spanish Agency of Medicines and Medical Devices (Identification code: L34LM-MM2GH-Y925U RJDHQ). The study has been performed in accordance with the ethical standards of the 1964 Declaration of Helsinki and its later amendments. This study is an observational, non-interventionist trial.

Informed consent statement: Signed informed consent was obtained from all patients.

Conflict-of-interest statement: Dr. Pacheco-Barcia reports grants from FSEOM and grants from Astra Zeneca during the conduct of the study; other from Eisai, other from Merck, other from Eli Lilly, other from Advanced accelerator applications, a Novartis company, grants from FSEOM and Merck, other from Roche, other from Eli Lilly, other from Bristol-Myers Squibb, other from Merck, other from Amgen, other from Merck Sharp and Dhome, other from Nutricia, other from Roche, other from Bayer, other from Amgen, other from Esteve, other from Eli Lilly, other from Roche, other from Bristol-Myers Squibb, grants from Ayuda Clínico Formativa AECC 2020, grants from FSEOM, outside the submitted work.

Data sharing statement: This database is available through a centralized web platform: www.neoetic.es. The code is available upon request to the authors. Code availability: Patients are identified by an encrypted code known only to the local researcher. The analysis code is available upon request to the authors.

STROBE statement: The study was undertaken according to the Strengthening the Reporting of Observational studies in Epidemiology (STROBE) guidelines.

Country/Territory of origin: Spain

ORCID number: Vilma Pacheco-Barcia 0000-0003-0141-1306; David Gomez 0000-0002-7265-0251; Berta Obispo 0000-0003-1214-6595; Luka Mihic Gongora 0000-0002-8371-4601; Raquel Hernandez San Gil 0000-0003-3426-7515; Patricia Cruz-Castellanos 0000-0002-9837-825X; Mireia Gil-Raga 0000-0002-4508-7395; Vicente Villalba 0000-0003-0284-3004; Ismael Ghanem 0000-0002-1859-0737; Paula Jimenez-Fonseca 0000-0003-4592-3813; Caterina Calderon 0000-0002-6956-9321.

S-Editor: Gong ZM
L-Editor: Filipodia
P-Editor: Gong ZM

REFERENCES

1 **World Health Organization International Agency for Research on Cancer (IARC)**. Globocan 2020: estimated cancer incidence, mortality and prevalence worldwide in 2020. Available from: https://gco.iarc.fr/today/data/factsheets/populations/900-world-fact-sheets.pdf
2 **World Health Organization International Agency for Research on Cancer (IARC)**. Globocan 2020: estimated cancer incidence, mortality and prevalence in Spain in 2020. Available from: https://gco.iarc.fr/today/data/factsheets/populations/724-spain-fact-sheets.pdf
3 **National Cancer Institute**. Cancer Stat Facts: Colorectal Cancer. 2022. Available from: https://seer.cancer.gov/statfacts/html/colorect.html
4 **DiMatteo MR**, Lepper HS, Croghan TW. Depression is a risk factor for noncompliance with medical treatment: meta-analysis of the effects of anxiety and depression on patient adherence. *Arch Intern Med* 2000; **160**: 2101-2107 [PMID: 10904452 DOI: 10.1001/archinte.160.14.2101]
5 **Greer JA**, Pirl WF, Park ER, Lynch TJ, Temel JS. Behavioral and psychological predictors of chemotherapy adherence in patients with advanced non-small cell lung cancer. *J Psychosom Res* 2008; **65**: 549-552 [PMID: 19027443 DOI: 10.1016/j.jpsychores.2008.03.005]
6 **Pinquart M**, Duberstein PR. Depression and cancer mortality: a meta-analysis. *Psychol Med* 2010; **40**: 1797-1810 [PMID: 20085667 DOI: 10.1017/S0033291709992285]
7 **Satin JR**, Linden W, Phillips MJ. Depression as a predictor of disease progression and mortality in cancer patients: a meta-analysis. *Cancer* 2009; **115**: 5349-5361 [PMID: 19753617 DOI: 10.1002/cncr.24561]
8 **Baqutayan SM**. The effect of anxiety on breast cancer patients. *Indian J Psychol Med* 2012; **34**: 119-123 [PMID: 23162185 DOI: 10.4103/0253-7176.101774]
9 **Stark DP**, House A. Anxiety in cancer patients. *Br J Cancer* 2000; **83**: 1261-1267 [PMID: 11044347 DOI: 10.1054/bjoc.2000.1405]
10 **Cameron LD**, Leventhal H, Love RR. Trait anxiety, symptom perceptions, and illness-related responses among women with breast cancer in remission during a tamoxifen clinical trial. *Health Psychol* 1998; **17**: 459-469 [PMID: 9776005 DOI: 10.1037/0278-6133.17.5.459]
11 **Calderón C**, Jiménez-Fonseca P, Hernández R, Mar Muñoz MD, Mut M, Mangas-Izquierdo M, Vicente MÁ, Ramchandani A, Carmona-Bayonas A. Quality of life, coping, and psychological and physical symptoms after surgery for non-metastatic digestive tract cancer. *Surg Oncol* 2019; **31**: 26-32 [PMID: 31493647 DOI: 10.1016/j.suronc.2019.08.009]
12 **Heidari S**, Babor TF, De Castro P, Tort S, Curno M. Sex and Gender Equity in Research: rationale for the SAGER guidelines and recommended use. *Res Integr Peer Rev* 2016; **1**: 2 [PMID: 29451543 DOI: 10.1186/s41073-016-0007-6]
13 **Clayton JA**, Tannenbaum C. Reporting Sex, Gender, or Both in Clinical Research? *JAMA* 2016; **316**: 1863-1864 [PMID: 27802482 DOI: 10.1001/jama.2016.16405]
14 **Maestre A**, Gonzálvez A, Carretero J. On the basis of sex and gender in healthcare. *Span J Med* 2021; **1**: 65-73 [DOI: 10.24875/SJMED.M21000007]
15 **Goldzweig G**, Andritsch E, Hubert A, Walach N, Perry S, Brenner B, Baider L. How relevant is marital status and gender variables in coping with colorectal cancer? *Psychooncology* 2009; **18**: 866-874 [PMID: 19061195 DOI: 10.1002/pon.1499]
16 **Kalff MC**, Dijksterhuis WPM, Verhoeven RHA, Wagner AD, Lemmens VEPP, van Laarhoven HWM, Gisbertz SS, van Berge Henegouwen MI. A population-based study on gender differences in tumor and treatment characteristics and survival of curable gastroesophageal cancer. *J Clin Oncol* 2020; **38** (15_suppl): 4550-4550 [DOI: 10.1200/JCO.2020.38.15_suppl.4550]
17 **Dijksterhuis WPM**, Kalff MC, Wagner AD, Verhoeven RHA, Lemmens VEPP, van Oijen MGH, Gisbertz SS, van Berge Henegouwen MI, van Laarhoven HWM. Gender Differences in Treatment Allocation and Survival of Advanced Gastroesophageal Cancer: A Population-Based Study. *J Natl Cancer Inst* 2021; **113**: 1551-1560 [PMID: 33837791 DOI: 10.1093/jnci/djab075]
18 **Kim HW**, Kim JH, Lim BJ, Kim H, Park JJ, Youn YH, Park H, Noh SH, Kim JW, Choi SH. Sex Disparity in Gastric Cancer: Female Sex is a Poor Prognostic Factor for Advanced Gastric Cancer. *Ann Surg Oncol* 2016; **23**: 4344-4351 [PMID: 27469120 DOI: 10.1245/s10434-016-5448-0]
19 **Yang D**, Hendifar A, Lenz C, Togawa K, Lenz F, Lurje G, Pohl A, Winder T, Ning Y, Groshen S, Lenz HJ. Survival of metastatic gastric cancer: Significance of age, sex and race/ethnicity. *J Gastrointest Oncol* 2011; **2**: 77-84 [PMID: 22811834 DOI: 10.3978/j.issn.2078-6891.2010.025]
20 **Najari BB**, Rink M, Li PS, Karakiewicz PI, Scherr DS, Shabsigh R, Meryn S, Schlegel PN, Shariat SF. Sex disparities in

cancer mortality: the risks of being a man in the United States. *J Urol* 2013; **189**: 1470-1474 [PMID: 23206422 DOI: 10.1016/j.juro.2012.11.153]

21 **Kim J**, Ji E, Jung K, Jung IH, Park J, Lee JC, Kim JW, Hwang JH, Kim J. Gender Differences in Patients with Metastatic Pancreatic Cancer Who Received FOLFIRINOX. *J Pers Med* 2021; **11** [PMID: 33573202 DOI: 10.3390/jpm11020083]

22 **Kim HI**, Lim H, Moon A. Sex Differences in Cancer: Epidemiology, Genetics and Therapy. *Biomol Ther (Seoul)* 2018; **26**: 335-342 [PMID: 29949843 DOI: 10.4062/biomolther.2018.103]

23 **Hohla F**, Hopfinger G, Romeder F, Rinnerthaler G, Bezan A, Stättner S, Hauser-Kronberger C, Ulmer H, Greil R. Female gender may predict response to FOLFIRINOX in patients with unresectable pancreatic cancer: a single institution retrospective review. *Int J Oncol* 2014; **44**: 319-326 [PMID: 24247204 DOI: 10.3892/ijo.2013.2176]

24 **Lambert A**, Jarlier M, Gourgou Bourgade S, Conroy T. Response to FOLFIRINOX by gender in patients with metastatic pancreatic cancer: Results from the PRODIGE 4/ ACCORD 11 randomized trial. *PLoS One* 2017; **12**: e0183288 [PMID: 28931010 DOI: 10.1371/journal.pone.0183288]

25 **Schmuck R**, Gerken M, Teegen EM, Krebs I, Klinkhammer-Schalke M, Aigner F, Pratschke J, Rau B, Benz S. Gender comparison of clinical, histopathological, therapeutic and outcome factors in 185,967 colon cancer patients. *Langenbecks Arch Surg* 2020; **405**: 71-80 [PMID: 32002628 DOI: 10.1007/s00423-019-01850-6]

26 Zentralinstitut für die kassenärztliche Versorgung in Deutschland. Available from: https://www.zi.de/fileadmin/images/content/PDFs_alle/Beteiligungsraten_2011_Deutschland_erw.pdf

27 **Kim SE**, Paik HY, Yoon H, Lee JE, Kim N, Sung MK. Sex- and gender-specific disparities in colorectal cancer risk. *World J Gastroenterol* 2015; **21**: 5167-5175 [PMID: 25954090 DOI: 10.3748/wjg.v21.i17.5167]

28 **Krishnan S**, Wolf JL. Colorectal cancer screening and prevention in women. *Womens Health (Lond)* 2011; **7**: 213-226 [PMID: 21410347 DOI: 10.2217/whe.11.7]

29 **Sun LM**, Liang JA, Lin CL, Sun S, Kao CH. Risk of mood disorders in patients with colorectal cancer. *J Affect Disord* 2017; **218**: 59-65 [PMID: 28458117 DOI: 10.1016/j.jad.2017.04.050]

30 **Mols F**, Schoormans D, de Hingh I, Oerlemans S, Husson O. Symptoms of anxiety and depression among colorectal cancer survivors from the population-based, longitudinal PROFILES Registry: Prevalence, predictors, and impact on quality of life. *Cancer* 2018; **124**: 2621-2628 [PMID: 29624635 DOI: 10.1002/cncr.31369]

31 **World Health Organization**. WHOQOL-HIV Instrument. Mental Health: evidence and research department of mental health and substance dependence. WHO: Geneva; 2012. Available from: https://apps.who.int/iris/bitstream/handle/10665/77776/WHO_MSD_MER_Rev.2012.03_eng.pdf?sequence=1&isAllowed=y

32 **Deimling GT**, Wagner LJ, Bowman KF, Sterns S, Kercher K, Kahana B. Coping among older-adult, long-term cancer survivors. *Psychooncology* 2006; **15**: 143-159 [PMID: 15880638 DOI: 10.1002/pon.931]

33 **Connor-Smith JK**, Compas BE. Coping as a moderator of relations between reactivity to interpersonal stress, health status, and internalizing problems. *Cognit Ther Res* 2004; **28**: 347-368 [DOI: 10.1023/B:COTR.0000031806.25021.d5]

34 **Subramaniam S**, Kong YC, Chinna K, Kimman M, Ho YZ, Saat N, Malik RA, Taib NA, Abdullah MM, Lim GC, Tamin NI, Woo YL, Chang KM, Goh PP, Yip CH, Bhoo-Pathy N. Health-related quality of life and psychological distress among cancer survivors in a middle-income country. *Psychooncology* 2018; **27**: 2172-2179 [PMID: 29856903 DOI: 10.1002/pon.4787]

35 **Marco DJT**, White VM. The impact of cancer type, treatment, and distress on health-related quality of life: cross-sectional findings from a study of Australian cancer patients. *Support Care Cancer* 2019; **27**: 3421-3429 [PMID: 30661203 DOI: 10.1007/s00520-018-4625-z]

36 **Tsunoda A**, Nakao K, Hiratsuka K, Yasuda N, Shibusawa M, Kusano M. Anxiety, depression and quality of life in colorectal cancer patients. *Int J Clin Oncol* 2005; **10**: 411-417 [PMID: 16369745 DOI: 10.1007/s10147-005-0524-7]

37 **Aminisani N**, Nikbakht H, Asghari Jafarabadi M, Shamshirgaran SM. Depression, anxiety, and health related quality of life among colorectal cancer survivors. *J Gastrointest Oncol* 2017; **8**: 81-88 [PMID: 28280612 DOI: 10.21037/jgo.2017.01.12]

38 **Sánchez R**, Alexander-Sierra F, Oliveros R. Relationship between quality of life and clinical status in patients with gastrointestinal cancer. *Rev Esp Enferm Dig* 2012; **104**: 584-591 [PMID: 23368650 DOI: 10.4321/S1130-01082012001100006]

39 **Oppegaard KR**, Dunn LB, Kober KM, Mackin L, Hammer MJ, Conley YP, Levine J, Miaskowski C. Gender Differences in the Use of Engagement and Disengagement Coping Strategies in Patients With Cancer Receiving Chemotherapy. *Oncol Nurs Forum* 2020; **47**: 586-594 [PMID: 32830804 DOI: 10.1188/20.ONF.586-594]

40 **von Elm E**, Altman DG, Egger M, Pocock SJ, Gøtzsche PC, Vandenbroucke JP; STROBE Initiative. The Strengthening the Reporting of Observational Studies in Epidemiology (STROBE) statement: guidelines for reporting observational studies. *J Clin Epidemiol* 2008; **61**: 344-349 [PMID: 18313558 DOI: 10.1016/j.jclinepi.2007.11.008]

41 **Derogatis LR**. Brief Symptom Inventory (BSI): Administration, Scoring and Procedures Manual. Minneapolis: NCS Pearson, Inc.; 1993

42 **Calderon C**, Ferrando PJ, Lorenzo-Seva U, Hernández R, Oporto-Alonso M, Jiménez-Fonseca P. Factor structure and measurement invariance of the Brief Symptom Inventory (BSI-18) in cancer patients. *Int J Clin Health Psychol* 2020; **20**: 71-80 [PMID: 32021621 DOI: 10.1016/j.ijchp.2019.12.001]

43 **Aaronson NK**, Ahmedzai S, Bergman B, Bullinger M, Cull A, Duez NJ, Filiberti A, Flechtner H, Fleishman SB, de Haes JC. The European Organization for Research and Treatment of Cancer QLQ-C30: a quality-of-life instrument for use in international clinical trials in oncology. *J Natl Cancer Inst* 1993; **85**: 365-376 [PMID: 8433390 DOI: 10.1093/jnci/85.5.365]

44 **Calderon C**, Ferrando PJ, Lorenzo-Seva U, Ferreira E, Lee EM, Oporto-Alonso M, Obispo-Portero BM, Mihic-Góngora L, Rodríguez-González A, Jiménez-Fonseca P. Psychometric properties of the Spanish version of the European Organization for Research and Treatment of Cancer Quality of Life Questionnaire (EORTC QLQ-C30). *Qual Life Res* 2022; **31**: 1859-1869 [PMID: 34928470 DOI: 10.1007/s11136-021-03068-w]

45 **Watson M**, Law MG, Santos M dos, Greer S, Baruch J, Bliss J. The Mini-MAC: further development of the mental adjustment to cancer scale. *J Psychosoc Oncol* 1994; **12**: 33-46 [DOI: 10.1300/J077V12N03_03]

46 **Calderon C**, Lorenzo-Seva U, Ferrando PJ, Gómez-Sánchez D, Ferreira E, Ciria-Suarez L, Oporto-Alonso M, Fernández-

Andujar M, Jiménez-Fonseca P. Psychometric properties of Spanish version of the Mini-Mental Adjustment to Cancer Scale. *Int J Clin Health Psychol* 2021; **21**: 100185 [PMID: 33363578 DOI: 10.1016/j.ijchp.2020.06.001]

47 **Richards MA**, Westcombe AM, Love SB, Littlejohns P, Ramirez AJ. Influence of delay on survival in patients with breast cancer: a systematic review. *Lancet* 1999; **353**: 1119-1126 [PMID: 10209974 DOI: 10.1016/S0140-6736(99)02143-1]

48 **Schroevers MJ**, Kraaij V, Garnefski N. Cancer patients' experience of positive and negative changes due to the illness: relationships with psychological well-being, coping, and goal reengagement. *Psychooncology* 2011; **20**: 165-172 [PMID: 20217657 DOI: 10.1002/pon.1718]

49 **Aminisani N**, Nikbakht HA, Shojaie L, Jafari E, Shamshirgaran M. Gender Differences in Psychological Distress in Patients with Colorectal Cancer and Its Correlates in the Northeast of Iran. *J Gastrointest Cancer* 2022; **53**: 245-252 [PMID: 33417199 DOI: 10.1007/s12029-020-00558-x]

50 **Gonzalez-Saenz de Tejada M**, Bilbao A, Baré M, Briones E, Sarasqueta C, Quintana JM, Escobar A. Association of social support, functional status, and psychological variables with changes in health-related quality of life outcomes in patients with colorectal cancer. *Psychooncology* 2016; **25**: 891-897 [PMID: 26582649 DOI: 10.1002/pon.4022]

51 **Braamse AM**, van Turenhout ST, Terhaar Sive Droste JS, de Groot GH, van der Hulst RW, Klemt-Kropp M, Kuiken SD, Loffeld RJ, Uiterwaal MT, Mulder CJ, Dekker J. Factors associated with anxiety and depressive symptoms in colorectal cancer survivors. *Eur J Gastroenterol Hepatol* 2016; **28**: 831-835 [PMID: 26928565 DOI: 10.1097/MEG.0000000000000615]

52 **Linden W**, Vodermaier A, Mackenzie R, Greig D. Anxiety and depression after cancer diagnosis: prevalence rates by cancer type, gender, and age. *J Affect Disord* 2012; **141**: 343-351 [PMID: 22727334 DOI: 10.1016/j.jad.2012.03.025]

53 **Kozak G**. Different strategies of managing neoplasia in the course of chosen cancers. *Anestezjol i Ratownictwo* 2012; **6**: 70

54 **Shapiro GK**, Mah K, de Vries F, Li M, Zimmermann C, Hales S, Rodin G. A cross-sectional gender-sensitive analysis of depressive symptoms in patients with advanced cancer. *Palliat Med* 2020; **34**: 1436-1446 [PMID: 32781931 DOI: 10.1177/0269216320947961]

55 **Trinquinato I**, Marques da Silva R, Ticona Benavente SB, Antonietti CC, Siqueira Costa Calache AL. Gender differences in the perception of quality of life of patients with colorectal cancer. *Invest Educ Enferm* 2017; **35**: 320-329 [PMID: 29767912 DOI: 10.17533/udea.iee.v35n3a08]

56 **Czerw A**, Religioni U, Banaś T. Perception of cancer in patients diagnosed with the most common gastrointestinal cancers. *BMC Palliat Care* 2020; **19**: 144 [PMID: 32943037 DOI: 10.1186/s12904-020-00650-w]

57 **Hansen IO**, Jess P. Possible better long-term survival in left versus right-sided colon cancer - a systematic review. *Dan Med J* 2012; **59**: A4444 [PMID: 22677242]

58 **Benedix F**, Kube R, Meyer F, Schmidt U, Gastinger I, Lippert H; Colon/Rectum Carcinomas (Primary Tumor) Study Group. Comparison of 17,641 patients with right- and left-sided colon cancer: differences in epidemiology, perioperative course, histology, and survival. *Dis Colon Rectum* 2010; **53**: 57-64 [PMID: 20010352 DOI: 10.1007/DCR.0b013e3181c703a4]

59 **Holch JW**, Ricard I, Stintzing S, Modest DP, Heinemann V. The relevance of primary tumour location in patients with metastatic colorectal cancer: A meta-analysis of first-line clinical trials. *Eur J Cancer* 2017; **70**: 87-98 [PMID: 27907852 DOI: 10.1016/j.ejca.2016.10.007]

60 **Majek O**, Gondos A, Jansen L, Emrich K, Holleczek B, Katalinic A, Nennecke A, Eberle A, Brenner H; GEKID Cancer Survival Working Group. Sex differences in colorectal cancer survival: population-based analysis of 164,996 colorectal cancer patients in Germany. *PLoS One* 2013; **8**: e68077 [PMID: 23861851 DOI: 10.1371/journal.pone.0068077]

61 **Franceschi S**, Gallus S, Talamini R, Tavani A, Negri E, La Vecchia C. Menopause and colorectal cancer. *Br J Cancer* 2000; **82**: 1860-1862 [PMID: 10839302 DOI: 10.1054/bjoc.1999.1084]

62 **Mueller F**, Büchel B, Köberle D, Schürch S, Pfister B, Krähenbühl S, Froehlich TK, Largiader CR, Joerger M. Gender-specific elimination of continuous-infusional 5-fluorouracil in patients with gastrointestinal malignancies: results from a prospective population pharmacokinetic study. *Cancer Chemother Pharmacol* 2013; **71**: 361-370 [PMID: 23139054 DOI: 10.1007/s00280-012-2018-4]

63 **Berg AK**, Buckner JC, Galanis E, Jaeckle KA, Ames MM, Reid JM. Quantification of the impact of enzyme-inducing antiepileptic drugs on irinotecan pharmacokinetics and SN-38 exposure. *J Clin Pharmacol* 2015; **55**: 1303-1312 [PMID: 25975718 DOI: 10.1002/jcph.543]

64 **Klein CE**, Gupta E, Reid JM, Atherton PJ, Sloan JA, Pitot HC, Ratain MJ, Kastrissios H. Population pharmacokinetic model for irinotecan and two of its metabolites, SN-38 and SN-38 glucuronide. *Clin Pharmacol Ther* 2002; **72**: 638-647 [PMID: 12496745 DOI: 10.1067/mcp.2002.129502]

65 **Wu H**, Infante JR, Keedy VL, Jones SF, Chan E, Bendell JC, Lee W, Zamboni BA, Ikeda S, Kodaira H, Rothenberg ML, Burris HA 3rd, Zamboni WC. Population pharmacokinetics of PEGylated liposomal CPT-11 (IHL-305) in patients with advanced solid tumors. *Eur J Clin Pharmacol* 2013; **69**: 2073-2081 [PMID: 23989300 DOI: 10.1007/s00228-013-1580-y]

66 **Cristina V**, Mahachie J, Mauer M, Buclin T, Van Cutsem E, Roth A, Wagner AD. Association of Patient Sex With Chemotherapy-Related Toxic Effects: A Retrospective Analysis of the PETACC-3 Trial Conducted by the EORTC Gastrointestinal Group. *JAMA Oncol* 2018; **4**: 1003-1006 [PMID: 29800044 DOI: 10.1001/jamaoncol.2018.1080]

67 **Czerw AI**, Religioni U, Deptała A, Walewska-Zielecka B. Assessment of pain, acceptance of illness, adjustment to life with cancer, and coping strategies in colorectal cancer patients. *Prz Gastroenterol* 2016; **11**: 96-103 [PMID: 27350836 DOI: 10.5114/pg.2015.52561]

68 **Hoyt MA**, Rubin LR. Gender representation of cancer patients in medical treatment and psychosocial survivorship research: changes over three decades. *Cancer* 2012; **118**: 4824-4832 [PMID: 22294480 DOI: 10.1002/cncr.27432]

World Journal of Gastrointestinal Oncology

Submit a Manuscript: https://www.f6publishing.com

World J Gastrointest Oncol 2022 October 15; 14(10): 2038-2047

DOI: 10.4251/wjgo.v14.i10.2038

ISSN 1948-5204 (online)

ORIGINAL ARTICLE

Observational Study

Droplet digital polymerase chain reaction assay for methylated ring finger protein 180 in gastric cancer

Guang-Hong Guo, Yi-Bin Xie, Tao Jiang, Yang An

Specialty type: Oncology

Provenance and peer review: Unsolicited article; Externally peer reviewed.

Peer-review model: Single blind

Peer-review report's scientific quality classification

Grade A (Excellent): 0
Grade B (Very good): B, B, B
Grade C (Good): 0
Grade D (Fair): 0
Grade E (Poor): 0

P-Reviewer: Albillos A, Spain; Valery PC, Australia; Wagner-Skacel J, Austria

Received: July 20, 2022
Peer-review started: July 20, 2022
First decision: August 20, 2022
Revised: August 21, 2022
Accepted: September 1, 2022
Article in press: September 1, 2022
Published online: October 15, 2022

Guang-Hong Guo, Department of Laboratory Medicine, The First Medical Center of Chinese PLA General Hospital, Beijing 100853, China

Yi-Bin Xie, Department of Pancreatic and Gastric Surgery, National Cancer Center/National Clinical Research Center for Cancer/Cancer Hospital, Chinese Academy of Medical Sciences and Peking Union Medical College, Beijing 100021, China

Tao Jiang, Medicine Innovation Research Division of Chinese PLA General Hospital, Beijing 100853, China

Yang An, Faculty of Hepato-Pancreato-Biliary Surgery, The Sixth Medical Center of Chinese PLA General Hospital, Beijing 100048, China

Corresponding author: Yang An, MD, Doctor, Faculty of Hepato-Pancreato-Biliary Surgery, The Sixth Medical Center of Chinese PLA General Hospital, No. 6 Fucheng Road, Haidian District, Beijing 100048, China. dr.anyang@163.com

Abstract

BACKGROUND

Gastric cancer (GC) is one of the most prevalent malignant tumors that endangers human health. Early diagnosis is essential for improving the prognosis and survival rate of GC patients. Ring finger protein 180 (RNF180) is involved in the regulation of cell differentiation, proliferation, apoptosis, and tumorigenesis, and aberrant hypermethylation of CpG islands in the promoter is strongly associated with the occurrence and development of GC. Thus, methylated RNF180 can be used as a potential biomarker for GC diagnosis.

AIM

To use droplet digital polymerase chain reaction (ddPCR) to quantify the methylation level of the RN180 gene. A reproducible ddPCR assay to detect methylated RNF180 from trace DNA was designed and optimized.

METHODS

The primer and probe were designed and selected, the conversion time of bisulfite was optimized, the ddPCR system was adjusted by primer concentration, amplification temperature and amplification cycles, and the detection limit of ddPCR was determined.

RESULTS

The best conversion time for blood DNA was 2 h 10 min, and that for plasma DNA was 2 h 10 min and 2 h 30 min. The results of ddPCR were better when the amplification temperature was 56 °C and the number of amplification cycles was 50. Primer concentrations showed little effect on the assay outcome. Therefore, the primer concentration could be adjusted according to the reaction system and DNA input. The assay required at least 0.1 ng of input DNA.

CONCLUSION

In summary, a ddPCR assay was established to detect methylated RNF180, which is expected to be a new diagnostic biomarker for GC.

Key Words: Gastric cancer; Ring finger protein 180; DNA methylation; Droplet digital polymerase chain reaction

Core Tip: Gastric cancer (GC) is one of the most prevalent malignant tumors that endangers human health. Early diagnosis is essential for improving the prognosis and survival rate of GC patients. Ring finger protein 180 (RNF180) is a newly discovered member of the ring finger protein family, and it is an important tumor suppressor gene involved in the construction of the E3 ubiquitin protein ligase in the ubiquitin proteasome system and ubiquitin degradation. Methylated RNF180 can be used as a potential biomarker for GC diagnosis. We aimed to evaluate the droplet digital polymerase chain reaction assay for methylated RNF180 in GC.

Citation: Guo GH, Xie YB, Jiang T, An Y. Droplet digital polymerase chain reaction assay for methylated ring finger protein 180 in gastric cancer. *World J Gastrointest Oncol* 2022; 14(10): 2038-2047
URL: https://www.wjgnet.com/1948-5204/full/v14/i10/2038.htm
DOI: https://dx.doi.org/10.4251/wjgo.v14.i10.2038

INTRODUCTION

Ring finger protein 180 (RNF180) is a newly discovered member of the ring finger protein family, and it is an important tumor suppressor gene involved in the construction of the E3 ubiquitin protein ligase in the ubiquitin proteasome system and ubiquitin degradation[1]. RNF180 affects many important physiological processes *in vivo*, including cell growth, differentiation, and tumorigenesis. RNF180 is expressed at low levels in gastric cancer (GC) tissue samples, and it is particularly crucial to the GC pathological stage and overall survival of patients[2]. Hypermethylation in the promoter region is the main mechanism of downregulation or silencing of RNF180 expression in tumors[3]. It is also associated with *Helicobacter pylori* (*H. pylori*) infection and GC prognosis[4,5]. Methylation of the RNF180 gene can be used as an independent diagnostic and prognostic biomarker in the clinic[6]. At present, the primary screening methods for GC in the clinic are upper gastrointestinal X-ray examination, gastrointestinal endoscopy, *H. pylori* antibody detection and plasma pepsinogen detection[7]. Tissue biopsy is the gold standard for pathological diagnosis of GC. The commonly used X-ray examination and endoscopy are not always well suited to the early diagnosis, *H. pylori* antibody and plasma pepsinogen are not specific enough, and the shortcomings of tissue biopsy are its invasiveness and heterogeneity. The recent development of liquid biopsy technology has been very promising in the early screening of tumors. It is a noninvasive procedure for diagnosis that utilizes circulating free DNA in body fluids and circumvents some of the limitations of conventional tissue biopsy[8,9].

Liquid biopsy has great clinical value for therapy evaluation and prognosis monitoring. Droplet digital polymerase chain reaction (ddPCR) is a novel absolute quantitative technique that divides the reaction system into thousands of units[10]. The fluorescence signal of each reaction unit is detected, and the original concentration is calculated according to a Poisson distribution. Liquid biopsy samples are from blood, urine, and other body fluids, but the tumor DNA content in these specimens is low[11]. Conventional PCR technology cannot meet the requirement of liquid biopsy. Compared with conventional PCR, ddPCR can achieve absolute quantification of trace nucleic acids and is more suitable for clinical liquid biopsy. In this study, a ddPCR assay to detect the methylated RNF180 gene was established and optimized for analyzing plasma and blood samples. It can be used for the screening and early diagnosis of GC and opens new possibilities to use methylated RNF180 as a biomarker of invasive GC.

Table 1 The limit of detection for droplet digital polymerase chain reaction

Input DNA (ng)	Conc (copies/μL)	Input DNA (ng)	Conc (copies/μL)
10	15.4	0.5	0.73
9	14	0.1	0.29
8	12.25	0.05	0
7	9.35	0.01	0
6	9.6	0.005	0
5	7.8	0.001	0
4	7.56	0.0005	0
3	4.53	0.0001	0
2	3.63	H_2O	0
1	1.4		

MATERIALS AND METHODS

Study subjects

The samples used in this study were blood samples from patients diagnosed between September 2020 and April 2021. Inclusion criteria: Complete clinicopathological data, clear imaging and pathological diagnosis, and absence of long-term radiotherapy, chemotherapy, and immunotherapy. The exclusion criteria were as follows: Patients with other types of tumors in addition to confirmed GC who had received long-term treatment.

DNA isolation

The samples were peripheral blood collected on an empty stomach in the morning, and EDTA was used as an anticoagulant. Upon collection, the blood samples were immediately aliquoted into 1.5 mL Eppendorf tubes at 200 μL/tube. Plasma samples were prepared by centrifuging blood at 1500 × g for 10 min. The samples were discarded if hemolysis or lipemia were observed. Plasma was aliquoted into 1000 μL Eppendorf tubes for subsequent experiments. DNA from 200 μL blood samples was extracted according to the instructions of the QIAamp Blood Mini Kit (Qiagen) and eluted in 84 μL Buffer AE. DNA was extracted from 1 mL of plasma sample according to the instructions of the QIAamp MinElute ccfDNA Mini Kit (Qiagen) and eluted in 24 μL ultrafine water. The concentration of double-stranded DNA (dsDNA) was measured by a Qubit dsDNA HS Assay Kit and Qubit 3.0 (Thermo Fisher).

Bisulfite conversion

A 20 μL DNA sample was transformed according to the instructions of the EZ DNA Methylation-Gold Kit (Zymo Research), and 22 μL M-Elution Buffer was added to the column matrix to elute DNA. PCR was performed in a thermal cycler with the lid temperature set at 105 °C. Thermal cycling condition was as follows: (1) 98 °C for 10 min; (2) 64 °C for 1 h 30 min, 1 h 50 min, 2 h 10 min, or 2 h 30 min; and (3) Hold at 4°C. The converted DNA was purified according to the cycle-Pure Kit instructions (Omega), and finally, 7 μL elution buffer was added. The single-stranded DNA (ssDNA) Assay Kit and Qubit 3.0 (Thermo Fisher) were used to determine the concentration of ssDNA.

Design of primers

Primers were designed based on the principle that unmethylated cytosine will transform into uracil after bisulfite treatment, while methylated cytosine remains unaltered. Primers and probes were designed so that they could distinguish between methylated and unmethylated sequences. The RNF180 gene sequence was obtained from National Center for Biotechnology Information. Then, the sequence was pasted into the methyl Primer Express software to find the CpG island, and methylation primers and probes were designed according to the transformed sequence. The 5′ end of the probes was modified with the FAM fluorophore, and the 3′ end was modified with BHQ1. Three pairs of primers were designed for ddPCR experiments and tested against 100% methylated control DNA (EpiTect PCR Control DNA Set, Qiagen). After repeated tests, the primers were screened according to their reproducibility, specificity, and detection rate. Then, unmethylated primers and probes were designed for subsequent experiments to calculate methylation rates.

Establishment and optimization of the ddPCR assay

The ddPCR assay was conducted under the same conditions with 100% methylated control DNA at the

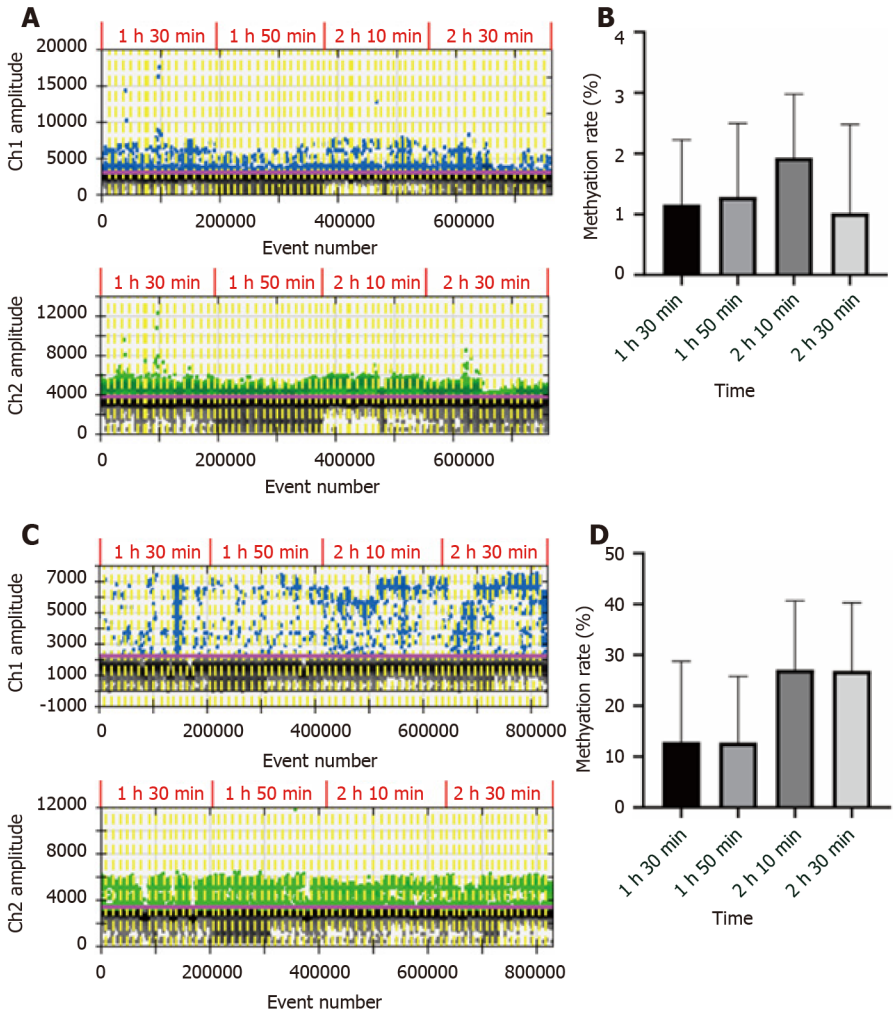

DOI: 10.4251/wjgo.v14.i10.2038

Figure 1 Conversion time of blood DNA and plasma DNA. A: The droplet digital polymerase chain reaction (ddPCR) results of 16 blood DNA samples converted for different times. Above: Fluorescence channel 1, methylation droplets; below: Channel 2, unmethylation droplets; B: Histogram of methylation rate of blood DNA samples at different conversion times; C: The ddPCR results of 16 plasma DNA samples; D: Histogram of methylation rates of plasma DNA samples.

initial input as shown in Table 1 to determine the lowest limit of detection (LOD). Simultaneously, to find the optimal ddPCR amplification condition, the amplification temperature was set at 56 °C and 59 °C, and the amplification cycles were set at 45 and 50. The ddPCR instructions recommended a final primer concentration of 700-900 nmol and a probe concentration of 250 nmol. Under the optimal cycling conditions, primer concentrations of 700, 750, 800, 850 and 900 nmol were tested to determine the optimal concentration. A negative control (EpiTect PCR Control DNA Set, Qiagen) and no-template control were included in each plate.

Twenty microliters of quantitative reaction was prepared, mixed with oscillation and briefly centrifuged to remove bubbles. The above reaction mixtures were added to the middle row of the droplet generating cartridge, and 70 μL ddPCR Droplet Reader Oil (BIO-RAD) was added to the bottom row. The reagents were placed smoothly in the droplet generator and the reaction was started. The liquid in the top row of the droplet generating cartridge was transferred to a 96-well plate and then placed into a heat sealer to seal with a film. After sealing, the 96-well plate was placed into a C1000 TouchTM Thermal Cycler (BIO-RAD) for PCR. QuantaSoft was opened after 30 min of preheating of the QX200 Droplet Reader (BIO-RAD). At the end of PCR, the 96-well plate was placed into the Droplet Reader and processed under the sample information setting. When finished, the program was run, and the data were analyzed after droplet reading.

RESULTS

Optimization of bisulfite conversion

The recommended conversion time was 2 h 30 min according to the instructions of the EZ DNA

Methylation-Gold Kit. However, due to the small amount of circulating free DNA in blood and plasma, and the loss after conversion, we decided to optimize the conversion time for our assay. DNA was extracted from the blood and plasma of 16 GC patients for this experiment. After determining the concentration of ssDNA, each DNA sample was divided into 4 conditions. For bisulfite conversion, the initial input amount of blood DNA was 500 ng, the initial input amount of plasma DNA was 10 ng, and the sample volume was adjusted to 20 μL with sterilized deionized water. The conversion time was set at 1 h 30 min, 1 h 50 min, 2 h 10 min or 2 h 30 min, and ddPCR assay was conducted in these 4 conditions. The results are shown in Figure 1. By comparing the methylation rates of the same samples subjected to various conversion times, we concluded that the optimal conversion time for blood DNA was 2 h 10 min, and the optimal time for plasma DNA was 2 h 10 min and 2 h 30 min. To streamline the experimental operation, the conversion time was set as 2 h 10 min in subsequent experiments.

Selection of primers

The primers designed for the methylated RNF180 gene was used to conduct ddPCR assays with 100% methylated control DNA, and the data that reached more than 10000 droplets were considered valid data. After repeating experiments, we chose one pair of primers and probes with the best result based on the reproducibility, specificity, and detection rate. The ddPCR results of the tested primers are shown in Figure 2. The second pair of primers with good specificity and reproducibility was selected according to the results shown in the figure. Subsequently, primers and probes for unmethylated RNF180 gene were designed to calculate the methylation rate of the sample.

DdPCR assays

Because of the low concentration of circulating DNA in plasma and inevitable DNA loss after bisulfite conversion, it is conceivable that the plasma trace DNA could not be detected. To address this concern, 100% methylated control DNA with gradient concentration (Table 1) was used to determine the minimum LOD of ddPCR. The results are shown in Figure 3A. The standard curve was drawn based on the above detection data, and the regression equation was $y = 1.5264x + 0.0881$, $R^2 = 0.9911$, as shown in Figure 3B. We speculated that methylation could not be detected when the input of DNA was less than 0.1 ng. After the bisulfite conversion of blood and plasma DNA, the ssDNA concentrations were all above 0.5 ng/μL. Therefore, ddPCR was reliable for the detection of circulating methylated DNA. To determine the optimal ddPCR amplification condition, the amplification temperatures of 56 °C and 59 °C were compared, and the amplification cycles or 45 and 50 were tested. The result is illustrated in Figure 4. The optimum amplification temperature was 56 °C and the optimum cycle number was 50. Under the reaction conditions of 56 °C and 50 cycles, the primer concentrations of 700 nmol, 750 nmol, 800 nmol, 850 nmol and 900 nmol were compared. As shown in Figure 5, there was little difference among the five primer concentrations; thus, it could be adjusted according to the reaction condition and DNA input amount.

DISCUSSION

According to the statistical report on global cancer incidence and mortality in 2020 issued by the International Agency for Research on Cancer, GC has been listed as the fifth most common malignant tumor in the world, with 1089103 new cases compared with the previous year. As GC is usually diagnosed at an advanced stage, it has a high mortality rate. GC accounted for 7.7% of total cancer deaths globally in 2020, making it the fourth most common cause of cancer-related deaths[12]. RNF180 is a tumor suppressor gene involved in many important physiological processes *in vivo*, such as cell growth, differentiation, and tumorigenesis[13]. When RNF180 was abnormally expressed, a variety of physical, chemical, and biological factors were affected, resulting in decreased gene expression or corresponding protein dysfunction. It has been confirmed that the inactivation of RNF180 is associated with apoptosis, tumor invasion and metastasis[14,15]. Downregulation of RNF180 gene expression was related to hypermethylation in the promoter region, and the methylated RNF180 gene played an important role in the occurrence, development, prognosis of GC and infection of *H. pylori*[16,17]. DNA methylation is the most common chemical modification of nucleic acids. Mechanistically, methyltransferases catalyze methylation by selectively adding the methyl group to cytosine of CG dinucleotide and turning it into 5-methyl cytosine. DNA methylation occurs mainly in DNA fragments with high CG content and between 300 and 3000 bp in length (CpG islands)[18]. Currently, many studies have confirmed that DNA methylation can cause alterations in chromatin structure and DNA stability, thereby controlling gene expression and participating in the regulation of many biological processes, such as aging, nervous system development, occurrence and development of cancer, tumor heterogeneity, and drug resistance[19,20].

Current methods of GC screening and diagnosis in clinical practice all have certain shortcomings, such as invasiveness, sampling deviation, low accuracy and specificity, and long detection time. Liquid biopsy is a noninvasive procedure that uses circulating free DNA, circulating tumor cells or other compounds in patients' body fluids for diagnosis. Currently, circulating tumor cells, exosomes and

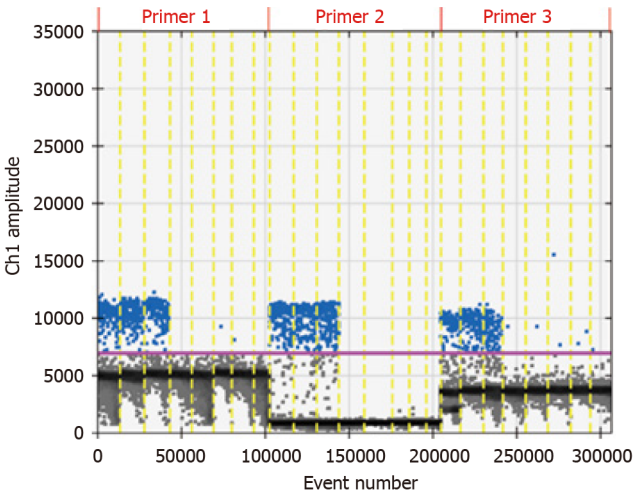

DOI: 10.4251/wjgo.v14.i10.2038

Figure 2 Fluorescence channel 1 results of methylated RNF180. The X-axis is the total number of droplets, the Y-axis is the fluorescence signal intensity, and the solid horizontal line (purple) is the signal threshold. The droplets with fluorescence signal intensity above the threshold line were positive droplets (blue). The droplets with fluorescence signal intensity below the threshold were negative droplets (gray).

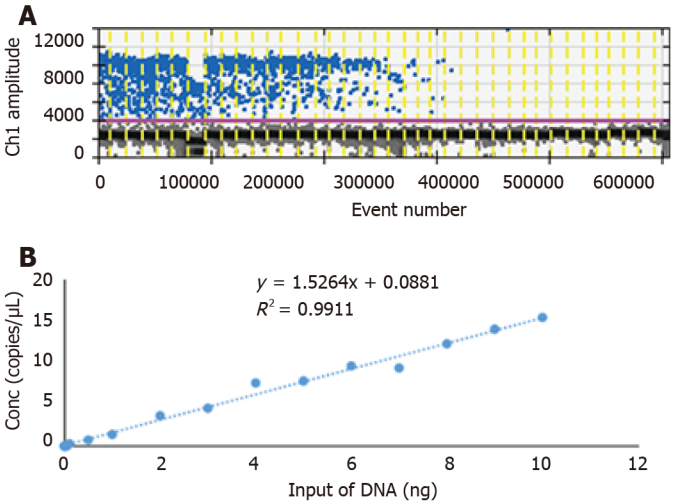

DOI: 10.4251/wjgo.v14.i10.2038

Figure 3 Limit of detection of droplet digital polymerase chain reaction. A: Diagram of the droplet digital polymerase chain reaction (ddPCR) results; B: Line graph of ddPCR limit of detection.

circulating nucleic acids are the main materials used in liquid biopsy of cancer. These circulating biomarkers are excreted from the tumor site into the blood, urine, saliva, or cerebrospinal fluid and can provide better insights into the evolution of tumor dynamics during treatment and disease progression. The most widely reported method has been detecting circulating free DNA in blood or plasma[21,22]. The detection of methylated DNA in GC patient plasma by liquid biopsy requires a highly sensitive and accurate method. DdPCR technology has the advantages of high accuracy, high sensitivity, and absolute quantitation and can be used to detect trace DNA. The ddPCR system emulsifies the aqueous PCR mixture into thermally stable oil droplets, while the real-time PCR of nucleic acid quantitation requires a standard curve obtained by diluting samples with known concentrations, which will be affected by laboratory and daily errors. A standard curve was not necessary for ddPCR, which can achieve absolute quantification by counting fluorescence-positive droplets and total droplets according to a Poisson distribution[23].

In this study, we developed a reliable ddPCR assay for the detection of methylated RNF180 in trace DNA. The results indicated that ddPCR could detect the methylated sites of trace circulating free DNA in plasma and achieve absolute quantification. When the DNA input was more than 0.1 ng, ddPCR could analyze the methylated sites of plasma DNA more accurately. This study proved that methylated RNF180 in blood or plasma can be further studied as a potential diagnostic biomarker of GC, and ddPCR assays of methylated DNA have promising applications in tumor screening and diagnosis. At present, this study only established a ddPCR detection method for the methylated RNF180 gene, but

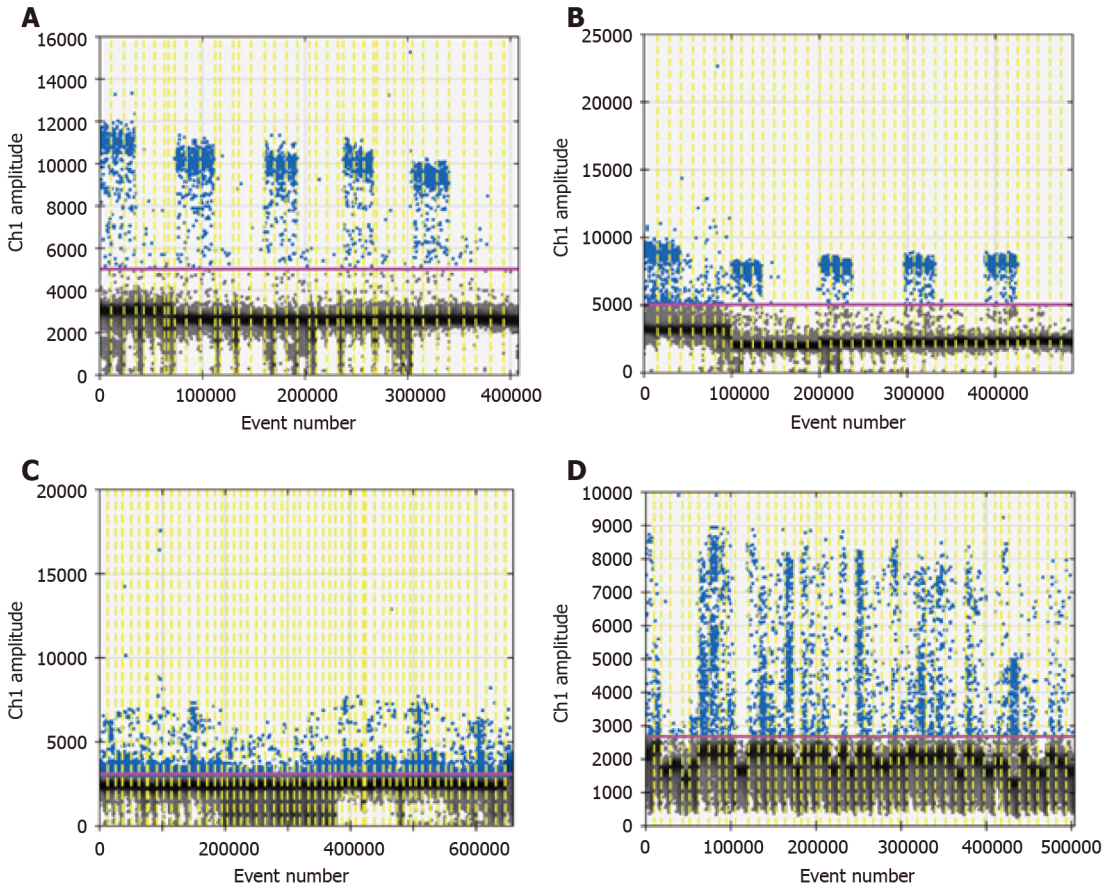

DOI: 10.4251/wjgo.v14.i10.2038

Figure 4 Optimization of amplification temperature and cycles. A and B: The droplet digital polymerase chain reaction (ddPCR) results of the amplification temperatures of 56 °C and 59 °C; C and D: The ddPCR results with 45 and 50 cycles of amplification.

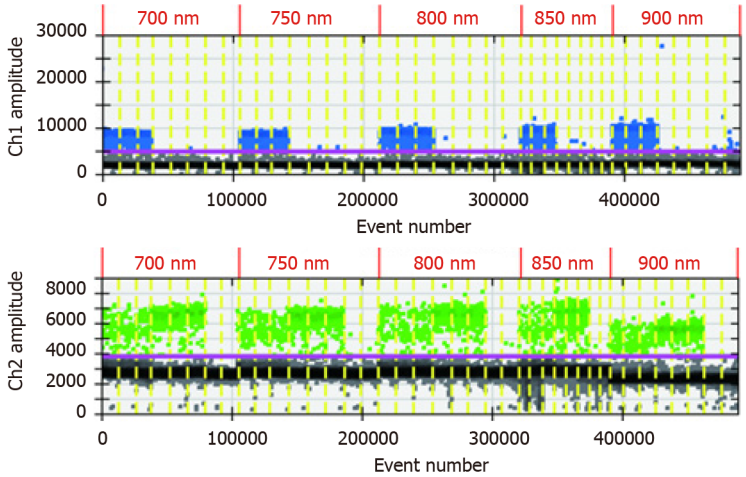

DOI: 10.4251/wjgo.v14.i10.2038

Figure 5 The droplet digital polymerase chain reaction results of different primer concentrations.

according to the experimental results, other methylated sites can also be analyzed by ddPCR technology. The subsequent detection of other GC methylation biomarkers in plasma can be explored.

CONCLUSION

In summary, a ddPCR assay was established to detect methylated RNF180, which is expected to be a new diagnostic biomarker for GC.

ARTICLE HIGHLIGHTS

Research background

Methylated ring finger protein 180 (RNF180) can be used as a potential biomarker for gastric cancer (GC) diagnosis.

Research motivation

Standard and sensitive of methylation detection methods for in plasma are urgently needed in clinical practice.

Research objectives

We aimed to use droplet digital polymerase chain reaction (ddPCR) to quantify the methylation level of the RNF180 gene. A reproducible ddPCR assay to detect methylated RNF180 from trace DNA was designed and optimized.

Research methods

The primer and probe were designed and selected, the conversion time of bisulfite was optimized, the ddPCR system was adjusted by primer concentration, amplification temperature and amplification cycles, and the detection limit of ddPCR was determined.

Research results

The best conversion time for blood DNA was 2 h 10 min, and that for plasma DNA was 2 h 10 min and 2 h 30 min. The results of ddPCR were better when the amplification temperature was 56 °C and the number of amplification cycles was 50. Primer concentrations showed little effect on the assay outcome. Therefore, the primer concentration could be adjusted according to the reaction system and DNA input. The assay required at least 0.1 ng of input DNA.

Research conclusions

In summary, a ddPCR assay was established to detect methylated RNF180, which is expected to be a new diagnostic biomarker for GC.

Research perspectives

The standard procedure of ddPCR in clinical practice should be performed and evaluated.

FOOTNOTES

Author contributions: Guo GH and An Y designed the study; Guo GH and Xie YB performed the research; Guo GH and Xie YB analyzed the date; Guo GH wrote the paper; Jiang T and An Y revised the manuscript for final submission; Guo GH and Xie YB contributed equally to this study; Jiang T and An Y are the co-corresponding authors.

Supported by the National Key Research and Development Program of China, No. 2020YFC2002700; the National Natural Science Foundation of China, No. 81972010; the CAMS Initiative for Innovative Medicine, No. 2016-I2M-1-007; and the Science Developing Funds of Navy General Hospital, No. CXPY201810.

Institutional review board statement: The study was reviewed and approved by the Ethics Committee of National Cancer Center/National Clinical Research Center for Cancer/Cancer Hospital, Chinese Academy of Medical Sciences and Peking Union Medical College.

Informed consent statement: The informed consent was waived by the Ethics Committee of National Cancer Center/National Clinical Research Center for Cancer/Cancer Hospital, Chinese Academy of Medical Sciences and Peking Union Medical College.

Conflict-of-interest statement: All the authors report no relevant conflicts of interest for this article.

Data sharing statement: No data was declared to share.

STROBE statement: The authors have read the STROBE Statement-checklist of items, and the manuscript was prepared and revised according to the STROBE Statement-checklist of items.

Country/Territory of origin: China

ORCID number: Guang-Hong Guo 0000-0002-0897-0410; Yi-Bin Xie 0000-0002-0255-3018; Tao Jiang 0000-0002-2127-9085; Yang An 0000-0002-2515-4562.

S-Editor: Wang JJ
L-Editor: A
P-Editor: Wang JJ

REFERENCES

1 **Ogawa M**, Mizugishi K, Ishiguro A, Koyabu Y, Imai Y, Takahashi R, Mikoshiba K, Aruga J. Rines/RNF180, a novel RING finger gene-encoded product, is a membrane-bound ubiquitin ligase. *Genes Cells* 2008; **13**: 397-409 [PMID: 18363970 DOI: 10.1111/j.1365-2443.2008.01169.x]
2 **Sun W**, Ma G, Zhang L, Wang P, Zhang N, Wu Z, Dong Y, Cai F, Chen L, Liu H, Liang H, Deng J. DNMT3A-mediated silence in ADAMTS9 expression is restored by RNF180 to inhibit viability and motility in gastric cancer cells. *Cell Death Dis* 2021; **12**: 428 [PMID: 33931579 DOI: 10.1038/s41419-021-03628-5]
3 **Wu Z**, Liu H, Sun W, Du Y, He W, Guo S, Chen L, Zhao Z, Wang P, Liang H, Deng J. RNF180 mediates STAT3 activity by regulating the expression of RhoC *via* the proteasomal pathway in gastric cancer cells. *Cell Death Dis* 2020; **11**: 881 [PMID: 33082325 DOI: 10.1038/s41419-020-03096-3]
4 **Han F**, Sun LP, Liu S, Xu Q, Liang QY, Zhang Z, Cao HC, Yu J, Fan DM, Nie YZ, Wu KC, Yuan Y. Promoter methylation of RNF180 is associated with H.pylori infection and serves as a marker for gastric cancer and atrophic gastritis. *Oncotarget* 2016; **7**: 24800-24809 [PMID: 27050149 DOI: 10.18632/oncotarget.8523]
5 **Deng J**, Liang H, Ying G, Zhang R, Wang B, Yu J, Fan D, Hao X. Methylation of CpG sites in RNF180 DNA promoter prediction poor survival of gastric cancer. *Oncotarget* 2014; **5**: 3173-3183 [PMID: 24833402 DOI: 10.18632/oncotarget.1888]
6 **Zhang X**, Zhang X, Sun B, Lu H, Wang D, Yuan X, Huang Z. Detection of aberrant promoter methylation of RNF180, DAPK1 and SFRP2 in plasma DNA of patients with gastric cancer. *Oncol Lett* 2014; **8**: 1745-1750 [PMID: 25202403 DOI: 10.3892/ol.2014.2410]
7 **Hamashima C**; Systematic Review Group and Guideline Development Group for Gastric Cancer Screening Guidelines. Update version of the Japanese Guidelines for Gastric Cancer Screening. *Jpn J Clin Oncol* 2018; **48**: 673-683 [PMID: 29889263 DOI: 10.1093/jjco/hyy077]
8 **Chivu-Economescu M**, Necula L, Matei L, Dragu D, Bleotu C, Diaconu CC. Clinical Applications of Liquid Biopsy in Gastric Cancer. *Front Med (Lausanne)* 2021; **8**: 749250 [PMID: 34651002 DOI: 10.3389/fmed.2021.749250]
9 **Cheung AH**, Chow C, To KF. Latest development of liquid biopsy. *J Thorac Dis* 2018; **10**: S1645-S1651 [PMID: 30034830 DOI: 10.21037/jtd.2018.04.68]
10 **Pinheiro LB**, Coleman VA, Hindson CM, Herrmann J, Hindson BJ, Bhat S, Emslie KR. Evaluation of a droplet digital polymerase chain reaction format for DNA copy number quantification. *Anal Chem* 2012; **84**: 1003-1011 [PMID: 22122760 DOI: 10.1021/ac202578x]
11 **Diefenbach RJ**, Lee JH, Rizos H. Methylated circulating tumor DNA as a biomarker in cutaneous melanoma. *Melanoma Manag* 2020; **7**: MMT46 [PMID: 32922728 DOI: 10.2217/mmt-2020-0010]
12 **Sung H**, Ferlay J, Siegel RL, Laversanne M, Soerjomataram I, Jemal A, Bray F. Global Cancer Statistics 2020: GLOBOCAN Estimates of Incidence and Mortality Worldwide for 36 Cancers in 185 Countries. *CA Cancer J Clin* 2021; **71**: 209-249 [PMID: 33538338 DOI: 10.3322/caac.21660]
13 **Han F**, Liu S, Jing J, Li H, Yuan Y, Sun LP. Identification of High-Frequency Methylation Sites in RNF180 Promoter Region Affecting Expression and Their Relationship with Prognosis of Gastric Cancer. *Cancer Manag Res* 2020; **12**: 3389-3399 [PMID: 32494203 DOI: 10.2147/CMAR.S246995]
14 **Cheung KF**, Lam CN, Wu K, Ng EK, Chong WW, Cheng AS, To KF, Fan D, Sung JJ, Yu J. Characterization of the gene structure, functional significance, and clinical application of RNF180, a novel gene in gastric cancer. *Cancer* 2012; **118**: 947-959 [PMID: 21717426 DOI: 10.1002/cncr.26189]
15 **Wang H**, Lu Y, Wang M, Wu Y, Wang X, Li Y. Roles of E3 ubiquitin ligases in gastric cancer carcinogenesis and their effects on cisplatin resistance. *J Mol Med (Berl)* 2021; **99**: 193-212 [PMID: 33392633 DOI: 10.1007/s00109-020-02015-5]
16 **Deng J**, Liang H, Zhang R, Hou Y, Liu Y, Ying G, Pan Y, Hao X. Clinical and experimental role of ring finger protein 180 on lymph node metastasis and survival in gastric cancer. *Br J Surg* 2016; **103**: 407-416 [PMID: 26805552 DOI: 10.1002/bjs.10066]
17 **Xie XM**, Deng JY, Hou YC, Cui JL, Wu WP, Ying GG, Dong QP, Hao XS, Liang H. Evaluating the clinical feasibility: The direct bisulfite genomic sequencing for examination of methylated status of E3 ubiquitin ligase RNF180 DNA promoter to predict the survival of gastric cancer. *Cancer Biomark* 2015; **15**: 259-265 [PMID: 25769451 DOI: 10.3233/CBM-150466]
18 **Lissa D**, Robles AI. Methylation analyses in liquid biopsy. *Transl Lung Cancer Res* 2016; **5**: 492-504 [PMID: 27826530 DOI: 10.21037/tlcr.2016.10.03]
19 **Liu C**, Jiao C, Wang K, Yuan N. DNA Methylation and Psychiatric Disorders. *Prog Mol Biol Transl Sci* 2018; **157**: 175-232 [PMID: 29933950 DOI: 10.1016/bs.pmbts.2018.01.006]

20 **Shinjo K**, Hara K, Nagae G, Umeda T, Katsushima K, Suzuki M, Murofushi Y, Umezu Y, Takeuchi I, Takahashi S, Okuno Y, Matsuo K, Ito H, Tajima S, Aburatani H, Yamao K, Kondo Y. A novel sensitive detection method for DNA methylation in circulating free DNA of pancreatic cancer. *PLoS One* 2020; **15**: e0233782 [PMID: 32520974 DOI: 10.1371/journal.pone.0233782]

21 **Petit J**, Carroll G, Gould T, Pockney P, Dun M, Scott RJ. Cell-Free DNA as a Diagnostic Blood-Based Biomarker for Colorectal Cancer: A Systematic Review. *J Surg Res* 2019; **236**: 184-197 [PMID: 30694754 DOI: 10.1016/j.jss.2018.11.029]

22 **Lehmann-Werman R**, Neiman D, Zemmour H, Moss J, Magenheim J, Vaknin-Dembinsky A, Rubertsson S, Nellgård B, Blennow K, Zetterberg H, Spalding K, Haller MJ, Wasserfall CH, Schatz DA, Greenbaum CJ, Dorrell C, Grompe M, Zick A, Hubert A, Maoz M, Fendrich V, Bartsch DK, Golan T, Ben Sasson SA, Zamir G, Razin A, Cedar H, Shapiro AM, Glaser B, Shemer R, Dor Y. Identification of tissue-specific cell death using methylation patterns of circulating DNA. *Proc Natl Acad Sci U S A* 2016; **113**: E1826-E1834 [PMID: 26976580 DOI: 10.1073/pnas.1519286113]

23 **Kuypers J**, Jerome KR. Applications of Digital PCR for Clinical Microbiology. *J Clin Microbiol* 2017; **55**: 1621-1628 [PMID: 28298452 DOI: 10.1128/JCM.00211-17]

World Journal of Gastrointestinal Oncology

Submit a Manuscript: https://www.f6publishing.com

World J Gastrointest Oncol 2022 October 15; 14(10): 2048-2060

DOI: 10.4251/wjgo.v14.i10.2048

ISSN 1948-5204 (online)

ORIGINAL ARTICLE

Prospective Study

Long-term follow-up of HER2 overexpression in patients with rectal cancer after preoperative radiotherapy: A prospective cohort study

Nan Chen, Chang-Long Li, Yi-Fan Peng, Yun-Feng Yao

Specialty type: Oncology

Provenance and peer review: Unsolicited article; Externally peer reviewed.

Peer-review model: Single blind

Peer-review report's scientific quality classification

Grade A (Excellent): A
Grade B (Very good): B, B
Grade C (Good): 0
Grade D (Fair): 0
Grade E (Poor): 0

P-Reviewer: Bartholomeyczik S, Germany; Shinozaki E, Japan; Yano M, Japan

Received: March 1, 2022
Peer-review started: March 1, 2022
First decision: April 19, 2022
Revised: May 17, 2022
Accepted: August 24, 2022
Article in press: August 24, 2022
Published online: October 15, 2022

Nan Chen, Chang-Long Li, Yi-Fan Peng, Yun-Feng Yao, Department of Gastrointestinal Surgery, Ward III, Key laboratory of Carcinogenesis and Translational Research (Ministry of Education/Beijing), Peking University Cancer Hospital and Institute, Beijing 100142, China

Corresponding author: Nan Chen, MD, PhD, Associate Professor, Department of Gastrointestinal Surgery, Ward III, Key laboratory of Carcinogenesis and Translational Research (Ministry of Education/Beijing), Peking University Cancer Hospital and Institute, No. 52 Fucheng Road, Haidian District, Beijing 100142, China. chennanpku@126.com

Abstract

BACKGROUND

The role of HER2 overexpression in rectal cancer is controversial.

AIM

To assess the role of HER2 overexpression in the long-term prognosis of rectal cancer.

METHODS

Data from patients with locally advanced rectal cancer who underwent total mesorectal excision after short-course radiotherapy at Beijing Cancer Hospital between May 2002 and October 2005 were collected. A total of 151 tissue samples of rectal cancer were obtained using rigid proctoscopy before neoadjuvant radiotherapy, followed by immunohistochemistry and fluorescence *in situ* hybridisation to determine the patients' HER2 expression status. Univariate and multivariate analyses of the associations between the clinicopathological factors and HER2 status were performed. Survival was estimated and compared using the Kaplan-Meier method based on HER2 expression status, and the differences between groups were verified using the log-rank test.

RESULTS

A total of 151 patients were enrolled in this study. A total of 27 (17.9%) patients were ultimately confirmed to be HER2-positive. The follow-up duration ranged from 9 mo to 210 mo, with a median of 134 mo. Distant metastasis and local recurrence occurred in 60 (39.7%) and 24 (15.9%) patients, respectively. HER2 positivity was significantly associated with the pre-treatment lymph node stage (pre-N) (P = 0.040), while there were no differences between HER2 status and age, sex, preoperative CEA levels (pre-CEA), T stage, and lympho-vascular invasion. In terms of prognosis, HER2 overexpression was correlated with distant meta-

stasis (P = 0.002) rather than local recurrence (P > 0.05). The multivariate analysis demonstrated that elevated pre-CEA [P = 0.002, odds ratio (OR) = 3.277, 97.5% confidence interval (CI): 1.543-7.163], post N(+) (P = 0.022, OR = 2.437, 97.5%CI: 1.143-5.308) and HER2(+) (P = 0.003, OR = 4.222, 97.5%CI: 1.667-11.409) were risk factors for distant metastasis. The survival analysis showed that there were significant differences between rectal cancer patients in terms of disease-free survival (DFS) [hazard ratio: 1.69 (95%CI: 0.91-3.14); P = 0.048] and overall survival (OS) [1.95 (1.05-3.63); P = 0.0077].

CONCLUSION

HER2 overexpression is a potential biomarker for predicting lymph node metastasis and distant metastasis, which are associated with worse long-term DFS and OS in rectal cancer patients with locally advanced disease.

Key Words: HER2; Rectal cancer; Distant metastasis; Local recurrence; Survival

Core Tip: Long-term follow-up of rectal cancer patients treated with neoadjuvant radiotherapy demonstrated that pre-treatment HER2 overexpression was significantly correlated with lymph node metastasis and long-term distant metastasis. Furthermore, HER2 overexpression, elevated CEA and lymph node positivity were independent risk factors, predictive for poorer survival.

Citation: Chen N, Li CL, Peng YF, Yao YF. Long-term follow-up of HER2 overexpression in patients with rectal cancer after preoperative radiotherapy: A prospective cohort study. *World J Gastrointest Oncol* 2022; 14(10): 2048-2060

URL: https://www.wjgnet.com/1948-5204/full/v14/i10/2048.htm

DOI: https://dx.doi.org/10.4251/wjgo.v14.i10.2048

INTRODUCTION

Colorectal cancer (CRC) is a great challenge for people worldwide and is the 3rd most commonly diagnosed cancer and the 2nd leading cause of cancer-related deaths. In China, the incidence and death rates of CRC are the 3rd and 5th highest, respectively[1,2]. In 2020, there were about 43340 new cases of rectal cancer in the United States each year, while this number was 376000 in China[2,3]. Due to its insidious onset, most patients are diagnosed with locally advanced disease, and approximately 20% of CRC patients have distant metastasis at the time of diagnosis[4]. A series of studies, including the SWEDISH RECTAL CANCER TRIAL in the 1990s[5], the CAO/ARO/AIO-94 trial performed in Germany in the early 21st century[6], and the subsequent EORTC22921 study[7], have shown the benefits of tumour regression, sphincter preservation, and decreased local recurrence, establishing the status of neoadjuvant radiotherapy. In recent years, the treatment mode of rectal cancer guided by TNM staging has been evolving; notably, the long-term survival rates have appeared to remain stable[8-10]. In addition, even patients with the same TNM stage may have different prognoses, prompting us to search for new therapeutic biomarkers to improve patient outcomes. In recent years, the molecular mechanisms of CRC have been further studied, and biological markers such as RAS and BRAF mutations have been identified as prognostic targets. In contrast, HER2, a member of the epidermal growth factor receptor family of receptor tyrosine kinases, is highly expressed in a variety of tumour cells. HER2 is currently considered a potential target for CRC therapy, as reported by previous findings [11]. Although there have been several studies on the role of HER2 in CRC, the results are controversial and lack long-term outcomes. The present study aimed to report the long-term outcomes of patients with HER2 overexpression in locally advanced rectal cancer with preoperative radiotherapy.

MATERIALS AND METHODS

Data from patients with locally advanced rectal cancer who underwent total mesorectal excision (TME) after short-course radiotherapy at the Beijing Cancer Hospital between May 2002 and October 2005 were collected. All patients underwent preoperative staging using magnetic resonance imaging, computed tomography, endorectal ultrasonography, and/or endoscopy. Each patient enrolled in our study satisfied the following criteria: (1) Age > 18 years; (2) Primary rectal adenocarcinoma below the

peritoneal folds; (3) Clinically staged as cT3-4 and/or N+ rectal tumours, with a tumour that could be resected radically; and (4) Willingness to participate in long-term follow-up. Patients were excluded if they: (1) Had synchronous tumours or a history of other malignant tumours within the previous 5 years; (2) Had a previous history of cytotoxic chemotherapy, previous pelvic radiation therapy, or a known hypersensitivity to any drug included in the treatment protocol; (3) Had a diagnosis of hereditary nonpolyposis colorectal carcinoma; (4) Were being treated with other experimental drugs or had previously participated in a clinical trial of other experimental agents for rectal carcinoma; and (5) Had clinical evidence of distant metastasis. There were no restrictions based on sex, race, or disability.

All patients received 30 Gy/10 F/2 W neoadjuvant radiotherapy (SIMENS PRIMUS 2916 Linear Accelerator), and radical surgeries (LAR or APR) were performed 2 wk after the end of radiotherapy, according to the TME principle. All patients received adjuvant chemotherapy (standard regimen, 5-FU or capecitabine) within 6 mo after surgery, according to the pathologic stage. Patient epidemiological information and primary tumour features, including distance from the anal verge and TNM stage before and after neoadjuvant radiotherapy, were collected prospectively. Regular follow-up visits were performed every 3 mo for the first 2 years, and then every 6 mo for a total of 5 years. After 5 years, follow-up was performed once per year. Follow-up examinations included blood tests for CEA and CA199, thoracic and abdominal/pelvic computed tomography or magnetic resonance imaging, and enteroscopy for timely detection of recurrence or metastasis. The study was approved by the medical ethics committee of the Peking University Cancer Hospital, and the requirement for informed consent was waived.

Immunohistochemical evaluation

All patients underwent rigid proctoscopy before neoadjuvant therapy, and a sufficient amount of tumour tissue was obtained. HER2 expression was evaluated using immunohistochemistry. Immunostained samples were examined and scored independently and in a blinded manner by two experienced pathologists. The scoring criteria were as follows[12]: 0 (no staining), 1+ (1%-25% positive cells), 2+ (26%-75% positive cells), or 3+ (76%-100% positive cells). A score of 0 or 1+ was considered negative (low expression) and a score of 3+ was considered positive (overexpression). In samples when the score was 2+ (moderate expression), fluorescence *in situ* hybridization (FISH) was performed to confirm the HER2 expression.

Statistical analysis

Data were analysed using R4.1.0 software. The 'survival' and 'survminer' package were used for statistical analysis, and the 'ggplot2' package was used for plotting. Categorical variables were assessed using the chi-square (2 × 2) or Fisher's exact test (2 × C) when applicable. Multivariate analysis was performed using a binary logistic regression model (forward: LR). Survival analysis was performed using the Kaplan-Meier method, and the differences between groups were verified using the log-rank test. P values < 0.05 were considered significant statistically.

RESULTS

In our previous reports, a total of 142 rectal cancer patients with locally advanced diseases were enrolled, followed by nine more patients meeting the inclusion criteria; finally, 151 patients were included in the final analysis (Figure 1). The mean age was 55.85 ± 13.26 years, with 93 (61.6%) men and 58 (38.4%) women. The patient characteristics are listed in Table 1.

The immunohistochemical results showed that HER2 over-expression was detected in 16.6% (25/151) of the tissue samples, with low expression (0-1+) in 73.51% (111/151) and moderate expression in 9.93% (15/151) of samples. In samples (n = 2) that scored 2+, we confirmed the positive expression of HER2 using FISH. A total of 27/151 (17.9%) samples were ultimately confirmed to have HER2 positivity. The median follow-up period for all patients was 134 mo. Distant metastasis and local recurrence occurred in 60 (39.7%) and 24 (15.9%) patients, respectively.

Correlation between HER2 overexpression and clinicopathological parameters

There were no significant differences between HER2 status and age, sex, preoperative CEA levels (pre-CEA), T stage, lymph-vascular invasion (LVI), and local recurrence. HER2 positivity was associated with pre-treatment N(+) stage (pre-N; P = 0.040) and distant metastasis (P = 0.002). Distant metastasis occurred in 66.7% (18/27) of HER2-positive patients compared to in 33.9% (42/124) of HER2-negative patients (Table 2).

Correlation between distant metastasis and clinicopathological parameters

Univariate analysis showed that pre-CEA, pre-treatment T stage (pre-T), post-treatment N status (Post-N), and HER2 status were correlated with distant metastasis (Table 3). These variables were further included in the binary logistic regression analysis, and the P value (0.052) of post-T was close to 0.05; therefore, it was also included in the multivariate analysis. The final analysis showed that elevated pre-

Table 1 Clinicopathological characteristics of the enrolled cohort (*n* = 151)

Characteristic	Result
Age diagnosis (yr)	55.85 ± 13.26
Gender (%)	
Male	93 (61.6)
Female	58 (38.4)
Distance to anal verge (cm) (%)	4.91 ± 2.04
> 6	45 (29.8)
≤ 6	106 (70.2)
Pre-CEA (%)	
Normal range	98 (64.9)
Elevated	53 (35.1)
Pre-T (%)	
T1	2 (1.3)
T2	10 (6.6)
T3	133 (88.1)
T4	6 (4.0)
Pre-N (%)	
N0	38 (25.2)
N+	113 (74.8)
Post-T (%)	
pT0	7 (4.6)
pT1	6 (4.0)
pT2	48 (31.8)
pT3	84 (55.6)
pT4	4 (4.0)
Post-N (%)	
pN0	89 (58.9)
pN+	62 (41.1)
Tumor regression grade (%)	
Grade 0	9 (6.3)
Grade 1	34 (23.9)
Grade 2	42 (29.6)
Grade 3	57 (40.1)
HER2 (%)	
-	124 (82.1)
+	27 (17.9)
LVI (%)	
+	20 (13.2)
-	131 (86.8)
Median follow-up period	134
Distant metastasis, number (%)	
Yes	60 (39.7)

No	91 (60.3)
Local recurrence, number (%)	
Yes	24 (15.9)
No	127 (84.1)

Pre-CEA: Preoperative CEA; LVI: Lympho-vascular invasion.

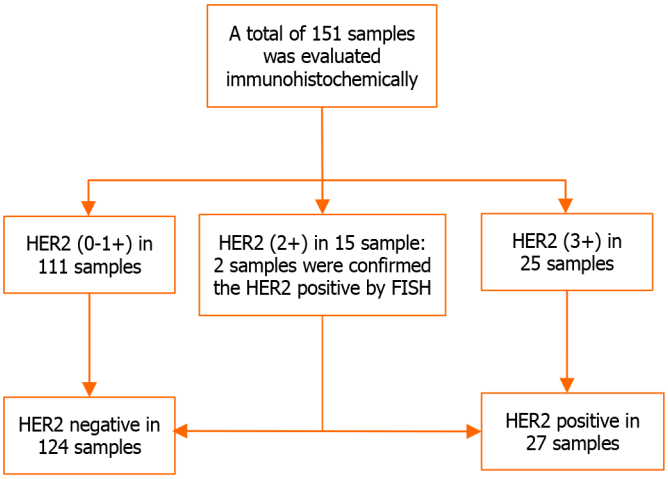

DOI: 10.4251/wjgo.v14.i10.2048

Figure 1 Flowchart of cohorts and the distribution of HER2 expression. FISH: Fluorescence *in situ* hybridization.

CEA [P = 0.002, odds ratio (OR) = 3.277, 97.5% confidence interval (CI): 1.543-7.163], post-N(+) (P = 0.022, OR = 2.437, 97.5%CI: 1.143-5.308), and HER2(+) (P = 0.003, OR = 4.222, 97.5%CI: 1.667-11.409) were risk factors for distant metastasis, as demonstrated in Table 4.

Survival analysis

The follow-up time ranged from 9 mo to 210 mo, with a median follow-up of 134 mo. During the follow-up period, 18 (66.7%) of the 27 HER2-positive patients experienced distant metastasis or recurrence, and 2 of these patients suffered from both metastasis and recurrence; thus, in terms of disease progression, there were a total of 18 (66.7%) distant metastases and 2 (7.4%) local recurrence events. The median disease-free survival (DFS) of HER2-positive patients was 43 mo. For HER2-negative patients, 57 (46.0%) out of 124 developed distant metastasis or recurrence. Death occurred in 20 (74.1%) of 27 HER2(+) patients, with a median overall survival (OS) of 58 mo, and in 60 (48.4%) of 124 HER2(-) patients, with a median OS of 133 mo. There were significant differences between the HER2-positive group and HER2-negative group with respect to both DFS [hazard ratio (HR): 1.69 (95%CI: 0.91-3.14); P = 0.048] and OS [1.95 (1.05-3.63); P = 0.0077], as shown in Figure 2A and B.

DISCUSSION

HER2, also known as C-erbB-2, neu, or p185, is a member of the EGFR/ErbB family. It is a transmembrane protein encoded by the HER2 proto-oncogene, which participates in the signalling transduction pathway leading to cell growth and differentiation, potentially affecting the invasion and migration of tumour cells in the network of tumorigenesis. Previous studies have confirmed that HER2 is one of a predictors for poor prognosis in breast cancer, gastric cancer, endometrial cancer, and other tumours, in which HER2 overexpression is associated with poorer tumour biological properties[13-17]. In recent years, HER2 overexpression has also been found in CRC tumours; however, the data reported in the literature vary greatly, with positivity rates of approximately 2.6%-17%[18-22]. The effects of HER2 on the prognosis of CRC are also controversial, and the relationship between HER2 and the prognosis of patients with CRC remains under discussion. Our study is a 10-year long-term follow-up report on the prognosis of HER2 overexpression in locally advanced rectal cancer, which is of great significance in exploring the role of HER2 in rectal cancer.

Table 2 Correlations among HER2 expression and the clinicopathological parameters

Variable	HER2- (%)	HER2+ (%)	χ^2	*P* value
Age (yr)			0.558	0.455
< 60	74 (59.7)	14 (51.9)		
≥ 60	50 (40.3)	13 (48.1)		
Sex			2.166	0.141
Male	73 (58.9)	20 (74.1)		
Female	51 (41.1)	7 (25.9)		
Pre-CEA			0.045	0.832
Normal range	80 (64.5)	18 (66.7)		
Elevated	44 (35.5)	9 (33.3)		
Distance to anal verge (cm)			0.236	0.627
> 6	38 (30.6)	7 (25.9)		
≤ 6	86 (69.4)	20 (74.1)		
Pre-T				0.694[1]
T1-2	11	1		
T3-4	113	26		
Pre-N			4.235	**0.040**
N0	27 (21.8)	11 (40.7)		
N+	97 (78.2)	16 (59.3)		
Post-T			1.583	0.208
T1-2	53	8		
T3-4	71	19		
Post-N			1.582	0.208
N0	76 (61.3)	13 (48.1)		
N+	48 (38.7)	14 (51.9)		
LVI				
+	17 (13.7)	3 (11.1)	0.002	0.962[2]
-	107 (86.3)	24 (88.9)		
Distant metastasis			9.959	**0.002**
+	42 (33.9)	18 (66.7)		
-	82 (66.1)	9 (33.3)		
Local recurrence			1.083	0.298[2]
+	22 (17.7)	2 (7.4)		
-	102 (82.3)	25 (92.6)		

[1]Fisher's exact test.
[2]Logistic regression model.
LVI: Lympho-vascular invasion.

Correlation between HER2 and local/distant metastasis of rectal cancer

In our study, the results from the correlation analysis using the chi-square test revealed that there were no significant differences between HER2 status and age, sex, pre-CEA, T stage, LVI, and local recurrence, which was consistent with the majority of previous reported results. Furthermore, HER2 positivity was associated with pre-N(+) (P = 0.040) and distant metastasis (P = 0.002), which is consistent with our previous short-term results[12]. Similar to our results, a study involving 1645 cases of primary colorectal adenocarcinoma showed that HER2 overexpression was associated with lymph node

Table 3 Correlations among distant metastasis and the clinicopathological parameters

Variable	Distant metastasis		χ^2	*P* value
	- (%)	+ (%)		
Age (yr)			0.121	0.728
< 60	52 (59.1)	36 (40.9)		
≥ 60	39 (61.9)	24 (38.1)		
Sex			0.446	0.504
Male	58 (62.4)	35 (37.6)		
Female	33 (56.9)	25 (43.1)		
Pre-CEA			9.704	**0.002**
Normal range	68 (69.4)	30 (30.6)		
Elevated	23 (43.4)	30 (56.6)		
Distance to anal verge (cm)			0.103	0.749
> 6	28 (62.2)	17 (37.8)		
≤ 6	63 (59.4)	43 (40.6)		
Pre-T				0.221[1]
T1-2	5	7		
T3-4	86	53		
Pre-N			0.001	1.000
N0	23 (60.5)	15 (39.5)		
N+	68 (60.2)	45 (39.8)		
Post-T			3.782	0.052
T1-2	43	18		
T3-4	48	42		
Post-N			7.995	**0.005**
N0	62 (69.7)	27 (30.3)		
N+	29 (46.8)	33 (53.2)		
LVI			1.014	0.314
+	10 (50.0)	10 (50.0)		
-	81 (61.8)	50 (38.2)		
HER2, number			9.959	**0.002**
-	82 (66.1)	42 (33.9)		
+	9 (33.3)	18 (66.7)		

[1]Fisher's exact test.

metastasis[23]. In addition, logistic regression was used to verify the predictive effect of HER2 overexpression on distant metastasis in rectal cancer. Univariate and multivariate analyses demonstrated that HER2 overexpression was associated with distant metastasis. The risk of distant metastasis in HER2-positive patients was 4.222 times higher than that in HER2-negative patients (P = 0.003, OR = 4.222, 97.5%CI: 1.667-11.409). We propose that these results suggest that overexpression of HER2 may promote the aggressiveness of rectal cancer. As in breast and gastric cancers, HER2 might play an important role in local failure and distant metastasis in patients with rectal cancer, featuring a higher possibility of lymph node metastasis.

Our results also showed that two other risk factors predictive of distant metastasis of rectal cancer were elevated pre-CEA (P = 0.002, OR = 3.277, 97.5%CI: 1.543-7.163) and post-N(+) (P = 0.022, OR = 2.437, 97.5%CI: 1.143-5.308). Studies have shown that pre-CEA is associated with neoadjuvant treatment response and clinical outcomes in patients with rectal cancer as a predictor of poorer prognoses[24-27].

Table 4 Multivariate logistic regression analysis results

Variable	Odds ratio	97.5%CI	*P* value
CEA level before radiotherapy			
Normal range	1		
Elevated	3.277	1.543-7.163	0.002
Post-treatment N			
N0	1		
N+	2.437	1.143-5.308	0.022
HER2			
-	1		
+	4.222	1.667-11.409	0.003

CI: Confidence interval.

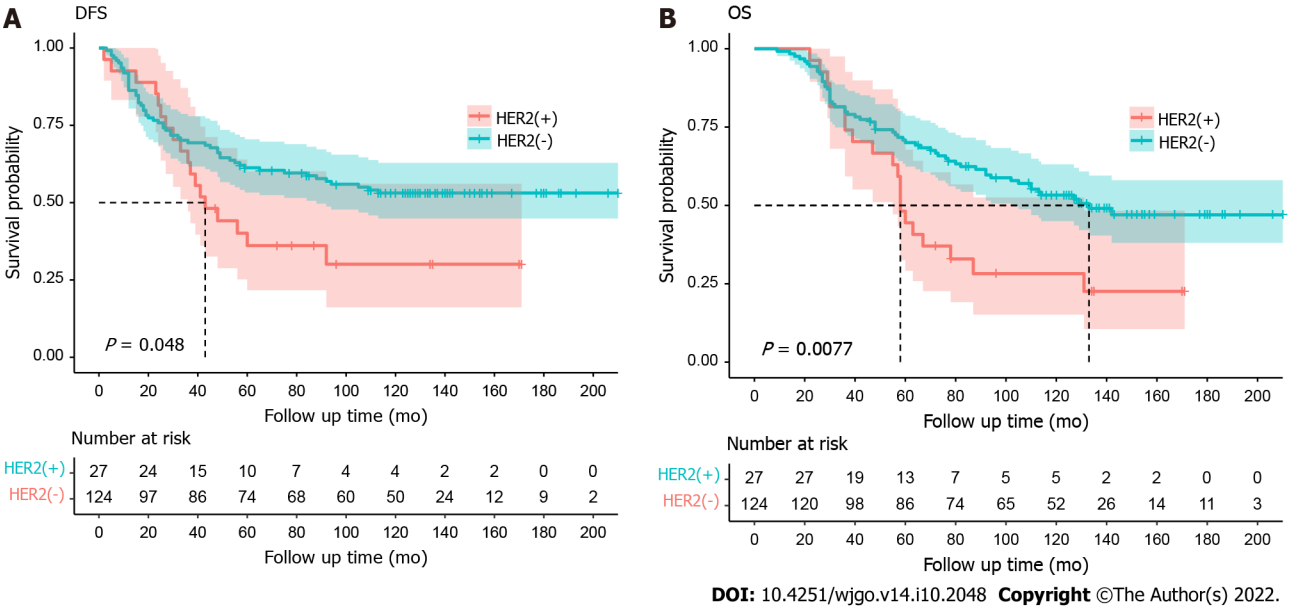

DOI: 10.4251/wjgo.v14.i10.2048

Figure 2 Kaplan-Meier survival analysis of disease-free survival and overall survival rates in relation to HER2 status. A: HER2 overexpression in rectal cancers is correlated with a shorter disease-free survival, *P* = 0.048; B: HER2 overexpression in rectal cancers is correlated with a shorter overall survival, *P* = 0.0077. DFS: Disease-free survival; OS: Overall survival.

Similarly, LN(+) status after neoadjuvant therapy was related to higher tumour stages and poorer treatment responses, which are obviously related to the prognoses of patients[28]. Therefore, we assumed that these might explain the increased rate of distant metastasis in elevated pre-CEA and post-N(+) patients.

Correlation between HER2 and long-term DFS/OS

A few studies have suggested that HER2 overexpression is a poor prognostic factor for CRC, playing an important role in its progression[29-31]. In the PETACC-8 trial, 1689 patients with stage III colon cancer received postoperative adjuvant chemotherapy. The results showed that HER2 overexpression was associated with a shorter time to recurrence [HR: 1.55 (95%CI: 1.02-2.36) *P* = 0.04] and shorter OS [HR: 1.57 (0.99-2.5) *P* = 0.05][32]. A meta-analysis of 1761 CRC patients from 11 studies by Li *et al*[33] showed that HER2 overexpression was negatively correlated with OS, and similar results were obtained in different subgroups, although the authors admitted that this effect might not be significant. However, some studies have shown that HER2 overexpression is not associated with the prognosis of CRC. In a large-pool study, three randomised controlled trials (the QUASAR, FOCUS, and PICCOLO trials) were analysed. Within a total of 3256 CRC patients enrolled, the results showed that there was no correlation between HER2 overexpression and survival (either progression-free survival or OS)[34].

Some studies have shown that cytoplasmic HER2-positive patients are associated with longer survival as an independent risk factor in Duke C stage patients[35]. In our short-term results report (median follow-up: 38 mo), the association between HER2 positivity and survival (DFS or OS) did not reach statistical significance. These results may be related to the short follow-up period. In this long-term study, with a median follow-up time of 134 mo, more events of distant metastasis or local recurrence occurred: 18 of 27 HER2-positive patients (66.7%) experienced disease progression, including 18 distant metastases and 2 Local recurrence events. There were significant differences between the HER2-positive and HER2-negative groups with respect to both DFS [HR: 1.69 (95%CI: 0.91-3.14); P = 0.048] and OS [HR: 1.95 (95%CI: 1.05-3.63); P = 0.0077] (Figures 1 and 2). The median DFS of HER2-positive patients was 43 mo. Of the 124 HER2-negative patients, 57 (46.0%) had distant metastases or recurrence events. Death occurred in 20 of 27 (74.1%) HER2-positive patients and 60 of 124 (48.4%) HER2-negative patients. The median OS was significantly shorter in HER2-positive patients than in HER2-negative patients (58 mo *vs* 133 mo). We hypothesis that HER2 overexpression, as a proto-oncogene, may be associated with increased tumour recurrence and poor prognosis. One explanation might be related to HER2's inhibition of tumour cell apoptosis, resulting in tumour cell proliferation and acceleration of tumour aggressiveness. This suggests that, in order to pay special attention to local recurrence or distant metastasis, regular postoperative follow-up might be particularly important for patients with HER2-positive diseases, thereby improving their long-term survival. It can also provide possible suggestions for the enhanced treatment of these patients (combined with targeted therapy).

Correlation between HER2 and anti-HER2 targeted therapy

Recurrence and distant metastasis have been the main causes of treatment failure for locally advanced rectal cancer, despite many efforts having been made. The effect of anti-HER2 targeted drugs, such as trastuzumab and lapatinib, on breast cancer with high HER2 expression has been confirmed by several international multicentre open randomised controlled studies[36,37]. Studies have shown that metastatic CRC with wild-type RAS and HER2 overexpression might benefit from HER2 dual-targeted therapy[38,39]. Other studies have shown that trastuzumab, a HER2 inhibitor, can inhibit colony formation in colon cancer cells and reduce the viability of CRC cells *in vitro*[40]. Although this study did not involve targeted therapy, the results demonstrated that HER2-positive patients were associated with a higher rate of distant metastasis, which was related to poorer DFS and OS. These findings imply that more active treatments for patients with HER2-positive rectal cancer with distant metastasis or locally recurrent diseases are warranted, such as chemotherapy combined with single-targeted or even dual-targeted therapy. Moreover, HER2 overexpression in CRC may not only be an important prognostic determinant but also a potential therapeutic factor; however, this needs to be investigated further. Given that HER2-positive tumour cells are more likely to be aggressive in nature, anti-HER2 treatment may be beneficial for improving patient outcomes.

This study had a few limitations. The results showed that 27 (17.9%) patients were confirmed to be HER2-positive, a rate higher than that reported in most previous studies. However, this result is still considerably consistent with the results of previous studies. Most studies demonstrated that the variability of HER2 positivity might be caused by non-uniform judgment criteria, cohort heterogeneity, small study populations, different regimes of preoperative chemoradiotherapy, antibody selection methods, staining platforms, and so on[41]. In this study, all patients underwent rigid proctoscopy before neoadjuvant therapy, and a sufficient amount of tumour tissue was obtained. All samples were evaluated using immunohistochemistry, and the evaluation criteria were similar to those used when evaluating HER2 expression in gastric cancer. Two experienced pathologists independently performed the blind examinations and scoring. For controversial results, the FISH method was used to verify the accuracy of the results and exclude the possibility of false positives. A possible reason for the high rate of positivity is the potential selection bias resulting from an inadequate number of patients from a relatively larger HER2-negative population. However, we believe that due to the higher aggressiveness and poor prognoses of HER2-positive patients, our results may be more meaningful when compared with the results of these negative patients.

CONCLUSION

In conclusion, a considerable proportion of patients with rectal cancer showed HER2 overexpression. HER2 overexpression plays an important role in rectal cancer, which may promote the aggressiveness of rectal cancer and may be a potential prognostic biological predictor. For rectal cancer patients receiving preoperative neoadjuvant radiotherapy, HER2 overexpression predicts lymph node metastasis and distant metastasis and is associated with worse long-term DFS and long-term OS.

ARTICLE HIGHLIGHTS

Research background

Predictive factors for long-term survival in locally advanced rectal cancer remained controversial. The roles of HER2 over-expression was still under discussion.

Research motivation

The effects of HER2 over-expression on the long-term survival was investigated in this prospective cohort study.

Research objectives

The associations between clinico-pathological factors and long-term survival were evaluated.

Research methods

Categorical variables were assessed using the Chi square (2 × 2) or Fisher's exact test (2 × C), when applicable. Multivariate analysis was performed using a binary logistic regression model (forward: LR). Survival analysis was performed by the Kaplan-Meier method, and the differences between groups were verified by log-rank test.

Research results

The immunohistochemical results showed that HER2 over-expression was detected in 16.6% (25/151) of the tissue samples. HER2 positivity was associated with the pre-treatment N(+) stage (Pre-N) (P = 0.040) and the distant metastasis (P = 0.002). There were significant differences between HER2 positive group and HER2 negative group with respect to both disease-free survival (DFS) [hazard ratio: 1.69 (95% confidence interval: 0.91-3.14); P = 0.048] and overall survival (OS) [1.95 (1.05-3.63); P = 0.0077].

Research conclusions

A considerable part of rectal cancer patients showed HER2 overexpression. HER2 overexpression plays an important role in rectal cancer, which may promote the aggressiveness of rectal cancer, and it may be a potential prognostic biological predictor. For those rectal cancer patients receiving preoperative neoadjuvant radiotherapy, HER2 overexpression predicts lymph node metastasis and distant metastasis, and it is associated with worse long-term DFS and long-term OS.

Research perspectives

For rectal cancer patients, with HER2 over-expression, conventional treatment combined with targeted therapy might be of help.

ACKNOWLEDGEMENTS

We gave special thanks to faculty members (Professor Gu J, Professor Wu AW, *etc*.) of Gastro-intestinal center Ward III, Beijing Cancer Hospital.

FOOTNOTES

Author contributions: Chen N and Li CL contributed equally to this paper; Chen N and Li CL drafted the manuscript; Chen N, Peng YF and Yao YF designed this study.

Supported by Beijing Municipal Administration of Hospitals Incubating Program, No. PZ2020027; and Beijing Talent Incubating Funding, No. 2019-4.

Institutional review board statement: The study was reviewed and approved by the Beijing Cancer Hospital Institutional Review Board (approval No. 2015KT33).

Clinical trial registration statement: This study is registered at Clinical trial registry of Beijing Cancer Hospital. The registration identification number is 2015KT33.

Informed consent statement: All study participants, or their legal guardian, provided informed written consent prior to study enrollment.

Conflict-of-interest statement: All the authors report no relevant conflicts of interest for this article.

Data sharing statement: No additional data are available.

CONSORT 2010 statement: The authors have read the CONSORT 2010 statement, and the manuscript was prepared and revised according to the CONSORT 2010 statement.

Country/Territory of origin: China

ORCID number: Nan Chen 0000-0002-0085-7472; Chang-Long Li 0000-0001-6665-2341; Yi-Fan Peng 0000-0002-6159-6088; Yun-Feng Yao 0000-0001-8433-0688.

Corresponding Author's Membership in Professional Societies: American Society of Colon and Rectal Surgeons, No. 24353.

S-Editor: Gao CC
L-Editor: A
P-Editor: Yuan YY

REFERENCES

1 **Benson AB**, Venook AP, Al-Hawary MM, Arain MA, Chen YJ, Ciombor KK, Cohen S, Cooper HS, Deming D, Garrido-Laguna I, Grem JL, Gunn A, Hoffe S, Hubbard J, Hunt S, Kirilcuk N, Krishnamurthi S, Messersmith WA, Meyerhardt J, Miller ED, Mulcahy MF, Nurkin S, Overman MJ, Parikh A, Patel H, Pedersen K, Saltz L, Schneider C, Shibata D, Skibber JM, Sofocleous CT, Stoffel EM, Stotsky-Himelfarb E, Willett CG, Johnson-Chilla A, Gurski LA. NCCN Guidelines Insights: Rectal Cancer, Version 6. 2020. *J Natl Compr Canc Netw* 2020; **18**: 806-815 [PMID: 32634771 DOI: 10.6004/jnccn.2020.0032]

2 **National Health Commission of the People's Republic of China**. Chinese Protocol of Diagnosis and Treatment of Colorectal Cancer (2020 edition). *Zhonghua Waike Zazhi* 2020; **58**: 561-585 [PMID: 32727186 DOI: 10.3760/cma.j.cn112139-20200518-00390]

3 **Siegel RL**, Miller KD, Jemal A. Cancer statistics, 2020. *CA Cancer J Clin* 2020; **70**: 7-30 [PMID: 31912902 DOI: 10.3322/caac.21590]

4 **Leufkens AM**, van den Bosch MA, van Leeuwen MS, Siersema PD. Diagnostic accuracy of computed tomography for colon cancer staging: a systematic review. *Scand J Gastroenterol* 2011; **46**: 887-894 [PMID: 21504379 DOI: 10.3109/00365521.2011.574732]

5 **Swedish Rectal Cancer Trial**, Cedermark B, Dahlberg M, Glimelius B, Påhlman L, Rutqvist LE, Wilking N. Improved survival with preoperative radiotherapy in resectable rectal cancer. *N Engl J Med* 1997; **336**: 980-987 [PMID: 9091798 DOI: 10.1056/NEJM199704033361402]

6 **Sauer R**, Fietkau R, Wittekind C, Rödel C, Martus P, Hohenberger W, Tschmelitsch J, Sabitzer H, Karstens JH, Becker H, Hess C, Raab R; German Rectal Cancer Group. Adjuvant vs. neoadjuvant radiochemotherapy for locally advanced rectal cancer: the German trial CAO/ARO/AIO-94. *Colorectal Dis* 2003; **5**: 406-415 [PMID: 12925071 DOI: 10.1046/j.1463-1318.2003.00509.x]

7 **Bosset JF**, Collette L, Calais G, Mineur L, Maingon P, Radosevic-Jelic L, Daban A, Bardet E, Beny A, Ollier JC; EORTC Radiotherapy Group Trial 22921. Chemotherapy with preoperative radiotherapy in rectal cancer. *N Engl J Med* 2006; **355**: 1114-1123 [PMID: 16971718 DOI: 10.1056/NEJMoa060829]

8 **van Gijn W**, Marijnen CA, Nagtegaal ID, Kranenbarg EM, Putter H, Wiggers T, Rutten HJ, Påhlman L, Glimelius B, van de Velde CJ; Dutch Colorectal Cancer Group. Preoperative radiotherapy combined with total mesorectal excision for resectable rectal cancer: 12-year follow-up of the multicentre, randomised controlled TME trial. *Lancet Oncol* 2011; **12**: 575-582 [PMID: 21596621 DOI: 10.1016/S1470-2045(11)70097-3]

9 **Kapiteijn E**, Marijnen CA, Nagtegaal ID, Putter H, Steup WH, Wiggers T, Rutten HJ, Pahlman L, Glimelius B, van Krieken JH, Leer JW, van de Velde CJ; Dutch Colorectal Cancer Group. Preoperative radiotherapy combined with total mesorectal excision for resectable rectal cancer. *N Engl J Med* 2001; **345**: 638-646 [PMID: 11547717 DOI: 10.1056/NEJMoa010580]

10 **Sauer R**, Becker H, Hohenberger W, Rödel C, Wittekind C, Fietkau R, Martus P, Tschmelitsch J, Hager E, Hess CF, Karstens JH, Liersch T, Schmidberger H, Raab R; German Rectal Cancer Study Group. Preoperative *vs* postoperative chemoradiotherapy for rectal cancer. *N Engl J Med* 2004; **351**: 1731-1740 [PMID: 15496622 DOI: 10.1056/NEJMoa040694]

11 **Hsieh AC**, Moasser MM. Targeting HER proteins in cancer therapy and the role of the non-target HER3. *Br J Cancer* 2007; **97**: 453-457 [PMID: 17667926 DOI: 10.1038/sj.bjc.6603910]

12 **Yao YF**, Du CZ, Chen N, Chen P, Gu J. Expression of HER-2 in rectal cancers treated with preoperative radiotherapy: a potential biomarker predictive of metastasis. *Dis Colon Rectum* 2014; **57**: 602-607 [PMID: 24819100 DOI: 10.1097/DCR.0000000000000107]

13 **Barros-Silva JD**, Leitão D, Afonso L, Vieira J, Dinis-Ribeiro M, Fragoso M, Bento MJ, Santos L, Ferreira P, Rêgo S, Brandão C, Carneiro F, Lopes C, Schmitt F, Teixeira MR. Association of ERBB2 gene status with histopathological

parameters and disease-specific survival in gastric carcinoma patients. *Br J Cancer* 2009; **100**: 487-493 [PMID: 19156142 DOI: 10.1038/sj.bjc.6604885]

14 **Kalogiannidis I**, Petousis S, Bobos M, Margioula-Siarkou C, Topalidou M, Papanikolaou A, Vergote I, Agorastos T. HER-2/neu is an independent prognostic factor in type I endometrial adenocarcinoma. *Arch Gynecol Obstet* 2014; **290**: 1231-1237 [PMID: 25022554 DOI: 10.1007/s00404-014-3333-2]

15 **Gravalos C**, Jimeno A. HER2 in gastric cancer: a new prognostic factor and a novel therapeutic target. *Ann Oncol* 2008; **19**: 1523-1529 [PMID: 18441328 DOI: 10.1093/annonc/mdn169]

16 **Kaptain S**, Tan LK, Chen B. Her-2/neu and breast cancer. *Diagn Mol Pathol* 2001; **10**: 139-152 [PMID: 11552716 DOI: 10.1097/00019606-200109000-00001]

17 **Gradishar WJ**, Moran MS, Abraham J, Aft R, Agnese D, Allison KH, Blair SL, Burstein HJ, Dang C, Elias AD, Giordano SH, Goetz MP, Goldstein LJ, Hurvitz SA, Isakoff SJ, Jankowitz RC, Javid SH, Krishnamurthy J, Leitch M, Lyons J, Matro J, Mayer IA, Mortimer J, O'Regan RM, Patel SA, Pierce LJ, Rugo HS, Sitapati A, Smith KL, Smith ML, Soliman H, Stringer-Reasor EM, Telli ML, Ward JH, Wisinski KB, Young JS, Burns JL, Kumar R. NCCN Guidelines® Insights: Breast Cancer, Version 4.2021. *J Natl Compr Canc Netw* 2021; **19**: 484-493 [PMID: 34794122 DOI: 10.6004/jnccn.2021.0023]

18 **Koeppen HK**, Wright BD, Burt AD, Quirke P, McNicol AM, Dybdal NO, Sliwkowski MX, Hillan KJ. Overexpression of HER2/neu in solid tumours: an immunohistochemical survey. *Histopathology* 2001; **38**: 96-104 [PMID: 11207822 DOI: 10.1046/j.1365-2559.2001.01084.x]

19 **Kruszewski WJ**, Rzepko R, Ciesielski M, Szefel J, Zieliński J, Szajewski M, Jasiński W, Kawecki K, Wojtacki J. Expression of HER2 in colorectal cancer does not correlate with prognosis. *Dis Markers* 2010; **29**: 207-212 [PMID: 21206005 DOI: 10.3233/DMA-2010-0742]

20 **Liu F**, Ren C, Jin Y, Xi S, He C, Wang F, Wang Z, Xu RH. Assessment of two different HER2 scoring systems and clinical relevance for colorectal cancer. *Virchows Arch* 2020; **476**: 391-398 [PMID: 31720832 DOI: 10.1007/s00428-019-02668-9]

21 **Meng X**, Huang Z, Di J, Mu D, Wang Y, Zhao X, Zhao H, Zhu W, Li X, Kong L, Xing L. Expression of Human Epidermal Growth Factor Receptor-2 in Resected Rectal Cancer. *Medicine (Baltimore)* 2015; **94**: e2106 [PMID: 26632727 DOI: 10.1097/MD.0000000000002106]

22 **Kountourakis P**, Pavlakis K, Psyrri A, Rontogianni D, Xiros N, Patsouris E, Pectasides D, Economopoulos T. Clinicopathologic significance of EGFR and Her-2/neu in colorectal adenocarcinomas. *Cancer J* 2006; **12**: 229-236 [PMID: 16803682 DOI: 10.1097/00130404-200605000-00012]

23 **Ingold Heppner B**, Behrens HM, Balschun K, Haag J, Krüger S, Becker T, Röcken C. HER2/neu testing in primary colorectal carcinoma. *Br J Cancer* 2014; **111**: 1977-1984 [PMID: 25211663 DOI: 10.1038/bjc.2014.483]

24 **Tarantino I**, Warschkow R, Worni M, Merati-Kashani K, Köberle D, Schmied BM, Müller SA, Steffen T, Cerny T, Güller U. Elevated preoperative CEA is associated with worse survival in stage I-III rectal cancer patients. *Br J Cancer* 2012; **107**: 266-274 [PMID: 22735902 DOI: 10.1038/bjc.2012.267]

25 **Park YA**, Lee KY, Kim NK, Baik SH, Sohn SK, Cho CW. Prognostic effect of perioperative change of serum carcinoembryonic antigen level: a useful tool for detection of systemic recurrence in rectal cancer. *Ann Surg Oncol* 2006; **13**: 645-650 [PMID: 16538413 DOI: 10.1245/ASO.2006.03.090]

26 **Moureau-Zabotto L**, Farnault B, de Chaisemartin C, Esterni B, Lelong B, Viret F, Giovannini M, Monges G, Delpero JR, Bories E, Turrini O, Viens P, Salem N. Predictive factors of tumor response after neoadjuvant chemoradiation for locally advanced rectal cancer. *Int J Radiat Oncol Biol Phys* 2011; **80**: 483-491 [PMID: 21093174 DOI: 10.1016/j.ijrobp.2010.02.025]

27 **Armstrong D**, Raissouni S, Price Hiller J, Mercer J, Powell E, MacLean A, Jiang M, Doll C, Goodwin R, Batuyong E, Zhou K, Monzon JG, Tang PA, Heng DY, Cheung WY, Vickers MM. Predictors of Pathologic Complete Response After Neoadjuvant Treatment for Rectal Cancer: A Multicenter Study. *Clin Colorectal Cancer* 2015; **14**: 291-295 [PMID: 26433487 DOI: 10.1016/j.clcc.2015.06.001]

28 **Mirbagheri N**, Kumar B, Deb S, Poh BR, Dark JG, Leow CC, Teoh WM. Lymph node status as a prognostic indicator after preoperative neoadjuvant chemoradiotherapy of rectal cancer. *Colorectal Dis* 2014; **16**: O339-O346 [PMID: 24916286 DOI: 10.1111/codi.12682]

29 **Osako T**, Miyahara M, Uchino S, Inomata M, Kitano S, Kobayashi M. Immunohistochemical study of c-erbB-2 protein in colorectal cancer and the correlation with patient survival. *Oncology* 1998; **55**: 548-555 [PMID: 9778622 DOI: 10.1159/000011911]

30 **Kapitanović S**, Radosević S, Kapitanović M, Andelinović S, Ferencić Z, Tavassoli M, Primorać D, Sonicki Z, Spaventi S, Pavelic K, Spaventi R. The expression of p185(HER-2/neu) correlates with the stage of disease and survival in colorectal cancer. *Gastroenterology* 1997; **112**: 1103-1113 [PMID: 9097992 DOI: 10.1016/s0016-5085(97)70120-3]

31 **Knösel T**, Yu Y, Stein U, Schwabe H, Schlüns K, Schlag PM, Dietel M, Petersen I. Overexpression of c-erbB-2 protein correlates with chromosomal gain at the c-erbB-2 Locus and patient survival in advanced colorectal carcinomas. *Clin Exp Metastasis* 2002; **19**: 401-407 [PMID: 12198768 DOI: 10.1023/a:1016368708107]

32 **Laurent-Puig P**, Balogoun R, Cayre A, Le Malicot K, Tabernero J, Mini E, Folprecht G, Van Laethem JL, Thaler J, Nørgård Petersen L, Sanchez E, Bridgewater J, Ellis S, Locher C, Lagorce C, Ramé JF, Lepage C, Penault-Llorca F, Taieb J. ERBB2 alterations a new prognostic biomarker in stage III colon cancer from a FOLFOX based adjuvant trial (PETACC8). *Ann Oncol* 2016; **27**: VI151 [DOI: 10.1093/annonc/mdw370.08]

33 **Li C**, Liu DR, Ye LY, Huang LN, Jaiswal S, Li XW, Wang HH, Chen L. HER-2 overexpression and survival in colorectal cancer: a meta-analysis. *J Zhejiang Univ Sci B* 2014; **15**: 582-589 [PMID: 24903996 DOI: 10.1631/jzus.B1300258]

34 **Richman SD**, Southward K, Chambers P, Cross D, Barrett J, Hemmings G, Taylor M, Wood H, Hutchins G, Foster JM, Oumie A, Spink KG, Brown SR, Jones M, Kerr D, Handley K, Gray R, Seymour M, Quirke P. HER2 overexpression and amplification as a potential therapeutic target in colorectal cancer: analysis of 3256 patients enrolled in the QUASAR, FOCUS and PICCOLO colorectal cancer trials. *J Pathol* 2016; **238**: 562-570 [PMID: 26690310 DOI: 10.1002/path.4679]

35 **Essapen S**, Thomas H, Green M, De Vries C, Cook MG, Marks C, Topham C, Modjtahedi H. The expression and prognostic significance of HER-2 in colorectal cancer and its relationship with clinicopathological parameters. *Int J Oncol*

2004; **24**: 241-248 [PMID: 14719098]

36 **Gianni L**, Dafni U, Gelber RD, Azambuja E, Muehlbauer S, Goldhirsch A, Untch M, Smith I, Baselga J, Jackisch C, Cameron D, Mano M, Pedrini JL, Veronesi A, Mendiola C, Pluzanska A, Semiglazov V, Vrdoljak E, Eckart MJ, Shen Z, Skiadopoulos G, Procter M, Pritchard KI, Piccart-Gebhart MJ, Bell R; Herceptin Adjuvant (HERA) Trial Study Team. Treatment with trastuzumab for 1 year after adjuvant chemotherapy in patients with HER2-positive early breast cancer: a 4-year follow-up of a randomised controlled trial. *Lancet Oncol* 2011; **12**: 236-244 [PMID: 21354370 DOI: 10.1016/S1470-2045(11)70033-X]

37 **Baselga J**, Bradbury I, Eidtmann H, Di Cosimo S, de Azambuja E, Aura C, Gómez H, Dinh P, Fauria K, Van Dooren V, Aktan G, Goldhirsch A, Chang TW, Horváth Z, Coccia-Portugal M, Domont J, Tseng LM, Kunz G, Sohn JH, Semiglazov V, Lerzo G, Palacova M, Probachai V, Pusztai L, Untch M, Gelber RD, Piccart-Gebhart M; NeoALTTO Study Team. Lapatinib with trastuzumab for HER2-positive early breast cancer (NeoALTTO): a randomised, open-label, multicentre, phase 3 trial. *Lancet* 2012; **379**: 633-640 [PMID: 22257673 DOI: 10.1016/S0140-6736(11)61847-3]

38 **Martinelli E**, Troiani T, Sforza V, Martini G, Cardone C, Vitiello PP, Ciardiello D, Rachiglio AM, Normanno N, Sartore-Bianchi A, Marsoni S, Bardelli A, Siena S, Ciardiello F. Sequential HER2 blockade as effective therapy in chemorefractory, HER2 gene-amplified, RAS wild-type, metastatic colorectal cancer: learning from a clinical case. *ESMO Open* 2018; **3**: e000299 [PMID: 29387480 DOI: 10.1136/esmoopen-2017-000299]

39 **Sartore-Bianchi A**, Trusolino L, Martino C, Bencardino K, Lonardi S, Bergamo F, Zagonel V, Leone F, Depetris I, Martinelli E, Troiani T, Ciardiello F, Racca P, Bertotti A, Siravegna G, Torri V, Amatu A, Ghezzi S, Marrapese G, Palmeri L, Valtorta E, Cassingena A, Lauricella C, Vanzulli A, Regge D, Veronese S, Comoglio PM, Bardelli A, Marsoni S, Siena S. Dual-targeted therapy with trastuzumab and lapatinib in treatment-refractory, KRAS codon 12/13 wild-type, HER2-positive metastatic colorectal cancer (HERACLES): a proof-of-concept, multicentre, open-label, phase 2 trial. *Lancet Oncol* 2016; **17**: 738-746 [PMID: 27108243 DOI: 10.1016/S1470-2045(16)00150-9]

40 **Conradi LC**, Spitzner M, Metzger AL, Kisly M, Middel P, Bohnenberger H, Gaedcke J, Ghadimi MB, Liersch T, Rüschoff J, Beißbarth T, König A, Grade M. Combined targeting of HER-2 and HER-3 represents a promising therapeutic strategy in colorectal cancer. *BMC Cancer* 2019; **19**: 880 [PMID: 31488078 DOI: 10.1186/s12885-019-6051-0]

41 **Guarini C**, Grassi T, Pezzicoli G, Porta C. Beyond RAS and BRAF: HER2, a New Actionable Oncotarget in Advanced Colorectal Cancer. *Int J Mol Sci* 2021; **22** [PMID: 34202896 DOI: 10.3390/ijms22136813]

World Journal of Gastrointestinal Oncology

Submit a Manuscript: https://www.f6publishing.com

World J Gastrointest Oncol 2022 October 15; 14(10): 2061-2076

DOI: 10.4251/wjgo.v14.i10.2061

ISSN 1948-5204 (online)

META-ANALYSIS

Combining of chemotherapy with targeted therapy for advanced biliary tract cancer: A systematic review and meta-analysis

Xue-Song Bai, Sheng-Nan Zhou, Yi-Qun Jin, Xiao-Dong He

Specialty type: Gastroenterology and hepatology

Provenance and peer review: Unsolicited article; Externally peer reviewed.

Peer-review model: Single blind

Peer-review report's scientific quality classification

Grade A (Excellent): 0
Grade B (Very good): B, B
Grade C (Good): C
Grade D (Fair): 0
Grade E (Poor): 0

P-Reviewer: Kapritsou M, Greece; Kitamura K, Japan; Tzeng IS, Taiwan

Received: June 8, 2022
Peer-review started: June 8, 2022
First decision: August 20, 2022
Revised: September 4, 2022
Accepted: September 13, 2022
Article in press: September 13, 2022
Published online: October 15, 2022

Xue-Song Bai, Sheng-Nan Zhou, Xiao-Dong He, Department of General Surgery, Peking Union Medical College Hospital, China Academy of Medical Science & Peking Union Medical College, Beijing 100730, China

Yi-Qun Jin, Affiliated Hangzhou First People's Hospital, Zhejiang University School of Medicine, Hangzhou 310000, Zhejiang Province, China

Corresponding author: Xiao-Dong He, Doctor, MD, Professor, Department of General Surgery, Peking Union Medical College Hospital, China Academy of Medical Science & Peking Union Medical College, No. 1 Shuaifuyuan, Dongcheng District, Beijing 100730, China.
hxdpumch@163.com

Abstract

BACKGROUND

Targeted therapy (TT) has resulted in controversial efficacy as first-line treatment for biliary tract cancer (BTC). More efficacy comparisons are required to clarify the overall effects of chemotherapy (CT) combined with TT and CT alone on advanced BTC.

AIM

To conduct a meta-analysis of the available evidence on the efficacy of CT combined with TT for advanced BTC.

METHODS

The PubMed, EMBASE, ClinicalTrials, Scopus and Cochrane Library databases were systematically searched for relevant studies published from inception to August 2022. Only randomized clinical trials (RCTs) including comparisons between the combination of gemcitabine-based CT with TT and CT alone as first-line treatment for advanced BTC were eligible (PROSPERO-CRD42022313001). The odds ratios (ORs) for the objective response rate (ORR) and hazard ratios (HRs) for both progression-free survival (PFS) and overall survival (OS) were calculated and analyzed. Subgroup analyses based on different targeted agents, CT regimens and tumor locations were prespecified.

RESULTS

Nine RCTs with a total of 1361 individuals were included and analyzed. The overall analysis showed a significant improvement in ORR in patients treated with CT + TT compared to those treated with CT alone (OR = 1.43, 95%CI: 1.11-1.86, P = 0.007) but no difference in PFS or OS. Similar trends were observed in the

subgroup treated with agents targeting epidermal growth factor receptor (OR = 1.67, 95%CI: 1.17-2.37, *P* = 0.004) but not in the subgroups treated with agents targeting vascular endothelial growth factor receptor or mesenchymal-epithelial transition factor. Notably, patients who received a CT regimen of gemcitabine + oxaliplatin in the CT + TT arm had both a higher ORR (OR = 1.75, 95%CI: 1.20-2.56, *P* = 0.004) and longer PFS (HR = 0.83, 95%CI: 0.70-0.99, *P* = 0.03) than those in the CT-only arm. Moreover, patients with cholangiocarcinoma treated with CT + TT had significantly increased ORR and PFS (ORR, OR = 2.06, 95%CI: 1.27-3.35, PFS, HR = 0.79, 95%CI: 0.66-0.94).

CONCLUSION

CT + TT is a potential first-line treatment for advanced BTC that leads to improved tumor control and survival outcomes, and highlighting the importance of CT regimens and tumor types in the application of TT.

Key Words: Advanced biliary tract cancer; Targeted therapy; Chemotherapy; Meta-analysis; Randomized controlled trial; First-line treatment

Core Tip: The clinical efficacy of adding targeted agents to first-line treatment of biliary tract cancer (BTC) remains unclear. Our study is the first meta-analysis of randomized clinical trials to evaluate the efficacy of the combination of targeted therapy (TT) with standard chemotherapy (CT) as first-line treatment in patients with advanced BTC. We assessed the efficacy of combined TT and CT in terms of objective response rate, progression-free survival and overall survival. Subgroup analyses were conducted based on different targeted agents, CT regimens and tumor locations.

Citation: Bai XS, Zhou SN, Jin YQ, He XD. Combining of chemotherapy with targeted therapy for advanced biliary tract cancer: A systematic review and meta-analysis. *World J Gastrointest Oncol* 2022; 14(10): 2061-2076
URL: https://www.wjgnet.com/1948-5204/full/v14/i10/2061.htm
DOI: https://dx.doi.org/10.4251/wjgo.v14.i10.2061

INTRODUCTION

Biliary tract cancer (BTC), including cholangiocarcinoma (CCA) (intrahepatic cholangiocarcinoma (iCCA), perihilar cholangiocarcinoma, or cholangiocarcinoma in the distal biliary tree) and gallbladder cancer (GBC), is a relatively rare invasive adenocarcinoma with a dismal prognosis. In recent decades, the incidence of BTC has shown a consistent increasing trend worldwide, particularly in Asian countries [1]. Surgery offers the only potentially curative treatment option for patients who have resectable disease. The high incidence of lymph node involvement and liver invasion are associated with worse clinical outcomes after surgery. However, given the frequent absence of symptoms and late diagnosis in patients with BTC, only a minority of patients (35% for CCA and 20% for GBC) are potential candidates for radical resection; even after resection with a negative surgical margin, the postoperative relapse rate is over 60%[2-4].

For patients with advanced BTC, including radically unresectable or metastatic adenocarcinoma[5], the available systemic therapeutics have limited effect, with a five-year survival of 4%[6,7]. Currently, the first-line treatment for advanced BTC remains gemcitabine-based chemotherapy regimens[1]. According to the ABC-02 trial in 2010, gemcitabine and cisplatin combination chemotherapy (CisGem) was verified to improve overall survival (OS), progression-free survival (PFS) and tumor control rate (TCR) compared with gemcitabine monotherapy in patients with CCA and GBC[6,8]. Gemcitabine and oxaliplatin (GemOx) combination therapy was also identified as an alternative to CisGem. The results of a phase III randomized controlled trial (RCT) in 2019 showed that modified GemOx might lead to a longer median OS (*P* = 0.57) and different toxicities than CisGem[9]. In addition, randomized phase 3 study trials evaluating efficacy have shown that the efficacy of gemcitabine and S1 combination regimens are noninferior to that of CisGem[10]. Nevertheless, no studies have verified if the superiority of such regimens over CisGem has statistical significance.

Due to the limited efficacy of current chemotherapy (CT) regimens for advanced BTC, new therapies need to be developed. In the past decade, through new parallel sequencing of malignancies, several genetic alterations and molecular characteristics for BTC have been further revealed, including isocitrate dehydrogenase (IDH)-1 and -2 mutations, fibroblast growth factor receptor (FGFR) fusions, neurotropic tyrosine kinase receptor fusions, V-raf murine sarcoma viral oncogene homolog B (BRAF) mutations and aberrations of human epidermal growth factor receptor (HER) family members[11-14]. Targeted

therapies (TTs) based on monoclonal antibodies or tyrosine kinase inhibitors associated with actionable genetic alterations in BTC are being extensively explored. Recently, combinations of CT and TT have been attempted to improve the prognosis for advanced BTC, but the clinical efficacy remains to be further evaluated[15].

Considering that the high heterogeneity and low incidence of BTC impede the recruitment of large cohorts of patients to identify effective targets and regimens in clinical trials, meta-analysis is needed to further assess the value of TT and investigate the survival benefits of this treatment. This study is the first meta-analysis of RCTs to evaluate the efficacy of the combination of TT with standard CT as first-line treatment for patients with advanced BTC.

MATERIALS AND METHODS

This systematic review and meta-analysis was conducted in accordance with the guidelines of the Preferred Reporting Items for Systematic Review and Meta-Analysis (PRISMA) statement guidelines and was prospectively registered in The International Prospective Register of Systematic Reviews (PROSPERO, https://www.crd.york.ac.uk/prospero/) platform (registration number CRD 42022313001).

Search strategy

A systematic literature search of the PubMed/MEDLINE, Clinical Trials, EMBASE, SOCPUS and Cochrane Library databases was conducted from inception to August 2022. Various combinations of the following search terms were used in the database searches: "biliary tract cancer", "gallbladder neoplasms", "cholangiocarcinoma", "molecular targeted therapy" and "antineoplastic agents". Reference Citation Analysis (https://www.referencecitationanalysis.com) was used to avoid missing relevant studies. In addition, we searched the reference lists of the included literature and potentially relevant studies to retrieve studies from other sources. The detailed search strategy and results are described in the supplement (Supplementary Table 1).

Selection criteria

Trials were eligible for inclusion if they met the following criteria: (1) Randomized controlled trials involving patients with BTC who were treated with targeted therapy and chemotherapy as first-line treatment; and (2) Advanced, unresectable, recurrent or metastatic BTC with PFS, OS, and/or objective response rate (ORR) reported. Studies involving the following were excluded: (1) No standard chemotherapy arm as a control; (2) Case reports, reviews, commentaries, notes and letters; and (3) Non-English language articles. Two independent reviewers conducted the assessment of all the searched studies. To avoid duplicate clinical data, the registration information in ClinicalTrials.gov was checked, and the most recent and most complete publication was incorporated.

Data extraction and quality assessment

Two authors independently extracted the data and information. In the event of a disagreement, the data source was checked, and a third reviewer was consulted to confirm the correct data. The following information was extracted: the first author's name, journal name, publication year, study period, national clinical trial number, institution and country. The detailed demographic characteristics included the number of patients, age, sex and disease site. Regarding therapeutic interventions, information on the treatment regimen was collected. The efficacy outcomes extracted included the ORR, PFS and OS. If the hazard ratios (HRs) of OS or PFS were not reported in the literature, Engauge Digitizer 4.1 was used to plot points on the survival curves and extract the HR values.

The risk of bias and quality of the RCTs were assessed by two independent authors in accordance with the criterion of the Cochrane risk of bias tool (ROB) including the following seven dimensions: blinding of participants and personnel (performance bias), blinding of outcome assessment (detection bias), incomplete outcome data (attrition bias), selective reporting (reporting bias) and other bias. A third author was consulted to resolve any disagreements.

Statistical analysis

Pooled HRs with 95%CIs were calculated for time-to-event data, including OS and PFS. Estimated odds ratios (ORs) were calculated for discrete variables, including the ORR and adverse events. The selection of a fixed- or random-effects model was based on the level of heterogeneity of the data, which was assessed by Cochran's Q-test and the Higgins I^2 statistic. A fixed effects model was adopted for $I^2 < 50\%$, and a random effect model was adopted for $I^2 > 50\%$. The potential bias of the publications was presented as funnel plots and measured using Egger's tests. Subgroup analysis was performed based on the different targets of the agents, CT regimens and location of the BTC. $P < 0.05$ was considered statistically significant. All statistical analyses of the extracted data were conducted with Review Manager 5.4.1 (Cochrane Collaboration, Oxford, United Kingdom).

RESULTS

Study search and selection

The PRISMA flowchart of the study search and selection process is presented in Figure 1. A total of 1654 records were retrieved in the initial search of PubMed, Embase, Scopus, Cochrane Library and ClinicalTrials.gov. A total of 621 records were duplicates and removed, and 1033 records were screened for eligibility using titles and abstracts. Of the 32 studies that underwent full-text assessment, nine RCTs met the prespecified inclusion criteria for the meta-analysis[16-24].

Study characteristics and quality assessment

The design characteristics of the nine clinical trials are summarized in Table 1. All 9 studies included were RCTs. Data on a total of 1361 patients were provided in the nine included trials. Eight targeted treatment regimens (ramucirumab, merestinib, panitumumab, cediranib, vandetanib, cetuximab, sorafenib and erlotinib) and three gemcitabine-based first-line CT regimens (CisGem, GemOx and gemcitabine) were used. Four of the studies were designed with blinding using CT plus placebo as comparators. All studies reported final data for ORR, PFS and OS as endpoints, with an acceptable sample size of patients and adequate length of follow-up. The quality assessment of the included articles was evaluated with the ROB (Supplementary Figure 1).

The descriptions of all the trial patients are presented in Table 2. Overall, the median age of the patients ranged from 59 to 68 years old. Most patients in these cohorts had unresectable disease with metastases. There was no difference between the CT group and CT combined with TT group in the distribution of age, sex, Eastern Cooperative Oncology Group performance status, disease status or primary tumor site.

Evaluation of efficacy

ORR: The ORR reported in the studies ranged from 19.3% to 44% in the CT + TT group and 10% to 39% in the CT group (Figure 2A). No significant heterogeneity was detected among studies, with I^2 = 44% and P = 0.06. Therefore, the fixed-effect model was adopted for the meta-analysis. The pooled data showed that CT + TT could significantly increase the ORR in BTC compared to CT (OR = 1.43, 95%CI: 1.11-1.86, P = 0.007). Subgroup analyses showed heterogeneity between different targeting molecules (I^2 = 60.5%, P = 0.05), implying that different therapeutic targets might an interaction effect on the ORR of BTC patients. CT + TT targeting for epidermal growth factor receptor (EGFR) might more effectively enhance the ORR in BTC than CT alone (Figure 2B, OR = 1.67, 95%CI: 1.17-2.37, P = 0.004), but no difference was found for agents targeting vascular endothelial growth factor receptor (VEGFR) (P = 0.29), mesenchymal-epithelial transition factor (MET) (P = 0.09) or VEGFR/EGFR (P = 0.41). No significant heterogeneity was detected in the ORR among subgroups of different CT regimens (I^2 = 14.5%, P = 0.31). In the GemOx subgroup, the ORR was higher in the CT + TT arm than in the CT-only arm (Figure 2C, OR = 1.75, 95%CI: 1.20-2.56, P = 0.004).

PFS: The median PFS ranged from 4.1 to 8.25 mo in the CT-only group and 3.0 to 8.0 mo in the CT combined with TT group. The overall pooled HR for OS was calculated based on a fixed-effect model (I^2 = 32%, P = 0.15). The results showed that the BTC patients in the group treated with CT + TT had a longer PFS than those treated with CT alone, but this difference was not statistically significant (Figure 3A, HR = 0.96, 95%CI: 0.85-1.08, P = 0.47). In the subgroup analysis, the selection of different CT regimens was found to have an interaction effect on PFS in BTC patients (I^2 = 70.0%, P = 0.04). When the CT regimen was GemOx, a remarkable survival benefit was observed in the CT + TT group compared to the CT-only group (HR = 0.83, 95%CI: 0.70-0.99, P = 0.03). Similar to the ORR results, when targeting EGFR, the combination of CT with TT still tended to lead to better PFS for BTC patients, although no statistical significance was observed (OR = 0.88, 95%CI: 0.75-1.03, P = 0.11) (P = 0.59 when targeting VEGFR, P = 0.21 when targeting VEGFR/EGFR, P = 0.49 when targeting MET).

OS: The median OS ranged from 9.5 to 20.07 mo in the CT-only group and 8.4 to 14.1 mo in the CT combined with TT group. Except for the Santoro *et al*[21]. study, all of the studies reported OS with HR data and events as outcomes. The fixed-effect model was applied, with I^2 = 0% and P = 0.53. The pooled data showed no significant improvement in the OS of BTC patients treated with CT + TT compared to those treated with CT alone (Figure 4A, HR = 1.04, 95%CI: 0.92-1.19, P = 0.50). Subgroup analysis among different molecular targets and CT regimens failed to show differences between CT and CT + TT (both I^2 = 0%).

Exploratory analysis

Exploratory analyses were performed to compare the effect of combining CT with TT according to the site of tumor origin (Figure 5). Among the 9 studies, two studies differentiated the data of PFS for GBC from BTC. Four studies reported PFS data for CCA [iCCA or extrahepatic cholangiocarcinoma (eCCA)]. After data pooling, heterogeneity was detected among subgroups in PFS according to tumor location (I^2 = 78.4%, P = 0.03), with no significant heterogeneity within subgroups (both I^2 = 0%). In the subgroup of patients with CCA, CT + TT conferred an improved ORR and PFS benefit compared to CT alone (ORR:

Table 1 Characteristics of trials included in the analysis

Ref.	NCT number	Country/regions	Study period	Number of patients		Chemotherapy regimen
				CT	CT + TT	
Valle *et al*[1], 2021	NCT02711553	18 countries and regions[a]	May, 2016 to Aug, 2017	101	106 102	CisGem
Vogel *et al*[17], 2018	NCT01320254	Germany	Jul, 2011 to Dec, 2015	28	62	CisGem
Leone *et al*[18], 2016	NCT01389414	Italy	Jun, 2010 to Sept, 2013	44	45	GemOx
Valle *et al*[19], 2015	NCT00939848	UK	Apr, 2011 to Sept, 2012	60	62	CisGem
Santoro *et al*[21], 2015	NCT00753675	Italy	Oct, 2008 to Sept, 2012	56	58	Gemcitabine
Chen *et al*[20], 2015	NCT01267344	China	Dec, 2010 to May, 2012	60	62	GemOx
Moehler *et al*[22], 2014	NCT00661830	Germany	May, 2008 to Jul, 2011	48	49	Gemcitabine
Malka *et al*[23], 2014	NCT00552149	France and Germany	Oct, 2007 to Dec, 2009	74	76	GemOx
Lee *et al*[24], 2012	NCT01149122	South Korea	Feb, 2009 to Aug, 2010	133	135	GemOx

[a]18 countries and regions include United States, Taiwan, South Korea, Turkey, Argentina, France, Russia, Spain, United Kingdom, Germany, Australia, Belgium, Hungary, Czech Republic, Sweden, Mexico, Denmark, Austria.

CT: Chemotherapy; TT: Targeted therapy; CisGem: Gemcitabine combined with Cisplatin; GemOx: Gemcitabine combined with Oxaliplatin; ORR: Overall response rate; OS: Overall survival; PFS: Progression-free survival.

OR = 2.06, 95%CI: 1.27, 3.35, P = 0.003; PFS: HR = 0.79, 95%CI: 0.66-0.94, P = 0.010). In contrast, the ORR and PFS did not differ among patients with GBC (ORR: P = 0.77, PFS: P = 0.30). The OS was similar between the CT and CT + TT groups for both CCA and GBC patients.

Assessment of publication bias

Publication bias was assessed by Egger's test and is presented as a funnel plot. Both the P value from Egger's test and the symmetry seen from the funnel plot indicate that there was no evidence of significant publication bias for ORR, PFS or OS in our meta-analysis (Figure 6, Egger's test, P = 0.756, 0.171, 0.706, respectively).

DISCUSSION

BTC tends to be diagnosed late and is associated with a poor prognosis. Currently, gemcitabine-based CT is still the standard first-line treatment for unresectable advanced BTC. However, the median survival in gemcitabine-treated BTC patients is only approximately 12 mo[13]. To further improve patient prognosis, more effective first-line strategies need to be explored[25]. Therefore, triple CT combinations such as with the addition of S-1 or nab-paclitaxel to the standard of care CisGem, 5-fluorouracil, irinotecan and oxaliplatin as well as some new agents such as NUC-1031 have also been evaluated in phase 2 clinical trials and demonstrated favorable safety profile[26-28]. Thereinto, gemcitabine, cisplatin plus S-1 showed survival benefits and higher risk ratio than gemcitabine, cisplatin. However, further exploration is required with phase III clinical trials for improving the clinical outcomes of advanced BTC patients. Recently, with the further understanding and exploration of the molecular characteristics of BTC, several actionable mutations have been identified and have changed the treatment paradigm for BTC. Currently, inhibitors targeting FGFR fusions and IDH-1 and -2 mutations have been tested in clinical trials with encouraging outcomes for pretreated CCA. As one of the most promising targets, the survival benefit of IDH-1 inhibitors as a second-line treatment option in IDH-1-mutated CCA has been demonstrated in a phase III clinical trial[29]. In addition, some pre-clinical and early clinical studies on other potential targets including HER-2, BRAF and ring finger protein 43 mutations are currently undertaken[30]. However, their efficacy as first-line treatment for BTC is still being evaluated in ongoing clinical trials (NCT02386397). Due to the lack of adequate patient selection, whether the addition of TT to first-line treatment improves prognosis compared with CT alone has been controversial to date.

Table 2 Patient characteristics in the included studies

Ref.	Design	Age, median	Males/females	ECOG 0/1-2	Locally advanced/metastatic	Primary tumour site
Valle *et al*[1], 2021	CisGem	59	53/48	61/39	2/98	iCCA, 55; GBC, 26; eCCA, 14; AoV, 5
	Ramucirumab	64	46/60	45/58	3/103	iCCA, 56; GBC, 24; eCCA, 18; AoV, 8
	Merestinib	62	48/54	52/50	4/98	iCCA, 60; GBC, 22; eCCA, 14; AoV, 6
Vogel *et al*[17], 2018	CisGem	59.5	14/14	11/17	5/17	GBC, 3; dCCA, 1; pCCA, 2; iCCA, 20; Others, 6
	Panitumumab	62	36/26	21/39	13/42	GBC, 11; dCCA, 7; pCCA, 2; iCCA, 41; Others, 6
Leone *et al*[18], 2016	GemOx	64.2	15/29	1/43	6/38	iCCA, 21; eCCA, 7; GBC, 16
	Panitumumab	63.9	17/28	0/45	8/37	iCCA, 21; eCCA, 12; GBC, 12
Valle *et al*[19], 2015	CisGem	64.5	28/34	28/34	8/54	iCCA, 15; eCCA, 24; GBC, 19; AoV, 4
	Cediranib	68	34/28	27/35	12/50	iCCA, 14; eCCA, 24; GBC, 20; AoV, 4
Santoro *et al*[21], 2015	Gemcitabine	64	25/31	34/21	NR	iCCA, 29; eCCA, 13; GBC, 7; AoV, 6
	Vandetanib	64.4	31/27	36/23	NR	iCCA, 31; eCCA, 10; GBC, 13; AoV, 4
Chen *et al*[20], 2015	GemOx	59	30/30	17/43	17/43	iCCA, 45; eCCA, 10; GBC, 5
	Cetuximab	61	28/34	18/44	23/39	iCCA, 44; eCCA, 9; GBC, 9;
Moehler *et al*[22], 2014	Gemcitabine	64.5	25/23	9/35	NR	GBC, 7; iCCA, 29
	Sorafenib	64	29/20	17/30	NR	GBC, 6; iCCA, 33
Malka *et al*[23], 2014	GemOx	62	42/32	27/43	15/59	iCCA, 46; eCCA, 14; GBC, 11; AoV, 0
	Cetuximab	61	43/33	35/36	17/59	iCCA, 49; eCCA, 8; GBC, 11; AoV, 1
Lee *et al*[24], 2012	GemOx	61	79/54	20/113	0/133	CCA, 84; GBC, 47; AoV, 2;
	Erlotinib	59	91/44	26/109	0/135	CCA, 96; GBC, 35; AoV, 4

ECOG: Eastern Co-operative Oncology Group; CisGem: Gemcitabine combined with Cisplatin; GemOx: Gemcitabine combined with Oxaliplatin; iCCA: Intrahepatic cholangiocarcinoma; GBC: Gallbladder carcinoma; eCCA: Extrahepatic cholangiocarcinoma; AoV: Ampulla of Vater; dCCA: Distal cholangiocarcinoma; pCCA: Perihilar cholangiocarcinoma; CCA: Cholangiocarcinoma.

This analysis pooled and analyzed data from a total of 1361 individuals from 9 RCTs to compare the effects of CT with TT or CT alone, in terms of the ORR, PFS and OS, as BTC treatment. Our results suggest that combination TT with CT as first-line systemic treatment for advanced biliary tract malignancies might be associated with beneficial outcomes in some situations.

Overall, our meta-analysis showed a significant improvement in the ORR in unselected patients treated with CT + TT compared to that in patients treated with CT (28.6% *vs* 20.7%). All the trials included adopted gemcitabine-based CT schedules for first-line systemic therapy, which is consistent with the current standards of care. Therefore, the ORR of CisGem was superior to that of gemcitabine alone, similar to in the phase III ABC-02 study[6]. Oxaliplatin is sometimes substituted for cisplatin. The adoption of GemOx as first-line CT is based on the fact that oxaliplatin is easier to administer than cisplatin, as it does not require excessive hydration and reduces the risk of renal toxicity, but maintains a similar efficacy to CisGem[6,31,32]. However, there has been no direct comparison or validated

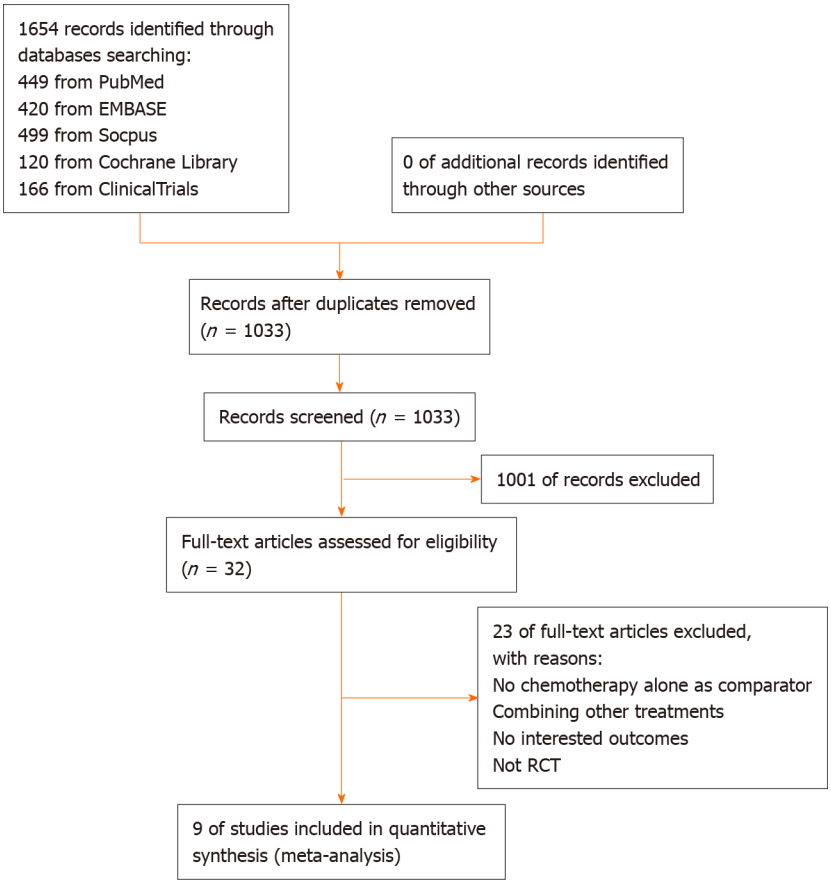

DOI: 10.4251/wjgo.v14.i10.2061

Figure 1 Flowchart of the study selection process. RCT: Randomized clinical trials.

superiority among different combinations (CisGem and GemOx) in advanced BTC. Our results demonstrate that combination TT with CT might significantly improve the ORR in BTC patients treated with GemOx (27.4% *vs* 17.7%, $P = 0.004$). Moreover, a similar significant advantage was observed in PFS for combination TT with CT, which we regard as a more unbiased outcome than OS, because OS is susceptible to the influence of subsequent therapies and other factors (HR = 0.83, $P = 0.03$)[33].

In the subgroup analysis of GemOx, the main driver of the OS benefit favoring the combination of TT and CT was the data from the study from Lee *et al*[24], in which erlotinib plus GemOx yielded a clear improvement in ORR (30% *vs* 15.8, $P = 0.005$) and a marginal superiority in PFS (5.8 mo *vs* 4.2 mo, HR = 0.80, 95%CI: 0.61-1.03, $P = 0.087$) compared with GemOx alone. Similar to our results, the PFS improved significantly with cetuximab plus gemcitabine treatment (HR = 0.66, 95%CI: 0.45-0.98, $P = 0.04$) in the study by Chen *et al*[20] that included Chinese patients. Unlike the other studies in this subgroup, Chen *et al*[20] adopted the modified GemOx regimen, which might have a better compliance rate than traditional GemOx, and observed a significantly longer treatment duration for GemOx plus cetuximab than for GemOx alone ($P = 0.01$). These results suggest that relatively mild CT regimens plus TT might be advantageous and beneficial for advanced BTC patients, especially Asian patients.

The heterogeneity of different anatomical locations and molecular profiles has been demonstrated to be associated with differences in clinicopathologic features and prognoses of advanced BTC. However, complete information about treatment and survival is usually absent in classifications that are based on molecular subtypes and anatomical location[34]. The subgroup analysis showed that the combination of EGFR agents with CT significantly improved the ORR compared with CT alone (30.3% *vs* 19.5%, $P = 0.004$), but no significant difference in PFS or OS was observed between the two groups. These results corroborate the finding of a pooled analysis by Eckel *et al*[35] that analyzed pooled data from 161 trials containing 6337 BTC patients treated with gemcitabine-based CT with or without TT. The study also demonstrates that the combination of EGFR-targeted agents with gemcitabine-based CT was more effective for tumor control and survival, with superior outcomes in the TCR, tumor progression and OS.

Nevertheless, most of the RCTs (except for the study from Chen *et al*[20]) could not independently validate a significant improvement with the combination of TT with CT. Given that differences in survival outcomes and molecular profiling have been reported between GBC and non-GBC BTCs, an exploratory analysis based on different tumor locations was conducted[6,36,37]. Previous studies have shown that patients with CCA tend to exhibit better chemosensitivity and prognoses than those with GBC[38]. Interestingly, in our meta-analysis, both the ORR and PFS in the iCCA and eCCA subgroups

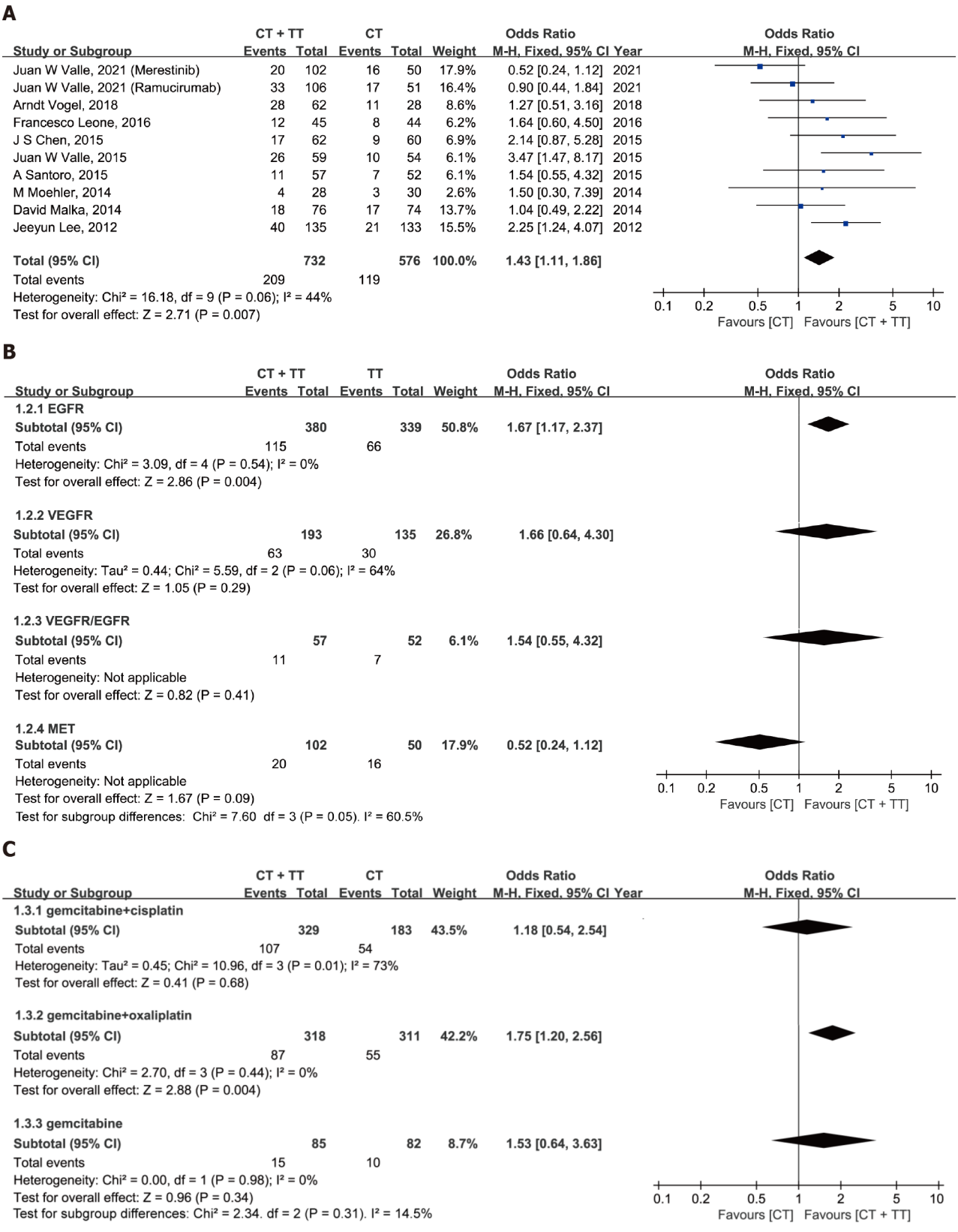

DOI: 10.4251/wjgo.v14.i10.2061

Figure 2 Forest plots on the assessment of objective response rate in biliary tract cancer patients treated with chemotherapy + targeted therapy or chemotherapy alone. A: Overall population; B: Subgroup analysis according to agent targets; C: Subgroup analysis according to chemotherapy regimens. CT: Chemotherapy; TT: Targeted therapy; EGFR: Epidermal growth factor receptor; VEGFR: Vascular endothelial growth factor receptor; MET: Mesenchymal-epithelial transition factor.

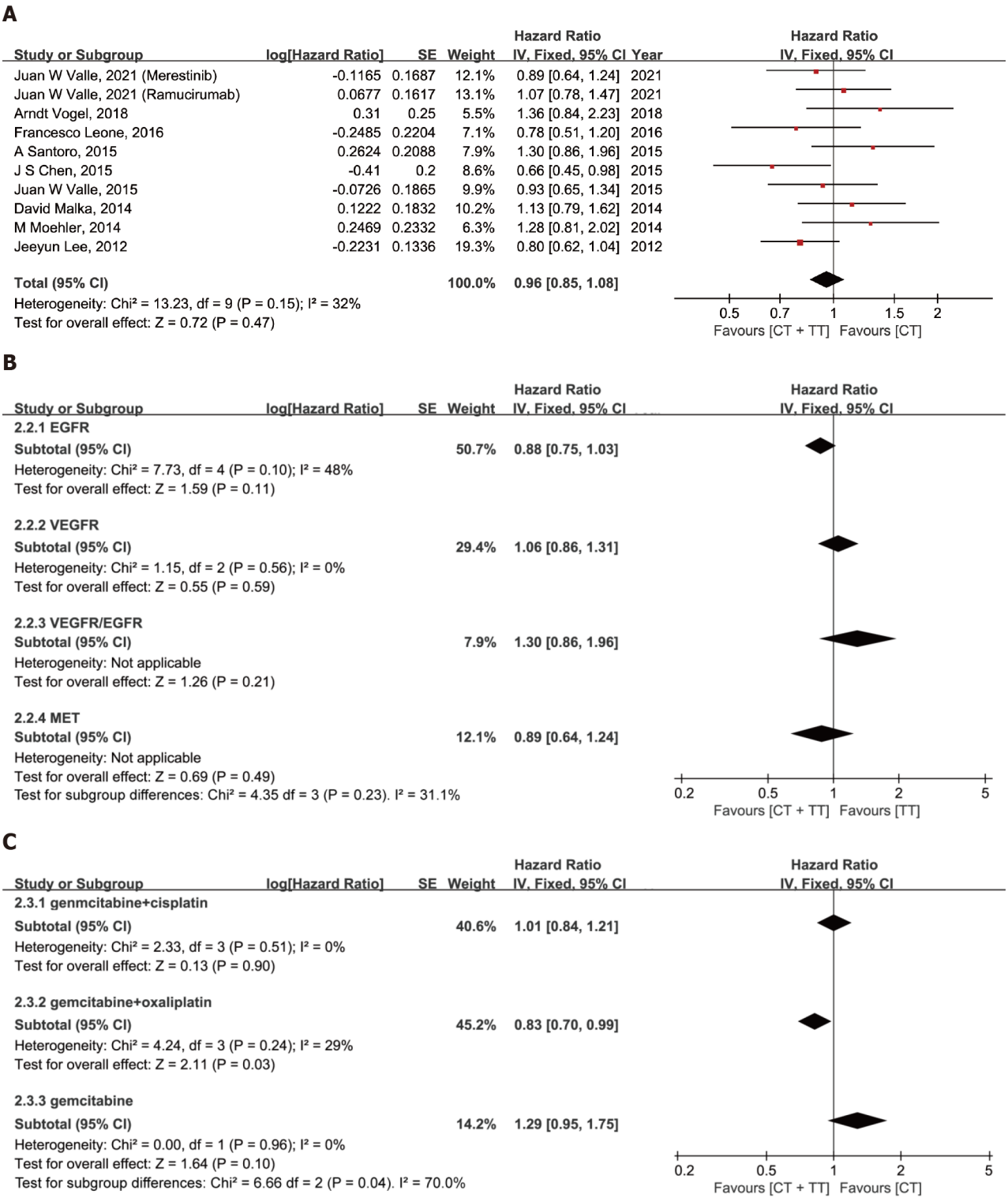

DOI: 10.4251/wjgo.v14.i10.2061

Figure 3 Forest plots on the assessment of progression-free survival in biliary tract cancer patients treated with chemotherapy + targeted therapy or chemotherapy alone. A: Overall population; B: Subgroup analysis according to agent targets; C: Subgroup analysis according to chemotherapy regimens. EGFR: Epidermal growth factor receptor; VEGFR: Vascular endothelial growth factor receptor; MET: Mesenchymal-epithelial transition factor.

improved with the combination treatment of TT with CT (*vs* CT alone) (P = 0.003, P = 0.010, respectively), but no difference in ORR or PFS was observed for the GBC subgroup (combination of TT with CT *vs* CT alone). Our results suggest that CCA might be associated with better treatment response and survival outcomes than GBC. Due to the different characteristics and patterns of CCA and GBC, more clinical data evaluating tumor location-specific outcomes should be reported in the future.

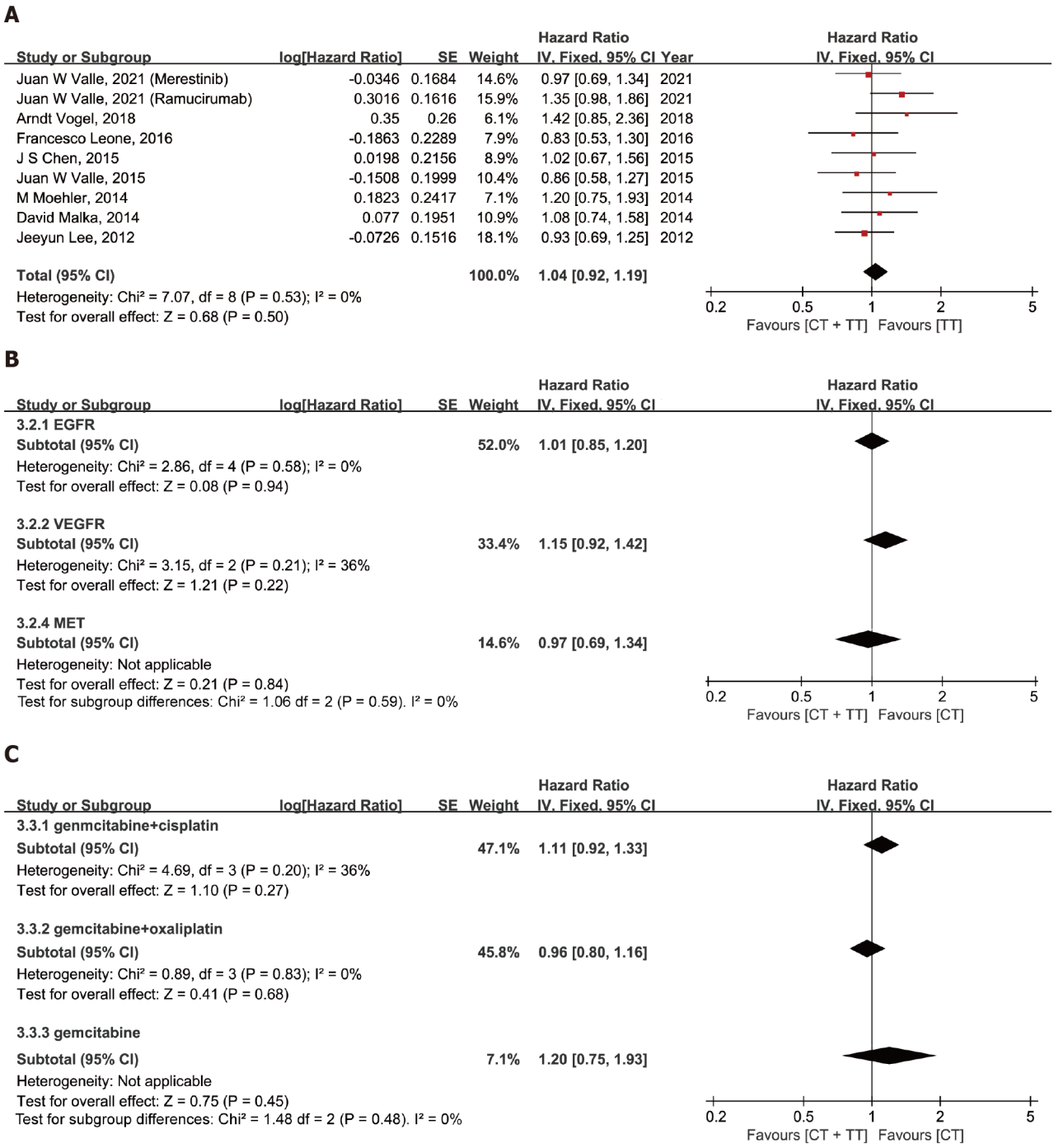

DOI: 10.4251/wjgo.v14.i10.2061

Figure 4 Forest plots on the assessment of overall survival in biliary tract cancer patients treated with chemotherapy + targeted therapy or chemotherapy alone. A: Overall population; B: Subgroup analysis according to agent targets; C: Subgroup analysis according to chemotherapy regimens. EGFR: Epidermal growth factor receptor; VEGFR: Vascular endothelial growth factor receptor; MET: Mesenchymal-epithelial transition factor.

Limitations

There are some potential limitations in our study. First, due to our strict inclusion criteria, only nine studies were included in the meta-analysis. Even so, the nearly symmetrical funnel plot and Egger's test indicated no evidence of publication bias. Second, the proportion of BTCs was imbalanced in terms of tumor location, which might have implications for overall tumor control and survival outcomes. Furthermore, the detailed data for subgroups of tumor location were incomplete, which might also influence the quality of the evaluation for overall outcomes. Moreover, the gender ratio, age and countries of patients were assumed to be similar, although they varied among the included studies. In addition, only English studies were included, which might result in a risk of language bias.

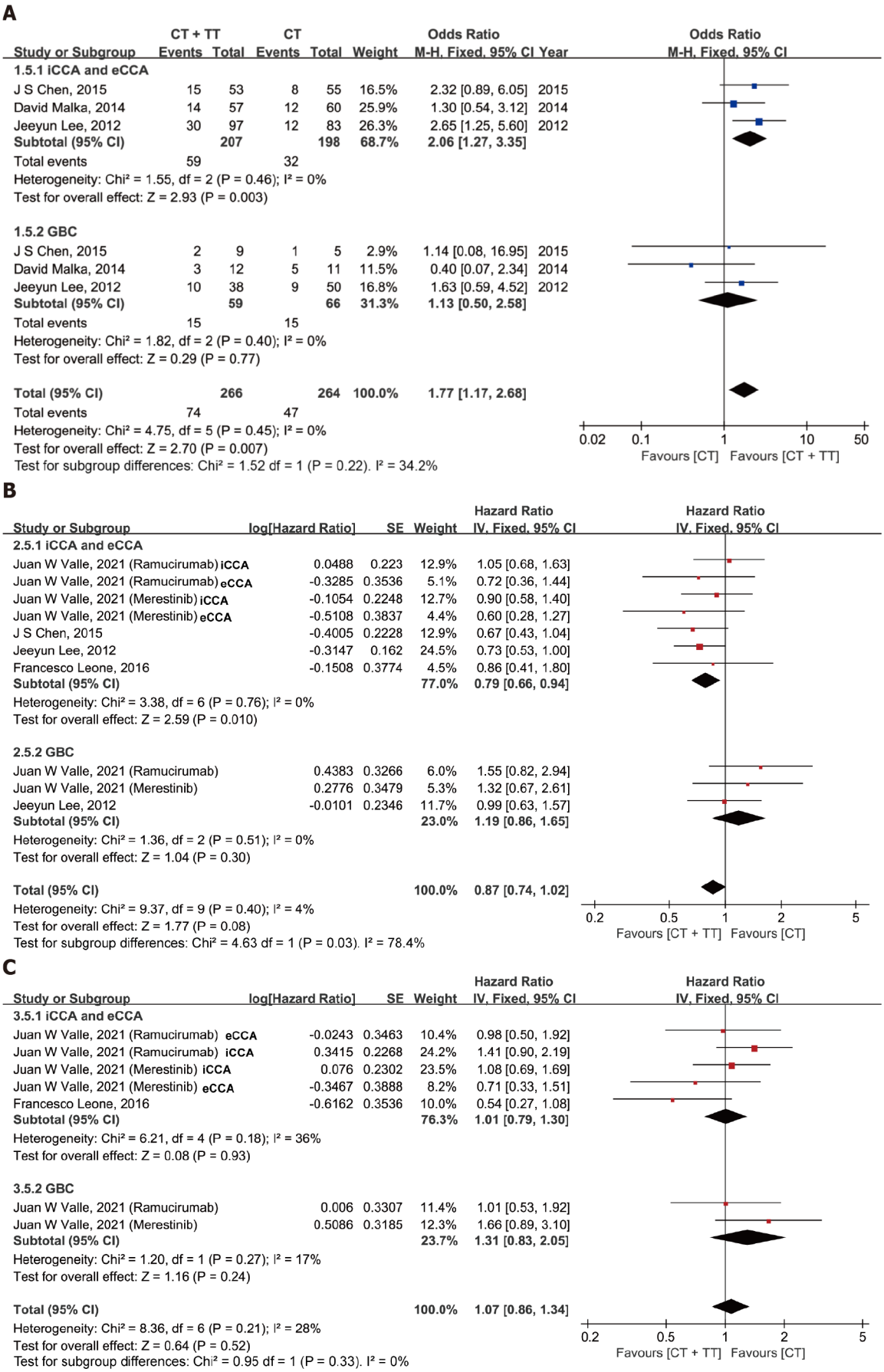

DOI: 10.4251/wjgo.v14.i10.2061

Figure 5 Forest plot comparing the efficacy of chemotherapy + targeted therapy and chemotherapy in different types of tumors. A:

Objective response rate; B: progression-free survival; C: Overall survival. CT: Chemotherapy; TT: Targeted therapy; iCCA: Intrahepatic cholangiocarcinoma; eCCA: Extrahepatic cholangiocarcinoma; GBC: Gallbladder cancer.

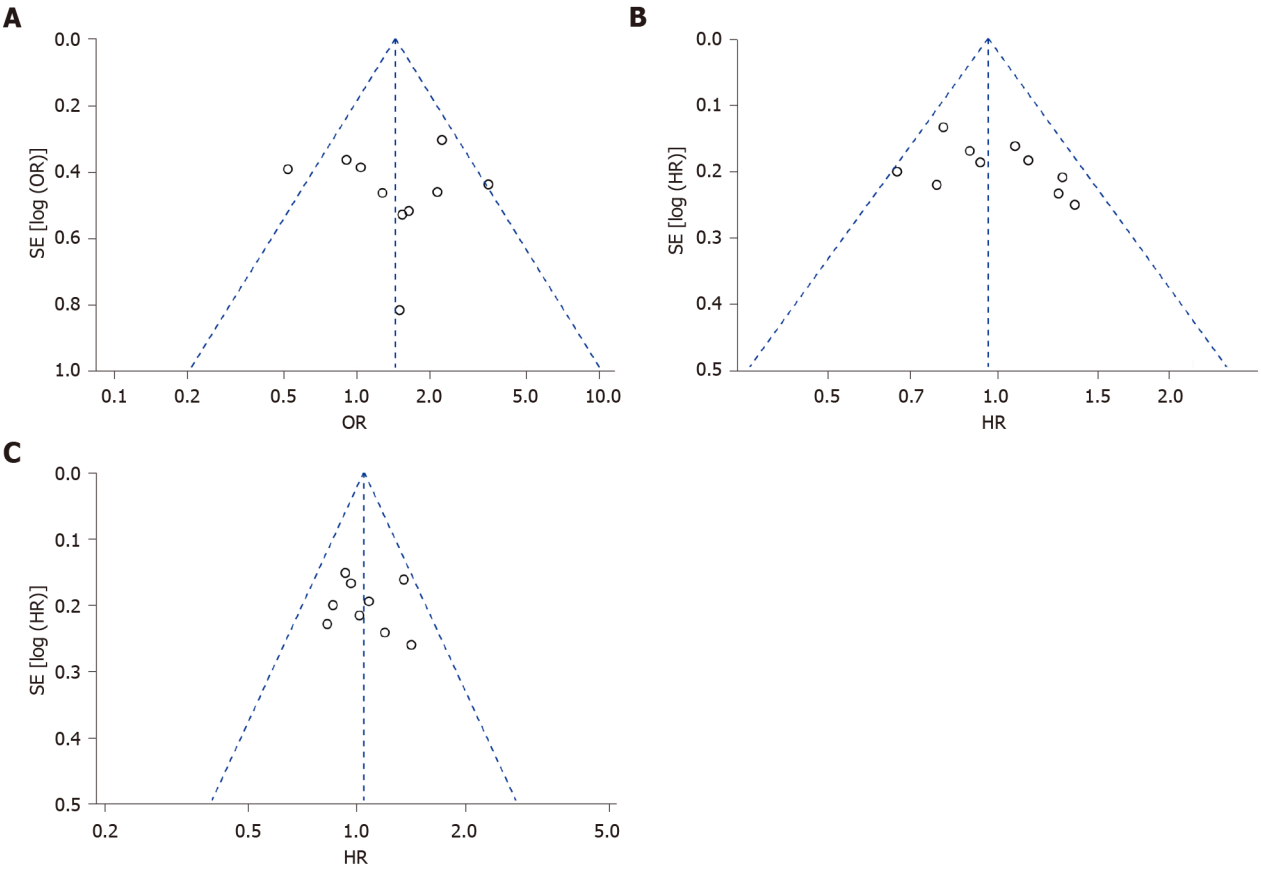

DOI: 10.4251/wjgo.v14.i10.2061

Figure 6 Funnel plot for the assessment of publication bias. A: Publication bias for objective response rate; B: Publication bias for progression-free survival; C: Publication bias for overall survival. HR: Hazard ratio.

CONCLUSION

In conclusion, this meta-analysis provides supporting clinical evidence for the promise of TT as first-line systemic therapy for advanced BTC. Gemcitabine-based CT combined with TT, especially agents targeting EGFR, could evidently increase the ORR for advanced BTC compared to CT alone. However, the higher ORR did not appear to translate into a significant benefit in PFS or OS in most of the prospective trials. Despite this, we identified that the CT regimen and tumor location had significant interactions in assessing the effect of TT in advanced BTC. CT combined with TT significantly improved the survival outcome of advanced BTC in patients who received GemOx as first-line treatment or those with CCA but not GBC. A deeper understanding of TT is required and the results are promising for the development of novel treatment strategies for advanced BTC. Our results help facilitate the design of future clinical trials for advanced BTC.

ARTICLE HIGHLIGHTS

Research background

The prognosis of patients with advanced biliary tract cancer (BTC) is poor. The clinical efficacy of combining chemotherapy (CT) with targeted therapy (TT) as first-line treatment remains controversial.

Research motivation

Currently, TT based on actionable genetic alterations in BTC are being extensively explored. However, the clinical efficacy of combination CT with TT as first-line treatment for advanced BTC is unclear. A meta-analysis is necessary to systematically and comprehensively evaluate the clinical value of TT for

advanced BTC.

Research objectives
The purpose of this meta-analysis was to explore the value of CT combined with TT as first-line treatment for advanced BTC.

Research methods
We systematically searched PubMed, EMBASE, ClinicalTrials, Scopus, and the Cochrane Library databases to screen and include randomized clinical trials (RCTs) on gemcitabine-based CT alone *vs* the combination of TT and CT as first-line treatment for advanced BTC. Review Manager 5.4.1 software was used to conduct the statistical analysis. Objective response rate (ORR), progression-free survival (PFS) and overall survival (OS) were analyzed as main outcomes. Subgroup analyses based on different targeted agents, CT regimens and tumor locations were performed.

Research results
Our meta-analysis showed a significant improvement in ORR in patients treated with CT + TT compared to those treated with CT alone (P = 0.007), but no difference in PFS or OS. Similar trends were observed in the subgroup treated with agents targeting EGFR (P = 0.004). Notably, patients who received a CT regimen of gemcitabine + oxaliplatin in the CT + TT arm had both a higher ORR (P = 0.004) and longer PFS (P = 0.03) than those in the CT-only arm. Moreover, patients with cholangiocarcinoma treated with CT + TT had significantly increased ORR and PFS.

Research conclusions
Our study is the first meta-analysis of RCTs to evaluate the efficacy of the combining TT with standard CT as first-line treatment for advanced BTC. The meta-analysis has demonstrated that CT + TT is a promising first-line treatment for advanced BTC that leads to improved clinical outcomes.

Research perspectives
In the future, more clinical studies are needed to explore the role of TT for advanced BTC. In addition, attention should be paid on the interactions of CT regimen and tumor location for assessing the clinical efficacy of TT in advanced BTC.

ACKNOWLEDGEMENTS

The authors thank Hai-Yu Pang for her support in statistical review of methodology and meta-analysis process. We thank Jie-Min Chen for his help in the process of editing and revising this work.

FOOTNOTES

Author contributions: Bai XS conceived the study idea; Bai XS, Zhou SN and Jin YQ conducted the literature searches and review of studies, performed data extraction, interpreted data analyses and drafted manuscripts; He XD advised on data interpretation, advised on ethodologies and helped performed statistical analysis of the manuscript; All authors interpreted data and wrote the report. All authors contributed to the article and approved the submitted version.

Supported by China Academy of Medical Science Innovation Fund for Medical Sciences, CIFMS, No. 2021-I2M-1-022-2021-S4.

Conflict-of-interest statement: All authors declare that the research was conducted in the absence of any commercial or financial relationships that could be construed as a potential conflict of interest.

PRISMA 2009 Checklist statement: The guidelines of the PRISMA 2009 Statement have been adopted.

Country/Territory of origin: China

ORCID number: Xue-Song Bai 0000-0001-8497-8468; Sheng-Nan Zhou 0000-0003-3198-7867; Yi-Qun Jin 0000-0001-6505-6206; Xiao-Dong He 0000-0002-6682-2926.

S-Editor: Zhang H
L-Editor: A
P-Editor: Zhang H

REFERENCES

1 **Valle JW**, Kelley RK, Nervi B, Oh DY, Zhu AX. Biliary tract cancer. *Lancet* 2021; **397**: 428-444 [PMID: 33516341 DOI: 10.1016/S0140-6736(21)00153-7]
2 **Rizvi S**, Khan SA, Hallemeier CL, Kelley RK, Gores GJ. Cholangiocarcinoma - evolving concepts and therapeutic strategies. *Nat Rev Clin Oncol* 2018; **15**: 95-111 [PMID: 28994423 DOI: 10.1038/nrclinonc.2017.157]
3 **Cao L**, Bridle KR, Shrestha R, Prithviraj P, Crawford DHG, Jayachandran A. CD73 and PD-L1 as Potential Therapeutic Targets in Gallbladder Cancer. *Int J Mol Sci* 2022; **23** [PMID: 35163489 DOI: 10.3390/ijms23031565]
4 **Ishihara S**, Horiguchi A, Miyakawa S, Endo I, Miyazaki M, Takada T. Biliary tract cancer registry in Japan from 2008 to 2013. *J Hepatobiliary Pancreat Sci* 2016; **23**: 149-157 [PMID: 26699688 DOI: 10.1002/jhbp.314]
5 **Chun YS**, Pawlik TM, Vauthey JN. 8th Edition of the AJCC Cancer Staging Manual: Pancreas and Hepatobiliary Cancers. *Ann Surg Oncol* 2018; **25**: 845-847 [PMID: 28752469 DOI: 10.1245/s10434-017-6025-x]
6 **Valle J**, Wasan H, Palmer DH, Cunningham D, Anthoney A, Maraveyas A, Madhusudan S, Iveson T, Hughes S, Pereira SP, Roughton M, Bridgewater J; ABC-02 Trial Investigators. Cisplatin plus gemcitabine *vs* gemcitabine for biliary tract cancer. *N Engl J Med* 2010; **362**: 1273-1281 [PMID: 20375404 DOI: 10.1056/NEJMoa0908721]
7 **Uson Junior PLS**, Majeed U, Yin J, Botrus G, Sonbol MB, Ahn DH, Starr JS, Jones JC, Babiker H, Inabinett SR, Wylie N, Boyle AWR, Bekaii-Saab TS, Gores GJ, Smoot R, Barrett M, Nagalo B, Meurice N, Elliott N, Petit J, Zhou Y, Arora M, Dumbauld C, Barro O, Baker A, Bogenberger J, Buetow K, Mansfield A, Mody K, Borad MJ. Cell-Free Tumor DNA Dominant Clone Allele Frequency Is Associated With Poor Outcomes in Advanced Biliary Cancers Treated With Platinum-Based Chemotherapy. *JCO Precis Oncol* 2022; **6**: e2100274 [PMID: 35666960 DOI: 10.1200/PO.21.00274]
8 **Valle JW**, Furuse J, Jitlal M, Beare S, Mizuno N, Wasan H, Bridgewater J, Okusaka T. Cisplatin and gemcitabine for advanced biliary tract cancer: a meta-analysis of two randomised trials. *Ann Oncol* 2014; **25**: 391-398 [PMID: 24351397 DOI: 10.1093/annonc/mdt540]
9 **Sharma A**, Kalyan Mohanti B, Pal Chaudhary S, Sreenivas V, Kumar Sahoo R, Kumar Shukla N, Thulkar S, Pal S, Deo SV, Pathy S, Ranjan Dash N, Kumar S, Bhatnagar S, Kumar R, Mishra S, Sahni P, Iyer VK, Raina V. Modified gemcitabine and oxaliplatin or gemcitabine + cisplatin in unresectable gallbladder cancer: Results of a phase III randomised controlled trial. *Eur J Cancer* 2019; **123**: 162-170 [PMID: 31707181 DOI: 10.1016/j.ejca.2019.10.004]
10 **Morizane C**, Okusaka T, Mizusawa J, Katayama H, Ueno M, Ikeda M, Ozaka M, Okano N, Sugimori K, Fukutomi A, Hara H, Mizuno N, Yanagimoto H, Wada K, Tobimatsu K, Yane K, Nakamori S, Yamaguchi H, Asagi A, Yukisawa S, Kojima Y, Kawabe K, Kawamoto Y, Sugimoto R, Iwai T, Nakamura K, Miyakawa H, Yamashita T, Hosokawa A, Ioka T, Kato N, Shioji K, Shimizu K, Nakagohri T, Kamata K, Ishii H, Furuse J; members of the Hepatobiliary and Pancreatic Oncology Group of the Japan Clinical Oncology Group (JCOG-HBPOG). Combination gemcitabine plus S-1 *vs* gemcitabine plus cisplatin for advanced/recurrent biliary tract cancer: the FUGA-BT (JCOG1113) randomized phase III clinical trial. *Ann Oncol* 2019; **30**: 1950-1958 [PMID: 31566666 DOI: 10.1093/annonc/mdz402]
11 **Valle JW**, Lamarca A, Goyal L, Barriuso J, Zhu AX. New Horizons for Precision Medicine in Biliary Tract Cancers. *Cancer Discov* 2017; **7**: 943-962 [PMID: 28818953 DOI: 10.1158/2159-8290.CD-17-0245]
12 **Jiao Y**, Pawlik TM, Anders RA, Selaru FM, Streppel MM, Lucas DJ, Niknafs N, Guthrie VB, Maitra A, Argani P, Offerhaus GJA, Roa JC, Roberts LR, Gores GJ, Popescu I, Alexandrescu ST, Dima S, Fassan M, Simbolo M, Mafficini A, Capelli P, Lawlor RT, Ruzzenente A, Guglielmi A, Tortora G, de Braud F, Scarpa A, Jarnagin W, Klimstra D, Karchin R, Velculescu VE, Hruban RH, Vogelstein B, Kinzler KW, Papadopoulos N, Wood LD. Exome sequencing identifies frequent inactivating mutations in BAP1, ARID1A and PBRM1 in intrahepatic cholangiocarcinomas. *Nat Genet* 2013; **45**: 1470-1473 [PMID: 24185509 DOI: 10.1038/ng.2813]
13 **De Lorenzo S**, Garajova I, Stefanini B, Tovoli F. Targeted therapies for gallbladder cancer: an overview of agents in preclinical and clinical development. *Expert Opin Investig Drugs* 2021; **30**: 759-772 [PMID: 33966562 DOI: 10.1080/13543784.2021.1928636]
14 **Bekaii-Saab TS**, Bridgewater J, Normanno N. Practical considerations in screening for genetic alterations in cholangiocarcinoma. *Ann Oncol* 2021; **32**: 1111-1126 [PMID: 33932504 DOI: 10.1016/j.annonc.2021.04.012]
15 **Casadio M**, Biancaniello F, Overi D, Venere R, Carpino G, Gaudio E, Alvaro D, Cardinale V. Molecular Landscape and Therapeutic Strategies in Cholangiocarcinoma: An Integrated Translational Approach towards Precision Medicine. *Int J Mol Sci* 2021; **22** [PMID: 34070643 DOI: 10.3390/ijms22115613]
16 **Valle JW**, Vogel A, Denlinger CS, He AR, Bai LY, Orlova R, Van Cutsem E, Adeva J, Chen LT, Obermannova R, Ettrich TJ, Chen JS, Wasan H, Girvan AC, Zhang W, Liu J, Tang C, Ebert PJ, Aggarwal A, McNeely SC, Moser BA, Oliveira JM, Carlesi R, Walgren RA, Oh DY. Addition of ramucirumab or merestinib to standard first-line chemotherapy for locally advanced or metastatic biliary tract cancer: a randomised, double-blind, multicentre, phase 2 study. *Lancet Oncol* 2021; **22**: 1468-1482 [PMID: 34592180 DOI: 10.1016/S1470-2045(21)00409-5]
17 **Vogel A**, Kasper S, Bitzer M, Block A, Sinn M, Schulze-Bergkamen H, Moehler M, Pfarr N, Endris V, Goeppert B, Merx K, Schnoy E, Siveke JT, Michl P, Waldschmidt D, Kuhlmann J, Geissler M, Kahl C, Evenkamp R, Schmidt T, Kuhlmann A, Weichert W, Kubicka S. PICCA study: panitumumab in combination with cisplatin/gemcitabine chemotherapy in KRAS wild-type patients with biliary cancer-a randomised biomarker-driven clinical phase II AIO study. *Eur J Cancer* 2018; **92**: 11-19 [PMID: 29413685 DOI: 10.1016/j.ejca.2017.12.028]
18 **Leone F**, Marino D, Cereda S, Filippi R, Belli C, Spadi R, Nasti G, Montano M, Amatu A, Aprile G, Cagnazzo C, Fasola G, Siena S, Ciuffreda L, Reni M, Aglietta M. Panitumumab in combination with gemcitabine and oxaliplatin does not

prolong survival in wild-type KRAS advanced biliary tract cancer: A randomized phase 2 trial (Vecti-BIL study). *Cancer* 2016; **122**: 574-581 [PMID: 26540314 DOI: 10.1002/cncr.29778]

19 **Valle JW**, Wasan H, Lopes A, Backen AC, Palmer DH, Morris K, Duggan M, Cunningham D, Anthoney DA, Corrie P, Madhusudan S, Maraveyas A, Ross PJ, Waters JS, Steward WP, Rees C, Beare S, Dive C, Bridgewater JA. Cediranib or placebo in combination with cisplatin and gemcitabine chemotherapy for patients with advanced biliary tract cancer (ABC-03): a randomised phase 2 trial. *Lancet Oncol* 2015; **16**: 967-978 [PMID: 26179201 DOI: 10.1016/S1470-2045(15)00139-4]

20 **Chen JS**, Hsu C, Chiang NJ, Tsai CS, Tsou HH, Huang SF, Bai LY, Chang IC, Shiah HS, Ho CL, Yen CJ, Lee KD, Chiu CF, Rau KM, Yu MS, Yang Y, Hsieh RK, Chang JY, Shan YS, Chao Y, Chen LT; Taiwan Cooperative Oncology Group. A KRAS mutation status-stratified randomized phase II trial of gemcitabine and oxaliplatin alone or in combination with cetuximab in advanced biliary tract cancer. *Ann Oncol* 2015; **26**: 943-949 [PMID: 25632066 DOI: 10.1093/annonc/mdv035]

21 **Santoro A**, Gebbia V, Pressiani T, Testa A, Personeni N, Arrivas Bajardi E, Foa P, Buonadonna A, Bencardino K, Barone C, Ferrari D, Zaniboni A, Tronconi MC, Cartenì G, Milella M, Comandone A, Ferrari S, Rimassa L. A randomized, multicenter, phase II study of vandetanib monotherapy *vs* vandetanib in combination with gemcitabine *vs* gemcitabine plus placebo in subjects with advanced biliary tract cancer: the VanGogh study. *Ann Oncol* 2015; **26**: 542-547 [PMID: 25538178 DOI: 10.1093/annonc/mdu576]

22 **Moehler M**, Maderer A, Schimanski C, Kanzler S, Denzer U, Kolligs FT, Ebert MP, Distelrath A, Geissler M, Trojan J, Schütz M, Berie L, Sauvigny C, Lammert F, Lohse A, Dollinger MM, Lindig U, Duerr EM, Lubomierski N, Zimmermann S, Wachtlin D, Kaiser AK, Schadmand-Fischer S, Galle PR, Woerns M; Working Group of Internal Oncology. Gemcitabine plus sorafenib *vs* gemcitabine alone in advanced biliary tract cancer: a double-blind placebo-controlled multicentre phase II AIO study with biomarker and serum programme. *Eur J Cancer* 2014; **50**: 3125-3135 [PMID: 25446376 DOI: 10.1016/j.ejca.2014.09.013]

23 **Malka D**, Cervera P, Foulon S, Trarbach T, de la Fouchardière C, Boucher E, Fartoux L, Faivre S, Blanc JF, Viret F, Assenat E, Seufferlein T, Herrmann T, Grenier J, Hammel P, Dollinger M, André T, Hahn P, Heinemann V, Rousseau V, Ducreux M, Pignon JP, Wendum D, Rosmorduc O, Greten TF; BINGO investigators. Gemcitabine and oxaliplatin with or without cetuximab in advanced biliary-tract cancer (BINGO): a randomised, open-label, non-comparative phase 2 trial. *Lancet Oncol* 2014; **15**: 819-828 [PMID: 24852116 DOI: 10.1016/S1470-2045(14)70212-8]

24 **Lee J**, Park SH, Chang HM, Kim JS, Choi HJ, Lee MA, Jang JS, Jeung HC, Kang JH, Lee HW, Shin DB, Kang HJ, Sun JM, Park JO, Park YS, Kang WK, Lim HY. Gemcitabine and oxaliplatin with or without erlotinib in advanced biliary-tract cancer: a multicentre, open-label, randomised, phase 3 study. *Lancet Oncol* 2012; **13**: 181-188 [PMID: 22192731 DOI: 10.1016/S1470-2045(11)70301-1]

25 **Adeva J**, Sangro B, Salati M, Edeline J, La Casta A, Bittoni A, Berardi R, Bruix J, Valle JW. Medical treatment for cholangiocarcinoma. *Liver Int* 2019; **39** Suppl 1: 123-142 [PMID: 30892822 DOI: 10.1111/liv.14100]

26 **Ioka T**, Kanai M, Kobayashi S, Sakai D, Eguchi H, Baba H, Seo S, Taketomi A, Takayama T, Yamaue H, Takahashi M, Sho M, Kamei K, Fujimoto J, Toyoda M, Shimizu J, Goto T, Shindo Y, Yoshimura K, Hatano E, Nagano H; Kansai Hepatobiliary Oncology Group (KHBO). Randomized phase III study of Gemcitabine, Cisplatin plus S-1 (GCS) *vs* Gemcitabine, Cisplatin (GC) for Advanced Biliary Tract Cancer (KHBO1401-MITSUBA). *J Hepatobiliary Pancreat Sci* 2022 [PMID: 35900311 DOI: 10.1002/jhbp.1219]

27 **Phelip JM**, Desrame J, Edeline J, Barbier E, Terrebonne E, Michel P, Perrier H, Dahan L, Bourgeois V, Akouz FK, Soularue E, Ly VL, Molin Y, Lecomte T, Ghiringhelli F, Coriat R, Louafi S, Neuzillet C, Manfredi S, Malka D; PRODIGE 38 AMEBICA Investigators/Collaborators. Modified FOLFIRINOX Versus CISGEM Chemotherapy for Patients With Advanced Biliary Tract Cancer (PRODIGE 38 AMEBICA): A Randomized Phase II Study. *J Clin Oncol* 2022; **40**: 262-271 [PMID: 34662180 DOI: 10.1200/JCO.21.00679]

28 **McNamara MG**, Bridgewater J, Palmer DH, Faluyi O, Wasan H, Patel A, Ryder WD, Barber S, Gnanaranjan C, Ghazaly E, Evans TRJ, Valle JW. A Phase Ib Study of NUC-1031 in Combination with Cisplatin for the First-Line Treatment of Patients with Advanced Biliary Tract Cancer (ABC-08). *Oncologist* 2021; **26**: e669-e678 [PMID: 33210382 DOI: 10.1002/onco.13598]

29 **Abou-Alfa GK**, Macarulla T, Javle MM, Kelley RK, Lubner SJ, Adeva J, Cleary JM, Catenacci DV, Borad MJ, Bridgewater J, Harris WP, Murphy AG, Oh DY, Whisenant J, Lowery MA, Goyal L, Shroff RT, El-Khoueiry AB, Fan B, Wu B, Chamberlain CX, Jiang L, Gliser C, Pandya SS, Valle JW, Zhu AX. Ivosidenib in IDH1-mutant, chemotherapy-refractory cholangiocarcinoma (ClarIDHy): a multicentre, randomised, double-blind, placebo-controlled, phase 3 study. *Lancet Oncol* 2020; **21**: 796-807 [PMID: 32416072 DOI: 10.1016/S1470-2045(20)30157-1]

30 **Lamarca A**, Barriuso J, McNamara MG, Valle JW. Molecular targeted therapies: Ready for "prime time" in biliary tract cancer. *J Hepatol* 2020; **73**: 170-185 [PMID: 32171892 DOI: 10.1016/j.jhep.2020.03.007]

31 **Fiteni F**, Nguyen T, Vernerey D, Paillard MJ, Kim S, Demarchi M, Fein F, Borg C, Bonnetain F, Pivot X. Cisplatin/gemcitabine or oxaliplatin/gemcitabine in the treatment of advanced biliary tract cancer: a systematic review. *Cancer Med* 2014; **3**: 1502-1511 [PMID: 25111859 DOI: 10.1002/cam4.299]

32 **Azizi AA**, Lamarca A, McNamara MG, Valle JW. Chemotherapy for advanced gallbladder cancer (GBC): A systematic review and meta-analysis. *Crit Rev Oncol Hematol* 2021; **163**: 103328 [PMID: 33862244 DOI: 10.1016/j.critrevonc.2021.103328]

33 **Jácome AA**, Castro ACG, Vasconcelos JPS, Silva MHCR, Lessa MAO, Moraes ED, Andrade AC, Lima FMT, Farias JPF, Gil RA, Prolla G, Garicochea B. Efficacy and Safety Associated With Immune Checkpoint Inhibitors in Unresectable Hepatocellular Carcinoma: A Meta-analysis. *JAMA Netw Open* 2021; **4**: e2136128 [PMID: 34870682 DOI: 10.1001/jamanetworkopen.2021.36128]

34 **Jusakul A**, Cutcutache I, Yong CH, Lim JQ, Huang MN, Padmanabhan N, Nellore V, Kongpetch S, Ng AWT, Ng LM, Choo SP, Myint SS, Thanan R, Nagarajan S, Lim WK, Ng CCY, Boot A, Liu M, Ong CK, Rajasegaran V, Lie S, Lim AST, Lim TH, Tan J, Loh JL, McPherson JR, Khuntikeo N, Bhudhisawasdi V, Yongvanit P, Wongkham S, Totoki Y, Nakamura H, Arai Y, Yamasaki S, Chow PK, Chung AYF, Ooi LLPJ, Lim KH, Dima S, Duda DG, Popescu I, Broet P, Hsieh SY, Yu

MC, Scarpa A, Lai J, Luo DX, Carvalho AL, Vettore AL, Rhee H, Park YN, Alexandrov LB, Gordân R, Rozen SG, Shibata T, Pairojkul C, Teh BT, Tan P. Whole-Genome and Epigenomic Landscapes of Etiologically Distinct Subtypes of Cholangiocarcinoma. *Cancer Discov* 2017; **7**: 1116-1135 [PMID: 28667006 DOI: 10.1158/2159-8290.CD-17-0368]

35 **Eckel F**, Schmid RM. Chemotherapy and targeted therapy in advanced biliary tract carcinoma: a pooled analysis of clinical trials. *Chemotherapy* 2014; **60**: 13-23 [PMID: 25341559 DOI: 10.1159/000365781]

36 **Lamarca A**, Frizziero M, McNamara MG, Valle JW. Clinical and Translational Research Challenges in Biliary Tract Cancers. *Curr Med Chem* 2020; **27**: 4756-4777 [PMID: 31971102 DOI: 10.2174/0929867327666200123090153]

37 **Ji JH**, Song HN, Kim RB, Oh SY, Lim HY, Park JO, Park SH, Kim MJ, Lee SI, Ryou SH, Hwang IG, Jang JS, Kim HJ, Choi JY, Kang JH. Natural history of metastatic biliary tract cancer (BTC) patients with good performance status (PS) who were treated with only best supportive care (BSC). *Jpn J Clin Oncol* 2015; **45**: 256-260 [PMID: 25628352 DOI: 10.1093/jjco/hyu210]

38 **Ben-Josef E**, Guthrie KA, El-Khoueiry AB, Corless CL, Zalupski MM, Lowy AM, Thomas CR Jr, Alberts SR, Dawson LA, Micetich KC, Thomas MB, Siegel AB, Blanke CD. SWOG S0809: A Phase II Intergroup Trial of Adjuvant Capecitabine and Gemcitabine Followed by Radiotherapy and Concurrent Capecitabine in Extrahepatic Cholangiocarcinoma and Gallbladder Carcinoma. *J Clin Oncol* 2015; **33**: 2617-2622 [PMID: 25964250 DOI: 10.1200/JCO.2014.60.2219]

World Journal of Gastrointestinal Oncology

Submit a Manuscript: https://www.f6publishing.com

World J Gastrointest Oncol 2022 October 15; 14(10): 2077-2084

DOI: 10.4251/wjgo.v14.i10.2077

ISSN 1948-5204 (online)

CASE REPORT

Disseminated carcinomatosis of the bone marrow caused by granulocyte colony-stimulating factor: A case report and review of literature

Kengo Fujita, Ayaka Okubo, Toshitsugu Nakamura, Nobumichi Takeuchi

Specialty type: Oncology

Provenance and peer review: Unsolicited article; Externally peer reviewed.

Peer-review model: Single blind

Peer-review report's scientific quality classification

Grade A (Excellent): A, A
Grade B (Very good): 0
Grade C (Good): 0
Grade D (Fair): D
Grade E (Poor): 0

P-Reviewer: Gao L, China; Guo F, China; Liu T, China

Received: May 21, 2022
Peer-review started: May 21, 2022
First decision: June 23, 2022
Revised: July 8, 2022
Accepted: August 21, 2022
Article in press: August 21, 2022
Published online: October 15, 2022

Kengo Fujita, Ayaka Okubo, Nobumichi Takeuchi, Department of Medical Oncology, Ina Central Hospital, Nagano 396-8555, Japan

Toshitsugu Nakamura, Department of Diagnostic Pathology, Ina Central Hospital, Nagano 396-8555, Japan

Corresponding author: Nobumichi Takeuchi, MD, PhD, Director, Doctor, Department of Medical Oncology, Ina Central Hospital, 1313-1 Ina, Nagano 396-8555, Japan.
ntakeuti@inahp.jp

Abstract

BACKGROUND

Disseminated carcinomatosis of the bone marrow (DCBM) is a widespread metastasis with a hematologic disorder that is mainly caused by gastric cancer. Although it commonly occurs as a manifestation of recurrence long after curative treatment, the precise mechanism of relapse from dormant status remains unclear. Granulocyte colony-stimulating factor (G-CSF) can promote cancer progression and invasion in various cancers. However, the potential of G-CSF to trigger recurrence from a cured malignancy has not been reported.

CASE SUMMARY

A 55-year-old Japanese woman was diagnosed with Ewing sarcoma localized on the fifth lumbar vertebrae 6 years after curative gastrectomy for T1 gastric cancer. After palliative surgery to release nerve compression, pathological diagnosis of the resected specimen was followed by curative radiation and chemotherapy. During treatment, G-CSF was administered 32 times for severe neutropenia prophylaxis. Eight months after completing definitive treatment, she complained of severe back pain and was diagnosed as multiple bone metastases with DCBM from gastric cancer. Despite palliative chemotherapy, she died of disseminated intravascular coagulation 13 d after the diagnosis. Immunohistochemical examination of the autopsied bone marrow confirmed a diffuse positive staining for the G-CSF receptor (G-CSFR) in the relapsed gastric cancer cell cytoplasm, whereas the primary lesion cancer cells showed negative staining for G-CSFR. In this case, G-CSF administration may have been the key trigger for the disseminated relapse of a dormant gastric cancer.

CONCLUSION

When administering G-CSF to cancer survivors, recurrence of a preceding cancer should be monitored even after curative treatment.

Key Words: Disseminated bone marrow carcinomatosis; Gastric cancer; Granulocyte colony-stimulating factor; Cancer survivor; Immunostaining; Case report

Core Tip: Disseminated carcinomatosis of the bone marrow (DCBM) is a rare manifestation of recurrence of a treated cancer, mainly gastric cancer. We reported a case of DCBM 8 years after curative surgery for T1 gastric cancer. Immunostaining for granulocyte colony-stimulating factor (G-CSF) receptor was diffusely positive in the relapsed lesions, but it was negative in the primary lesion. The administration of G-CSF during treatment for Ewing sarcoma within 2 years before the relapse could have been the trigger for the gastric cancer recurrence. G-CSF administration in patients with history of cancer could be a risk factor for recurrence.

Citation: Fujita K, Okubo A, Nakamura T, Takeuchi N. Disseminated carcinomatosis of the bone marrow caused by granulocyte colony-stimulating factor: A case report and review of literature. *World J Gastrointest Oncol* 2022; 14(10): 2077-2084
URL: https://www.wjgnet.com/1948-5204/full/v14/i10/2077.htm
DOI: https://dx.doi.org/10.4251/wjgo.v14.i10.2077

INTRODUCTION

Disseminated carcinomatosis of the bone marrow (DCBM) is a rare metastatic disorder that originates from gastric cancer in about 90% of cases[1-4]. Although the reported incidence of bone recurrence from curatively resected gastric cancer was 0.7%-2.1%, 13.4%-17.6% of autopsied gastric cancer cases had bone metastasis[5-9]. The duration between primary surgery and DCBM diagnosis was reportedly longer than 5 years in 66.7% of cases[10]. Therefore, disseminated tumor cells (DTCs) could stay in a prolonged subclinically dormant status. However, the precise mechanisms of this metachronous relapse are not well-known[11].

We reported a case of DCBM 8 years after curative surgery of T1 gastric cancer. Within 2 years prior to the relapse, definitive treatment with multiple granulocyte colony-stimulating factor (G-CSF) infusions for Ewing sarcoma was administered. We focused on the relationships between G-CSF administration and gastric cancer relapse.

CASE PRESENTATION

Chief complaints

A 55-year-old woman followed up for cured Ewing sarcoma at the outpatient oncology department of our hospital complained of pain all over the body, especially in the lumbar area.

History of present illness

The patient's pain started 8 mo after completing chemotherapy for Ewing sarcoma. The lumbar pain extended to the upper back and right shoulder for several weeks.

History of past illness

The patient had undergone curative distal gastrectomy with lymphadenectomy for early gastric cancer (T1aN1M0)[12], and completed a 5-year postoperative follow-up without any signs of recurrence based on tumor markers, gastroduodenoscopy, and computed tomography (CT) scans. Seven years after the gastrectomy, she had persistent pain on the right hip joint and right lumbar area, which was attributed to a soft tissue tumor on the right fifth lumbar vertebra seen on CT and magnetic resonance imaging (MRI). The pathologic diagnosis of the palliatively resected tumor was Ewing sarcoma, which was confirmed by chromosomal analysis of *ESWR1* break apart. After induction radiotherapy (50.4 Gy/28 Fr), she received adjuvant chemotherapy with 8 courses of vincristine (16 mg in total), 4 courses of doxorubicin (344 mg in total), 8 courses of cyclophosphamide (13840 mg in total), 33 courses of ifosfamide (81.2 mg in total), and 32 courses of etoposide (2240 mg in total). Six times of red blood cell

(RBC) transfusion were required for grade 4 anemia. Grade 4 neutropenia was treated with antibiotics and 18 doses of 2700 μg of filgrastim (filgrastimBS®, Nippon Kayaku, Tokyo, Japan). For severe neutropenia prophylaxis, 14 doses of 50.4 mg of pegfilgrastim (G-Lasta®, Kyowa Kirin, Tokyo, Japan) were given (Figure 1). After completion of chemotherapy, CT and MRI revealed no residual tumor.

Personal and family history

The patient had no prior history of smoking or alcohol consumption. There was no relevant family history in relation to this case report.

Physical examination

On admission, the patient's temperature was 36.3 °C, heart rate was 82 beats per minute, respiratory rate was 19 breaths per minute, blood pressure was 122/86 mmHg, and oxygen saturation at room air was 95%. Our primary clinical consideration was bone metastasis from recurrent Ewing sarcoma or gastric cancer.

Laboratory examinations

Laboratory examinations showed evident increases in serum alkaline phosphatase (ALP) at 8081 IU/L (normal, 106-322 IU/L) and pancytopenia (RBC 2.23 × 10^{12}/μL, hemoglobin 7.2 g/dL, white blood cell 8500/μL with 69% neutrophils, and platelet 2.9 × 10^{4}). The following tumor markers were elevated: Carcinoembryonic antigen (CEA) at 120.3 ng/mL (normal, < 5 ng/mL) and carbohydrate antigen 125 (CA125) at 45.5 U/mL (normal, < 35 U/mL). Notably, the ALP range was 1000-1500 IU/L during chemotherapy for Ewing sarcoma and remarkably increased when the patient complained of pain (Figure 1). Additionally, the CEA and CA125 were normal throughout the five-year follow-up of the resected gastric cancer but were not available during the treatment for Ewing sarcoma.

Imaging examinations

Bone scintigraphy, using technetium-99m hydroxymethylene diphosphonate, revealed an increased uptake in the spine, limbs, pelvis, and skull and decreased radioactivity in the kidneys (Figure 2). These characteristic image findings are called superscans (also termed super bone scans and super scan patterns) and can indicate bone marrow involvement[13,14].

MULTIDISCIPLINARY EXPERT CONSULTATION

Bone marrow biopsy from the iliac crest revealed adenocarcinoma, which seemed to be a recurrence from gastric cancer. The immunohistochemical findings of the adenocarcinoma cells were as follows: CK7(+), CK20(+), MUC2(-), MUC5AC(+), MUC6(focal+), CDX2(−), and CA19-9(−). The results were identical to those of the primary lesion of the resected stomach 8 years prior, except for CDX2, which was focally positive in the primary lesion.

Postmortem autopsy revealed the following metastatic lesions from gastric cancer: (1) Bilateral bronchopulmonary lymph nodes; (2) Scattered minute tumor emboli in the lungs; and (3) Diffuse bone marrow infiltration in the vertebrae (cervical, thoracic, and lumbar), ribs, and iliac bone. There were no recurrences of gastric cancer in the peritoneal cavity and stomach and of Ewing sarcoma all over the body. The histological and immunohistochemical findings of the autopsied bone marrow were identical to those of the bone marrow biopsy. To further investigate the mechanism of relapse, additional immunostainings on the primary and relapsed bone marrow lesions were done using anti-G-CSF antibody (clone 5.24, 1:600, Sigma-Aldrich, St. Louis, Missouri, United States) and anti-G-CSF receptor (G-CSFR) antibody (1:300, Bioss antibodies, Woburn, Massachusetts, United States). Immunostaining for G-CSF was negative in both lesions. In contrast, G-CSFR was diffusely positive in the cytoplasm of the cancer cells in the relapsed lesions but was negative in the primary lesion (Figure 3).

FINAL DIAGNOSIS

The final diagnosis was DCBM from gastric cancer that was curatively resected 8 years prior.

TREATMENT

Weekly intravenous chemotherapy that comprised methotrexate 140 mg, fluorouracil 840 mg, and calcium folinate 12 mg per course was started but needed to be stopped on day 7 because of deteriorating general condition of the patient[15-18].

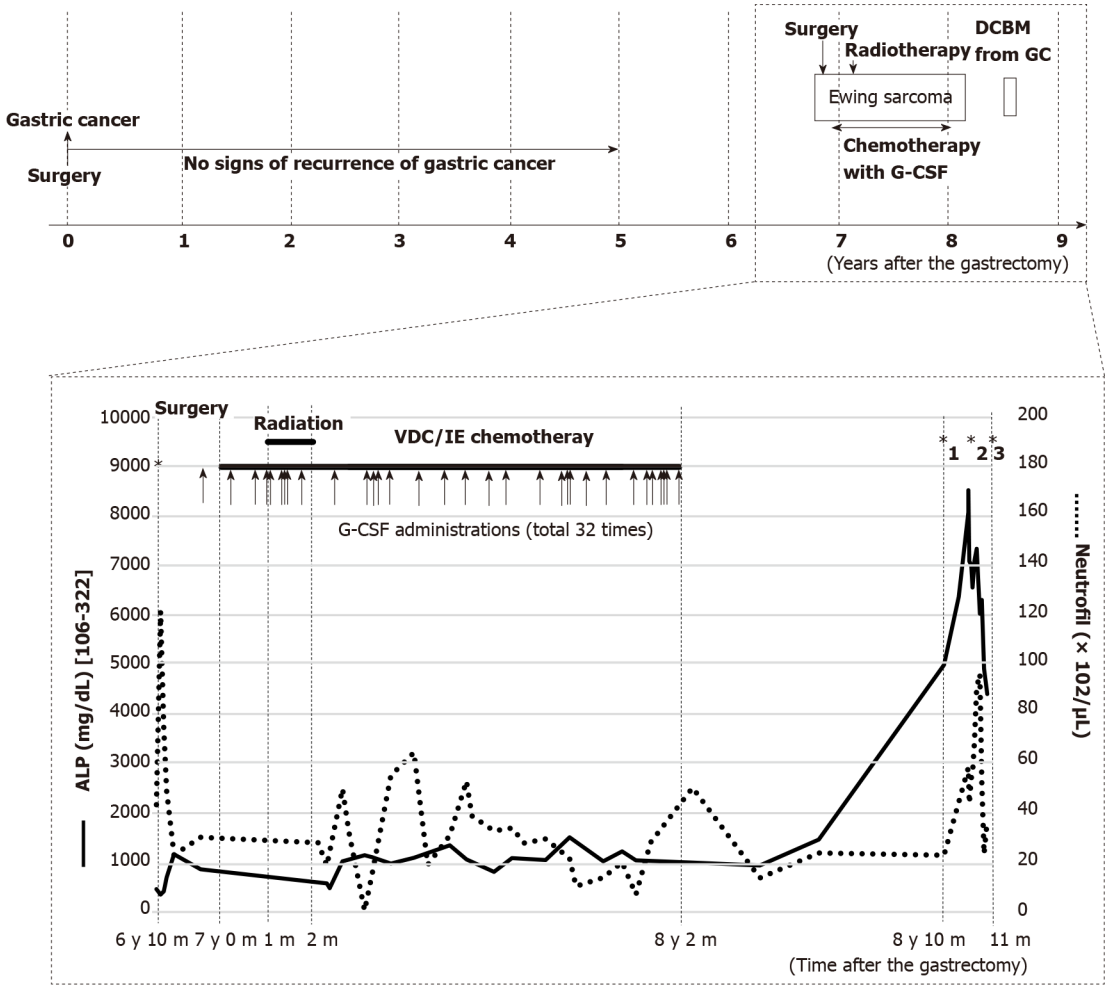

DOI: 10.4251/wjgo.v14.i10.2077

Figure 1 Clinical course after gastrectomy. During the five-year follow-up of resected gastric cancer, there are no signs of recurrence based on tumor markers, computed tomography, and gastroduodenoscopy. Eight months after completing chemotherapy with granulocyte colony-stimulating factor administration for Ewing sarcoma, disseminated carcinomatosis of the bone marrow (DCBM) from gastric cancer is diagnosed. Alkaline phosphatase is moderately elevated during the treatment of Ewing sarcoma and remarkably increased when the patient complained of lumbar pain, which led to the diagnosis of DCBM.∗1: Complaint of pain; ∗2: Bone marrow biopsy; ∗3: Died of DCBM. G-CSF: Granulocyte colony-stimulating factor; DCBM: Disseminated carcinomatosis of the bone marrow; ALP: Alkaline phosphatase; VDC/IE: Vincristine, doxorubicin, cyclophosphamide/ifosfamide, etoposide; GC: Gastric cancer.

OUTCOME AND FOLLOW-UP

Despite chemotherapy, disseminated intravascular coagulation progressed, and the patient died 13 d after the diagnosis of DCBM.

DISCUSSION

This case suggested the potential of G-CSF administration to cause recurrence presenting as DCBM from a curatively resected gastric cancer 8 years prior. Although the precise mechanism of DCBM as a manifestation of a metachronous recurrence of cured cancer is unclear, recent studies have indicated the reactivation of dormant DTCs by various factors, which are mainly related with angiogenesis and the immunologic antitumor surveillance system[19-23]. The administration of G-CSF has been reported to be one of the factors that can promote cancer progression and invasion in various cancers[24], and this interaction was confirmed *in vivo* using gastric cancer cells expressing G-CSFR[25]. However, previous clinical documentations have seldom documented that G-CSF could trigger recurrence of cured malignancies. In this report, we focus on the direct and indirect effects of G-CSF on the metachronous relapse of cured malignancies.

G-CSF can directly promote the proliferation and spread of gastric cancer cells, especially those with stem-like properties, such as CD44 and aldehyde dehydrogenase expression, by activating G-CSFR and the RERK1/2 and RSK1 phosphorylation pathways[26,27]. In the present case, G-CSFR staining was negative in the primary lesion but was diffusely positive in the relapsed lesion. This observation

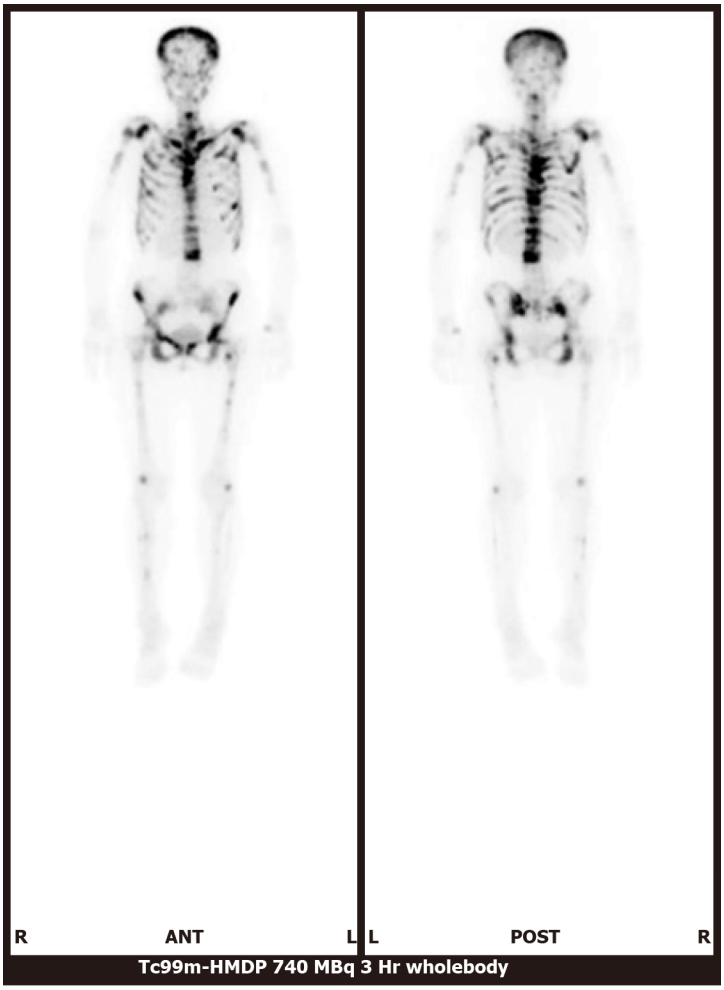

DOI: 10.4251/wjgo.v14.i10.2077

Figure 2 Bone scintigraphy using 99 m technetium-hydroxymethylene diphosphonate. There is increased uptake in the spine, limbs, pelvis, and skull and decreased uptake in the kidneys.

provided two possible explanations. First, a small amount of slow growing G-CSFR-positive gastric cancer cells could survive in a dormant state for a long period. Second, residual DTCs may develop and express G-CSFR throughout years of dormant state. G-CSF can promote the growth of solid tumors not only through G-CSFR on tumor cells but also by modulating immune cell activities or bone remodeling. G-CSF can activate myeloid derived suppressor cells and regulate T cells and macrophages, both of which can lead to the progression of solid tumors by suppressing CD8-positive T cells[28-31]. In addition, G-CSF can accelerate bone infiltration of tumor cells by activating osteoclasts and inhibiting osteoblasts[32,33]. These direct and indirect effects of G-CSF could be a positive trigger for the reactivation of dormant cancer cells.

About 90% of gastric cancer cases have positive G-CSFR staining, and some cancers have been reported to express G-CSFR[27,34]. G-CSF administration for the second primary cancers could be a risk factor for recurrence of a preceding G-CSFR-expressing primary cancer that was assumed to be cured for a long time. Therefore, G-CSF administration should be performed carefully in patients who have a preceding cancer. Considering the high incidence of G-CSFR-expressing gastric cancer, no other similar cases of gastric cancer recurrence caused by G-CSF have been reported. The possibility of G-CSF causing recurrence of a preceding cancer might have been overlooked. Because this one case is not enough to accurately evaluate the risk of G-CSF to cause recurrence, further research on the interaction between G-CSF and tumor proliferation and relapse are needed.

CONCLUSION

G-CSF administration in cancer survivors could be a risk factor for recurrence of a preceding cancer, even after curative treatment.

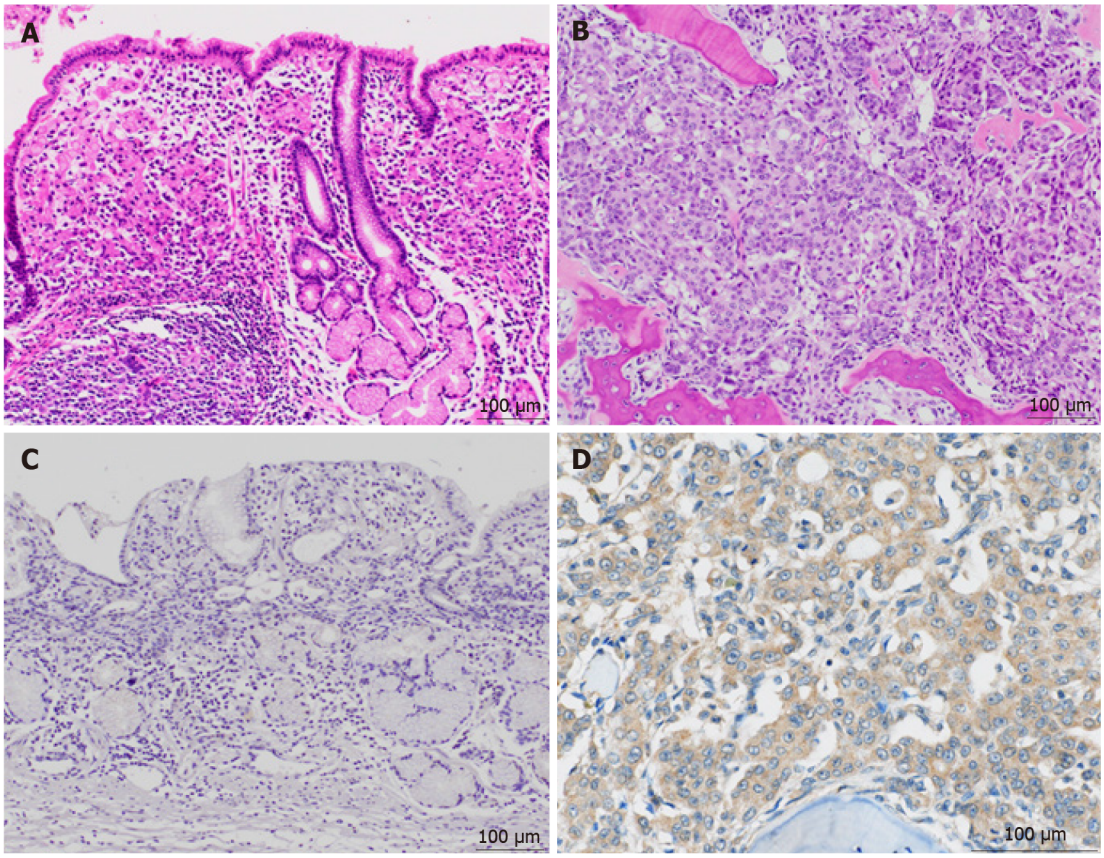

DOI: 10.4251/wjgo.v14.i10.2077

Figure 3 Histologic and immunohistochemical images of the primary and relapsed lesions. A: Histology of the primary gastric specimen shows moderately to poorly differentiated adenocarcinoma and, partially, signet cell carcinoma (hematoxylin and eosin); B: On autopsy, the metastatic bone marrow lesion shows corresponding adenocarcinoma (hematoxylin and eosin); C: Immunohistochemical staining for granulocyte colony-stimulating factor receptor (G-CSFR) is negative in the primary lesion; D: Immunohistochemical staining for G-CSFR is diffusely positive in the bone marrow metastatic lesion.

ACKNOWLEDGEMENTS

The authors thank Ms. Ayumi Karasawa, Mr. Yusuke Kohno, and Ms. Sayuri Hirashima for their excellent technical assistance.

FOOTNOTES

Author contributions: Fujita K and Okubo A collected and interpreted clinical data, reviewed the literatures, and drafted a manuscript; Nakamura T was involved in pathological diagnosis and revised the manuscript critically for intellectual content; Takeuchi N was the patient's primary oncologist and revised the manuscript critically for intellectual content; and all authors critically revised the report, commented on drafts of the manuscript, and approved the final report.

Informed consent statement: Informed written consent was obtained from the patient's family members for publication of this report and any accompanying images.

Conflict-of-interest statement: All the authors report no relevant conflicts of interest for this article.

CARE Checklist (2016) statement: The authors have read the CARE Checklist (2016), and the manuscript was prepared and revised according to the CARE Checklist (2016).

Country/Territory of origin: Japan

ORCID number: Nobumichi Takeuchi 0000-0001-9953-785X.

S-Editor: Wang JJ
L-Editor: A
P-Editor: Wang JJ

REFERENCES

1 **Iguchi H**. Recent aspects for disseminated carcinomatosis of the bone marrow associated with gastric cancer: What has been done for the past, and what will be needed in future? *World J Gastroenterol* 2015; **21**: 12249-12260 [PMID: 26604634 DOI: 10.3748/wjg.v21.i43.12249]
2 **Kikuchi Y**, Matsuzaki M, Tokura N, Kanayama K, Kanayama M, Shiratori M, Shinohara M, Igarashi Y, Sumino Y, Nakano K. Disseminated carcinomatosis of the bone marrow due to gastric cancer: Analysis of cases at Toho University and in Japan. *J Med Soc Toho* 2010; **57**: 127-136
3 **Ubukata M**, Seshimo A, Aratake K, Miyake K, Amano K, Ueda Y, Kameoka S. A case of disseminated carcinomatosa of the bone marrow from gastric cancer occurring 5 years after a curative resection. *J Jap Surg* 2012; **37**: 1120-1125 [DOI: 10.4030/jjcs.37.1120]
4 **Hasuda N**, Koshizuka K, Oyachi N, Takano K, Matsumoto M. A case report of disseminated carcinomatosis of the bone marrow from early gastric cancer 4 years after operation. *J Jap Surg Assoc* 2008; **69**: 355-359 [DOI: 10.3919/jjsa.69.355]
5 **Kobayashi M**, Okabayashi T, Sano T, Araki K. Metastatic bone cancer as a recurrence of early gastric cancer -- characteristics and possible mechanisms. *World J Gastroenterol* 2005; **11**: 5587-5591 [PMID: 16237749 DOI: 10.3748/wjg.v11.i36.5587]
6 **Mikami J**, Kimura Y, Makari Y, Fujita J, Kishimoto T, Sawada G, Nakahira S, Nakata K, Tsujie M, Ohzato H. Clinical outcomes and prognostic factors for gastric cancer patients with bone metastasis. *World J Surg Oncol* 2017; **15**: 8 [PMID: 28061855 DOI: 10.1186/s12957-016-1091-2]
7 **Rhee J**, Han SW, Oh DY, Im SA, Kim TY, Bang YJ. Clinicopathologic features and clinical outcomes of gastric cancer that initially presents with disseminated intravascular coagulation: a retrospective study. *J Gastroenterol Hepatol* 2010; **25**: 1537-1542 [PMID: 20796152 DOI: 10.1111/j.1440-1746.2010.06289.x]
8 **Etoh T**, Baba H, Taketomi A, Nakashima H, Kohnoe S, Seo Y, Fukuda T, Tomoda H. Diffuse bone metastasis with hematologic disorders from gastric cancer: clinicopathological features and prognosis. *Oncol Rep* 1999; **6**: 601-605 [PMID: 10203599 DOI: 10.3892/or.6.3.601]
9 **Turkoz FP**, Solak M, Kilickap S, Ulas A, Esbah O, Oksuzoglu B, Yalcin S. Bone metastasis from gastric cancer: the incidence, clinicopathological features, and influence on survival. *J Gastric Cancer* 2014; **14**: 164-172 [PMID: 25328761 DOI: 10.5230/jgc.2014.14.3.164]
10 **Okuno T**, Yamaguchi H, Kitayama J, Ishigami H, Nishikawa T, Tanaka J, Tanaka T, Kiyomatsu T, Hata K, Nozawa H, Kawai K, Kazama S, Ishihara S, Sunami E, Watanabe T. A case of disseminated carcinomatosis of the bone marrow originating from gastric cancer 3 years after intraperitoneal chemotherapy against peritoneal carcinomatosis. *World J Surg Oncol* 2016; **14**: 107 [PMID: 27080037 DOI: 10.1186/s12957-016-0851-3]
11 **Ubukata H**, Motohashi G, Tabuchi T, Nagata H, Konishi S. Overt bone metastasis and bone marrow micrometastasis of early gastric cancer. *Surg Today* 2011; **41**: 169-174 [PMID: 21264750 DOI: 10.1007/s00595-010-4389-7]
12 **Amin MB**, Greene FL, Edge SB, Compton CC, Gershenwald JE, Brookland RK, Meyer L, Gress DM, Byrd DR, Winchester DP. The Eighth Edition AJCC Cancer Staging Manual: Continuing to build a bridge from a population-based to a more "personalized" approach to cancer staging. *CA Cancer J Clin* 2017; **67**: 93-99 [PMID: 28094848 DOI: 10.3322/caac.21388]
13 **Pour MC**, Simon-Corat Y, Horne T. Diffuse increased uptake on bone scan: super scan. *Semin Nucl Med* 2004; **34**: 154-156 [PMID: 15031814 DOI: 10.1053/j.semnuclmed.2003.12.005]
14 **Lin CY**, Chen YW, Chang CC, Yang WC, Huang CJ, Hou MF. Bone metastasis versus bone marrow metastasis? *Kaohsiung J Med Sci* 2013; **29**: 229-233 [PMID: 23541269 DOI: 10.1016/j.kjms.2012.08.038]
15 **Takashima A**, Shirao K, Hirashima Y, Takahari D, Okita NT, Nakajima TE, Kato K, Hamaguchi T, Yamada Y, Shimada Y. Sequential chemotherapy with methotrexate and 5-fluorouracil for chemotherapy-naive advanced gastric cancer with disseminated intravascular coagulation at initial diagnosis. *J Cancer Res Clin Oncol* 2010; **136**: 243-248 [PMID: 19727819 DOI: 10.1007/s00432-009-0655-8]
16 **Hamaguchi T**, Shirao K, Yamamichi N, Hyodo I, Koizumi W, Seki S, Imamura T, Honma H, Ohtsu A, Boku N, Mukai T, Yamamoto S, Fukuda H, Yoshida S; Gastrointestinal Oncology Study Group of Japan Clinical Oncology Group. A phase II study of sequential methotrexate and 5-fluorouracil chemotherapy in previously treated gastric cancer: a report from the Gastrointestinal Oncology Group of the Japan Clinical Oncology Group, JCOG 9207 trial. *Jpn J Clin Oncol* 2008; **38**: 432-437 [PMID: 18515821 DOI: 10.1093/jjco/hyn043]
17 **Murad AM**, Santiago FF, Petroianu A, Rocha PR, Rodrigues MA, Rausch M. Modified therapy with 5-fluorouracil, doxorubicin, and methotrexate in advanced gastric cancer. *Cancer* 1993; **72**: 37-41 [PMID: 8508427 DOI: 10.1002/1097-0142(19930701)72:1<37::aid-cncr2820720109>3.0.co;2-p]
18 **Wils JA**, Klein HO, Wagener DJ, Bleiberg H, Reis H, Korsten F, Conroy T, Fickers M, Leyvraz S, Buyse M. Sequential high-dose methotrexate and fluorouracil combined with doxorubicin--a step ahead in the treatment of advanced gastric cancer: a trial of the European Organization for Research and Treatment of Cancer Gastrointestinal Tract Cooperative Group. *J Clin Oncol* 1991; **9**: 827-831 [PMID: 2016625 DOI: 10.1200/JCO.1991.9.5.827]
19 **Hen O**, Barkan D. Dormant disseminated tumor cells and cancer stem/progenitor-like cells: Similarities and opportunities. *Semin Cancer Biol* 2020; **60**: 157-165 [PMID: 31491559 DOI: 10.1016/j.semcancer.2019.09.002]

20 **Triana-Martínez F**, Loza MI, Domínguez E. Beyond Tumor Suppression: Senescence in Cancer Stemness and Tumor Dormancy. *Cells* 2020; **9**: 346 [PMID: 32028565 DOI: 10.3390/cells9020346]

21 **Saleh T**, Bloukh S, Carpenter VJ, Alwohoush E, Bakeer J, Darwish S, Azab B, Gewirtz DA. Therapy-Induced Senescence: An "Old" Friend Becomes the Enemy. *Cancers (Basel)* 2020; **12**: 822 [PMID: 32235364 DOI: 10.3390/cancers12040822]

22 **Jahanban-Esfahlan R**, Seidi K, Manjili MH, Jahanban-Esfahlan A, Javaheri T, Zare P. Tumor Cell Dormancy: Threat or Opportunity in the Fight against Cancer. *Cancers (Basel)* 2019; **11**: 1207 [PMID: 31430951 DOI: 10.3390/cancers11081207]

23 **Aguirre-Ghiso JA**. Models, mechanisms and clinical evidence for cancer dormancy. *Nat Rev Cancer* 2007; **7**: 834-846 [PMID: 17957189 DOI: 10.1038/nrc2256]

24 **Theron AJ**, Steel HC, Rapoport BL, Anderson R. Contrasting Immunopathogenic and Therapeutic Roles of Granulocyte Colony-Stimulating Factor in Cancer. *Pharmaceuticals (Basel)* 2020; **13**: 406 [PMID: 33233675 DOI: 10.3390/ph13110406]

25 **Baba M**, Hasegawa H, Nakayabu M, Shimizu N, Suzuki S, Kamada N, Tani K. Establishment and characteristics of a gastric cancer cell line (HuGC-OOHIRA) producing high levels of G-CSF, GM-CSF, and IL-6: the presence of autocrine growth control by G-CSF. *Am J Hematol* 1995; **49**: 207-215 [PMID: 7541602 DOI: 10.1002/ajh.2830490306]

26 **Fan Z**, Li Y, Zhao Q, Fan L, Tan B, Zuo J, Hua K, Ji Q. Highly Expressed Granulocyte Colony-Stimulating Factor (G-CSF) and Granulocyte Colony-Stimulating Factor Receptor (G-CSFR) in Human Gastric Cancer Leads to Poor Survival. *Med Sci Monit* 2018; **24**: 1701-1711 [PMID: 29567938 DOI: 10.12659/MSM.909128]

27 **Morris KT**, Khan H, Ahmad A, Weston LL, Nofchissey RA, Pinchuk IV, Beswick EJ. G-CSF and G-CSFR are highly expressed in human gastric and colon cancers and promote carcinoma cell proliferation and migration. *Br J Cancer* 2014; **110**: 1211-1220 [PMID: 24448357 DOI: 10.1038/bjc.2013.822]

28 **Pilatova K**, Bencsikova B, Demlova R, Valik D, Zdrazilova-Dubska L. Myeloid-derived suppressor cells (MDSCs) in patients with solid tumors: considerations for granulocyte colony-stimulating factor treatment. *Cancer Immunol Immunother* 2018; **67**: 1919-1929 [PMID: 29748897 DOI: 10.1007/s00262-018-2166-4]

29 **Karagiannidis I**, Jerman SJ, Jacenik D, Phinney BB, Yao R, Prossnitz ER, Beswick EJ. G-CSF and G-CSFR Modulate CD4 and CD8 T Cell Responses to Promote Colon Tumor Growth and Are Potential Therapeutic Targets. *Front Immunol* 2020; **11**: 1885 [PMID: 33042110 DOI: 10.3389/fimmu.2020.01885]

30 **Karagiannidis I**, de Santana Van Vilet E, Said Abu Egal E, Phinney B, Jacenik D, Prossnitz ER, Beswick EJ. G-CSF and G-CSFR Induce a Pro-Tumorigenic Macrophage Phenotype to Promote Colon and Pancreas Tumor Growth. *Cancers (Basel)* 2020; **12** [PMID: 33036138 DOI: 10.3390/cancers12102868]

31 **Motallebnezhad M**, Jadidi-Niaragh F, Qamsari ES, Bagheri S, Gharibi T, Yousefi M. The immunobiology of myeloid-derived suppressor cells in cancer. *Tumour Biol* 2016; **37**: 1387-1406 [PMID: 26611648 DOI: 10.1007/s13277-015-4477-9]

32 **Li S**, Li T, Chen Y, Nie Y, Li C, Liu L, Li Q, Qiu L. Granulocyte Colony-Stimulating Factor Induces Osteoblast Inhibition by B Lymphocytes and Osteoclast Activation by T Lymphocytes during Hematopoietic Stem/Progenitor Cell Mobilization. *Biol Blood Marrow Transplant* 2015; **21**: 1384-1391 [PMID: 25985917 DOI: 10.1016/j.bbmt.2015.05.005]

33 **Li S**, Zhai Q, Zou D, Meng H, Xie Z, Li C, Wang Y, Qi J, Cheng T, Qiu L. A pivotal role of bone remodeling in granulocyte colony stimulating factor induced hematopoietic stem/progenitor cells mobilization. *J Cell Physiol* 2013; **228**: 1002-1009 [PMID: 23042582 DOI: 10.1002/jcp.24246]

34 **Yeo B**, Redfern AD, Mouchemore KA, Hamilton JA, Anderson RL. The dark side of granulocyte-colony stimulating factor: a supportive therapy with potential to promote tumour progression. *Clin Exp Metastasis* 2018; **35**: 255-267 [PMID: 29968171 DOI: 10.1007/s10585-018-9917-7]

World Journal of Gastrointestinal Oncology

Submit a Manuscript: https://www.f6publishing.com

World J Gastrointest Oncol 2022 October 15; 14(10): 2085-2087

DOI: 10.4251/wjgo.v14.i10.2085

ISSN 1948-5204 (online)

CORRECTION

Correction to "Genome-wide CRISPR-Cas9 screening identifies that hypoxia-inducible factor-1a-induced CBX8 transcription promotes pancreatic cancer progression *via* IRS1/AKT axis"

Bu-Wei Teng, Kun-Dong Zhang, Yu-Han Yang, Zeng-Ya Guo, Wei-Wei Chen, Zheng-Jun Qiu

Specialty type: Oncology

Provenance and peer review: Unsolicited article; Externally peer reviewed.

Peer-review model: Single blind

Peer-review report's scientific quality classification

Grade A (Excellent): A
Grade B (Very good): B
Grade C (Good): C
Grade D (Fair): 0
Grade E (Poor): 0

P-Reviewer: Liu H, United States; Solimando AG, Italy; Trna J, Czech Republic

Received: April 6, 2022
Peer-review started: April 6, 2022
First decision: June 12, 2022
Revised: June 15, 2022
Accepted: September 13, 2022
Article in press: September 13, 2022
Published online: October 15, 2022

Bu-Wei Teng, Department of General Surgery, Shanghai General Hospital of Nanjing Medical University, Shanghai 200080, China

Bu-Wei Teng, Department of General Surgery, Lianyungang Clinical College of Nanjing Medical University/The First People's Hospital of Lianyungang, Lianyungang 222061, Jiangsu Province, China

Kun-Dong Zhang, Yu-Han Yang, Zeng-Ya Guo, Wei-Wei Chen, Zheng-Jun Qiu, Department of General Surgery, Shanghai General Hospital, Shanghai 200080, China

Corresponding author: Zheng-Jun Qiu, MD, Chief Doctor, Director, Surgeon, Department of General Surgery, Shanghai General Hospital, No. 100 Haining Road, Shanghai 200080, China. zhengjun.qiu@shgh.cn

Abstract

Correction to "Genome-wide CRISPR-Cas9 screening identifies that hypoxia-inducible factor-1a-induced CBX8 transcription promotes pancreatic cancer progression *via* IRS1/AKT axis" (PMID: 34853645 PMCID: PMC8603463 DOI: 10.4251/wjgo.v13.i11.1709). In this article, the picture of Figure 6C was misused due to our carelessness while typesetting. We corrected this mistake, and replaced the incorrect image with the correct one.

Key Words: Correction; Error; Figure; CRISPR-Cas9

Core Tip: Correction to "Genome-wide CRISPR-Cas9 screening identifies that hypoxia-inducible factor-1a-induced CBX8 transcription promotes pancreatic cancer progression *via* IRS1/AKT axis."

Citation: Teng BW, Zhang KD, Yang YH, Guo ZY, Chen WW, Qiu ZJ. Correction to "Genome-wide CRISPR-Cas9 screening identifies that hypoxia-inducible factor-1a-induced CBX8 transcription promotes pancreatic cancer progression *via* IRS1/AKT axis". *World J Gastrointest Oncol* 2022; 14(10): 2085-2087
URL: https://www.wjgnet.com/1948-5204/full/v14/i10/2085.htm
DOI: https://dx.doi.org/10.4251/wjgo.v14.i10.2085

TO THE EDITOR

After confirming the figures in our manuscript, we were surprised to find a mistake in Figure 6C[1]. It was an unintentional error that occurred when we typeset the images. We have replaced the incorrect images with the correct Figure 6C (Figure 1). Figure 6D-E was based on the correct image and does not need to be changed. We assure you that this mistake does not change the meaning of the picture or the conclusion of the manuscript. We apologize for our careless mistake, which has caused great inconvenience.

DOI: 10.4251/wjgo.v14.i10.2085

Figure 1 We replaced the incorrect images with the correct Figure 6C in "Genome-wide CRISPR-Cas9 screening identifies that hypoxia-inducible factor-1a-induced CBX8 transcription promotes pancreatic cancer progression *via* IRS1/AKT axis."

FOOTNOTES

Author contributions: Teng BW found and corrected the misused figure; Zhang KD, Yang YH, Guo ZY, Chen WW, and Qiu ZJ checked the correction.

Conflict-of-interest statement: There are no conflicts of interest to report.

Country/Territory of origin: China

ORCID number: Bu-Wei Teng 0000-0002-9555-2830; Kun-Dong Zhang 0000-0002-2232-2153; Yu-Han Yang 0000-0002-3717-5088; Zeng-Ya Guo 0000-0001-8310-5147; Wei-Wei Chen 0000-0001-8325-5663; Zheng-Jun Qiu 0000-0002-8318-847X.

S-Editor: Chen YL
L-Editor: Filipodia
P-Editor: Chen YL

REFERENCES

1 **Teng BW**, Zhang KD, Yang YH, Guo ZY, Chen WW, Qiu ZJ. Genome-wide CRISPR-Cas9 screening identifies that hypoxia-inducible factor-1a-induced *CBX8* transcription promotes pancreatic cancer progression *via* IRS1/AKT axis. *World J Gastrointest Oncol* 2021; **13**: 1709-1724 [PMID: 34853645 DOI: 10.4251/wjgo.v13.i11.1709]

Published by **Baishideng Publishing Group Inc**
7041 Koll Center Parkway, Suite 160, Pleasanton, CA 94566, USA
Telephone: +1-925-3991568
E-mail: bpgoffice@wjgnet.com
Help Desk: https://www.f6publishing.com/helpdesk
https://www.wjgnet.com